UNSW SYDNEY

Natural Organics Removal using Membranes

Author:
Schäfer, Andrea Iris

Publication Date:
1999

DOI:
https://doi.org/10.26190/unsworks/21834

License:
https://creativecommons.org/licenses/by-nc-nd/3.0/au/
Link to license to see what you are allowed to do with this resource.

Downloaded from http://hdl.handle.net/1959.4/20695 in https://unsworks.unsw.edu.au on 2026-09-03

Natural Organics Removal Using Membranes

Doctor of Philosophy (PhD)
October 1999

Andrea Iris SCHÄFER

UNESCO Centre for Membrane Science and Technology
Chemical Engineering and Industrial Chemistry
The University of New South Wales
Sydney NSW 2515, AUSTRALIA









CERTIFICATE OF ORIGINALITY

I hereby declare that this submission is my own work and that, to the best of my knowledge and belief, it contains no materials previously published or written by another person, nor material which to a substantial extent has been accepted for the award of any other degree or diploma at UNSW or any other educational institution, except where due acknowledgement is made in the thesis.

I also declare that the intellectual content of this thesis is the product of my own work, except to the extent that assistance from others in the project's design and conception or in style, presentation and linguistic expression is acknowledged.

Andrea Iris Schäfer

REVIEW PANEL

1. **Prof. Menachem Elimelech**, Yale University, Environmental Engineering, New Haven, Cinneticut, USA. menachem.elimelech@yale.edu

2. **Prof. Mark Wiesner**, Rice University, Environmental Science and Engineering, Houston, Texas, USA. wiesner@rice.edu

3. **Dr. Pierre Aimar**, Université Paul Sabatier, Laboratoire Génie Chimique, Toulouse, France. aimar@dr14.cnrs.fr

Schäfer, Andrea Iris
Natural Organics Removal using Membranes
PhD Thesis, UNSW, UNESCO Centre for Membrane Science and Technology, Chemical Engineering.
Copyright © 1999 all rights reserved.

ISBN 0 7334 0652 1

ABSTRACT

Membrane processes are increasingly used in water treatment. Experiments were performed using stirred cell equipment, polymeric membranes and synthetic surface water containing natural organics, inorganic colloids and their aggregates, and cations.

All processes could remove a significant amount of natural organics. Pretreatment with ferric chloride was required to achieve significant organic removal with MF and high MWCO UF.

Additionally, fouling mechanisms for the three processes were investigated. Crucial parameters were aggregate characteristics (fractal structure, stability, organic-colloid interactions), solubility of organics and calcium, and hydrodynamics.

In MF, fouling by pore plugging was most severe. Variations in solution chemistry changed the aggregation state of the colloids and/or natural organic matter and dramatically affected rejection and fouling behaviour.

UF membrane fouling was mainly influenced by pore adsorption and could improve natural organics rejection significantly. Coagulant addition shifted fouling mechanism from pore adsorption to cake formation. Aggregate structure was most significant for flux decline.

In NF, rejection of natural organics involved both size and charge exclusion. Fouling was caused by precipitation of a calcium-organic complex and could be avoided by pretreatment with metal salt coagulants.

Thorough chemical characterisation of the organics used demonstrated that only size and aromaticity can be related to fouling.

The study is concluded with a process comparison based on a water quality parameter and a cost comparison. Treatment cost of microfiltration with chemical pretreatment was similar to that of nanofiltration at a comparable natural organics rejection.

ACKNOWLEDGEMENTS

I would like to thank my supervisors, Tony Fane, and David Waite, for their time, scientific input, personal skills, guidance, and continued support for all my 'special projects', which allowed almost complete freedom and creativity. May our scientific co-operation and friendship carry on.

Thanks to the undergraduate students who contributed with experimental work to this project - without you the broad scope of this work would not have been possible: Netty Sugiharto (UNSW), Osar Hassum-Tenara (UNSW), Torben Schlieckau (Uni Hamburg, Germany), Axel Heuer, Rainer Mauch, Martina Fischer, Ursula Schwicker (all Uni Stuttgart, Germany), Emmanuelle Aoustin (ENSCM, France) - you taught me a great deal!

The German Academic Exchange Council (DAAD) and the CRC for Water Quality and Treatment deserve special gratitude for making it all possible with scholarships, as well as project and travel funding. The Australian Government is thanked for an OPRS scholarship.

Thanks to those who helped with technical and scientific support in the UNESCO Centre for Membrane Science and Technology (UNSW), Chemical Engineering Workshop (UNSW), Australian Water Quality Centre (Australia), CSIRO Molecular Science (Australia), Civil Engineering (UNSW), Waite Institute (Australia), Centre for Particle Technology (UNSW), Food Technology (UNSW), Microbiology (UNSW), Surface Chemistry (UNSW), Electron Microscope Unit (UNSW), Photovoltaics Special Research Centre (UNSW), ATA Scientific (Australia), DOC Labor Stefan Huber (Germany), IWW Uni Duisburg (Germany), Millipore (Australia), Fluid Systems (San Diego, US), Memtec (Australia), University of Lappeenranta (Finland), Gosford City Council (Australia). It is greatly appreciated.

My gratitude to the international membrane family - always the same crowd who meets and hangs out at all these conferences. It is a very special feeling to be at membrane conferences and many of you were and are great mentors. Thanks to Dr. Rudi Graf (Berghof GmBH, Germany) who made me fall in love with membranes 10 years ago.

Thanks to my friends and family - thanks for accepting me going my own way; for being there when I needed you; and, thanks for writing, visiting and caring, especially during the hard times.

A very special thanks to Bryce for your love. Thanks for the uncountable support in almost unbearable struggles with administration and immigration, putting up with moods, listening to worries, fulfilling my countless expectations, proof-reading, and all this while doing your own dissertation!

Thanks for those who were spiritual teachers and gave this time a 'philosophical' touch, participating in the struggle of confidence, questioning, frustration, curiosity, enthusiasm, disappointment, persistence, search for happiness and grief. Thanks to the callers from Lifeline for helping me keep my feet on the ground, my mind well connected to life, and putting my 'giant' problems into the context of real life.

Finally, thanks to nature, the bush, the sea, creatures such as birds and dolphins, the mountains and the weather, all so present in Australia to be enjoyed to help relax and get away. May I be able to return a favour one day by using my knowledge to protect you from technological nonsense which is progressing so unquestioned.

It was worth it!

DEDICATION

This thesis is dedicated to my dad, Rainer Schäfer, from whom I inherited some of the characteristics which were so essential to complete this PhD - commitment, persistence, and a fighting spirit – and who cannot be there anymore to see the outcome of his efforts.

This thesis is also in remembrance of those other friends and family who we lost during its completion – Steve Robbo, Hans Kraft, Niels, and Irene Schäfer – and in expectation of a new family member due to arrive in early 2000.

May we accept the natural cycle of life.

CONTENTS

Abstract i

Acknowledgements iii

Dedication v

Chapter 1 – *Introduction* 1

Chapter 2 – *Characterisation of Natural Organics - A Review* 5

2.1 INTRODUCTION 6

2.2 DEFINITION OF NATURAL ORGANICS 7

2.2.1 Nature of Different Natural Organics 7
2.2.2 Definition of Compounds 7

2.3 ORIGIN OF NATURAL ORGANICS 8

2.3.1 Chemical Formation, Humification and Aging 8
2.3.2 Biological Activity 8
2.3.3 Soil and Vegetation 9
2.3.4 Weather and Seasonal Variations 9
2.3.5 Lake Waters versus Freshwater Streams 9
2.3.6 Groundwater 9
2.3.7 Pollution by Human Activity 9
2.3.8 Availability for Research 10

2.4 EXTRACTION OF NATURAL ORGANICS FROM WATERS 10

2.4.1 Ion Exchange Resin 10
2.4.2 Reverse Osmosis 11
2.4.3 Desalting 12
2.4.4 Purification 12

2.5 CHARACTERISATION OF NATURAL ORGANICS 13

2.5.1 Concentration Measurements of Natural Organics 13
2.5.2 Aromaticity and Reactivity 13
2.5.3 Hydrophobicity 14
2.5.4 Size, Molecular Weight, Radii of Gyration, Polydispersity 14
2.5.5 Diffusion Coefficient 19
2.5.6 Elemental Analysis and Structure 19
2.5.7 Functional Groups 20

2.5.8 Charge and Acidity 21
2.5.9 Solubility and Aggregation of Natural Organics 22
2.5.10 Micelle Formation of Natural Organics and Surfactant Characteristcs 23
2.5.11 Structure/Fractal Dimension of Natural Organics 23

2.6 FRACTIONATION OF NATURAL ORGANICS 24

2.6.1 Particulate/Dissolved Organic Carbon Separation 24
2.6.2 FA/HA Separation 24
2.6.3 Size/MW Fractionation 24
2.6.4 Hydrophilic/Hydrophobic Fractionation 24

2.7 VARIATIONS OF NATURAL ORGANICS CHARACTERISTICS WITH SOLUTION CHEMISTRY 25

2.7.1 Effect of Organic Concentration 25
2.7.2 Effect of Ionic Strength 25
2.7.3 Effect of pH 26

2.8 INTERACTIONS OF NATURAL ORGANICS WITH OTHER SOLUTES 26

2.8.1 Cations 26
2.8.2 Trace Metals 27
2.8.3 Interactions with Other Compounds 27

2.9 INTERACTIONS OF NATURAL ORGANICS WITH COLLOIDS 28

2.9.1 Characterisation of Natural Organics and Colloid Systems 28
2.9.2 Organic Adsorption onto Colloids 29
2.9.3 Colloid Stabilisation and Mobilisation 31
2.9.4 Aggregate Formation and Structure 32

2.10 NATURAL ORGANICS IN WATER TREATMENT 32

2.10.1 Drinking Water Standards 32
2.10.2 Treatability of Natural Organics by different Processes 33
2.10.3 Disinfection By-Product Formation 33
2.10.4 Bacterial Regrowth, Biofilms and Conditioning Films 33
2.10.5 Membrane Fouling 34

2.11 SUMMARY 35

2.12 CONCLUSIONS 37

Chapter 3 - *Membrane Review* *39*

3.1 INTRODUCTION AND OVERVIEW 40

3.2 FUNDAMENTAL PRINCIPLES AND MECHANISMS 42

3.2.1 Microfiltration (MF) 43
3.2.2 Ultrafiltration (UF) 47
3.2.3 Nanofiltration (NF) 48
3.2.4 Reverse Osmosis (RO) 50

3.3 MEMBRANES 53

3.3.1 Membrane Materials for MF and UF 53
3.3.2 Membrane Materials for NF and RO 53
3.3.3 TFC Membrane Modification in NF 53
3.3.4 Membrane Selection, Testing and Evaluation 54

3.4 REJECTION OF NATURAL ORGANICS AND COLLOIDS 55

3.4.1 Microfiltration (MF) 55
3.4.2 Ultrafiltration (UF) 55
3.4.3 Nanofiltration and Reverse Osmosis 57
3.4.4 Variation of Rejection due to Fouling 62

3.5 FOULING BY NATURAL ORGANICS AND COLLOIDS 63

3.5.1 Organic Fouling 63
3.5.2 Inorganic Fouling or Scaling 68
3.5.3 Colloid and Particle Fouling 69

3.6 MEMBRANE AND FOULING LAYER CHARACTERISATION 75

3.6.1 Microscopic Techniques 75
3.6.2 Surface Charge 76
3.6.3 Hydrophobicity and State of Water 76
3.6.4 Deposit Morphology and Surface Analysis 77

3.7 FOULING CONTROL 78

3.7.1 Pretreatment for Rejection Increase and Fouling Prevention 78
3.7.2 Backwashing, Backflushing, and Operation Mode 82
3.7.3 Membrane Cleaning 83

3.8 MEMBRANE PROCESS APPLICATIONS IN WATER TREATMENT 84

3.8.1 Membrane Processes versus Conventional Treatment 84
3.8.2 Membranes versus other Alternatives 85
3.8.3 Microfiltration 85
3.8.4 Ultrafiltration 86
3.8.5 Nanofiltration and Reverse Osmosis 86
3.8.6 Hybrid Membrane Processes 87
3.8.7 Cost 88

3.9 CONCLUSION 89

Chapter 4 - *Materials and Methods* *91*

4.1 CHEMICALS AND BACKGROUND SOLUTION 92

4.2 ORGANICS 92

4.3 HEMATITE COLLOIDS (α-FE_2O_3) 93

4.4 MEMBRANES 93

4.4.1 Microfiltration Membranes 94
4.4.2 Ultrafiltration Membranes 94

4.4.3 Nanofiltration Membranes 94

4.5 FILTRATION EQUIPMENT 96

4.5.1 Microfiltration Equipment 96
4.5.2 Ultrafiltration Equipment 96
4.5.3 Nanofiltration Equipment 97

4.6 GENERAL ANALYTICAL METHODS 98

4.6.1 pH Value 98
4.6.2 Conductivity 98
4.6.3 Inductively Coupled Plasma Atomic Emission Spectroscopy (ICP-AES) 98
4.6.4 Ion Chromatography (IC) 99

4.7 ORGANICS CHARACTERISATION 99

4.7.1 Dissolved Organic Carbon (DOC) 99
4.7.2 UV/VIS Spectroscopy 99
4.7.3 Titration 100
4.7.4 Elemental Analysis 101
4.7.5 XAD Fractionation 101
4.7.6 Cation Content of Organics 102
4.7.7 High Performance Size Exclusion Chromatography (HPLC-SEC) 102
4.7.8 Ultrafiltration Fractionation 104
4.7.9 Liquid Chromatography – Organic Carbon Detection (LC-OCD) 107
4.7.10 Humic Solubility and Aggregation 112
4.7.11 Viscosity 113
4.7.12 Matrix Assisted Laser Desorption/Ionisation (MALDI) 114
4.7.13 Diffuse Reflectance Fourier Transform Infrared Spectroscopy (DRIFT) 114

4.8 SOLUTION PREPARATION 116

4.8.1 Stable Hematite Colloids in Absence of Organics 116
4.8.2 Colloids at pH 3 with Organics 116
4.8.3 Reaction Limited Aggregation (RLA) 117
4.8.4 Diffusion Limited Aggregation (DLA) 117
4.8.5 SPO: Aggregates with Organics 117
4.8.6 OPS: Colloids Stabilised with Organics 117
4.8.7 Coagulation 118

4.9 PARTICLE AND AGGREGATE CHARACTERISATION 120

4.9.1 Zeta Potential and Mobility of Particles 120
4.9.2 Particle Size and Structure Analysis/Fractal Dimension (Malvern) 122
4.9.3 Aggregate Size 122
4.9.4 Aggregate Structure 124
4.9.5 Photon Correlation Spectroscopy (PCS) 126

4.10 MEMBRANE AND DEPOSIT CHARACTERISATION 127

4.10.1 Zeta Potential of Membranes 127
4.10.2 Field Emission Scanning Electron Microscopy (FESEM) 128
4.10.3 Electron Dispersive Spectra (EDS) 129

4.10.4 X-Ray Photoelectron spectroscopy (XPS) 130
4.10.5 Contact angle measurements 130
4.10.6 Determination of Membrane Mass Deposit 130

Chapter 5 – *Microfiltration* *131*

5.1 INTRODUCTION 132

5.2 FILTRATION PROTOCOL 133

5.3 MEMBRANE CHARACTERISATION 134

5.4 MF OF ORGANICS IN THE ABSENCE OF INORGANIC COLLOIDS 136

5.5 MF OF INORGANIC COLLOIDS IN THE ABSENCE OF ORGANICS 137

5.5.1 Effect of primary particle size 137
5.5.2 Effect of pH 138
5.5.3 Effect of Aggregation 138

5.6 INORGANIC COLLOIDS AT PH 3 WITH ORGANICS 141

5.7 MF OF AGGREGATED COLLOIDS WITH ADDITION OF ORGANICS (SPO) 142

5.7.1 Effect of membrane type 142
5.7.2 Effect of organic type and concentration 142
5.7.3 Effect of primary particle size 143
5.7.4 Effect of calcium concentration 143
5.7.5 Effect of stirring 145
5.7.6 Effect of pH 145
5.7.7 Effect of transmembrane pressure 146

5.8 MF OF STABILISED COLLOIDS (OPS) 148

5.8.1 Effect of membrane type 148
5.8.2 Effect of organic type and concentration 148
5.8.3 Effect of primary particle size 149
5.8.4 Effect of calcium concentration 149
5.8.5 Effect of pH 149

5.9 BLOCKING LAW ANALYSIS 150

5.9.1 Stable Colloids in the Absence of Organics 150
5.9.2 Aggregated Colloids with subsequent Addition of Organics (SPO) 151
5.9.3 Stabilised Colloids (OPS) 153

5.10 MF OF $FECL_3$-COAGULATED SOLUTIONS 154

5.10.1 Microfiltration of Coagulated Organic Solutions 155
5.10.2 Microfiltration and Coagulation of Particle Suspensions 156

5.11 SUMMARY 158

5.12 CONCLUSION 160

Chapter 6 – *Ultrafiltration* *161*

6.1 INTRODUCTION **163**

6.2 FILTRATION PROTOCOL **163**

6.2.1 Fractionation and Rejection Experiments 163
6.2.2 Aggregation Experiments 163
6.2.3 Fouling Experiments 163

6.3 MEMBRANE CHARACTERISATION **164**

6.3.1 Pure Water Flux 164
6.3.2 Molecular Weight Cut-Off or Pore Size 164
6.3.3 Membrane Surface Roughness 165
6.3.4 Membrane Surface Charge 166

6.4 REJECTION AND FRACTIONATION EXPERIMENTS **167**

6.4.1 Effect of Ionic Strength 167
6.4.2 Effect of pH 167
6.4.3 Effect of Organic Concentration 168
6.4.4 Effect of Calcium Concentration 170
6.4.5 Effect of Organic Type 170
6.4.6 Cation Rejection by UF 171
6.4.7 UV_{254nm}/DOC Ratio 172
6.4.8 Comparison of UF fractionation and Size Exclusion Chromatography (SEC) 172
6.4.9 Chemical Analysis of the UF Fractions using LC-OCD 175

6.5 FILTRATION OF INORGANIC AGGREGATES **178**

6.5.1 Theoretical Considerations 178
6.5.2 Effect of KCl 180
6.5.3 Effect of $CaCl_2$ 182
6.5.4 Effect of pH 183
6.5.5 Effect of IHSS Fulvic Acid 184
6.5.6 Aggregate Characteristics and their Effect on Membrane Filtration 185

6.6 FILTRATION OF ORGANICS AND CALCIUM **190**

6.6.1 Calcium Concentration 190
6.6.2 Organic Type 192
6.6.3 Effect of Flux on Fouling 194
6.6.4 Blocking Law Analysis 195

6.7 FILTRATION OF INORGANIC COLLOIDS AND ORGANICS **197**

6.7.1 Stable Colloids in the Absence of Organics 197
6.7.2 Aggregates in the Absence of Organics 198
6.7.3 Colloids Stabilised by Organics (OPS) 199
6.7.4 Aggregates in Presence of Organics (SPO) 201
6.7.5 Comparison of Membrane Deposits formed by OPS and SPO Systems 203

6.8 COAGULATION PRETREATMENT **204**

6.8.1 Effect of Ferric Hydroxide Flocs on Flux in the Absence of Organics 204
6.8.2 Effect of Ferric Chloride on Rejection and Flux 205
6.8.3 Coagulation of OPS Systems 206
6.8.4 Coagulation of SPO Systems 208
6.8.5 Blocking Law Analysis 208

6.9 SUMMARY 211

6.10 CONCLUSION 214

Chapter 7 – *Nanofiltration* *215*

7.1 INTRODUCTION 216

7.2 FILTRATION PROTOCOL 216

7.2.1 Membrane Compaction and Baseline 216
7.2.2 Protocol for Rejection Experiments 217
7.2.3 Protocol for Recycle Experiments 217

7.3 MEMBRANE CHARACTERISATION 219

7.3.1 Effect of Temperature on Water Flux 219
7.3.2 Membrane 'Pore Size' 220
7.3.3 Membrane Surface Charge 221
7.3.4 Surface Roughness 224
7.3.5 Contact Angle 224

7.4 REJECTION EXPERIMENTS 226

7.4.1 Salt Rejection in the Absence of Organics 226
7.4.2 Organics and Salt Rejection in Synthetic Surface Water Solutions 228

7.5 FOULING CONSIDERATIONS 238

7.5.1 Mass Balance for Deposit Calculations 238
7.5.2 Estimation of Adsorption of Organics on Membrane Surface 238
7.5.3 Concentration Polarisation and Osmotic Pressure 239
7.5.4 Mass Transfer Coefficient and Wall Concentration 240
7.5.5 Osmotic Pressure in Solutions and Boundary Layer 242
7.5.6 Solubility of Calcium and Natural Organic Matter (NOM) 243

7.6 FOULING EXPERIMENTS 244

7.6.1 Effect of Background Electrolyte 244
7.6.2 Effect of Organic Type 247
7.6.3 Effect of Calcium Concentration 248
7.6.4 Critical Fouling Conditions 251
7.6.5 Effect of Organic Concentration and Type 253
7.6.6 Effect of pH 258
7.1.1 Effect of Transmembrane Pressure 260
7.6.7 Effect of Inorganic Colloids 262

7.7 COAGULATION PRETREATMENT 265

7.7.1 Effect of Organic Type 265
7.7.2 Effect of Ferric Chloride on Treatment of Solutions containing Colloids and HA 266
7.7.3 Effect of Ferric Chloride Addition at Critical Fouling Conditions 268
7.7.4 Permeate LC-OCD Analysis 269
7.7.5 Suggested Mechanisms 270

7.8 MEMBRANE DEPOSIT MORPHOLOGY STUDIES 272

7.8.1 Electronmicroscopy 272
7.8.2 XPS Analysis 274
7.8.3 Contact Angle 275

7.9 SUMMARY 276

7.10 CONCLUSION 280

Chapter 8 - *Process Comparison* *281*

8.1 INTRODUCTION 282

8.2 PURE WATER MEMBRANE CHARACTERISTICS 282

8.3 REJECTION OF ORGANICS AND CALCIUM 283

8.3.1 Rejection of Organics and Cations 283
8.3.2 Rejection Mechanisms 285

8.4 FOULING BY ORGANICS, CALCIUM AND COLLOIDS 285

8.4.1 Organics and Calcium 285
8.4.2 Colloidal Systems 287

8.5 FERRIC CHLORIDE PRETREATMENT 288

8.5.1 Effect on Rejection 288
8.5.2 Effect on Flux 290

8.6 PROCESS RELIABILITY AND WATER QUALITY 291

8.6.1 Dependence of Product Quality on Organic Type and Solution Chemistry 291
8.6.2 Water Quality 291

8.7 MEMBRANE AREA REQUIREMENTS AND COST 293

8.7.1 Membrane Cost 293
8.7.2 Membrane Requirements 294
8.7.3 Water Quality and Membrane Cost 295
8.7.4 Effect of Ferric Chloride Pretreatment 296

8.8 ENVIRONMENTAL CONSIDERATIONS 298

8.8.1 Energy Requirements 298
8.8.2 Chemicals Addition 298
8.8.3 Concentrate Disposal 299
8.8.4 Health Aspects 300
8.8.5 Treatment Considerations 301

8.9 CONCLUSION 301

Chapter 9 – *Summary & Conclusion* *303*

Chapter 10 - *Further Research* *309*

Appendix 1 - *Concentration of Natural Organic Matter* *313*

A1.1 SELECTION OF CONCENTRATION METHOD 314

A1.1.1 Conventional Methods 314
A1.1.2 Concentration using Membranes 314
A1.1.3 Comparison of Membrane and Adsorption Concentrates 314
A1.1.4 Method Selection 315

A1.2 SURFACE WATER SOURCE 316

A1.2.1 Choice of Location 316
A1.2.2 Raw Water Characteristics 317

A1.3 MEMBRANE PROCESS OPERATION 318

A1.3.1 Microfiltration and Reverse Osmosis Equipment 318
A1.3.2 Membrane Process Operation 319
A1.3.3 Freeze Drying 320
A1.3.4 Analysis 320

A1.4 RESULTS 321

A1.4.1 Flux and Water Permeability 321
A1.4.2 Organic Carbon Rejection 322
A1.4.3 Rejection of Conductivity 324
A1.4.4 pH Value 325
A1.4.5 Cation Analysis 326
A1.4.6 Overall Rejection 327
A1.4.7 MF Backwash Efficiency 329
A1.4.8 Membrane Cleaning and Storage 329
A1.4.9 Mass Balance 329

A1.5 CONCLUSION 331

Appendix 2 - *Filtration System Characterisation* *333*

A2.1 FILTRATION SYSTEM DESIGNS 334

A2.1.1 Perspex Stirred Cell 334
A2.1.2 Stainless Steel Stirred Cell 335

A2.2 MASS TRANSFER IN STIRRED CELLS 335

A2.3 SHEAR IN A CYLINDRICAL CHAMBER STIRRED BY A RADIAL FLOW IMPELLER 335

A2.3.1 General Description of Flow 335
A2.3.2 Theoretical Analysis for Shear Prediction in Stirred Cell 336
A2.3.3 Implications of Shear on Agglomerates in Solution 339

Appendix 3 - *Hematite Preparation (α-Fe_2O_3)* *341*

A3.1 SYNTHESIS OF HEMATITE PARTICLES 342

A3.2 CHARACTERISATION OF HEMATITE PARTICLES 343

Appendix 4 - *Instrument Calibration* *347*

A4.1 ORGANIC CARBON ANALYSIS 348

A4.1.1 Introduction 348
A4.1.2 Principle 348
A4.1.3 Oxidation Efficiency and Choice of Standards 348
A4.1.4 Operation Mode 350
A4.1.5 Detection Limit 351
A4.1.6 Errors and Interferences 351

A4.2 UV/VIS ABSORBANCE 353

A4.2.1 Method 353
A4.2.2 Absorbance Characteristics of NOM 354
A4.2.3 Errors and Interferences 355

Appendix 5 - *Solution Speciation using MinteqA2* *357*

A5.1 INTRODUCTION 358

A5.2 MINTEQA2 SPECIATION CODE 358

A5.2.1 Availability of software and data input 358

A5.3 SPECIATION RESULTS 359

A5.3.1 pH calculations as a function of partial CO_2 pressure 359
A5.3.2 Solution Speciation 360
A5.3.3 Calcium Precipitation 361
A5.3.4 Speciation of Systems Containing Organics 362
A5.3.5 Comments on the membrane boundary layer concentrations 364

A5.4 CONCLUSION 365

Glossary & Symbols 367

References 373

Index 401

Thesis Related Publications 407

Curriculum Vitae 409

Chapter 1

INTRODUCTION

Surface water treatment is a controversial issue. A healthy balance between possible risks, such as immediate microbiological contamination and long-term carcinogenic effects due to disinfection by-products, and the treatment costs is required. Another issue of concern relates to drinking water standards, which seem unreasonably strict in some countries and practically absent in others. The price people are required to pay for their water varies with the standards.

What quality of water do we really need? This leads us to environmental considerations; how much energy is reasonable to use for water treatment, how much chemical addition can be justified? Do we really need to treat all the water we use? Are we running out of water and should we start to think about reuse or focus more on water savings? Are we stuck in a vicious circle of increasing pollution and conditions which require more and more treatment?

Obviously not all of these questions can be answered in one thesis. This is a thesis about treatment, a somewhat fundamental study about what we can achieve with treatment now and what inhibits treatment efficiency. The focus is on treatment by alternative membrane processes. What is different is the attempt to compare and evaluate options on the basis of productivity (capital and maintenance cost), energy consumption and chemical requirements. The results apply to the water that needs to be treated to achieve specified standards: that part of drinking water which cannot be replaced with greywater. The results cannot replace a rethinking and optimisation of water usage and demand management.

Many processes are available to tackle the challenge of providing a safe and affordable drinking water. Case studies typically present one particular surface water and one treatment process. It seems that there is an urgent need to carry out research in a manner that provides comparable results which apply to a 'general' surface water and which allow an objective comparison of relevant treatment processes. A clear understanding of the 'science' of a natural water system and the 'engineering' of treatment and their interaction seems essential.

Looking at water treatment developments in recent years, it is apparent that the most advanced treatment options are membrane processes. Membranes remove contaminants (depending on the membrane, anything from bacteria, viruses, particles to dissolved organics and salt) by physical retention, when the water is forced with an applied pressure through the membrane. Membranes are fairly new to the water industry and yet their growth in applications is tremendous. This is due to a steadily decreasing manufacturing cost, a relatively small footprint compared to conventional treatment, a potential for reduction of chemicals usage and very low maintenance requirements. Yet the performance of membranes is far from ideal. An artificial membrane cannot achieve the sophisticated performance and long lifetime of membranes we often see in nature. This gives us an idea of the potential there is for improving the humble state of current commercial membranes.

Pressure driven membrane processes (microfiltration (MF), ultrafiltration (UF) and nanofiltration (NF)) allow the production of high quality drinking waters. Natural organics need to be removed to increasingly low levels, as they are precursors of carcinogenic disinfection by-products. While MF, UF, and NF can remove natural organics to some extent, pretreatment is required for MF to achieve sufficient removal, and the higher operating pressures in NF may limit process economics. Fouling by

surface water components such as natural organics, inorganic colloids, and multivalent ions is a threat to performance and efficiency of all three processes.

The aim of this thesis is to investigate these pressure-driven membrane processes towards their

- potential to remove natural organic matter (NOM),
- critical fouling conditions,
- the structure of the deposit formed in and on the membranes.

An understanding of critical fouling conditions and examination of fouling morphology will then lead to improved performance, which will reflect in a reduced energy and/or chemicals requirement of existing membranes. It may also explain why membranes do not perform 'ideally' and how this can be improved.

It is anticipated that under certain conditions all three processes are capable of producing a high quality drinking water. For microfiltration this requires a pretreatment step. The optimal process or process combinations may depend on the raw water characteristics and the desired product water quality.

Classical studies of membrane filtration have tended to consider humic substances (HS) and multi-valent ions. Initial experiments (designed to concentrate NOM as described in detail in Appendix 1) showed a drastic flux decline of the microfiltration process. Analysis of the fouling layer followed and the result (discussed in Chapter 2) suggested a change in the planned research strategy: there was a very obvious need to include inorganic colloids in the study.

Multi-valent ions interact with organics, inorganic colloids and membranes. Real systems are very complex. An effort to simplify natural systems without losing important factors has been made and the systems were characterised thoroughly.

Parameters of importance are those variables of a natural surface water

- humic substances (HS)/ Natural organic matter (NOM) (concentration, type, characteristics)
- mono- and multivalent salts (concentration, type)
- pH and ionic strength
- inorganic colloids (concentration, size, aggregate characteristics, charge)

and those of a membrane process,

- hydrodynamics (stirring), transmembrane pressure (flux),
- membrane (material, 'pore size' , surface charge, surface roughness).

The aggregate characteristics of colloids and flocs such as structure and size are of particular concern. Natural waters contain inorganic colloids embedded in organic matrices and the colloids may be in various aggregation states or simply stabilised by the organics.

It was anticipated that the filtration behaviour could be improved by changing the aggregate characteristics and influencing the conformation of the organic molecules.

In this thesis, the initial chapters provide an introduction with a description of the organics (Chapter 2), the membrane processes (Chapter 3), and a general materials and methods section (Chapter 4). This is followed by the results of the different processes, microfiltration (Chapter 5), ultrafiltration (Chapter 6), and nanofiltration (Chapter 7). The following chapter (Chapter 8) is then dedicated to finding common trends in these processes and pointing out potential implications of the results, their application to understanding hybrid membrane processes, and cost issues and product quality issues. Final chapters include conclusions (Chapter 9) and outlook with suggestions for further research (Chapter 10) will conclude the project.

The study shows a to date unique comparison of the three available processes MF, UF and NF for identical feed solutions. The scope of the work is summarised schematically in Figure 1.1.

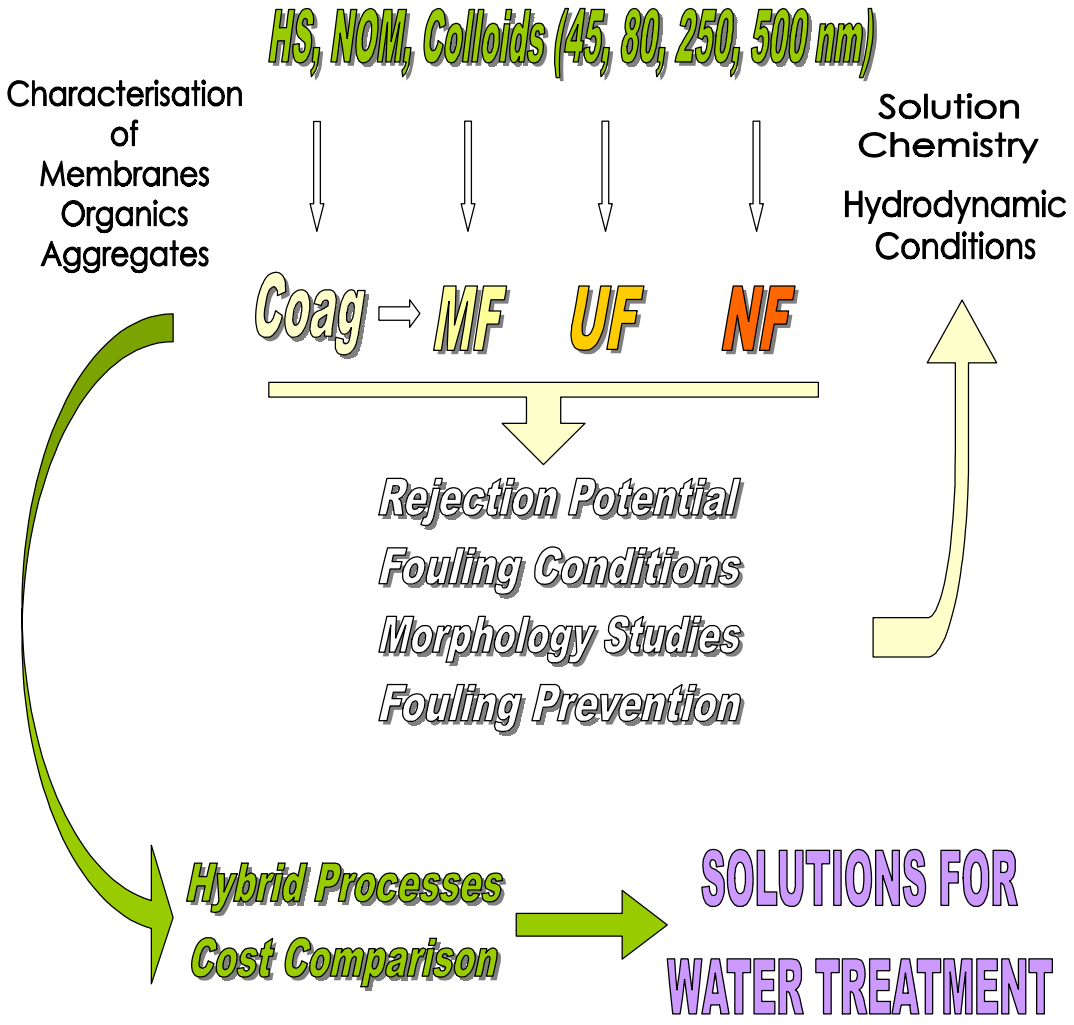


Figure 1.1 *Schematic description of the 'NOM removal using membranes' research scope*

Chapter 2

CHARACTERISATION OF NATURAL ORGANICS A REVIEW

In this chapter, natural organics will be defined and their origin described. Different options of natural organics sources for research are discussed.

Then characterisation methods will be reviewed and characteristics described. These characteristics are relevant for the treatment of waters containing natural organics and can often be related to removal and fouling. In many treatment studies such characteristics are neglected.

Methods to obtain natural organics from surface waters, their purification and fractionation will be reviewed. Many of the techniques described were used in this study. Subsequently, this lead to the selection of a suitable process for NOM concentration for this study (see Appendix 1).

The variation of the natural organics characteristics with changes in solution chemistry, their interaction with cations and other compounds and their interactions with inorganic colloids will also be discussed. These interactions occur in natural waters and may also influence treatability. A brief description of colloid characterisation and aggregation mechanisms is also given.

Finally a brief overview is given over the issues of natural organics in water treatment. These issues include disinfection by-product formation, biofouling and conditioning films as well as treatment process options.

2.1 INTRODUCTION

Humic substances (HS) research has been through a renaissance in recent years after it became recognised that these compounds are the precursors of chlorination disinfection by-products, such as trihalomethanes, haloacetic acids and chlorophenols. Much research has been done on the use of alternative oxidants such as chloramines, UV and ozone, but all, if efficient disinfectants, cause by-products. The by-products might be of a completely different family, but are potentially carcinogenic and not always well known. This implies that it is safer to remove the natural organics during treatment and prior to disinfection. Further problems associated with natural organics are taste and odour, and their association with pollutants such as hydrophobic organics (e.g. pesticides) and heavy metals. Some organics contribute to biological regrowth and thus enhance microbiological health risks.

Natural organics and their characteristics are important issues in water treatment research. A large number of studies in the literature have either used very specific, rather undefined natural organics or operationally defined compounds somewhat modified by their extraction process. In engineering studies, HSs are very popular as a model compound for a "natural foulant". A trend can be seen to work with unfractionated samples, however the comparability of such studies is poor.

Books have been written about HSs, which are the dominant fraction of natural organic matter (NOM). The International Humic Substances Society (IHSS) has been founded, but a common structure of a HS has not yet been widely accepted. The large variety of size, functional groups and origin makes researchers' lives difficult and analytical methods remain complex and often lead to irreproducible results. The amount of literature available on HSs is extensive, but the quality of research done is often limited to the methods of analysis available and raw water samples used. Results are mostly incomparable due to the use of very different source materials and extraction methods.

The sources of these substances contributed to a number of disputes in the literature. Inexpensive commercial HSs are generally of unknown origin and their relation to surface water organics is questionable. IHSS standard and reference material is unaffordable for medium and large scale research. Self-concentrated NOM is specific with respect to its origin and research results can not be compared to other aquifiers, unless the impact of each component is studied and the NOM itself is well characterised.

The removal of HSs remains a challenge in water treatment, with the promising goal of reducing a long term chronic exposure of large parts of the population to carcinogenic chemicals. The challenges are the production of a high quality drinking water and the maintenance of high efficiencies in treatment due to natural organics fouling.

2.2 DEFINITION OF NATURAL ORGANICS

2.2.1 Nature of Different Natural Organics

Natural organics, especially humic acid (HA) and fulvic acid (FA) contribute to the natural colour of water, which becomes visible if the dissolved organic carbon (DOC) concentration is higher than approximately 5 mgL^{-1}. It is for that reason that natural organics removal is often referred to as colour removal. Surface water DOC contains about 45% FA, 5% HA, 25% low molecular weight (LMW) acids, 5% neutral compounds, 5% bases and 5% contaminants (Thurman (1983)). An average organic composition of a natural water is shown in Figure 2.1. However, the quantitative amount of each fraction changes is very case specific.

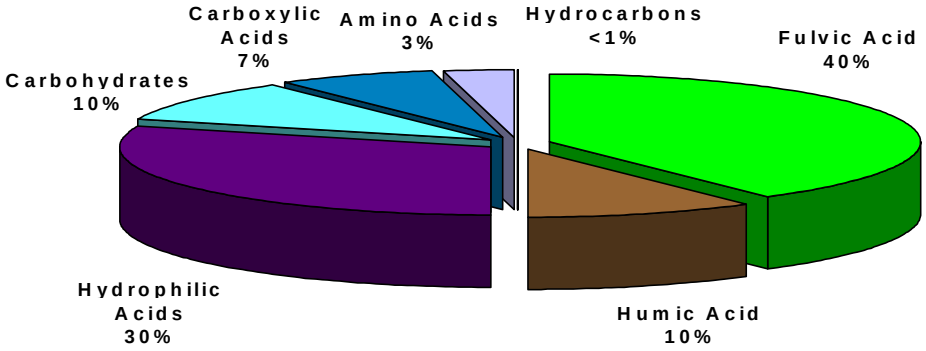


Figure 2.1 *Composition of an Average River Water (5 mgL^{-1} DOC) (Thurman (1983)).*

Hydrophilic acids represent about 30% of NOM and are sometimes called "hydrophilic HSs". This part of NOM is the least characterised and is more difficult to isolate and purify. Volatile fatty acids or sugar acids could be part of this component (Thurman (1983)). To study the impact of these hydrophilic HSs on water treatment processes, both complete NOM samples and fractions such as HS need to be considered. It is therefore important not to concentrate on HSs only, but also compare to NOM. Organic matter also occurs in natural waters as dissolved molecules, as suspended sediments in the form of coated particles and on coated bottom sediments (Thurman (1983)). This colloid-organic interaction will be addressed specifically in a later section (2.9).

2.2.2 Definition of Compounds

Three different compounds make up HSs: Humin (defined as insoluble), humic acid (HA, insoluble at a pH of 1) and fulvic acid (FA, soluble at any pH). Other names used to describe HS are ulmic, hymatomelanic, gray humic, brown humic, crenic, apocrenic or yellow acid (Swift (1985)).

Aqueous natural organics are operationally defined with their properties depending on the concentration method used. In general, NOM is the complete content of organics in a natural water as shown in Figure 2.1. This NOM is generally obtained by concentrating or drying a surface water sample. HA and FA are fractions of NOM and require a fractionation process for separation.

The definition of soil HS is all the material that can be extracted from soil with 0.1 M NaOH. HA can be precipitated at pH <2.0, whereas FA remains in solution. The study of soil HSs is much older than that of aqueous HS (Thurman (1983)) and many methods have been developed for soil materials.

Aqueous HSs are defined differently to soil HS. Aqueous HS are, by operational definition hydrophobic organic acids. It is the fraction of NOM that adsorbs under certain conditions (pH 2.0) on XAD8 resin (Leenheer (1981)). The organic matter adsorbed is subsequently desorbed with aqueous NaOH and acidified again to fractionate HA from FA. At a pH of < 2.0, HA will precipitate, leaving FA in the supernatant (Leenheer (1981)). A hydrophilic fraction has been seperated by adsorption at pH 2 on XAD4 resin after previous removal of the hydrophobic acid fraction on XAD8 (Leenheer (1996)). Hydrophilic acids contain large portions of sugars, amino acids and amino sugars (Krasner *et al.* (1996)).

2.3 ORIGIN OF NATURAL ORGANICS

The origin of aquatic HSs (or the natural synthesis of HSs (humification)) is unclear. In the literature, different models are proposed, including the pathways biodegradation of plant and animal material, plant biopolymer decay, condensation-polymerisation reactions, lignin biodegradation, amino acid sugar interactions and many others (Schulten and Schnitzer (1995)). Küchler *et al.* (1994) state that a lack of light, nutrients and clay for adsorption as well as an anaerobic environment cause a high organic matter content. Selected parameters are summarised here in order to highlight their relevance to possible changes in treatment behaviour.

2.3.1 Chemical Formation, Humification and Aging

Humification describes the two most fundamental processes in the formation of humic matter; polymerisation and the emergence of unsaturated structures (Ziechmann (1980)). Both biotic and abiotic processes can cause humification. Different theories of the source of stream HS have been presented and one theory is that HA is a continuation of FA polymerisation. Stream HS is generally younger, less aromatic, lower in molecular weight (MW) and less intense in colour compared to soil HS (Malcolm (1985)). However, it is not generally accepted that humification is the only existing process. Peuravuori and Pihlaja (1998) found that larger size organics somewhat resemble the smaller molecules, but the structural units are not linked in regular sequence and are thus not real polymers.

Ageing is an important issue for sample storage. Huber (unpublished) reported an increase in molar mass and unsaturated structures (measured by an increased UV/DOC ratio) of a diluted humic rich lake sample on storage for two weeks. However, this could also indicate a natural aggregation process (as described in further detail in section 2.5.9).

2.3.2 Biological Activity

HSs are formed during anaerobic degradation processes in the sediments (Kastelan-Macan and Petrovic (1996)). DOC is high where microbiological activity and plant degradation are high (Thurman (1983)). HS can be used as fertilisers, indicating some kind of bioavailability (Wilson (1988)). In summer, when temperatures are higher, the microbiological activity increases. This generally results in larger and more aromatic organic compounds as aliphatic organics are easily accessible to microorganisms.

2.3.3 Soil and Vegetation

The origin of NOM in a surface water depends on the origin of the water itself and the surrounding environment of the river or lake. An average river water could, for example, be composed of snow melt, groundwater and rainfall –all very low in DOC- and canopy drip, interstitial water, emergent plants and lake water -rich in DOC (Thurman (1983)). Differences in HS character occur for high/low water flow and analysis of different soils, cow manure and plant leachates (all potential sources of HSs in water) indicates the dependence on origin (Cotsaris *et al.* (1988)). Collins *et al.* (1986) stated that a higher carbohydrate content is found in HS from soil rather than those found in water.

The geochemistry of soils has an impact on the HS characteristics. Some soils retain certain fractions of natural organics, and components of plants and microbes are present in different fractions depending on the soil conditions (Wilson (1988)). Sandy soils, which do not adsorb anionic organic matter very well, would be expected to contribute a high concentration of natural organics to infiltrating waters (Thurman (1983)). Very common in Australia are Eucalyptus species which have a waxy cuticle that contributes to a higher fraction of lignins and polyphenolic compounds (Hart *et al.* (1988)).

2.3.4 Weather and Seasonal Variations

Seasonal variations in the composition of aquatic organic matter (AOM) were determined for different rivers. It was found that carboxylic acid content becomes higher as a consequence of higher rainfall, which washes natural organics out from the soil. Krasner *et al.* (1996) reported an increase of DOC, UV, and fluorescence after heavy rain. This peak in HS concentrations was confirmed by Alarcon Herrera (1994) and Frimmel and Hesse (1996). Temperature variations over the seasons alter various processes such as precipitation/coagulation, carbonate and oxygen content, and biological activity, which all influence organic composition. Owen *et al.* (1993) however reported little seasonal variations for non-eutrophic systems. Stratification was also expected to cause changes in organic characteristics.

During summer, organic matter decomposition by microorganisms occurs in soils and aromatic structures (humification end products) become more important than aliphatic structures (Clair *et al.* (1996)). Natural UV radiation may lead to the break down of some compounds.

2.3.5 Lake Waters versus Freshwater Streams

The composition of a river water varies constantly, whereas lake waters would be expected to be a little more stable (Thurman (1983)). Martin-Mousset *et al.* (1997) found waters from reservoirs generally richer in DOC than river waters. Conditions in lakes however will be very dependent on stratification behaviour or occurrence of algal blooms.

2.3.6 Groundwater

Surface waters are more aromatic than groundwaters due to a generally lower microbiological activity in groundwaters. FA from groundwater was found to be smaller and more homogeneous than found in surface waters (Pettersson *et al.* (1994)).

2.3.7 Pollution by Human Activity

Human activities, such as agriculture and industry, lead to the pollution of waters due to the input of nutrients and chemicals. Additionally, sewage treatment plants release small, aliphatic organics. The occurrence of such human activities can be seen in the characteristics of the organic carbon content of natural waters. For example, large European rivers (Seine, Rhine, Main) contain significant quantities of

small, aliphatic organics, while unpolluted wetlands and swamps show a predominance of large and highly aromatic organics (Huber (1998)).

2.3.8 Availability for Research

HSs can be purchased from a few commercial chemical companies (Aldrich, Fluka, etc.). The origin of these products or the method of extraction is unknown, but are probably derived from soil, coal or peat. Characteristics and quality vary from batch to batch and the colour of these products is very dark. Commercial HAs often have a high ash content. HA and FA from soils and waters are usually very different from the commercial ones (Malcolm and MacCarthy (1986)). Commercial products are often much larger in size and need to be purified. They were also found to be very similar to peat and should not be used to simulate water HSs behaviour (Malcolm and MacCarthy (1989)). Other authors found that commercial HS contain a large amount of residual components and a much lower nitrogen content than typical aqueous HS. Their use for studies has not been recommended (Legube *et al.* (1990)).

HSs can also be purchased through the International Humic Substances Society (IHSS) at a very elevated price. Standard and reference material of known origin and character can be obtained and the material has been widely used and characterised (Averett *et al.* (1989)). The reference material may also vary from batch to batch. The equivalents of aquatic or stream humic material are Suwannee River HA and FA. The Suwannee River drains the Okefenokee Swamp in south-eastern Georgia (USA) and contains high DOC (30-80 mgL^{-1}) and low inorganic solutes (Serkiz and Perdue (1990)).

The use of this well defined material allows the comparison of results from other laboratories. Note that this does not guarantee results which are applicable to every other river water, since compositions vary greatly and depend on other components present in water.

Another option is extraction from local natural waters and this is often the only option for larger scale research. The use of a surface water should be avoided due to its variability over time.

2.4 EXTRACTION OF NATURAL ORGANICS FROM WATERS

Processes available for the extraction of natural organics from waters include vacuum distillation, freeze-drying, freeze concentration, co-precipitation, ultrafiltration, reverse osmosis (RO), solvent extraction, sorption, anion exchange, and non-ionic macroporous sorbents (Aiken (1985)). Many of these methods include chemical treatment that may alter the HS characteristics. In this section, the most common methods for the processing of large samples will be described. An important issue in NOM extraction is the recovery of organics. Minimising the loss of certain fractions, such as small compounds which are difficult to treat, is also important.

2.4.1 Ion Exchange Resin

XAD resin was proposed as a standard method for the preparative isolation of aquatic HSs (Thurman and Malcolm (1981)). The XAD8 resin was found to be best to extract HS from stream water without the extraction of other organic and inorganic constituents (Malcolm (1985)). The adsorbed dissolved organic matter is desorbed from the resin with either aqueous NaOH or a water-methanol-ammonia mixture. Recoveries of 75 to 100% were reported (Serkiz and Perdue (1990), Collins *et al.* (1986)).

This resin, however, mainly retains hydrophobic acids, whereas hydrophilic acids are better retained by XAD4 and are lost if only a XAD8 resin is used. Biodegradable DOC is adsorbed to a lesser degree on both resins than the non-biodegradable DOC (Agbekodo and Legube (1995)).

Legube *et al.* (1990) doubted that the HS obtained still showed raw water HS characteristics, since a number of chemical steps are involved in the process. Recovery of FA decreased rapidly with the increased volume treated.

A diethylaminoethyl (DEAE) weak anion exchange resin has been used prior to XAD8 resin to avoid acidification in extraction. It was suspected that XAD8 and DEAE resins both adsorb a similar fraction of organic carbon given the very similar characteristics of samples extracted with these methods (Pettersson (1994)). DEAE has been reported to have a low anion exchange capacity and poor flow characteristics, which may limit the use of DEAE for large scale processing (Aiken (1985)).

Morran *et al.* (1996) have used a magnetic resin to extract NOM with about 80% of DOC was recovered. It is however likely that the smallest size fractions were lost in the process (Newcombe and Drikas (1996)).

It is obvious that these methods, although widely used, have their limitations. The use of ion exchange resin is very time consuming due to the long resin preparation procedure. Changes in pH and ionic strength for adsorption and regeneration may change the HS characteristics considerably. Recoveries are not stable and are low for LMW compounds.

2.4.2 Reverse Osmosis

RO membranes have a very small molecular weight cut-off (MWCO) and are expected to retain a large fraction of LMW compounds, such as amino acids or sugars, and are therefore useful for extracting a representative mixture of NOM from surface waters. For nanofiltration studies it is important to retain the LMW fraction, as these molecules could be major contributors of pore plugging in membrane filtration. Pure HS solution cannot be obtained from such a mixture with a the salt content of the sample depending on its origin.

Serkiz and Perdue (1990) were the first to report the successful use of RO to isolate NOM from river water. Polyamide (PA) membranes on a polysulphone (PS) support were used. Freshwaters were pretreated with a cation exchange resin and, due to a low salt content, no further desalination was required. Concentrates were then freeze dried. Recoveries of about 90% were achieved. The method appears to be well suited for NOM removal with the possibility of subsequent use of XAD for separation of FA and HA from the NOM. The method can be applied to freshwaters containing DOC in the range of 3 to 40 mgL^{-1}. Problems of the method include the presence of residual inorganics such as H_2SO_4 and $Si(OH)_4$.

Since the early studies of Serkiz and Perdue (1990) RO has been used in several studies to extract NOM from surface waters. This physical separation avoids chemical alterations of the target substances, but the extract needs to be desalted and may contain bacteria or plankton. A portable RO plant might be used and large quantities can be concentrated quickly (Clair *et al.* (1996)). RO membrane rejection for DOC was determined to be greater than 95%, but losses due to plumbing design can be great. Precipitation occurred in most samples. The pK_a of acidic groups in the permeate was rather high, which indicated some kind of selectivity of the membrane. PS membrane material showed a higher recovery than CA (Clair *et al.* (1991)). RO followed by UF to fractionate the concentrated

material has been used for groundwater studies. The groundwater was modelled with four substances, among them Aldrich HA, which was retained to 97%. The recovery of smaller ions was strongly pH and ionic strength dependent, being close to 100% at pH 7-8, and dropping off linearly with pH (Crum *et al.* (1996)). To achieve high recoveries of LMW compounds, it is necessary to keep the pH neutral, therefore cation exchange prior to RO needs to be avoided.

Sun *et al.* (1995) used a portable reverse osmosis unit to extract HSs from river waters. It has been shown that excellent recoveries of small organic acids was achieved, when they were present as anionic species. However, there is still no good procedure to remove inorganic anions from the concentrate. Rejection for LMW anions is better with sodium rather than hydrogen ions in solution. This suggested the use of a cation exchange resin after the RO rather than before if inorganic precipitation is not a problem. Fouling was found to have no effect on rejection. This might even lower the degree of organics precipitation due to a higher pH. However other authors report that the use of a Dowex-50 cation exchange resin prior to concentration with RO avoided precipitations on the membrane (Serkiz and Perdue (1990)).

In applying reverse osmosis for NOM extraction, the choice of an appropriate river water, preferably high in DOC and low in salt content, is important. Also the choice of a suitable membrane with maximised rejection is critical to avoid the loss of small organics with the permeate. The drawbacks of this method are the concentration of salts and other contaminants. This generally results in a product of high ash content and the salt can lead to precipitation in the concentrate. Particles in the surface water also need to be removed prior to concentrations however this can be achieved with microfiltration (MF).

2.4.3 Desalting

After NOM has been concentrated it needs to be desalted if the extraction method did not already include this step. Desalting can be difficult since inorganic and organic ions of a similar size need to be separated. The only option to desalt the concentrate is cation exchange, which unfortunately either decreases the pH or only exchanges multivalent for monovalent ions. Ions which are complexed by the organics cannot be exchanged. Crum *et al.* reported a decrease in cation resin exchange efficieny at a lower pH (Crum *et al.* (1996)). It can also be expected that some organics will be lost in a cation exchange process.

UF with a MWCO of 500 Da was used to desalt NOM concentrated with a magnetic resin but high losses of LMW NOM were reported (Hepplewhite (1995), Newcombe *et al.* (1996), Crum *et al.* (1996)). UF of such a MWCO is also likely to retain salt to some degree. If fractionation is employed prior to desalting, the desalting step may be limited to the lowest MW fraction, thus minimising the loss of organic matter.

2.4.4 Purification

Serkiz and Perdue (1990) reported successful treatment of H_2SO_4 and $Si(OH)_4$ residues in the RO concentrate with an ion retardation resin with a high affinity for strong acids, but losses of organics were reported.

Aldrich HA requires purification prior to use. This can be done by dissolution in 0.01 M NaOH to precipitate contaminants. HA is then precipitated from the supernatant at pH 2.0 and collected by

filtration (Crum *et al.* (1996)). Another method is to use a high MWCO UF membrane and dialyse or filtrate an organic stock solution to remove the undesired high molecular weight (HMW) compounds.

2.5 CHARACTERISATION OF NATURAL ORGANICS

The characterisation of natural organics is important in order to understand treatment behaviour and to compare results to other waters. The main characteristics of natural organics are molecular weight, functional groups, hydrophobicity and charge. Results obtained are often relative, depending on the method used and thus vary greatly, even for identical compounds. It seems impossible to measure absolute values and it is therefore important to determine a repeatable method to achieve comparable results and, where possible, apply different methods.

2.5.1 Concentration Measurements of Natural Organics

Organic Carbon

A sum parameter for organic matter is total organic carbon (TOC) or dissolved organic carbon (DOC). However, DOC or TOC will not give any information about the HS content if mixed organic substances are used, such as NOM. DOC/TOC analysis can be problematic, especially at low concentrations (several 100 μgL^{-1}), where contamination due to washwater, chemicals, atmosphere, and sample vials can be higher than the value of interest. Different methods of DOC/TOC analysis are available, but only the UV/persulfate oxidation methods appears successful for determination of low concentrations (Greenberg *et al.* (1992), Koprivnjak *et al.* (1995)). Errors are generally high at low levels (Hambsch (1992)). Recent developments, however, overcome some of the problems and detection limits of μgL^{-1} are possible (Huber (1992), Huber (unpublished)).

Kainulainen *et al.* (1994) determined correlation coefficients for different analytical methods (TOC, $KMnO_4$), colour, and fractions of humic matter were determined. Correlations were poor for smaller molecules, and NF and $KMnO_4$ produced the best results. Many oxidation processes transform larger humic molecules into smaller, more active fractions that are non-detectable.

UV/Vis Absorbance

UV absorbance has been used for reasons of simplicity in many pilot plant studies. However, UV measures the aromatic compounds preferentially and does not give correct results if the aromaticity is altered, as is the case in most treatments. Values will be overestimated, as most treatment processes preferentially remove aromatic compounds. UV absorbance can therefore not be used to measure treatment efficiency.

The UV/TOC ratio is often used to determine the humic fraction in the organic matter or to determine the aromaticity of a sample. Different wavelengths of UV absorbance are used to measure colour (see Appendix 4).

Fluorescence

Fluorescence can also be measured for LMW compounds to determine concentrations, but discrepancies between UV and fluorescence were found for different MWs (Jucker and Clark (1994)) and, again, results would vary if samples are fractionated during treatment. Belin *et al.* (1993) found a higher fluorescence of smaller compounds such as FA and hydrophilic acids, compared to HA. A shift of intensity to shorter wavelengths with increasing salinity has been observed in fluorescence

spectroscopy. The shift has been related to a decrease in the extent of conjugation of the fluorescing chromophores (Alberts *et al.* (1995)).

2.5.2 Aromaticity and Reactivity

UV absorbance at particular wavelengths can be related to the presence of specific chromophores. Absorbance at 254 nm can be mainly correlated to the amount of double bonds in aromatic rings (Pettersson *et al.* (1994)) and, thus, to the aromaticity of a sample, whereas absorbance at 436 nm is more related to the concentration of unsaturated C=C, C=O, and N=O units, chinones, keto-enol-tautomerie and complexed iron. Absorbance was observed to be highly pH dependent (Abbt-Braun *et al.* (1990)). Eaton (1995) subsequently developed a standard method to measure UV absorbance of natural waters. Korshin *et al.* (1997b) correlated absorbance characteristics to the reactivity of aromatic moieties with chlorine. Also, absorbance decreases after chlorination (Korshin *et al.* (1996)).

UV is associated with the multi-aromatic content of HS. While the fact that there are differences for various molecular weight groups makes this analysis inapplicable for concentration determination in treatment, as a shift in MW will occur (Jacangelo *et al.* (1992)). However, this shift may give information about the change in aromaticity and the nature of organics during treatment. HA is more aromatic than FA, and FA is more aromatic than hydrophilic acids (Krasner *et al.* (1996)).

2.5.3 Hydrophobicity

Hydrophobicity describes how much a molecule 'dislikes' water. It is therefore closely linked to its solubility. A hydrophilic compound is highly soluble in water, whereas a hydrophobic compound is more soluble in an organic solvent. Consequently, the partitioning coefficient of the organics between organic solvents such as octanol and water can be used to measure hydrophobicity. The phenolic groups are more soluble in octanol, whereas the carboxylic groups are more soluble in water (Clark and Jucker (1993)). The low concentrations of organics in natural waters made the determination of a partitioning coefficient difficult, especially at neutral pH when both FA and HA were very water soluble. According to Cotsaris *et al.* (1988), 58-74% of organics in the water were hydrophilic. Hydrophobic groups were mainly one or two ring aromatic compounds, but according to Leenheer (1985) hydropobic effects were small.

2.5.4 Size, Molecular Weight, Radii of Gyration, Polydispersity

Size, molecular weight, radii of gyration and polydispersity are all interrelated. Size is an important characteristic in water treatment, as diffusion coefficients and removal efficiencies are directly dependent on the size of a solute. A large number of methods exist to measure these important parameters though results vary greatly. Each method has its own limitations.

For example, HA and FA from soil were observed in the 10 to 300 kDa (HA) and 3 to 100 kDa (FA) range (Johns *et al.* (1993)). In another study, 50 to 60% of FA was found to be larger than 10 kDa (Legube *et al.* (1990)). The MW of FA was found to be 650 to 950 Da and for HA of 2000 to 3000 Da (Malcolm (1985)). In yet another study the average MW of stream HS is believed to be about 600 Da, with a maximum of 2000 Da (Leenheer (1985)). Many other researchers have determined a lower MW, which might indicate that aggregates or micelles were measured in the previous examples, if not associates of the organics with inorganic particulate matter (Leenheer *et al.* (1989)). Results are often dependent on standards used. An overview of the more common methods will be given here. A range of methods is required to obtain meaningful results, requiring great analytical effort.

Chromatographic Techniques (Gel Permeation, Size Exclusion)

Gel permeation chromatography (GPC) relies on the fact that molecules which are smaller than the pore size of the gel matrix are retarded in their passage through the column. Larger molecules which cannot penetrate pores are excluded and pass through the column more rapidly (Wershaw and Aitken (1985)). GPC depends on the MW standards used if a size is to be determined. It also depends on the electrophoretic mobility of the organics, which may vary with their size (De Nobili and Fornasier (1996)). Adsorption effects and charge interactions make a quantitative analysis difficult, and these need to be controlled by electrolyte addition (Huber (unpublished)). This results in a 'salt peak' in the chromatograms due to the difference in salt content of eluent and sample, and may also cause a variation of the sample characteristics.

Chromatographic techniques are very commonly used in the characterisation of natural waters (Aoyama (1996a, 1996b), Huber (unpublished), Shaw *et al.* (1994), Mori (1988), Becher *et al.* (1985), Amy *et al.* (1987)). However, most authors use different techniques, detectors, standards and eluents, making the comparison of results difficult.

For example, the molecular weight distribution of natural organics was determined with high pressure liquid chromatography (HPLC) and polystyrene sulfonate (PSS) standards (Pettersson *et al.* (1994)). High Pressure Size Exclusion Liquid Chromatography (HPSEC) was used to determine MW and results compared well to vapour pressure osmometry and flow field-flow fractionation (FFF).

Polydispersity is the ratio of weight average MW to number average MW. Chin (1995) found polydispersity to be small (<2.0 for FA and <2.5 for HA) (Chin (1995)). This was confirmed by Beckett *et al.* (see Table 2.1).

Humic material from bank filtered lake water has been divided into six fractions using size exclusion chromatography (SEC) coupled with HPLC and UV absorbance (254 nm), and a MW of around 10 kDa was determined (Kainulainen *et al.* (1994)). Shaw *et al.* (1994) used gel filtration chromatography (GFC) to study apparent molecular size and found a decrease in size with decreasing pH.

Frimmel and Hesse (1996) combined gel permeation liquid chromatography (GPLC) with UV and DOC detectors to separate natural organics into different groups. This was possible due to the relatively high sensitivity of the detectors used.

Huber (unpublished) described the direct injection size exclusion chromatography (DISEC) approach. This approach relies on the understanding of various effects to extract more information than just size from SEC. No high ionic strength eluent was used. Ion exclusion lead to an early elution of anionic acids. This effect was decreased in the presence of ions in the eluent. Hydrophobic interactions (non-electrostatic interactions between nonpolar (aromatic) groups of the solute and the column) are shielded by the charged functional groups of a molecule, but if the charge is shielded by electrolytes the hydrophobic effects become stronger. The DISEC method allows the quantification of important chemical functionalities of NOM. HS, HS hydrolysates, low molecular mass acids, low molecular mass neutrals and amphiphilics and polysaccharides may be separated by this method. This method was further developed into the liquid chromatography organic carbon detection (LC-OCD) approach which is described in Chapter 4.

Ultrafiltration Fractionation and Dialysis

Ultrafiltration (UF) is a membrane process which retains solutes mostly by size exclusion (see Chapter 3 for a detailed description of mechanisms). Retention is determined by the geometric properties of pores, the size of the solute, and concentration polarisation (Goldsmith (1971)). The molecular weight cut-off (MWCO) of these membranes is determined by the manufacturer using uncharged molecules such as dextrans at relatively high concentrations (Hazlett (1990), Readman (1991)). A series of membranes are required, which are of identical material, but have different MWCOs. Furthermore the membrane material should be hydrophilic (thus regenerated cellulose rather than polysulfone) to avoid loss of organics to the membrane by adsorption and the pore size distribution should be narrow. The results need to be corrected for the change of concentration in the cells over time (Logan and Jiang (1990)). Charge effects may also be important.

While this method is commonly used (De Nobili and Fornasier (1994), Küchler *et al.* (1994), Mazid (1988), Belin *et al.* (1993), Shaw *et al.* (1994), Burba *et al.* (1998), Buffle *et al.* (1978), Crum *et al.* (1996), Aiken (1984), Amy *et al.* (1987), Reinhard (1984), Amy *et al.* (1992), Hepplewhite (1995)), most authors have used different filtration protocols for their fractionation experiments. Cells can be operated in series (cascade) or in parallel, volumes and concentrations are varied, and some authors refill the cell with pure water to keep the cell concentration constant. All these factors influence the results obtained, and solution chemistry, pH, and ionic strength may also influence results. Generally reported size results are above the expected sizes of FA and HA. UF MWCOs used are usually 0.5-1, 3, 5, 10, 30 kDa.

NOM from an Australian reservoir was fractionated into five different size fractions using UF. The estimated loss during the fractionation process was 10% (Newcombe and Drikas (1996)). Serkiz and Perdue (1990) reported losses of 30 to 40% during UF fractionation - even in the lowest MW fraction.

The fractionation of synthetic groundwater (adipic acid, EDTA, β-cyclodextrin, Aldrich HA) was studied with UF and dialysis. It was found that the fractions can only be obtained if the cell volume was kept constant until at least 700ml permeate were produced. This indicated that dialysis alone could not achieve satisfactory fractionation (Crum *et al.* (1996)).

Newcombe *et al.* (1996) fractionated Australian NOM into six fractions with UF. The different fractions exhibited highly varying characteristics. Carboxyl groups were similar in all fractions, but a gradual transformation from high colour, high branched structure, and low carbohydrate content to rather long chain aliphatic carbon occurred from high to low MW fractions. O-alkyl carbon content (related to carbohydrates), decreased with a reduction of size, showing a higher degradability of high MW compounds. These results indicated that fractionation did not occur because of size only. Very similar trends were found for different freshwaters with the same method (Hepplewhite (1995)).

Collins *et al.* (1986) used five stirred UF cells in parallel to determine the apparent MW of HS. This method was found to provide a relative comparison for samples. Shaw *et al.* (1994) compared UF with dialysis. UF showed larger compounds in the permeate, whereas only smaller compounds than the MWCO were found with dialysis. Dialysis is purely diffusion controlled. This was attributed to the effects of pressure and stirring in UF which may have lead to a sub-division of molecules, although diffusion coefficients could also have played a major role.

Aster *et al.* (1996) set-up an analytical, multistage ultrafiltration to allow the on-line separation of aqueous HSs into six MW fractions. Burba *et al.* (1998) extended this method to metal-organic

complexes. A multi-channel pump was used to transport the 10 mL sample across the membranes. Resultsindicated that better recoveries for high MW compounds were obtained with UF than GPC.

Aiken (1984) evaluated UF for two different membranes to determine the MW of FA. From the literature, it was noted that researchers using UM10 observed that 50% or more of FA were greater than 10kDa, whereas researchers using PM10 found a significantly lower proportion (3-36%). Standards of MW 2000 and 5000 were mostly retained by the 10kDa MWCO membranes. This indicated that to accurately compare data, membranes need to be evaluated carefully prior to use. Little correlation was found between UF and GPC (Leenheer (1985)) which is not surprising considering the different nature of the methods. However, Ephraim *et al.* (1996) found a positive correlation between the two methods and found size effects stronger for larger compounds. Amy *et al.* (1987) determined stronger pH effects in GPC than in UF, but measured larger MW with GPC than UF. This surprising effect could be due to the choice of standards and eluent. The effect of ionic environment is also important as noted by Kwak and Nelson (1977) who reported that the retention by UF membranes was reduced significantly in 1M NaCl. Staub *et al.* (1984) recommended an ionic stregth greater than 0.1 M to reduce charge effects.

Buffle *et al.* (1978) found UF to be better than GPC as the adsorption capacity is lower. Cascade filtration is recommended to avoid MWCO changes due to adsorption effects, and concentrations less than a few hundred mgL^{-1} are essential. The washing method, where the concentrate volume is kept constant with distilled water, produced better results than the concentration method. Electrolyte concentration, pH, and pressure difference were reported to play a minor role. The major source of error is the membrane itself and a new membrane should be used for each filtration. Belin *et al.* (1993) fractionated samples using UF and XAD and found very similar fluorescence characteristics of the fractions obtained.

The different examples show that the development of a standard method is somewhat needed.

Ultracentrifugation

Ultracentrifugation relies on intermolecular charge repulsion by the addition of salt to the samples (Swift (1985)). Other methods are the use of UF membranes in the centrifuge vials. In an ultracentrifuge study, FA was determined to be in the 825 to 1500 Da range, and HA in between 1920 and 4750 Da (Wilkinson *et al.* (1993)). These results appear plausible. Ultracentrifugation was studied and determined to be suitable for direct measurement of natural waters, if no other molecules that absorb at 280 nm, such as proteins, are present (Wilkinson *et al.* (1993)). Analytical centrifugation was rarely used, but is regarded as promising (Leenheer (1985)).

Flow Field-Flow Fractionation

Flow field-flow fractionation (flow FFF) was developed by Beckett and Hart (1988) to determine the MW distribution of humic and fulvic acid. This method determines the diffusion coefficient which is then correlated to the MW with standards of known solutions, such as polystyrenesulphonate. A different result was obtained, compared to size exclusion chromatography when using Aldrich humic acids. In Becketts study the complexity of this kind of analysis is demonstrated by Beckett and Hart (1988) and different methods are questioned.

FFF was applied to determine MW distributions for different Australian water sources, Aldrich HA, and the Suwannee River FA and HA reference materials. FA samples had a lower polydispersity than HA, where polydispersity is defined as the molecular weight average divided by the number average.

Beckett *et al.* observed that aqueous HSs often do not show a peak at all due to their large polydispersity (Beckett *et al.* (1987), Beckett (1989)).

Table 2.1 displays results for Suwannee River samples and Aldrich humate. The lower polydispersity of FA was confirmed in the current study (see Chapter 4).

Table 2.1 *MW, diffusion coefficient and polydispersity for Suwannee River HSs and Aldrich humate (Beckett et al. (1987)).*

Organic Type	MW (FFF)	MW (other method*)	D_{max} [m^2s^{-1}]	Polydispersity M_W/M_N [-]
Suwannee HA	1490	1500	$4.10 \cdot 10^{-10}$	2.78
Suwannee FA	860	750	$3.23 \cdot 10^{-10}$	1.66
Aldrich HA	3270	-	-	4.72

* vapour pressure osmometry and low angle X-ray scattering.

Dynamic Light Scattering

Dynamic light scattering has been used to determine the size of HS (De Nobili and Contin (1994)). It appears as if the size of aggregates, rather than molecules, is measured. Since no size can be determined of UF fractions, the authors assume that these smaller size fractions do not form aggregates. Sizes measured depend on pH and ionic strength; with high pH and ionic strength increasing the size of species. Size is calculated from the measured diffusion coefficient using the Stokes-Einstein equation (Shinozuka and Nihei (1994)) and values were in the 50-200 nm range, which clearly indicates aggregation.

For light scattering experiments, the choice of the laser is critical. Natural organics can be fluorescent compounds when excited by lower laser wavelengths. This interferes with measurements. This effect can be minimised by the choice of a red laser. Additionally, given the low concentrations required to avoid molecule interactions, aggregation or multiple scattering of these small compounds, a very powerful laser is required.

Small Angle X-Ray Scattering

The angular distribution and intensity of scattered X-rays are a function of size and shape of molecules (Aiken (1984), Aiken *et al.* (1990)). The radius of gyration is measured which is then compared to standards of known molecular weight to obtain molecular weight data.

Membrane Osmometry

Membrane osmometry has been used to determine average molecular mass (Tombacz and Meleg (1990)). This method, however, is limited to a molecular mass range of 10^4 to 10^6 (Shaw (1991)) and would therefore appear less useful for aqueous organic matter.

Electron Microscopy

While electron microscopy has been widely used for the characterisation of colloidal systems in conjunction with natural organics (Leppard *et al.* (1990), Wilkinson *et al.* (1995)), its quantitative use for size determination of natural organics has been very limited (Bailey *et al.* (1997)). However, the technique has been successfully demonstrated for molecular weight determination of other (however purer) compounds (Engel (1978)). On membranes, organics are not distinguishable from the

membrane polymer unless associated with colloids or in aggregated state. Transmission electron microscopy (TEM) has been used by Krasner *et al.* (1996) and small spherical units (1-2 nm) of organic matter were seen. Larger, more fibrous materials were also seen. This was confirmed by Fiella *et al.* (1993). The very small colloids are embedded in organic matrices which makes them difficult to detect by other techniques (see also section 2.9.1).

Other Techniques

Laser-Desorption Fourier-Transform Mass Spectrometry (LD FTMS) was used by Rice and Weil (1994) to analyse FA. The results are absolute values and oligosaccharides were identified. The size range measured was 342 to 1476 Da. At high laser powers all molecules were fragmented. While these techniques result in absolute results, they are rarely used for natural organics, most likely due to their complexity and lack of availability of instruments.

In summary, chromatographic techniques and UF are the most commonly used methods for MW determination. Whereas chromatographic techniques are limited by the availability of standards and detectors used, UF is limited by the compounds used for MWCO determination of the membrane manufacturers, relatively large volumes required, and possible charge interactions between membranes and solutes. It would appear to be sensible to use several different characterisation techniques to achieve reliable results.

2.5.5 Diffusion Coefficient

The diffusion coefficient of natural organics is related to the size of the molecules. Worch (1993) published a formula to relate MW with size for organic molecules (see Eqn. (2.1)). The size can then be related to diffusion coefficient by using the Stokes Einstein equation (see Appendix 5). While this method assumes spherical shapes, it allows the estimation as equivalent spheres.

$$D_S = 3.595 \cdot 10^{-14} \frac{T}{\eta \cdot M^{0.53}} \qquad (2.1)$$

Cornel *et al.* (1986) measured diffusion coefficients of HA in dilute solutions and found a decrease with increased molecular weight. This contradicts the above method and the anomalous behaviour was attributed to artifacts in the size measurements. Diffusivity increased with increasing ionic strength and decreasing pH. This could be attributed to the change in shape of the molecules as will be further explained in section 2.7. Diffusion coefficients were in the order of 1 to 2.5 · 10^{-10} m^2s^{-1} for 50 to 100 kDa and 0.5 · 10^{-10} m^2s^{-1} for 1 kDa UF fractions, respectively. The diffusion coefficients for Suwannee River materials are shown in Table 2.1.

2.5.6 Elemental Analysis and Structure

The elemental composition of natural organics varies from source to source and is different for NOM, FA, and HA. Values published for Suwannee River Reference FA and HA, DOM and Aldrich HA are shown in Table 2.2. For NOM, or DOM in this case, the analysis is more complex due to a generally very high ash content. The DOM was extracted with RO and contains a higher proportion of polar aliphatic substances (e.g. carbohydrates, proteinaqueous compounds). This was expected, as XAD extracts more hydrophobic compounds (Serkiz and Perdue (1990), Clair *et al.* (1996)). These values have been approximately confirmed in other studies (Thurman and Malcolm (1981), Reedy (1989)).

However, other authors found the average carbon content of river water samples to be 55% (HA) and 45% (FA) (Küchler *et al.* (1994)), which is probably a degree of variation to be expected.

Table 2.2 *Elemental Composition of Suwannee River HS, DOM ([1]Campbell and Malcolm (1985) and commercial Aldrich HA ([2]Shinozuka and Nihei (1994)).*

HS	C [%]	H [%]	O [%]	N [%]	P [%]	S [%]	O+S [%]	ash [%]
Suwannee HA [1]	54.34	4.08	39.43	1.08	0.01	0.68		3.38
Suwannee FA [1]	53.5	4.24	41.29	0.69	0.01	0.59		0.38
Suwannee DOM 04/87 [1]	49.19	4.45	-	0.80	-	-	45.56	2.42
Suwannee DOM 10/88 [1]	48.79	4.44	-	0.90	-	-	45.87	6.14
Aldrich HA [2]	56	4.3	-	0.9	-	-	-	-

The structures of HA and FA are not yet determined. A combination of many techniques is required to determine the structure of HSs. Schulten *et al.* have employed pyrolysis-gas chromatography with electron impact and field ionisation mass spectrometry (Py-GC/MS), in-source pyrolysis-field ionisation mass spectrometry (Py-FIMS), ^{13}C CP/MS NMR, oxidative and reductive degradation, colloid chemical methods, and electron microscopy to develop a carbon network structure for soil HS (Schulten (1994), Schulten and Schnitzer (1993)). The elemental composition of HA was $C_{308}H_{328}O_{90}N_5$ for a MW of 5540 Da. This indicates of the complexity of such compounds and the extensive techniques required. If carbohydrates or proteinaceous materials are bonded covalently with HA, %C content decreases and %O content increases.

Aqueous humics are generally smaller. Reddy *et al.* (1989) estimated an elemental composition of $C_{34.3}H_{33.1}O_{19.2}$ for FA of MW 750. Leenheer *et al.* (1989) proposed three structural models for FA but suggested that a large diversity of structures is likely to exist.

While such analysis are not the subject of this study, it is important to note that the structure of a compound does influence retention by membranes and the conformation in the boundary layer which influences flux.

2.5.7 Functional Groups

Functional groups are determinants of characteristics such as chemical binding, UV absorption, charge, hydrophobic interactions and solubility. Major functional groups of HSs are carboxylic acids, phenolic hydroxyl, carbonyl and hydroxyl groups (Thurman (1985)) Some authors also suggested the presence of sulphonic functional groups (Nyström *et al.* (1995)). The distribution of carbon amongst different functional groups for a number of organics is shown in Table 2.3. FA is clearly more aliphatic and less aromatic than HA. The least and most aromatic representatives of NOM concentrates obtained with RO are also described and show a much higher carbohydrate and aliphatic content, whereas aromatic structures are less.

Nuclear resonance spectroscopy is one method which can be applied to gain functional group information. ^{1}H, ^{13}C NMR with results of Norwood and Christman (1987) demonstrating that the lignin/phenolic structure is only a minor fraction of the organic carbon. ^{13}C NMR was used to determine the percentage of carbon in each functional group for five size fractions of NOM. The

amount of carbon in O-alkyl groups increased sharply with MW, varying between 25 and 50%. The carboxyl groups contained around 15% carbon (Newcombe and Drikas (1996)). Collins *et al.* (1986) found that the carboxyl content of HS was inversely related to MW.

Table 2.3 *Different Structural C Percentages of River HSs (Clair et al. (1996)).*

Organic Type	Aliphatic	Carbohydrate	Aromatic	Carboxyl	Other
Suwannee FA	31	19	23	18	9
Suwannee HA	23	19	37	14	7
NOM least aromatic	38	42	5	13	2
NOM most aromatic	37	27	12	19	5

2.5.8 Charge and Acidity

Charge and acidity are directly related to the functional group content. Natural organics are generally considered as weak acids with several carboxylic groups. They may also contain some phenolic functional groups. These groups give the molecules their charge, which increases in negativity with increasing pH. Most HA groups are dissociated at a pH>4.0 and carry a negative charge (Nyström *et al.* (1995)). At low pH the solubility of these compounds decreases due to the poor dissociation of the carboxylic acid groups. Carboxylic groups can be titrated to calculate the charge per mg DOC. Due to the wide range of compounds present, no clear equivalence point can be determined, but a plot of Δcharge as a function of ΔpH was found to be similar for all NOM fractions (Newcombe and Drikas (1996)). Surface potential measurements as a function of pH and ionic strength showed two levels, one corresponding to the carboxylic, the other one to the phenolic group (Tombacz and Meleg (1990)).

The presence of salts in NOM often disturbs charge titration. Tipping *et al.* (1988) determined a lower charge of NOM compared to purified species due to strongly bound metal ions.

HA is more soluble than FA at higher pH. HA has more phenolic groups than FA and is more hydrophobic. FA has a higher carboxylic acidity than HA (Küchler *et al.* (1994)) and therefore a higher charge. The carboxylic group concentration for FA, extracted from surface water, was determined to be 5.2 to 6.9 meqg^{-1}. Jucker and Clark (1994) showed the activity of carboxylic and phenolic groups and a change in molecular structure with HS concentration. Other authors report that functional groups of FA and HA are very similar and their negative charge increases with pH with pKa values of 2.5 to 3.5 and 4 to 5, for highly and moderately acidic carboxyl groups, respectively, and 9 to 10 for phenolic groups (Malcolm (1985)). Edwards *et al.* (1996) found that NOM extracted from lake water had a total acidity of 10.7 to 14.1 meqg^{-1} TOC. This was divided into weak (pKa $\geq$ 8.0), strong (3.0 $\leq$ pKa $\leq$ 8.0) and very strong (pKa $\leq$ 3.0) acids and the following proportions were found: 15-22% very strong, 64-75% strong and 9-17% weak acids. It was believed that paired functionalities are responsible for these unexpected results. Analogous paired structures were present in FA. The contribution of strong acids in this water was very surprising, since most researchers neglect HS charge at a pH lower than 3.0. However, accurate determination of acidic functional groups is problematic because of the starting and stopping values of titration. It is usually assumed that carboxylic acids dissociate in the pH range of 3 to 6. Very strong acids and weak acids are not measured if the titration is carried out in the pH range

of 3 to 8. Using monomeric and polymeric malic acid standards, it was noticed that polymerisation creates molecules with a weaker acidity, showing that they will not be measured in the usual titration range (Edwards *et al.* (1996)).

A relationship between molecular dimension and acidity has been reported (Perie *et al.* (1995)). The smaller the molecular dimension, the more acidic is the isoelectric point. The pK_a of a HS depends on the size of the molecule because of two effects: the field effect, which decreases pK_a due to charge delocalisation, and H-bonding, which increases the pK_a (Cabaniss (1995)). Two carboxylic acid groups on one aromatic ring will decrease the pK_a value of the first acid group and thus make it a stronger acid. Carboxyl content of NOM was estimated to be one per seven carbon atoms (14%) (Thurman (1985)). A comparative study has been carried out using wet chemical analysis and ^{13}C NMR. Carboxylic group content is lower for titrations than for NMR, with NMR results being closer to total acidity (Rasyid *et al.* (1992)). Potentiometric and conductiometric titrations of $1gL^{-1}$ HS with NaOH were used in this thesis to determine functional group concentrations of Suwannee River HS (Clark and Jucker (1993)). Results are summarised in Chapter 4.

The charge of natural organics determines their interaction with membranes, cations, colloids and their solubility. Charge is therefore a very relevant characteristic for water treatment and the distinction between the charges of functional groups is of particular interest in the interpretation of pH effects on membrane rejection and fouling.

2.5.9 Solubility and Aggregation of Natural Organics

The solubility of natural organics is an important issue in membrane processes where concentration polarisation is a common effect. Concentration polarisation may lead to gel layer formation if the solubility is exceeded. Solubilities of mixtures are difficult to determine. Many parameters influence solubility; FA is, by definition, more soluble than HA at low pH. The complexation with metal ions (see section 2.8) also influences solubility. Metal complexes of FA are more soluble than those of HA due to the lower MW and the higher charge of FA. The solubility of each compound depends on the saturation of the complex with metal ions (Stevenson (1985)). Tipping *et al.* (1988) established a direct relationship between solubility and charge of HA.

Trivalent and some bivalent cations can precipitate HSs under the right pH conditions from dilute solutions. Precipitation or aggregation of organics with cations is facilitated at low temperatures, most likely due to the coprecipitation effect with carbonates (Steinberg and Muenster (1985)). However carbonates are more soluble at low temperatures.

Aggregation occurs due to an increase in ionic strength, which shields organic charge. The high MW components aggregate preferentially (Mayer (1985)). Calcium can enhance aggregation of NOM (Tipping and Ohnstad (1984b), Yan and Zydney (1999)). According to Tipping and Ohnstad (1984a), as the pH decreased below 5 the solubility decreased due to complexation with the cation, where high molecular weight compounds were least soluble. Low MW compounds remained non-aggregated in solution even when complexed with calcium. Precipitation of the HSs occurred when functional groups are neutralised or complexed. The critical coagulation concentration was in the order of 2 to 3 mM $CaCl_2$.

An ionic strength increase in water treatment occurs, for example, in the membrane boundary layer or along RO modules. In natural systems this occurs when freshwaters mix with seawater.

The aggregation kinetics have been reported to be rapid (aggregates of about 1 μm form within one hour), visible and settling aggregates form over two days (Mayer (1985)). UV measurements showed changes in aggregation. Hering and Morel (1988) observed aggregate formation during calcium titrations of HA. Tombacz and Regdon (1984) reported humics aggregation as mostly irreversible. Depending on the solution chemistry, HSs can either be fully dissolved (treated as polyelectrolytes), associated as loose aggregates or form micelles. As a function of pH, ionic strength and metal ions concentration organic cations either form compact aggregates or organocomplexes.

Natural organics also readily adsorb onto mineral matter which transforms the organic into particulate form. Depending on the size of the mineral colloid, it will remain in suspension or settle. This issue will be addressed separately (refer to section 2.9).

2.5.10 Micelle Formation of Natural Organics and Surfactant Characteristcs

Strongly polar molecules like surfactants can form micelles in solution. Natural organics are amphiphilic molecules (possess both hydrophobic and hydrophilic groups). In a micelle they would arrange to form a hydrophobic core with a hydrophilic outer shell. It has been suggested that FA forms micelles in solution (Clark and Jucker (1993)). Childress and Elimelech (1996) showed evidence of surfactant characteristics of some natural organics where humics make membranes more hydrophilic. Leenheer *et al.* (1989) reported surface-active properties of aqueous HSs. A difference in mobility was explained by the possible formation of micelles.

However, micelle formation of FA appears unrealistic, since for micelle formation a very polar molecule is required. FA has a rather evenly distributed charge, which would allow some sort of polarisation, but the formation of real micelles is questionable.

2.5.11 Structure/Fractal Dimension of Natural Organics

The conformation of natural organic molecules under various solution conditions is of particular interest in water treatment, as the structure of the molecules may influence their packing and water permeability. The fractal dimension reflects the space occupied by the disordered system. Senesi *et al.* described a method using a UV/VIS spectrophotometer to measure the fractal dimension of humic aggregates (Senesi (1994), Senesi *et al.* (1994, 1996, 1997)). At low pH the aggregates were of a compact, collapsed, less porous structure, whereas at a higher pH they were more expanded, open, and of "fluffy" structure. While the method appeared to work well for the published data, the simultaneous variation of absorbance, fluorescence, and scattering casts some doubt on the method.

In fact, Hongve and Åkesson (1998) suggest the use of wavelengths >800 nm to measure turbidity in order to avoid interference from absorbing substances. The fractal analysis suggested by Senesi (1994) was carried out over the entire UV/Vis range. A more useful approach could be static light scattering with an appropriate laser. Overall little work has been reported on the conformation of humic molecules (as opposed to their aggregates) (Mayer (1985)).

Rice and Lin (1994) measured fractal geometry by small-angle x-ray scattering. In solid state, the fractal dimensions were between 2 and 3 which confirms the visual observations of Krasner *et al.* (1996) (see section 2.5.4). While in the solid state the organics were surface fractals, in solution they are expected to become mass fractals. Österberg and Mortensen (1994) measured fractal structure using small angle neutron scattering (SANS). At lower temperatures ($<8^0$C) loose aggregates are formed (fractal

dimension <1.85), which indicated fast aggregation. On temperature increase, the fractal dimension increases to up to 2.35 (21^0C). Reported aggregate sizes were 0.9 to 1.5 nm.

2.6 FRACTIONATION OF NATURAL ORGANICS

Fractionation of natural organics is required to link characteristics to treatment behaviour. Leenheer *et al.* (1989) expressed an urgent need to separate the complex mixture of HSs into more homogeneous fractions in order to understand its nature and properties. The fractionation of HS in terms of MW, functional groups, elemental composition, and other characteristics, is limited by methods and patience (Swift (1985)).

2.6.1 Particulate/Dissolved Organic Carbon Separation

Particulate organic carbon (POC) can be easily separated from dissolved organic matter using a 0.45 μm filter. This operation distinguishes the parameters TOC and DOC by definition. If a 0.45 μm organic filter is used for sample preparation, large volumes of pure water need to be filtered to eliminate any organic contamination of the sample from possible membrane coatings. However, this method cannot remove small colloids from the solutions (see Chapter 5) or even separate organic aggregates which are smaller than 450 nm.

2.6.2 FA/HA Separation

HA can be precipitated from natural waters by lowering the pH value to 1.0, while the FA remains in solution (Bourbonniere and van Halderen (1989)). FA has an increased carboxyl and decreased aliphatic content which explains its higher solubility in water than HA (Rasyid *et al.* (1992)). The acidification step used to precipitate HA, hydrolysed the carbohydrates and altered the subsequent analysis (Clair *et al.* (1996)).

A more common method used for aqueous organics is the resin adsorption step (XAD8, XAD4), which was described in section 2.4.1 and can be used for concentrates to isolate the desired compounds. This method also requires acidification to separate FA from HA.

2.6.3 Size/MW Fractionation

For size or MW fractionation, essentially the same methods as described in section 2.5.4 can be applied as a preparative technique. Limitations are often the low concentrations of fractions, necessitating a concentration step which may induce sample alteration.

The need for large volumes of material often leads to a scale-up of systems. With UF, for example, hollow fibre systems and stirred cells have been compared for the concentration and fractionation of HS. Kwak and Nelson (1977) showed that retention increased with pressure, decreased with ionic strength and was not concentration dependent. Hollow fibres proved ineffective for UF fractionation compared to flat sheet membranes due to clogging and indiscriminate retention effects (Küchler *et al.* (1994)).

2.6.4 Hydrophilic/Hydrophobic Fractionation

The fractionation into hydrophobic and hydrophilic components can be significant, for example in the study of adsorption effects with membranes of different hydrophobicity.

Fractionation of HS with NaCl depends on the charge of a molecule and its ability to aggregate (Tombacz and Meleg (1990)) and a fractionation by hydrophobicity will be obtained. However this method will change the ionic strength of the sample and a preparative use of this method is not possible. NaCl would also cause a size fractionation and separation of effects may not be possible.

Alternatively XAD resins can be used as described in section 2.4.1. This method is aimed specifically at hydrophobic compounds. DOC and biodegradable DOC (BDOC) were fractionated by Agbekodo and Legube (1995) into hydrophobic/hydrophilic fractions using XAD8 (hydrophobic) and XAD4 (hydrophilic) resins. With the XAD8 resin, essentially all HSs are adsorbed, whereas XAD4 adsorbs all kind of organics.

2.7 VARIATIONS OF NATURAL ORGANICS CHARACTERISTICS WITH SOLUTION CHEMISTRY

Natural organics change their shape according to solution conditions including the concentration of the organics, the ionic strength and the pH. Two extremes of molecule shapes are common - rigid spherocolloids and flexible linear molecules (Ghosh and Schnitzer (1980)).

2.7.1 Effect of Organic Concentration

Changes in molecular shape due to organic concentration are due to variations in viscosity. If viscosity changes linearly with concentration, there are no configurational changes expected. However, if relationships are non-linear, configurational changes take place. Ghosh and Schnitzer (1980) determined a critical concentration, 3.5 to 5 gL^{-1}, below which these changes occur. Above this concentration the organics behave like spherocolloids or uncharged rigid colloids as they have no space to expand. The solubility of organics due to concentration effects was not addressed by Ghosh and Schnitzer (1980). These results correspond well to structure analysis, where the fractal dimension of solid HS was around 3, thus more or less spherical.

This may be of importance in membrane filtration, where significant changes in concentration may take place in the boundary layer, where molecular conformation may influence gel layer permeability. However it may only be relevant for feeds of high NOM, high recovery and significant concentration polarisation.

2.7.2 Effect of Ionic Strength

HSs change from linear to spherical form on increasing ionic strength. This is due to the neutralisation of anionic carboxylic acid and phenolic groups by the cations of the added salt. At high organic concentrations this effect was not observed, probably because of high HS concentration that allowed the change in shape without salt (Agui *et al.* (1992)). Size depends on ionic strength - the higher the ionic strength, the smaller the molecule (Jucker and Clark (1994)). Ghosh and Schnitzer (1980) found molecules fully uncoiled at low ionic strength of 1 mM NaCl, whereas at 50 to 100 mM NaCl the structure was fully coiled. This corresponds to brackish water conditions, seawater would be about 600 mM.

At the low ionic strengths ($I=0.5 \cdot 10^{-3}$), typical of natural waters, FA and HA were found to be very large (Clark and Jucker (1994)). The hydrodynamic diameters of HSs were found to vary between 15

and 1.7 nm at an ionic strength of 0.4 mM and 1 M, respectively (O'Melia (1989)). The effect of ionic strength was found to disappear for LMW FAs (Pettersson *et al.* (1994)). The size of a HS molecule might be an important factor for membrane fouling. At a high ionic strength, the retention of LMW compounds might decrease significantly.

2.7.3 Effect of pH

pH alters the charge of the organic molecules and a variation in charge effects a different repulsion between the functional groups. This alters the conformation of the molecules. Shaw *et al.* (1994) measured a decrease in size of HSs with decreasing pH. Ghosh and Schnitzer (1980) attributed a linear colloid behaviour at pH 6.5 with complete dissociation of the organics. At higher pH values, some association of macromolecules occurred due to an increase of free radical content with pH. Not all molecules participated in these associations. While HA is not soluble at low pH, FA remains soluble but partially aggregates at pH 2.

2.8 INTERACTIONS OF NATURAL ORGANICS WITH OTHER SOLUTES

Most pollutants in natural waters are associated with natural organics. In surface waters, natural organics co-preciptitate with calcium carbonate. Organics are also known to inhibit calcite precipitation (Steinberg and Muenster (1985)). In the following sections reported interactions between natural organics and cations, trace metals and other compounds such as pesticides are summarised.

2.8.1 Cations

Cations in conjunction with natural organics enhance membrane fouling. This effect, although being generally accepted, is not well understood. Therefore, the interactions of natural organics and cations are of particular importance. The effect of cations on natural organics' solubility was discussed in section 2.5.9.

Cations interact with natural organics in two manners; site specific strong binding and weak binding which is the presence of counter-ions in the vicinity of the organic molecule or electrostatic attraction (Leenheer *et al.* (1989)). The two binding mechanisms are not independent of each other. Weak binding is present in all molecules and increases with carboxylic acid content and the structural arrangement of these groups, whereas strong binding is very organic specific and is not always present. Kango and Zutshi (1986) reported a broad variability with the source of HSs in interaction characteristics with calcium. The complexation of natural organics with calcium may lead to stable complexes or aggregation according to Liao and Randtke (1986). Cabaniss and Shuman (1988) reported that about 50% of FA in a natural environment may be associated with calcium and magnesium, but that such associations may be destroyed in a extraction process. Complexation may be measured using UF fractionation (Staub *et al.* (1984)), as described in section 2.5.4. Brun *et al.* (1994) attributed complexation of natural organics with calcium to the dissociation of functional groups. This would indicate few interactions below pH 5 and an involvement of phenolic groups. Ephraim *et al.* (1994) found a decrease of calcium binding by FA with increasing ionic strength. Results were higher when measured with UF, rather than calcium selective electrodes. Tipping *et al.* (1988) reported an effect of total organic charge on binding capacity. Aluminium did not compete with calcium for sites, which

indicated specific interactions. The HS-Ca complex formation was directly proportional to pH and the acidity of functional groups (Armirbahman and Olson (1995)).

Calcium and magnesium have a large impact on the binding of HSs to negatively charged particles and surfaces encountered in water treatment (Tipping and Heaton (1983)). Chandrakanth and Amy (1998) suggested that calcium preferentially interacts with oxygen-containing functional groups.

The interactions with calcium vary the organic size depending on the organic concentration. Metal complexation showed an increase in size in UF fractionation (Aster *et al.* (1996)). The ions present in river water were measured simultaneously with UF fractionation to ascertain how they interact with HSs of various sizes (Küchler *et al.* (1994)). In concentrated solutions aggregate formation is favoured, while for low concentrations intramolecular contractions result in smaller sizes (Engebretson and von Wandruszka (1994)). Huber (unpublished) reported a decrease in measured size with calcium bicarbonate addition.

Hering and Morel (1988) showed different binding characteristics of IHSS and Aldrich HA. Also, varying binding mechanisms were suggested for different ions which indicates specific binding. Burba *et al.* (1998) found that Fe and Al are evenly distributed in all MW fractions. These results contradict the findings of Hoffmann *et al.* (1981) who found that trace metals interact most with the intermediate size range of organics (1-10 kDa) whereas calcium and magnesium were found predominantly in the lower molecular size range.

The interaction of natural organics with cations result in various species, but due to the unknown equilibrium constants and the different interactions by various organics involving several mechanisms, the available data is limited. Matlack (1992) modelled the interactions of natural organics with cations in order to determine speciation. He found a general underestimation of the interactions by speciation software due to the assumption of competition between cations.

Little literature has been published on the binding energy of calcium and natural organics. Clark *et al.* published binding energies between calcium and natural organics measured by XPS as 349.2 to 349.7 eV (Clark and Jucker (1993)). However, it was not specified in which chemical state calcium and HSs were and much more work is needed to identify the species involved.

2.8.2 Trace Metals

Organics are responsible for the transport of trace metals in the natural environment. While most monovalent ions are fully dissolved in natural waters, multivalent ions are often associated with small inorganic colloids of less than 10 nm in size. Some of the trace metals form soluble complexes with organic ligands, and others associate with organics as colloids. The distribution of trace metals in surface waters can be determined using UF fractionation (see section 2.5.4). Tanizaki *et al.* (1992) found that iron is mostly associated with colloidal materials, as iron tends to be stabilised by naturally occurring organic and inorganic colloids. Heavy metals associate with natural organics in a similar manner and their transport in the environment is also enhanced.

2.8.3 Interactions with Other Compounds

Numerous studies have been performed concerning the binding characteristics of HS with organic or inorganic toxins. These toxins, which occur in natural waters, bind to HSs and can cause problems once they are released (Alberts *et al.* (1994)). HSs bind to hydrophobic and amphipathic micropollutants, such as herbicides and pesticides (Wilkinson *et al.* (1993)). This was confirmed by

Frimmel *et al.* (1994) who stated that HSs increase the solubility of hydrophobic pesticides. Zhou and Rowland (1997) showed an increased uptake of hydrophobic pollutants by suspended particles that were coated with natural organics. Murphy *et al.* (1990) confirmed this increased uptake for coated hematite and kaolinite, and attributed variations between the two primary particles in sorption characteristics to different orientations of the HSs.

This pollutant uptake is an important effect in water treatment, where the retention of such colloids and the resulting stress could cause a release of such pollutants.

2.9 INTERACTIONS OF NATURAL ORGANICS WITH COLLOIDS

Inorganic colloids in surface waters may be the oxy/hydroxides of Mn, Fe, Al and Si, as well as carbonates and clays, with a size range from a few nanometres up to millimetres (Thurman (1985), Morel and Hering (1993)). Such colloids have been extensively characterised and modelled (Ledin *et al.* (1995), Wilkinson *et al.* (1995), Filella *et al.* (1993), Leppard *et al.* (1990), Filella and Buffle (1993), Perret *et al.* (1994), Newman *et al.* (1994)). Colloids in a natural environment often have a negative surface charge and occur in large organic matrices. Solution chemistry and surface properties control the colloidal stability of these natural particles.

According to Filella and Buffle (1993), colloids <80nm coagulate rapidly, particles >0.9 μm sediment quickly, while those inbetween coagulate slowly and settle eventually. Particles that settle in the aquifier are not usually encountered in water treatment, although aggregation may occur during treatment. Submicron particles are of particular importance due to their high specific surface area, which allows the adsorption of many compounds and their stability.

The interactions between colloids, organics, and multivalent ions suggest the importance of these phenomena in the membrane filtration behaviour of natural waters containing colloids and organics.

2.9.1 Characterisation of Natural Organics and Colloid Systems

Visual Techniques

Wilkinson *et al.* (1995) used transmission electron microscopy (TEM) to visualise NOM-colloid aggregates. The technique showed filamentous matrices, which interact with small spherocolloidal inorganic particles. Aggregation of organics and colloids continued until one large aggregate was formed. Such behaviour accounts for the presence of large matrices of organics and colloids in natural systems. Diffusion coefficients are higher for more compact structures. At high ionic strength and low pH coiled structures form (fractal dimension 1.8), whereas linear chains or loose matrices are otherwise formed (fractal dimension close to 1.0). Krasner *et al.* (1996) also showed TEM photos of such matrices and aggregates in a natural water.

Particle Analysis

Particle analysis is often difficult in natural systems due to the presence of larger particles which necessitates fractionation of the samples. Also, the particles present are often unstable and the concentrations of submicron particles are low. Concentration variations were given by Filella and Buffle (1993) as between 0.1 mgL^{-1} in sea- or groundwater to 10 gL^{-1} in a river. Iron containing particles are, according to the authors, very common and occur in sizes of 2-450 nm. Colloids smaller than 50

nm in diameter are often embedded in large organic matrices. These sizes are significantly smaller than those of colloids usually studied in water treatment research.

Fractal Dimension

Fractal dimension relates density and size of an aggregate. The determination of fractal dimensions by light scattering is limited to very well defined systems. Light scattering analysis becomes invalid for aggregates in a size range where settling becomes important (>1 μm) or for polydisperse systems. Thill *et al.* (1998) have developed a method using confocal scanning laser microscopy for such aggregates, which are common in natural systems. Zhang and Buffle (1996) used TEM for fractal dimension analysis.

Of particular interest in water treatment is the permeability of aggregates. When aggregates deposit on a membrane, flux is determined by the resistance of the formed cake. Furthermore, the drag force on the colloid is determined by the aggregate porosity. Veerapaneni and Wiesner (1997) predicted the resistance to fluid flow as a function of fractal dimension. They determined that fluid flow through the aggregates decreased with increasing fractal dimension.

Grout *et al.* (1998) question the description of natural samples by simple power laws. According to these authors natural systems are often multifractal which means the fractal dimension varies for different size scales. Veerapaneni and Wiesner (1997) studied the effect of filtration velocity on the fractal dimension of deposits formed by 69 nm colloids. Fractal dimensions increased with increased velocities where a lower head loss was measured. this was attributed to columnar structures formed.

2.9.2 Organic Adsorption onto Colloids

Colloids in the natural environment commonly have a negative surface charge due to an adsorbed layer of NOM, which can lead to stabilisation of the colloids (Tiller and O'Melia (1993), Beckett and Le (1990)). The interactions of colloids and organics are important for water treatment and the various properties of the organics result in adsorption via several mechanisms, including electrostatic interaction, specific chemical affinity, and hydrophobic interactions (Amal *et al.* (1992)). The HSs can adsorb at the colloid surface in loops or tails, depending on the solution chemistry, and thus alter the surface morphology of the inorganic colloids. FA has been reported to be less adsorbed than larger compounds by Amirbahman and Olson (1995). Amirbahman and Olson (1993) related the different adsorption rates for various organics to the altered conformations of the organics.

Au *et al.* (1999) described organic adsorption on hematite as a complexation between organic functional groups and neutral oxide sites. It was hypothised that a layer of NOM forms on the surface regardless of solution chemistry and possibly regardless of the particle surface characteristics. Gu *et al.* (1994) suggested that ligand exchange (surface complexation) between carboxyl and hydroxyl functional groups was the main mechanism for NOM-iron oxide surface interactions. However, it is possible that a number of mechanisms play a role, including anion exchange (electrostatic interaction), hydrophobic interaction, entropic effect (flocculation is more likely at a lower temperature), hydrogen bonding, and cation bridging. The authors determined that the amount adsorbed increased at low pH, which corresponds to the results of Fairhurst *et al.* (1995) for hematite.

Fairhurst *et al.* (1995) found that adsorption of HA at 5 mgL^{-1} (as organic carbon) on 50 mgL^{-1} hematite decreased with increasing pH from 65% at pH 2 to 10% at pH 10. The apparent point of zero charge (pH_{pZC}) of the colloids was shifted from pH 8 (no HA) to a pH <2. Such charge inversion of colloids

has been attributed to the free functional groups on the HA, which do not interact with the colloids (Julien *et al.* (1994)). These researchers studied the adsorption of organics with various numbers of functional groups on preformed flocs, and demonstrated that the zeta potential of colloids with adsorbed organics that only had one functional group was zero. These results mean that humic-covered hematite would be negatively charged in most situations, and that the resulting charge depends on the organic type. Au *et al.* (1999) measured adsorption densities of HA on hematite of 1.25 to 0.25 mg m^{-2} (pH4 to pH10), and a hydrodynamic layer thickness of the adsorbed layer of 1 to 3 nm. Tipping (1981) found a decrease in humics adsorption on hematite with increased pH, and an increase of adsorption with calcium concentration at any pH. Chandrakanth *et al.* (1996) modelled NOM-calcium-alumina interactions and found that alumina and calcium compete for NOM. By analogy, this means that hematite and calcium may compete for NOM sites. FA and NOM were found to adsorb to a similar extent, but hydrophobic fractions were adsorbed preferentially. This was confirmed by Korshin *et al.* (1997). Pettersson *et al.* (1994) observed the adsorption of particles to decrease with increasing MW and postulated that this could be a reason for a lower HS content of groundwaters that had a long contact time with minerals.

Gu *et al.* (1996a, 1996b) also determined that NOM fractions compete for adsorption onto mineral surfaces when sites are limited, with more aromatic compounds being sorbed preferentially. Edwards *et al.* (1996) found that organic acids that contain paired functionalities sorb more strongly onto mineral surfaces. Strong acid groups form more stable complexes. Dissolved FAs have a strong affinity to bind to hydroxylated sites on mineral surfaces (Kastelan-Macan and Petrovic (1996)). Suess (1973a, 1973b) studied the interaction of organic compounds with calcium carbonate, and observed monolayer adsorption (0.1 to 1.5 mg m^{-2} carbon); organo-calcium complexes on calcite grains existed. The effect of alumina particles on NOM was studied and modelled by Chandrakanth *et al.* (1996) as a function of pH, ionic strength, ion concentration (calcium, HCO_3) and preozonation. Adsorption equilibria of NOM and particles were rapid and alumina competed with calcium for adsorption sites of NOM. NOM was modelled successfully as a triprotic acid.

2.9.3 Colloid Stabilisation and Mobilisation

Colloid stability depends on colloid charge and, to a lesser extent, on steric effects. Colloids in the absence of specifically adsorbing species are characterised by their point of zero charge (pzc), and when pH equals pzc their stability is minimal. In the presence of adsorbing species, colloids are characterised by their isoelectric point (IEP). At the IEP all positive and negative surface charges of the surface are balanced. Inorganic surfaces such as clays and metal oxides can be significant adsorbants. HSs can stabilise particles in water, reverse their charge, and incorporate bivalent ions in the fixed part of the double layer. Stabilisation leads to an increased mobility and the presence of natural matter in a surface water may mobilise inorganic materials from the sediments (Ryan and Elimelech (1996)). The degree of stability depends on the amount of organics adsorbed. According to Liang and Morgan (1990) a small amount of organics can decrease stability due to charge neutralisation, whereas a larger amount adsorbed leads to charge reversal and restabilisation. Fulvic acid was used to study the impact of HSs on particles in solution. Particle charge inversion occurred at FA concentrations of 0.25 to 0.5 mgL^{-1}, creating unstable particles and a thick deposit on the filter medium. Higher concentration increased negative charge, enforced charge repulsion, and decreased the amount deposited. Removal and headloss increased with deposit build-up. Removal efficiencies for natural waters varied from 30 to

60%, depending on the concentration of organics (Prasanthi *et al.* (1995)). Hematite particles in a natural environment are usually stable, as destabilised colloids settle rapidly. Song *et al.* (1994) addressed the masking of colloid surface heterogeneity by dissolved organic matter. This can enhance colloidal mobility. Kretzschmar *et al.* (1997) showed that HSs also stabilise kaolinite colloids.

The mobility of geothite in water was measured as a function of HS concentration and the presence of calcium. The mobility is highly concentration dependent up to a calcium concentration of 2 mgL^{-1}. The effect of bivalent ions is not great for high HS concentrations and low ion content (Tipping and Heaton (1983)).

Tiller and O'Melia (1993) studied the colloidal stability of hematite in the presence of NOM and various model organic compounds. Adsorption increased with the molecular weight and the hydrophobicity of the compound. The presence of calcium only had a small effect on NOM adsorption at low ionic strength (I=0.01M), but destabilised the NOM coated particles at high ionic strength (I=0.1M). Colloid behaviour at low ionic strength, as in typical surface water, is dominated by double layer interactions. Major bivalent cations destabilised particles, and these particles then aggregated easily and adhered to surfaces. At intermediate ionic strength, corresponding to aquatic systems, calcium could react with HS functional groups, and alter conformations in the macromolecular adsorbed layer. This reduced its charge and thickness, increased adsorption, and enhanced coagulation and deposition, due to a reduced colloidal stability (O'Melia (1989)). According to Liang (1988) aggregation was affected by chemical interactions between bivalent ions and surface-adsorbed humics. Such interaction occur as surface waters move into the sea.

Armirbahman and Olson (1995) showed that the presence of Ca^{2+} ions reduced the stability of organic coated hematite particles, due to charge screening and complex formation with two humic functional groups. The electrophoretic mobility of hematite particles coated with organics decreased with calcium concentration. A clear distinction between electrostatic, hydrophobic, and steric interactions could not be ascertained, since these effects were considered to be interrelated. Calcium destabilised particles with an adsorbed organic layer. Electrostatic effects were found to dominate particle stabilisation by NOM in natural waters (Tiller and O'Melia (1993)). Tipping and Ohnstad (1984) suggested that calcium could contribute to bridging flocculation, where very high molecular weight HSs or organic fibrils could also contribute to bridging.

2.9.4 Aggregate Formation and Structure

Aggregation of colloids depends on many parameters, such as pH, ionic strength, primary colloid size, stirring, and the presence of dissolved organic matter. A few technical terms will be defined here. Perikinetic flocculation occurs for small colloids that are controlled by Brownian motion and not influenced by stirring. Orthokinetic flocculation occurs under conditions where colloids are larger than 1 μm, stirring becomes important. Shear determines the aggregate size (Jung *et al.* (1995)). There are two distinct regimes in irreversible aggregation. Diffusion limited aggregation (DLA), or fast aggregation, occurs when interparticle repulsion is low. Reaction limited aggregation (RLA) is slower and takes place when a repulsive barrier exists. Lin *et al.* (1989) suggested that these regimes are universal or independent of the chemical details of the primary colloids. Zhang and Buffle (1996) anticipated that aggregates grow mainly through collision with other aggregates (or clusters), rather than through primary colloid addition. Fractal dimensions at low ionic strength (RLA) were significantly higher, 2.1, than those measured at high ionic strength (DLA, 1.8). Aggregates restructure due to shear,

but only at large length scales, whereas for small length scales aggregates remain their original structure (Lin *et al.* (1990)). At large length scales an increase in fractal dimension was apparent. Gregory (1998) also stated that restructuring resulted in denser aggregates and that denser flocs were less prone to break-up. If flocs have fractal character their density will decrease with size. The structure of hematite aggregates and their formation kinetics were studied in the presence of FA. Two cases were expected; compact structure and slow aggregation at low temperature and low salt concentration, and loose, tenuous aggregates due to rapid aggregation at high temperature and high salt concentration.

Boller and Blaser (1998) divided flocs into two classes - those which are prone to breakage (500-2000 μm), and flocs which are hard to rupture (<100 μm) under water treatment conditions.

Dynamic light scattering was applied for aggregation kinetics analysis and static light scattering for aggregate structure. Amal *et al.* (1992) found three aggregation kinetics regimes. At low salt and FA concentrations (ratios 3:1 or 4:1), no growth occurred due to repulsion, at moderately higher concentration, growth increased and at high concentrations (ratios above 10:1 to 20:1), rapid coagulation took place and became independent of salt concentration.

Particles of different attributes, such as characteristic surface or charge, need to be investigated to be able to predict treatment performance. The impact of particle content on fouling of tight membranes is not clear in the literature, but it is generally assumed that particles play a major role in fouling. These effects need to be understood prior to optimising membrane pretreatment.

2.10 NATURAL ORGANICS IN WATER TREATMENT

2.10.1 Drinking Water Standards

In the United States, current Stage 1 Major Contaminant Level (MCL) of total trihalomethanes (THMs) and five haloacetic acids (HAA5) are at 80 and 60 μgL^{-1}, respectively. At Stage 2 this will be lowered to 40 and 30 μgL^{-1} (US EPA (1998), Dal-Cin *et al.* (1995)). In Germany maximum admissible THM concentrations are as low as 10 μmL^{-1} (McCann (1999)).

However, drinking water standards do not exist in Australia and the 1996 guidelines are currently being reviewed, including THMs for the first time. The 1987 guidelines are still not commonly applied (Vitanage *et al.* (1996)).

This results in higher treated water qualities in countries like the US or Europe, where standards are generally very high and source waters of poor quality due to high population densities.

2.10.2 Treatability of Natural Organics by different Processes

Treatment aims to meet drinking water guidelines. The removal of disinfection by-products (DBPs) and biodegradable organics are primary targets. Taste and odour compounds are also important.

An overview of the current water treatment situation was given by Jacangelo *et al.* (1995). Three processes appeared most relevant for HS removal: activated carbon, nanofiltration, and enhanced coagulation. Another, relatively recent treatment option was the use of magnetic ion exchange resin, which has been specifically developed for NOM removal (Morran *et al.* (1996)). Treatment options considered by Allgeier and Summers (1995c) were coagulation, alternative disinfectants, ozonation, biotreatment, granulated activated carbon (GAC) and membranes. GAC and nanofiltration have been

demonstrated to be the most effective, but also the most expensive Ion exchange was not been considered by these authors. Ødegaard *et al.* (1999) other authors state that ion exchange is an expensive treatment option compared to other processes.

A variety of hybrid processes can also be used, such as pretreatment of powdered activated carbon (PAC), coagulation, conventional treatment, resin or cartridge filtration followed by ion exchange, adsorption, or membranes.

Membrane processes have the advantage of being simple, requiring little space, and can be operated with minimal chemical addition and maintenance. Membrane processes are now considered as cost competitive with an outlook to even better and cheaper membranes. Application volumes increase exponentially and it appears sensible to select membrane processes as the main focus of this study.

2.10.3 Disinfection By-Product Formation

Disinfection of drinking water is required when the water contains organic matter that could promote bacterial regrowth in a distribution system. Disinfection of water that contains organic matter, such as HSs, produces so called disinfection by-products (DBPs). By-products of chlorination are best known, but other oxidation processes such as chloramines, UV, or ozonation all produce different kinds of by-products. When considering health effects, a balance is required between epidemiological (waterborne diseases such as hepatitis A, cholera, salmonellosis, typhoid and gastro-enteritis) and chronic (causing cancer or birth defects) risks originating from either a lack of disinfection or disinfection, respectively (Cowie *et al.* (1996)). A minimal risk can be achieved by eliminating organic compounds in water treatment, achieving a low chlorination requirement and a low DBP formation potential. Methods which are able to achieve this high quality are available, but are often uneconomic, especially in Australia where drinking water is relatively cheap (about 80c per m^3).

Disinfection by-products (DBPs) include trihalomethanes, haloketones, haloacetonitriles, haloacetic acids, and other chlorinated compounds. If ozone pretreatment is applied, ozonation by-products can be formed, one of them being bromate (Tal and Amy (1991)).

The different chlorination by-products have been described in detail by Hashimoto (1995). The risk of chlorination by-products in relation to current regulations was discussed, and alternative disinfectants were investigated by Regli *et al.* (1995). Kronberg (1999) attributes the mutagenic character of DBPs to various chlorohydroxyfuranones (CHFs). The concentrations critical for human health are largely unknown. Main chlorination reaction products of natural waters were summarised by Jiminez *et al.* (1993) and a model for the THM formation developed. An empirical kinetic equation was established for the formation of THM from HA and hypochlorite at a different pH.

The higher the UV absorbance of a sample, the higher its by-product forming potential, although FA and hydrophilic acids react with chlorine to a similar extent (Krasner *et al.* (1996)). According to Singer (1999), DBP formation is directly proportional to UV absorbance.

This implies that UV absorbing compounds need to be removed preferentially, although all organics seem to be prone to reaction with chlorine.

2.10.4 Bacterial Regrowth, Biofilms and Conditioning Films

Organic matter in waters can be a nutrient for biological growth in distribution systems which causes microbiological health risks. Gauthier *et al.* (1999) suggested that organic matter is responsible for loose deposits in distribution systems with a high chlorine consumption. This is another driving force for

organics removal. However, it appears as if the most bioavailable fraction of natural organics is also the most difficult to remove.

Martin-Mousset *et al.* (1997) found that about 15% of DOC is biodegradable. Agbekodo and Legube (1995) found that HA was 7% degradable and of average bioassimilability, while FA was not biodegradable. Similar trends were determined for HSs (Louis *et al.* (1995)). Carbohydrates are very degradable and it was found that about 40% of carbohydrates in stream water were bound to HSs. In studies that used NOM, contains a higher biodegradable portion due to non-humic components such as amino acids or sugars.

Another study suggested that FA and HA were microbiologically decomposed in anaerobic and aerobic environments, and the rate is slower when the oxygen content of FA decreased. This indicated that the oxygen is used by the microorganisms (Pettersson (1994)).

Hambsch (1992) examined biological growth in different surface waters with a new method based on a measure of cell concentration with turbidity. The effect of ozone on biodegradability was studied, showing an increase due to ozone treatment. The non-humic fraction of river water was determined to be far more degradable.

These findings imply a strong need to remove the smaller fraction of natural organics if regrowth potential is to be controlled.

2.10.5 Membrane Fouling

Of particular interest in this study is the fouling of membrane processes by natural organics. Fouling depends on the characteristics of the natural organics. A detailed review of the characteristics of interest is required to highlight the factors that may influence membrane fouling. Membrane filtration behaviour is addressed in detail in Chapter 3.

2.11 SUMMARY

A summary of key characteristics of natural organics and the possible implications of these characteristics on treatment is shown in Table 2.4. The effect of some of these characteristics on membrane treatment is investigated in more detail in Chapter 3.

Table 2.4 *Key characteristics of natural organics and their interactions with other water constituents as described in this chapter.*

Characteristic	Trends	Relevance to Treatment
Definition	HA: adsorbed by XAD8 resin and precipitated at pH 2; FA: adsorbed by XAD8 resin and soluble at pH 2; Hydrophilic fraction: adsorbed by XAD4 resin; NOM: all fractions, generally concentrated by reverse osmosis	Aquatic organics are operationally defined by the method of concentration
Composition	Particulate (POC) and dissolved (DOC)	POC and DOC are removed by different processes (MF removes POC, but not DOC)
Concentration	0 to 50 mgL^{-1}	Concentration determines how much DOC needs to be removed and may impact treatment efficiency (e.g., more fouling at higher concentration)
Aromaticity/ Hydrophobicity	Larger compounds (HA) are more aromatic and hydrophobic than FA. NOM also contains the hydrophilic fraction	Hydrophobic compounds are easier to remove by conventional processes (coagulation/ flocculation) and may cause more severe membrane fouling. Hydrophobicity also influences rejection by membranes
Size/Molecular Weight (MW)	Size and MW are very dependent on origin	Small organics are harder to remove by membrane processes
Polydispersity	HA is more polydisperse than FA. Values range from 1.7 to 4.7.	Treatment is easier to predict for a less polydisperse sample
Diffusivity	Diffusivity is related to size with smaller molecules having a higher diffusivity. Values are in the order of 2 to $5 \cdot 10^{-10}$ m^2s^{-1}	Diffusivity governs transport of organics away from the membrane to avoid fouling and in some processes rejection is determined by diffusifity
Elemental Composition	50 to 55% C, 4% H, 40 % O, 1% N and traces of P, S, other compounds and ash. Ash is higher for NOM compared to FA and HA	unknown
Molecular Structure	unknown	Influences rejection by membranes (see Chapter 3) and possibly conformation in the boundary layer, which influences flux

Functional Groups	Aliphatic, carbohydrate, aromatic and carboxyl. Contents depends on origin. FA and NOM are more aliphatic, HA more aromatic	Functional groups determine the interactions between molecules, cations, and colloids, as well as their interactions with membranes
Charge and Acidity	Determined by dissociation of carboxylic and phenolic functional groups. Carboxylic content 3 to 6 meqg^{-1} and phenolic content 1.5 to 3 meqg^{-1}. HA has more phenolic groups, FA more carboxylic, but is very case dependant	Charge determines rejection in some membranes and the solubility of compounds. Charge also influences the interaction with other solutes and adsorption on colloids and membranes
Solubility and Aggregation	FA is, by definition, more soluble than FA. Low pH and high ionic strength decreases solubility. Multivalent ions are more effective in enhancing aggregation. A critical coagulation concentration of 2-3 mM $CaCl_2$ with natural organics was reported	The solubility determines whether compounds precipitate on the membrane surface when the boundary layer concentration increases or the pH is adjusted to avoid inorganic precipitation
Structure/ Fractal Dimension	Fractal dimensions which describe the structure of natural organicss were reported to be between 2 and 3. Results were on aggregates - no results for non-aggregated organics were reported	Structure and fractal dimension determine packing and water permeability of a deposit.
Effect of Solution Chemistry	Natural organics change their shape as a function of solution chemistry from coils to linear molecules as pH increases and ionic strength decreases	The shape of the molecules determines the conformation on the membrane as well as rejection by more porous membranes
Interaction with Cations and Trace Metals	Cations form complexes with natural organics and also bind weakly via a charge shielding effect. The more charged or dissociated the organics, the more interactions	Cation organic interactions influence the speciation and cations also enhance the adsorption of organics on membranes. The interaction with trace metals determines the transport of trace metals in natural systems
Interactions with other Compounds	Natural organics also interact with other compounds such as micropollutants or pesticides. Natural organics increase the solubility of such compounds	Natural organics influence the retention of micropollutants by membranes
Adsorption onto Colloids	Adsorption of natural organics on inorganic colloids decreases with pH. Natural organics adsorb to some extent under most conditions, resulting in a hydrodynamic layer thickness of 1 to 3 nm and very negatively charged colloids.	The adsorption of natural organics onto colloids may be used to enhance organics retention by membranes
Colloid Stabilisation and Mobilisation	The adsorption of natural organics often leads to colloid stabilisation due to the high charge of the adsorbed organics. Multivalent ions can destabilise these stable colloids	Stabilised colloids are not retained by MF if the primary colloids are smaller than the membrane pores

2.12 CONCLUSIONS

These studies verify a variation of HS composition and characteristics with many parameters, being different for every river or lake of interest. This makes it difficult to predict treatment efficiency. A detailed characterisation will always be required, but a seasonal variation also needs to be considered.

The choice of a representative source of NOM for research in water treatment represents an initial challenge, and finding the relevant characteristic that can be determined easily to predict treatability is the second.

The study of natural organics, their origin, and characteristics, lead to the selection of natural organic sources and an extraction method for this study. The selection of a water source relatively high in organics, low in alkalinity and with an unpolluted environment was determined as being essential. However, the source needs to represent realistic local conditions. The extraction method of choice was RO with a MF pretreatment. Method and results are shown in Appendix 1. Additionally, IHSS reference material was chosen for comparison as a range of fundamental research studies was planned.

A broad range of fractionation and characterisation methods was then selected (see Material and Methods, Chapter 4) in order to obtain a comprehensive picture of the natural organics characteristics and overcome drawbacks of the individual methods.

Chapter 3

MEMBRANE FILTRATION REVIEW

In this chapter, membrane filtration in water treatment is reviewed. The aim is to assess the current status and reveal gaps in knowledge from the wealth of literature. The background on models and principles is summarised for the relevant processes; microfiltration (MF), ultrafiltration (UF), and nanofiltration (NF). Reverse osmosis is briefly considered to put NF, which is often described as a process "in between" UF and RO, in perspective.

After a brief description of membrane materials, membrane rejection and fouling will be addressed. Both rejection of and fouling by natural organics and inorganic colloids, will be a major focus of this work. A further issue is the characterisation of clean and fouled membranes as well as fouling control.

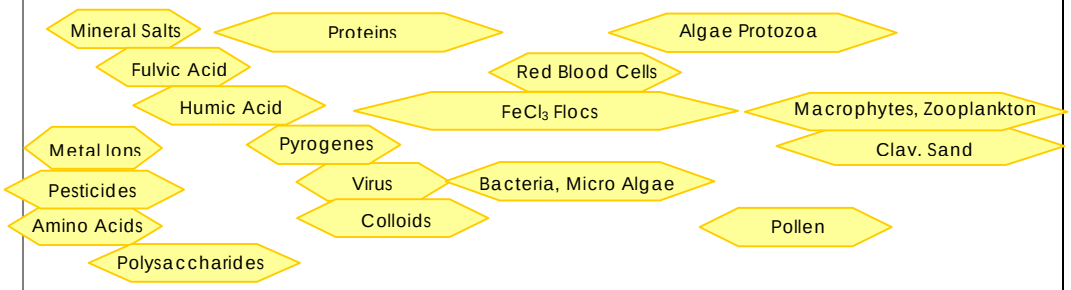
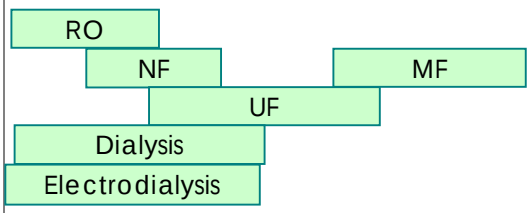
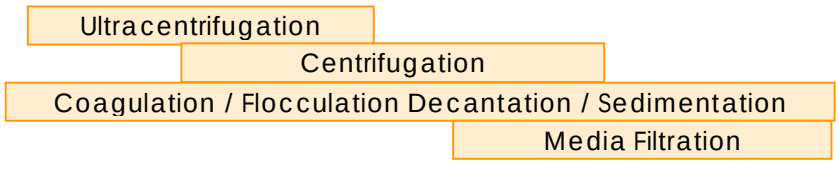
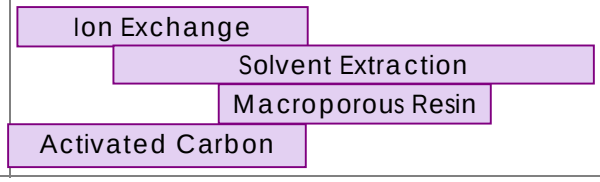
The last sections describe membrane application issues in water treatment. The processes have been compared in terms their volume of application and recent growth. This is obviously linked to treatment cost, an issue which will also be addressed briefly. Problems which have arisen in previous pilot plant or full scale studies will be part of the fouling studies in this thesis, where effects can be investigated on a smaller scale. Issues of concentrate disposal or treatment and membrane integrity are not discussed in this review. The concluding remarks address research needs and plans for this project.

3.1 INTRODUCTION AND OVERVIEW

There are many processes available for water treatment. Process selection depends on the required water quality, and therefore which solutes or particles are to be retained. Of course the treatment cost also plays a major role in process selection. Unfortunately, environmental criteria - such as reduction of chemical addition or alternative operation modes, which allow the use of alternative energies – are, at best, only indirectly considered in cost evaluations which precede process selection.

Conventional physico-chemical treatment involving addition of coagulants and sand filtration, competes with membrane separation processes, but often fails in the treatment of waters containing large amounts of natural organic matter. In Table 3.1, an overview of common processes as well as the sizes of solutes and particles of interest is presented.

Table 3.1 *Overview of treatment processes and solute/particle dimensions (Cheryan (1986), Agbekodo (1994)).*

	Atomic Force Microscopy	Electron Microscope	Optical Microscope	Visible			
	Dissolved Matter		Colloids		Suspended Matter		
	Ions	Molecules	Macromolecules		Microparticles		Macroparticles
Molecular Weight [Da]	100	1000	10000	100000			
Size [µm]	0.001	0.01	0.1	1	10	100	1000
Solute/Particle Dimension							
Membrane Separation Process							
Physico-Chemical Separation Process							
Separation Process with Change of Phase							
Chemical Separation Process							

As can be seen, membrane separation processes cover the entire size range, from suspended solids to mineral salts and small organics. Membrane processes also compete with some other processes such as activated carbon, ion exchange and to some extent coagulation and filtration.

Of the process options considered, microfiltration (MF) is the membrane process with the largest pores. It is generally used for waters of high turbidity, and low colour or organics content. MF can remove bacteria and "turbidity". MF is also a common pretreatment process for NF and RO. The fact that MF pores are relatively large allows cleaning methods, such as air backflush or permeate backwash, which remove deposits from pores and surface.

Ultrafiltration (UF) has only recently been recognised in water treatment and is becoming increasingly popular due to its ability to remove turbidity, microorganisms, and viruses, especially when issues such as *Giardia* and *Cryptosporidium* are of concern (Jacangelo *et al.* (1995a)). The removal of dissolved organics is limited with UF.

Nanofiltration (NF) is a relatively new process, though while the number of applications is growing rapidly, the transport mechanisms are still poorly understood (Raman *et al.* (1994)). NF shows a high selectivity between mono- and multivalent ions. Its popularity in water treatment stems from its softening abilities and high organics (and micropollutant) rejection.

Reverse Osmosis (RO) is used primarily in desalination, or for waters where micropollutants are difficult to remove with other processes. RO removes both mono- and multivalent ions. However, for surface waters no full demineralisation is usually required and NF is more economic at a similar organics removal.

Pressure driven membrane processes do not retain dissolved gases such as CO_2 (Rohe *et al.* (1990)) and some taste and odour compounds.

3.2 FUNDAMENTAL PRINCIPLES AND MECHANISMS

In this section, the main models for membrane processes are summarised. This allows a basic understanding of rejection and deposition principles and underlines the importance of certain parameters in the different processes. The four membrane types, MF, UF, NF, and RO, are considered in separate sections.

Table 3.1 illustrates that the separation between the different processes is not precise, as the processes overlap. Therefore, filtration and separation models are generally applicable to more than one process. Often several phenomena are operative simultaneously and which one dominates depends on the membrane and the solute or particle in question. Concepts such as the resistance-in-series model, the osmotic pressure model or concentration polarisation are principles which are applicable to any membrane operation. These will be described in the MF section.

Rejection (R_i) is defined by equation (3.1). This definition is the apparent rejection calculated from the bulk concentration c_B and the permeate concentration c_P, for sample i. The true membrane rejection is higher due to concentration changes in the boundary layer. However, the values of concentration in the boundary layer are not accessible.

$$R_i = 100 \cdot \left(1 - \frac{c_{Pi}}{c_{Bi}} \right) \tag{3.1}$$

The most critical parameter in the characterisation of membranes is their flux. For the characterisation of clean membranes flux is measured with MilliQ water as 'pure water flux'. The definition of the instantaneous flux is given in equation (3.2), where V is the filtrate volume, t the filtration time, and A the membrane surface area.

$$J \equiv \frac{1}{A} \frac{dV}{dt} \tag{3.2}$$

Alternatively the hydrodynamic permeability (L_V) can be used to describe water throughput. This parameter is very useful when different processes or transmembrane pressures are to be compared, as it is normalised by the transmembrane pressure ΔP.

$$L_V = \frac{J}{\Delta P} \tag{3.3}$$

Both, flux and rejection tend to vary with time. The underlying mechanisms are described below by a summary of models for each process. Some models apply to several processes and others only to a particular process under certain conditions. The application of models requires caution as membrane-solute interactions will depend on many factors. These include solute size, charge and morphology; membrane pore size, charge, surface roughness and chemical characteristics; solution chemistry; and, hydrodynamics, which influence permeation drag, shear forces, and cake compaction.

A surface water system is complex and cannot easily be explained by simplified models, especially when solute-solute interactions are poorly understood. Nevertheless, the awareness of existing models is essential to recognising trends and to develop model extensions and improvements.

3.2.1 Microfiltration (MF)

Rejection Mechanisms

Physical sieving is believed to be the major rejection mechanism for MF with water convecting through the membrane due to an applied transmembrane pressure. The deposit or cake on the membrane can act as a self-rejecting layer, and retain even smaller particles or solutes than would be expected to be removed given the pore size of the membrane ("dynamic membrane"). Thus a fouled MF membrane may have UF rejection characteristics and flux may decline significantly due to the build-up of this deposit.

Electrostatic interactions, dispersion forces, and hydrophobic bonding may play some role in rejection. Little is known about effects such as particle adhesion, deposit compressibility, particle shape, and particle mixtures.

Filtration Models

Pure water flux under laminar conditions through a tortuous porous barrier may be described, according to Carman (1938) and Bowen and Jenner (1995), by equation (3.4).

$$J = \frac{\Delta P}{\eta R_M} \tag{3.4}$$

ΔP is the transmembrane pressure difference, η the dynamic solvent viscosity, and R_M the clean membrane resistance (i.e. the porous barrier). Units of the symbols are explained in the symbols section at the end of this thesis.

The **Resistance in Series Model** describes the flux of a fouled membrane. This is given in equation (3.4). The resistances R_{CP}, R_P and R_C denote the additional resistances which result from the exposure of the membrane to a solution containing particles or solute. R_{CP} is the resistance due to concentration polarisation, R_P the internal pore fouling resistance, and R_C the resistance due to external deposition or cake formation. These resistances are usually negligible in RO, where the osmotic pressure effects become more important (Fane (1997)). However, the osmotic pressure can also be incorporated into R_{CP}.

$$J = \frac{\Delta P}{\eta (R_M + R_{CP} + R_P + R_C)} \tag{3.5}$$

The **Osmotic Pressure Model,** as shown in (3.6), is an equivalent description for macromolecules according to Wijmans *et al.* (1985). $\Delta\Pi$ is the osmotic pressure difference across the membrane.

The osmotic pressure difference can usually be neglected in MF and UF, since the rejected solutes are large and their osmotic pressure small. However, even polymeric solutes can develop a significant osmotic pressure at boundary layer concentrations (Ho and Sirkar (1992)). This naturally implies that the resistance in series model (equation (3.4)) would be more appropriate in MF, while the osmotic pressure model (equation (3.6)) may be more useful in NF and RO. Both models have been applied to UF.

$$J = \frac{\Delta P - \Delta\Pi}{\eta R_M} \tag{3.6}$$

Reversible flux decline can be reversed by a change in operation conditions, and is referred to as concentration polarisation. Irreversible fouling can only be removed by cleaning, or not at all. Irreversible fouling is caused by chemical or physical adsorption, pore plugging, or solute gelation on the membrane.

Concentration Polarisation is the accumulation of solute due to solvent convection through the membrane and was first documented by Sherwood (1965). It appears in every pressure driven membrane process, but depending on the rejected species, to a very different extent. It reduces permeate flux, either via an increased osmotic pressure on the feed side, or the formation of a cake or gel layer on the membrane surface. Concentration polarisation creates a high solute concentration at the membrane surface compared to the bulk solution. This creates a back diffusion of solute from the membrane which is assumed to be in equilibrium with the convective transport. At the membrane, a laminar boundary layer exists (Nernst type layer), with mass conservation through this layer described by the **Film Theory Model** in equation (3.7) (Staude (1992)). c_F is the feed concentration, D_S the solute diffusivity, c_{BL} the solute concentration in the boundary layer and x the distance from the membrane.

$$-Jc_P + Jc_F + D_S \frac{dc_{BL}}{dx} = 0 \qquad (3.7)$$

A schematic of the concentration profiles and the mass balance leading to equation (3.7) is shown in Figure 3.1, where δ is the boundary layer thickness.

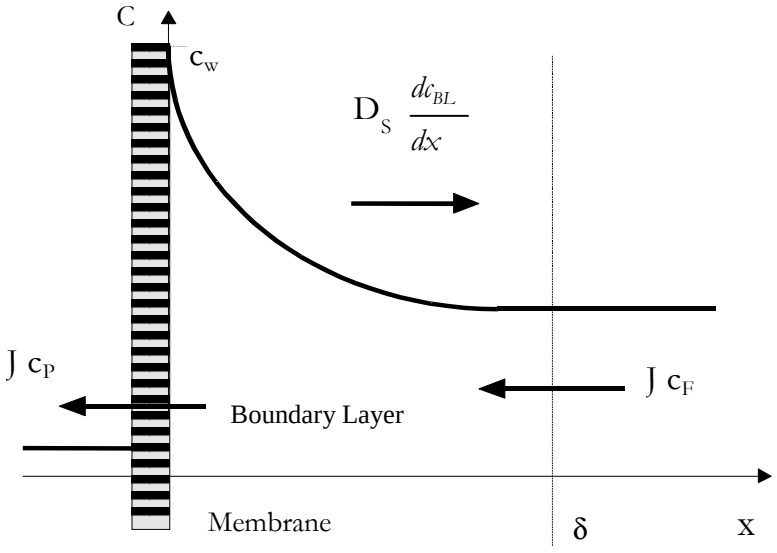


Figure 3.1 *Concentration Polarisation.*

After integrating with the boundary conditions $c = c_W$ for $x = 0$ and $c = c_b$ for $x = \delta$ for similar solute and solvent densities, constant diffusion coefficient, and constant concentration along the membrane, equation (3.7) can be derived. The wall concentration which determines adsorption is c_W, gel formation or precipitation, and k_S the solute mass transfer coefficient as defined in equation (3.9),

$$J = k_S \ln \frac{(c_W - c_P)}{(c_B - c_P)} \qquad (3.8)$$

$$\text{where} \quad k_S = \frac{D_S}{\delta}. \tag{3.9}$$

Concentration polarisation can be minimised with turbulence promoters on the feed side of the membrane, such as spacers or introduction of crossflow.

The **Gel Polarisation Model** is based on the fact that at steady state flux reaches a limiting value, where increases in pressure no longer increase the flux. According to the Gel Polarisation model, at this limiting value, the solubility limit of the solute in the boundary layer is reached and a gel formed. For 100% rejection, the expression for this limiting flux (J_{lim}) is described by equation (3.10). c_G is the gel concentration, beyond which the concentration in the boundary layer cannot increase.

$$J_{\text{lim}} = k_S \ln \frac{c_G}{c_B} \tag{3.10}$$

The model does not include membrane characteristics, and tends to predict a lower flux than observed. An improvement can be achieved in using D_S for the gel layer rather the bulk solution (Bowen and Jenner (1995)). McDonogh *et al.* (1984, 1989) modified this model and included charge effects. Bacchin *et al.* (1995) included effects of pH and ionic strength on surface interactions.

Belfort *et al.* (1994) proposed five stages of fouling. These are, (1) fast internal sorption of macromolecules, (2) build-up of a first sublayer, (3) build-up of multisublayers, (4) densification of sublayers, and (5) increase in bulk viscosity. The fifth stage can be neglected for dilute suspensions like surface water. The dependence on particle size can be described as

$d_{particle} \ll d_{pore}$: deposit on pore walls, restricting pore size

$d_{particle} \simeq d_{pore}$: pore plugging or blockage

$d_{particle} > d_{pore}$: cake deposition, compaction over time.

For particles much smaller than the membrane pores, internal deposition eventually leads to the loss of pores. Particles of a similar size to the membrane pore will cause pore blockage. Particles larger than the pores will deposit as a cake, with the porosity depending on a variety of factors including particle size distribution, aggregate structure and compaction effects. The process of small particles adsorbing in the pores may be a slow process compared to pore plugging, where a single particle can completely block a pore and therefore flux decline should be more severe for the latter case.

Hermia (1982) introduced the **Filtration Laws,** which aim to describe fouling mechanisms. The models are valid for unstirred, dead-end filtration (deposition without cake disturbance due to shear and no gravity settling) and complete rejection of solute by the membrane (but obviously allowing pore penetration). Under conditions where permeate drag dominates, the effect of stirring may be negligible. The constant pressure filtration law is shown in equation (3.11).

$$\frac{d^2t}{dV^2} = k\left(\frac{dt}{dV}\right)^n \tag{3.11}$$

The basic equation leads to four filtration models have been derived by Hermia (1982). By plotting t/V and Exp(t) over filtration time t and volume V, it is possible to determine which filtration mechanism is

dominant. According to Bowen *et al.* (1995), all mechanisms occur in a complete filtration experiment either successively or superimposed due to pore and particle size size distributions.

The **Complete Blocking Model** (pore blocking) is valid for particles which have a very similar size to the pores. The particles seal the pores and do not accumulate on each other. The constant pressure filtration law can be written as

$$\frac{d^2t}{dV^2} = k\left(\frac{dt}{dV}\right)^2 \tag{3.12}$$

which, on integration, gives $V = J_0\left(1-e^{-kt}\right)$ (3.13)

where J_0 is the initial flux. The **Standard Blocking Model** (Pore Constriction Model) describes pore blocking for particles that are much smaller than the pores. Particles pass through the pores and deposit on the surface of the pores. The pore volume will decrease proportionally with the filtrate volume.

$$\frac{d^2t}{dV^2} = k\left(\frac{dt}{dV}\right)^{3/2} \tag{3.14}$$

$$\frac{t}{V} = \frac{k}{2}t + \frac{1}{J_0} \tag{3.15}$$

The **Intermediate Blocking Model** describes long term adsorption. Every particle reaching a pore will contribute to blockage and particles accumulate on each other. Again, the modified constant pressure filtration law is

$$\frac{d^2t}{dV^2} = k\left(\frac{dt}{dV}\right) \tag{3.16}$$

and the integration $kV = \ln(1+kt\,J_0)$ (3.17)

The **Cake Filtration Model** describes the filtration of particles which are much larger than the pores and will be retained, without entering the pores. The particles deposit on the membrane surface contributing to the boundary layer resistance. Included in this model is deposition due to concentration polarisation.

$$\frac{d^2t}{dV^2} = k \tag{3.18}$$

$$\frac{t}{V} = \frac{k}{2}V + \frac{1}{J_0} \tag{3.19}$$

Another model, known as the **Solids Flux Model,** was developed by Belfort *et al.* (1994)**.** This was proposed for sticky particles, which do not backmigrate from the membrane to the bulk solution and cause irreversible fouling. The constant b describes the characteristics of the sublayer and Φ_S the solids volume fraction in the feed.

$$J = J_0\, e^{-b\Phi_S} \tag{3.20}$$

In the filtration of aqueous solutions, all of these models may be combined and their importance in the overall filtration behaviour may change over time. The particle size has a strong influence and only very little is known about the filtration of mixtures where a variety of particle sizes and shapes are present in solution. In most publications, single filtration laws are considered, while very little work has been done on the coupling of different processes.

3.2.2 Ultrafiltration (UF)

UF can be used to remove colloids and macromolecules. UF can be used as a pretreatment to NF or RO, which may lengthen the filtration cycle of these processes compared to a MF pretreatment.

Rejection Mechanisms

As in MF, physical sieving is an important rejection mechanism in UF and convection dictates solvent passage. The deposit can also act as a self-rejecting layer and charge interactions, as well as adsorption, may play an important role.

Rejection is usually evaluated with macromolecules of different molecular weights, such as dextrans or proteins, which leads to the determination of a molecular weight cut-off (MWCO).

Filtration Models

The **Mechanical Sieving Model (Ferry)** suggests hindered transport of solute due to convection, limited by steric effects (Braghetta (1995)). Rejection is determined by the ratio of solute macromolecular diameter to pore diameter, λ.

$$R=[\lambda(2-\lambda)]^2 \quad \text{for} \quad \lambda<1 \tag{3.21}$$

$$R=1 \quad \text{for} \quad \lambda\geq 1 \tag{3.22}$$

$$\text{with} \qquad \lambda=\frac{d_{solute}}{d_{pore}} \tag{3.23}$$

The model does not account for solute velocity drag, diffusional limitations, or concentration effects at the membrane surface.

The **Modified Sieving Rejection Model** (Munch *et al.* (1979)), accounts for the double layer thickness surrounding a charged solute which leads to a modified λ.

$$\lambda=\frac{d_{solute}+2\kappa^{-1}}{d_{pore}-2\kappa^{-1}} \tag{3.24}$$

$$\text{with} \qquad \kappa^{-1}=\left[\frac{\varepsilon k_B T}{8\pi z^2 e^2 N_A c_S}\right]^{\frac{1}{2}} \tag{3.25}$$

This double layer thickness, or Debye length, κ^{-1} will affect the packing of colloids on a membrane (McDonogh (1984)). ε is the dielectric constant, k_B the Boltzmann constant, T the absolute temperature, z the ion valence, e the fundamental electron charge, N_A the Avogadro constant and c_S

the electrolyte concentration. The double layer thickness is strongly influenced by the solution ionic strength.

The **Pore Flow Model** uses the **Hagen-Poiseuille Equation** to describe solvent flow through cylindrical pores of the membrane. No membrane characteristics other than pore size or pore density are accounted for, and neither limitation of flux due to friction nor diffusion is considered. Flux occurs due to convection under an applied pressure. The equation is derived from the balance between the driving force pressure and the fluid viscosity, which resists flow (Braghetta (1995), Staude (1992)). Solvent flux (J) is described by equation (3.26) and solute flux (J_S) by equation (3.27), where r_p is the pore radius, n_p the number of pores, τ the tortuosity factor, Δx the membrane thickness and σ the reflection coefficient.

$$J = \frac{\pi \, \Delta P \, r_P^{\,4} \, \tau \, n_P}{8 \, \eta \, \Delta x} \tag{3.26}$$

$$J_S = (1-\sigma) \, J \, c_F \tag{3.27}$$

The flow rate is predicted to be proportional to pressure and proportional to the fourth power of pore radius. Two mechanisms were proposed for solute transport, physical sieving and equilibrium partitioning between solute in pores and outside pores.

Bhattacharjee and Datta (1996) predicted mathematically that the resistance due to solute backtransport was responsible for flux decline, whereas osmotic pressure, as well as cake and gel formation were negligible. Rosa and dePinho (1994) used different sized organics to model mass transfer resistance as a function of pore size distribution. Transport for the relatively high concentrations was typical for pore flow (steric and hydrodynamic forces) and good agreement between model and experimental data was achieved. Huisman *et al.* (1997) studied the effect of temperature and ionic strength on UF membrane resistance. Temperature showed no effect, although the permeability increased with ionic strength. This was attributed to lower zeta potentials and thinner double layers – thus electroviscous effects.

In Chapter 6, additional models covering filtration through cakes will be described.

3.2.3 Nanofiltration (NF)

NF is a process located between UF and RO. Some authors refer to NF as charged UF (Simpson *et al.* (1987)), softening, low pressure RO (Rohe *et al.* (1990)), or do not distinguish at all between NF and RO. NF is generally expected to remove 60 to 80% of hardness, >90% of colour, and all turbidity. The process has the advantage of low operating pressures compared to RO, and a high rejection of organics compared to UF. Monovalent salt is not retained to a significant extent, however this is not normally required in water treatment of surface water. Rejection of membranes is usually evaluated by the manufacturer with NaCl or $MgSO_4$ solutions, as opposed to a MWCO specification as in UF.

Rejection Mechanisms

Both, charge and size are important in NF rejection. At a neutral pH most NF membranes are negatively charged, while they might be positively charged at low pH (Zhu *et al.* (1995), Peeters (1997)). The principal transport mechanisms of NF are depicted in Figure 3.2.

Physical sieving (steric hindrance) is the dominant rejection mechanism in NF for colloids and large molecules, whereas the chemistries of solute and membrane become increasingly important for ions and lower molecular weight organics. The mechanisms, however, are still poorly understood. Macoun (1998) summarised NF rejection mechanisms as follows

- **Wetted Surface** – water associates with the membrane through hydrogen bonding and molecules which form hydrogen bonds with the membrane can be transported,
- **Preferential Sorption/Capillary Rejection** – the membrane is heterogeneous and microporous, electrostatic repulsion is based on different electrostatic constants in solution and membrane,
- **Solution Diffusion** – membrane is homogeneous and non-porous, solute and solvent dissolve in the active layer and diffusion determines transport,
- **Charged Capillary** – the electric double layer in pores determines rejection, ions of same charge as membrane are attracted and counter-ions are rejected due to the streaming potential,
- **Finely Porous** – membrane is a dense material punctured by pores, transport is determined by partitioning between bulk and pore fluid.

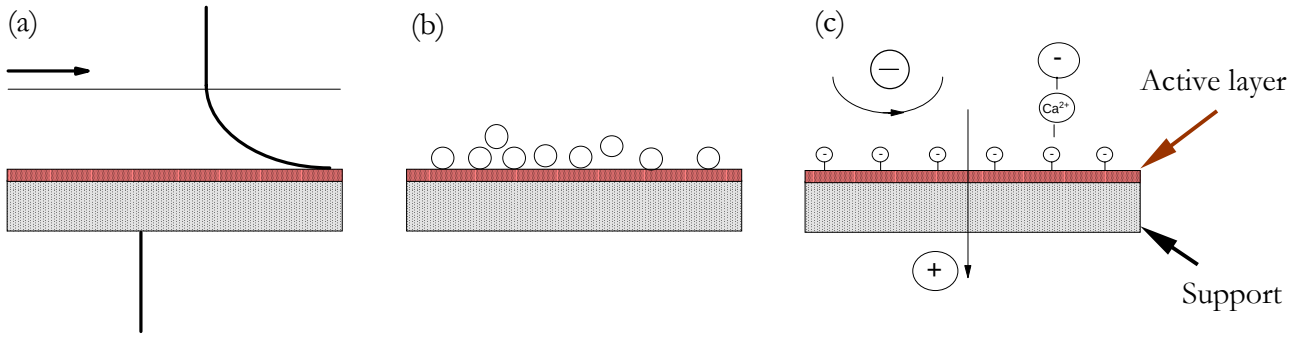


Figure 3.2 *Transport phenomena in NF, (a) concentration polarisation (b) sieving (c) charge effects (e.g. charge repulsion or electric double layer formation).*

The normally negatively charged membranes may also function to a limited extent as a cation-exchange membrane (Mallevialle *et al.* (1996)).

Filtration Models

UF and RO models may all apply to some extent to NF. Charge, however, appears to play a more important role than for other pressure driven membrane processes. The **Extended-Nernst Planck Equation** (equation (3.28)) is a means of describing NF behaviour. The extended Nernst Planck equation, proposed by Deen *et al.* (1980), includes the Donnan expression, which describes the partitioning of solutes between solution and membrane. The model can be used to calculate an effective pore size (which does not necessarily mean that pores exist), and to determine thickness and effective charge of the membrane. This information can then be used to predict the separation of mixtures (Bowen and Mukhtar (1996)). No assumptions regarding membrane morphology are required (Peeters (1997)). The terms represent transport due to diffusion, electric field gradient and convection respectively. J_{Si} is the flux of an ion i, $D_{I,P}$ is the ion diffusivity in the membane, R the gas constant, F the Faraday constant, ψ the electrical potential and $K_{I,c}$ the convective hindrance factor in the membrane.

$$J_{Si} = -D_{i,p}\frac{dc_i}{dx} - \frac{z_i c_i D_{i,p}}{R \cdot T} \cdot F \cdot \frac{d\Psi}{dx} + K_{i,c} c_i J \qquad (3.28)$$

The equation predicts solute rejection as a function of feed concentration, ion charge, convection across the membrane, and solute diffusion (Braghetta (1995)). The model has proven to be successful for modelling the solute transport in simple electrolyte solutions, although its applicability in the presence of organics is questionable.

Wang *et al.* (1995b) developed the model further to account for the transport phenomena of organic electrolytes, thus combining electrostatic and steric hindrance effects. The steric hindrance pore model suggested by Nakao *et al.* (1982) was incorporated into the modified Nernst Planck equation.

For mixed solutions, hindered diffusivity becomes more significant. The rejection depends on electrolyte concentration and the membrane charge increases with salt concentration. This indicates co-ion adsorption on the membrane, and, in fact the effective membrane charge was described as a Freundlich isotherm as a function of bulk concentration by Bowen and Mukhtar (1996).

The **Fine Porous Model** as presented by Xu and Spencer (1997), describes equilibrium and non-equilibrium factors of rejection. Only coupling between solvent and solute is taken into account, and no solute-solute coupling is permitted. Equilibrium parameters dominated separation, and these are described by the reflection coefficient σ in equation (3.28), where k_M is the solute mass transfer coefficient in the membrane.

$$R = 1 - \left[1 + \left(\frac{\sigma}{1-\sigma}\right) \cdot \left(1 - e^{-\frac{J}{k_M}}\right) \cdot e^{-\frac{J}{k_S}}\right]^{-1} \qquad (3.29)$$

The **Steric Hindrance Pore Model** was published by Wang *et al.* (1995a). This model also allows the calculation of an effective pore radius and the ratio of membrane porosity to membrane thickness.

As can be seen with the various models, the determination of an effective pore size has become an issue. This is due to the fact that NF pores are too small to be measured directly by various methods as in MF or UF.

3.2.4 Reverse Osmosis (RO)

In RO, the osmotic pressure of a solution has to be overcome by an applied transmembrane pressure to achieve solvent flux and separation. Recovery (ratio of product/feed) has a high impact on flux and rejection, and both decrease with increasing recovery.

Rejection Mechanisms

Physical sieving applies to colloids and large molecules. Apart from that, rejection is a function of the relative chemical affinity of the solute to the membrane material. Ion rejection follows the lyotropic series, which means that rejection is increased with the increased hydrated radius of the ion. The order of the ions, however, may change due to ion pairing, complexation, or other solute-solute interactions, and it is, therefore, difficult to predict rejection for mixtures of ions. The rejection behaviour in the presence of organics, or even of organics themselves is poorly understood and only trends can so far be noted. Rejection is usually evaluated with NaCl or $MgSO_4$ solutions.

Filtration Models

At this stage three models have been used to describe RO. They are all valid for ideal membranes only, but were shown to be valid in practice under certain conditions.

The **Preferential Sorption/Capillary Flow Model** (Sourirajan and Matsuura (1985)) is based on the assumption that a layer of water sorbs at the membrane surface, creating a deficit of solute at the surface. The membrane is viewed as a microporous medium, and transport is controlled by the surface chemistry of the membrane and water transport through the membrane. Ions with large hydrated radii are retained better, since they also have to overcome more energy to strip off the water. Ions diffuse through the layer of structured water at the membrane surface and through water cluster channels in the membrane (Staude (1992)), where B is the pure water permeability of the membrane.

$$J = B(\Delta P - \Delta\Pi) \tag{3.30}$$

The model predicts an increase of solute flux with increasing feed concentration, whereas solute flux appears to be independent of pressure. Higher operating pressure increases the total rejection, however, due to increased solvent flux.

The **Irreversible Thermodynamics Model** (Kedem and Katchalsky (1958)) is founded on coupled transport between solute and solvent and between the different driving forces. The entropy of the system increases and free energy is dissipated, where the free energy dissipation function may be written as a sum of solute and solvent fluxes multiplied by driving forces. L_V is the hydrodynamic permeability of the membrane, $\Delta\Pi_W$ the osmotic pressure difference between membrane wall and permeate, L_S the solute permeability and c_{MS} the average solute concentration across the membrane.

Solvent flux $$J = L_V(\Delta P - \sigma\Delta\Pi_W) \tag{3.31}$$

Solute flux $$J_S = L_S\Delta\Pi + (1-\sigma)Jc_{mS} \tag{3.32}$$

with $$\sigma \equiv \left(\frac{\Delta P}{\Delta\Pi}\right)_{J=0} \tag{3.33}$$

Solute flux increases with solvent flux (and pressure) and with increasing osmotic pressure.

The **Solution Diffusion Model** assumes that solute and solvent dissolve in the membrane, which is imagined as a dense, non-porous layer. The membrane also has a layer of bound water at the surface, due to its low dielectric constant. The solute and solvent have different solubility and diffusion coefficients in the membrane, and rejection of solute depends on its ability to diffuse through structured water inside the membrane (Staude (1992)). All solutes diffuse independently, driven by their chemical potential across the membrane. It is the same as the irreversible thermodynamics model for the case where no coupling occurs. This model has lost credibility in the past due to neglected membrane imperfections, membrane-solute interactions, and solute-molecule interactions (no convection, no external forces, no coupling of flow) (Braghetta (1995)).

Solute flux is pressure independent and selectivity increases with pressure. A modified version of the model includes advective transport through pores and diffusion.

The equation for solvent flux is derived from Fick's law of diffusion, Henry's law of chemical potential, and Van't Hoff's equation for osmotic pressure. In equations (3.34) and (3.35) $c_{m,W}$ is the concentration

of water in the membrane, $V_{m,W}$ the partial molar volume of water, Δx the membrane thickness, k the distribution coefficient and D_M the solute diffusivity in the membrane.

Solvent flux
$$J = \frac{Dc_{m,W}V_{m,W}}{RT\Delta x}(\Delta P - \Delta\Pi) \tag{3.34}$$

Solute flux
$$J_S = \frac{k D_M}{\Delta x}\Delta c_S \tag{3.35}$$

Donnan Equilibrium and Electroneutrality Effects for charged membranes are based on the fact that charged functional groups attract counter-ions. This leads to a deficit of co-ions in the membrane and the development of Donnan potential. The membrane rejection increases with increased membrane charge and ion valence. This principle has been incorporated into the extended Nernst-Planck equation, as described in the NF section. This effect is responsible for the shift in pH, which is often observed in RO. Chloride passes through the membrane, while calcium is retained, which means that water has to shift its dissociation equilibrium to provide protons to balance the permeating anions (Mallevialle *et al.* (1996)).

3.3 MEMBRANES

The choice of membrane for fouling and rejection studies is crucial. Ko and Pellegrino (1992) pointed out that some membranes exhibit low fouling regardless of their rejection. For other membranes, their flux is controlled by osmotic pressure effects, which is indicative of rejection. Lainé *et al.* (1989) pointed out that the most important membrane characteristic is probably hydrophilicity.

3.3.1 Membrane Materials for MF and UF

Common membrane materials for MF were summarised by Belfort *et al.* (1994) and by Ho and Sirkar (1992). The surface morphologies and porosities vary greatly. Most membranes carry a negative charge to repel the colloids, which are usually negatively charged in natural systems. As the membrane pore size decreases the membrane resistance increases and a reduction in thickness of the active layer is required. This is achieved by producing asymmetric membranes or by mounting a thin layer on a more porous support (Noble and Stern (1995)). While MF membranes are symmetric, UF membranes are mostly asymmetric due to the smaller pore size.

3.3.2 Membrane Materials for NF and RO

A comprehensive RO and NF membrane materials overview was published by Petersen (1993). NF membranes may be porous or non-porous depending on the material (Peeters (1997)). Polymeric membranes are also amphoteric, which means they have basic and acidic functional groups. RO membranes, able to produce high flux and rejection, contain two features: ring structures to supply hydrophilic voids, and functional groups with unshared electron pairs to enhance water transport. Resistance to chlorine can be a problem (Glater *et al.* (1994)). The importance of chlorine resistance was confirmed by Yaroshchuk and Staude (1992) who reviewed the properties and applications of charged RO (also named NF) membranes. Applications ranged from water softening at low pressure to separation of organics as a function of their pK_a value.

Thin film composite (TFC) membranes possess a polyamide (PA) layer on an asymmetric polysulphone (PS) support. Many TFC membranes now demonstrate chlorine resistance (Kawada *et al.* (1987), Tran *et al.* (1989)), although polyamide generally has a very low chlorine resistance (Glater *et al.* (1994)). While PS membranes are generally more chlorine resistant (Allegrezza *et al.* (1987)), PS is hydrophobic and more prone to fouling. Cellulose acetate (CA) membranes are another large group of NF and RO membranes. While CA membranes often exhibit low fouling and reasonable chlorine tolerance, their biodegradability is high.

The TFC membranes used in this study were developed by Takigawa *et al.* (1995) for organic rejection at ultra-low pressures. Further characteristics are provided in Chapter 4.

3.3.3 TFC Membrane Modification in NF

Organic acids with carboxylic functional groups are often added to the membrane solutions to adjust pH. Other impurities on the membrane surface can also influence membrane charge. At low pH, amine salts and monomeric polyamides are positively charged. Anionic surfactants are negatively charged at low pH. At higher pH, carboxylic functional groups and surfactants deprotonate and carry a negative charge (Elimelech *et al.* (1994)). Kulkarni *et al.* (1996) modified TFC membranes with acids and alcohol

to increase flux while maintaining high rejection. This was attributed to a greater membrane hydrophilicity.

3.3.4 Membrane Selection, Testing and Evaluation

The choice of membranes is critical and this requires careful evaluation. To save costs of testing, many operators try to perform bench-scale rather than pilot-scale experiments for an initial process evaluation. Stirred cell systems are commonly used for research purposes.

Allgeier and Summers (1995a) developed a rapid bench-scale membrane test (RBSMT) for NF membranes (NF70) to simulate high water recoveries on a small scale with minimal test solution. High recoveries were achieved with a recycling pump, and full-scale flow was simulated with feed spacers and permeate carriers, identical to spiral wound modules commonly used in large scale plants. Membrane compaction with pure water was carried out for several days to obtain steady state. Three different river waters were processed, and fouling occurred quickly, with irreversible fouling occurring in the first few cycles. Flux increased after chemical cleaning, whereas rejection was optimal just before cleaning. The test took four days per membrane and required 60 L of test water. This test was applied to evaluate flux and rejection under conditions close to full-scale systems. NF met the requirements for disinfection by-product (DBP) control (Allgeier and Summers (1995c)). The RBSMT was not able to test long term membrane fouling or biofouling (Allgeier (1996)). Gusses *et al.* (1996) compared the RBSMT with pilot tests and a good agreement in rejection and fouling was found.

DiGiano (1996) suggested a batch-recycle membrane test as an alternative. The test operates in batch mode by recirculating both feed and permeate. The advantage of this test is the lower feed volume required (3 L versus 60 to 200 L for the RBSMT). Moulin (1993) described a dynamic membrane test, that allows determination of the suitability of a membrane to obtain the required health standards (cytotoxicity).

The characteristics of eleven different NF membranes were summarised by Rautenbach and Gröschl (1990). Traditional softening membranes were compared to high flux type membranes. Fu *et al.* (1995) characterised eight membranes from different manufacturers and of various materials. Trisep TS80 and Nitto Denko NTR7450 were chosen for pilot studies. Performances were comparable, but the latter membrane was better for removal of trihalomethane precursors (THMPs).

3.4 REJECTION OF NATURAL ORGANICS AND COLLOIDS

3.4.1 Microfiltration (MF)

Unfouled MF does not retain natural organics unless they are associated with particulates and measured as turbidity. This means that a pretreatment step, such as coagulation, is required. MF can remove *Giardia* and *Cryptosporidium* but the extent of removal of *Cryptosporidium* depends on size, adsorption and cake layer built-up. Jacangelo *et al.* (1995a) observed that fouling of MF membranes increased rejection of various species. Consequently, Kumar *et al.* (1998) found a significant removal of trihalomethanes (THMs) by MF in an extended pilot study.

The retention of natural organics has to date not been studied on a small scale, although fouling of natural organics has been investigated (Yuan and Zydney (1999)). The high degree of fouling observed may well indicate that some organics are retained, especially since fouling was attributed to organics aggregation and surface deposition.

The magnitude of rejection of colloids smaller than the MF pore size is also unclear, as is the retention of possibly fragile colloid-organic matrices, as described in Chapter 2.

3.4.2 Ultrafiltration (UF)

Rejection of natural organics by UF membranes has been discussed briefly in the natural organics characterisation and size fractionation by UF section of Chapter 2. The MWCO ranges from 0.5 to 300 kDa in UF and this governs retention of natural organics.

Hagmeyer *et al.* (1996) reported that DOC removal varied between 26 and 37% for UF in long term operation. Jacangelo *et al.* (1993) found UF with a MWCO of 100 kDa ineffective for substantial by-product precursor removal. Ødegaard and Thorsen (1989) used MWCO 3 kDa cellulose acetate membranes to remove colour in water treatment. Faivre *et al.* (1992) found that UF could not remove sufficient organic matter, even at a MWCO of 1 kDa, and concluded that NF was required. For significant organics rejection, a MWCO below 20 kDa was required (Thorsen *et al.* (1997)). Lainé *et al.* (1990) showed that no THMPs were removed by UF, and this was confirmed by Clark and Heneghan (1991). All of these works are somewhat contradictory. One reason for this could be the variation of organic size and the different MWCOs used.

Lainé *et al.* (1989) pointed out that for UF to be economic, MWCOs of no less than 10 to 50 kDa should be applied. This contradicts the MWCO required for significant natural organics rejection. Wiesner *et al.* (1992) and Côté (1995) published DOC removal as a function of MWCO. Wiesner *et al.* found a near linear decline, while Côté showed a steep decline in rejection between 1 and 10 kDa. The graphs were based on a review of publications and represent the MWCO dependence well.

Rejection also depends on the solution chemistry and characteristics of the organics. For low concentration filtration, as found in surface waters, rejection generally decreases with pressure (Goldsmith (1971)). For higher concentrations, rejection may increase due to a number of reasons-pore closure by the solute, or the concentrated solution in the boundary layer may act as a 'dynamic membrane'. UF is believed not to retain ions, unless associated with organics, and charge effects are not incorportated into any UF model, although some authors do report charge effects. For example, Staub *et al.* (1984) examined UF for organics complexation measurements. Negative molecules were best retained by the negatively charged membranes, and linear, flexible molecules were less retained

than rigid molecules. Some positively charged ions were adsorbed by the membranes. Stirring increased the rejection of organics similar in size to the membrane pores. Overall, steric, charge, and hydration energy factors were involved in separation. Hydration energy was only important if the size of the molecule was similar to the pore size. Complexes pass the membranes more easily, as their charge is more neutral.

Küchler and Miekeley (1994) measured retentions of purified Aldrich HA and a soil FA for a 1 kDa membrane, and rejection was 80-90% for HA and 60-70% for FA. Identical results were found for a 10 kDa membrane, showing a size exclusion effect. The retention increased with pH and decreased with ionic strength for FA (1 kDa). For HA, these effects were less significant. Ion rejection by the 1 kDa membranes was observed and depended on the ion characteristics. Values of 8% were reported for sodium chloride and 32% for sodium carbonate. Calcium chloride was not investigated. This study also indicated the presence of charge effects. Kabsch-Korbutowicz and Winnicki (1996) studied HA and iron rejection using porous ion exchange membranes (UF). Up to 98% of HA, 95% of Fe and 45% of Mn was removed. Ions were removed when complexed with the organics. Bacchin *et al.* (1996) reported salt rejection of a 300 kDa UF membrane due to a deposit of 0.7 μm bentonite platelets. This was attributed to cake geometry and charge repulsion. Salt retention decreased with salt concentration. A high retention was obtained at neutral or high pH and low ionic strength in UF of weak electrolytes. This was due to charge repulsion or a required electroneutrality in retentate and permeate (Bailey *et al.* (1995)).

Kilduff and Weber (1992) determined a dependence on ionic strength for the rejection of random-coil polymers or natural humic molecules. Concentration polarisation also changed rejection. This influences the results obtained in rejection experiments and size determination methods such as fractionation.

Jacangelo *et al.* (1992) investigated UF for HS removal and two membranes (50 and 100 kDa) showed no significant difference in TOC and UV removal. Removals of 20 to 25 % TOC was achieved. In long term tests, a linear relationship between raw water TOC and permeate TOC was obtained. The small difference for the two membranes and small removal indicate that a high proportion of the river HS has a MW of smaller than 50 kDa, as one would expect from other studies and the review in Chapter 2.

UF was tested for the filtration of FA, HA, and a Calcein model solution. FA and Calcein retention increased with pH and decreased with ionic strength, while HA rejection was constant. Anion retention was proportional to charge. A FA and HA retention of >70% was obtained (Küchler and Miekeley (1994)).

The above results show that charge, size, MWCO, and solution chemistry all play key roles in UF rejection of natural organics.

Colloids are retained effectively by UF due to the small pore sizes of the membranes, compared to MF. However, if colloids are very small, then pore penetration can occur. Kim *et al.* (1993) found a higher colloid rejection in stirred conditions using silver sol. Particle penetration into the membrane was highest at low salt concentrations. In the absence of salt, particle-membrane interactions dominated, whereas at high salt concentrations aggregation enhanced rejection.

The rejection of both MF and UF can be increased by an appropriate pretreatment (see pretreatment section). This raises the question of whether substantial organics removal using either MF/UF with pretreatment or NF is more economic.

3.4.3 Nanofiltration and Reverse Osmosis

The MWCO of NF and RO is in the 100 to 1000 Da range with "pores" < 1 nm in diameter. Organics rejection is therefore expected to be high. According to van der Bruggen *et al.* (1999), differences in rejection between membranes are clearly visible for compounds which exhibit about 50% rejection. Taylor and Mulford (1995) found TOC removal in NF to be sieving-controlled, and, thus independent of pressure and recovery. The rejection of inorganic solutes was diffusion limited.

Bowen *et al.* (1997) suggested different mechanisms for small ions and uncharged solutes. While Donnan partitioning described ion rejection well, steric effects were important for uncharged solutes such as organic molecules. It was found that the effective pore size determined with uncharged organic solutes was applicable for ions, but not vice versa. It appears worthwhile to address the rejection of different solutes in the following sections separately.

Ion rejection and streaming potential (see section 3.6.2) are characterisation methods for dense membranes (Peeters (1997)). Both charge and size are important. Peeters *et al.* (1995) studied NF rejection mechanisms using streaming potential measurements with salt solutions and organics. The effect of size exclusion and surface charge could be distinguished with this method. The use of different salts resulted in distinct differences of streaming potential and zeta potential of NF membranes. This was found to be in accordance with salt retention: the higher the zeta potential, the higher the retention (Peeters *et al.* (1996)).

NF membranes tend to allow the passage of monovalent ions. This means that the osmotic pressure that has to be overcome is lower than in RO (Bourbigot and Bablon (1993)). The rejection mechanism of ions is now well understood and several models allow accurate predictions, with the extended Nernst-Planck equation being the most popular (Tsuru *et al.* (1991a, 1991b), Hall *et al.* (1997), Pontalier *et al.* (1997)). In single solutions rejection follows the lyotropic series (Mallevialle *et al.* (1996)). The variation of membrane charge with pH and the transport of hydrogen and hydroxide ions also need to be considered, as these ions take part in the pH dependent transport mechanism observed by Hall *et al.* (1997b). At pH 2, the rejection of chlorine is lower than at pH values of 4 and 6, while that of sodium and calcium is increased. This indicates the importance of the hydrogen ion in the transport process (Hall *et al.* (1997a)).

Hagmeyer and Gimbel (1993) observed the RO permeate had a lower pH than the feed for solutions of pH <7 and a higher permeate than feed pH at pH >7. The authors explained this by a lower CO_3^{2-} rejection at high pH, however this is unlikely due to membrane charge. Jeantet and Maubois (1995) explained that for negatively charged membranes anions govern rejection, whereas for neutral membranes steric effects dominate. At positive charge, the anions showed negative rejection and the multivalent cations governed rejection. Negative rejection gives rise to concentration of a solute in the permeate, or its permeation at a rate faster than that of water. This phenomenon has been reported by several authors (Tsuru (1991a, 1991b), Ratanatamskul (1996), Jeantet and Maubois (1995), Peeters (1997)), and could be explained for negative anion rejection using the extended Nernst-Planck equation. The model, however, failed to explain the negative cation rejections that were also observed by Peeters (1997). According to Tsuru *et al.* (1991a, 1991b), it is the monovalent co-ion that shows

negative rejection under certain conditions. For a negatively charged membrane this is mostly chloride. Ratanatamskul *et al.* (1996) reported negative rejection to occur for monovalent anions when multivalent anions are present, especially when membrane charge was low. High temperature could enhance this effect. Rejection mechanism studies for the Filmtec NF40 were carried out by Macoun *et al.* (1991) and the hydration forces dominated the rejection mechanism, besides coulombic and dielectric forces.

Kastelan-Kunst *et al.* (1997) deduced a very narrow pore size distribution of around 6Å for the FT-30 membrane. The number of pores was somewhat related to permeability, but RO could not be described as a sieving process. The interactions between membrane, organic solutes, and water molecules determined separation. Lipp *et al.* (1994) found the ion rejection of FT30 PA composite membranes to increase with pressure and decrease with ion concentration if no fouling layer was present. Kotelyanskii *et al.* (1998) suggested that the anion limits salt transport for the FT30 membrane. High salt rejection was attributed to the difference in salt and ion mobilities in the membrane. Ratanatamskul *et al.* (1996) determined that a decrease in rejection at very low pressures could be compensated for by an increased membrane charge. Simpson *et al.* (1987) found a decrease in rejection with increased ion concentration, and attributed this to charge shielding. Rejection was very dependent on solute speciation, which varies with pH adjustment, leading to different permeate qualities. Complexation of cations with EDTA lead to an increased ion rejection. A similar effect would be expected if ions complexed with natural organics.

Speciation is the determination of the distribution of species in solution under various solution conditions, which influence dissociation of solutes and their interactions. A number of software packages are available to facilitate the calculations (see Appendix 5). While most membrane research neglect such solute-solute interactions, it appears that these interactions may have a very critical influence on membrane filtration as solute size and charge are modified. Of particular interest in membrane filtration of natural waters is the speciation of the carbonate system. As shown above, NF rejection depends on the ion charge and size, and these are both dependent on speciation. Simpson *et al.* (1987) studied the effect of pH on NF behaviour considering speciation. At neutral pH monovalent bicarbonate (HCO_3^-) predominated and rejection was low, whereas at high pH divalent carbonate (CO_3^{2-}) predominated and rejection was high. This high anion rejection also increased sodium rejection, and the increased osmotic pressure at higher rejections resulted in lower flux. A higher pH on the feed side of RO modules suggests that CO_2 is retained to a lesser extent than the other carbonate species.

In summary, key parameters to ion rejection are the membrane "pore" size, charge, pH, ion charge and size, flux and pressure, concentration, solute-solute interactions, composition of mixtures, and speciation. While models have been successful in explaining some results, the entire rejection mechanism is still poorly understood.

Organic Rejection

Rejection of organics may be determined by size and charge as well as the same parameters that govern ion rejection. In addition, factors such as molecular conformation and structure may play a role.

Early studies of RO reported that the rejection of organics increased with molecular weight and branching in a homologous series (Eisenberg and Middlebrooks (1985)). It was also suggested that phenol rejection is low. Rejection of macromolecules or aggregated compounds was 80 to 99%,

whereas the rejection of volatile compounds was only 14 to 40%. Generally, rejection increased when molecules were larger, sterically complex, or polyfunctional. This meant that ionisable compounds were rejected to a greater extent than hydrophobic compounds. The rejection of small organic molecules depended on structure and size, as well as charge and dipole moment of the molecules. Van der Bruggen *et al.* (1998) found that retention increased with molecular diameter, decreased with molecule polarity, and that concentration had no effect on retention. In another study of 30 to 700 Da compounds using NF membranes, van der Bruggen *et al.* (1999) demonstrated that polarity of a molecule reduced its retention. This was explained as an electrostatic attraction of the dipole towards the NF membrane which thus facilitated entrance into the pores. This effect was identical for membranes of both negative and positive charge with only the direction of the dipole changing. Negatively charged molecules were retained better due to Donnan exclusion by the negatively charged membrane. Positively charged molecules were retained less than negative or neutral molecules. Individual membranes exhibited significant differences in the extent to which size and charge determined rejection.

Duranceau and Taylor (1992) investigated the removal of synthetic organic compounds. Rejection was a function of molecular weight, and for smaller compounds of charge. Chian and Fang (1976) determined steric and polar effects in the organic separation of RO. Results from a single solution could not be extrapolated to mixtures. Rejection increased with size, branching, polarity, and pressure. The importance of hydrogen bonding was membrane dependent (Fang and Chian (1975)). Huang *et al.* (1998) observed a low aliphatic acid rejection by RO - rejection increased with size, crosslinking, and hydrogen bonding ability. Laufenberg *et al.* (1996) studied the retention of carboxylic acids and their mixtures by RO. The presence of other acids reduced the retention of compounds that were poorly retained, and increased the retention of compounds that were strongly retained. This was attributed to intermolecular interactions.

Mallevialle *et al.* (1996) summarised the following trends in organics rejection by RO as follows.

- rejection increases with increased molecular weight and branching
- compounds with an ionised group are rejected better than those without an ionised group
- rejection is greater if functional groups are dissociated (effect of pH)
- synthetic organic compounds (SOCs), phenolic compounds, and low MW chlorinated hydrocarbons are poorly rejected (e.g. some herbicides and insecticides)
- compounds that are very prone to hydrogen bonding are less effectively removed (e.g. alcohols, aldehydes, acids, urea)
- interactions with NOM significantly increase SOC removal
- rejection of organic acids improved when present as salt
- non-polar membranes are more effective at removing low MW compounds
- no dissolved gases are retained (may be a problem for odour control)
- steric and polar effects are specific for each compound.

Chelation also influenced rejection, and this was explained by Szabó *et al.* (1996) by a variation of the diffusivity by chelation. The chelation ability of a compound depended on the steric position of the functional group. Chelation and complexation are very important effects in the filtration of natural organics and multivalent ions. Considering the complexity of organic rejection, it appears obvious that rejection of natural organics will vary greatly from source to source. While the larger compounds would be expected to be retained by steric effects, smaller and uncharged compounds could potentially exhibit a lower rejection. Overall, the rejection of natural organics by NF and RO is expected to be 90 to 95%, but due to variations with membrane and organic characteristics lower results have also been published.

Wiesner *et al.* (1992) noticed that the solution diffusion model had a lower predictive capacity for organic solutes than for sieving effects. Guizard *et al.* (1991) introduced a reflection factor to describe the NF heteroporosity, in order to estimate the extent to which either of the processes (diffusion or sieving) is involved.

Disinfection by-product removal by NF was studied by Amy *et al.* (1993a). Pretreatment by UF was required and THMs were more efficiently removed than HAAFP (haloacetic acid forming potential) and CHFPs (chloral hydrate forming potential). Agui *et al.* (1992) studied HSs removal from water using a RO membrane and monitored pH and ionic strength effects. The HSs dissolved in water were considered to be similar to FAs (which were believed to dominate in surface waters). Three molecular weight groups were determined between 0.1 and 180 kDa. Adding NaOH to the solution caused the two higher MW groups to combine. Rejection was higher at neutral pH (90%), rather than acidic pH (60-75%), and the rejection was concentration dependent. The reasons for this solvent dependent behaviour were attributed as adsorption, hydrogen-bonding, or electrostatic attraction. The presence of trivalent ions enhanced the rejection of the 3.5 to 40 kDa organics fraction. This was attributed to changes in the macromolecular configuration of humic matter, as at higher ionic strength the molecules form coils (Agui *et al.* (1992)). However, the reported rejections are relatively low for RO. DiGiano (1996) found that the hydrophilic fraction of NOM did not associate with the membrane in a way to cause flux decline, but the affinity of that fraction to water resulted in reduced rejection. Nilson and DiGiano (1996) also found that the hydrophobic fraction is retained best, while the rejection of the hydrophilic fraction decreased with time. Nyström *et al.* (1995a) attributed NF rejection to the free volume in membranes. The presence of $FeCl_3$ caused a decrease in organic retention. Braghetta *et al.* (1997) determined a strong effect of charge on the rejection of NOM by loose NF membranes. The pH and ionic strength not only influenced NOM rejection due to the variation of molecule conformation, but also due to changes in membrane tightness. Taylor *et al.* (1987) found a MWCO of 400 Da to be ideal for THM precursor removal from groundwaters. A lower MWCO did not improve removal, while a larger MWCO reduced removal. RO was tested as a function of operating parameters, such as pressure, flow rate, membrane 'pore size', and solution pH, for the removal of HS. Pressure had no impact on HS rejection, but did effect water flux and inorganic salt retention. The solute concentration influenced rejection for some membranes, with the membranes themselves having the greatest effect on retention (Ødegaard and Koottatep (1982)). Allgeier and Summers (1995b) found a large variation in rejection for different surface waters. Rejection increased rapidly in the first 10 to 20 hours and was then stable. A concentration polarisation layer of charged molecules (HAs) enhanced charge repulsion and decreased transport of bulk TOC. A significant fraction of PEG (used as an organic model compound) of a molecular weight range 0.5 to 3 kDa was found in the permeate, and the chain structure of the molecules permitted this transport. For some waters, the organic matter hydrophobicity

decreased significantly, while the permeate shifted towards the non-humic fraction. A hydrophilic membrane was expected to remove the non-polar humic fraction better. Improved rejections for some river waters were explained by a high interaction of the 0.5-3 kDa humic fractions with the membrane, creating high resistance and self-rejecting capability (Allgeier and Summers (1995b)).

The NF70 membrane achieved good results for high and medium molecular weight organic matter. The low molecular weight fraction (<500 Da) was removed least (Amy *et al.* (1990)). According to Agbekodo and Legube (1995) a MWCO of 200 to 300 Da retains more micropollutants than any other current process. There is, however, a fraction of organic matter that can pass through the membrane, with molecular weights of up to 500 Da. Small organic compounds such as aminoacids, sugars, aldehydes, and fatty and aromatic acids, are not likely to be retained. These compounds are biodegradable and may contribute to bacterial regrowth in a distribution system. Logically, NF was found to increase the ratio of LMW compounds in DOC and BDOC of the product water.

Braghetta (1995) measured a reduction in rejection of DOC at low pH and high ionic strength for a sulphonated polysulphone hollow fibre NF membrane (1 kDa). This was attributed to the compaction of the membrane, the more compact structure of NOM molecules, and the densely packed layer of NOM at the membrane surface at low pH. The pH of the feed can influence the rejection behaviour of a membrane significantly, especially near the isoelectric point of a solute. If the same molecule changed its charge, it was able to pass through the membrane. Effective charge of a membrane depends on pH and ionic strength, which influence functional group dissociation and double layer effects. If the membrane has a high negative charge, which is normally the case at high pH and low ionic strength, the repulsion of functional groups will be strong, creating much free space and high flux. This will also influence rejection, being lowest at low pH. At low ionic strength, the impact of NOM concentration was low. Using neutral PEG standards it was shown that variations in rejection and flux were due to changes in the membrane matrix (Braghetta and DiGiano (1994)).

In summary, NF and RO achieve extremely high natural organics rejection compared to MF and UF. The compliance of NF with surface water requirements appears unproblematic. However, the rejection mechanisms are not well understood. Solution chemistry, organic characteristics, membrane charge, and the presence of inorganics, seem to be major factors.

Micropollutant Rejection

The rejection of micropollutants, such as herbicides and pesticides are a major driving force for the implementation of NF, although the reduction can be difficult due to the hydrophobic character of many of these compounds. While micropollutant rejection will not be investigated in this project, a brief review of micropollutant rejection abilities of NF membranes is included due to the importance of natural organics. Two ultra-low pressure RO membranes were compared (TFC-S, TFC-ULP, Fluid Systems). Both membranes showed different salt rejections, but pesticides were removed to a very high degree (>94%) (Takigawa *et al.* (1995)). The rejection abilities of NF towards micropollutants have been successfully demonstrated in many studies (Bourbigot and Bablon (1993), Ventresque and Bablon (1996), Bourbigot (1996)).

In contrast, Hofman *et al.* (1995) reported that NF was not able to remove pesticides well enough, and that an activated carbon post-treatment was necessary, while RO showed a higher pesticide removal. The rejection dependence of membrane material was much greater for NF than RO.

NOM type and concentration as well as inorganic ions influenced atrazine rejection. Rejection increased in the presence of NOM and decreased with ionic strength (Devitt *et al.* (1998)). Agbekodo *et al.* (1996) investigated the effect of NOM on atrazine and simazine removal. NOM increased rejection from 50% to 90 - 100%, when the NOM concentration was increased from 0.4 to 3.6 mgL^{-1}, respectively. This was explained by complexation and the transformation of the hydrophobic pesticides to negatively charged molecules. The free atrazine rejection was diffusion limited, while the atrazine in conjunction with NOM was rejected due to sieving. Devitt *et al.* (1994) confirmed the enhanced rejection of atrazine in the presence of NOM. These authors attributed the atrazine removal to interior adsorption in the NOM molecules. Devitt and Wiesner (1998) also reported that atrazine rejection decreased with ionic strength. Berg *et al.* (1997) related pesticide rejection to convection and steric hindrance rather than diffusion. The molecule cross-section determined the rejection, and dissociated molecules were also rejected better. Rejection increased with pH. CA membranes were not suitable for organic micropollutant removal (Hofman *et al.* (1997)).

Chang *et al.* (1994) compared MF, UF, and NF for arsenic removal. NF removed 16 to 97% at recoveries of 15 to 90%. UF could not remove arsenic, while MF with a coagulation pretreatment showed a dependence on organic carbon concentration. At low coagulant dosages organics impaired removal, while at high dosages removal was enhanced by the organics. De Witte (1996) published a 96% atrazine rejection by NF.

This brief overview illustrates the importance of operating conditions and the presence of natural organics on micropollutant rejection. Once again, solute-solute interactions are critical in the determination of removal of specific compounds. This highlights the importance of studying holistic systems, rather than single model compounds.

3.4.4 Variation of Rejection due to Fouling

Apart from solute-solute interactions, the deposition of foulants on the membrane can alter rejection. Rejection can increase due to a lower porosity of the fouling layer or pore constriction, or decrease due to a higher concentration in the boundary layer (concentration polarisation effect).

For example, Lipp *et al.* (1994) showed that organic fouling layers of humic substances increased salt rejection independent of HS concentration, whereas an inorganic fouling layer (iron hydroxide) decreased salt rejection. Rejection also increased with pH, as the fouled membranes became more negatively charged at high pH. This result was very interesting, indicating that an organic fouling layer was able to hold back inorganic components. DiGiano *et al.* (1994) showed that permeation of TOC increased with time, indicating the presence of diffusion together with convection. Fouling by macromolecules, especially pore fouling, also increased organic rejection over time (Fane *et al.* (1983)).

3.5 FOULING BY NATURAL ORGANICS AND COLLOIDS

Generally, membranes with larger pores exhibit a greater flux decline as filtration proceeds. This is due to the significantly higher intrinsic fluxes and the increased possibility of internal fouling. It should be noted that flux decline is not necessarily fouling. Concentration polarisation, or osmotic pressure effects can appear as fouling, and so can membrane compaction. Careful experimental design is therefore necessary to distinguish fouling from other effects. Fouling can also change rejection behaviour of membranes. While fouling is commonly observed in membrane processes, its origin is not always well understood. Consequently, Wiesner *et al.* (1992) described research needs in NF as mainly the chemical definition of organic foulants, the role of calcium in fouling, fouling prevention with chemical and physical pretreatments, and the study of the mechanisms, economic modelling, and concentrate disposal.

Baker *et al.* (1995) summarised fouling in surface water treatment by NF as a combination of inorganic precipitation or scaling, colloid fouling, organic adsorption, and biofouling. While interactions between solutes and the membranes are poorly understood, it is thought that effects like charge interactions, bridging, and hydrophobic interactions may play an important role. NOM, including HSs, are believed to play a major role in the fouling process. UF flux decline occurred, firstly, due to a gel forming when the solubility limit is exceeded in the concentration polarisation layer, or, secondly, because of adsorption (Matthiasson (1983)).

The assessment of fouling and its prediction in NF is not readily apparent due to the presence of so many parameters. Reiss and Taylor (1995) compared three parameters used to investigate fouling - silt density index (SDI), modified fouling index (MFI), and the linear correlation of the water mass transfer coefficient (MTC). Three different NF pilot systems were used with different pretreatments including activated carbon and MF. No correlation between the different parameters was obtained, indicating that the filtration laws on which the models are based on might not be valid for NF. Hence, these parameters need to be used with caution.

The different foulants and their possible interactions with membranes will be described in the following sections. While biofouling is also important, especially in the long term, it is believed that biofouling occurs generally after organic, inorganic and colloid fouling. The initial fouling may even influence biofouling due to the formation of a "conditioning film". This study is limited to the initial deposition.

3.5.1 Organic Fouling

Organic fouling depends on the organic characteristics. Research to date focuses on the identification of a "critical" organic fraction, which then can be eliminated to prevent fouling.

DiGiano *et al.* (1994) found that a MW of greater than 30 kDa was responsible for NF fouling. The flux history indicated a change in the fouling mechanism after 20h operation, possibly due to an interaction of the hydrophobic and hydrophilic fraction. Wiesner *et al.* (1992) identified four NOM categories which are strong foulants - proteins, aminosugars, polysaccharides, and polyhydroxyaromatics. Maartens *et al.* (1998) observed greater fouling for a more heterogeneous organic sample in UF, which consisted of a mixture of smaller and larger compounds, compared to a sample that contained only larger compounds. Amy and Cho (1999) identified polysaccharides as dominant foulants in UF and NF. However, polysaccharide concentration in surface waters is relatively low. Kaiya *et al.* (1996) found

compounds larger than 100 kDa to be major foulants in MF. Mackey (1999) studied the fouling of UF and NF membranes (cellulose ester and TFC-SR) by various model compounds, such as polysaccharides, polyhydroxyaromatics, and proteins. The larger compounds (polysaccharides and proteins) caused more fouling, and in mixtures the fouling increased.

This result was confirmed by Berg and Smolders (1989), who studied protein mixtures. Higher fouling of mixtures was attributed to molecule charge, rather than size effects and resulting differences in molecular packing. This is of interest in surface water treatment, as described in Chapter 2, since natural organics are a mixture of compounds with extremely varied characteristics. A study with Suwannee River NOM showed a very high flux decline at low pH. This was explained by a larger macromolecular packing density (gel-layer), due to the spherocolloidal shape of NOM at this pH, while at neutral pH the effect was low and mainly a long term phenomenon (Braghetta and DiGiano (1994)).

Nilson and DiGiano (1996) measured little fouling due to the hydrophilic fraction in NF. However, the unfractionated sample, however, showed greater flux decline than the hydrophobic fraction alone. The proposed reasons for this difference were given as an interaction between the two fractions, modification due to fractionation, or the loss of a specific fraction to the XAD resin. Although the largest MW fraction was responsible for fouling, the large size of the foulants prevented them from penetrating into the pores, and fouling was therefore reversible.

Once again the above results emphasise the importance of solute-solute interactions. Membrane characteristics and operating conditions also affect fouling.

DiGiano *et al.* (1994) studied fouling with a hollow fibre NF PS membrane (1 kDa). The membrane surface was treated to be hydrophilic. An increase in crossflow velocity greatly decreased flux decline, and the same effect was observed by decreasing TOC concentration. The membrane resistance was directly related to the amount of TOC removed from the fouled surface. Thorsen *et al.* (1993) recommend the use of highly hydrophilic membranes with a pore size of 1-2 nm and low operating pressure to reduce fouling in the filtration of soft waters high in organics. Fouling was worst for positively charged membranes which interact strongly with the negatively charged organics (Nyström *et al.* (1996)). In a later study Thorsen *et al.* (1997) found hydrophilic membranes to be more fouling resistant, while pore size did not affect fouling.

Reversible fouling was caused by cake formation and irreversible fouling from organics adsorption. The static adsorption test showed that the hydrophobic membranes suffer a high pure adsorptive flux loss, whereas the hydrophilic membrane is almost unaffected by adsorption. Hollow fibre studies showed a high irreversible fouling for PS membranes, but coagulation significantly enhanced flux recovery (Clark and Heneghan (1991)).

NOM was found to be less important for fouling than previously considered, following experiments with extracted NOM spiked into the feed. Six different membranes were tested and fouling was modelled using reversible and irreversible fouling coefficients, calculated from mass transfer coefficients (Champlin and Hendricks (1995)). This study seems to contradict most other studies in finding a lesser extent of fouling. A possible explanation might be a lack of inorganics in the permeate used.

Inorganic ions enhance fouling during water treatment with membranes. In the NF of conventionally treated water, the adsorption of macromolecules was followed by the adhesion of a biofilm. The inorganic deposit was determined to be mainly calcium, phosphorous (due to pretreatment), and

minorities of aluminium and iron (Baker *et al.* (1995)). Hong and Elimelech (1997) showed that fouling by NOM is increased in the presence of calcium ions, at decreased pH, and increased ionic strength. Additionally, the authors noted that permeation drag and electrostatic double layer repulsion control fouling. The addition of EDTA reduced such fouling. Hiemstra *et al.* (1997) concluded from pilot trials that iron deposition and HA adsorption were the main causes of NF fouling.

Calcium can be expected to create a more compact fouling layer and thus enhance flux decline. Mallevialle *et al.* (1989) used various MF and UF membranes to evaluate the irreversible fouling of HS. Flux decreases of up to 90% were observed in the initial stages of filtration. An analytical scheme to analyse water and the deposit was established. Fouling could be linked to the organic matrix of HS, and carbohydrates, proteins, and polyhydroxy aromatic compounds were believed to be the major contributors.

Yuan and Zydney (1999) found that humic substances, despite their small size, can cause a significant flux decline of MF membranes. This was attributed to aggregates deposited on the membrane surface. Prefiltration improved flux decline, but reaggregation occurred at increased calcium concentrations. An initial deposit of organics facilitated further deposition.

In summary, a number of organic fouling mechanisms occur. The most important ones being initial adsorption, precipitation and gel formation, and the interaction with multivalent cations. Large organics appear to foul membranes most, and for mixtures fouling is consistently worse, indicating solute-solute interactions. Organic fouling has been studied mostly for UF and NF, with MF being rarely studied.

Adsorption

Adsorption is the physico-chemical interaction between solutes and the membrane. The adsorption of organics, or more specifically humic substances, is considered a major fouling mechanism in water treatment. NOM can either adsorb in the structure of the cake and give the cake cohesion, or in the bulk of the membrane. These interactions are strongly influenced by membrane solute affinities and the reversibility is slow.

However, it is not well established to what extent adsorption can account for the fouling observed.

Adsorption can vary membrane charge. Jucker and Clark (1994) measured zeta potentials of hydrophobic UF membranes before and after adsorption. Hydrophobic compounds exhibited a preferential adsorption and zeta potentials became less negative after adsorption. The change in contact angle of the membranes before and after adsorption was also measured and was smaller, the more HS was adsorbed. HA and FA were on the same curve for the adsorption/contact angle relationship. Adsorption kinetics showed that FA adsorbed more quickly than HA due to a higher diffusivity, whereas HA adsorbed to a greater extent as a result of a greater number of attachment sites on the bigger molecules. Adsorption increased with concentration. Calcium interacted between HA and the membrane, and more calcium was required at a higher pH due to the larger pH difference. Adsorption seemed to first appear in pores (high energy sites), then on the skin. Adsorption isotherms of Suwannee River FA and HA were also determined for UF membranes by Clark and Jucker (1993). The effect of calcium was greater for HA. More porous membranes showed a larger flux decline. Phosphate groups from the buffer solution competed with calcium for adsorption. This study illustrated the importance of the choice of an adequate background solution, as ions from a buffer

solution can compete for adsorption and results in different effects. Adsorption was also dependent on the solubility of the organics, and a lower solubility lead to higher adsorption. The behaviour at low pH was attributed to changes in solubility (Clark and Lucas (1998)). Braghetta and DiGiano (1994) found a greater adsorption of organics on the membrane at low pH due to a higher packing density. Adsorption also increased with ionic strength.

The effect of HA adsorption on hydrophilic (CA and TFC) membranes for a pH range of 2 to 10 was demonstrated by Elimelech *et al.* (1994). The surface charge became more negative over the entire pH range for both membrane types and reached values of –30 mV at pH 2, down to –45 mV and –50 mV at pH 10 for the CA and TFC membranes, respectively. This shows that adsorption is not limited to hydrophobic surfaces.

The work of Childress and Elimelech (1996) established that humic substances also adsorb on hydrophilic membranes very rapidly, and that the membrane surface potential becomes more negative due to the humic substances. Calcium facilitates the adsorption of negatively charged organics onto negative surfaces. This indicated some charge neutralisation effect or specific interaction. Childress and Elimelech (1997) studied adsorption of HS and surfactants on NF membranes using streaming potential measurements. Large HS molecules adsorbed preferentially, especially in the presence of calcium. Surfactants formed hemicelles at the surface. This study is very relevant for HS as some natural organics may have surfactant characteristics (see Chapter 2).

Crozes *et al.* (1993a) found that the adsorption on a porous membrane was much higher than that on a flat piece of the same material. Adsorption and flux decline occurred after contacting the membranes with the solutes in the absence of flux. This indicated a higher adsorption with a larger membrane area. Maartens *et al.* (1998) found that larger organics adsorbed faster to UF membranes and reduced the pore size more effectively. Non-polar groups were the main cause of protein fouling, arising from adsorption on PS and polyethersulphone monopolar membranes. Hydrophilic membranes were expected to reduce fouling problems (Gourley *et al.* (1994)).

The adsorption of organic compounds is an important process, however, adsorption alone would only be responsible for a relatively thin deposit layer. After this initial adsorption, the solutes see the "new" membrane characteristics, which are determined by the solute. It appears as if gel formation or cake deposition are more important long term problems.

Precipitation and Gel Formation

Concentration polarisation, as described in the previous section, can become irreversible if a gel is formed, which can be the case when solute solubilities are exceeded. Concentration polarisation depends strongly on solute concentration and operational conditions, such as pressure and stirring. Fouling of 'tight' UF and NF membranes tends to occur more on the surface than in pores – similar to MF and 'loose' UF. Cake formation is usually reversible and can, as in MF, form a second membrane.

Surprisingly, Ødegaard and Thorsen (1989) demonstrated that HS concentration and pressure, which influence precipitation and gel formation, had no influence on flux. The fouling layer thickness was calculated with pressure drop and flow. The film was soft, dark brown, and loosely connected to the surface.

Wijmans *et al.* (1984) indicated that osmotic pressure limitations are more likely in the UF of low molecular weight organic solutes, whereas for high molecular weight solutes, gel formation was more important.

Tu *et al.* (1997) predicted NF flux by incorporating a gel-layer into the concentration polarisation model. Results corresponded well to filtration experiments with tannic acid. Gill *et al.* (1988) showed that viscosity effects in the boundary layer are more important than diffusivity. Concentration factors in UF of macromolecules were 40 to 400 times. A similar effect can be expected for large natural organic molecules. Kim *et al.* (1992b) showed cake formation for low initial fluxes, and aggregation for high initial fluxes in protein UF. This demonstrated that solute-solute interactions in the boundary layer are important.

The mass transfer coefficient (MTC) describes the accumulation of solute at the membrane surface. It is determined by the hydrodynamic conditions at the surface and flux.

Duranceau and Taylor (1993) modelled the MTC and found a direct relationship of MTC with solute charge and molecular weight. Nyström *et al.* (1995a) found that tighter NF membranes foul less, and that a charge repulsion between membrane and foulant also reduced fouling. Gel formation was described as a symbiotic effect of salts and organics. Multivalent ions fouled the membrane when combined with an organic. HA fouled the membrane at lower pH values, when it was partly undissociated. A gel formed on the membrane surface if a high concentration was applied. Nyström *et al.* (1994) filtered HA with 3 mgL^{-1} iron and while a gel layer was formed, flux decline occurred at pH 7, but not at pH 10. The low fouling at high pH was attributed to the absence of pore penetration.

While gel formation and precipitation are reported frequently as the source of fouling in all membrane processes, only a small amount of work has been done on a quantitative determination of gel layer concentration and the solubility of natural organics. Naturally, flux or transmembrane pressure are important for concentration polarisation, which seems to be the major factor in gel formation. The MTC can also describe this, as was shown above. Organic characteristics such as solubility and hydrophobicity require further investigation as do their interaction with ions. The solubilities of HS and their complexes with salts are relatively unknown, as was discussed in Chapter 2.

Pore versus Surface Fouling

Many authors distinguish between pore and surface fouling. Cleaning is more effective if fouling occurs on the membrane surface. However, in many cases it is difficult to distinguish between the two mechanisms. The blocking laws described in section 3.2.1 for MF and UF have a limited use to distinguish between pore and surface fouling, but for NF this distinction is practically impossible (Bowen *et al.* (1995), Kim *et al.* (1993)). By definition, these models are limited for applications in dead-end, unstirred filtration. Song (1998) described the initial rapid flux decline in MF and UF as pore blocking, whereas a slower, more gradual process was attributed to cake formation.

Mackey (1999) observed a greater fouling in UF than NF, and proposed both pore and surface fouling. The fluxes of UF at the end of the experiments were close to those of NF. The greater fouling in the UF case was attributed to pore fouling evidenced by an initial very steep decline in flux.

Pore blocking requires a initial low retention of the solute. While retention may increase due to cake formation, this increase in retention especially at early stages of filtration can indicate pore fouling.

Effect of Multivalent Cations

Multivalent ions have been reported to enhance adsorption and fouling in general. Possible interactions are bridging and charge neutralisation between membrane and organic (both are usually negatively charged), chelation, complexation, and aggregation (in the bulk and boundary layer), and co-precipitation of organics and inorganic precipitates.

Speth *et al.* (1996) investigated foulants on NF membranes after conventional treatment. Foulants had a specific fingerprint, different to the organics in the feedwater. The deposit was also rich in aluminium, calcium, iron, magnesium, sodium, and silica. Mallevialle *et al.* (1989) analysed membrane deposits and found a higher ash content in the deposits compared to the raw water.

Multivalent ions are believed to enhance natural organics adsorption. The effect depends on the organic type. Clark and Jucker (1993) determined that the effect of calcium on FA is lower than with HA. Binovi (1983) found that the gel layer formed on RO membranes was composed primarily of organics and iron. Nyström *et al.* (1994) filtered HA with 3 mgL^{-1} iron and while a gel layer was formed, the flux decline was low.

Mackey (1999) studied the effect of iron (5 mgL^{-1} or 0.09 mM) and calcium (50 mgL^{-1} or 1.25 mM) on fouling of polygalacturonic acid (PgA). Surprisingly, calcium and iron did not significantly enhance fouling. Aggregation was suggested as a fouling mechanism for the concentrations which were close to the solubility limit.

3.5.2 Inorganic Fouling or Scaling

Membrane scaling is the precipitation of ions on the membrane resulting in flux decline. This occurs when salt, rejected by the membrane, passes the solubility limit in the boundary layer. This effect is therefore of importance in NF and even more so in RO. Natural organics may influence this scaling.

Potts *et al.* (1981) summarised the most critical inorganics for RO to be calcium, magnesium, carbonate, sulfate, silica, and iron. Scaling is more important in RO than NF due to the higher rejection of ions, which also increases the osmotic pressure gradient across the membrane. Anti-scalants are often added or the pH adjusted to a lower value to prevent precipitation. High oxygen levels in the feed can also cause the precipitation of metal oxides. Removal or complexation of calcium may also prevent scaling, as well as a reduction of recovery. Allgeier and Summers (1995b) adjusted pH for scale control using the Langelier Saturation Index (LSI) in NF.

Inorganic solutes can cause fouling due to precipitation on and in the membrane due to hydrolysis and oxidation during filtration (Mallevialle *et al.* (1996)). Boffardi (1997) experimented with scale and deposit control in RO. Chemical treatment with several anti-scalants was effective in inhibiting scaling. Khatib *et al.* (1997) found amorphous iron and silica responsible for UF fouling by lake water. Adhesion of the gel was facilitated by reduction of the electrostatic repulsion. Binovi (1983) found the silt density index (SDI) insensitive to dissolved metals, such as iron or silica, as it only measured solids large enough to be measured as turbidity.

Boerlage *et al.* (1997) investigated the effect of organic matter on barium sulphate scaling. Solutions were generally oversaturated indicating a metastable zone. Crystalisation inhibition by natural organics was recognised as a possibility requiring further investigation. Overall, there appears to be a definite lack of research in the area of natural organics effects on inorganic precipitation, co-precipitation of inorganics and natural organics, as well as the precipitation of calcium-organic complexes. The limited

evidence suggests that under some conditions organics inhibit inorganic fouling and under other conditions inorganics enhance organic fouling.

3.5.3 Colloid and Particle Fouling

Colloids are defined as particulates in the size range of 1 nm to 1 μm (Potts *et al.* (1981)). Below that range, particulates are dissolved solids. While this size range includes organic matter, this section is mainly devoted to inorganic colloids. Fouling depends on colloid size and membrane pore size. A number of models exist for colloidal fouling and these were summarised by Bowen and Jenner (Bowen and Jenner (1995)). Here, major mechanisms and forces on colloids will be summarised.

A particle in the feed stream will be exposed to a number of forces and the resulting force will determine the particle's destiny. The forces are dependent on the particle size (Altmann and Ripperger (1997)).

A feed stream can be analysed for its fouling potential by measuring its SDI, zeta potential, and by elemental analysis. Severe fouling is expected for zeta potentials close to zero, high SDI, and large amounts of multivalent ions with a low solubility. The SDI, however, is limited to particles retained by a 0.45 μm microfilter, and the effect of fine colloids is probably underestimated by this analysis. The modified fouling index (MFI) was adjusted by Boerlage *et al.* (1997) for use with UF membranes. This was so that fouling could be predicted, taking into account smaller colloids, which may be more relevant in RO fouling.

Particle Deposition and Deposit Morphology

Three mechanisms are important for the backtransport of particles from a membrane. For small solutes and submicron colloids, **Brownian Diffusion** (determined by the Stokes-Einstein equation (Sethi and Wiesner (1997)) dominates backtransport of the colloids from the membrane into the bulk solution. **Inertial Lift,** which is caused by the presence of a wall is important for large particle sizes and high shear rates. **Shear Induced Diffusion** is an orthokinetic mechanism also more important for larger colloids.

Sethi and Wiesner (1997) predicted a most unfavourable size of 0.4 μm where the backtransport, considering all mechanisms, was at a minimum and thus the resulting flux lowest. When also considering cake permeability as a function of particle size, this minimum shifted to 0.01 - 0.1 μm. The dependence on membrane pore size and initial flux was not addressed in this study. Chellam and Wiesner (1998) pointed out the complicating effects of polydispersity on the use of such models. Most natural systems are polydisperse.

In a further study, Chellam and Wiesner (1997) showed that the specific resistance of the deposit increased with shear rate and decreased with initial flux. This implied that the deposit structure is also important. Additionally, Veerapaneni and Wiesner (1994) simulated the deposition of particles on permeable surfaces. Small particles ($\ll$1 μm) and low fluid velocities favoured the formation of loose deposits on the surface, while particles >1 μm formed dense deposits. These results show the impact of colloid size on particle packing and thus the permeability of the deposit. Particle-particle interactions, however, were neglected.

Particle-particle and particle-membrane interactions can be described with the Derjaguin-Landau-Verwey-Overbeek (DLVO) theory which combines van der Waals and electrostatic double layer interactions. While these theories generally apply for smooth surfaces, Bhattacharjee *et al.* (1998) have

modified the model for rough surfaces, which appears to be a more realistic approach for natural organics, colloids, and membranes. For rough or heterogeneous surfaces, interaction energies were considerably lower than for smooth surfaces. However, rough surfaces allowed the deposition of more particles (Elimelech (1999)).

Critical Flux or Pressure and Effect of Membrane 'Pore Size'

Most membrane colloid studies focus on cake control. This results in models which are often considered as independent of pore size. Particle deposition models do not include the issue of whether the cakes affect permeability. However, pore size and operating conditions have an impact on fouling. Pore size is related to flux. Howell (1995) introduced the concept of critical flux in MF. Transmembrane pressure increases flux and accelerates fouling. A critical flux exists, below which there is no fouling. This critical flux is a function of particle size (or, better, the ratio of particle to pore size), hydrodynamics, and membrane-colloid interactions. When fouling occurs at higher fluxes, the flux eventually stabilises at the critical flux value. The critical flux declines for decreasing diffusivity of particles or macromolecules. For small particles ($\ll 1$ μm), Brownian diffusion plays an important role. For particles > 1μm shear induced diffusion dominates, and for the intermediate size range charge interactions between membrane and particles are believed to dominate.

While this critical flux phenomena is generally accepted in MF and UF, some authors also mention limiting fluxes in NF (Levenstein *et al.* (1996)). Cohen and Probstein (1986) determined a characteristic permeation velocity below which no fouling was observed in the RO of colloids. Bacchin *et al.* (1995) defined a critical flux for the MF, UF, and RO of large colloids. The critical flux J_{crit} is a function of diffusion and the potential barrier between particles ν_B as shown in equation (3.36), where δ is the boundary layer thickness and D the particle diffusivity.

$$J_{crit} = \frac{D}{\delta} \ln\left(\frac{\nu_B}{\delta}\right) \tag{3.36}$$

For fluxes greater than this critical flux all the colloidal matter is deposited, while below this flux nothing is deposited (Bacchin (1994)). The predicted critical flux was higher than other models for colloids in the range 0.1 to 10 μm. The observed critical flux will depend on the depolarising mechanism (diffusion, lift, electrokinetic interaction, etc.). For smaller colloids, adsorption becomes important. In calculations of limiting fluxes, Field and Aimar (1993) concluded that changes of viscosity in the boundary layer were more important than changes in diffusivity. An ideal flux was defined as a flux where no fouling occurred. Hwang *et al.* (1998) referred to a critical pressure, above which the compressive forces between particles were overcome and particles come in contact with each other. This directly influenced cake porosity. It was also found that the cake closer to the membrane had a more compact structure than the cake on the bulk side. Cake porosity increased with ionic strength up to a maximum at 10 mM and then decreased. Song (1998) described an initial pore blocking, due to fluxes higher than critical pressure at the MF and UF module entrance. The equilibrium operating pressure lead to an absorption of excessive pressure by the formed cake. Song and Elimelech (1995) demonstrated the pressure and particle size dependence of cake formation due to concentration polarisation. The critical pressures for 1 nm, 0.1 μm and 1 μm colloids were 10^6 Pa, 10 Pa, and 10^{-2} Pa, respectively. These were indeed low pressures for membrane filtration, especially for larger colloids. Li *et al.* (1998, 1999) showed that the most suitable model for critical flux of supermicron particles was

shear induced diffusivity by using an in-situ direct observation technique. While negligible particle deposition occurred below critical flux, near the critical flux deposition was significant, while above the critical flux layers of particles were formed.

Due to the importance of particle and membrane pore sizes the following sections are split into the different membrane processes.

Microfiltration

MF is the process with the largest pores and highest fluxes. This means that the flux is affected by larger particles and permeation drag, which is the convective force dragging the particles towards the membrane, is strongest. Due to the fact that MF is designed for turbidity removal, a lot of research is available on this topic. Solution chemistry (pH, ionic strength, and the presence of organics that stabilise colloids) can have a significant effect on rejection and flux decline. High ionic strength can cause colloid aggregation, which may increase the porosity of the deposit and decrease its resistance to flux.

Tarleton and Wakeman (1993) showed that small particles in mixtures determined the flux decline in crossflow MF. For overlapping pore and particle size, fouling occurred as a combined effect of pore and surface blockage. For large particles, a dynamic membrane was formed, which retained smaller particles and prevented their penetration into pores. This effect may be observed in the MF of surface water, where colloids eventually enhanced the rejection of organics. In another work, Tarleton and Wakeman (1994a) described the effect of aggregation near the isoelectric point of particles. This lead to cake formation at the membrane surface, whereas stable colloids caused irreversible fouling due to accumulation in the membrane pores accompanied by low rejection. It is the deposit formed on the membrane, not the membrane itself, which governs flux and rejection after an initial filtration period (1994b). Chang *et al.* (1996) studied the effect of particle size (latex, 0.1 to 3 μm) and their mixtures on MF behaviour. Flux increased with particle size for the range studied. The balance between lift force and permeation drag determines layer deposition on a membrane (Altmann and Ripperger (1997)). The lift force depends on shear and increases with particle size. The solvent velocity, particle size and density determine permeation drag. Submicron particles are preferentially transported to the membrane by permeation drag (Bowen and Jenner (1995), Li *et al.* (1998)).

For aggregates, their density and structure might play an important role. The effect of aggregate structure on flux in UF has been reported by Schmitz *et al.* (1993). The authors modelled particle aggregation at the membrane surface and found a more complete space filling in the cake for particles that are re-entrained due to crossflow shear. Kim *et al.* (1993) studied the MF and UF of silver colloids (10 nm) in dilute suspension. At very low and at high salt concentrations, cake formation occurred and rejection was high. For intermediate salt concentrations of 1 to 10 mM NaCl, particles penetrated into the pores with minimal cake formation. Stirred filtration created a more finely dispersed cake, whereas unstirred conditions permitted aggregation. This was attributed to the altered conditions at the membrane surface. Shear may play an important role in aggregate size, especially if no time for equilibration of aggregation is allowed prior to filtration. The results indicate the importance of aggregation. Chen *et al.* (1997) studied the MF of silica colloids. Substantial transmission of particles was observed, which delayed cake formation.

Amirbahman and Olson (1995) analysed the deposition kinetics of hematite coated with humic matter in a quartz bed filter as a function of calcium concentration. At high ionic strength and low pH, tightly

packed conformations were achieved due to a loss in configurational energy. Calcium decreased the stability of the coated particles and increased their adsorption onto quartz. Hematite of 170 nm diameter and an isoelectric point of 6.5 has been used. Two different phenomena occurred; the screening of the surface charge due to calcium in the diffuse double layer, and the complex formation of calcium with free or surface-bound HS functional groups. HA coated particles were more stable than FA coated particles.

Moaddeb and Koros (1997) described the deposition of silica on polymeric MF membranes as non-uniform. This means that cake characterisation is difficult as a cracks could vary the results. Meagher *et al.* (1996) stated that attractive interaction between membranes and particles would cause a flux decline, even if the particles were aggregated. Aggregation reduced the flux decline if there was no attraction between the membranes and colloids. The authors outlined the restrictions of the gel polarisation model, as the porosity of the deposit is not accounted for in the model. It was also suggested that the resistance of the gel layer is more important than the particle-surface interaction (what is often referred to as adsorption).

High surface porosity of membranes increased the fouling tendency and rigid particles caused a lower flux decline than compressible particles, such as bacteria (Fane (1997)). Due to the large pore sizes of MF, internal fouling can be very important. Fane *et al.* (1993) described different types of cakes that form on MF membranes in the filtration of biomass. Abiotic particles could form a low or high voidage cake, which was determined by the solution chemistry. In contrast, biomass particles formed a cake on the membrane in which the extracellular bacterial polymers (EPS) filled the void space and controlled the cake resistance. This model is somewhat similar to inorganic colloids coated with humic acid, which added adhesive characteristics to the smooth colloid surfaces and fill the space between the inorganic colloids.

In summary, although the MF of colloids is generally well understood, the literature is somewhat limited in the areas of filtration of colloids much smaller than the membrane pore size, and in systems where aggregation occurs. Systems are, in this regard, often poorly characterised, especially in the presence of humic substances. As shown in Chapter 2 organics stabilise inorganic colloids at sizes much smaller than pores, and their behaviour in MF or surface waters is largely unknown.

Ultrafiltration

A significant amount of UF research has been focused on particle size and charge, and their effects on filtration performance (McDonogh *et al.* (1989)). However in UF, aggregation or stability effects have been rarely studied. Aggregation and stabilisation by natural organics are a key effect in natural systems.

Fane (1984) reported a flux minimum for colloids of 0.1 μm in UF. This minimum was explained by a balance between Brownian diffusion at low particle size and shear at larger sizes. McDonogh *et al.* (1995) studied the UF (10 kDa) of colloids of different charge and size (PS 95 and 290 nm; silica 12 and 23 nm). Flux increased with colloid size for PS, but for silica a decrease with size was observed. Flux passed through a minimum as particle charge was increased. The high fluxes at low charge were attributed to larger particle sizes due to coagulation and aggregation, and at higher charge a larger repulsion of the particles in the cake. Bacchin *et al.* (1996) reported a decrease in UF (300 kDa) flux with increased ionic strength for kaolinite. This was explained by a reduction of cake porosity, due to decreased repulsion and increased particle size from coagulation. A lower cake resistance was reported for salt concentrations above the critical coagulation concentration. Harmant and Aimar (1996)

predicted that after a critical amount of deposition, the deposition characteristics would change depending on particle-particle interactions. Close contact between the particles resulted in cohesive cakes. Harmant (1996) stated that colloid aggregation in the boundary layer occurred after a threshold value of deposition. After aggregation, deposition was irreversible due to the close particle-membrane contact. Irreversible fouling was prevented if the colloid concentration remained under a critical concentration in the boundary layer. Bacchin (1994) found an increase in cake resistance with ionic strength up to the critical coagulation concentration. Beyond that concentration resistance decreased dramatically. This was explained by the combined effects of lower porosity, increased particle size, and enhanced deposition at high ionic strength. Belfort *et al.* (1976) attributed greater flux at higher ionic strengths to a particle size effect, presumably aggregates had formed in the bulk. As shown above, the results are quite contradictory with regard to ionic strength.

Jönsson and Jönsson (1996a) investigated the effect of colloid stability on fouling of UF (25 kDa) membranes. Stable suspensions (below 1 M NaCl at 4 gL^{-1} silica, 12 nm) exhibited a reversible flux decline and thus concentration polarisation, while aggregates caused irreversible fouling. Jönsson and Jönsson (1996b) also developed a fluid flow model that allowed the calculation of concentration profiles at the membrane as a function of electrolyte concentration. Assuming hexagonal packing, the volume fraction reached a maximum at high NaCl concentration (1M), but concentration dropped rapidly with distance from the membrane. At low ionic strength the volume fraction of silica colloids (6 nm) was lower in the membrane boundary layer compared to the high ionic strength, but the layer thicker. The osmotic pressure of colloids as a function of ionic strength ranged between 2 and 23 kPa at a volume fraction of 20%. Yiantsios and Karabelas (1998) confirmed these results for UF and RO - stable colloidal systems caused less fouling. However, the observed results could also be an osmotic effect due to the higher ionic strength, particularly for the RO experiments.

Fane *et al.* (1982) discussed the possibility of UF flux enhancement by particulates. It was found that rigid particles larger than 1 μm could enhance flux. Cohesive and compressible particles, even if large, would cause flux reduction. Milonjic *et al.* (1996) filtered hematite suspensions and found that increased pressure and stirring lead to a increased flux. Chudacek and Fane (1984) measured deposit layers of several μm on UF membrane by macrosolutes and silica colloids.

Kim *et al.* (1993) used the blocking laws to show that colloidal fouling in UF was a two stage process - internal deposition followed by cake formation. Stirred conditions caused a greater flux decline, which was attributed to different levels of concentration, and thus aggregation in the boundary layer. Fu and Dempsey (1997) filtered FA and colloids. The authors observed that the flux was a function of the nature of colloids in the cake, while a decrease in zeta potential increased adsorption. Kim *et al.* (1994a) investigated the importance of pore size on flux decline in the UF of kaolin mixed with various organics, such as humic substances. If the organics were larger than the membrane pore size, they caused a more significant flux decline. In a later study by Kim and Hosomi (1996a), the flux decline of humic substances with a number of UF membranes was found to be independent of the molecular weight to membrane pore size ratio. This was attributed to the change in kaolin size distribution in the presence of organics. Nazzal and Wiesner (1993) studied flux decline of ceramic membranes in the presence of silica and humic substances. Humic substances created a higher reduction in flux than the silica colloids - the humic substances masked effects of pH and ionic strength.

Nanofiltration and Reverse Osmosis

NF and RO membranes do not have pores larger than 1 nm and it is often the case that the double layer of charged particles is likely to be larger than this. Therefore, if colloids contribute to NF and RO fouling, then this is likely to occur via the formation of a dense gel layer on the membrane, which involves molecules which occupy the interparticle space. Colloidal fouling of NF and RO membranes is not as well understood as in MF and UF, where colloids and particulates are major foulants.

NF and RO 'pores' are small and internal fouling by colloids is unlikely. The deposition of colloids on tight membranes may increase the boundary layer concentration, and give rise to an increased flux decline due to osmotic effects or cake resistance.

Chellam *et al.* (1997b) found that colloidal materials caused more fouling than organics in NF. Elimelech *et al.* (1997) noted the importance of membrane roughness on colloid fouling, however the mechanism of this fouling is poorly understood. Bentonite was used to study the effect of suspended solids on RO membranes. The estimated result was, that up to a concentration of 100 mgL^{-1} at 10 bar, bentonite had no effect on membrane flux. Bentonite concentrations of 1 to 3000 mgL^{-1} were studied, causing severe flux decline at higher concentrations (Ødegaard and Koottatep (1982)). These concentrations are extreme for surface water conditions.

Zhu and Elimelech (1995) studied RO fouling using aluminium oxide colloids (13 nm) and their aggregates. Fouling increased with ionic strength and in the presence of organic matter. The fouling was mostly reversible. When colloids were unstable their deposition onto previously retained particles was facilitated.

Elimelech *et al.* (1997) compared TFC and CA membranes for colloidal fouling using non-aggregated suspensions of colloidal silica (0.24 μm). The TFC membranes exhibited greater fouling. This was attributed to the greater surface roughness, which lead to an increased attachment on the membrane. The rejection characteristics of the two membranes were not published. Zhu and Elimelech (1997) used colloidal silica (120 nm) and found permeation drag to be the dominant fouling mechanism. Surface roughness increased deposition, which was explained by a distribution of surface energies. Fouling also increased with ionic strength and particle concentration. Zhu (1996) studied the fouling of TFC and CA membranes with a number of different colloidal systems. Particle fouling caused a decreased ion rejection due to enhanced concentration polarisation for some membranes. Flux was, overall, very important for colloid deposition. Ionic strength was also very important, where cake resistance increased with ionic strength. Zhu *et al.* (1995) used silica and kaolinite to study the effects of colloids on fouling of RO membranes. Salt rejection decreased with increased particle concentration. The fouling layer hindered backdiffusion and increased concentration polarisation. The extent of colloidal fouling was determined to be greater at high ionic strength, since the double layer repulsion is then reduced and deposition increased. Permeation drag was found to play an important role in colloidal fouling, especially at high ionic strength when double layer repulsion is low.

Cohen and Probstein (1986) studied RO fouling with dissolved ferric hydroxide. Stable colloids caused a higher flux decline than aggregates, which formed a more porous deposit. Jackson and Landolt (1973) suggested that the flux decline due to iron hydroxide in RO is governed by nucleation and growth of the iron oxides. Nucleation was a function of flux, particle size, and the number of available sites on the membrane. Growth was determined by flux, polymerisation rate, and shear forces. At very high and low pH, far from the isoelectric point, fouling is most severe due to the presence of small colloids.

Coagulated suspensions hardly fouled the membranes. Belfort (1980) precoated RO membranes with a diatomaceous earth layer to prevent fouling. The improved fluxes were explained as a protection of pin holes from submicron particles.

3.6 MEMBRANE AND FOULING LAYER CHARACTERISATION

Fouling is a very crucial parameter in process efficiency, and the analysis is not always straightforward. Flux decline provides a good indication of the extent of fouling, but the mechanism needs to be analysed by other means. In more open membranes the bubble point method could be used to measure the pore size reduction. For tighter UF membranes a similar method, based on biliquid porosimetry, can be used, but this becomes inapplicable for NF, due to its very tight structure. For NF and RO, the use of models is required to determine effective pore size (see section 3.2.3). For example, Bowen and Mukhtar (1996) used the extended Nernst-Planck equation to determine effective membrane thickness, effective charge density, and effective membrane pore size. These parameters are difficult to determine for NF and RO membranes. Wang *et al.* (1995a) successfully used the steric hindrance model.

3.6.1 Microscopic Techniques

Electron Microscopy

Electron microscopy requires dry samples for analysis. While field emission scanning electron microscopy (FESEM) analyses surfaces, transmission electron microscopy looks at membrane cross sections at a slightly higher resolution. Methods have been described by Kim *et al.* (1992a). Kim *et al.* (1994b) used gold and silver particles to characterise protein fouling layers. This technique allowed the distinction between pore and surface fouling of MF and UF membranes.

Atomic Force Microscopy (AFM)

AFM allows the surface characterisation of membranes in a dry and wet state. While resolution is better than in electron microscopy, the depth of focus is much smaller. More sophisticated techniques also allow force measurements between the tip, or objects mounted on the tip, such as colloids or organics, and membranes (Bowen *et al.* (1998)). While some authors have successfully used AFM to show NF pores (Bowen *et al.* (1997)) and determined their surface radius, a major drawback of the technique is that very smooth membranes are required to achieve very high resolutions and that the pore sizes determined are surface pore sizes and not the effective pore sizes required for prediction of separation. Most membranes do not meet the smooth surface criteria. Bowen *et al.* (1997) nevertheless demonstrated successfully that some NF membranes do have distinct pores. Knoell *et al.* (1999) used AFM to determine aspect ratios, pore perimeters, pore length and width, and the number of pores per area.

Direct Observation through the Membrane (DOTM)

Li *et al.* (1998, 1999) developed a technique that allows visual in-situ observation of colloids depositing on membranes. The technique is limited to transparent membranes, but allows the study of particle deposition and particle-membrane interactions. Light microscopy was satisfactory for super-micron particles, but fluorescence microscopy was required for sub-micron bacteria (0.5 μm).

3.6.2 Surface Charge

The membrane charge plays an important role in solute rejection, and charge effects become more important for tighter membranes. Bowen *et al.* (1997) showed that the charge of NF membranes is acquired by co-ion uptake from solution. Charge and rejection increase with salt concentration due to co-ion adsorption (Bowen and Mukhtar (1996)). Wang *et al.* (1995a) calculated the fixed charge density of NF membranes as a function of NaCl concentration and found a near linear increase. Ratanatamskul *et al.* (1997) showed that ion uptake by the membrane increased with concentration, and thus membrane charge increased to maintain electroneutrality.

Donnan Potential Measurement

Higa *et al.* (1998) measured the Donnan potential at a membrane interface. They found that the effective charge density was the same for all ions tested. The potential in the system was determined by the counter-ion with the highest valence. Takagi *et al.* (1996) determined Donnan potential from zeta potential. Donnan potential was very large compared to zeta potential, due to the low pore volume of RO membranes. The effective charge was due to chloride adsorption, as the CA membrane possessed no fixed charge. Adsorption on the surface and in pores was identical.

Streaming Potential

Membrane charge is commonly acquired by streaming potential measurements, from which the zeta potential can be calculated (Peeters (1997)). Charge of a membrane influence rejection and fouling. The isoelectric point of a membrane can be determined, when streaming potential is measured as a function of pH. Streaming potential can be measured through pores or along the surface. When pores are smaller, the pore streaming potential is difficult to determine and calculations often result in severe underestimations (Bowen and Cao (1998)). Pihlajamäki (1998) constructed apparatuses for streaming potential measurements through pores and along surfaces. The methods were used for clean and fouled membranes.

Kim *et al.* (1996b) compared streaming potential and electroosmosis measurements for MF and UF membranes over the pH range 4 to 7. Values for electroosmosis were higher but showed no charge reversal. Streaming potentials were similar in magnitude for MF and UF. An increased electrolyte concentration resulted in a decrease of potential. Electroosmosis was found to be unreliable for membranes with small pore sizes (Zander *et al.* (1995)).

Causserand *et al.* (1994) demonstrated that streaming potential can also be used to assess fouling, as the surface potential often changes to the foulant characteristics.

Uranyl Acetate Adsorption

Knoell *et al.* (1999) used uranyl cation adsorption to determine the amount of sulphonate groups on membranes. A linear correlation between uranyl adsorption and sulphonate groups was found, and also a heterogeneity of their distribution was observed.

3.6.3 Hydrophobicity and State of Water

Contact Angle

Contact angle measurements determine the hydrophobicity of membranes - the higher the hydrophobicity the greater the expected adsorption (Gourley *et al.* (1994)). Contact angle measurements also give information about the wettability of a membrane, which determines flux (Kulkarnie *et al.*

(1996)). While the sessile drop (or water droplet) technique is the conventional method, Bouchard *et al.* (1997) established that the use of three different reference liquids could give valuable information about surface energies. Different bonds were responsible for HS adsorption on TFC and CA membranes. Jucker and Clark (1994) found that hydrophobic UF membranes become more hydrophilic after the adsorption of humic substances. Combe *et al.* (1999) challenged this relationship between hydrophobicity and HS adsorption. The authors proposed that increased adsorption was not related to hydrophobicity (or membrane charge), but to the number of surface sites on the membrane. Zander *et al.* (1995) observed the contact angle to be independent of pH and ionic strength variations in the range of surface water conditions.

State of Water

The state of water in a membrane can become important for RO membranes as it is often related to rejection. Murphy and dePinho (1995) studied the state of water in RO and UF membrane active layers using attenuated total reflection fourier transform infrared spectroscopy (ATR-FTIR). Water content increased with porosity, and the structure of the water was dependent on average pore size. Large clusters of water were linked to low salt rejection, whereas low association of water in clusters indicated a low permeability to salt.

3.6.4 Deposit Morphology and Surface Analysis

Mallevialle *et al.* (1989) described a range of surface analytical techniques that are available for foulant identification. Many techniques that are currently being used for organics characterisation (see Chapter 2) can potentially be used for membrane deposit characterisation.

Structure and Fractal Dimension

The determination of cake porosity and fractal dimension of membrane deposits is difficult. While filtration laws can be applied, most assume a constant porosity.

Veerapaneni and Wiesner (1997) studied the fractal dimension of a membrane deposit by re-suspending the cake and performing static light scattering. Control experiments showed that the structure did not change due to the re-suspension.

X-Ray Photoelectron Spectroscopy (XPS)

XPS is a useful technique to determine the chemical state of a deposit. In theory, this technique is ideal to determine whether calcium is bridging natural organics and membrane, or if co-precipitation or complex deposition occurred. In practise, this has been attempted by Jucker and Clark (1994), and binding energies where published. Unfortunately due to the unknown binding energies of the possible compounds a clear distinction is not yet possible (see also Chapter 2).

Fourier-Transform Infrared Spectrometry (FTIR)

Fourier transformation infrared spectroscopy (FTIR) can be used for the characterisation of clean and fouled membranes. Pihlajamäki (1998) used FTIR to determine adsorption sites on membranes. UF membrane materials were characterised for fouling with FTIR to distinguish differences in surface layers, streaming potential (conformational changes of proteins/aggregates), and contact angle (adsorption kinetics) measurements. Maximum fouling was found at a zeta potential near zero (Nyström *et al.* (1995b)).

Markers

Fouling with proteins has been measured with ^{14}C marked proteins. Fouling was much higher for hydrophobic membranes like PA and PS, compared to CA. An inflection point in the adsorption isotherms indicated that two mechanisms of adsorption existed. A relationship between adsorption and hydraulic permeability existed (Matthiasson (1983)).

3.7 FOULING CONTROL

Fouling can be controlled by altering the operating conditions (see section 3.5.3 for critical flux and pressure), chemicals addition (see inorganic fouling section 3.5.2) or by pretreatment. In this section the focus is on pretreatment.

3.7.1 Pretreatment for Rejection Increase and Fouling Prevention

Various processes are available for pretreatment of membrane processes. These methods are either aimed at rejection enhancement or fouling prevention. The majority of the techniques target different compounds, and thus need to be tailored to a specific water and application.

Some of the available options are powdered activated carbon, UV/ozone, magnetite, lime softening, ion exchange, conventional media filtration, and coagulation with inorganic and polymeric coagulants.

Cartridge Filtration

Filtration is required in some UF and in NF/RO processes. This is mainly because spiral wound modules cannot tolerate large particulates due to their very thin channels. Also, coarse particles may damage membranes under high shear conditions. Filters applied are usually in the 1-25 μm range, aimed at suspended solids (Suratt (1993)).

Conventional Treatment

Conventional treatment or media filtration can reduce the suspended solids load by a factor of two (Suratt (1993)). This value seems very low and depends on the suspended solids characteristics. Gusses *et al.* (1997) stated that conventional treatment was not a sufficient pretreatment for NF. A combination of coagulation, ozonation, and biological treatment was a better alternative. Glucina *et al.* (1997) confirmed the inadequacy of conventional pretreatment for NF. UF pretreatment was more effective than MF in the long term regarding flux, while rejection of the NF membrane was independent of pretreatment.

Coagulation/Flocculation

Coagulation is part of the conventional water treatment process of coagulation, sedimentation and filtration. As stricter drinking water standards are implemented, enhancement or optimisation of coagulation processes will be required. While coagulation cannot always meet guidelines, it can enhance organics rejection by membranes and in some cases reduce fouling (Jacangelo *et al.* (1995b)). Coagulation is a water treatment process that also occurs in the natural environment (Crosby *et al.* (1993)). The mechanism of natural organics removal varies with pH and coagulant dose. For coagulation as a pretreatment, iron or aluminium sulphate are commonly used to increase cake porosity (Jacangelo *et al.* (1995b)). The addition of a polyelectrolyte can also enhance ion rejection in NF (Levenstein *et al.* (1996)).

According to Dennett *et al.* (1996), adsorption, charge neutralisation, and sweep coagulation are predominant mechanisms in water treatment. Sweep coagulation involves the formation of a solid precipitate. At neutral a pH sweep coagulation would be expected, whereas at a very low pH restabilisation can occur. Removals of up to 95% using UV absorbance were achieved and attributed to a combination of mechanisms. Organic concentration was 13 mgL^{-1} as DOC and coagulant dose 10 to 100 mgL^{-1} $FeCl_3 \cdot 6H_2O$. Surface water treatment with MF achieved good disinfection (turbidity and *Giardia*), and with coagulation pretreatment 60% THMP removal could be achieved. The effect of coagulation on MF efficiency negligible, and no additional removal was achieved with a higher dosage (Vickers *et al.* (1993)). Experiments with the same membranes were carried out for surface waters with a very varying turbidity (0.5 to 110 NTU). Flux declined at very high turbidity, but aluminium, iron, and pathogens were removed as well, when turbidity reduced to 0.1-0.3 NTU and organics to 20-30% TOC (Moulin and Tazi-Pain (1993)).

To remove appropriate amounts of natural organics in conventional treatment, high dosages are needed. This is called enhanced coagulation. Krasner and Amy (1995) reported a higher removal by ferric chloride than by alum. This result was confirmed by Crozes *et al.* (1995) and Jacangelo *et al.* (1995b). The pH is also an important parameter, and at pH below 6 removal could be increased significantly. Vickers *et al.* (1995) defined the optimum pH region as pH 5 to 6. Larger MW and hydrophobic compounds are removed preferentially by coagulation (McCoy (1993), Jacangelo *et al.* (1995b)). Iron coagulants were found to outperform alum. The presence of divalent cations can reduce the coagulant dose, due to neutralisation of natural organics.

Amorphous ferric oxyhydroxides (or ferrihydrites) form and adsorb natural organic matter similar to other colloids. However, the specific surface areas of such amorphous materials are very high (159-234 m^2g^{-1}), which makes them attractive for water treatment. In natural waters, colloid surface areas ranged from 6.4 to 164 m^2g^{-1}. As the precipitates age, they develop more crystalline structures and such ageing affects surface area and pore size. Lo and Waite (1998) determined that denser aggregates were formed under stirring, which was more important than the effect of salt. The size of ferric oxyhydroxide precipitates (in the absence of organics) ranged from 10 nm at low pH to 700 nm at high pH. Flocculation can be induced by a reduction in surface charge (e.g. by pH increase).

Coagulant dosages in water treatment are usually determined by the natural organics content, rather than particle concentration. According to O'Melia *et al.* (1999) other factors are organic type, type of coagulant, pH, hardness, and temperature. Ferrihydrites may be recycled and reused in a water treatment system for waste reduction (Schultz *et al.* (1987)). Volcheck *et al.* (1993) used polymers to remove metal ions with MF. Separation was attributed to the formation of a polymer layer inside membrane pores and on the surface. UF was recommended for future work to ensure polymer recovery. Chen *et al.* (1998) determined an increased removal of organics by UF in the presence of calcium, magnesium, manganese, and iron. Iron was most effective in removal enhancement.

Hillis *et al.* (1996) used ferric sulphate with MF. The optimum coagulant dosage (for conventional treatment) was different to the optimum MF dosage, with slightly more coagulant being required to obtain optimum filtration. A THMP removal of greater than 80% was achieved. Wiesner *et al.* (1989) used polyaluminium chloride (PAC) coagulation prior to MF to increase humics rejection. The formation of larger particles prior to MF reduced foulant penetration into pores. Organic rejections of organics of >95% were reported. Bian *et al.* (1999) also used PAC to increase UF rejection.

A membrane process (MF/UF) as a separation process for coagulated water has the advantage that breakthrough does not occur, in contrast to conventional filtration. TOC removal varies from 5 to 70%, but increases if optimised. The optimisation of NOM removal is possible, as the removal of turbidity, particles, and microorganisms is guaranteed with a membrane process and is not interlinked with NOM removal. Lower dosages may not be required, as the settlability of a floc is not important. Coagulation facilitates the backwash of a deposit (Vickers *et al.* (1995)). UF PS membranes have been tested for TOC removal from surface waters. Different methods for fouling prevention and the impact of calcium and clays were tested. The combination of HA and calcium caused severe fouling, and a further increase in calcium concentration increased the reversible part of fouling. The greatest fouling occurred for HA, calcium, and clay in solution, irreversible fouling being increased by the addition of clay. Preventive measures, such as lime softening and coagulation, decreased this fouling, but only coagulation could reduce irreversible fouling significantly and increase TOC removal. Coagulation made filtration pressure dependant, and the TOC in the permeate increased with cake layer build-up (Hagstrom (1988)).

Coagulation and MF have also been used by Tang *et al.* (1994) in secondary wastewater reuse. Ravindran *et al.* (1993) used alum coagulation and MF and coagulation increased both flux and rejection. Thompson (1994) used flocculation prior to membrane filtration to reduce colour, optimise backwash efficiency, and reduce fouling. Alum was applied as the coagulant. A linear relationship between floc size and flux was found. Under the optimum dose level of alum, both the standard blocking model and cake filtration model were applicable, while above the optimum dose, the complete blocking model was valid. At a pH less than 6, colour removal improved, but fouling increased. The specific surface area of a floc increased with lower pH, and the higher the dosage, the smaller the floc. Air from backwash caused flotation of the backwash liquid. Break-through of coagulant occurred for very high concentrations. The optimum flocculant dose level coincided with the isoelectric point, and the presence of minerals increases the required dosage (Thompson (1994)).

Patel *et al.* (1994) employed a combined process of coagulation and MF to avoid a disinfection post-treatment. The coagulation step was used to eliminate phosphorous, arsenic, and viruses, to avoid fouling, decrease particle accumulation on the membrane surface, and improve backflush characteristics. MF pilot plant studies in constant permeate flux mode showed that turbidity, particles, and faecal coliforms could be removed, but TOC removal was unreliable. Crossflow MF showed no difference to dead-end filtration, and both methods were similar to or better than sand filtration. Results with coagulation and MF improved phosphorous and turbidity removal, but the process was not optimised. The treatment lead to a reduction of chlorine demand in the product water.

MF with a PAC pretreatment was compared to UF for slightly polluted river water. Almost no difference was observed for the two processes. Coagulation was necessary to maintain a high MF flux. THMPF was removed at 0-50% (Kunikane *et al.* (1994)).

Lahoussine-Turcaud *et al.* (1990) simulated surface water with dispersions of dissolved organic matter and colloids. PAC was used as a coagulant before UF. Different models of particle deposition were considered, and the deposit and flux decline increased with particle size up to a size of 3 μm, with greatest flux decline at 0.2 μm. The simulated river water contained tannic acid (as small compounds), calcium, HA, and kaolin in tap water. Coagulation improved filtration behaviour, while in Seine river

water fouling was only marginally controlled by the coagulant. This was attributed to the presence of small organic compounds.

Bedwell *et al.* (1988) studied fouling mechanisms for surface water that was treated by lime softening, and rich in humic and fulvic acids. HA and FA caused problems in the filter cake and in interactions with the nylon membrane. A coloured deposit was clearly visible due to its colour, and good performance correlated with precipitate (very low and very high pH), rather than the soluble salts. At a neutral zeta potential the particles aggregated easily, and acid cleaning showed no effect, whereas surfactants were very effective. Other observations were that oxidation increased filterability, smaller humic materials seemed to increase aggregation, and that shear was found to be an important factor that destroys aggregates in crossflow filtration.

Activated Carbon Adsorption

Crozes *et al.* (1993a, 1993) reported reduced fouling of a hydrophilic UF membrane after powdered activated carbon (PAC) pretreatment. PAC appeared to adsorb the fraction of organics that were responsible for fouling. For a hydrophobic membrane, flux decline remained severe despite pretreatment. Jacangelo *et al.* (1995c) used PAC and found that fouling was retarded, but not completely inhibited. High dosages were required to achieve high precursor removal. Pretreatment of MF with PAC could achieve good atrazine control, but increased flux decline Clair *et al.* (1997). In contrary, Wetterau *et al.* (1995) showed that PAC pretreatment reduced fouling. According to DiGiano *et al.* (1994), PAC only adsorbed the middle fractions of MW and fouling increased with PAC contact time.

Clark and Heneghan (1991) tested UF, both with and without pretreatment, of lake water with coagulation and PAC. A backflush was employed to remove short-term flux loss and static adsorption tests were employed to characterise irreversible fouling. UF alone removed turbidity perfectly, whereas no THMFP was removed without pretreatment. PAC performed better than coagulation, removing 80-85% of THMFP.

DiGiano *et al.* (1993) reduced NF fouling by the addition of coal particles as turbulence promoters, which decreased NOM fouling. Particles of 0.3 μm exhibited the largest fouling tendency, and the range of 5 to 75 μm was studied for turbulence promotion. Depending on their size, particles and colloids can enhance or prevent fouling. Effects to be considered are Brownian diffusion, lateral migration, and shear-induced diffusion. The role of particles in flux enhancement has been studied with anthracite coal particles. The fluidised particles were expected to act as detached, inert turbulence promoters. The smallest particles (0.3 μm) had the largest tendency to foul the membrane, due to slower backtransport from the surface. Particles increased the flux at low crossflow velocities.

Laîné *et al.* (1990) used a hydrophobic and a hydrophilic membrane to remove turbidity, organic matter, and THMPs from lake water. UF was compared to coagulation+UF, PAC+UF, and coagulation+PAC+UF. While no THMPs were removed with UF alone, 30% rejection was achieved with coagulation as pretreatment, and 85% with PAC pretreatment. Additionally, the resistance of the cake layer was improved significantly if two pretreatments were applied. Baudin and Anselme (1995) applied a combination of PAC and UF for river water treatment. PAC was added to a recirculation loop to obtain a higher adsorption efficiency ("Cristal" process). Taste and odours were successfully removed, and the process performed better than conventional GAC treatment.

Johannsen (1993) studied organics adsorption on activated carbon. Results indicated that smaller and less UV-absorbing compounds adsorb more easily, adsorption increases at lower pH, and, therefore, removal of natural organics depends strongly on their origin. These results show that pretreatment can be targeted at small or large compounds by using adsorption or coagulation, respectively.

Solomon *et al.* (1993) carried out an extensive investigation of UF with a wide range of pretreatments (MF, GAC, Al coagulation, biofiltration (sandfilter), ozone+biofiltration) to observe organic matter, DBP precursor, and turbidity removal from natural waters. Hydrophobic membranes were used to study fouling effects. Low molecular weight HS appeared to be easy to remove biologically, and low MW polysaccharides caused irreversible fouling. Static adsorption tests showed a smaller effect than pure water flux decline. MF and GAC were not able to remove fouling matter, whereas alum coagulation, biofiltration, and ozone+biofiltration increased water production by 50-100%, due to a better backflush efficiency. Van der Hoek *et al.* (1995) investigated RO with different pretreatments for natural waters. Scaling was found to be a serious problem and the anti-scalant additive was suspected of increasing biological and organic fouling. MFI and DOC were significantly reduced with extended pretreatment of ozone+biological activated carbon and slow sand filtration. Activated carbon pretreatment improved the disposability of the concentrate.

Iron Oxide Adsorption

Iron oxide adsorption can be combined with UF to increase rejection of natural organics and reduce fouling. Chang (1996) found UF fouling by NOM independent of organic size, affinity towards iron oxide adsorption, and pH. Chang and Benjamin (1995) increased the UF rejection of natural organics from 10 to 20% without pretreatment, to 50 to 85% with iron oxide particle (IOP) addition. At the same time, fouling decreased significantly. Chang (1996) added heated iron oxide particles (HIOPs) prior to UF and anticipated that the particles protected the membranes from NOM deposition. The HIOPs were regenerated, but the sorption capacity was affected.

Chang and Benjamin (1996) also found that iron oxide particles cannot selectively adsorb certain NOM fractions, which are responsible for fouling. While unheated IOPs were a fresh precipitate of unknown particle size, the HIOPs were somewhat aged and the size range was 0.5 to 50 μm. Flux decline with the unheated IOPs was high and irreversible, but was reduced with the HIOPs due to adsorption of NOM on the particles and prevention of gel formation. However, fouling subsequently occurred on the HIOP layer. The dose of the particles was 170 mgL^{-1} as Fe, which is higher than the dose in coagulation, however the IOPs can be reused. Heating the particles would make them less amorphous. A more recent study by Chang *et al.* (1998) on regeneration, showed a 30 fold regeneration with negligible sorption properties. Chang *et al.* (1997) subsequently developed a process in which the iron oxide adsorption is carried out in a separate filtration bed prior to membrane filtration. This prevents contact of the particles with the membranes. The filter media used was iron oxide coated sand or olivine (IOCM). Adsorption was most effective at acidic pH values. Head-loss was lower than for sand filtration and pretreatment more effective.

3.7.2 Backwashing, Backflushing, and Operation Mode

Microfiltration

The relatively large pores of MF allow the removal of the deposit using air backflush or permeate backwash. Crossflow, rather than dead-end filtration mode, can be used to control the thickness of the

deposit. However, for aqueous (dilute) solutions, dead-end filtration is often preferred due to significantly lower energy requirements (pumping).

In a pilot test, Kumar *et al.* (1998) found that almost 10% of the production capacity was lost due to cleaning and backwashes. This indicates the importance of optimisation of these processes. Magnesium oxide slurries were used to optimise a MF process in intermittent operation. Concentration polarisation disappeared after a short cessation of feed flow. The start-stop cycle was optimised, and the mean flux was increased by 100% (White and Lesecq (1993)). The principle of an effective permeate backwash is described for a MF plant for wastewater. A longer duration of the backwash pulse had no effect, whereas shortening the backwash duration and interval with an increased pressure gives a better cleaning effect. This also leads to a higher production time. A maximum velocity of backpulse through the pores, at the lowest possible time is required (van Duijn (1996)). The backwash efficiency and TOC removal can be increased significantly with the addition of a coagulant (Ben-Aim and Peuchot (1991), Dittrich and Gnirβ (1995)).

Ultrafiltration

Permeate backwash is a possible means to remove cake deposit in UF. The choice of a more hydrophilic membrane can decrease adsorption significantly and changes in the solution chemistry can impact on the deposit structure and porosity.

Nakatsuka and Ase (1995) found backwash most effective if the backwash pressure is more than double the operating pressure. An increase in crossflow velocity also lead to higher flux, but at the cost of higher energy consumption. Hagmeyer *et al.* (1996) optimised the backwash interval to 30 sec every 30 minutes. Efficiency could be further increased with the duration and frequency, but at the cost of recovery.

Jönsson (1993) studied shear rate and flux interruption for fouling control. While shear only marginally restored flux, the interruption of permeate flow was a successful technique. Lipp *et al.* (1997) discussed backwashing and while chlorine was most effective in restoring flux, the formation of THMs in the backwash needs to be considered. Crozes *et al.* (1995) observed a lower effectiveness of backwash if the operating pressure was higher. Operating conditions such as low pressure and high crossflow could limit reversible fouling, which resulted in a reduction of irreversible fouling.

Nanofiltration

Bian *et al.* (1999) reduced the concentration polarisation and fouling in NF by vibrations. Mallubhotla *et al.* (1998) reduced the concentration polarisation by constructing helical modules from tubular membranes.

In NF, a key factor is pretreatment, which can be conventional sand filtration, MF, or UF. It is believed however, that conventional filtration does not remove particulate matter sufficiently to prevent severe fouling.

3.7.3 Membrane Cleaning

Finally, fouling can be removed to a certain extent by chemical cleaning. Changes in solution chemistry can minimise fouling (pH far from isoelectric point, low I), as can low pressure operation, high crossflow velocity, selection of modules, and hydrophilic membranes (Fane (1997)).

Pure water can be used to remove loosely associated solutes from the membrane. For irreversible fouling, chemicals are required. The chemicals to be used depend on the foulant in question and the resistance of the membrane to the cleaning agent (Trägårdh (1989)). This requires an understanding of the fouling mechanism if cleaning was to be optimised. Maartens *et al.* (1998) determined that a combination of alkaline solutions with detergents were effective in removing organic foulants in UF. Cleaning, however, reduced rejection of the membranes (which was restored with filtration) and membrane lifetime. Speth *et al.* (1996) found acid cleaning very effective due to the inorganic component in fouling. Ødegaard and Thorsen (1989) suggested a washing routine for RO membranes, however the cleaning frequency appeared rather high. Alborzfar *et al.* (1998) used an alkaline solution to remove NOM deposits, and both acidic and alkaline cleaning to remove inorganic precipitation.

3.8 MEMBRANE PROCESS APPLICATIONS IN WATER TREATMENT

An overview of the application and volume treated by membrane processes is given in Table 3.2. The increase in recent years is obvious. At this stage, there is still more RO than MF and UF being used in potable water treatment (Wiesner *et al.* (1992)).

Table 3.2 *Overview of pore size, operating pressure, application and production volumes for 1994 and 1998 ([1]Mallevialle et al. (1996), [2]Aptel (1998), [3] Fane (1999), [4] Aptel and Laîné (1998)).*

Process	Pore Size [nm]	Operating Pressure [MPa]	Application	Municipal Drinking Water Production (1994)[1] [m^3d^{-1}]	Municipal Drinking Water Production (1998)[2, 3, 4] [m^3d^{-1}]
MF	macropores >50nm (100nm)	0.05 - 0.5	turbidity removal	31 000	500 000
UF	mesopores 2-50 nm (10nm)	0.05 - 0.5	turbidity and macromolecule removal	63 000	600 000
NF	micropores <2nm	0.1 - 1.5	surface & ground waters of high hardness and organics	500 000	1 000 000
RO	non-porous (?)	5 - 8 (2x osmotic pressure)	desalination of sea- and brackish water	3 000 000	10 000 000

3.8.1 Membrane Processes versus Conventional Treatment

The optimum coagulation conditions (i.e. pH) were found to be the same as in conventional treatment for removal, but optimal flux in membrane treatment requires further optimisation. Vickers *et al.* (1995)

compared the combination of coagulation with membranes to coagulation in conventional treatment. The advantages of membrane treatment were a lower coagulant dose, as particulates will be removed by the membranes and no settlable flocs are required.

Vickers *et al.* (1997) found that MF with coagulation pretreatment produced very similar results to conventional treatment with respect to DBP precursor removal. The advantage of MF was the simultaneous removal of *Cryptosporidium* and *Giardia*. Crossflow MF was found to be the superior technology to coagulation and filtration for a remote area water supply, and colour and turbidity were removed perfectly (Holland and Nash (1995)).

Nilson and DiGiano (1996) stated that NF was cost-competitive with conventional treatment for small systems. Conventional treatment was not always able to meet surface treatment requirements. Ericsson and Trägårdh (1996) reported a higher and more consistent drinking water quality for NF, compared to conventional treatment with activated carbon. UF did not remove sufficient colour, and NF also outperformed UF combined with GAC. The costs of NF were slightly higher than conventional filtration combined with activated carbon. Ødegaard and Thorsen (1989) stated that the cost of RO was competitive with conventional treatment for small systems, where waters high in colour were to be treated. Lipp *et al.* (1997) compared UF combined with lime filtration to conventional treatment, and the largest cost fraction shifted from maintenance to membranes, while overall capital and operating costs remained comparable.

A life cycle assessment study, carried out by Sombekke *et al.* (1997), compared conventional filtration and GAC with NF. The NF performed better in health and quality aspects and worse in environmental impact, due to concentrate treatment and energy requirements. NF could outperform conventional treatment if green energy could be used.

3.8.2 Membranes versus other Alternatives

Dal-Cin *et al.* (1995) described ozonation plus granulated activated carbon (GAC) as a viable alternative to membranes, however costs were higher. These authors also reviewed the use of membranes for drinking water applications. NF appeared to be the most attractive membrane process with a good balance between natural organics removal and flux. The lower operating pressures contributed to large cost savings compared to RO.

Pilot studies of surface water treatment using membranes are reported very frequently in the literature. Many full scale applications also exist. With the increase in water quality regulations such installations are expected to become increasingly abundant (Jacangelo *et al.* (1997)). Levi *et al.* (1997) described a "satellite" system, where water was treated locally using UF and NF. This avoided contamination by long distribution systems.

3.8.3 Microfiltration

MF units are widely used for turbidity removal (Hillis (1997), Tsatsaronis and Durham (1996), Ho *et al.* (1995)). Ho *et al.* (1995) installed a MF unit for turbidity and fine particles were removed satisfactorily. However, the true colour could not be removed completely without pretreatment. In the case of blue-green algae blooms, a GAC unit was used as post-treatment.

MF can be operated in dead-end or crossflow filtration mode, with the latter being of advantage if the material filtered is likely to plug the membrane. The tangential flow sweeps fouling material off the surface. The disadvantage is that the high flow rate requires more energy and this operation mode is

often reserved for feed waters with a high solids content. In surface water treatment this may be necessary, for example, after a heavy rain event.

MF, with its high potential for colloid removal, is an ideal pretreatment for processes using tighter membranes. Material removed will be held back by the membrane and partly form a deposit.

3.8.4 Ultrafiltration

UF only became popular in water treatment very recently, primarily because of its ability to remove viruses. The first plant was constructed in 1988 (Aptel (1995)). Since then, UF has been widely installed and unit costs have been reduced, with many large scale suppliers available (Doyen (1997)).

3.8.5 Nanofiltration and Reverse Osmosis

NF is often more appropriate than RO in water treatment as the product is not fully demineralised (Côté (1995)). NF has been demonstrated frequently on pilot scale to be effective in by-product removal (Mulford *et al.* (1990), Agbekodo *et al.* (1994), Ericsson *et al.* (1996), Watson and Hornburg (1989), Faivre *et al.* (1992), Alborzfar *et al.* (1998), Legube *et al.* (1995)) and many NF plants operate worldwide (Jensen and Thorsen (1995)). The largest NF plant was installed in Paris, France, after extensive pilot operations (Côté *et al.* (1993), Ventresque *et al.* (1997)). The decision to build this plant was based on a significant reduction in chlorine demand and a reduction of micropollutants compared to other processes, such as ozone combined with GAC. Low levels of pesticides are required in Europe. The membranes used exhibited high calcium and alkalinity permeabilities, which made the process more economic. Treatment costs were about 30% higher than GAC adsorption with an ozone pretreatment (Bourbigot *et al.* (1993), Ventresque and Bablon (1996), Randon *et al.* (1994)). A prototype is now operating in Méry-sur-Oise, with the production of the full-scale plant being 340 000 m^3/d with sand-filtered feed (Kopp and Chandriaux (1993)). NF achieved 90% removal of DOC, BDOC, and pesticides (Bourbigot (1994)). The NF membranes used are Filmtec TFCs tailored to achieve the optimum balance of organic removal and inorganic passage. Gagliardo *et al.* (1997) compared TFC and CA membranes, and found TFC membranes to be more economic, and the rejection and flux were higher at identical operating pressures. Reiss *et al.* (1997) also found that TFC membranes outperformed CA on rejection. It was pointed out that variations in flux and rejection of small membrane areas were large, which supported the need for pilot studies.

An NF pilot plant was operated with a MF pretreatment to remove THMPs from highly organic groundwater. The 100 μgL^{-1} THM standard was easily achieved. This process was compared to other options such as oxidant substitution, coagulant, and GAC. No other process could compete with ultra-low pressure NF (Watson and Hornburg (1989)).

A NF plant was installed for water treatment in a small community. CA membranes were used due to their hydrophilic characteristics, for which reduced fouling was reported. UF, as an alternative treatment, could only be effective with either a PAC or coagulant pretreatment, which makes operation more complex and generates a waste stream. Excellent product qualities concerning TOC, UV 254 nm, THMFP, and colour were achieved and maintenance was easy (Rachwal *et al.* (1994)). Fu *et al.* (1994) tested numerous membranes and observed that an increased rejection of charged organics and calcium carbonate scale occurred, together with organic fouling.

NF and low MWCO UF were compared for colour removal and both proved to be efficient (Arenillas *et al.* (1995)). NF was able to remove 95% of chlorinated organic compounds from pulp and paper

plant effluent (Afonso *et al.* (1992)). NF (NF70) was used on industrial scale, after sand filtered surface water treatment, to prevent organohalide formation and microbiological growth in the distribution system. Water was prefiltered for large particles. Anti-scalants were applied and the membranes were chemically cleaned biannually. Excellent water quality and good disinfection levels were obtained (Kopp *et al.* (1993)). Results after nine months operation showed excellent permeate quality (Legube *et al.* (1995)).

NF, UF, RO, and ozone oxidation were compared for the removal of colour and DBPs from groundwater. The UV/TOC ratio was used to determine the humic content of the total organics. The ratio decreased due to oxidation, which means that non-humic by-products are formed, and the average molecular weight decreased. NF showed good results, between the low rejection of UF and the high pressure of RO. NF removed about 50% TOC, all humic UV, and 88% colour. The overall removal was higher than with ozone, where humic substances were directly transformed into by-products. The disadvantage of NF was the requirement of a post-treatment step for H_2S odours (Tal and Amy (1991)).

NF was found to be a very good treatment for a groundwater high in sulphates, hardness, and sodium, although the concentrate disposal was a problem (Dard *et al.* (1995)).

Different treatment processes, such as coagulation and sand filtration, oxidation, NF, granular activated carbon, and biologically activated carbon were compared by Legube *et al.* (1995).

Van der Meer *et al.* (1996) developed a process design model for NF. The lower salt retention of NF permitted a different operation mode, and recirculation could replace a second stage. This operation lead to a higher permeate concentration and energy requirements. Van der Meer and van Dijk (1997) also developed a spiral-wound module design model for NF, which indicated that modules in NF need to be different to RO, due to the higher fluxes. Capillary modules were recommended due to the absence of spacers. DaCosta (1993) optimised spacer design. While these designs generally optimise flux and hydrodynamics, fouling has not yet been considered.

The disadvantage of a NF treatment is the high energy cost, and the generation of waste streams that need further treatment prior to disposal (Wale and Johnson (1993)). However, the generated waste stream is only a concentration of the natural components of surface water, and not a sludge of added chemicals as in coagulation or PAC. Moreover all water treatment processes inevitably produce a waste (residue stream). Product water stabilisation may also be of concern in NF, and more so, in RO. Kasper (1993) discussed different possibilities of membrane filtrate stabilisation and water disinfection.

3.8.6 Hybrid Membrane Processes

The use of a combined membrane system of MF/UF plus NF seems to be the most promising innovation (Jacangelo *et al.* (1995b)).

MF and UF have been compared as a pretreatment step for NF in colour removal. MF obtained poor colour removal (80%) and flux reduction is higher for the higher flux membranes (MF) (Chang *et al.* (1995)). Chellam *et al.* (1997) compared MF and UF (10 kDa) as pretreatment for NF and found no difference, but both performed significantly better than conventional pretreatment, which was attributed to colloid removal. A low flux and high recovery operation was recommended for NF. UF has been used as a pretreatment to RO in water treatment (Kamp (1995)). Amy *et al.* (1993) stated that to guarantee low fouling of NF, pretreatment with MF or UF was required. MF was only moderately

effective in particulate removal. Lozier and Jones (1997) operated a MF and NF hybrid system. MF reduced particle fouling of the NF, but NF fouling remained high. Both TFC and CA membranes showed similar fouling. Chellam *et al.* (1997b) suggested that dual membrane systems (MF/UF plus NF) could reduce NF fouling. Conventional pretreatment was not sufficient.

Rautenbach and Gröschl (1990) described NF as a pretreatment step to RO to increase the recovery of the RO process, due to the removal of scaling agents by NF. NF also has the advantage that a concentrate of a relatively low salinity is produced which may be used for irrigation, reducing the quantity of concentrate to be disposed (Dal-Cin *et al.* (1995)).

3.8.7 Cost

Membrane processes and membranes have changed significantly in recent years. The membrane characteristics required depend on the application as described in previous sections. NF represents an interesting trade-off between the high energy requirement RO and the low rejection UF. If waters are turbid, but not coloured or polluted with micropollutants, MF is an attractive, low cost, option. Total treatment costs (capital and operating) in water treatment applications are summarised for the four processes in Table 3.3.

Table 3.3 *Typical operation parameters for membrane processes in water treatment. Values are ranges given by different authors (Côté (1995), Jacangelo et al. (1999), Wiesner et al. (1994), Nyström et al. (1995a), Lozier and Jones (1997), Clair et al. (1997), Ericsson et al. (1996), Taylor et al. (1987), Ødegaard and Thorsen (1989), Hagmeyer et al. (1996), Pickering and Wiesner (1993), Chellam et al. (1998), Sethi and Wiesner (1995), Tan and Sudak (1992)).*

Process	Flux [$Lm^{-2}h^{-1}$]	Operating Pressure [bar]	Permeability [$Lm^{-2}h^{-1}bar^{-1}$]	Recovery [%]	Total Cost [US$$m^{-3}$]	Capacity [m^3d^{-1}]
Conventional	2 000-10 000	0.1-2.0	-	-	0.85-0.15	380-17 000
Conventional+ O_3+GAC	-	-	-	-	1.15-0.55	380-17 000
MF	68-170, 100-1 000	0.3-2.1, 0.2-2	60-250	90-98	0.10-0.11, 0.21-0.49, 0.03-0.27	8700 4800
UF	68-170, 50-200	0.5-2.1, 1-5	60-250	90-98	0.45-0.20, 0.10-0.21, 0.04-0.14	380-17 000, 2880-55200
NF	25-34, 20-50, 10-100	5.2-8.6, 5-20	5-10	75-95	0.85-0.30, 0.34-0.96, 0.16-0.53	380-17 000
RO	12-25, 10-50	10.3-103, 20-80	<5	50-80	0.23-0.92*	-
MF/UF+NF	17-34	2.5-5	-	-	0.74	-

* low pressure and brackish water, not desalination applications. Costs for desalination 1.06-2.11 US$$m^{-3}$.

According to Durham (1997), RO process costs reduced by 30 to 40% after the development of MF pretreatment. Pickering and Wiesner (1993) concluded their cost modelling with the comments that cost is largely a function of flux, as flux determines the membrane area to be installed. At small design capacities (2000 m^3h^{-1}), MF and UF costs were competitive with conventional treatment. UF was less costly than MF for larger facilities (>20 000 m^3h^{-1}). Chellam *et al.* (1998) also published a sharp decrease in total NF cost with an increased recovery. Vigneswaran and Fane (1998) described the lower end of production costs as 0.33, 0.28 and 0.18 US$$m^{-3}$, and since the development of the submerged MF system the costs for MF decreased to 0.07 to 0.10 US$$m^{-3}$ (Fane (1999)).

Sethi and Wiesner (1995) modelled the cost of MF and UF processes and found a sharp increase for recoveries higher than 90%. The importance of particle size in cost evaluation was also pointed out, and cost also increased with particle concentration. UF was cost competitive with conventional treatment for low particle concentrations (up to 20 mgL^{-1}), if particles are 0.1 μm on average. The presence of larger colloids improved flux (and cost), while small foulants like NOM made the process less economic.

According to Khow *et al.* (1997), NF is cost-competitive with conventional processes up to plant sizes of 10 000 m^3/day. Filteau and Moss (1997) developed a cost model for evaluation of NF and RO processes.

3.9 CONCLUSION

From this review it appears that the application of theoretical models to natural organics separation and fouling would be premature. Model substances are required, but it appears that they do not to give similar fouling as the surface water mixture.

Ion rejection studies are not an objective of this study. However, the ion rejection of the system used and the variation of ion rejection due to fouling are important issues. Improvement in our understanding of boundary layer mechanisms seems more appropriate at this stage. Issues worthy of further investigation are,

- MF of colloids smaller than the pores and colloid-organic systems
- Rejection characteristics of fouled membranes
- Mechanism of calcium-organic fouling (bridging, complexation, co-precipitation)
- Effect of organic aggregation on flux
- Effect of MWCO on fouling and rejection mechanism
- Importance of solute-solute interactions on deposit morphology
- Influence of solute-solute interactions on gel layer formation
- Concentration polarisation effects for "dilute" surface water systems
- Separation of charge and size effects for organics and ion separation and the effect of speciation
- Effect of pretreatment on membrane processes for rejection enhancement and fouling control.
- Colloidal fouling experiments with model colloidal systems and known aggregation behaviour

- Distinction between pore and surface fouling
- How changes in a membrane module effect fouling and rejection due to higher concentration and lower flow
- Which organics are not retained and how pretreatment can target these compounds

From a thorough understanding of fouling mechanisms, a well designed cleaning scheme can be developed. This seems however beyond the scope of this study. The choice of hydrophilic membranes is essential. As discussed in Chapter 2, many NOM parameters remain unknown and will be unknown for a given water. It would be useful to more clearly define those NOM characteristics that correlate with rejection and fouling characteristics. It is also important that research be carried out close to surface water conditions rather than in model systems (provided excessive complexity does not preclude results interpretation).

Small scale fouling studies are necessary. Many pilot studies have shown that membrane processes work in principle, but that fouling can be a difficult problem. Large units often do not permit the variation of enough parameters and results are often contradictory.

Further it appears that a study of the range of membrane processes at comparable conditions is needed with a thorough characterisation of the membranes used. This comparative study would then allow the identification of a process for a given feed water condition which is most economic and which exhibits an acceptable health risk. This thesis is a contribution to this comparison of membrane processes for water treatment.

Chapter 4

MATERIALS & METHODS

In this chapter the materials used (chemicals, organics, colloids, membranes and filtration equipment) are described. Membrane characteristics as provided by the manufacturer are summarised. Solution preparation and analytical methods are also presented, including the methods used for organics, aggregate, and membrane deposit characterisation.

Filtration protocols are described in the relevant chapters, microfiltration, ultrafiltration and nanofiltration, respectively. Membrane characteristics such as surface charge and morphology are also presented in these chapters.

Some methods which required special attention, such as concentration of NOM, drawings and hydrodynamic analysis of the filtration equipment, synthesis of hematite colloids, instrument calibration (DOC and UV), and solution speciation are shown in Appendix 1, 2, 3, 4, and 5, respectively.

4.1 CHEMICALS AND BACKGROUND SOLUTION

All chemicals used were of analytical grade from Ajax Chemicals. 1M HCl, NaOH, and NaCl solutions were used for pH and ionic strength adjustments. For some experiments, KCl or $CaCl_2$ were used as the electrolyte. This is indicated in the relevant results section. Dextran standard (MW 1000 Da), which was used for NF pore size comparison, was purchased from Fluka, Australia.

MilliQ water was produced with a six step method; MilliRO, Super-C Carbon Cartridge, Ion Exchange Cartridge, Ion Exchange Cartridge, Organex-Q Cartridge, Milli-Pak Filter. For DOC analysis and standards, water from a regularly sterilised MilliQplus system was used. The MilliQ quality was >18 MΩ/cm.

Experiments were carried out in a background buffer solution that was chosen as a simple model of natural surface waters, with a monovalent and divalent cation and a background electrolyte to allow pH adjustment without changing ionic strength. The concentration of the cation calcium, was selected after the analysis of the Mooney Mooney Dam surface water. The composition of this water is shown in Appendix 1. The composition of the model system is summarised in Table 4.1. This background solution was used in all experiments, if not otherwise indicated. The species in solution as a function of solution chemistry is described in Appendix 5.

Table 4.1 *Background buffer solution composition ("stock").*

Compound	Molecular Weight [Da]	Concentration [mM]	Concentration [mgL^{-1}]	Purpose
$NaHCO_3$	84	1	84	Buffer
NaCl	58.5	20	$2.935 \cdot 10^3$	Background electrolyte
$CaCl_2$	111.5	0.5	56	Representative of dominant multivalent ions present

4.2 ORGANICS

Humic substances were purchased from the International Humic Substances Society (IHSS, USA). Suwannee River Stream Reference humic (HA) and fulvic acids (FA) were used.

The organics are extensively characterised by IHSS (Averett *et al.* (1989)). As a third organic, 5000L of surface water from the Mooney Mooney Dam (Brisbane Water National Park, NSW, Australia) were concentrated using microfiltration (MF) and reverse osmosis (RO) and freeze dried. The procedure is described in Appendix 1. Aldrich HA, a commercially available product (Sigma Aldrich, Australia) was used for comparison in some experiments. This HA is not from a aqueous source, but nevertheless frequently used in the literature.

Further characterisation is reported in the organics characterisation section below. An overview over some characteristics is also sown in Chapter 2. The organics were prepared as 100 mgL^{-1} organic carbon stock solutions by mixing the dry powder with MilliQ water without increasing the pH. The solutions were stored at 4^0C in the dark. The amount of powder required for 100 mL stock solution was 18.4 mg, 18.6 mg and 200 mg for HA, FA and NOM respectively. This reflects the carbon content of the organics.

4.3 HEMATITE COLLOIDS (α-Fe_2O_3)

Hematite was selected as a model colloid in this study due to its well understood aggregation behaviour, the monodisperse, spherical nature of the colloids and the fact that the synthesis of colloids of various primary particle sizes (40 to 500 nm) is possible. While silica and clays may be more abundant in surface waters, hematite appears to be a good compromise between real systems and a simple model compound.

The synthesis of monodispersed, spherical hematite colloids of four primary particle sizes is described in detail in Appendix 3. The main properties of these colloids are also given in Appendix 3.

4.4 MEMBRANES

Commercially available flat sheet membranes were selected. The primary selection criterium was that the membrane be made of a hydrophilic material, which adsorbs less organics than more hydrophobic polymers. For comparison, the membranes used are listed in Table 4.2 with their pore size or molecular weight cut-off (MWCO) as specified by the manufacturer.

Table 4.2 *Characteristics of MF, UF and NF membranes used in experiments.*

Process	Supplier	Type	Typical Operating Pressure [bar]	Specifications Pore Size [μm] Molecular Weight Cut-Off [kDa]	Pure Water Flux [$Lm^{-2}h^{-1}$]	Surface Charge at pH 8 [mV]
MF	Millipore	GVWP	1	0.22 μm	7970 ± 290	-21.1
		GVHP	1	0.22 μm	8090 ± 320	-9.8
UF	Millipore	PLHK	1	100 kDa	1320 ± 40	-17.3
		PLTK	1	30 kDa	390 ± 20	-16.4
		PLGC	3	10 kDa	65 ± 5	-7.5
		PLCC	3	5 kDa	28 ± 3	-14.3
		PLBC	3	3 kDa	22 ± 2	-9.2
		PLAC	3	1 kDa	15 ± 2	-11.6
NF	Fluid Systems	CA-UF	5	-	50 ± 4	-11.0
		TFC-SR	5	-	46 ± 6	-21.8
		TFC-S	5	-	49 ± 6	-6.5
		TFC-ULP	5	-	19 ± 3	-19.4

This characterisation is relatively vague, as different methods are used by each manufacturer (Readman (1991), Thorsen *et al.* (1997)). As a more comparable parameter, the pure water fluxes as determined in the experiments are also given, as well as the membrane zeta potential at pH 8. A new membrane was used for each experiment (except for fractionation experiments).

The results of surface charge measurements of the membranes as a function of pH, pure water fluxes and electronmicrographs are shown in the MF, UF, and NF chapters, respectively.

4.4.1 Microfiltration Membranes

Two microfiltration membranes (Millipore, hydrophilic (GVWP) and hydrophobic (GVHP)) with nominal pore sizes of 0.22 μm were used. The hydrophilic membrane is a modified hydrophobic membrane. The hydrophilic membrane was chosen for most experiments because hydrophilic membranes have a reduced adsorption capacity towards hydrophobic organics (Jucker and Clark(1994)). The membrane material is a modified polyvinylidene fluoride (PVDF).

The hydrophobic membrane was soaked in a 50% ethanol solution for 10 minutes to wet the pores and then rinsed with MilliQ water. All membranes were soaked in warm MilliQ water for 30 minutes prior to use to remove any organic contamination.

4.4.2 Ultrafiltration Membranes

Ultrafiltration was used for fouling, rejection, and fractionation experiments. The fractionation experiments require membranes with very low adsorption characteristics to reduce loss of organics on the membranes. It was thus necessary to find low fouling membranes, which are available in a range of membrane molecular weight cut-offs (MWCO). The Millipore "PL series" fulfil the low adsorption condition and they are available in seven MWCOs in the range from 1 kDa to 300 kDa. The fractionation membranes selected were the PLAC, PLBC, PLCC, PLGC, PLTK, and PLHK with MWCOs of 1, 3, 5, 10, 30, and 100 kDa, respectively. Fouling and rejection experiments were carried out with the 10 and 100 kDa membranes.

These regenerated cellulose membranes on a non-woven polypropylene substrate are described by the manufacturer as low protein-binding and hydrophilic. The MWCO (as described in Table 4.2) is determined by a range of Dextran markers. A MWCO of 10 kDa means that 90% of markers with a molecular weight greater than 10 kDa were retained.

Prior to use, the membranes were soaked in 0.1 M NaOH for 30 minutes and flushed with 3.4 L of MilliQ water in order to remove the glycerin preservative, which can strongly interfere with UV and DOC analysis. Alternatively, flushing the membrane with 1L MilliQ also removed the glycerin sufficiently.

4.4.3 Nanofiltration Membranes

Nanofiltration membranes were received from Fluid Systems in San Diego, USA (now Koch Membrane Systems). Thin film composite membranes were chosen due to their low fouling characteristics compared to polysulphone membranes used in other studies. The CA-UF membrane is, as the name suggests, classed as a UF membrane and the material is cellulose acetate. However, it is treated as a NF membrane here as it is often used for similar applications according to the manufacturer, and also because it exhibits some salt rejection. Membrane characteristics as given from

the supplier are summarised in Table 4.3. The cut-off was specified to be about 5 kDa and the material is non-ionogenic. The active layer of this membrane is about 150 nm. CA membranes have generally a 50% lower flux than TFC membranes, but are cheaper.

The TFC membranes are chemically modified to render the membranes more hydrophilic, but more details were not available. All three membranes have different additives and post-treatments in the manufacturing process. The manufacturer estimates the thickness of the active layer of the TFC membranes to be 150 to 200 nm. For the TFC-SR membrane a different monomer was used compared to the other TFC membranes. While the TFC-S and TFC-ULP membranes are made from metaphenylene diamine with acid chloride (a benzene ring with two to three carboxylic acid groups), the TFC-SR membrane is fabricated from a mixture of cyclo-aliphatic amine with acid chloride. This means that the TFC-S and TFC-ULP have both positive and negative functional groups, whereas the TFC-SR membrane has negative functional groups only. Marker tests with 1% lactose (180 Da) solutions at pH 6-7 showed a rejection of 94.4% and 90.6% for the TFC-SR and TFC-S membranes, respectively. Rejection of the membrane is expected to be higher (Takigawa (1999)).

Table 4.3 *Membrane Information from Fluid Systems Corporation (now Koch Membrane Systems), San Diego.*

	TFC-S	TFC-SR	TFC-ULP	CA-UF
Material	TFC Polyamide (PA) on Polysulfone (PS) base	TFC proprietary PA on PS base, coated with PVA (dye to check for damage)	TFC PA on PS base	Cellulose Diacetate
Test Conditions	1 g/L NaCl, 2.5 g/L $MgSO_4$ 25^{0}C pH 7.5 5.6 bar	1 g/L NaCl 2.5 g/L $MgSO_4$ 25^{0}C pH 7.5 5.6 bar	2 g/L NaCl 25^{0}C pH 7.5 7 bar	tap water 3.5 bar
Flux	14.7 L/m^{2}h	14.7 L/m^{2}h	14.7 L/m^{2}h	16.5 L/m^{2}h
pH range	4-11	4-11	4-11	4-6
Rejection	95% hardness, 85% Cl	98.5% hardness, 30% Cl	98.5% Cl	Not specified
Design Application	NF or softening of municipal water at ultralow pressure; up to 45^{0}C	nanofiltration or softening of municipal water at ultralow pressure; up to 1 ppm Cl_2; up to 45 ^{0}C	Industrial or municipal water ultralow pressure	Surface water at moderate pressure if chlorination desired (up to 1 ppm Cl_2)
Design Pressure	5.6 bar (560 kPa)	5.6 bar (560 kPa)	3.5-12.25 bar (560-1225 kPa)	3.5 bar (560 kPa)
Storage Medium	0.5% sodium meta bisulfite, MilliQ after wash	dry MilliQ after wash	dry MilliQ after wash	unknown
Pretreatment	wash with MilliQ	wash with warm MilliQ to remove PVA coating	soak in MilliQ	wash with MilliQ

All membranes were stored in a refrigerator (4 ^{0}C) in plastic bags in the medium in which they arrived, and sealed. A few membranes of each type were cut out, pretreated and then placed in a petrie dish in the refrigerator for use in experiments.

4.5 FILTRATION EQUIPMENT

Stirred cell systems were selected for the experimental work for a number of reasons; (i) volumes are small which is required for the use of IHSS reference material, (ii) membrane samples are small which allows the use of a new membrane for each experiment, (iii) the solution chemistry can be precisely controlled, (iv) experiments are relatively short and thus the investigation of a great number of parameters is possible, and (v) the concentration in the cell represents the concentration in a crossflow module (recovery about 70%). A comparison of mass transfer values was demonstrated in the case of NF in Chapter 7. Drawings of the filtration equipment are shown in Appendix 2. A hydrodynamic analysis is also shown in Appendix 2.

4.5.1 Microfiltration Equipment

All experiments were carried out in a magnetically stirred batch cell (volume of 110 mL, membrane area $15.2 \cdot 10^{-4}$ m^2) at a pressure of 100 kPa (if not otherwise indicated), pressurised with nitrogen gas. A reservoir of 1.5 L volume was connected to the stirred cell. A photo of a Perspex stirred cell with reservoir, manufactured in the university workshop, is shown in Figure 4.1.



Figure 4.1 *Perspex stirred cell with reservoir.*

All stirred experiments were stirred at 270 rpm (measured with a Philips PR 9115/00 stroboscope). A balance and stop watch were used to measure permeate volume. Experiments were conducted at a temperature of 25 ± 1 ^{0}C.

4.5.2 Ultrafiltration Equipment

The same system as described in the MF section and shown in Figure 4.1 was used for all rejection, fouling, and fractionation ultrafiltration experiments. The balance was connected to a PC for flux data collection.

4.5.3 Nanofiltration Equipment

Nanofiltration experiments were carried out in a stainless steel stirred cell with an Amicon magnetic stirrer on a magnetic heater plate (Industrial Equipment & Control, Australia). The calibration is shown in Figure 4.2.

The volume of the cell was 189 mL, the inner diameter 56.6 mm (resulting in a membrane surface area of $21.2 \cdot 10^{-4}$ m^2). The stirrer speed could be varied from about 200 to 2000 rpm, with a setting of 400 rpm used routinely. The stirrer speed was measured using a Philips PR 9115/00 stroboscope. One side of the stirrer bar was labelled to avoid measuring of half rotations.

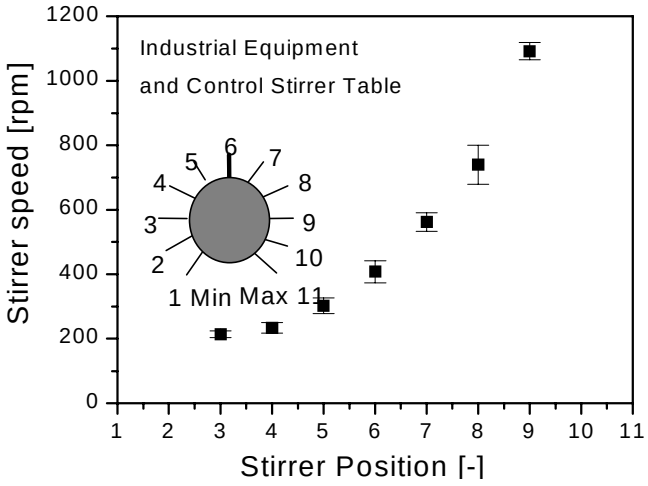


Figure 4.2 *Calibration of magnetic stirrer table.*



Figure 4.3 *Stainless steel stirred cell set-up.*

The stirred cell was pressurised with instrument grade air. Air was used (rather than N_2), to provide CO_2 for the carbonate buffer. pH changes due to the high pressure air were estimated to be less significant than with N_2 (see Appendix 5 for details). A photo of the set-up is shown in Figure 4.3 and a schematic in Figure 4.4.

The cell was equipped with a pressure gauge mounted in the stainless steel line after the air cylinder, a stainless steel reservoir with a volume of 2 L, a pressure release valve, a fluid inlet and outlet connection, a pressure safety valve, and a refill opening on top of the reservoir. On top of the stirred cell, a fluid inlet connection, a pressure release valve and a temperature probe fitting were mounted. The temperature was measured with a PT 100 probe, connected to a Kane-May KM 330 indicator.

To control the temperature inside the cell, it was placed in a 2 L plastic beaker, through which tap water was circulated continuously. The temperature was kept constant (unless otherwise indicated) at 20 ^{0}C ± 1 ^{0}C. Permeate flux was measured by weight with a Mettler-Toledo PR 2002 (0.1 to 2100g) balance, which was connected to a PC equipped with Mettler-Toledo BalanceLink software.

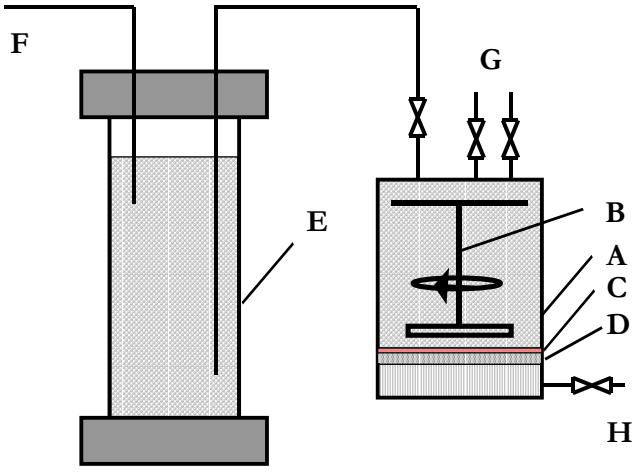


Figure 4.4 *Stainless steel stirred cell set-up. A: stirred cell, volume 185 mL; B: magnetic stirrer (Amicon, driven by magnetic stirrer table); C: membrane; D: stainless steel porous support; E: reservoir volume 2000 mL, F: pressurised instrument air inlet, G: feed inlet, pressure release and safety valves; H: permeate outlet (to balance and PC).*

4.6 GENERAL ANALYTICAL METHODS

4.6.1 pH Value

A Beckman glass electrode (Ag/AgCl) was used for solution preparations and no contamination was observed. The electrode was only used in samples after DOC analysis and was cleaned prior to use for pH adjustment.

4.6.2 Conductivity

Conductivity was measured using a Lutron CD-4303 portable instrument.

4.6.3 Inductively Coupled Plasma Atomic Emission Spectroscopy (ICP-AES)

A Perkin Elmer Optima 3000 Spectrometer was used to determine the cation content of solutions. Samples and multielement standards (0, 1, 10 and 100 mgL^{-1}) were diluted with 5% nitric acid. All vials used were cleaned with 1 M sulphuric acid. Detection limits are 3, 5, 0.1, 5, and 70 μgL^{-1} for Fe, Al, Ca, Na, and K, respectively.

The particle sol and filtration samples were diluted 1:1 with HCl (36%) and heated (in a closed sample vial) to dissolve the colloidal hematite. These samples were then analysed directly.

4.6.4 Ion Chromatography (IC)

IC was used for chloride determination for NF rejection experiments. Anions could not be analysed using IC, as humic substances interfere with the analysis (Hoffmann *et al.* (1986)). A Millipore Waters Model 590 instrument was used with a Model 430 Conductivity detector. The eluent used was 0.68 gL^{-1} boric acid (H_3BO_3), 0.235 gL^{-1} gluconic acid anhydride ($C_6H_{10}O_6$) and 0.3 gL^{-1} lithium hydroxide ($LiOH \cdot 6\ H_2O$).

4.7 ORGANICS CHARACTERISATION

4.7.1 Dissolved Organic Carbon (DOC)

Dissolved organic carbon was analysed using a Skalar 12 instrument. The method is based on UV-persulphate oxidation and described in detail in Appendix 4. The DOC of every sample was measured as a routine analysis.

For samples containing colloids, aggregates or flocs the measured value is total organic carbon (TOC). None of the samples were filtered as this would lead to loss of organics.

4.7.2 UV/VIS Spectroscopy

A Varian Cary 1E UV/VIS Spectrophotometer was used to evaluate the method and for further standard analysis. Spectra of UV/VIS in the range from 190 to 500nm were obtained and correlations established with DOC analysis. The method is further described and evaluated in Appendix 4. UV/VIS was also a routine analysis and the wavelength was used in rejection calculations.

At low wavelength (190 nm region), absorption by inorganics is observed. This is strong in the case of unpurified Mooney Mooney NOM and absent in the purified IHSS samples. The ion content of all samples is shown in section 4.7.6.

The UV/VIS spectrum of NOM is attributed mainly to absorption of light energy by aromatic compounds and can be broken into a series of transition bands, similar to those published for benzene (Korshin *et al.* (1997b)). Three transition bands can be distinguished for each aromatic chromophore in NOM - the local excitation (LE) band, the benzenoid (Bz) band, and the electron-transfer (ET) band. The peaks vary in their height, width, and centre location depending on the composition of the NOM (Kaeding (1998)). The presence of these various peaks can be recognised in the shoulders on the spectra as shown in Figure 4.5, however detailed analysis was not considered warranted.

From Figure 4.5, it can be seen that the (probably) soil-derived Aldrich HA (purified with a 100kDa UF membrane) has the largest UV/VIS absorbance, followed by IHSS and the NOM HA fraction which are surprisingly similar. The FA fraction of Mooney Mooney NOM has a higher absorbance than the unpurified NOM, which can be explained given the NOMs relatively high content of hydrophilic acids of a very low absorbance. The IHSS FA also has a slightly lower absorbance over the complete wavelength range.

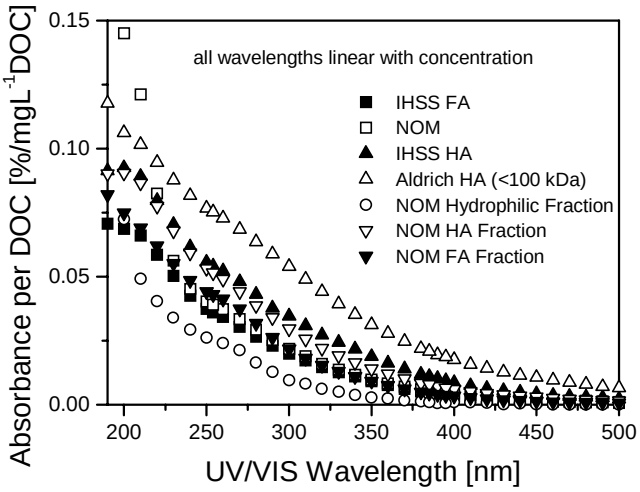


Figure 4.5 *UV Spectra of the organics used.*

4.7.3 Titration

The NOM sample, which was concentrated as described in Appendix 1, was titrated using a Metrohm automatic titrator. The titrator was operated in dynamic titration mode. The samples were acidified from ambient pH to pH 2.8 with 0.1 M HNO_3 and subsequently alkalised with 0.1 M NaOH to pH 10. It was assumed that at pH 2.8 all acidic functional groups will be saturated, whereas at pH 10 all carboxylic and half of the phenolic groups were dissociated. The limitations of these assumptions were discussed in Chapter 2.

The titration vessel was purged with nitrogen to eliminate CO_2. From the volume and molarity of added base and the mass of titrated DOC, the content of acidic functional groups can be calculated. Carboxylic acid content was calculated from the amount of base added until the end-point was reached. Phenolic acid content was calculated as twice the difference in titrant required to change the pH of the titrate from 8 to 10, since it was assumed that at pH 10 only half the phenolic groups were dissociated. A solution of a concentration of 20 mgL^{-1} as DOC NOM were titrated. The error due to the salt content of NOM is likely to be high.

Table 4.4 describes the acidity and size of the three organics used and the average molecular weight as found in the literature (for IHSS organics and purified Aldrich HA) or as measured (for NOM). The reported MW will be verified later (see section 4.7.7) by analysis.

Table 4.4 *Acidity and average molecular weight of the organics ([1]Jucker and Clark (1984),[2]Beckett et al. (1987), [3]Hering and Morel (1988),[4]analysed by titration (see above), [5]Clark and Jucker (1993), [6]Childress and Elimelech (1996)).*

Type of Organic	Acidity [meq.g^{-1}]		Average Molecular Weight [kDa]		
	Carboxylic	Phenolic			
IHSS FA	3.4[1] 5.4[5] 6.1	1.5[1] 2.0[5]		750[2]	
IHSS HA	4.0[1] 4.1[6]	2.9[1] 2.1[6]	1100[3]	1500[2]	1200[4]
Purified Aldrich HA	3.3[6]	2.5[6]		> 50 000[6]	
Mooney Mooney NOM	5.1[4]	1.3[4]		< 1000[4]	

4.7.4 Elemental Analysis

Elemental analysis of the IHSS reference material was provided by IHSS with purchase of the organic material. The elemental analysis was performed for IHSS by Huffman Laboratories (Wheat Ridge, CO, USA). Results are summarised in Table 4.5.

Table 4.5 *Elemental analysis results of the organics used.*

Sample [%]	C	H	O	N	S	P	Total	H_2O	Ash
Stream HA Reference	52.89	4.14	43.40	1.17	0.58	<0.01	102.2	9.8	3.46
Stream FA Reference	53.04	4.36	43.91	0.75	0.46	<0.01	102.5	8.9	0.98
Mooney Mooney NOM	6.3	-	-	-	-	-	-	-	-

The Mooney Mooney Dam NOM was also to be analysed by IHSS. However, the wet digestion method which is used for HA and FA cannot be applied directly to NOM and is currently being revised. The method to be developed will also analyse the ash composition.

4.7.5 XAD Fractionation

The XAD fractionation method is the classic concentration method for humic substances (see also Chapter 2). The IHSS HA and FA samples were isolated using this method. This procedure was therefore used to obtain humic substances from the Mooney Mooney NOM. The fractions were used for NOM concentration and for experimental work.

A stock solution of about 4 g NOM in 500 mL water was prepared, resulting in a solution concentration of 291 mgL^{-1} as DOC or a total mass of 145.5 mg organic carbon. The solution was then desalted using an Amicon YC05 membrane (molecular weight cut-off 500 Da). According to Amicon, this UF membrane does retain large salts such as phosphates and sulphates, but does not retain a significant amount of smaller-sized salts. 310 mL of permeate were collected and discarded, resulting in a loss of 5.0 mg organics (as DOC). Thus, 2.5% of organics, could be considered smaller than the membrane pores.

The remaining solution volume of 190 mL was fractionated using the method of Leenheer (1981, 1996). Results are presented for the NOM sample in Figure 4.6.

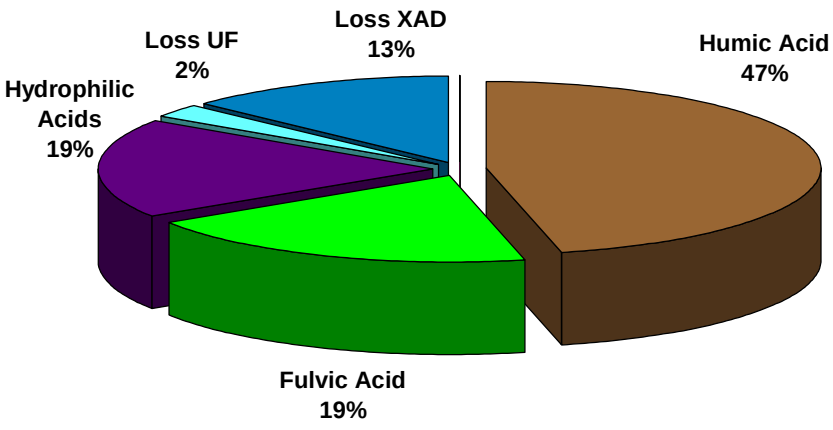


Figure 4.6 *Composition of Mooney Mooney Dam NOM in percent.*

The sample has a high proportion of HA (47%) compared to fulvic and hydrophilic fractions (19% each). This could account for the high microbiological activity in the Mooney Mooney Dam, which would result in a consumption of the more accessible fulvic and hydrophilic compounds. The relatively high loss of organics in the XAD procedure is probably due to the presence of particulate organic matter.

4.7.6 Cation Content of Organics

The cation content of the organic samples was determined using ICP-AES (see section 4.6.3 for analytical details). Results are shown in Table 4.6.

The values per 100 mg DOC show the high salt content of NOM and its fractions. While the IHSS samples and the XAD extracted HA and FA fractions of NOM are very low in cation content, the NOM, the hydrophilic fraction of NOM, and the purified Aldrich HA have all very high cation contents. The hydrophilc fraction has accumulated the entire salt content of the NOM sample. This does not mean that all ions are associated with the hydrophilic fraction, but due to the purification method all ions remain in the hydrophilic sample. This needs to be considered when treatment data of this sample are interpreted.

Table 4.6 *Cation content of organics used. The salt content is per amount of DOC due to the stock solution concentration. Values in brackets are per 100 mgL^{-1} DOC, thus mg cations per 100 mg DOC.*

	IHSS HA	IHSS FA	NOM	NOM HA	NOM FA	NOM Hydrophilic	Aldrich 100 kDa
DOC [mgL^{-1}]	100	100	100	250.3	114.5	22.1	12
Al [mgL^{-1}]	0.10 (0.10)	0.02 (0.02)	0.58 (0.58)	0.24 (0.10)	0.07 (0.06)	0.47 (2.13)	0.28 (2.33)
Ca [mgL^{-1}]	0.22 (0.22)	0 (0)	62.6 (62.6)	0.61 (0.24)	0.24 (0.21)	48.6 (219.9)	0.94 (7.83)
Fe [mgL^{-1}]	0.11 (0.11)	0 (0)	1.41 (1.41)	0.46 (0.18)	0.36 (0.31)	1.2 (5.43)	0.15 (1.25)
Na [mgL^{-1}]	1.52 (1.52)	0.23 (0.23)	296 (296)	3.16 (1.26)	3.54 (3.09)	244 (1104.1)	12.3 (102.5)
K [mgL^{-1}]	0.55 (0.55)	0.41 (0.41)	52.4 (52.4)	2.16 (0.86)	1.19 (1.04)	1.43 (6.47)	0.47 (3.92)

4.7.7 High Performance Size Exclusion Chromatography (HPLC-SEC)

Size exclusion chromatography (SEC) enables the determination of the molecular size of organic molecules. Samples were filtered through a 0.45 μm filter (Gelman Sciences Acrodiscs) prior to analysis. The membrane filter material was Supor (Polyether-sulphone).

SEC was performed according to the method of Chin *et al.* (1994). A Shodex KW802.5 SEC column (Waters Corp., Milford, MA., USA) was used and a Waters liquid chromatography system consisting of the following components was used for the analysis: Waters 501 high pressure pump, Waters 717 autosampler, InterAction column temperature control oven, Waters 484 UV/VIS detector, and Waters Millenium 2.0 computer software package.

The mobile phase consisted of 200 mM phosphate at pH 6.8, adjusted to an ionic strength of 0.1 M with high purity NaCl. The eluent was filtered through a preconditioned 0.22 μm membrane filter to prevent interference from particulates. The system was operated at 1.0 mL/min and 30^{0}C, with 200 μL

injections and detection at 260 nm. The mobile phase was degased for 30 minutes in an ultrasonic bath prior to use.

The system was calibrated using polystyrene sulphonates (PSS) (Polysciences, NJ, USA). 1 gL^{-1} standards were prepared (35, 18, 8, 4.6 kDa). Blue Dextran, a high molecular weight polysaccharide (approx. 2 000 kDa) and an acetone solution (1%) were used to determine the column's void volume and total permeation volumes, respectively. The PSS's were detected at 224 nm (see Figure 4.7), the acetone at 280 nm and the Blue Dextran at 260 nm. All samples were detected well inside the 15 min/sample run time.

$$Molecular\ Weight = 10^{(\text{Slope of Line} \cdot \text{RetentionTime})} + Intercept\ of\ the\ Line. \qquad (4.1)$$

The log of the molecular weight versus peak retention time for the PSS standards were plotted and consistently yielded a straight line. By using the calibration equation:

The raw detector response versus retention time were converted to graphs of detector response versus apparent molecular weight. The molecular weight determined for the organics used in this work is shown in Figure 4.8. A number of observations can be made.

Surface water is the water from Mooney Mooney Dam prior to concentration and freeze drying, whereas NOM is the redissolved powder of the same water. A small, but nevertheless clear, increase in molecular weight can be seen. It is thus obvious that the organic is being modified even using this comparably "soft" concentration method.

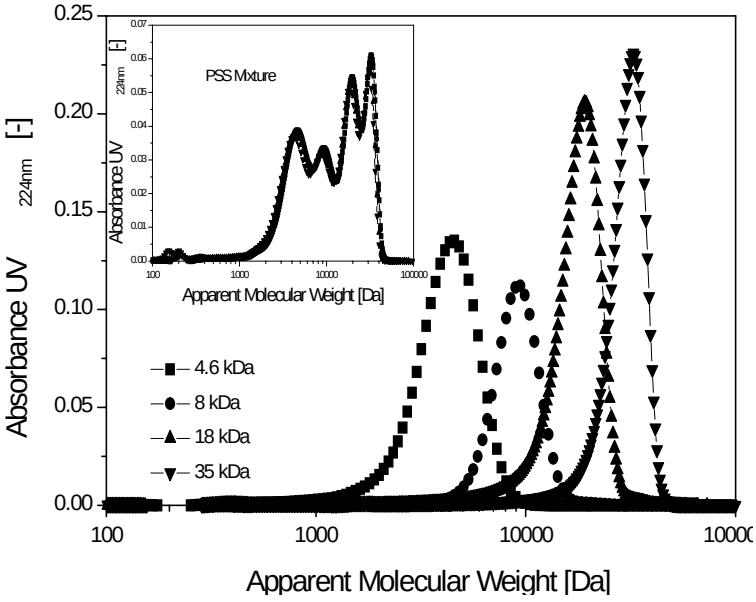


Figure 4.7 *HPLC-SEC PSS standards in single solutions and as a mixture.*

The Aldrich HA has the largest size. Once this organic is purified by filtration through a 100 kDa MWCO UF membrane, the size becomes comparable to the other organics. Of the purified compounds, IHSS HA is the largest organic, and surface water the smallest. All organics have a size distribution. The narrow peak at 300 Da is the salt peak. IHSS FA has a broader size distribution than IHSS HA. Table 4.7 shows a summary of the peak molecular weight values. The values are the peak height MW as determined from Figure 4.8.

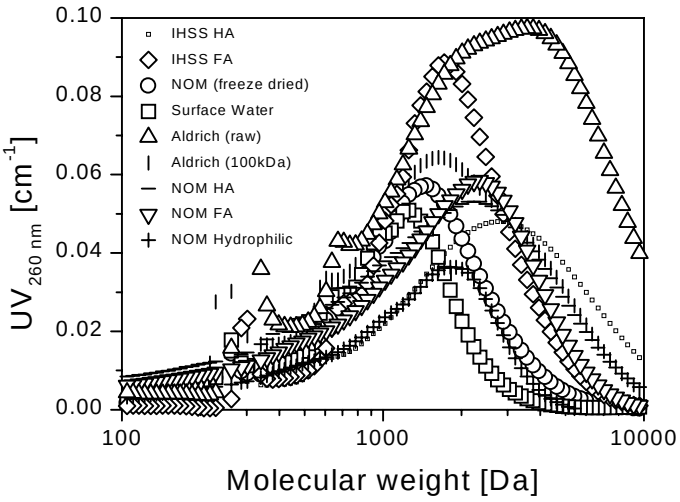


Figure 4.8 *Size distribution of the organics used determined by SEC (all organics measured in background solution).*

The Suwannee River (IHSS) organics are large compared to the surface water and NOM samples. This could be due to the high initial organic concentration in the Suwannee River and its swampy nature.

The method does not give 'true' results due to the use of UV absorbance as the detection method. This method preferentially analyses larger compounds selectively (see Chapter 2), and is therefore likely to overestimate MW results.

Table 4.7 *Molecular weight [MW] of the organics used (as peak value from* **Figure 4.8***).*

Organic	IHSS HA	IHSS FA	Aldrich Raw	Aldrich Filtered	Surface Water	NOM	NOM HA	NOM FA	NOM Hydrophilic
MW [Da]	3000	1800	4000	1500	1100	1200	2050	2300	1800

The large values obtained for the NOM fractions (analysed in a different batch as the NOM) cannot be explained with the overestimated MW. The reason for the discrepancy with other techniques are unclear and points out possible problems due to calibration.

4.7.8 Ultrafiltration Fractionation

Ultrafiltration is another method for the determination of the molecular weight, or more correctly, size of organics. The results often compare poorly to SEC results, as the methods emphasise different characteristics of the organics. Charge effects can be important in UF and SEC. Both can be suppressed by adjusting the ionic strength of the samples, but this will also influence the size and the conformation of the molecules. In order to understand better the impact of solution chemistry on the UF fractionation result, the method was examined thoroughly. Two filtration protocols were tested for analytical fractionation of samples; serial and parallel fractionation. UF fractionation could not produce samples large enough in concentration for further experimentation, at least not at volumes and concentrations at which the rejection is not influenced. Preparative fractionation was thus not used, as the concentration of permeate samples would have been necessary, which was not feasible at the volumes required. The transmembrane pressure for fractionation was 300 kPa for the 1,3,5 and 10 kDa membranes and 100 kPa for the 30 kDa membrane. Membranes were used several times in fractionation, given the small volumes filtered.

Parallel Fractionation

In parallel fractionation the same feed sample is fed to the five membranes in parallel (see Figure 4.9). Permeate and retentate are then collected for analysis. The feed volume is in this case 100 mL, and 35 mL permeate were collected then the filtration was stopped.

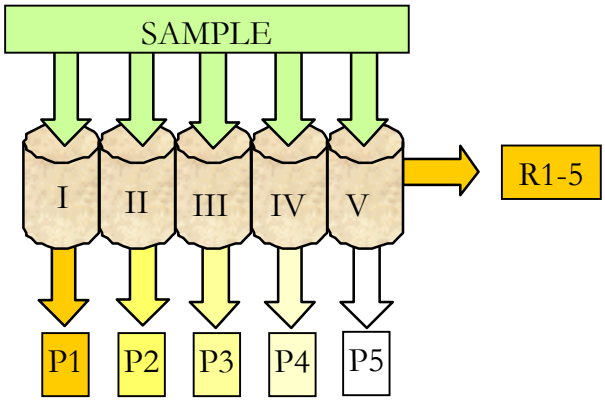


Figure 4.9 *Schematic of parallel fractionation through membranes I, II, III, IV and V. Five permeates (P1 to P5) and five retentates (R1 to R5) are produced.*

Table 4.8 *Calculation of percentage in a molecular weight fraction.*

Molecular weight fraction [kDa]	Contents [%]
> 30	$((c_F - c_{P30}) \cdot c_F^{-1}) \cdot 100$
10-30	$((c_{P30} - c_{P10}) \cdot c_F^{-1}) \cdot 100$
5-10	$((c_{P10} - c_{P5}) \cdot c_F^{-1}) \cdot 100$
3-5	$((c_{P5} - c_{P3}) \cdot c_F^{-1}) \cdot 100$
1-3	$((c_{P3} - c_{P1}) \cdot c_F^{-1}) \cdot 100$
< 1	$c_{P1} \cdot c_F^{-1} \cdot 100$

Serial Fractionation

In serial fractionation the permeates are filtered subsequently through the next membrane (see Figure 4.10). 400 mL of feed sample are used and 35 mL of each permeate are sampled. The volumes filtered per stage are listed in Table 4.9.

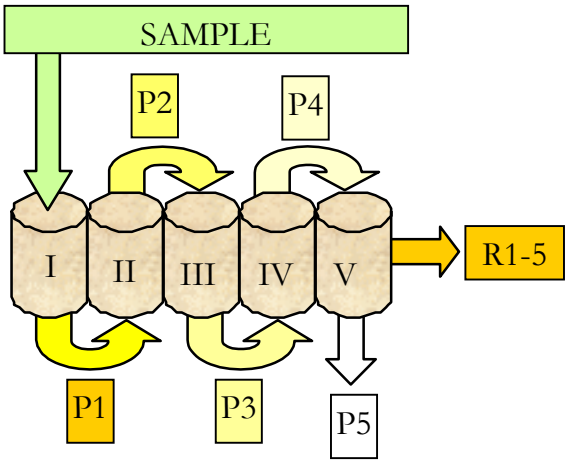


Figure 4.10 *Schematic of serial fractionation through membranes I, II, III, IV and V. Five permeates (P1 to P5) and five retentates (R1 to R5) are produced.*

Table 4.9 *Feed and permeate volumes for each stage of serial fractionation.*

Membrane MWCO [kDa]	Feed Volume [mL]	Permeate Volume [mL]
30	400	320
10	285	228
5	193	154
3	119	95
1	60	48

Comparison of Serial and Parallel Fractionation

Surface water concentrate at a feed concentration of 15 mgL^{-1} as DOC was used in background solution to compare both fractionation procedures. A difference in the results is expected, because the feed solutions are different for both approaches. In parallel fractionation the large molecules will possibly hinder the permeation of small ones through the membranes, and thus result in an overestimation of molecular size.

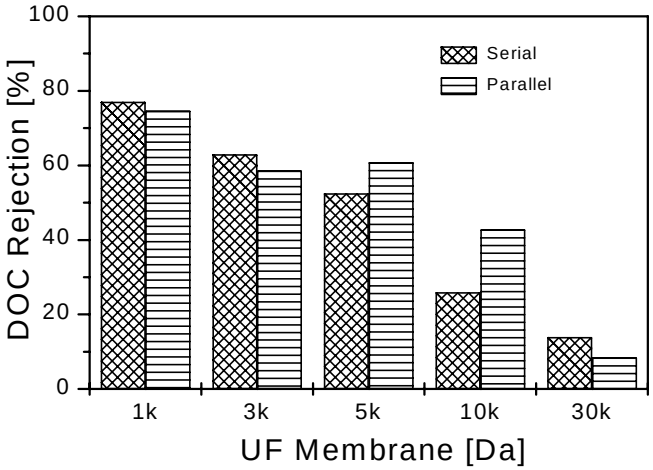


Figure 4.11 *DOC rejection (NOM concentrate) for serial and parallel fractionation in comparison (the rejection was calculated with the permeate and feed concentration, it is thus not the true rejection of the membranes which would be calculated with bulk concentrations).*

It can be seen that the difference between the two methods is minimal and for further fractionation the parallel approach was used due to its shorter time requirements. Results for parallel fractionation for all organics used are shown in Figure 4.12 as the percentage of DOC in the permeate. See Chapter 6 for rejection results.

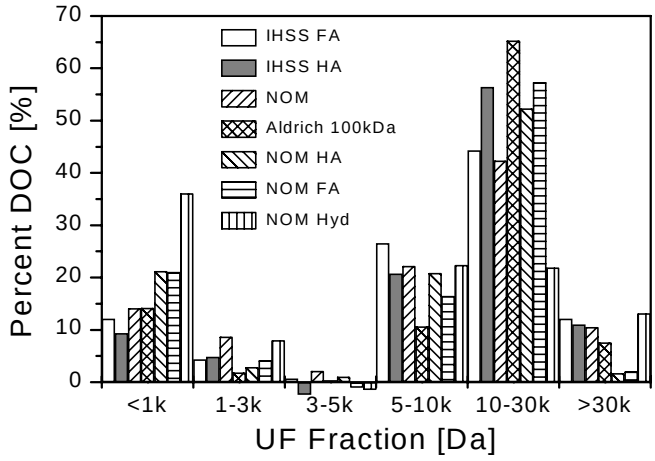


Figure 4.12 *Ultrafiltration fractionation results for the organics used (all in background solution).*

The IHSS materials, HA and FA, are very similar in size according to UF. The rejection of HA is only slightly higher, and the difference is most apparent for the 5 and 10 kDa membranes. The pores of these membranes seem to be closest to the size of the organic molecules. NOM has a 5 to 15% lower rejection. Again, differences are most apparent with the 10 kDa membrane. The three NOM fractions are all very different; the HA and FA fraction are again very similar and larger than the NOM. FA appears to be a little larger than the HA, which was not expected. This could indicate that charge effects are important in UF fractionation. The hydrophilic fraction is, as expected, the smallest compound and rejection even of the 1 kDa membrane is as low as 75%.

The purified Aldrich material (prefiltered through a 100 kDa membrane) was comparable to the other compounds and closest in size to IHSS HA. The raw Aldrich material was not UF fractionated, as the 100 kDa membrane retained 95% of the DOC. Rejection of all membranes would thus be >95%.

One of the disadvantages of this method is that it cannot be presented as a size result due to the different rejection values. However, the method gives valuable results in terms of rejection by different membranes which can be used for treatment efficiency and give an idea about a required MWCO to retain organics.

4.7.9 Liquid Chromatography – Organic Carbon Detection (LC-OCD)

This method was developed by Stefan Huber (Karlsruhe, Germany) and consists of three size exclusion chromatography columns which divide the organic carbon into several fractions as a function of size, but also hydrophobic and ionogenic characteristics. A sample of up to 3 mL is injected into the instrument and filtered in-line with a 0.45 μm filter. The deposit on the filter is backwashed after 5 minutes and directly analysed with the TOC analyser to determine the particulate organic carbon content (POC).

The organic carbon detector used is based on a thin film reactor principle ("Gräntzel" type). The inorganic carbon is removed by a stripping process in the top of the reactor. The organic carbon is oxidised to CO_2 using a radiological method of splitting water molecules radiated with light at 185 nm. This method is more efficient than the persulphate method, which was used for routine analysis (see Appendix 4 for oxidation efficiencies). The CO_2 was analysed using non-dispersive IR. The detection limits are in the low μgL^{-1} concentrations. UV absorbance was also analysed in parallel. Samples were diluted prior to injection. The samples used were 100 mgL^{-1} as DOC stock solutions of IHSS HA and FA, as well as NOM. For the other solutions stock solutions as available were used; 12.. 100 mgL^{-1} as DOC for purified Aldrich (100 kDa), 250.3 mgL^{-1} as DOC for NOM HA, 114.5 mgL^{-1} as DOC for NOM FA, 22.1 mgL^{-1} as DOC for the NOM hydropilic fraction. Samples were diluted; IHSS-HA 1:50, IHSS-FA 1:50, Aldrich 100 kDa permeate 1:10, NOM 1:50, NOM HA fraction 1:100, NOM FA fraction 1:50 and the NOM hydrophilic fraction 1:10. Results are shown in Figure 4.13 and Table 4.10.

CDOC is the chromatographable fraction of TOC, which means the hydrophilic and amphiphilic fraction of DOC. Results were calculated using peak area. HOC is the hydrophobic fraction. The humic substances peak was used for molecular weight determination by fitting a symmetrical Poisson distribution to the peak, which allows determination of average weight MW (Mw) and average number (Mn). The Mw/Mn ratio gives an indication of the width of the size distribution.

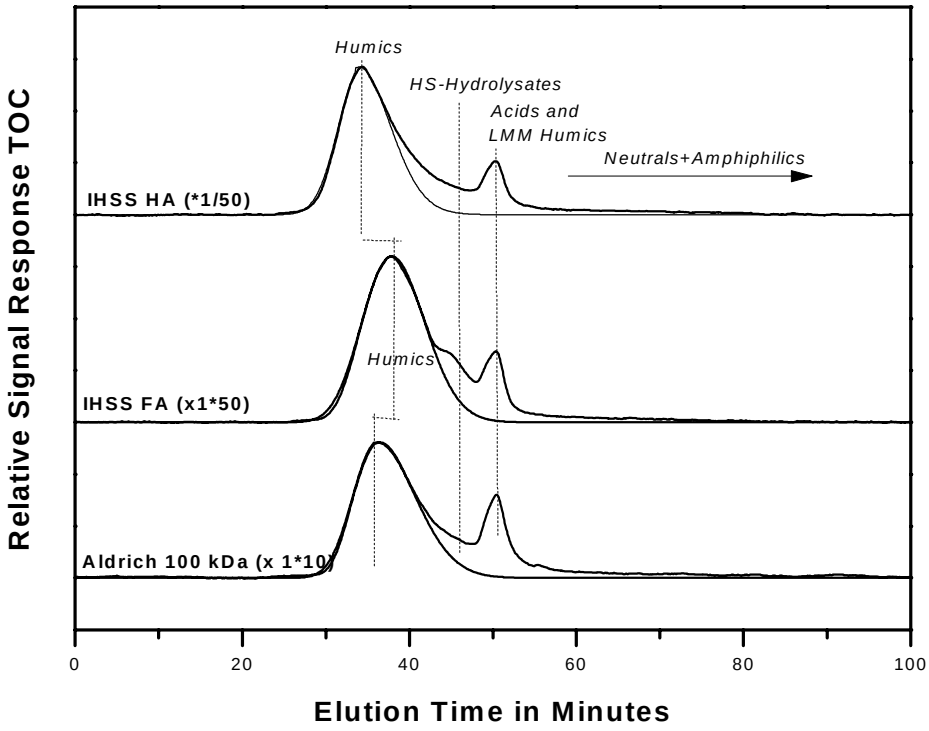


Figure 4.13 *LC-OCD results of IHSS HA, IHSS FA, and purified (100 kDa) Aldrich sample. Dilutions are of 100 mgL^{-1} as DOC stock solutions in MilliQ water for the IHSS samples and 12 mgL^{-1} as DOC for the Aldrich sample.*

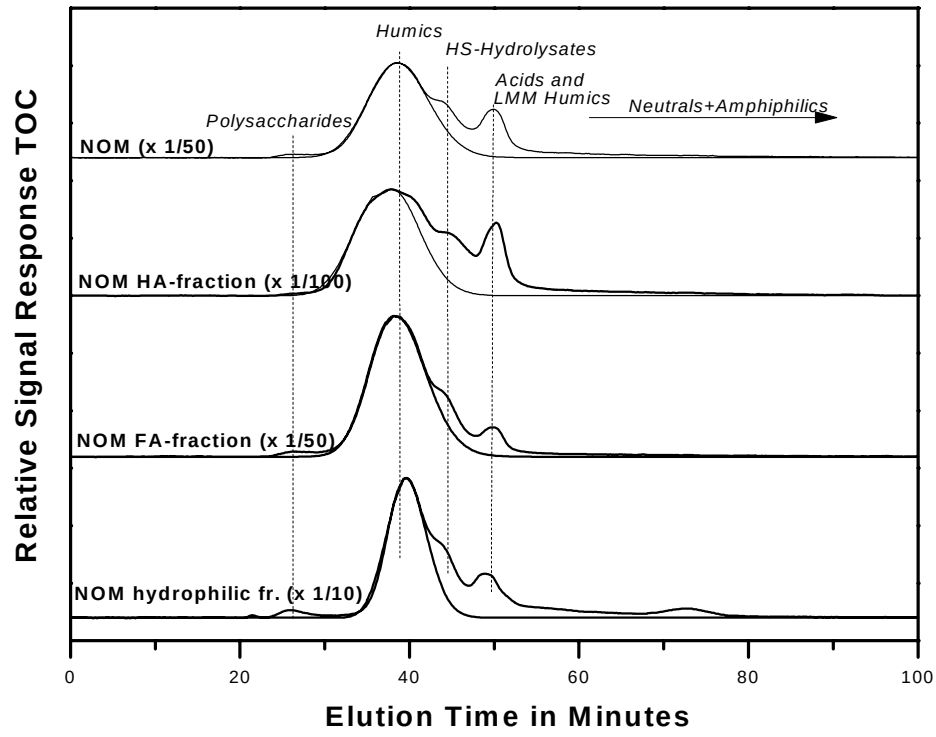


Figure 4.14 *LC-OCD results of the NOM and its HA, FA and hydrophilic fractions. Dilution is for the following stock solutions; NOM 100 mgL^{-1} as DOC, 250.3 mgL^{-1} as DOC for NOM HA, 114.5 mgL^{-1} as DOC for NOM FA, and 22.1 mgL^{-1} as DOC for the NOM hydrophilic fraction.*

SAC is the UV absorbance at 254 nm, CSAC is the UV absorbance of the chromatographable fraction. The faction UV/DOC, or SAC/OC, was calculated from the humic substance fraction and represents the aromaticity of the sample.

HS-hydrolysates are probably formed in waters by very slow UV oxidation. It is assumed that these compounds are highly substituted aromatic and conjugated acids, or they also may be intermediates in the formation of HS. Low molecular weight acids are C1 to C5 anions. The low molecular weight neutrals and amphiphilics are compounds like alcohols, aldehydes, ketones, and amino acids. Polysaccharides (UV inactive) are the EPS of algae and bacteria. They are a sign of biological activity.

The IHSS HA shows a very large size and the presence of some polysaccharides which were extracted with the XAD resin. It is a possibility that the IHSS is partly aggregated when kept in a stock solution at 100 mgL^{-1} as DOC. The Aldrich sample contains large amounts of hydrophobic compounds, as well as low molecular weight neutrals and amphiphilics. This indicates that this sample is chemically different. The sample has also a very high aromaticity. The IHSS HA and FA differ mainly in the presence of polysaccharides and inorganic colloids in the HA sample, as well as in size and aromaticity. No major chemical distinction can be made by the fractions.

The Gosford NOM contains hardly any polysaccharides and mostly pedogenic HS, which indicates a "bog lake". Again, aromaticity and size are the most clear distinctions between the fractions, but the values are lower than those of the Suwannee River IHSS samples.

Overall, the fractionation of the samples (using XAD methods) is not complete, neither in the case of the IHSS samples, nor in the case of the Gosford NOM. Therefore, there will always be an overlap of compounds, which is likely to make interpretation of results difficult.

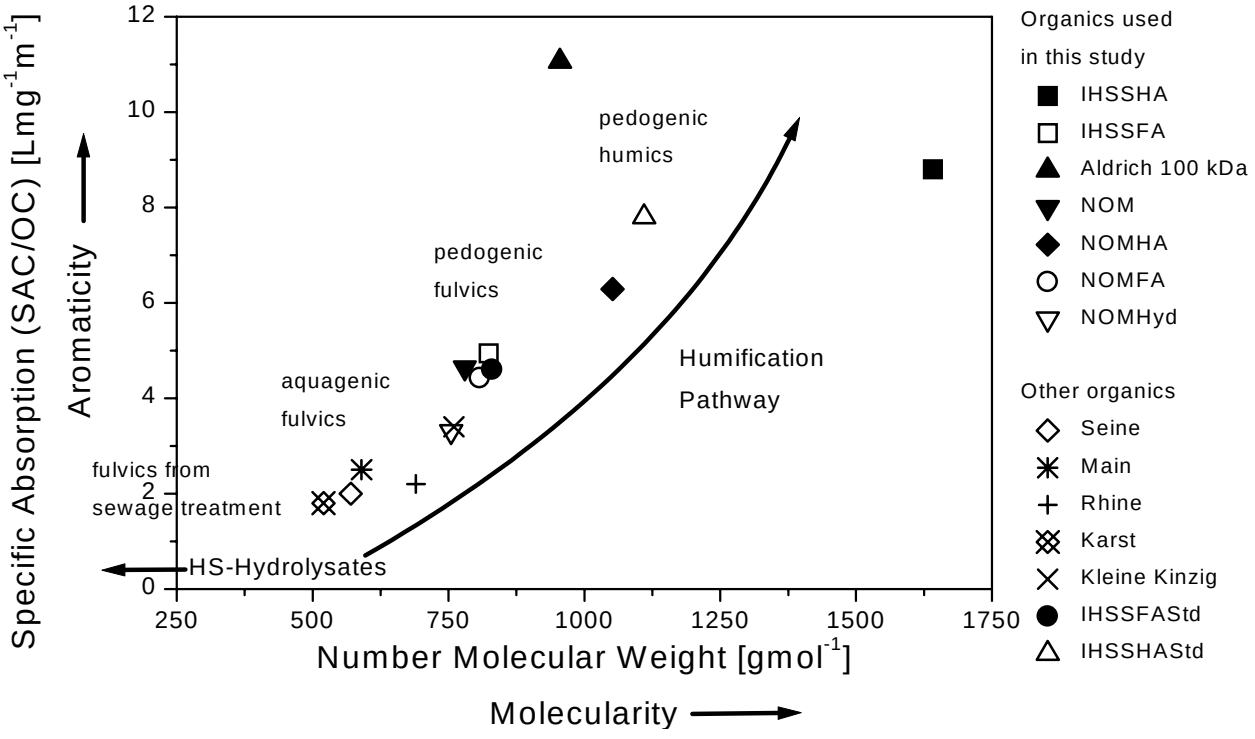


Figure 4.15 *Humification diagram for the natural organics as used in this study and other organics as reported by Huber (1998).*

Table 4.10 *Results of the LC-OCD analysis for the natural organics used in this study.*

	IHSS HA	IHSS FA	Aldrich 100kDa	Gosford NOM	Gosford HA Fraction	Gosford FA Fraction	Gosford Hydropohilic Fraction
TOC [μgL^{-1}]	72.5	83.9	16.9	118.7	309.4	136.3	26.4
DOC [% of TOC]	100	100	99.7	100	100	100	100
CDOC [% of TOC]	100.1	100.1	91.1	97.9	100	100.1	98
HOC [% of TOC]	-0.1	-0.1	8.5	2.1	0	-0.1	2.0
POC [% of TOC]	0	0	0.3	0	0	0	0
Humics (HS) [% of CDOC]	73.5	81.2	76.2	72.9	65.2	82.8	63.0
HS Hydrolysates [% of CDOC]	18.5	12.4	13.0	15.9	25.2	10.3	21.2
Low molecular mass acids [% of CDOC]	0	0	0	2.1	1.9	0.2	0.3
LMM neutrals and amphiphilics [% of CDOC]	6.6	6.4	10.8	8.2	7.7	4.6	13.2
Polysaccharides [% of CDOC]	1.4	-	-	0.9	-	2.0	2.2
CSAC [m^{-1}]	565.7	395.1	164.3	465.4	1505.9	557.0	66.2
Humics (HS) [% of CSAC]	83.0	85.3	79.0	84.5	84.3	89.9	81.5
HS Hydrolysates [% of CSAC]	12.1	13.3	13.7	13.3	13.1	8.3	15.0
Low molecular mass acids [% of CSAC]	1.8	0.5	2.8	-	-	-	-
LMM neutrals and amphiphilics [% of CSAC]	0.5	0.9	4.5	2.2	2.6	0.7	2.8
Inorganics; UV active colloids [% of CSAC]	2.8	-	-	-	-	1.0	0.8
Mw [$gmol^{-1}$]	2748	1532	1814	1381	1857	1381	970
Mn [$gmol^{-1}$]	1641	824	955	780	1052	807	755
Mw/Mn [-]	1.67	1.86	1.90	1.77	1.76	1.63	1.28
SAC/OC of Humics [$L(mg.m)^{-1}$]	8.8	4.94	11.06	4.64	6.29	4.43	3.3

Aromaticity can be drawn over molecularity in the humic substances diagramm as shown in Figure 4.15. This allows the comparison of humic substances of different sources and an understanding of the likely nature of the samples.

The further a sample towards the top right corner of the diagram, the more it is humificated. Pedogenic HS are biologically regarded as inert and very aged. Aquagene organics are products of biological degradation of bacteria and algae, as well as marine origin or from wastewater treatment plants.

While the NOM and its fractions and the IHSS FA lie nicely in the region of FA isolates and pedogenic surface waters, Aldrich 100 kDa permeate and IHSS HA lie well outside this region. The NOM sample lies well above the samples from European rivers such as the Seine, Main, Rhine, and Karst. This can be explained with a relatively high input of small organics from wastewater treatment plants which are discharged into these rivers. Smaller and probably "purer" rivers such as the Steinbach or Kleine Kinzig are located close to the hydrophilic and FA fraction of NOM.

The Aldrich sample has a unusually high aromaticity, whereas the IHSS HA has an extremely high molecularity. Both, high aromaticity and molecularity indicate a biologically stable water with organics easily removable by coagulation.

Results for MW at the concentrations analysed, diffusivity as calculated after Worch (1993) and molecular radii, calculated from diffusivity by using the Stokes Einstein are shown in Table 4.11. Substituting the Stokes Einstein equation into the relationship developed by Worch (1993) and shown in Chapter 2 results in equation (4.2).

$$r = 2.037 \cdot 10^{-11} \cdot M^{0.53} \quad \text{in [m]} \tag{4.2}$$

Table 4.11 *Acidity, average molecular weight of the organics used as determined by LC-OCD, diffusivity and molecular radii as calculated after Worch (1993) and Stokes Einstein at 20 ^{0}C.*

Type of Organic	Stock Solution Concentration [mgL^{-1} as DOC]	Concentration for Analysis [mgL^{-1} as DOC]	Molecular Weight [g mol^{-1}]	Diffusivity [g mol^{-1}]	Molecule Radius [nm]
IHSS HA	100	2.0	2747	$1.48 \cdot 10^{-10}$	1.35
IHSS FA	100	2.0	1532	$2.01 \cdot 10^{-10}$	0.99
Aldrich 100 kDa Permeate	12	1.2	1814	$1.84 \cdot 10^{-10}$	1.08
Mooney NOM	100	2.0	1381	$2.13 \cdot 10^{-10}$	0.94
NOM HA Fraction	250.3	2.5	1857	$1.82 \cdot 10^{-10}$	1.10
NOM FA Fraction	114.5	1.1	1318	$2.18 \cdot 10^{-10}$	0.92
NOM Hydrophilic Fraction	22.1	2.2	970	$2.56 \cdot 10^{-10}$	0.79

The results correspond very well to the SEC results except for the NOM fractions where the LC-OCD results make more sense. The molecule size is in the 0.7 to 1.4 nm size range which is close to tight UF and NF membrane pore size if the relation ship which was developed by Worch is valid for natural organics.

4.7.10 Humic Solubility and Aggregation

Solubility of the organics was measured by preparing a sample of varying organic type, concentration, salt composition, and pH. Solutions were prepared in 20 mL sample vials, rapidly shaken after addition of the various stock solutions, pH adjusted and then the UV scans to measure the aggregation of the organics were carried out after 1, 5 and 24 h.

Aggregate sizes were measured using PCS (see section 4.9.5), structure using the 'humic fractal method' (described below), and 15 mL of the samples were then centrifuged to measure the solid content. Organic concentrations of 25-75 mgL^{-1} as DOC, pH 3.5 to 10, calcium chloride concentrations of 0-25 mM were tested.

Precipitation occurred at the pH extremes at which investigations were undertaken, i.e. at pH 3.5 and pH 10. The nature of the solids formed at these two pH extremes was very different. At low pH, only HA (not FA and NOM) precipitated. Calcium had no effect on this precipitation, which was observed even in the absence of calcium. This effect could be explained by the low solubility of HA, compared to FA at low pH.

A RC5B Sorvak (DuPont) refrigerated superspeed centrifuge was used at 13000 rpm (G=25 000) for 30 min at 20^0C. Nalgene 50 mL PPCO Oak Ridge Centrifuge tubes were used (De Nobli and Contin (1994)). After centrifugation, 14 mL of supernatant were separated from the solid precipitate and analysed with the samples prior to centrifugation for DOC concentration.

After centrifugation a mass balance was carried out. 20 to 40% of HA were lost to the solid fraction in the presence of 25 mM calcium. Precipitation is highest at high pH, when the solubility of calcium is lowest. For all other organics and conditions the amount of organics in the solid fraction is low (<10 %) which shows that the organic solubility is high and that calcium is required to precipitate the organics. It also means that it is likely that a specific HA-calcium complex precipitates. If aggregation was the case this would also be achievable with NaCl which is not the case, even at very high concentrations.

Aggregation of the organics was studied using a UV/VIS spectrophotometer as described by Senesi *et al.* (1994, 1996, 1997). Turbidity was calculated from the absorbance results. Samples were measured as a function of time. The method assumes a constant absorbance of the samples, which can be problematic and is valid for large aggregates only (Senesi *et al.* (1994)). For this reason no fractal dimension data were calculated, but log turbidity versus log wavelength plots served to investigate the relative structure density of organic aggregates and the change in structure with time. Changes in structure with time (samples were also refrigerated over night) were only observed for HA in the presence of calcium at medium and low pH. This result is shown in Figure 4.16.

Aggregation of the calcium-organic systems generally increased at low temperature (4^0C). Due to the higher calcium carbonate solubility at low temperature, this precipitate must be a calcium-organic compound. The precipitation of calcite and the formation of calcium-organic complexes as a function of solution chemistry is discussed in Appendix 5. Organics can inhibit inorganic precipitation, but, given the high degree of uncertainty in calcium-organic complexation constants and the lack of data on calcite-organic interactions, definitive prediction of the effect of NOM on calcite precipitation was not possible.

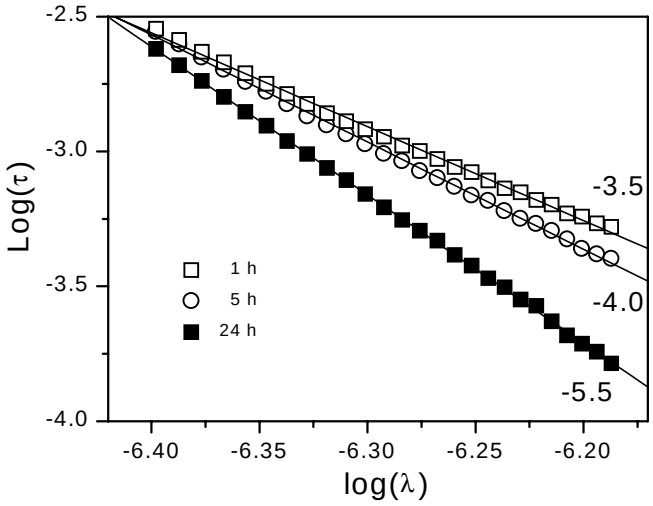


Figure 4.16 *Log turbidity versus log wavelength plot for a solution containing 25 mgL^{-1} HA, 25 mM $CaCl_2$ at pH 7.2.*

A variation of structure was observed for HA at low pH, indicating that aggregation/precipitation is occurring over several hours after mixing. In the presence of large amounts of NaCl (75 mM), foam formation was observed. The aggregates formed were very large (see section 4.9.5).

Both HA and FA were removed from solution in the presence of 25 mM calcium chloride at pH 10. At this pH, calcite precipitates and the interactions between organics and calcium are strongest. In the absence of calcium no precipitation occurred at pH 10. This may indicate the precipitation of a calcium-organic compound, co-precipation of organics with calcite or, simply adsorption of organics onto calcite surface sites.

4.7.11 Viscosity

Viscosity was measured using a Haake VT 500 instrument with a NVSt cell at 25^{0}C. Representative samples of feed solutions used in various experiments produced the results given in Table 4.12. The results appear to be slightly underestimated (water at 25^{0}C should have a viscosity of 0.89 10^{-4} Pa s), but relative changes can be seen, especially for the RO concentrate. It can be expected that viscosity effects will play a role in the treatment of surface waters, especially at the high concentrations expected in the boundary layer near the membrane surface and with changes in temperature.

Table 4.12 *Viscosity of various solutions. The value of MilliQ water is lower than the expected value of 0.89 at 25^{0}C.*

Substance at 25^{0}C	Viscosity ±5% [10^{-4} Pa s]
MilliQ Water	0.80
Surface Water (Gosford)	0.89
RO Concentrate (last sample, see Appendix 1)	0.96
10 ppm Hematite, 5 ppmC FA pH 2.9	0.95
10 ppm Hematite, 5 ppmC FA pH 7.5	0.89
10 ppm Hematite, 5 ppmC FA pH 9.2	0.91

4.7.12 Matrix Assisted Laser Desorption/Ionisation (MALDI)

MALDI enables determination of the chemical composition and chemical structure of a sample. The sample is ionised into positive and negative ions using a laser. Maldi heats organic compounds in the matrix very rapidly leading to vaporisation of the ionised molecules before decomposition can occur.

The time of flight of the generated ions is measured, which allows determination of the molecular weight of compounds. For the ionisation step the sample must be prepared in a supporting matrix. The matrix used was 9-nitroanthracene. To check the method, control runs of the matrix were undertaken containing bovine serum albumin (BSA). The signal was not suppressed or altered due to the presence of the matrix compound. Five organics were analysed (Table 4.13), and for most of the organics very large ions were observed at an excellent resolution even at large size.

Table 4.13 *MALDI results for different organics.*

Organic	Smallest Peak [m/z] *	Largest Peak [m/z] *
Aldrich HA	567	148 600
IHSS HA	< 1000	72 300
IHSS FA	591	2 500
NOM	< 1000	198 100
Fluka HA	990	152 700

* mass-charge ratio

The results are somewhat surprising if one considers the molecular weights measured with other methods. SEC and UF fractionation may "lose" these extremely large compounds or their concentration may simply be too small to be measured. Very distinct peaks were founds for all organics in the size range of about 1000 m/z. The IHSS FA is the only compound for which no extremely large ions were analysed. The presence of salt should not disturb the analysis, however a more detailed study of this method may be of advantage.

Nuclear magnetic resonance spectroscopy (^{13}C CP/MAS Solid State NMR) and Fourier transform infrared spectroscopy (FT-IR) were also performed for the freeze dried NOM sample. The results were both very noisy and paramagnetic compounds such as iron and manganese interfered with the ^{13}C NMR analysis. After 20 h of run time the sample showed mostly alkyl and alkyl-oxygen carbon, thus very little aromatic compounds.

4.7.13 Diffuse Reflectance Fourier Transform Infrared Spectroscopy (DRIFT)

DRIFT provides information about the nature and arrangement of functional groups in NOM. DRIFT analysis was carried out using a Nicolet Magna 750 Spectrometer with a KBr filter and an MCP/B detector. The dry sample was mixed with granulated KBr (Merck, Spectroscopic Grade) to 5 w/w %). Instrument settings were 64 scans, gain 4 cm and data spacing of 1.928 cm^{-1}.

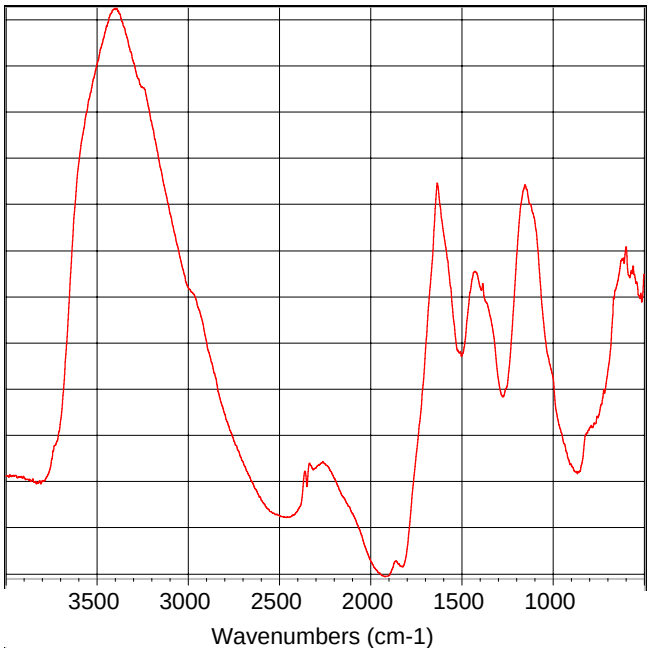


Figure 4.17 *DRIFT spectrum of Mooney Mooney NOM (y-scale is absorbance, with arbitrary unit).*

The result shown in Figure 4.17 is very typical for NOM. The peak heights give relative information about the concentration of groups.

The strong absorption in the 3200-3500 cm^{-1} region is due H-bonded groups such as -CH, -OH, and -NH. The shoulder peak at 2900 cm^{-1} is likely to be aliphatic methylene groups (fatty acids, waxes). Peaks in the 1650 to 1750 cm^{-1} region can be attributed to the C=O of quinones, ketones, and maybe aromatic C=C vibrations, which are very weak. Carboxylates are found in the 1600 cm^{-1} region and also show a small peak at 1440 cm^{-1}, and aliphatic oxygen (esters, ethers and alcohols (carbohydrates) in the 1100 cm^{-1} region. The peak at 1400 cm^{-1} may be either aryl or aliphatic CH.

Peaks at 3400 cm^{-1} (sharp) and 1650 cm^{-1} are due to phenolic groups and the peak for methylene (3000 cm^{-1}) is small, which is typical of FAs. Peaks in the 2800 to 3000 cm^{-1} region are an indication of CH_2 and CH_3, which is typical for tree litter leachate (cellulose) (Page (1998)).

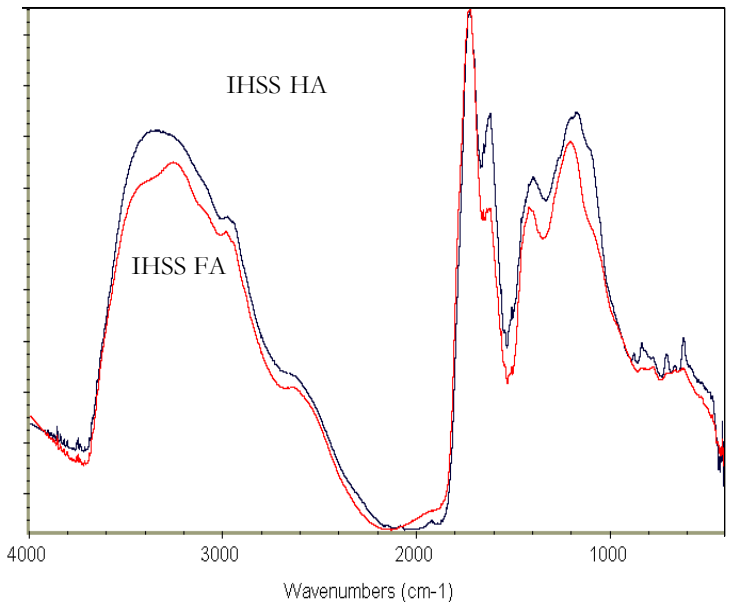


Figure 4.18 *DRIFT Spectrum of IHSS FA and HA (y-scale is absorbance, with arbitrary unit).*

Looking at the pure humic compounds shown in Figure 4.18, the phenolic peak is sharpest for the NOM and is also significantly higher than in the IHSS samples. The IHSS HA has a clearly higher phenolic content than the IHSS FA. The carboxylic acid content is more obvious in the IHSS HA sample than in the FA, and no such peak is apparent in the NOM sample. It appears that the IHSS HA also contains more of the compounds stated by Page (1998) to be aliphatic alcohol (and thus the fraction which is difficult by conventional treatment).

While the samples give reasonable qualitative information, the differences between the different organics appear to be very small. Unfortunately, the method does not allow quantitative determination of functional group content.

4.8 SOLUTION PREPARATION

If not indicated otherwise, solutions consisted of 1 mM $NaHCO_3$, 0.5 mM $CaCl_2$, and 20 mM NaCl as a background electrolyte. For experiments in which the calcium concentration was varied, the conductivity was adjusted to 2 $mScm^{-1}$. For all other experiments a background solution as detailed above was used. 1M NaOH, HCl, and NaCl were used for pH and ionic strength adjustment. The colloidal sols were ultrasonified for 15 minutes prior to solution preparation.

The humic substances were kept in 100 mgL^{-1} (as organic carbon) stock solutions at 4 ^0C for short periods of time. Solutions which did not contain colloids or coagulants were prepared by adding appropriate quantities of stock solutions into MilliQ water. Solutions which did contain colloids or coagulants require a little more attention and their preparation method as well as solution characterisation is described in the following sections.

Feed solutions containing inorganic colloids and organics were prepared in two different orders (SPO, OPS), both of which could be naturally occurring scenarios when rivers of various origins flow through different environments, or when rivers mix. The preparation procedures are described below.

Figure 4.19 depicts hematite colloids in possible aggregation and colloid-organic interaction stages. The pictures are obviously simplifications, but nevertheless help to understand the different filtration behaviour of these particulate assemblages.

4.8.1 Stable Hematite Colloids in Absence of Organics

To examine the filtration behaviour of stable particles without organics, the particles were dispersed into MilliQ water pre-adjusted to pH 3 or 12 in the absence of salt. At this pH, the particles are far from their point of zero charge and thus mostly stable and dispersed due to electrostatic repulsion (see Figure 4.19A). The density of hematite is 5.24 gcm^{-3} (Liang (1988)) and their aggregation kinetics have been studied extensively (Amal (1991)).

4.8.2 Colloids at pH 3 with Organics

To understand the effect of organics on the primary particles, another set of experiments far from surface water conditions (no electrolyte solution and pH 3) was carried out. At this pH the colloids are initially stable. When the organics are added, the surface charge is reversed resulting in aggregation. This was confirmed with microfiltration, after which large aggregates were found on the membrane

surface (results not shown). Some of the organics are not very soluble at this pH and thus only a partial adsorption occurs.

Here the colloids are prepared as in the previous paragraph and the organics are then added from the stock solution. The solution was left stirring for about 2 hours to allow completion of the adsorption process.

4.8.3 Reaction Limited Aggregation (RLA)

Reaction limited (slow) aggregation occurs when repulsion between colloids is strong (thus at low to moderate salt concentrations). The colloidal aggregates have time to interpenetrate and thus compact aggregates of high mechanical strength form (see Figure 4.19B).

To produce such aggregates, a solution of hematite was prepared (with a well ultrasonified colloid sol), the solution chemistry adjusted to the desired values and salt added. This solution was left to aggregate overnight in a 2 L container and stirred at 270 rpm. Most experiments were carried out at pH 3 at various KCl concentrations.

4.8.4 Diffusion Limited Aggregation (DLA)

Diffusion limited (rapid) aggregation occurs when colloid surface charge is low or screened (high ionic strength). The resulting aggregate structure is loose and tenuous, mechanically weak, and prone to shear restructuring. A simplified DLA aggregate is shown in Figure 4.19C.

To produce such aggregates, a solution of hematite was prepared (with a well ultrasonified colloid sol), the solution chemistry adjusted to the desired values and salt added. This solution was left to aggregate overnight in container and stirred at 270 rpm. Most experiments were carried out at pH 3 with various KCl concentrations.

4.8.5 SPO: Aggregates with Organics

This order of mixing the solution allows the colloids to aggregate, as determined by the background solution pH and ionic strength, before the organics are added. When the organics are now added to these preformed aggregates, the organic will adsorb on the aggregate surface as shown in Figure 4.19D.

500 mL (for a total of 1L solution) of background solution at double concentration was prepared. The particles were added and the mixture stirred at 270 rpm for 10 minutes. Then 500 mL of double concentrated organic solution was added and stirred at 270 rpm for approximately 17 hours. The pH was adjusted prior to mixing the solutions and pH and conductivity were measured prior to the start of the filtration experiment.

4.8.6 OPS: Colloids Stabilised with Organics

During this mixing order, the particles adsorb the organics onto their surface before they can aggregate. The systems were generally stable due to steric stabilisation or charge effects. Aggregation of the particles with inverted surface charge may still be possible, especially in the presence of calcium ions or if the colloid surface is only partially covered. Partial coverage by the organics results in charge neutralisation rather than reversal. Three scenarios were observed in this study. Firstly, IHSS FA and HA caused stabilisation of the colloids due to charge repulsion (high negative charge due to organics) and steric effects (see Figure 4.19E). Secondly, NOM caused simultaneous stabilisation and aggregation

due to the presence of salt in the NOM (Figure 4.19F). And finally, when calcium was added after stabilisation of the colloids, destabilisation occurs due to charge screening or organic-calcium interactions (Figure 4.19G).

500 mL of organics at double concentration was prepared, and the pH adjusted. The particles were added and the mixture stirred at 270 rpm for one hour. Then 500 mL of double concentrated background salt solution of adjusted pH was added and stirred at 270 rpm over night. The pH was adjusted prior to mixing the solutions and pH and conductivity were measured prior to the start of the filtration experiment.

4.8.7 Coagulation

Two sets of equipment were used for coagulation experiments - a conventional jar testing apparatus with six 500 mL cylindrical beakers with an overhead stirrer each, and a Heidoloph RZ R2021 overhead stirrer. The paddle was identical for both stirrer types (1 cm by 4 cm rectangular plate). The jar tests were used for screening tests and MF experiments. In that case the $FeCl_3$ was added from a 20 mM (5.4 gL^{-1} $FeCl_3$ $6H_20$) stock solution, the solution was then rapidly mixed at 100 rpm for 2 minutes and then at 25 rpm for 20 minutes. The method was adapted from Dennett *et al.* (1996).

With the single overhead stirrer, the solutions were stirred for 2 minutes at 100 rpm, then for 20 minutes at 35 rpm (minimum of stirrer). No pH adjustment was made after the addition of ferric chloride.

At 100 mgL^{-1} $FeCl_3$ in general no visible flocs formed. The solution was dark yellow in colour. At 25 mgL^{-1} flocs formed rapidly. The flocs partly floated or settled and broke very easily. The floc formation could be influenced by solution chemistry.

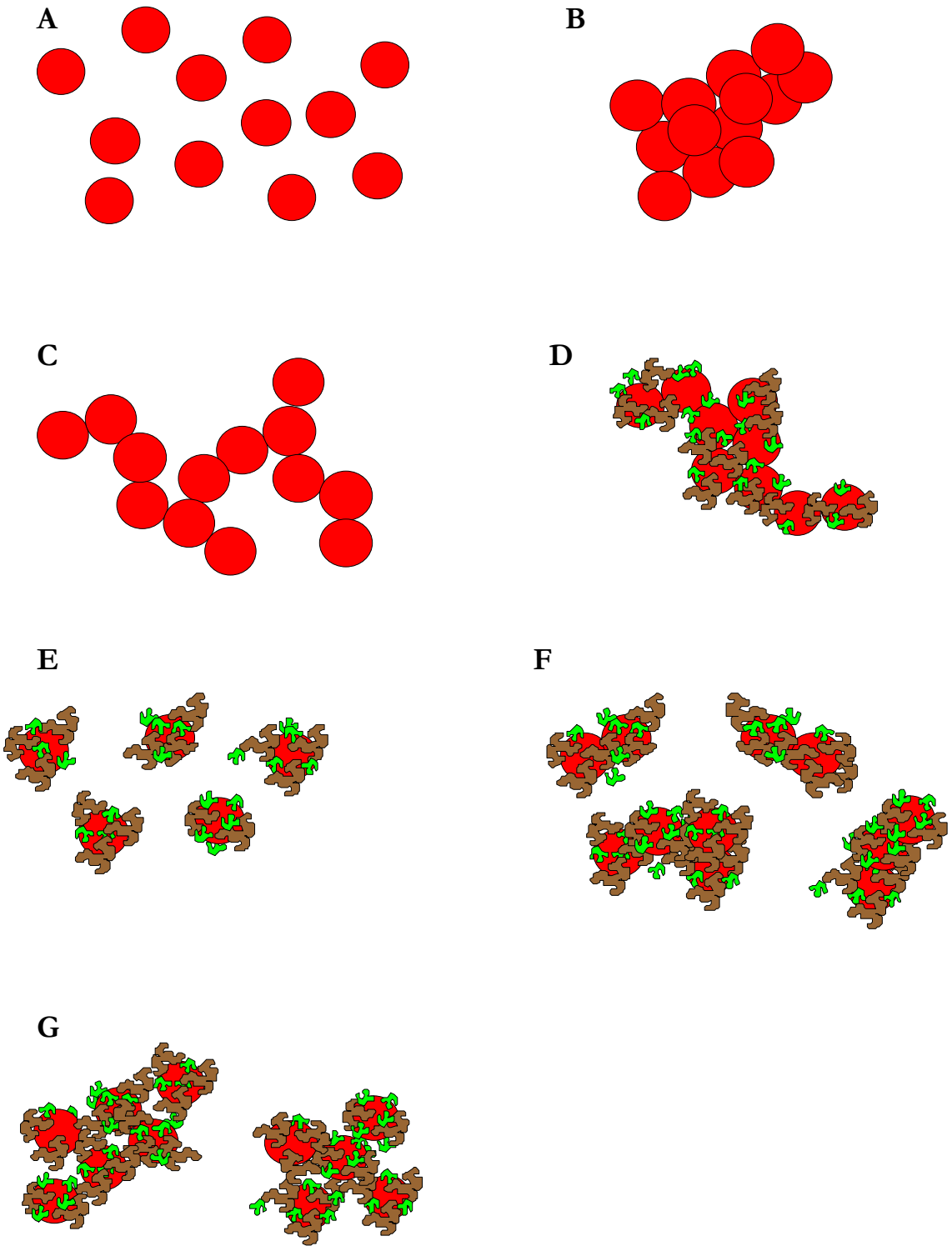


Figure 4.19 *Postulated structures (A) stable hematite colloids in absence of organics, (B) reaction limited aggregation (RLA), (C) diffusion limited aggregation (DLA), (D) SPO: aggregates with organics, (E) OPS: colloids stabilised with organics, (F) OPS: colloids stabilised with NOM, (G) OPS: colloids stabilised with organics and destabilised with calcium.*

4.9 PARTICLE AND AGGREGATE CHARACTERISATION

4.9.1 Zeta Potential and Mobility of Particles

A Coulter Delsa 440 Zeta Sizer was used to measure the particle mobility from which zeta potential was calculated. The method is based on the movement of charged particles inbetween two electrodes, imposing current or voltage. The samples samples were equilibrated for at least 12 hours at a defined solution chemistry prior to analysis which was carried out at 25 ^{0}C.

The following sections discuss results of this analysis. The zeta potential of hematite particles as a function of pH in MilliQ water are shown in Figure 4.20. The isoelectric point of hematite is observed to be about pH 7.0, which compares favourably with the previously reported values of about 6.5 (Amirbahman and Olsen (1995), Matijevic and Schreiner (1978)) and 8.5 (Tiller and O'Melia (1993)). Particle charge depends on the particle size with larger particles having a lower charge. At a pH of 3, colloids will have a high positive charge, resulting in their relative stability. At a pH of 11-12 their charge will be reversed (i.e. very negative) and particles again stabilised. Experiments in which the size effect of primary particles was to be examined, were therefore conducted at pH 3 or 12 to minimise aggregation effects. Particle properties for the three colloid types used are shown in Appendix 3.

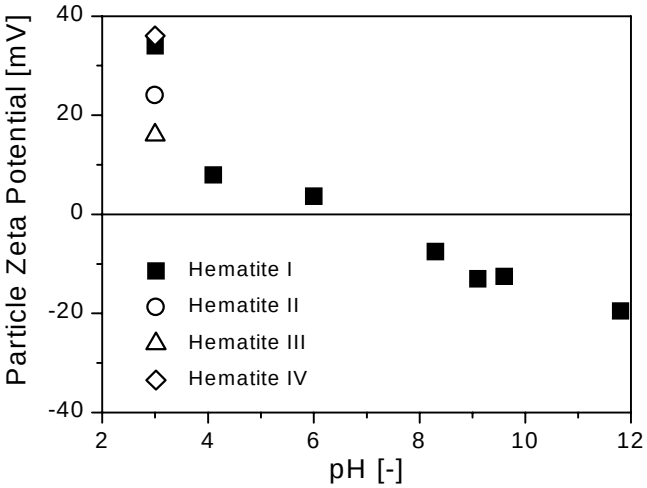


Figure 4.20 *Zeta potential of hematite colloids as a function of pH in absence of organics and salt solution.*

Amal *et al.* (1992) and other authors (see Chapter 2) have previously demonstrated a hematite charge reversal by organics at pH 3, which is also shown in Figure 4.21. In contrast, at pH 8, the charge is not reversed, since at this pH the particles already have a negative charge. However, the negative charge is substantially increased with increased organics concentration. The majority of the present experiments were carried out at pH 8 and it was found that 0.8 mgL^{-1} (as organic carbon) was sufficient to lower the particle zeta potential by 20 mV, from -13 mV to -33 mV. An increase in organic concentration to 5 mgL^{-1} (as organic carbon) decreased the zeta potential only a further 3 mV, showing that particle coating was almost complete. At pH 8, both the organic matter and the hematite were negatively charged. It appears that adsorption of organic matter, either by strong specific "surface complexation" or by non-electrostatic means such as hydrophobic interactions or calcium bridging, has superimposed the charge associated with the organic onto the colloid. HA was more efficient in charge reversal than FA (results not shown). This corresponds to the results of Liang (1988), who determined that molecules with a longer carbon chain had a greater effect on colloid stability. Amirbahman and Olson

(1995) reported a smaller residual charge for particles coated with HA, compared with FA. NOM was least efficient in charge reversal (results not shown), possibly due to the fact that the NOM was not purified and might be complexed with inorganics, thus having less groups available for binding.

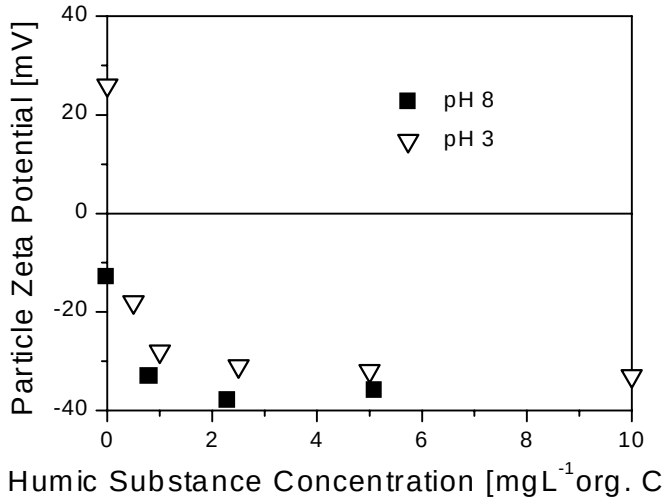


Figure 4.21 *Zeta potential of hematite colloids at pH 3 without background solution with FA and at pH 8 in presence of background solution with HA.*

The order of mixing of particles, organics and salt had a large impact on the zeta potential, as shown in Figure 4.22. The presence of background solution lowered the point of zero charge (compare Figure 4.20 and Figure 4.22). Organics adsorbed onto particles after aggregation (SPO) resulted in a more negative zeta potential, whereas if organics were adsorbed on particles first (OPS), the zeta potential was less negative. The importance of the mixing order shows that the pre-aggregated particles (SPO) act as larger particles that have a lower specific surface area, so that less organics are needed to reverse their surface charge. This is supported by the fact that the surface potential is stable as a function of organic concentration for SPO, whereas the zeta potential decreases with OPS with organic concentration.

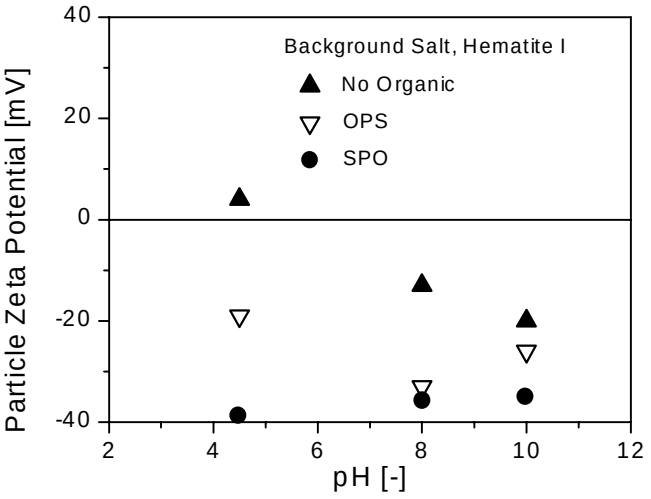


Figure 4.22 *Zeta potential of hematite colloids prepared without organics and with organics in different mixing orders (OPS: organics-particles-salt, SPO: salt-particles-organics).*

The calcium ions in solution could play an important role in modifying surface charge. They would tend to shield part of the negative hematite charge as suggested above, or act as a bridge between organics and particles and increase adsorption through ternary surface complex formation. Calcium was reported by Liang (1988) to increase hematite aggregation and by Tiller and O'Melia (1993) to

destabilise coated particles. Calcium was found to neutralise colloid charge in the absence of organics (about 4 mM of $CaCl_2$ were required, see Figure 4.23). The zeta potential of SPO aggregates became less negative (5 mV) in the presence of 4 mM $CaCl_2$ (probably due to calcium-organic interactions). For OPS the scatter in results was large, probably due to interactions of colloids and a varied mobility of the colloid-organic associates.

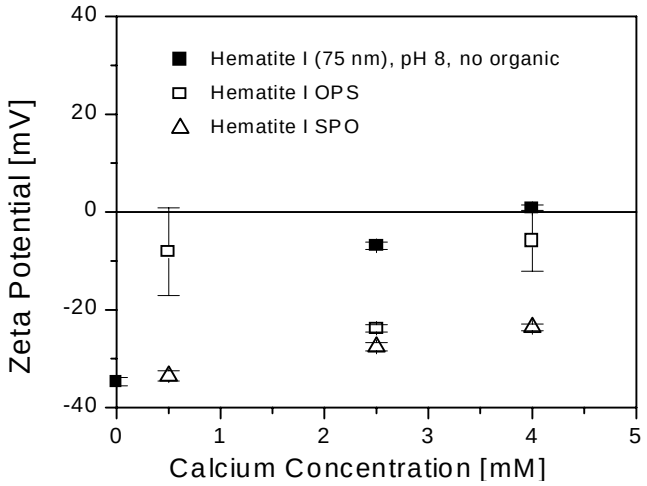


Figure 4.23 *Zeta potential of hematite colloids as a function of calcium concentration, at pH 8 with background solution.*

4.9.2 Particle Size and Structure Analysis/Fractal Dimension (Malvern)

Particle size and aggregate fractal dimension were measured with a Malvern Instruments Mastersizer/E. A 100 mm lens was used to measure particle sizes between 200 nm and 110 μm (the 45 mm lens allowed particle analysis from 50 nm to 80 μm). Measurements were taken immediately after filling the cell to avoid settling effects, and no stirring was applied.

Since the aggregation process is a function of time, samples of the feed suspension were taken prior to the filtration experiments and immediately analysed with the Malvern Mastersizer. Size distribution information was directly available from the instrument output.

4.9.3 Aggregate Size

Aggregate size depends on solution chemistry, hydrodynamic conditions when aggregates are formed, and the presence of organics. To understand the aggregation formation, at first simple systems were looked at, that is 10 mgL^{-1} hematite, pH 3 and ionic strength varied using KCl. The critical coagulation concentration for KCl in these systems was 65 mM as shown in Chapter 6.

Size distributions typical of aggregates formed under low and high salt concentrations either side of the critical coagulation concentrations (c.c.c.) are shown in Figure 4.24 and Figure 4.25, respectively.

Interestingly, two peaks were consistently observed in the size distributions for aggregates formed under reaction limited (low salt) conditions, with one grouping of aggregates in the 0.1-1.0 μm size range and another grouping in the 20-100 μm range. This latter group of aggregates typically exhibited a mode size in the volume-based size distribution of around 30-50 μm. In comparison, aggregates formed at salt concentrations greater than the c.c.c. exhibited only one major peak in the volume-based size distribution, with mode sizes typically around 8-10 μm.

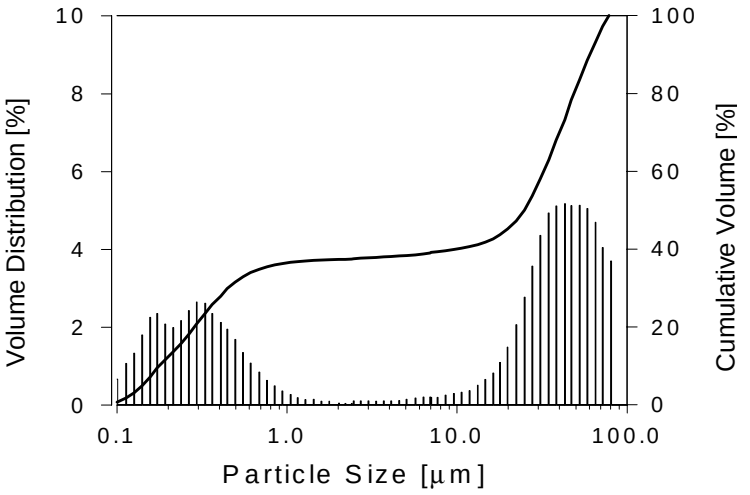


Figure 4.24 *Volume based size distributions of hematite aggregates formed at 10 mM KCl (pH 3, stirrer speed 220 rpm).*

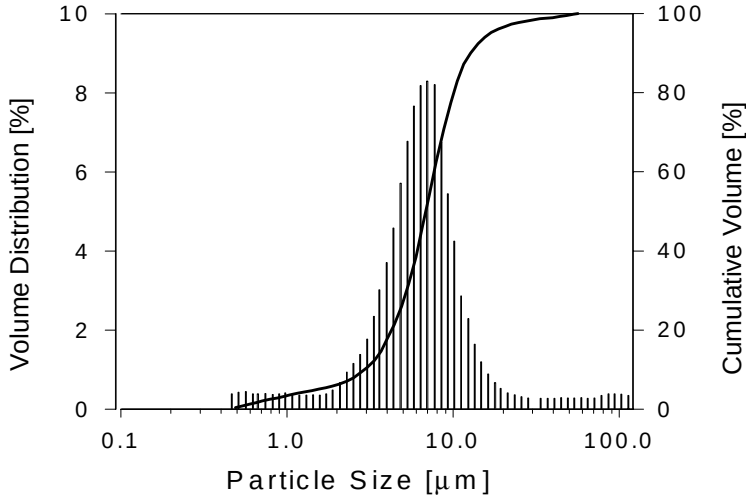


Figure 4.25 *Volume based size distributions of hematite aggregates formed at 100 mM KCl (pH 3, stirrer speed 220 rpm).*

In more applied experiments more complex systems were used. Particle size analysis was only possible in the SPO mixing order. In the OPS order, the aggregates were too small and the scattered light intensity was very low.

The size distributions observed are very different from the well defined systems at pH 3, and are shown in Figure 4.26. The aggregation is less controlled and more heterogeneous. A higher calcium concentration leads to smaller aggregates. At 0.5 mM $CaCl_2$ the bulk volume consists of larger aggregates, but there was also a larger amount of very small aggregates present.

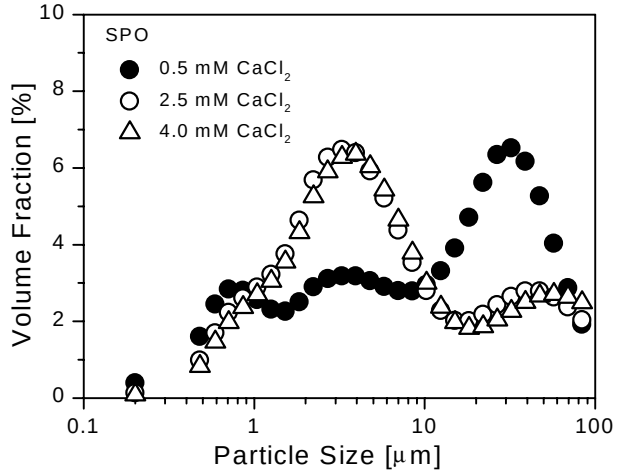


Figure 4.26 *Particle size distribution for SPO hematite systems as a function of calcium concentration (10 mgL^{-1} Hematite I, 5 mgL^{-1} HA as DOC).*

For the systems mixed in OPS order, no size was measured. The Malvern instrument signal was too low for these systems. Since the rejection of these stabilised systems was so low in MF, it is assumed that the size of these colloids is not larger than primary colloids plus an adsorbed organic layer (thickness 1 to 2 nm).

In the coagulation experiments in the absence of particulates, large flocs were formed for some ferric chloride concentrations used and no visible flocs were seen in others. The flocs were very weak and easily broken when solutions were filled into the measuring cell or the filtration equipment. This is reflected in the particle size distributions. At 100 mgL^{-1} $FeCl_3$ flocs formed less due to restabilisation of the solutions, whereas at 25 mgL^{-1} floc formation was rapid and large flocs were visible. Figure 4.27 shows the size distribution results. At the high dosage, flocs were visible in the size analysis although they are not visible in the suspensions (results were repeatable). They are obviously much smaller than at the lower dosage, where flocs are larger than the upper limit of the instrument (which is limited by settling effects).

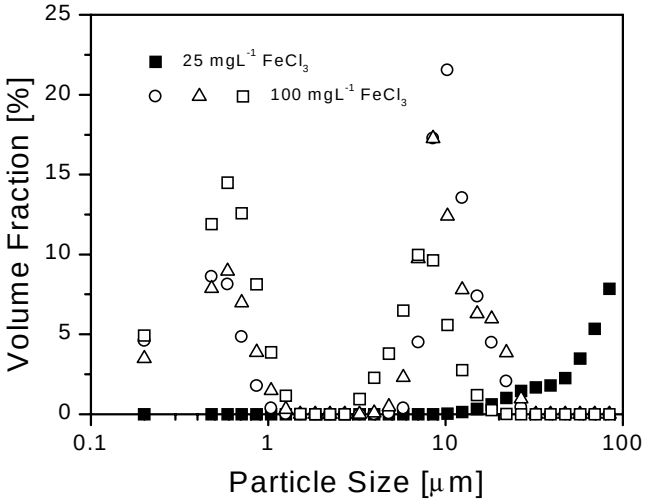


Figure 4.27 *Floc size distribution for two ferric chloride concentrations and HA (5 mgL^{-1} HA in background solution, pH 8); analysis was repeated three times at 100 mgL^{-1} $FeCl_3$.*

4.9.4 Aggregate Structure

Aggregate structure is an important characteristic with respect to aggregate filterability. Aggregate structure was also measured with the Malvern Mastersizer. Log-log plots of light intensity (I) versus wave vector (Q) were used to determine fractal dimension, which is a measure of the structure of aggregates. Jung *et al.* (1995) have described this procedure and demonstrated that this technique produces reliable structural information for aggregates of monodisperse particles in an appropriate size range.

Results of previous static light scattering studies on colloidal hematite aggregates formed under conditions identical to those used here (Amal *et al.* (1992), Zhang and Buffle (1996)) revealed two distinct structural regimes. Under reaction limited aggregation (RLA) conditions, relatively compact aggregates were obtained, while under diffusion limited aggregation (DLA) conditions, somewhat more open particle assemblages were observed. This association of aggregate structure and aggregation kinetics has now been widely reported for a range of colloidal systems (Lin *et al.* (1989)). Fractal dimensions of 1.83 ± 0.07 and 2.2 ± 0.1 were determined using static light scattering by Zhang and

Buffle (1996) for hematite aggregates prepared under DLA and RLA conditions, respectively. These values are consistent with those reported for other colloidal systems (Lin *et al.* (1990), Sposito (1997)).

Plots show scattered light intensity as a function of wave number $Q = (4\pi n/\lambda) \sin(\theta/2)$ where n is the refractive index of the medium, θ is the angle of scatter from the incident beam, and λ is the wavelength of the incident beam (for a He-Ne laser, λ = 632.8 nm). Linear fits to selected "power law" regions of the data are shown as is the resultant computed contribution to scattering by a cohort of small aggregates at high Q.

The results of small angle light scattering studies on the same set of aggregates, generated under low and high salt (KCl) concentrations, are shown in Figure 4.28, below. The intensity of these samples is very low, as samples were diluted to avoid any multiple scattering. These results are consistent with the size distribution data with scattering from two distributions of particles evident in the 10 mM KCl results and from one distribution at 100 mM KCl. The scattering data in the 10 mM KCl case at low wavenumber (Q) is attributable to the larger sized cohort of particles (larger particles scatter light both more intensely and at smaller angles than do smaller particles), while the low intensity contribution at high Q is attributable to the cohort in the sub-micron size range. While power law scattering is evident in both low and high salt concentration cases (confirming the presence of fractal structure), extraction of definitive structural information is non-trivial given the complexity of these systems. Thus, for the 10 mM KCl case, which should be RLA, a linear region in the log I vs. log Q plot can be defined and provides a scattering exponent of 2.34 ± 0.02 similar to those of Zhang and Buffle (1996). However, the choice of data points is rather subjective given the presence of the high Q contribution.

Similarly, in the 100 mM KCl case, a linear region can be defined and a scattering exponent of 2.20 ± 0.01 obtained, but departure from linearity occurs at high Q (where the slope of the log I vs. log Q plot approaches 1.8 (closer to that of Zhang and Buffle(1996)), again rendering the choice of data points somewhat subjective.

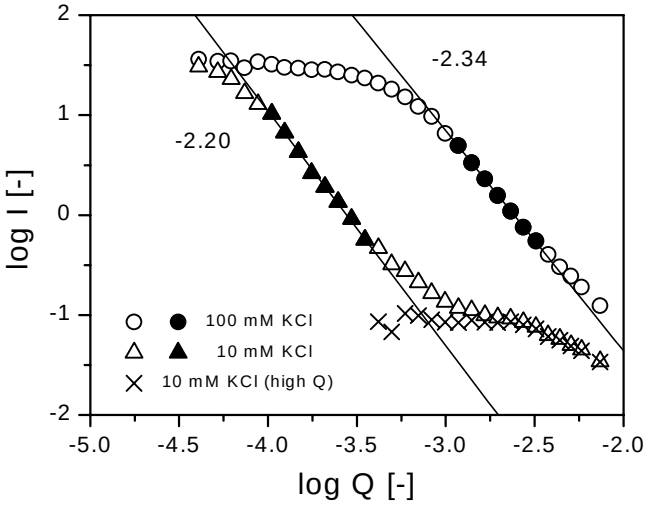


Figure 4.28 *Results of small angle static light scattering studies of hematite aggregates formed at 10 mM and 100 mM KCl (pH 3, stirrer speed 220 rpm).*

For the complex systems used to model surface waters, the aggregation cannot be explained so easily. Figure 4.29 shows the log I versus log Q plot for the SPO system when the calcium concentration was

varied. At high calcium concentration the smaller aggregates are denser, whereas the larger aggregates are somewhat looser. It is difficult to say a priori which aggregates dominate in filtration in this case.

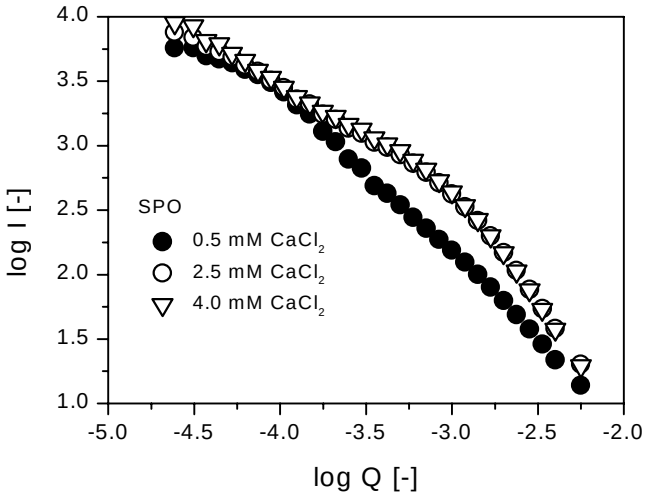


Figure 4.29 *Scattering intensity over scattering vector; the slope of the graph is related to the density of the aggregates; SPO aggregates (hematite) as a function of calcium concentration.*

When hydrous ferric oxide particles are coagulated, very large flocs can form and their structure also depends on the electrolyte (in this case ferric chloride) concentration. Although the scatter in data is considerable (probably due to floc break-up), a large difference between precipitates formed at low (25 mgL^{-1} ferric chloride) and high (100 mgL^{-1}) can be seen in Figure 4.30. The flocs formed at low ferric chloride concentration have a higher slope and are thus denser than the flocs formed faster at a higher concentration due to the restabilisation. However it is unclear if the small precipitates (100 mgL^{-1} conditions) show fractal behaviour at all, as the relationship should be linear (see Figure 4.30).

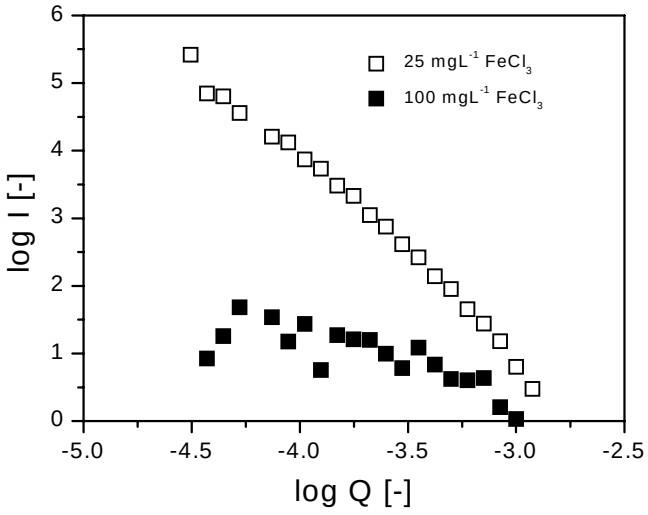


Figure 4.30 *Scattering intensity over scattering vector; the slope of the graph is related to the density of the aggregates; ferric chloride flocs with 5 mgL^{-1} as DOC HA, pH 8.*

4.9.5 Photon Correlation Spectroscopy (PCS)

PCS measures the diffusion coefficient of particles in the size range between 3 nm and a few micrometres. Particle size measurements for particles and/or aggregates smaller than 1 μm were performed on a Malvern Photon Correlation Spectrometer (PCS) Autosizer 4700 (633 nm, 5 mW, He-Ne laser). It is essentuial to use a red laser due to the fluorescence spectra of the humic substances (Goldberg and Weiner (1989)). A round quartz cell was used and temperature adjusted to 25^0C. The method measures the diffusion coefficient (Brownian motion) of particles and is limited to about 3 nm

at the lower end and, due to sedimentation, to about 3 μm at the upper end. Particle size is determined from the mass using Stokes-Einstein equation (thus number measurements are potentially incorrect as a spherical shape is assumed in the calculations). The presence of large particles disturbs the analysis.

The method was used to measure the size of primary hematite colloids (see Appendix 3) and the solubility of organics in the presence of calcium. The latter results can be summarised in a number of points. Firstly, no particulates were measured for FA. FA was prepared at pH 3, pH 6, in the presence of 75 mM NaCl, and in the presence of 25 mM $CaCl_2$ at pH 8 and 10. Aggregation or precipitation were not observed under any of these conditions. This indicates that the interaction between FA and calcium is minimal and that FA is very soluble, even at high salt conditions.

For NOM, particulates were present at all conditions, at low pH (3.5) and high pH (10). This shows that NOM is not fully soluble after freeze drying at any conditions. This can be explained with precipitation of organics at low pH and precipitation of inorganics at high pH. When the salt concentration ($CaCl_2$ or NaCl) was increased the colloids measured became very large, presumably due to aggregation phenomena. Very large flocs were visible and the precipitates were too large for correct PCS analysis (1-10 μm).

For HA, at low pH (3.5), particulates were measured in the absence and presence of calcium. Calcium increased the measured particulate size, indicating aggregation of organic colloids. At pH 8 particles formed in the absence of calcium, which shows that there may be some undissolved HA. At pH 10, no particulates were measured and the HA was fully dissolved. Once calcium was added at pH 10, particulates were measured, possibly confirming the co-precipitation of organics with calcite. In the presence of 25 mM calcium, particles are smallest at pH 8 and largest at pH 3.5. Organic concentration did not have a measurable effect on the size of the colloids, and at 25 mM $CaCl_2$ particles formed at 25, 50, and 75 mgL^{-1} HA as DOC.

Although PCS gave interesting insights into organic precipitation or aggregation, the measured values were not absolute. The scattering intensity was very low, due to the low concentration and very small colloid sizes. A more powerful instrument is required to confirm results and to obtain quanitative data.

An alternative instrument available (NICOMP Model 370) uses a more powerful laser (argon ion, 20 mW, 488 nm). This laser, although more powerful, cannot be used for the analysis of humic substances or NOM, as the wavelength lies in the fluorescence excitation and emission spectra of the organics. Results would thus be incorrect.

4.10 MEMBRANE AND DEPOSIT CHARACTERISATION

4.10.1 Zeta Potential of Membranes

Streaming potential was measured using a Brookhaven Instruments Corp. (Holtsville, NY, USA) BI-EKA commercial instrument which has a crossflow slit geometry. Childress and Elimelech (1996) and Elimelech *et al.* (1994) described the measuring cell and the principle in detail. For comparison, another surface potential analyser was used as constructed and described by Pihlajamäki (1998). The streaming potential, from which the zeta potential can be calculated with the Helmholtz-Smoluchowski equation, was measured in the presence of 10 mM NaCl, 1 mM $NaHCO_3$ and 0.5 mM $CaCl_2$, unless otherwise

indicated. The instrument used for pore zeta potential analysis is also described by Philajamäki (1998). Results are presented in the membrane characterisation section of each chapter together with the electrolyte solutions used for the measurements.

4.10.2 Field Emission Scanning Electron Microscopy (FESEM)

FESEM was used to characterise the surface roughness of clean membranes, and to examine membrane deposits and colloids. Results are shown in the relevant chapters. FESEM also proved useful in characterising surface water composition when filtered through a NF membrane, as shown in Figure 4.31 and Figure 4.32. Results showing similar colloidal organic matrixes were also obtained by Wilkinson *et al.* (1995) and Filella and Buffle (1993) after far more complex sample preparation, but slightly higher resolution. This is described in more detail in Chapter 2.

Surfaces of the specimen were thin coated with chromium after freeze drying, following the method of Kim *et al.* (1990, 1992). For intersections, membranes were freeze dried, broken in the frozen state (under liquid nitrogen) and the intersection then coated with a thin layer of chromium. The samples were then viewed with a Hitachi S-900 field emission scanning electron microscope (FESEM) at 2-4 kV. Figure 4.32 shows a close-up electronmicrograph of one of the larger colloids in the organic matrix.

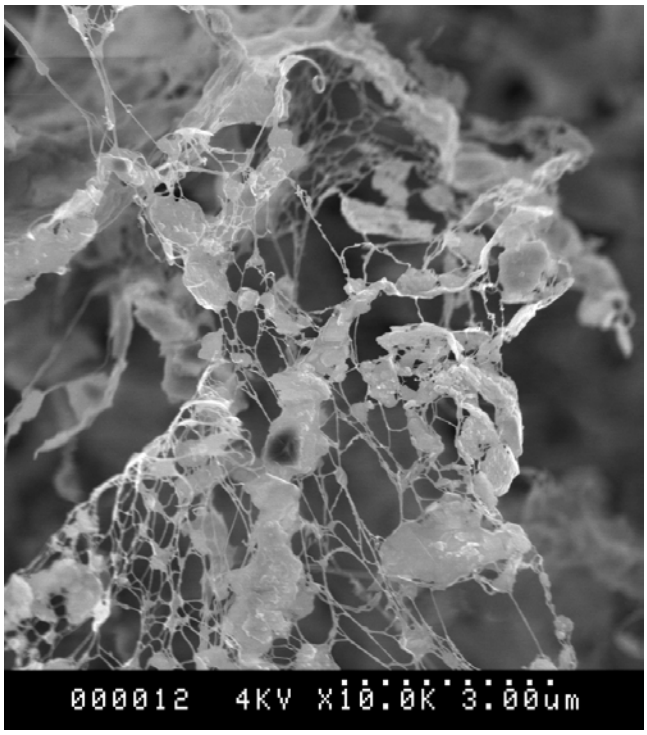


Figure 4.31 *Electronmicrograph of surface water colloids and organics. The colloids are embedded in an organic matrix.*

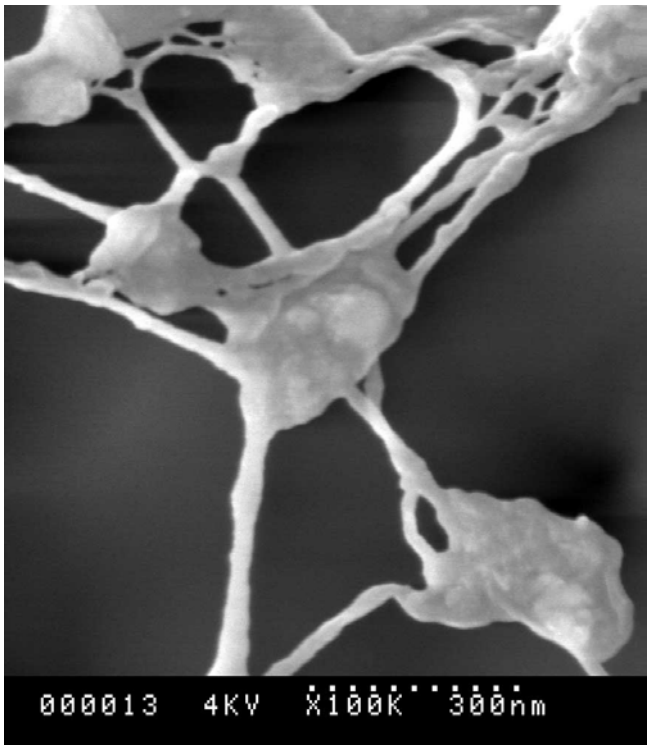


Figure 4.32 *Organic coated colloid from surface water. The colloids were shown to contain Al, Si, and Fe.*

4.10.3 Electron Dispersive Spectra (EDS)

Electron dispersive spectra allows the selective elemental analysis of objects seen on samples while viewed with an electron microscope. This was used to examine the particulates shown in Figure 4.32.

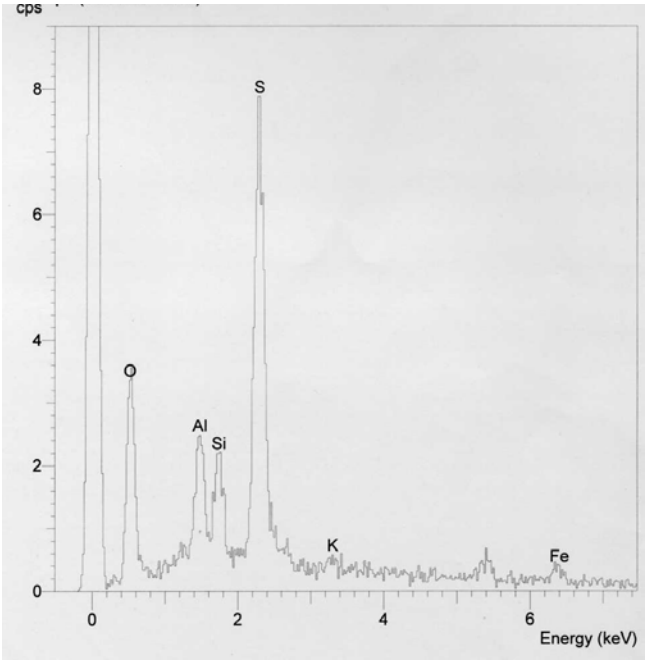


Figure 4.33 *EDS spectrum of a colloid as shown in Figure 4.32.*

The large sulphur peak is from the polysulphone membrane support (the organics were analysed on an NF membrane). This was confirmed by analysing the clean membrane. For the membrane the sulphur peak is higher (9.2 cps), carbon is visible (1 cps) and oxygen is lower (1.3 cps). None of the Al, Si, and Fe were visible. EDS does not easily measure compounds such as carbon and oxygen. However the

increased oxygen peak for the particle indicates that we are looking at oxides. The lower limit of EDS (and XPS) is about 1 atome %.

4.10.4 X-Ray Photoelectron spectroscopy (XPS)

A KRATOS XSAM800 instrument with a MgKα X-ray source (1253.6 eV proton energy, no monochromator) was used to analyse clean membranes and surface deposits. The pass energy was 40 eV in fixed analyser transmission (FAT) mode. No sample preparation was required for XPS. Results of this analysis are presented in Chapter 7.

4.10.5 Contact angle measurements

Contact angles of clean and fouled dry membranes were measured. Contact angle can give an indication of the hydrophobicity of a membrane surface. The surface roughness, however, will also influence the contact angle and so can hydration. The measurement of contact angles on dry membranes must be treated with care, as for some membranes the results are very different (Bouchard *et al.* (1997).

The medium used was MilliQ water. The angle between water droplet surface and membranes was measured using a light microscope, thus the "conventional sessile drop technique" was applied. The methods have been reviewed in Chapter 3.

4.10.6 Determination of Membrane Mass Deposit

This method was used for UF membranes only, since these membranes separate from the support material when drying. The cake mass was measured by separating the membrane skin and accumulated cake from the membrane support after drying for 1.5 h at 80 ^{o}C and weighed. The weight of the clean membrane skin was determined to be 17.5 $\pm$ 0.2 mg for a 15.2 $\cdot$ 10^{-4} m^2 membrane area.

Mass of cake accumulated was determined under selected suspension conditions in separate runs. This involved cessation of the experiment after passage of a known volume of permeate, followed by careful removal of the liquid above the cake and determination of the cake mass.

Chapter 5

MICROFILTRATION

Surface waters contain colloids and natural organic matter, largely composed of humic substances. The effect of natural organic matter (NOM) and humic substances (IHSS stream humic and fulvic acid reference material) on the deposition and rejection of inorganic colloids (hematite) by GVWP and GVHP microfiltration (MF) membranes is studied. Parameters of interest are solution pH, ionic strength, calcium concentration, primary colloid size (75, 250 and 500 nm), organic type and concentration, as well as membrane type and hydrophobicity, aggregate characteristics and colloid stability.

The method of preparation of the equilibrated suspensions, and thus their aggregation state, has a large influence on the rejection of the colloids and their aggregates, as well as the association of the particles with the membrane material and flux decline. The systems studied are grouped into (a) organics in the absence of inorganic colloids, (b) stable (non-aggregating) primary particles, (c) primary particles at pH extremes with organics, (d) particles stabilised with organics, (e) particles pre-aggregated in electrolyte solution prior to adsorption of organics, and (f) organics solutions and hematite suspensions coagulated with ferric chloride ($FeCl_3$).

Extreme pH conditions and pre-adsorption of organics onto the particle surface creates very stable systems and the rejection of the colloids is then reduced significantly. Reduced rejection leads to a penetration of the particles into the pores and adsorption on the pore walls. In this case, the flux decline is dependent on colloid size, with the size closest to the membrane pore size causing the highest flux decline. In the presence of organics, membrane-colloid charge interaction and adsorption are reduced and rejection decreases for stable colloids.

For aggregates, the presence of organics causes a higher flux decline. The presence of calcium leads to an increased flux for hematite aggregates, and a decreased flux for stable colloid-organic systems due to destabilisation of the systems and subsequent increase in rejection. The mechanical stability of the formed aggregates is great, with breakage only being observed at pressures well above typical MF operating conditions.

Coagulant addition significantly increases both organics rejection and flux decline. The rejection was very dependent on organic type and varied between 50 and 90%. The cake resembles the deposit observed with a surface water.

5.1 INTRODUCTION

MF can remove particles above a certain size (often referred to as turbidity) from surface waters. The removal of organics is possible if they are associated with particulates. This can be achieved by a coagulation/flocculation processes or by the adsorption of organics onto particles.

MF pores are relatively large (0.2 μm in diameter for the membranes used) with fouling usually occcurring because of particles rather than organics. Particle fouling of MF has been studied extensively as was shown in Chapter 3. Usually particles that are bigger than the pores are chosen in membrane studies. What has not been studied is the effect of organics on small colloidal systems and the relation to fouling. It is these small colloids which were found in the deposit on a MF membrane after surface water filtration (see Figure 5.1). In the membrane deposit, single particles in the size range around 100 nm, particle agglomerates, and a gel-like, probably organic, deposit can be seen. As was shown in Chapter 4, the visible colloids are of inorganic nature and are embedded in an organic matrix.

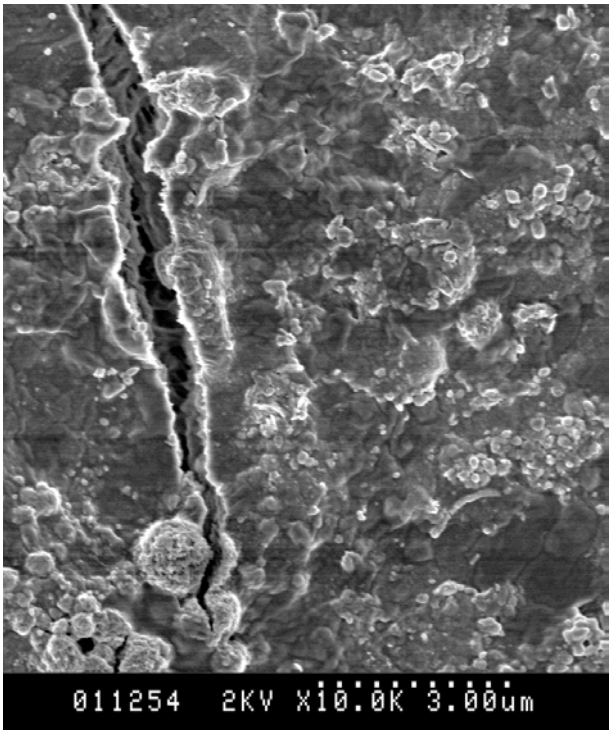


Figure 5.1 *Electronmicrograph of surface water from Mooney Mooney Dam (Gosford, NSW) on a GVWP MF membrane.*

The three key questions for this chapter are:

(i) What effect has particle stability on rejection of submicron particles (of diameter much smaller than the pore size)?

(ii) What effect has aggregation on rejection and flux?

(iii) To what extent can coagulation/flocculation influence organic/colloid rejection and flux?

The rejection of small colloids and organics obviously addresses the issue of the treated product water quality, but also has implications for further treatment steps - for example, when MF is used as a pretreatment to nanofiltration. The rejection and flux values that can be achieved lead to questions of

economic competitiveness with alternative treatments, such an UF and NF, which are more complete barriers to small colloids and organics.

Parameters of interest are solution pH, ionic strength, calcium concentration, primary colloid size (75, 250, and 500 nm), organic type and concentration, as well as membrane type and hydrophobicity, aggregate structure, and colloid stability.
Initially the membrane was tested with organics and 'model' primary particles in order to establish a baseline. As the chapter proceeds the systems become more and more complex and approach the properties of a 'real' surface water. The success of this can be observed in the similarity of the membrane deposit for a surface water and the 'synthetic' mixture.

5.2 FILTRATION PROTOCOL

Pure water flux was determined for each membrane using 3 L MilliQ water. The last 100 mL of filtrate were analysed for TOC as a control sample for organic contamination. The cell was then filled with the feed solution, the stirring switched to 270 rpm, and the pressure adjusted to 100 kPa (unless indicated otherwise). Two types of filtration protocols were used, a *standard* and a *recycle* protocol. Pure water flux was determined after the **recycle** experiments only, using 1 L of MilliQ water.
For **standard** experiments samples were taken from the feed solution, three subsequent permeate solutions (270 mL each), and the concentrate (sampled using a pipette in order to avoid disturbance of the deposit on the membrane). About 1 L of feed solution was filtered per experiment. The equipment was further flushed with MilliQ water after the membrane was removed.
For *recycle* experiments, the above procedure was repeated three times. The permeate was collected, sampled and filtered another two times without redispersion of the cake. Samples were taken during each recycle step and the total feed volume was about 1.5 L. Membrane flux averaged over an interval of filtration was calculated as

$$J(t) = \frac{V(t)}{A \cdot t} \tag{5.1}$$

and the flux behaviour in the *standard* experiments is given as the ratio of permeate flux after 800mL permeate collection to initial pure water flux

$$Flux\ ratio = \frac{J_{800\,mL}}{J_{W0}}. \tag{5.2}$$

For the *recycle* experiments, flux behaviour is described as flux decline, calculated as

$$Flux\ decline = 100 \cdot \left(1 - \frac{J_{Wf}}{J_{W0}}\right). \tag{5.3}$$

'Flux decline' is therefore the decline in pure water flux of the membranes before and after the experiments. The majority of experiments performed were recycle experiments. The apparent rejection was calculated using the following equation. c_{pi} is the concentration of permeate sample i taken directly from the membrane and not from the permeate container. It is thus the permeate concentration averaged over the filtration interval required to collect the sample. The concentration in the batch cell was measured at the end of each experiment.

$$R_i = 100 \cdot \left(1 - \frac{c_{pi}}{c_{bi}}\right) \tag{5.4}$$

Then c_{bi} was estimated for the mean permeate sample times via linear interpolation between feed and concentrate concentration. For the recycle experiments, the concentration was corrected for sampling. The deposition of solute (iron and organic carbon) on the membrane was calculated with equation (5) based on mass balance, where m is the mass of deposit.

$$m = c_F \cdot V_F - c_c \cdot V_{cell} - \sum_{i=1}^{9} c_{Pi} \cdot V_{Pi} \tag{5.5}$$

The loss of solute to cell walls is neglected. The error of this method is estimated to be ± 1% absolute mass deposit, which indicates that relative errors are high when the mass deposited is low.

5.3 MEMBRANE CHARACTERISATION

The zeta potential of both membranes in a clean state and of the pretreated GVHP membrane are illustrated as a function of pH in Figure 5.2. Electronmicrographs of the respective membrane surfaces are shown in Figure 5.3A and B.

It can be seen that the GVWP and GVHP membranes have similar morphology but very different surface charge characteristics. Pretreatment of the GVHP membrane with 50% ethanol solution (EtOH) changes the membrane potential significantly. After this treatment GVWP and GVHP membranes exhibit similar zeta potentials at high pH.

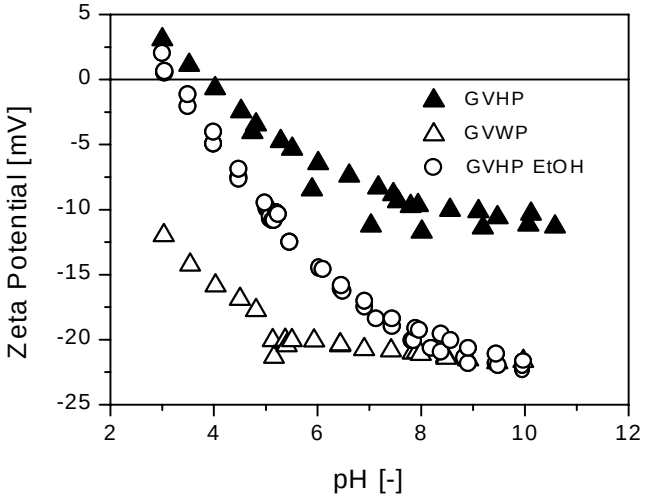


Figure 5.2 *Zeta potential of clean membranes (a) GVHP, (b) GVWP, (c) GVHP pretreated with 50% ethanol solution.*

The more hydrophilic GVWP membrane has a higher negative charge, which decreases towards low pH, but is negative over the complete pH range. The hydrophobic GVHP membrane has a slight positive charge at low pH, a pH_{pzc} of 4, and a stable value of about -10 mV is reached at pH 7. The pretreated GVHP membrane has a slight positive charge at low pH and reaches - 22 mV at high pH, which is similar to the GVHP membrane at low pH and to the GVWP at high pH.

From an applications view point, it should be noted that the membranes are negative over most of the relevant pH range. Similar results were obtained by Kim *et al.* (1994), who measured the zeta potential through the pores rather than along the surface. However, the isoelectric points determined by those authors were 3.7 and 4.4 to 5.3 for the GVWP and GVHP membranes, respectively.

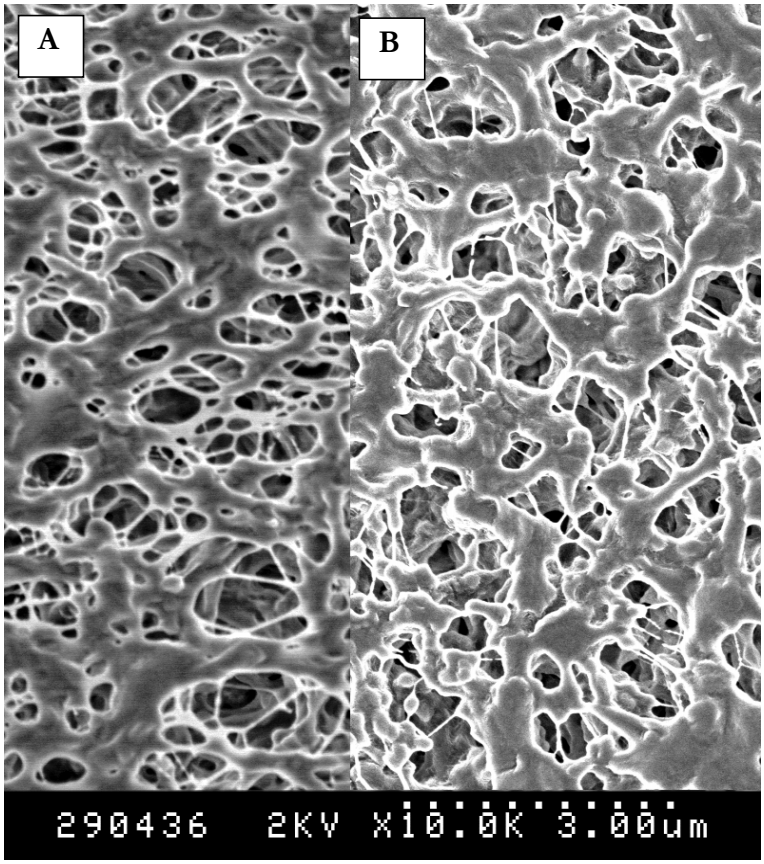


Figure 5.3 *Electronmicrographs of clean membranes (A) GVWP and (B) GVHP.*

The pure water fluxes (at a transmembrane pressure of 1 bar) for both membranes are summarised in Table 5.1. The flux under these conditions is very high and it can be assumed that permeation drag in experiments with suspensions would dominate over forces such as lateral migration (Li *et al.* (1998)). The flux of the GVWP membrane is slightly lower at high pH, when the membrane has a negative charge. For the pretreated GVHP membrane, flux remains relatively stable. Initial fluxes are higher for the GVWP membrane, but for pH 8 when the zeta potential for both membranes is the same, the flux is also the same. It is possible that the GVWP membrane loses its hydrophilicity at high pH.

Table 5.1 *Pure water flux of clean MF membranes at a transmembrane pressure of 100 kPa.*

Membrane	pH [-]	Flux [$Lm^{-2}h^{-1}$]	Average Flux [$Lm^{-2}h^{-1}$]
GVWP	4.5	8110	-
GVWP	8	7874	7968 ± 288
GVWP	10	6378	-
GVHP	8	5116	-
GVHP + EtOH	4.5	8796	-
GVHP + EtOH	8	7924	7803 ± 308
GVHP + EtOH	10	8875	-

5.4 MF OF ORGANICS IN THE ABSENCE OF INORGANIC COLLOIDS

All three types of organics were filtered in the absence of colloids to investigate the extent of any flux decline caused by the organics alone. The results are summarised in Table 5.2. Experiments were

conducted at 2.5 mM $CaCl_2$. Humic acid (HA) showed the highest flux decline (78%), compared to fulvic acid (FA, 15%) and NOM (37%). In the absence of calcium, this flux decline is reduced significantly (11% compared to 78%). This suggests that HA interacts with calcium to form materials that bind to the membrane, and either render the surface more hydrophobic or partially block the pores. The effect of calcium would be either an electrostatic or a complexation effect. The significant flux decline for NOM can be attributed to a high content of HA in the NOM, and the higher concentration of inorganic salt already present in the NOM (see Chapter 4).

The deposition of organics on the membranes is due to either adsorption from solution or deposition due to rejection. The latter would be the case if the organics were large enough to be retained by the membrane matrix. It is likely that a portion of the NOM is present in colloidal form. In addition, HA is less soluble than FA and may not be fully dissolved. Calcium is expected to cause aggregation of particulate organics. This was reported by Yuan and Zydney (1999) for a sample of large organics (Aldrich HA). These workers reported that the deposition occurred on the membrane surface, which was attributed to aggregation. However, considering the small size of such molecules and aggregates, this is unlikely for the systems used in this study.

Table 5.2 *Deposition of organics on membrane in the absence of inorganic colloids (5 mgL^{-1} DOC).*

Membrane	$CaCl_2$ [mM]	Organic Type	Deposit [% DOC]	Deposit [% UV_{254nm}]	Rejection* [% DOC]	Rejection* [% UV_{254nm}]	Flux decline [%]
GVWP	2.5	HA	13	8	10.1	4.0	78
GVHP	2.5	HA	17	11	16.1	5.9	75
GVWP	0	HA	11	3	13.6	0	11
GVWP	2.5	FA	4	1	7.2	0.3	15
GVWP	2.5	NOM	22	5	17.1	1.8	37

* rejection is low and could be attributed to deposition, which is not considered in rejection calculations and this leads to considerable error (overestimation) in rejection data.

The more hydrophobic membrane (GVHP) is observed to induce a slightly higher deposition than the hydrophilic membrane, indicating the influence of hydrophobic interactions. A similar effect has previously been reported by Jucker and Clark (1994) for hydrophobic UF membranes. UV analysis confirms the trends observed with DOC analysis, except for NOM. This suggests that the deposition of colloids, as well as organic adsorption, may be important in the case of NOM. For purified organics (FA and HA) adsorption is important, which is enhanced in the presence of calcium. The adsorption would screen the organic charge and enhance hydrophobic interactions. It could also enhance bridging effects between negatively charged organics and negatively charged membranes, or cause particulate organic aggregation due to charge screening. The deposition mechanism most likely involves a combination of the above. More deposition with the less negatively charged membranes suggests, however, that hydrophobic effects play a role.

The results confirm the presence of an 'organic' cake, observed in the filtration of surface water. Flux decline is very high considering the small amount of organics deposited, as it would take a considerable amount of time to fill the membrane pores with the small organics. In a surface water system, particles

are also important contributors to membrane fouling (as was shown in Figure 5.1). The colloidal systems of interest were described and characterised in Chapter 4.

5.5 MF OF INORGANIC COLLOIDS IN THE ABSENCE OF ORGANICS

5.5.1 Effect of primary particle size

The flux decline as a function of primary particle size for particles at pH 3 without salt solution (and thus stable), and at pH 8 with salt solution (and thus aggregated) is shown in Figure 5.4. The SPO and OPS results in this figure will be discussed later.

The flux at pH 3 passes through a minimum at a primary particle size of 250 nm. Fane (1984) observed a minimum flux as a function of particle size for ultrafiltration of colloids. This was ascribed to a transition from polarisation control by Brownian diffusion (decrease with particle size) to inertial lift (increase with particle size). However, this does not seem to explain our results with MF of hematite. Table 5.3 (no 1, 3, 4, 6, 9) summarises rejection data for a range of experimental conditions, including those in Figure 5.4. At pH 3 all primary particles have high rejection, including hematite I, which at 75 nm is much smaller than the pore size. Figure 5.5A and Figure 5.5B show electron micrographs of the surface and cross section respectively of the membrane after filtration of 800 mL of hematite I solution at pH 3. Colloids can be seen adsorbed at the top surface and the internal surface of the membranes, which suggests that the high rejection (low transmission) may be due to adsorptive removal. This may be due to the fact that at pH 3 the membrane is negatively charged and the hematite is positive.

The high flux ratio for hematite I is presumably because the dilute feed results in slow flux decline by gradual pore closure. The high flux ratio for the largest colloids, hematite III (500 nm), is probably because this particle forms a surface cake of relatively high permeability, resulting in slow flux decline. For the intermediate colloid, hematite II (250 nm), the particle size is similar to the pore size and most readily leads to pore plugging and obstruction. This causes the rapid flux decline, as seen in the lower flux ratio in Figure 5.4. The electronmicrograph of the membrane cross section for hematite III is shown in Figure 5.5C. This shows a dense cake layer, blocking pores and particle penetration into the membrane.

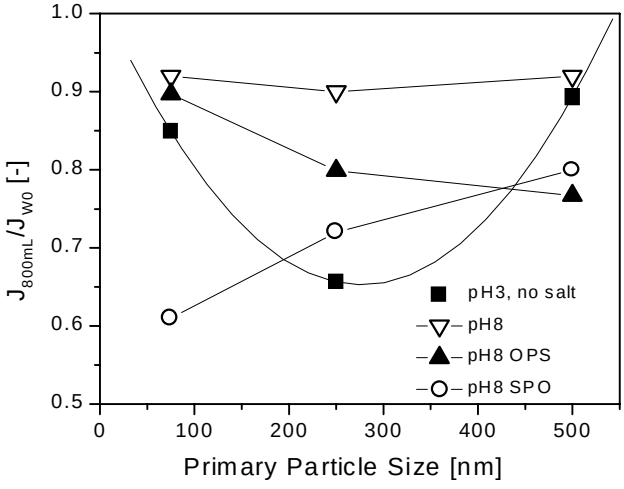


Figure 5.4 *Flux ratio (flux after collection of 800 mL permeate over pure water flux) as a function of primary colloid size for stable colloids (pH3), aggregates in the absence of organics (pH8), stabilised colloids (OPS), and aggregates (SPO).*

Table 5.3 *Rejection of Fe and UV absorbance at 254 nm (after collection of 400 mL permeate volume, GVWP membrane).*

No	Experimental Conditions	Fe Rejection [%] and UV_{254nm} Rejection [%]					
	All 10 mgL^{-1} hematite	Hematite I		Hematite II		Hematite III	
		Fe	$UV_{254\ nm}$	Fe	$UV_{254\ nm}$	Fe	$UV_{254\ nm}$
1	pH 3, MilliQ	99	99	93	97	93	99
2	pH 12, MilliQ	85	51	-	-	-	-
3	pH 8, background salt	97	66	-	-	-	-
4	pH 3, 5 mgL^{-1} [x] HA	97	44	96	37	95	26
5	5 mgL^{-1} HA, SPO[*], pH 4.5	90	42	-	-	-	-
6	5 mgL^{-1} HA, SPO[*], pH 8	95	43	93	25	93	21
7	5 mgL^{-1} HA, SPO[*], pH 10	88	45	-	-	-	-
8	5 mgL^{-1} HA, OPS, pH 4.5	54	41	-	-	-	-
9	5 mgL^{-1} HA, OPS[*], pH 8	11	6	92	39	94	12
10	5 mgL^{-1} HA, OPS, pH 10	6	5	-	-	-	-
11	5 mgL^{-1} FA, OPS, pH 8	0	7	-	-	-	-
12	5 mgL^{-1} NOM, OPS, pH8	23	15	96	38	97	15

[*] OPS = mixing order organics-particles-salt; SPO = mixing order salt-particles-organics

[x] all as organic carbon

5.5.2 Effect of pH

In order to study the effect of charge, hematite I was filtered with both GVWP and GVHP membranes at pH12. At this pH both membranes and hematite have a negative charge of similar magnitude (-20mV). Rejection is slightly reduced for both membranes compared to pH3 (see Table 5.3, no 2 for the GVWP value), however the membranes do adsorb hematite to a large extent and eventually achieve full rejection. For these conditions, flux declined 75-80% at pH 3, and 95% at pH 12. Fane *et al.* (1988) have previously reported a decrease in flux of an inorganic membrane with increased pH and more negative zeta potential. The same effect can be seen in this case, where the hematite colloids form an 'inorganic' membrane with a more negative zeta potential at pH 12. This effect will be further investigated in Chapter 6.

It should be noted that the zeta potential is an average value for the surface potential, and does not account for individual surface functional groups. Therefore it is possible that there are remaining positive groups even in the presence of organics, which do interact with the membrane surface.

Also, the operation of MF at a very high flux may bring the colloids in very close contact with the membrane surface. Then the repulsive forces might be overcome, inducing the colloids to adhere to the membrane due to short range forces (Van der Waals interactions).

Alternatively, the continued adsorption, even in the presence of electrostatic repulsive effects, may indicate strong specific binding between colloid-metal centres and membrane functional groups. Once the flux has declined to 2 - 20% of its initial value, electrokinetic interactions could increase rejection.

5.5.3 Effect of Aggregation

Experiments were carried out in the presence of electrolyte solution and pH 8 (in this case to provide a baseline for the aggregation experiments with organics). The rejection of the 75 nm colloids was complete, as shown in Table 5.3 (no 3). Figure 5.4 shows that after aggregation the flux ratio is high (>90%) and independent of primary particle size. Aggregation reduces flux decline. This is similar to observations reported by Kim *et al.* (1993) with colloidal silver on addition of electrolyte.

The aggregates were mechanically strong and did not break at the membrane surface in the standard (100kPa) experiments. Breakage of some of the aggregates occurred at a relatively high pressure of 300 kPa, with a 20 to 25% lower rejection. Results are shown later in the SPO section (Figure 5.11). The flux results are not shown, but the flux decline was very similar (50%) to that obtained in other experiments where 100 kPa was applied.

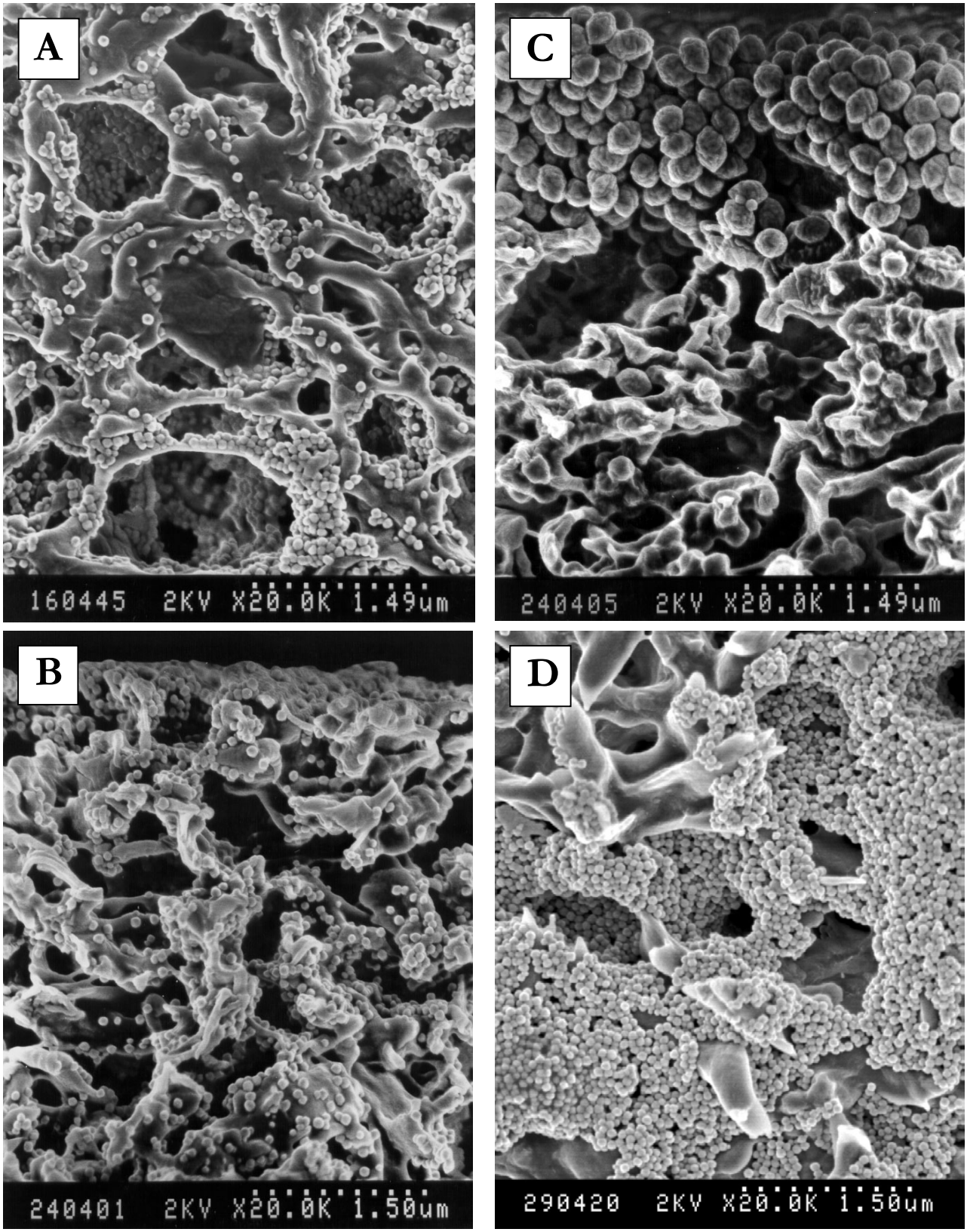


Figure 5.5 *Electronmicrograph of (A) the membrane surface and (B) the cross-section for hematite I (75 nm, pH3, no organics), (C) the cross-section for hematite II (250 nm); (all 10 mgL^{-1} hematite, GVWP membrane), and (D) the membrane surface for aggregates (SPO).*

5.6 INORGANIC COLLOIDS AT PH 3 WITH ORGANICS

To understand the effect of organics on the primary particles, another set of experiments far from surface water conditions (pH 3 with no electrolyte solution) was carried out.

In the presence of 5 mgL^{-1} (as organic carbon) HA, rejection of colloids was higher and flux decline lower than in the absence of organics. Results are shown in Table 5.3 (No 4) and Table 5.4. Organic rejection increased compared to filtration in the absence of colloids (compare Table 5.2).

These effects can be attributed to the adsorption of organics on the colloids, which increases negative colloid charge and depletes organics in the permeate to some extent, as well as the low solubility of HA at this pH and thus the filtration of the aggregates or the precipitate.

The colloid charge was shown in Chapter 4. At pH 3 some organics will adsorb, but due to the low dissociation of organic functional groups the charge of the organics will be low. This means that the charge of the colloids will be reversed ineffectively and aggregation occurs. This was indeed observed in Figure 5.6.

Table 5.4 *Flux and rejection of colloids at pH 3 in MilliQ and in the presence of organics (5 mgL^{-1} HA).*

Colloid	Membrane	DOC Rejection [%]	Fe Rejection [%]	DOC Deposit [% DOC]	Fe Deposit [% Fe]	Flux Decline [%]
I (MilliQ)	GVHP	-	87	-	94	66
I (MilliQ)	GVWP	-	99	-	100	74
I	GVHP	32	99	17	56	53
I	GVWP	17	97	0	74	70
II	GVWP	23	96	0	95	86
III	GVWP	20	95	13	92	54

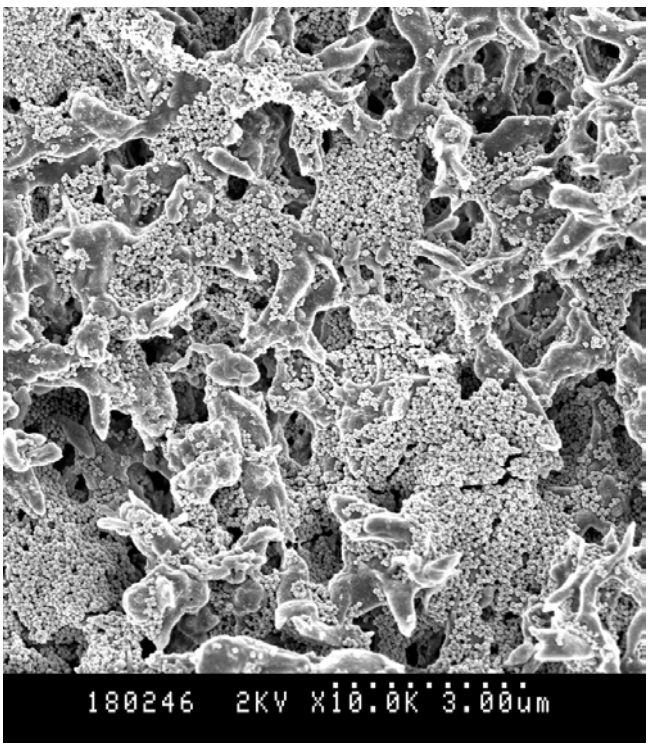


Figure 5.6 *Electronmicrograph of inorganic colloids (hematite I) in the presence of 5 mgL^{-1} as DOC HA at pH 3 (resolution half of that in* **Figure 5.5***).*

5.7 MF OF AGGREGATED COLLOIDS WITH ADDITION OF ORGANICS (SPO)

In this mixing order, particles aggregate and then adsorb organics on their surface. A very different deposit occurs on the membrane, when this mixture is filtered. This is shown in Figure 5.5D, which depicts the deposition of large aggregates rather than the single particles of Figure 5.5A. The effects of membrane type, organic type and concentration, colloid size, as well as solution chemistry (pH and calcium concentration) will now be examined for this system. The solution chemistry influences the size and structure of the aggregates. Other factors likely to influence aggregation, for example stirring and transmembrane pressure, are also investigated.

5.7.1 Effect of membrane type

Due to the importance of cake formation and flux dependence on deposition, membrane type was not examined in this section. It was anticipated that aggregate characteristics were more important than membrane type.

5.7.2 Effect of organic type and concentration

The organic type does not have an influence on flux and colloid rejection with this particle preparation method. Flux declines 75-85% for all organics and the rejection of colloids is high (greater than 90%). The results are summarised in Table 5.5 (No 1, 8, 9) and Figure 5.7A. Rejection drops a little after pressure release (cycles 2 and 3 in Table 5.5), possibly indicating some aggregate breakage or concentration polarisation effects.

Table 5.5 *Deposition and rejection of hematite colloids, organic rejection, and flux decline as a function of organic type and concentration, calcium concentration and pH (GVWP membrane, SPO).*

No	Organic Conc. [mgL^{-1} as DOC]	Calcium Conc. [mM]	Hematite	pH [-]	Deposition [% Fe]	Organic Rejection [% DOC]	Flux Decline [%]	Rejection [% Fe] after cycles 1, 2, 3		
1	5 HA	0.5	I	8	91	17	74	96	86	86
2	10 HA	0.5	I	8	93	11	75	94	90	91
3	20 HA	0.5	I	8	88	6	81	88	92	90
4	5 HA	2.5	I	8	95	13	64	97	91	85
5	5 HA	4	I	8	97	12	60	99	98	94
6	5 HA	0.5	I	4.5	92	8	80	90	84	72
7	5 HA	0.5	I	10	87	29	73	88	85	76
8	5 FA	0.5	I	8	93	5	78	95	89	87
9	5 NOM	0.5	I	8	94	8	84	96	88	80
10	5 HA	0.5	II	8	94	12	63	94	94	88
11	5 HA	0.5	III	8	87	6	40	88	77	80

As shown in Table 5.5 (No 1, 2, 3), HA concentration was varied from 5 to 20 mgL^{-1} DOC, but the increase in concentration had only a marginal effect on colloid rejection. The aggregates were not redispersed due to the addition of organics, which stabilised the particles in the OPS case. The deposition of DOC (results not shown) on the membrane increases with concentration, but colloid deposition is constant at about 90%. Organic rejection decreases with increased concentration,

presumably due to the decrease in adsorption on the colloids, and flux decline increases with a higher HA concentration.

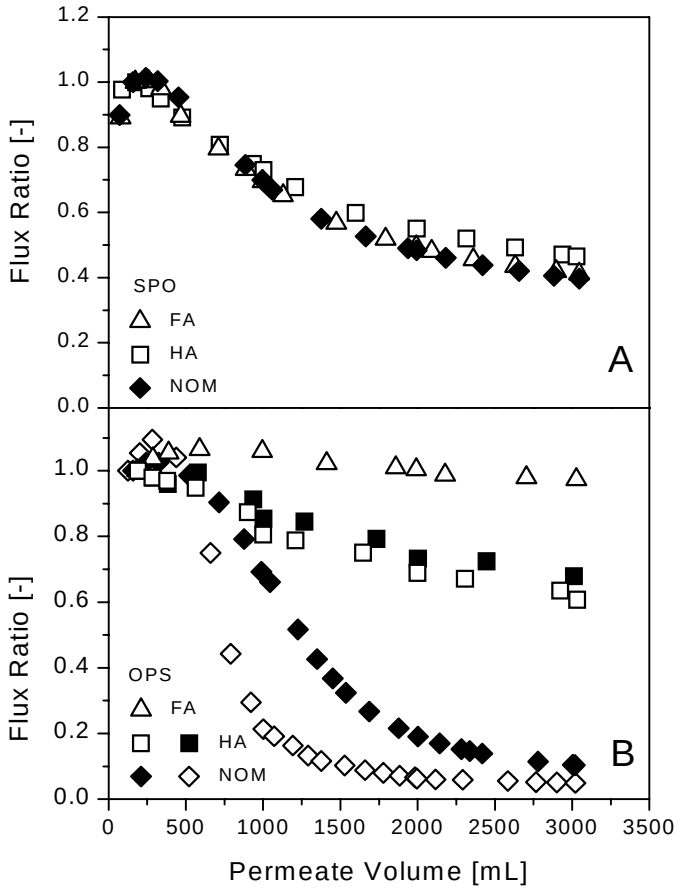


Figure 5.7 *Flux ratio (flux divided by initial flux), for different organic types (GVWP membrane), (A) for stabilised colloids (OPS) and (B) for aggregates (SPO).*

5.7.3 Effect of primary particle size

Primary particle size has an effect on the deposition of organics, with 12, 9, and 6% of organics being deposited for 75, 250, and 500 nm primary colloids, respectively. Organic rejection increased with decreasing colloid size (see Table 5.3, No 1, 10, 11), which can be explained by increased adsorption for a higher specific surface area of the smaller colloids.

Colloid rejection is almost complete for all sizes as shown in Table 5.3, and deposition is in the order of 90%. Flux decline increases with decrease in primary particle size (see Figure 5.4). This is most likely attributable to the formation of a cake of lower porosity with more interstitial organics.

5.7.4 Effect of calcium concentration

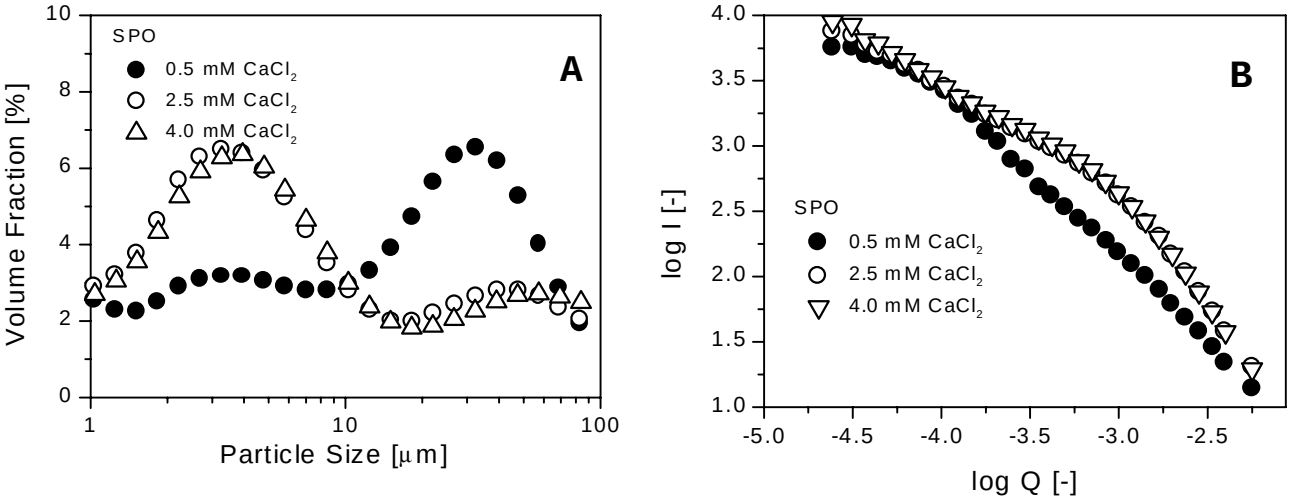
When the calcium concentration in the background electrolyte was increased, flux decline was lower. Results are shown in Table 5.5 (No 1, 4, 5) and Figure 5.9A. The UV_{254nm} rejection drops significantly over time at higher calcium concentrations, which could indicate a detachment of some individual colloids from the aggregates. Colloid deposition increases with increasing calcium concentration, and very interestingly, the flux also increases.

These results suggest that aggregate characteristics, such as structure, have an effect on flux as also shown in Chapter 6. The addition of larger amounts of electrolyte causes the colloids to aggregate faster due to a reduction in charge repulsion. Faster aggregation results in looser aggregates, which can also induce larger flux.

The variation of the particle size with calcium concentration is shown in Figure 5.8A. Surprisingly, at a higher calcium concentration the aggregate size is smaller (3-4 μm versus 30-40 μm at low calcium concentration), possibly as a result of a greater extent of breakup of the more tenuous flocs formed at high salt concentrations. However, the volume fraction of submicron particles is also lower at high calcium concentration.

It is very likely that higher calcium concentration leads to the formation of looser aggregates, as has been shown for well defined systems in Chapter 4. Figure 5.8B shows the I versus Q plot (of which the slopes are related to aggregate density) for the different aggregates as a function of calcium concentration. Aggregate size is inversely related to the scattering vector Q. It appears that larger aggregates have a denser structure at lower salt concentration, while at the higher salt concentration the small ones are denser.

Figure 5.8 *(A) Particle size distribution for as a function of calcium concentration (10 mgL^{-1} Hematite I, 5 mgL^{-1} HA as DOC and (B) Scattering intensity over scattering vector; the slope of the graph is related to the density of the aggregates.*



This does not show a strong trend as the comparison between aggregates below and above the critical coagulation concentration (determined to be about 30 mM, see Chapter 4), but in this case a higher salt concentration forms very dense and small aggregates. These results indicate the need for a more detailed investigation. The interpretation of scattering data for polydisperse systems is questionable at this stage and very little is known about the aggregation of systems at a pH close to the isoelectric point, in the presence of calcium and organics.

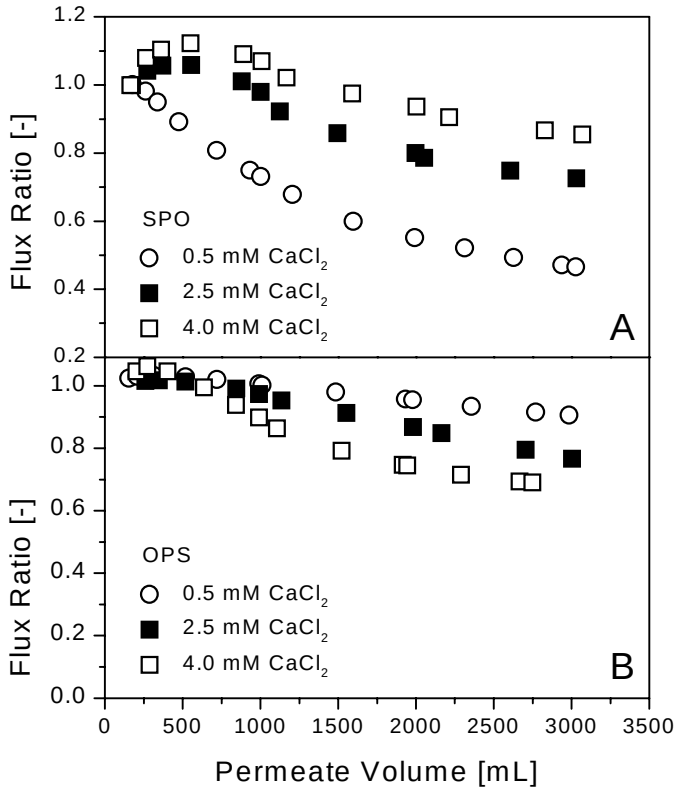


Figure 5.9 *Flux ratio as a function of calcium concentration (A) for stabilised colloids (OPS) and (B) for aggregates (SPO, GVWP membrane).*

5.7.5 Effect of stirring

In this mixing order, particles are deposited as a cake. Stirring may be important in partially removing the deposit, or preferentially classifying the particles with smaller ones in the cake, as reported by Altmann and Ripperger (1997). Stirring was varied from 0 to 540 rpm. Flux is a little lower at 0 and 540 rpm, compared to 270 rpm, and rejection decreased more over the filtration volume in the unstirred experiment. This suggests that concentration polarisation effects are operative and smaller particles may deposit preferentially at 540 rpm. However, overall it appears that concentration polarisation effects (and impact of shear on the boundary layer thickness) are minimal, with the deposition being dominated by permeation drag. Deposition is identical (92%) for all three stirring conditions. This behaviour is expected at the high fluxes used in these experiments.

5.7.6 Effect of pH

The effect of pH is shown in Figure 5.10A and results are summarised in Table 5.5 (No 1, 6, 7). Low pH causes the largest flux decline, which corresponds to the observations at pH3 with organics. Organics deposition is 10, 12, and 44%, at pH 4.5, 8, and 10, respectively. At low pH the organics are less soluble, and thus have less functional groups available for colloid-organic interactions. Therefore, precipitates would deposit together with organics adsorbed on hematite. Tipping (1981) reported a decrease in adsorption of organics on hematite with increased pH (see also Chapter 2). The increase in organics deposition at higher pH must, therefore, be attributed to the deposition of calcium-organic complexes with the colloids.

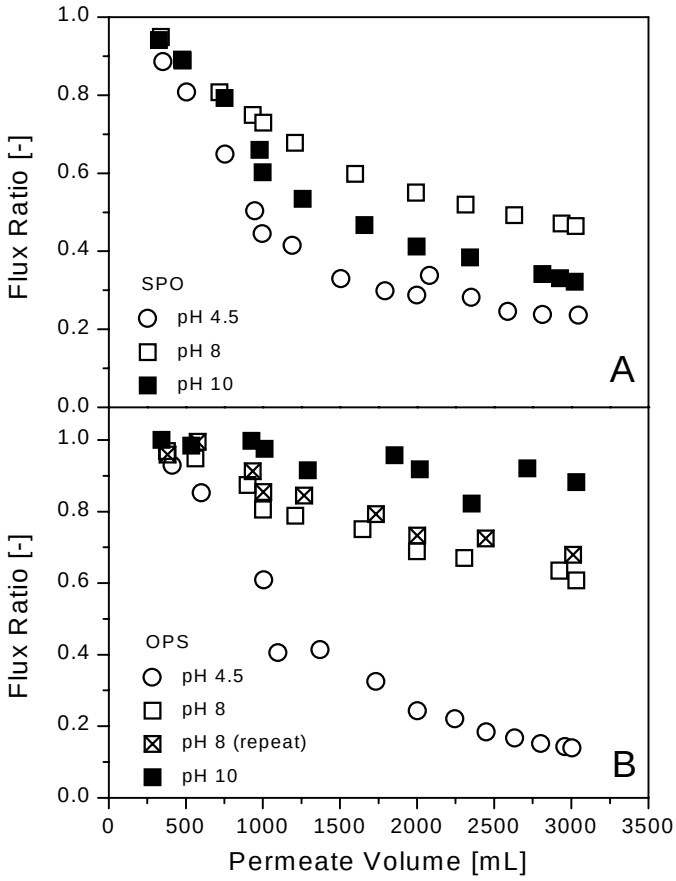


Figure 5.10 *Flux ratio as a function of pH (A) for stabilised colloids (OPS) and (B) for aggregates (SPO, GVWP membrane).*

5.7.7 Effect of transmembrane pressure

Flux increases with transmembrane pressure, thus increasing convection and permeation drag. This is expected to cause increased deposition of particles if they are larger than the size of the pores and if permeation drag is the limiting deposition factor. Increased permeation drag increases the force on the aggregates during deposition and an excessive permeate pressure can lead to aggregate break-up, which may result in a reduced rejection.

The flux decline was identical for all pressures (80% decline) and the flux increased linearly with pressure. In each case, about the same amount of cake was deposited (same volume filtered) and the invariance of flux with pressure implies that an incompressible cake exists. The colloid rejection as a function of filtrate volume for the four transmembrane pressures is shown in Figure 5.11A in the absence of organics (as discussed earlier) and in Figure 5.11B with organics. The first three points represent the first filtration cycle. The pressure was then released, and points four and seven are the first points of filtration cycles two and three, respectively. The recycle results suggest that pressure increase leads to break-up of the aggregates. Low rejection occurs at the start of the filtration cycles, after the pressure was released, the cells refilled and filtration resumed. The resulting flux increase would facilitate transport of the smaller or broken aggregate fractions through the membrane before larger aggregates deposit again and retain small fractions. A decline of rejection indicates some concentration polarisation (see first cycle at 300 kPa) with filtration time, but this decrease is much lower than that at the start of the new cycle. If concentration polarisation was dominating, rejection would drop at the end of a cycle rather than at the start.

The presence of organics appears to facilitate aggregate break-up. Flux decline is independent of transmembrane pressure and it is therefore assumed that the cake is not compacted. The aggregate

break-up is also reflected in the deposition of hematite as shown in Table 5.6. Deposition is reduced when aggregates break and rejection decreases. The break-up of the aggregates may be either due to, firstly, the force on the aggregates during filtration or, secondly, to the force of the expanding membrane on the cake when the pressure is released.

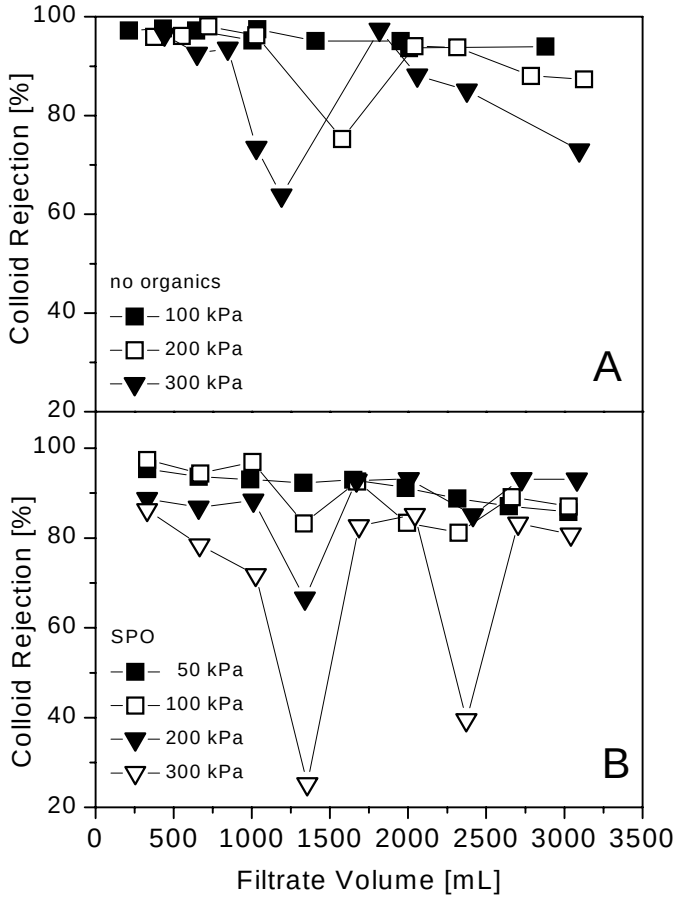


Figure 5.11 *(A) Iron rejection as a function of transmembrane pressure (Hematite I, no organics) and (B) Iron rejection as a function of transmembrane pressure (SPO, GVWP membrane).*

Table 5.6 *Deposition and rejection of hematite colloids as a function of transmembrane pressure (GVWP membrane, SPO).*

Transmembrane Pressure [kPa]	Flux Decline J_w/J_{w0} [%]	Deposition [% Fe]	Rejection [% Fe] after cycles 1, 2, 3		
50	74	93	94	92	87
100	74	91	96	86	86
200	79	85	88	84	90
300	80	78	79	64	68

Overall, the recycle experiments showed that concentration polarisation effects were negligible - if they were significant, flux would increase after permeate recycle. Concentration changes in the cell due to filtration do not seem important either.

5.8 MF OF STABILISED COLLOIDS (OPS)

In this mixing order (OPS), particles are generally stable due to the presence of adsorbed organics on their surface. Effects of membrane type, organic type and concentration, colloid size, as well as solution chemistry (pH and calcium concentration) will now be examined for this system. The effects of pressure and stirring were not examined for the OPS system, as no cake was formed in most cases.

5.8.1 Effect of membrane type

Given the fact that aggregation in the presence of NOM caused major flux decline and not adsorption (see next paragraph), it is evident that the membrane type did not play a major role. Small differences were observed in the deposition of solute, with slightly higher values of deposition for the more hydrophobic GVHP membrane. This again corresponds to the results reported by Jucker and Clark (1994).

5.8.2 Effect of organic type and concentration

Figure 5.7B shows results of flux ratio (flux divided by initial flux) as a function of organic type. A quite distinctive difference between the fluxes for the three different organic types can be observed, with FA resulting in very little flux decline and NOM causing almost complete loss of flux.

The difference between NOM and FA or HA is primarily the presence of salts in the NOM powder, which is in this case more important than the characteristics of the different organic species (see Chapter 4 for quantity and types of salt in the NOM powder). The salt leads to aggregation of some colloids prior to stabilisation, and this generates the most detrimental conditions for flux decline. This can probably be attributed to the formation of very small aggregates that can effectively block the membrane pores, and this is supported by the initially very low rejection of colloids (Table 5.7, no 9).

Table 5.7 *Deposition and rejection of hematite colloids, organic rejection, and flux decline as a function of organic type and concentration, calcium concentration and pH (GVWP membrane, OPS).*

No	Organic conc. [mgL^{-1} as DOC]	Calcium conc. [mM]	Hematite	pH [-]	Deposition [% Fe]	Organic Rejection [% DOC]	Flux Decline [%]	Rejection [% Fe] after cycles 1, 2, 3		
1	5 HA	0.5	I	8	18	1	22	11	8	6
2	10 HA	0.5	I	8	4	2	10	0	3	0
3	20 HA	0.5	I	8	10	3	28	5	5	1
4	5 HA	2.5	I	8	27	31	50	12	12	16
5	5 HA	4	I	8	96	28	69	92	90	76
6	5 HA	0.5	I	4.5	71	22	83	54	60	69
7	5 HA	0.5	I	10	7	18	17	6	3	1
8	5 FA	0.5	I	8	18	7/7*	11/16*	15	10	4
9	5 NOM	0.5	I	8	75	7/7*	95/95*	24	84	95
10	5 HA	0.5	II	8	89	7	55	86	83	81
11	5 HA	0.5	III	8	88	9	40	94	93	92

* repeated

Zeta potential measurements show that particles coated with NOM have the greatest negative charge (results not shown). This supports the hypothesis that salts present in the NOM allow the colloids to

aggregate simultaneously with stabilisation by the organics, which reduces surface area and forms very small aggregates (doublets and triplets, <0.2 μm). The relatively small aggregates would be captured in the pores very easily, leading to the detrimental flux declines observed. Rejection and deposition data of hematite confirm these observations (see Table 5.7, No 1, 8, 9).

The organic concentration was varied (Table 5.7, No 1, 2, 3) and this resulted in a change in particle charge and aggregation. Flux was found to be directly related to deposition of colloids on the membrane and rejection of colloids, both of which are lowest at 10 mgL^{-1} (as DOC).

5.8.3 Effect of primary particle size

Flux decline was most severe for hematite II (250 nm). This was also observed for organic-free particles stabilised at pH 3, and particles at pH 3 with organics (see Figure 5.4). Hematite I showed less flux decline compared to Hematite II and III (high flux ratio) and rejection has now, in the presence of organics, dropped to almost zero (see Table 5.7, 1, 10, 11). For hematite II, initial rejection of colloids is not complete (80%), which indicates pore penetration and rejection decreases when pressure is released in recycle experiments. This can be explained by the fact that the membrane has a pore size distribution, allowing some of the 250 nm colloids to pass through. The deposition results are similar for hematite II and III, for which about 89% are deposited. Flux is higher for hematite III than II (Table 5.7, No 11 vs 10) due to the larger colloid size resulting in a cake with larger "voids". Deposition of hematite II is larger than for hematite I with NOM, but the flux is higher (Table 5.7, No 10 vs 9). This confirms that small colloids, once retained, cause a much more severe flux decline. It should be noted here that small colloids will eventually block pores. However, this was not achieved for FA and HA, with the rejection remaining low, even after the filtration of 3L (Table 5.7, No 7 and 8).

5.8.4 Effect of calcium concentration

Experiments were carried out at 0.5, 2.5, and 4 mM $CaCl_2$. Results are shown in Figure 5.9B, and the trend observed is to that of the SPO data. Calcium can destabilise colloids that were stabilised by organics. This was observed to occur at a concentration between 2.5 and 4 mM $CaCl_2$, with a resultant increase in colloid rejection from 15 to 95% and a greater flux decline, as shown in Table 5.7 (No 1, 4, 5). This corresponds to the effect of calcium on stabilised colloids reported by Amirbahman and Olson (1995), which was described in more detail in Chapter 2. Deposition increased with calcium concentration, which indicates that the destabilisation is always present to some extent. The calcium was added after the colloids were stabilised with HA, which is a different scenario to NOM, where salt (which is in the NOM powder) is added simultaneously. In this case, the calcium provides a full destabilisation of the organic-coated colloids at 4 mM, leading to complete rejection and deposition.

5.8.5 Effect of pH

pH has a strong effect on flux and deposition (see Table 5.7, No 1, 6, 7). At pH 4.5 flux is lowest and deposition highest and these results are plotted in Figure 5.10B. Zeta potential measurements showed lowest colloid charge at low pH. Aggregation is therefore most likely at this pH, which would increase deposition. The results are very similar to aggregation of colloids with NOM. This is supported by an increased rejection of colloids at pH 4.5 (Table 5.7, No 6 vs 1,7). At pH 10 the organics are most soluble, adsorb strongly on the colloids, and thus readily stabilise them and result in low rejection and deposition, and high flux.

In summary, there are two scenarios which cause the most severe flux decline. Firstly, poorly soluble organics at low pH (4.5) or in the presence of salt, which is often the case with surface waters, and secondly small colloids, that partially aggregate. Particles prepared with organics in the OPS order exhibit a low flux decline for the small colloids, due to a low rejection and an incomplete adsorption within the pores. The solution chemistry is important, as pH influences the adsorption of organics and, thus, particle stabilisation. Additionally, calcium can destabilise the previously stable colloids.

5.9 BLOCKING LAW ANALYSIS

Blocking laws were described in detail in Chapter 3. In Table 5.8 the blocking laws are summarised. As the flux in the MF experiments was very high, stirring had no effect and deposition was near complete, it can be assumed that applying the blocking laws is valid. However, the laws would tend to be less valid for the OPS system, rejection was very low.

A number of experiments were selected for the analysis. Plotting t/V and Exp(t) over filtration time and volume allows the determination of which filtration mechanism is valid. This analysis was applied here to verify the observations of rejection and flux decline as a function of primary particle size.

Table 5.8 *Constant Pressure Filtration Laws (Hermia (1982), Bowen et al. (1995)).*

Law	Equation	Description
Complete Blocking (pore blocking)	$V = \frac{J_0}{k_{CB}}\left(1-e^{-k_{CB}t}\right)$	Particles do not accumulate on each other and particles arriving at the membrane will seal pores, $d_{particle} \simeq d_{pore}$
Intermediate Blocking (long term adsorption)	$V = \frac{J_0}{k_{IB}}\ln(1+k_{IB}t)$	Particles do accumulate on each other and seal membrane pores, $d_{particle} \simeq d_{pore}$
Standard Blocking (direct adsorption)	$\frac{t}{V} = \frac{1}{J_0} + \frac{k_{SB}}{J_0}t$	Particles deposit on the internal pore walls, decreasing the pore diameter, $d_{particle} << d_{pore}$
Cake Filtration (boundary layer resistance)	$\frac{t}{V} = \frac{k_{CF}}{4J_0^2}V + \frac{1}{J_0}$	Particles are retained due to sieving and form a cake on the surface, deposition occurs on other particles, all membrane area is already blocked, $d_{particle} > d_{pore}$

Results for the blocking law analysis are shown in the following sections for stable colloids in the absence of organics, and for both SPO and OPS cases.

5.9.1 Stable Colloids in the Absence of Organics

The filtration of these primary colloid systems was described in section 5.5. The colloids of a size closest to the membrane pore size resulted in the greatest flux decline, as this was attributed to pore plugging. In contrast, the smaller colloids were too small to fill up pores effectively at the volumes filtered, and the larger colloids formed a cake on the membrane surface. These suggestions were confirmed with electronmicrographs (see Figure 5.6).

Blocking law analysis is shown in Figure 5.12 and Figure 5.13 for the three different primary colloid sizes.

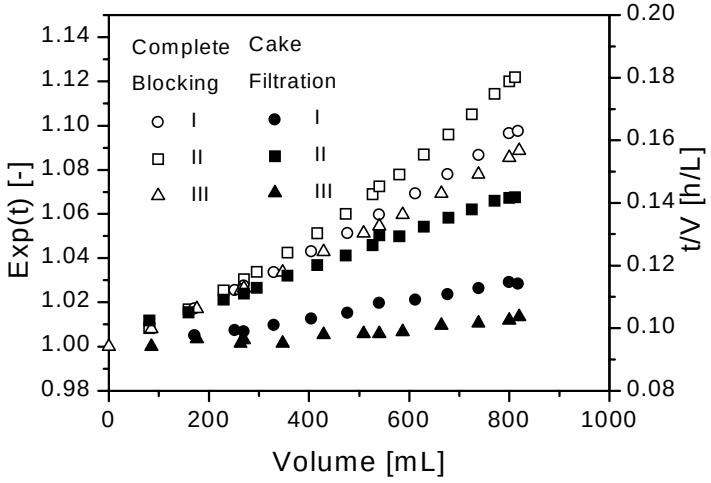


Figure 5.12 *Complete Blocking and Cake Filtration law for stable hematite colloids at pH 3.0 as a function of colloid size.*

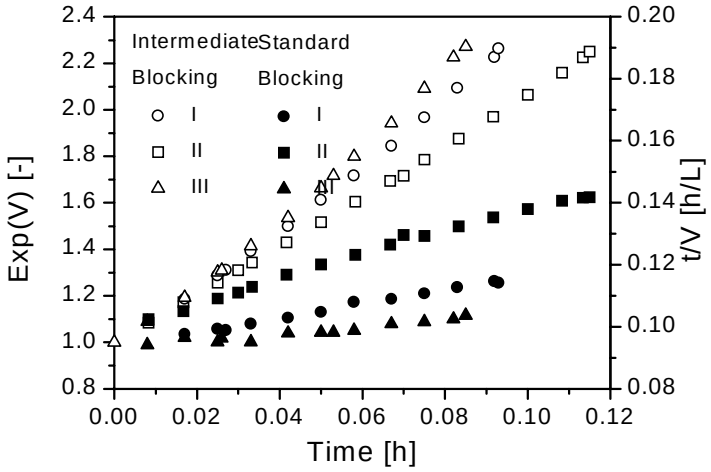


Figure 5.13 *Intermediate and Standard Blocking Filtration law for stable hematite colloids at pH 3.0 as a function of colloid size.*

The graphs show a linear relationship for all blocking laws for at least one section of the graph. This implies that all four mechanisms are valid if the blocking laws apply. None of the mechanisms can be eliminated. The slopes of the lines can be related to the resistance of filtration (see Table 5.8 for detailed description of the slope). Particles II (250 nm) show the steepest slope for most mechanisms.
It was not the aim of this study to quantify the mass transfer coefficients or filtration resistances, but rather to identify which blocking law was applicable. This is not possible, unless one proposes the theory that all blocking laws occur simultaneously or sequentially.

5.9.2 Aggregated Colloids with subsequent Addition of Organics (SPO)

The filtration of these aggregates was described in detail in section 5.7. The conclusion was that the aggregates are larger than the membrane pores and are retained on the membrane surface, forming a cake. This was also confirmed by electronmicroscopy (see Figure 5.6).
In this section, the blocking law analysis for SPO systems is shown as a function of pH (Figure 5.14 and Figure 5.15) and primary colloid size (Figure 5.16 and Figure 5.17).
Again, all graphs show linear relationships, indicating the possible presence of all four mechanisms to some extent. This could be true as the aggregation is most likely incomplete, leaving some small colloids for contribute to pore adsorption and pore blocking.

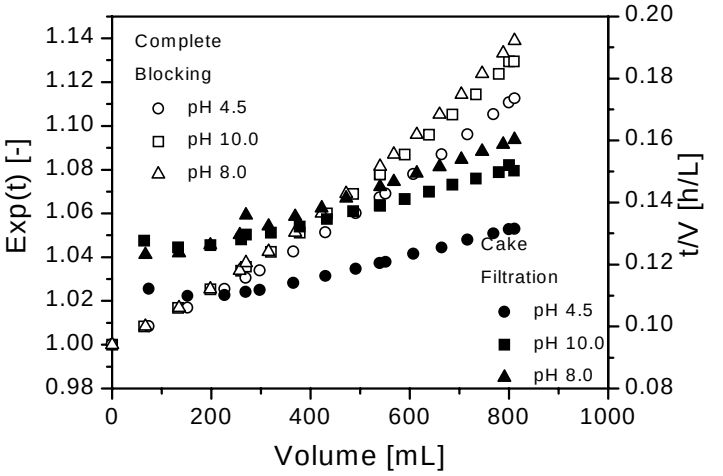


Figure 5.14 *Complete Blocking and Cake Filtration law for hematite aggregates at varying pH with 5 mgL^{-1} as DOC HA and SPO mixing order.*

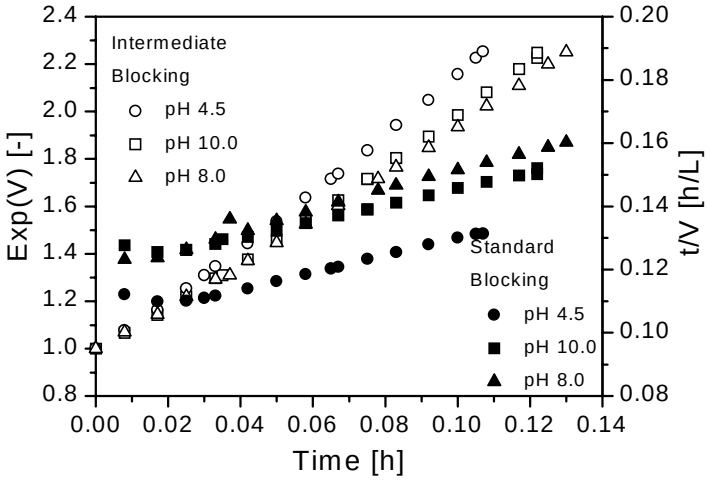


Figure 5.15 *Intermediate and Standard Blocking Filtration law for hematite aggregates at varying pH with 5 mgL^{-1} as DOC HA and SPO mixing order.*

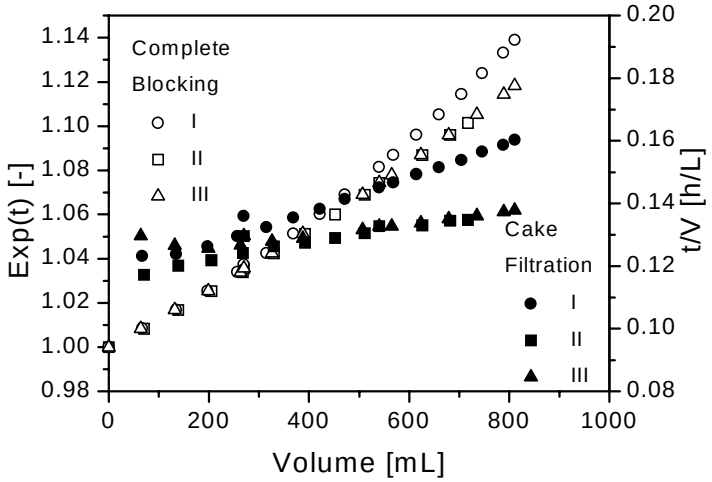


Figure 5.16 *Complete Blocking and Cake Filtration law for hematite aggregates as a function of primary colloid size with 5 mgL^{-1} as DOC HA and SPO mixing order.*

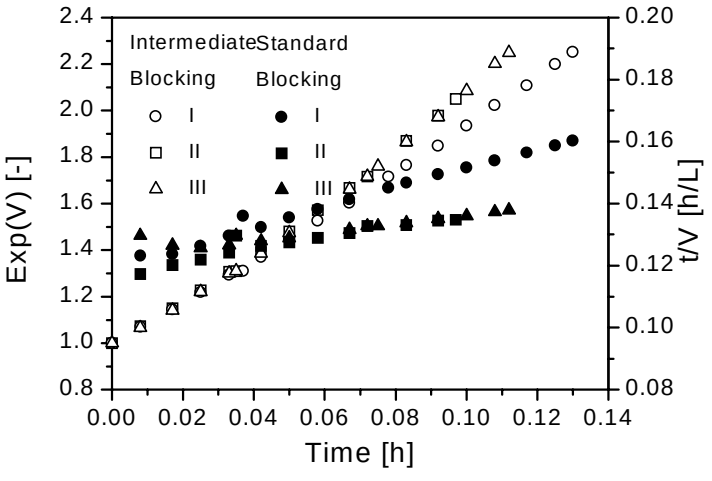


Figure 5.17 *Intermediate and Standard Blocking Filtration law for hematite aggregates as a function of primary colloid size with 5 mgL^{-1} as DOC HA and SPO mixing order.*

5.9.3 Stabilised Colloids (OPS)

The filtration and rejection of stabilised colloids (OPS) was shown in section 5.8. The stable colloids have a high negative surface charge and are not retained by the MF membranes. Adsorption on the membrane material is minimal - much less than in the absence of organics and at pH 3.

Results of the blocking law analysis are shown as a function of pH for the smallest colloids (Hematite I, 75 nm) and as a function of primary colloid size at pH 7 to 8 in Figure 5.18 and Figure 5.19, and Figure 5.20 and Figure 5.21, respectively.

All relationships are linear in at least one part of the graph, however, the cake filtration relationship is constant. This means that no cake is formed, which is indeed the observed situation during these experiments. While the overall linear relationships appear unrealistic, this shows that the blocking laws may indicate the correct mechanism - all filtration phenomena occur simultaneously or sequentially, except in the OPS case of small colloids where no cake formation occurs.

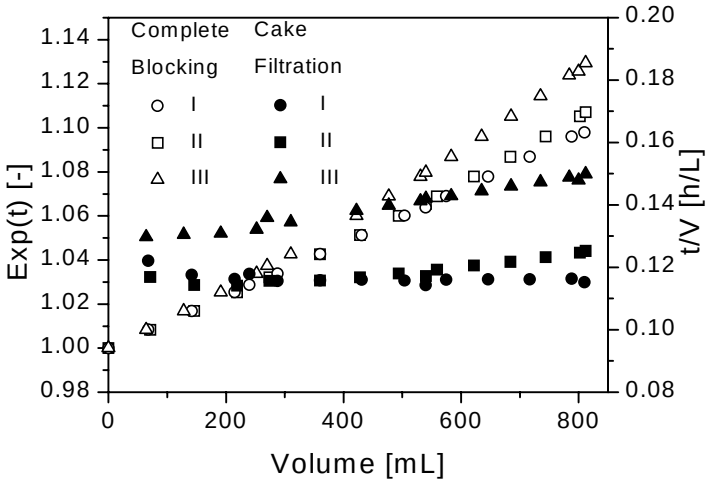


Figure 5.18 *Complete Blocking and Cake Filtration law for hematite aggregates at varying pH with 5 mgL^{-1} as DOC HA and OPS mixing order.*

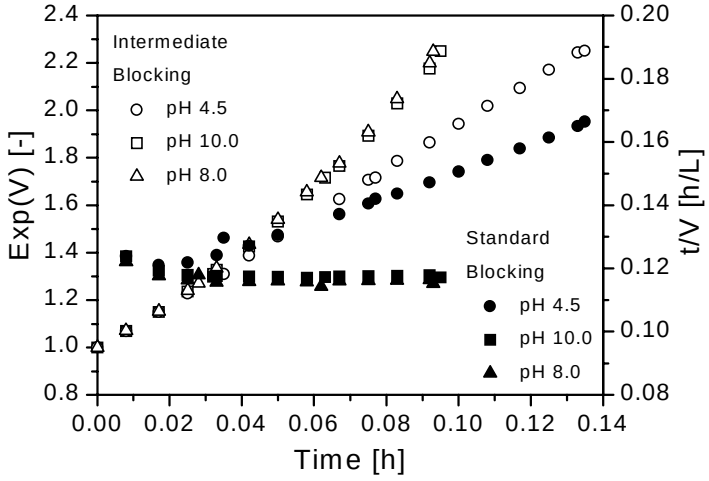


Figure 5.19 *Intermediate and Standard Blocking Filtration law for hematite aggregates at varying pH with 5 mgL^{-1} as DOC HA and OPS mixing order.*

As a function of primary colloid size the observation made is similar - for the small colloids (75 nm), no cake formation is observed. For the 250 nm colloids cake formation is slightly higher but very close to zero, whereas for the large particles (500 nm) cake filtration is clearly evident.

All other mechanisms are present as in all other cases (SPO, pH 3).

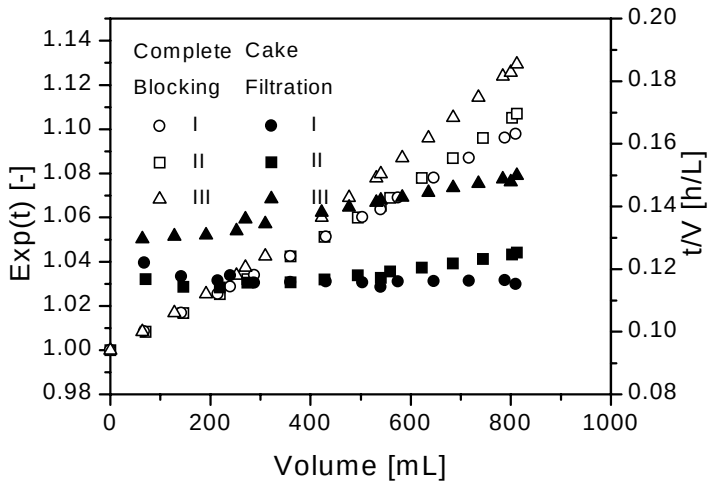


Figure 5.20 *Complete Blocking and Cake Filtration law for hematite aggregates as a function of primary colloid size with 5 mgL^{-1} as DOC HA and OPS mixing order.*

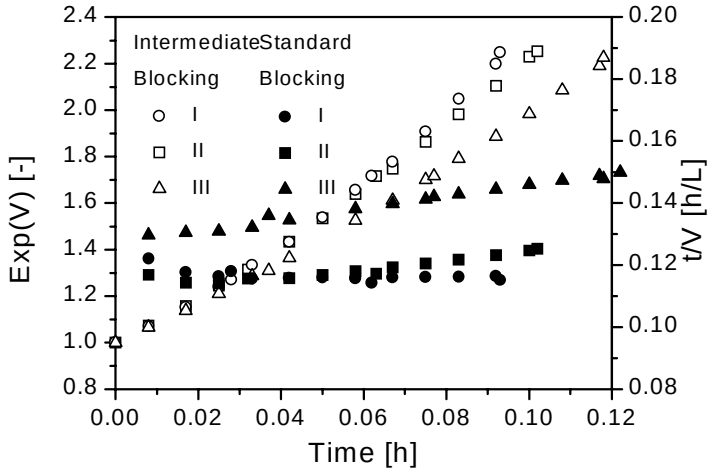


Figure 5.21 *Intermediate and Standard Blocking Filtration law for hematite aggregates as a function of primary colloid size with 5 mgL^{-1} as DOC HA and OPS mixing order.*

The blocking law analysis showed that particles do accumulate, block pores, and adsorb at the membrane surface, although cake formation is not always visible. Also, it is unknown how the model reacts to cake formation inside pore entrances. This is a possible scenario and may have a similar effect as the cake formed on the surface. A more quantitative analysis of the blocking laws of the systems used appears useful.

5.10 MF OF $FeCl_3$-COAGULATED SOLUTIONS

As shown in section 5.4, MF only removes a very small amount of dissolved organics. To increase the organics rejection with MF, the organics need to be transformed into particulates. This can be done by coagulation, which, combined with conventional filtration, is currently the most abundant water treatment process. The interest in this investigation was to be able to compare the flux and rejection achieved with MF and pretreatment to other membrane processes (see following chapters).

Ferric chloride was chosen as the coagulant due to its higher efficiency of removing NOM and alkalinity than alum, as summarised in Chapter 3. Ferric chloride added to an aqueous solution will start a continuous process of hydrolysis, complexation, polymerisation, solation, precipitation, and gelation according to Tang et al. (1994). The various species created will interact with other solution components such as particulates or NOM. Coagulation/flocculation can be driven by double layer compaction, charge neutralisation, bridging, entrapment into the precipitate (sweep flocculation), or adsorption onto the precipitate (Crozes *et al.* (1995b)). The speciation depends strongly on solution

chemistry parameters, such as pH, ionic strength, buffer capacity, type of particulates and organics, and $FeCl_3$ concentration. At a high coagulant dose (and high pH), the dominant process of NOM removal is adsorption onto ferric hydroxide flocs, and at low dosage (and low pH), insoluble complexes such as humates or fulvates would be formed (co-precipitation) (Krasner and Amy (1995), Dennett *et al.* (1996)).

5.10.1 Microfiltration of Coagulated Organic Solutions

The coagulation was carried out in jar testing equipment prior to MF. No settling of the colloids was permitted, in order to simulate direct injection. The coagulation method was adapted from Dennett *et al.* (1996).

In this study, the pH after coagulant addition of about 4-5 corresponds to the optimum pH for NOM removal as shown in Figure 5.22. The removal varies between 0% and >90%, depending on pH and organic type. Clearly at low pH removal is highest and the hydrophobic HA is removed best.

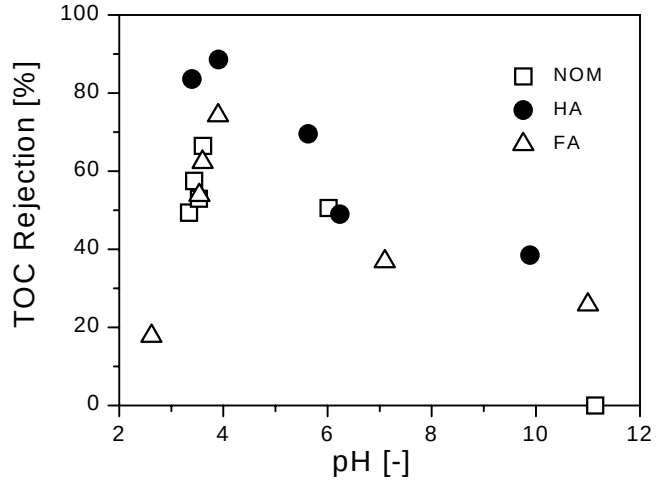


Figure 5.22 *TOC rejection as a function of feed pH for the three different types of organics (25 mgL^{-1} $FeCl_3$, 5 mgL-1 organic carbon).*

Removal increases gradually with an increase in organic concentration. Figure 5.23 shows the results for a ferric chloride concentration of 25 mgL^{-1}, indicating that the process is selective towards a fraction of NOM. The difference in removal for different organic types shows that hydrophobic compounds are preferentially removed. Since NOM contains a mixture of organics and salts the removal is lower. The solubility of the HA is lower than that of the FA, and interactions with colloids are stronger for the more hydrophobic humic acid (Gu *et al.* (1994), see also Chapter 2).

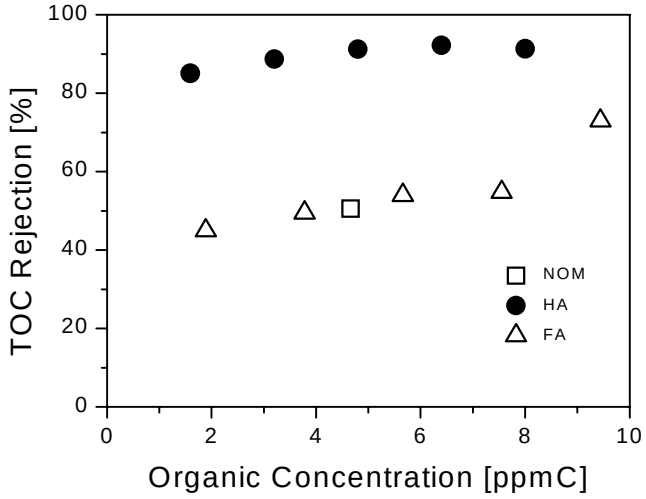


Figure 5.23 *TOC rejection as a function of feed organic concentration for the three different types of organics (25 mgL^{-1} $FeCl_3$, pH 4.5).*

$FeCl_3$ dosage also influences organic rejection as shown in *Figure 5.24*. While only very little TOC is removed in the absence of coagulant, rejection is highest at 25 mgL^{-1} for IHSS HA and at about 50 mgL^{-1} for IHSS FA and NOM. An increased dosage leads to a steady decline in TOC rejection. Lo and Waite (1998) measured smaller particle sizes (as low as 10 nm) at high dosage when the iron precipitates restabilise. This may explain the lower organic rejection at such coagulant concentrations. In this case iron rejection would also be reduced.

At the lower dosage of 25 mgL^{-1}, $FeCl_3$ flocs are visible. These flocs were observed to break up during the filtration process. Restabilisation of the precipitate occurred at 100 mgL^{-1} $FeCl_3$.

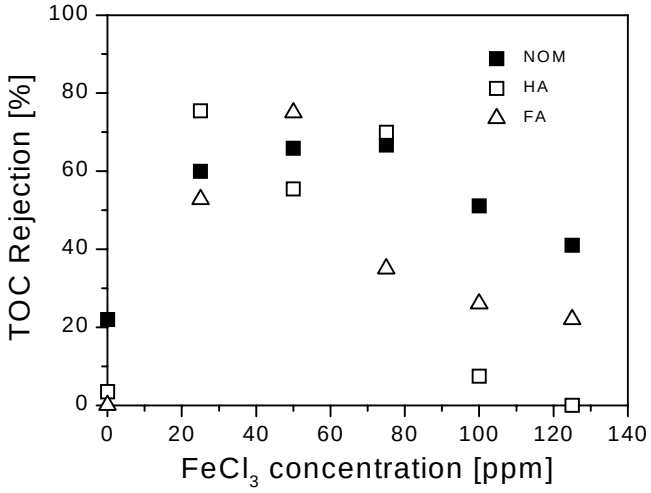


Figure 5.24 *TOC rejection as a function of $FeCl_3$ dosage for three different organic types (5 mgL^{-1} as TOC).*

Flux behaviour for two dosages (25 and 100 mgL^{-1} $FeCl_3$) is shown in Figure 5.25. Flux stabilises at about 30% of the initial value at the low dosage (except for the OPS). At the high dosage, the experiment was interrupted when the flux declined to below 10%. This is most likely a combined effect between increased particle load, floc characteristics, and possible pore plugging.

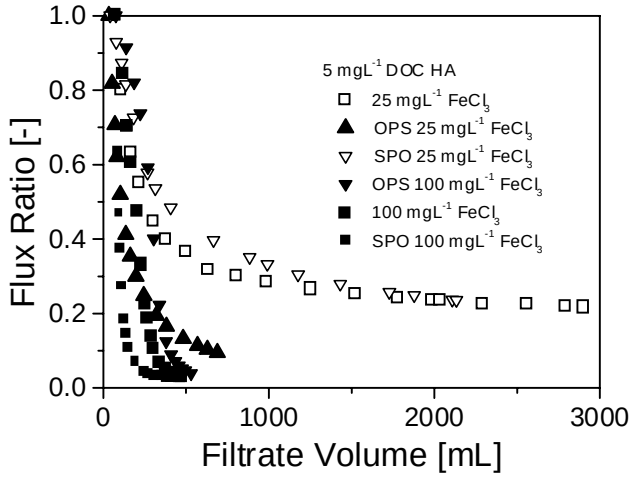


Figure 5.25 *MF flux ratio over filtrate volume after jar tests with solutions containing 5 mgL^{-1} dissolved organic carbon (HA).*

5.10.2 Microfiltration and Coagulation of Particle Suspensions

To simulate a real surface water the previously described systems, containing organics and either stabilised or aggregated inorganic colloids, were now coagulated.

The rejection of TOC and iron for recycle jar tests is shown in Table 5.9. The values differ from the initial experiments in organic concentration which is now higher (12.5 mgL^{-1} as DOC). At the higher ferric chloride dosage, the rejection is consistently lower, which indicates pore penetration of the ferric hydroxide flocs with an initially low rejection. Gradually pores block, a cake forms, and rejection goes up. This effect is also reflected in the flux as shown in Figure 5.25. Organic rejection is higher in the presence of colloids, salt, and high ferric chloride dosages.
Iron rejection is initially very low at the high dosage but increases rapidly to near 100%. Such low initial rejections would lead to contamination of the product water, especially if a backwash is carried out frequently.

Table 5.9 *Rejection of iron and TOC as a function of organic type, colloid system and coagulant dosage (12.5 mgL^{-1} DOC organic). pH was not adjusted.*

Organic Type	Colloids	$FeCl_3$ [mgL^{-1}]	Fe Rejection 1* [%]	Fe Rejection 2* [%]	TOC Rejection 1* [%]	TOC Rejection 2* [%]
HA	-	25	100	99.0	10.0	10.8
HA	-	100	55.9	97.4	44.9	70.5
FA	-	25	100	100	32.9	44.2
FA	-	100	41.9	97.5	23.7	72.2
NOM	-	25	99.8	99.5	40.7	38.0
NOM	-	100	98.0	99.0	80.1	86.6
HA	OPS	25	98.7	99.6	80.7	77.1
HA	OPS	100	44.1	95.7	43.5	91.8
HA	SPO	25	100	100	78.7	85.9
HA	SPO	100	85.7	98.1	73.1	90.1

* sample 1 and 2 respectively, thus samples for first 270 mL of permeate and second 270 mL.

In some cases, flux decline was observed to be detrimental when coagulant was added to the solution prior to MF. The difference between the various solutions was significant - at 25 mgL^{-1}, with or with out aggregates, a stable flux was reached. At this lower dosage, the solid load on the membrane is smaller and the flocs are larger.
This should also be the case when the stable OPS colloids are coagulated. However, it seems as if the coagulant is not totally efficient towards these colloids, and that some can form small particles, which penetrate into pores. The flux value corresponding to the flux ratio of 0.27 in Figure 5.25 is about 850 $Lm^{-2}h^{-1}$, which is high for MF in absolute terms.
An electronmicrograph of the membrane deposit in the presence of 25 mgL^{-1} $FeCl_3$ and 5 mgL^{-1} DOC HA is shown in Figure 5.26A, and an electronmicrograph of a deposit of 25 mgL^{-1} $FeCl_3$, 10 mgL^{-1} hematite and 5 mgL^{-1} DOC HA in Figure 5.26B. A thick cake is formed on the membrane, and in the presence of hematite this cake is very similar to the cake observed in surface water treatment (Figure 5.1).

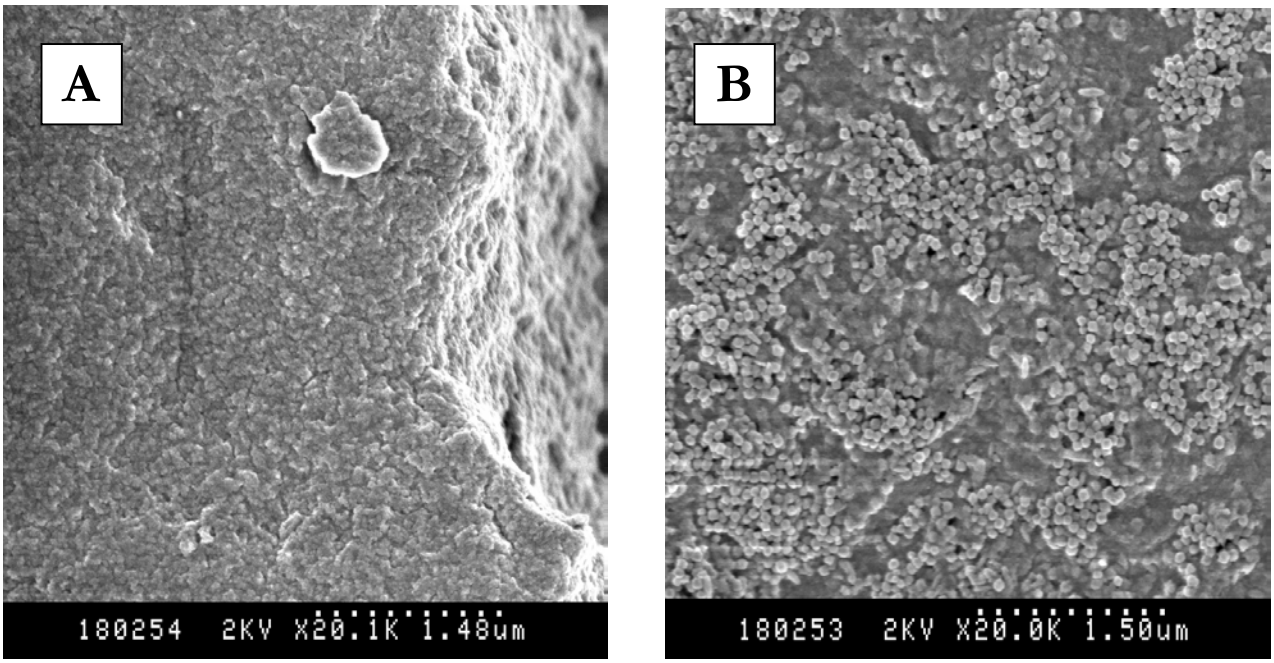


Figure 5.26 *Electronmicrograph of membrane deposit after filtration of a solution containing (A) 25 mgL^{-1} $FeCl_3$, 5 mgL^{-1} DOC humic acid and (B) 25 mgL^{-1} $FeCl_3$, 5 mgL^{-1} DOC humic acid and 10 mgL^{-1} hematite aggregates.*

MF with ferric chloride pretreatment increased NOM removal substantially. However, the process efficiency (towards organic removal) is very dependent on the nature of the organic matter. In a surface water the composition of organics changes constantly, and thus the treatment efficiency cannot be readily predicted. Careful monitoring and control would be required to maximise organics removal.

5.11 SUMMARY

The present study contributes to an understanding of MF membrane fouling under conditions where permeation drag dominates. Real surface water systems have been simulated with inorganic colloids and natural organics in various aggregation states. The systems studied were grouped into (a) organics in the absence of inorganic colloids, (b) stable primary particles, (c) primary particles at pH extremes with organics, (d) particles stabilised with organics, (e) particles pre-aggregated in electrolyte solution prior to adsorption of organics, and (f) solutions coagulated with ferric chloride ($FeCl_3$).

Filtration of colloids at pH extremes served as a baseline of colloids, which are neither aggregated nor stabilised by an adsorbed organic layer. As expected from the literature review, the particle size closest to the membrane pore size (250 nm) caused largest flux decline. Rejection occurred in this case due to a combination of hydrophobic, specific, and van der Waals forces, and could not be explained by charge interaction only. Blocking law analysis showed evidence of pore blocking, cake formation, adsorption and pore closure at some stage of the filtration process.

At pH conditions closer to that of surface waters and in the presence of an electrolyte solution, the colloids aggregate and are fully rejected. In this case, the flux decline depends on the deposition on the

membrane rather than primary colloid size. This corresponds more or less to a surface water of high turbidity, but no organic content.

Once the organics are added, there are two cases to be distinguished. In the first case, the colloids are first aggregated in the electrolyte solution before mixing with the organics. The organics adsorb on the aggregate surface and fouling is increased compared to aggregates in the absence of organics. In the second case, colloids are first mixed with the organics, then with the electrolyte solution. Steric or charge stabilisation of the colloids occurs due to adsorption of organics on the colloid surface. Rejection now drops to almost zero and fouling depends totally on the primary colloid size. Rejection could be increased in this case by destabilisation of the colloids using calcium. In this case, the blocking laws showed that no cake is formed on the membrane surface.

Comparing OPS and SPO in Figure 5.7 (effect of organic type), Figure 5.9 (effect of calcium concentration), and Figure 5.10 (effect of pH) showed important differences between the two systems in terms of flux. The organic type has no effect for SPO, whereas for OPS flux decline is less for FA and HA and very high for NOM. Calcium has opposite effects on both systems. For OPS calcium increases flux decline due to destabilisation effects, whereas for SPO the flux decline is lower at higher calcium concentrations. This is presumably due to a different structure of the initial aggregates. pH also shows differences. While for SPO pH can affect aggregate structure, in the OPS case it affects colloid stability and thus greatest flux decline occurs when colloids partly aggregate.
Blocking law analysis showed that cake formation is absent in the OPS case due to the very low rejection and deposition.

Most severe fouling was observed when the smallest (75 nm) colloids were mixed with NOM, which contains salt and organics. In this case aggregation and stabilisation effects occur at the same time producing very small aggregates which are detrimental to flux. This is the condition closest to 'real' surface water, where detrimental flux decline is often observed.

Ferric chloride pretreatment could achieve organics removal up to 90%. The removal depends strongly on solution chemistry, organic type and concentration, and the characteristics of the formed flocs. Performance is difficult to predict if the number of parameters change rapidly as in a normal surface water. Iron rejection is low at high dosage when the flocs are very small. These flocs penetrate into the membranes and cause most detrimental flux decline.

The flux of the coagulated suspensions could not be manipulated by colloid or aggregate addition at high dosage. At low dosage, the flocs formed were large enough to be retained by the membrane, and the addition of aggregates did not cause higher flux decline. The presence of stable colloids did cause flux decline, most likely due to pore penetration.

The addition of hematite as an adsorbent neither caused an improvement of rejection nor reduced flux decline due to the low adsorbable amount on the hematite, as was shown in Chapter 2.

5.12 CONCLUSION

Overall, the result with the greatest impact on water treatment is the low rejection of the stabilised colloids. Due to their low settlability, these systems will be most abundant in most streams and chemically pretreated feedwaters.

These results have application to real systems, for which inorganic colloids and organics will mix very differently, forming a diversity of aggregates and stable colloids. The characterisation of the colloid-organic associates in natural water is clearly critical in predicting likely MF behaviour.

Such characterisation is rarely carried out in membrane research and the characterisation itself is limited by the methods available for such systems, which are very dilute and relatively polydisperse.

Ferric chloride addition could improve organic rejection to values comparable with UF and NF. However, the process is potentially unreliable due to the dependence of rejection and flux on organic type and concentration, solution chemistry, and floc characteristics.

Chapter 6

ULTRAFILTRATION

Ultrafiltration (UF) rejection and fractionation experiments showed that rejection depends on ionic strength, pH, organic concentration, calcium concentration, and most importantly, organic type. Membranes with a lower molecular weight cut-off (five membranes with cut-offs between 1 kDa and 30 kDa were used) produce waters with a lower UV/DOC ratio. This selective removal of UV absorbing compounds was confirmed with liquid chromatography organic carbon detection. The effect of ionic strength was demonstrated to target specific compounds, with humic substances being retained preferentially. Charge and size do play a role in the rejection of organic compounds by UF. The filtration protocol and cell concentration also influence rejection, which is of particular importance when UF is used for organic characterisation.

Looking at the effect of aggregate structure on UF flux (100 kDa membrane), a close coupling between the structure and size of hematite flocs formed in suspension and the permeability of the cake that accumulates on UF membranes is observed. Specific resistances of cakes formed from flocs generated under diffusion limited aggregation (DLA) conditions are at least an order of magnitude lower than cakes formed from flocs generated under reaction limited aggregation (RLA) conditions. Similar effects are observed whether the aggregation regime is controlled by salt concentration, pH, or added organic anions. This dramatic difference in cake resistance is considered to arise from the size and fractal properties of the hematite assemblages. The ease of fluid flow through these assemblages will be influenced both by the fractal dimension of the aggregates and by their size relative to primary particle size (since for fractal aggregates, porosity increases as the size of the aggregate increases). The size and strength of aggregates are also important determinants of the relative effects of permeation drag, shear induced diffusion and inertial lift. This results, in the studies reported here, in relatively similar rates of particle deposition for both rapidly and slowly formed aggregates. The results presented here suggest that control of cake permeability (and mass) via control of aggregate size and structure is an area with scope for further development, though the nature and extent of compaction effects in modifying the fractal properties of aggregates generated in suspension requires attention.

Fouling experiments with colloid systems, as described in Chapter 4, were performed with the 10 kDa and 100 kDa membranes. The 10 kDa membrane showed very little flux decline and stable rejection. This was attributed to the initially much lower flux and the smaller pores, which allow less pore penetration. Calcium concentration and organic type (in the absence of colloids) confirmed the importance of aggregation, as flux decline increased when organics aggregated and rejection increased. This effect was most abundant with IHSS HA, the largest and most hydrophobic compound (some solubility and aggregation characteristics were shown in Chapter 4).

Stable primary colloids (with no organics) showed a dependence of flux on Debye length, which varies with pH/ionic strength. Aggregates which were formed under conditions closer to natural waters than those described above, did not show any flux decline. This is due to the formation of loose aggregates under such conditions. Aggregates of OPS order (stabilised colloids) showed, overall, a higher flux decline than aggregates of SPO order (colloids which were allowed to aggregate prior to mixing with organics. High calcium concentrations were detrimental in either case, presumably due to coagulation of non-adsorbed organics.

Ferric hydroxide precipitates resulted in flux decline, depending on the dosage, which determines charge and structure. High dosage (100 mgL^{-1} ferric chloride) caused severe flux decline, even for the 10 kDa membrane. This flux decline worsened when stirring was stopped. The presence of colloids (OPS or SPO) did not influence this flux decline. However, at low dosage (25 mgL^{-1} ferric chloride) no significant flux decline was observed under any conditions. This indicates that flocs of a very different nature are formed (compared to the coagulation by calcium), which do not have an impact on flux.

Overall, the UF experiments indicated that flux is very dependent on the structure of the deposit, which was determined by the solute or colloid characteristics and their interaction in suspension. Organic rejection is more reliable for tighter membranes (10 kDa) and flux is more stable. Coagulation pretreatment can improve flux and rejection, however the performance depends on floc characteristics.

6.1 INTRODUCTION

Ultrafiltration (UF) membranes have pore sizes in the range of 2 – 100 nm and are, therefore, able to remove viruses, bacteria, colloids, and larger particulate matter from suspensions. Partly because of their ability to produce a treated water free of pathogens, the use of UF membranes in the treatment of waters and wastes is increasing, but high capital and operating costs still remain a critical factor in limiting their more extensive application (Mallevialle *et al.* (1996)). Important factors in determining these costs are the magnitude of permeate flux that can be achieved and the frequency of membrane cleaning.

Therefore, the objective of this chapter is to identify the factors that influence UF rejection and flux decline. Six membranes of identical material are investigated.

6.2 FILTRATION PROTOCOL

6.2.1 Fractionation and Rejection Experiments

For fractionation experiments, the perspex stirred cells (see Chapter 4 for equipment description) were operated directly from the nitrogen bottle without a reservoir. Membranes were floated in a beaker of MilliQ water, skin side down, for at least one hour to remove the glycerin coating. Then at least 300mL of MilliQ water were filtered through the membrane. The filtrate was analysed with UV and DOC to confirm full removal of glycerin. The membranes were reused up to 5 times and stored in 0.1 % sodium azide at 4^0C. Pure water flux was measured after the filtration of 500 mM of MilliQ water prior to each experiment. The filtration protocols for serial and parallel fractionation were described in Chapter 4. In this Chapter parallel fractionation results will be shown.

6.2.2 Aggregation Experiments

Hematite suspensions were equilibrated at various defined pH, salt, and fulvic acid concentrations for 17 hours with stirring at 220 rpm prior to membrane filtration.

Prior to use, the membranes were soaked in 0.1 M NaOH for 30 minutes and flushed with 3.4 L of MilliQ water in order to remove the preservative glycerin. The experiments were conducted with transmembrane pressures in the range of 0 to 300 kPa and a temperature of 25°C. The stirring speed in most experiments was set to 520 rpm. The feed volume was inserted into the stirred cell from two reservoirs (about 1.5 L) connected in series as shown in Chapter 4.

6.2.3 Fouling Experiments

Two filtration protocols were used for fouling experiments, one for the 10 kDa membrane and another for the 100 kDa membrane. The different fluxes did not allow the filtration of similar volumes.

All experiments were stirred at 270 rpm unless otherwise indicated. A feed reservoir of 1.5 L was connected to the stirred cell to provide extended filtration volume. Pure water flux was measured after the filtration of 1 L of MilliQ water for both membranes.

For the 10 kDa membrane, 225 mL of feed solution were introduced into the reservoir. Pressure was adjusted to 300 kPa. A total of 150mL were filtered (three permeate samples of 50mL each were taken), leaving 75mL of retentate.

For the 100 kDa membrane, 450 mL of feed solution were introduced into the reservoir. Pressure was adjusted to 100 kPa and the filtration cell was filled up. The permeate was sampled once (sample volume 50 mL) and then recycled into the reservoir together with the retentate and filtration was repeated. This was repeated a third time. This recycling experiment enabled the separation of concentration polarisation effects from fouling effects. The 110 mL of retentate was then also sampled.

Pure water flux was measured again after each experiment with approximately 300 mL and 1000mL of MilliQ filtered for the 10kDa and 100kDa membranes, respectively. Membrane samples were kept in a petrie dish for deposit analysis.

The amount M of solute or colloid deposited (in mg) on the membranes was calculated by using mass balance (see equation (6.1)), where V_F, V_R, and V_{Pi}, are the volumes of feed, retentate and permeate (sample i), respectively, and c_F, c_R, and c_{Pi} the concentrations of feed, retentate and permeate.

$$M = V_F \cdot c_F - \sum_i (V_{Pi} \cdot c_{Pi}) - V_R \cdot c_R \tag{6.1}$$

This can also be described as percent of mass in feed solution deposited ($M_{\%}$)

$$M_{\%} = 100 \cdot \frac{M}{V_F \cdot c_F} \tag{6.2}$$

The results for DOC should be treated with care, as the error is expected to be large, especially at low concentrations. This is due to the analytical method and risk of contamination of the samples.

6.3 MEMBRANE CHARACTERISATION

The regenerated cellulose UF membranes used were described in Chapter 4. These membranes were selected due to their hydrophilicity, which should show reduced adsorption of organic compounds (Jucker and Clark (1994)).

6.3.1 Pure Water Flux

The pure water fluxes of all UF membranes used at the transmembrane pressure applied are summarised in Table 6.1. Also shown are other membrane characteristics, including molecular weight cut-off (MWCO), estimated pore size, and measured surface charge.

The pure water fluxes are very different; at the low MWCOs (PLAC, PLBC and PLCC) fluxes and permeabilities are lower than those of NF membranes (see Chapter 7). The higher MWCO membranes are well below the MF pure water fluxes (see Chapter 5), but certainly in the area of MF fluxes in full-scale systems. This demonstrates the continuity in membrane characterisation.

6.3.2 Molecular Weight Cut-Off or Pore Size

The molecular weight cut-off (MWCO) was specified by the manufacturer based on dextran experiments (see Chapter 4). The nominated pore size was estimated from the MWCO using the relation given by Worch (1993), which is also shown in Chapter 2. The pore sizes range from 1 to 10 nm. This is based on dextran rejection and does not account for variations of retentions with molecular shape.

Table 6.1 *Molecular weight cut-off, pore size, pure water flux, operating pressure and surface charge of the UF membranes used.*

Membrane Type	MWCO [kDa]	Pore Radii [nm]*	ΔP [kPa]	Pure Water Flux [$Lm^{-2}h^{-1}$]	Permeability [$Lm^{-2}h^{-1}bar^{-1}$]	Membrane Resistance [m^{-1}]	Surface Charge (pH 8) [mV]
PLAC	1	0.94	300	15 ± 2	5.0	$7.18 \cdot 10^{10}$	-11.6
PLBC	3	1.42	300	22 ± 2	7.3	$4.90 \cdot 10^{10}$	-9.2
PLCC	5	1.91	300	28 ± 3	9.3	$3.85 \cdot 10^{10}$	-14.3
PLGC	10	2.59	300	65 ± 5	21.7	$1.66 \cdot 10^{10}$	-7.5
PLTK	30	4.81	100	390 ± 20	390	$0.09 \cdot 10^{10}$	-16.4
PLHK	100	9.10	100	1320 ± 40	1320	$0.03 \cdot 10^{10}$	-17.3

* calculated after Worch (1993).

6.3.3 Membrane Surface Roughness

The regenerated cellulose membranes generally have a very smooth surface. Electronmicrographs of the two membranes used for fouling experiments are shown in Figure 6.1A and B. A higher resolution electronmicrograph of the most porous membrane is shown in Figure 6.2. For the tighter membrane no pore structure was visible. The regenerated cellulose is a very unstable material under the electron beam in the microscope (note the low beam energies 2 to 4 kV used). The voids seen on the surface can be attributed to surface roughness. It is not possible to identify effective pore sizes from surface images, but for the PLHK membrane in Figure 6.2 pore openings can be seen and the estimate of a pore radius of about 9 nm in Table 6.1 appears possible.

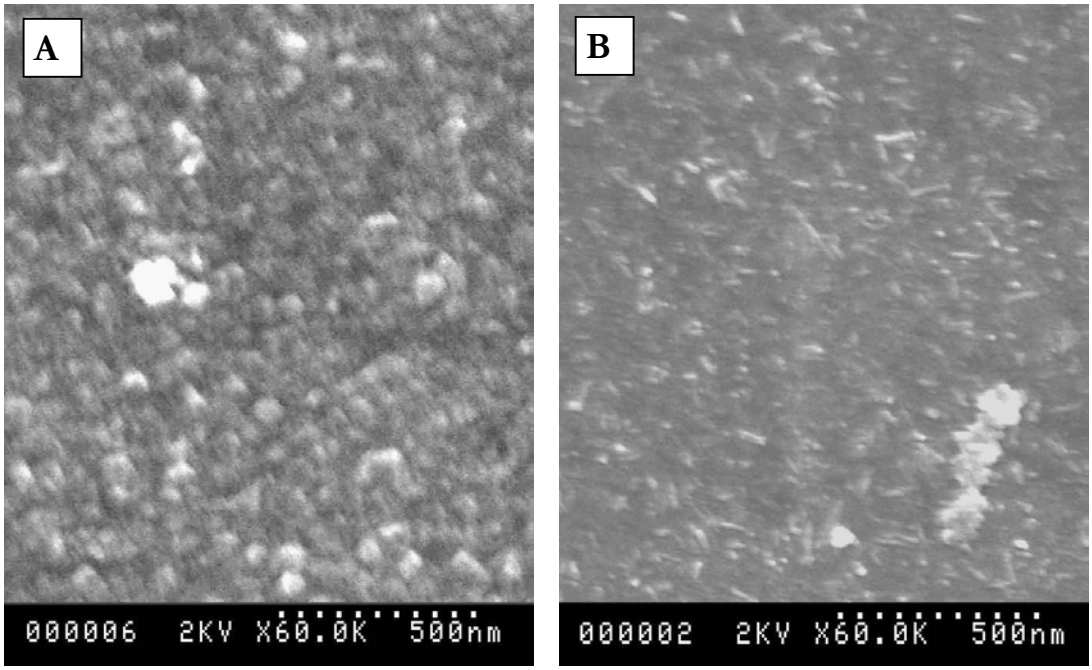


Figure 6.1 *Electronmicrograp of the clean (A) PLHK (100 kDa) and (B) PLGC (10 kDa) membranes.*

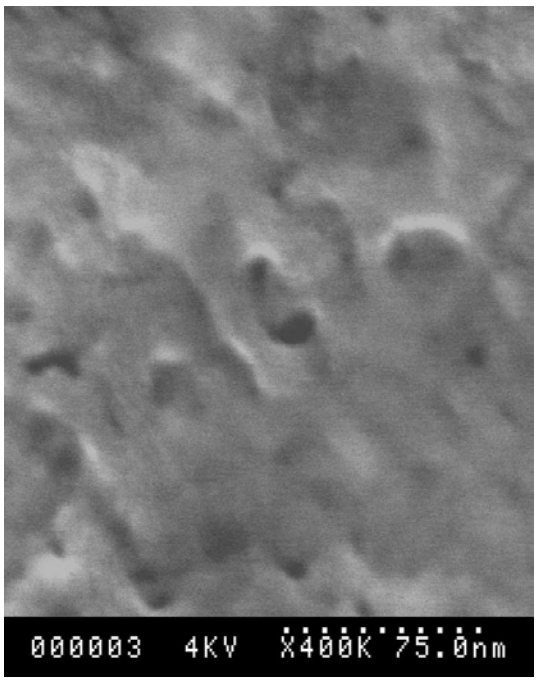


Figure 6.2 *Electronmicrograph of the PLHK membrane (MWCO 100 kDa).*

6.3.4 Membrane Surface Charge

The membrane surface potential was measured in 1 mM KCl solution. The results are shown in Figure 6.3. The surface charge at pH 8 is also given in Table 6.1. The membranes have a point of zero charge between pH 3 and pH 4. While the absolute value of the charge at pH 8 is higher than expected for UF membranes, no relationship between observed MWCO and surface charge can be established. The results contradict the work of Braghetta (1995), who stated that regenerated cellulose membranes are uncharged. However, Clark and Jucker (1993) reported a non-zero, higher (less negative) zeta potential for regenerated cellulose membranes compared to polysulphone materials.

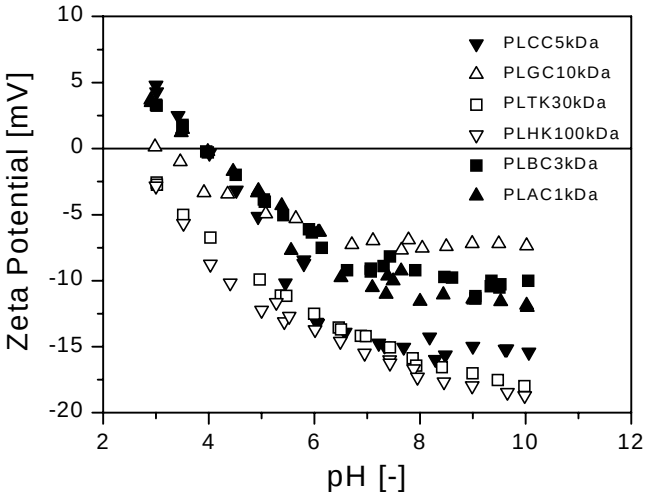


Figure 6.3 *Zeta potential of the UF membranes in 1 mM KCl.*

UF is believed to reject principally on a size exclusion basis. However, as described later, the 3 kDa and 5 kDa membranes have a very similar rejection for the charged organic molecules. This can be attributed to charge interactions, as the 5 kDa membrane has the higher charge.

6.4 REJECTION AND FRACTIONATION EXPERIMENTS

6.4.1 Effect of Ionic Strength

The ionic strength influences DOC rejection considerably (see Figure 6.4). DOC rejection decreases up to 20% on increasing NaCl concentrations from 1.7 to 60 mM (corresponding to a conductivity variation from 0.35 to 7.7 $mScm^{-1}$). The effect of ionic strength on DOC rejection may be attributed to the increased coiling that these large organic molecules will undergo as shielding of functional groups occurs.

When the ionic strength increases the charge on the organic molecules is increasingly shielded. The functional groups make the molecules stretch to linear orientation at high charge and at low charge these molecules curl up and eventually aggregate. Repulsive electrostatic interactions between a charged molecule and a charged membrane would also be expected to decrease at higher ionic strength and thus a closer approach of the similarly charged organic molecules to the membrane surface with subsequent more facile entrainment of these molecules in permeate flowing through the membrane.

Staub *et al.* (1984) reported that flexible linear molecules pass more easily through porous membranes than their spherocolloidal counterparts. This contradicts the results observed here and may indicate that charge effect are observed.

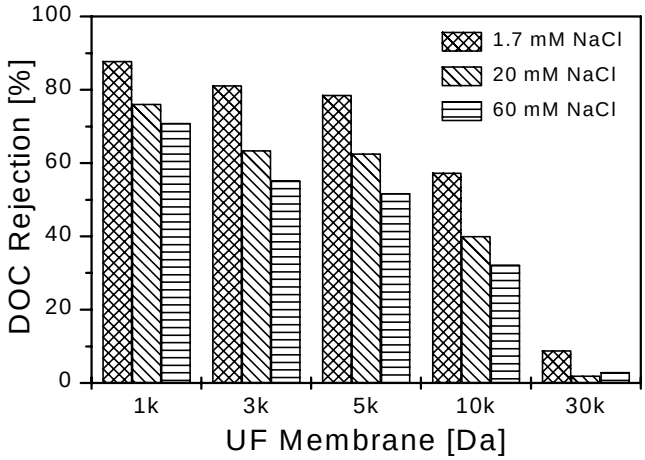


Figure 6.4 *DOC rejection as a function of ionic strength (15 mgL^{-1} NOM concentrate, pH 7).*

These effects were further investigated by size exclusion analysis (SEC) of the fractions (see section 6.4.8) and by liquid chromatography – organic carbon detection (LC-OCD) (see section 6.4.9).

6.4.2 Effect of pH

Similar to ionic strength, the pH changes the charge of the organic molecules, and potentially their shape and size. However, Ghosh and Schnitzer (1980) stated that at low organic concentrations (such as the ones used here or common in natural waters) the effect of pH is much less significant than that of ionic strength. This was confirmed here with the results shown in Figure 6.5 and Figure 6.6. The effect of pH, both at low and high ionic strength, is minimal and probably within experimental error. This could be due to a coupling of two phenomena with opposite effect, as with increasing pH (and thus increasing charge) the organics have a linear flexible shape, but also a more negative charge. While the rejection of uncharged linear flexible molecules was shown to be decreased (Staub *et al.* (1984)), in this work the increased charge may in fact lead to an increased rejection. This is obvious for the 5 kDa

membrane which has a higher MWCO, but a similar or higher rejection. This is attributed to the increased charge of this membrane as was shown in Figure 6.3 (the MWCO of these membranes was determined using uncharged dextran molecules).

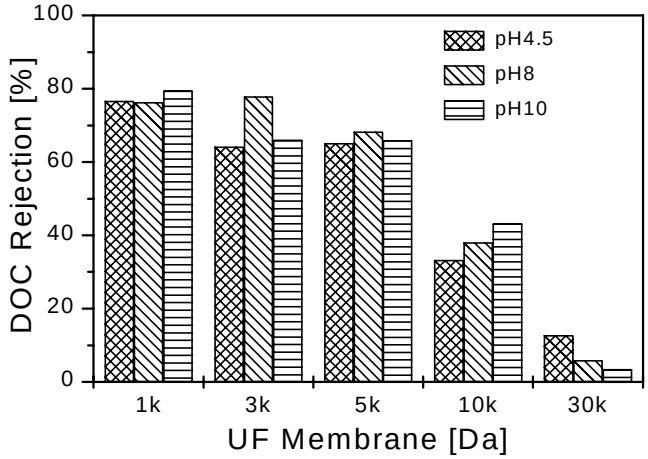


Figure 6.5 *DOC rejection as a function of pH (15 mgL^{-1} NOM concentrate, 20 mM NaCl).*

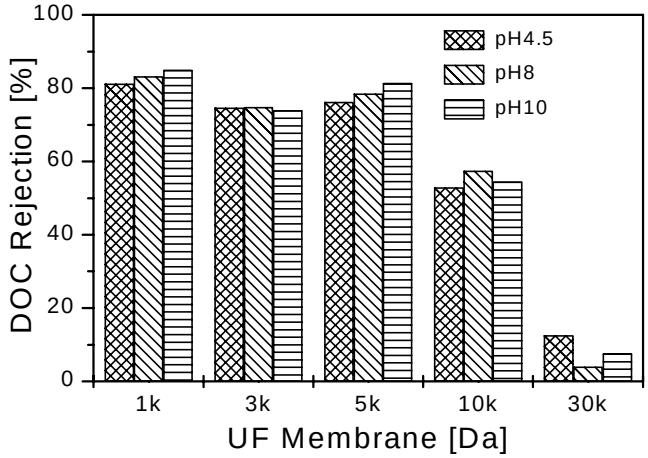


Figure 6.6 *DOC rejection as a function of pH (15 mgL^{-1} NOM concentrate, no NaCl).*

6.4.3 Effect of Organic Concentration

Fractionation of natural organics is often carried out on water samples of different origin or on concentrates. This section aims to demonstrate that the result obtained in fractionation is dependent on the concentration of the feed sample as well as on the filtration protocol used for fractionation. Ghosh and Schnitzer (1980) examined the impact of organic concentration on structure and size. However, the concentrations these authors regard as "high" are in the gL^{-1} range, and it is therefore not surprising that these effects were not observed in the more realistic concentration range investigated here.

Figure 6.7 shows a decrease in flux as a function of organic concentration for the most open membrane. This indicates a clear concentration polarisation effect.

Rejection increases with the filtered volume (see Table 6.2) due to an increase in the bulk concentration, but permeate concentration also increases. The increased permeate concentration is a result of concentration polarisation. A higher concentration in the boundary layer facilitates the permeation of compounds (both organics and membranes have a size distribuntion). Further reasons for this increased rejection could be pore closure which results in a reduced sieving coefficient (which is the ratio of permeate concentration to bulk concentration) or the change in the size distribution in the

bulk due to the loss of smaller species to the permeate.

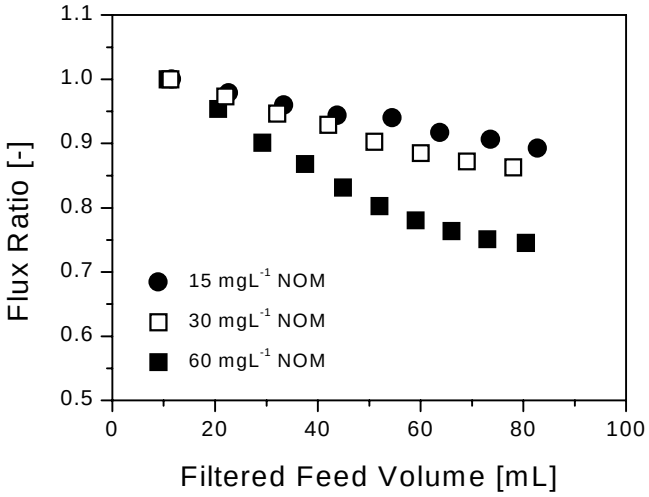


Figure 6.7 *Flux ratio as a function of NOM concentration (30 kDa membrane, 20 mM NaCl, pH 7).*

Table 6.2 *Rejection for the five UF membranes as a function of permeate volume (15 mgL^{-1} NOM concentrate, 20 mM NaCl, pH 7).*

Permeate Volume [mL]	1 kDa [%]	3 kDa [%]	5 kDa [%]	10 kDa [%]	30 kDa [%]
35 mL	80	69	70	57	30
55 mL	83	74	73	58	36
75 mL	86	79	76	68	44
95 mL	95	91	91	87	80

Figure 6.8 shows the effect of organic concentration on DOC rejection, when the ionic strength is adjusted to a common value of 20 mM NaCl. The variation is minimal, demonstrating that the organic concentration, typical or slightly higher than for surface waters, has no effect. However, as shown above, if concentrates with varying ionic strength are treated, rejection varies significantly.

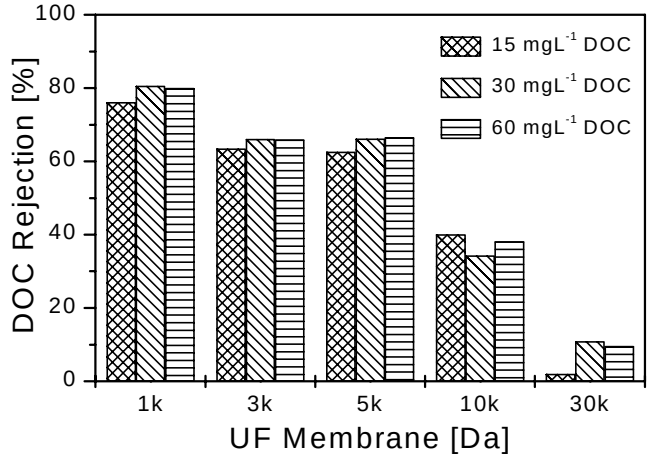


Figure 6.8 *Effect of organic concentration on DOC rejection (15 mgL^{-1} NOM concentrate, 20 mM NaCl, pH 7).*

6.4.4 Effect of Calcium Concentration

Calcium screens the organic charge and leads to a different shape of the molecules. Additionally, calcium forms complexes with organics or leads to aggregation of organic colloids. All these interactions will effect the organic size. Therefore, in a water that contains a different amount of calcium the size of the organics may appear different, although it may be identical to the organic in a different sample.

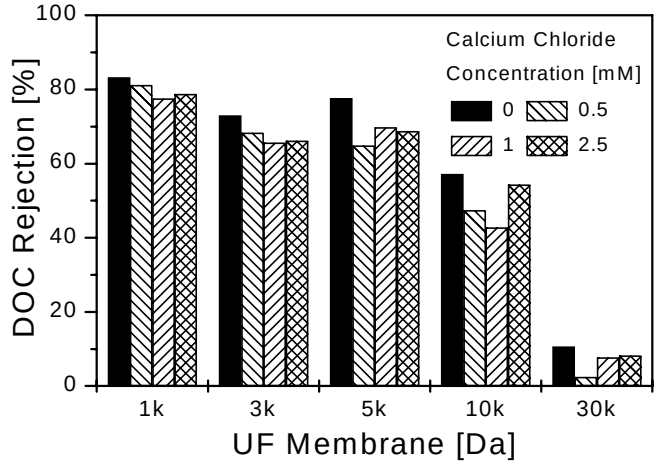


Figure 6.9 *Effect of calcium concentration on DOC rejection (15 mgL^{-1} DOC NOM concentrate, 20 mM NaCl, 1 mM $NaHCO_3$, 0.5 mM $CaCl_2$, pH 8).*

While as a general trend, the organic rejection decreases with calcium rejection (Figure 6.9), the effect observed is relatively small. A more detailed assessment of filtration of organics in the presence of calcium is given in section 6.6.

6.4.5 Effect of Organic Type

UF fractionation results for the different organics used have previously been shown in Chapter 4, where they were presented as percentages in certain fractions. Here results are presented as rejection by the different membranes (Figure 6.10). The rejection of the hydrophilic NOM fraction is low for all membranes, even the 1 kDa membrane reaches only 67% rejection. Overall, the rejection of IHSS HA is the highest. The 1 kDa, 3 kDa, and 5 kDa membranes exhibit a very similar rejection behaviour and the pattern of rejection of organics is identical. A rejection of about 80% in these cases.

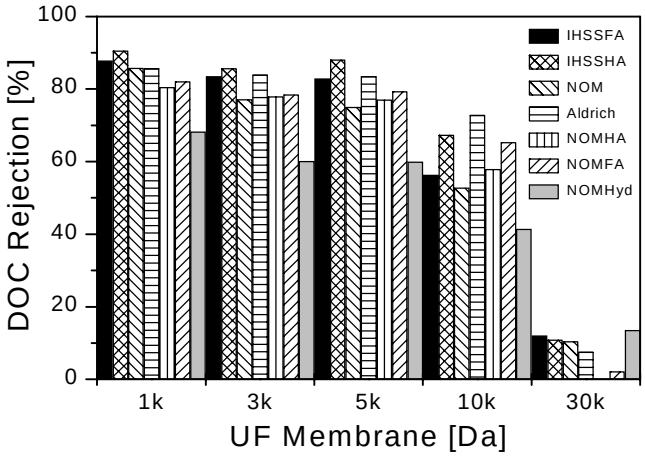


Figure 6.10 *Rejection of the organics by different UF membranes (15 mgL^{-1} DOC, 20 mM NaCl, 1 mM $NaHCO_3$, 0.5 mM $CaCl_2$, pH 8).*

As indicated previously for the 5 kDa membrane, charge effects may cause an increased rejection. For the 10 kDa membrane, rejection is 5-20% lower (than found for the 5 kDa membrane), but the pattern is again the same.

The size of the organics is important (see Chapter 4 for more detail on organic molecular weight and size). The mass average molecular weight of the organics follows the order IHSS HA > NOM HA > Aldrich HA 100 kDa permeate > IHSS FA > NOM > NOM FA > NOM hydrophilic fraction with sizes ranging feom 2747 to 970 Da (molecule radii of 1.35 to 0.79 nm). Membrane pore radii are shown to vary from 0.94 to 9.1 nm in Table 6.1.

The greatest difference in rejection occurs between the 10 kDa and the 30 kDa membrane. Rejection drops to about 10% for the 30 kDa membrane, followed by rejections near zero by the 100 kDa membrane (results not shown). These results indicate that a 5 kDa membrane is ideal if 80% of organics are to be removed. A tighter membrane shows no improvement and operates at a lower flux whilst a more open membrane has a very low rejection. The hydrophilic fraction is overall less retained and a tighter membrane (such as NF or RO) will be required to successfully remove this fraction. It has to be noted here, however, that the hydrophilic fraction has, due to the fractionation method used, an increased ionic strength (see Chapter 4 for fractionation method and salt content). The hydrophilic fraction is the fraction that is biologically most available, whereas chlorination by-product formation occurs preferentially for larger, more aromatic compounds.

6.4.6 Cation Rejection by UF

UF membranes are generally believed not to retain ions. However, some authors have reported ion rejection (Küchler and Miekeley (1994)). Cations, especially multivalent cations and trace metals do interact with humic substances (Klein *et al.* (1990)) and these inorganics would consequently be retained with that organic fraction.

As can be seen in Figure 6.11, calcium rejection is about 15% for the 1kDa membrane. Rejection decreases with the increasing MWCO of the membranes. IHSS FA and Aldrich 100 kDa samples seem to show an increased cation rejection.

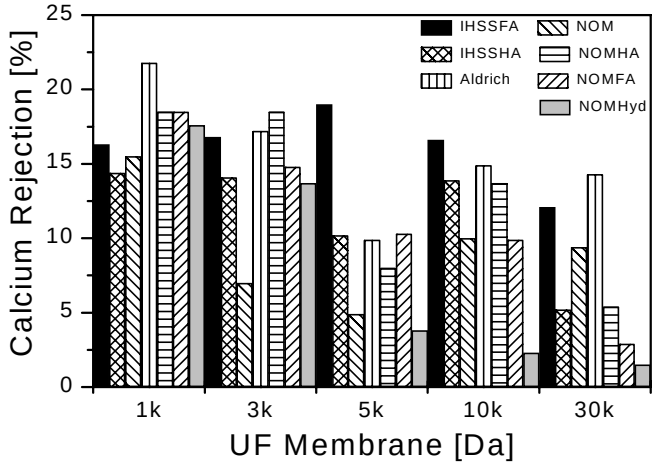


Figure 6.11 *Rejection of calcium by UF membrane in the presence of different organics (15 mgL^{-1} DOC, 20 mM NaCl, 1 mM $NaHCO_3$, 0.5 mM $CaCl_2$, pH 8).*

The higher rejection of the tighter membranes either indicates a stronger association with the smaller compounds, or a cation rejection by these membranes. Since the rejection of organic was identical for the 1 kDa, 3 kDa, and 5 kDa membranes, this is most likely a retention of calcium by the membrane. This effect examined by a filtration of the pure salt solution (see Table 6.3). The calcium rejection in the absence of organics is slightly lower than in the presence of organics. This shows that the organics do interact with the calcium and that UF does retain salts such as calcium, especially for low MWCOs.

Also the membrane charge may increase (become more negative) in the presence of organics which

may increase ion rejection.

Table 6.3 *Calcium rejection by the UF membranes in the absence of organics (20 mM NaCl, 1 mM $NaHCO_3$, 0.5 mM $CaCl_2$, pH 8).*

Membrane [kDa]	1	3	5	10	30
Calcium Rejection [%]	13.1	13.5	1.9	2.5	2.8

6.4.7 UV_{254nm}/DOC Ratio

The UV_{254nm}/DOC ratio describes the aromaticity of a sample. The higher the ratio, the more aromatic is the sample. The ratio decreased in the permeates with decreasing MWCO of the membranes which shows a clear relation between organics molecular weight and aromaticity, larger organics are more aromatic and are retained better. Figure 6.12 shows an example of this generally observed trend.

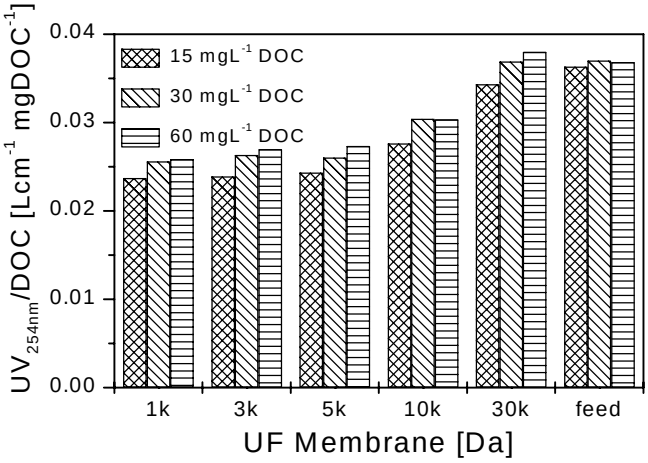


Figure 6.12 *Effect of membrane type on UV_{254nm}/DOC ratio in permeates at different organic concentrations (15 mgL^{-1} NOM concentrate, 20 mM NaCl, pH 7).*

6.4.8 Comparison of UF fractionation and Size Exclusion Chromatography (SEC)

All samples from fractionation experiments were analysed with size exclusion chromatography (SEC) to compare if there is a 'true' size effect. The SEC technique was optimised to reduce charge interactions between the organics and the column. This resulted in an analysis at relatively high ionic strength (see Chapter 4 for method description). A few selected results are presented here using the examples of varied ionic strength (which exhibit the largest effects in UF fractionation).

Figure 6.13 to Figure 6.18 show the SEC results for the ionic strength experiment for the 1 kDa, 3 kDa, 5 kDa, 10 kDa, 30 kDa permeates and the feed samples, respectively. The y-axis in the SEC graphs is the concentration of the sample, as determined by UV absorbance. This measurement is selective as it preferentially measures larger, more aromatic compounds. Unfortunately, at the time when this research was carried out, no analyser with DOC analysis was available. Such analysis is difficult as the concentrations are very low. As a result small, non-absorbing compounds are lost in SEC analysis.

The leftmost peak (lowest molecular weight, 100Da) is the 'salt peak' which includes salts from samples and the buffer. The different figures identify an overlay of three major peaks in the NOM sample, which become more or less abundant in the different permeates.

For the 1 kDa membrane (Figure 6.13), the concentration of the sample is obviously lowest. Two organic peaks are visible, one at 400-500 Da and another one at 800-900 Da. The smaller MW peak is

the highest in concentration. Unfortunately, the method does not allow chemical identification of these peaks. It is most likely that these low molecular weight compounds are neutral and amphiphilic in character. This fraction was identified to be about 13.2% of DOC in Chapter 4, however their UV absorbance is low (2.8% of absorbance). This means that this fraction is underestimated with the SEC method.

For the 3 kDa membrane (Figure 6.14) the same peaks are visible, but now the 700-800 Da peak is the highest. Interestingly, for the 5 kDa membrane (Figure 6.15), this effect is reversed, which suggests that the 700-800 Da peak may be a charged fraction which is retained more by the more charged 5 kDa membrane.

The trend continues with the 10 kDa membrane (Figure 6.16), the small peak at 400-500 Da is still there, the peak at 700-800 Da dominates, now accompanied by a shoulder at around 1000 Da. In the 30 kDa permeates (Figure 6.17) this 'new' peak clearly dominates and the sample is not very different to the feed samples (Figure 6.18).

In assessing the effect of ionic strength it should be noted that the results of SEC analysis of the feed samples at different ionic strengths are identical. This means that any 'size' difference which the different ionic strength may induce, is fully reversible once the samples are injected into the relatively strong ionic environment of the SEC analysis.

Alternatively, it could be argued that ionic strength change is having a negligible effect on size and/or shape of the organic molecules with effects of ionic strength on the ultrafilterability of organic molecules being due to alteration in charge screening. These two effects are difficult to separate though, if anything the UF results favour a charge explanation.

The SEC results confirm that the concentration of organics in the permeate increases with an increase in ionic strength, in accord with the observed decrease in rejection in the UF fractionation on ionic strength increase.

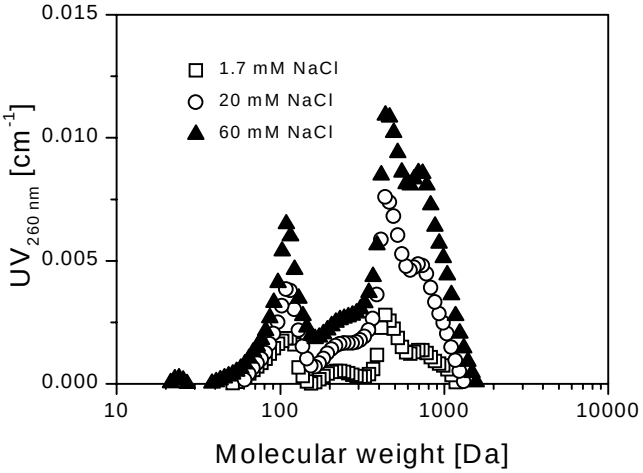


Figure 6.13 *SEC results of permeates of the 1 kDa UF membrane at varied salt concentration (15 mgL^{-1} NOM concentrate).*

For the 1 kDa membrane the small organic peak dominates for all ionic strengths, whereas for the 3 kDa membrane this changes. At high ionic strength the two peaks are identical, whereas at low ionic strength the small peak is higher. This shows that a higher ionic strength allows larger compounds to pass through the membrane. Above it was described that this peak may be retained more by the 5 kDa

membrane due to charge effects. If this was the case then the same explanation applies here. The 5 kDa membrane shows more or less the same trend as the 3 kDa membrane.

For the 10 kDa membrane the same shift is observed with the increase in ionic strength, whereas the 30 kDa membrane shows no shift (it does not retain organics at all).

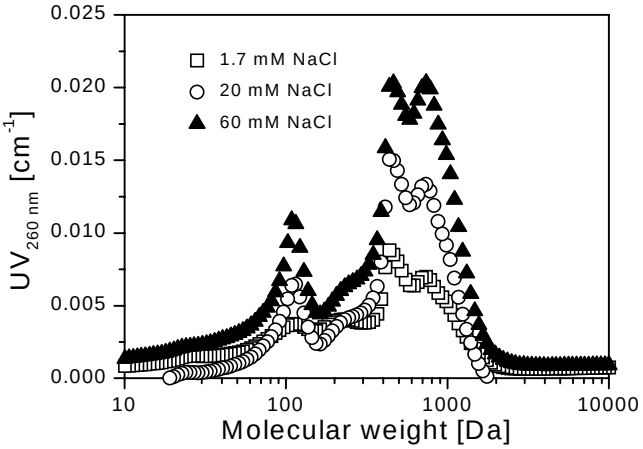


Figure 6.14 *SEC results of permeates of the 3 kDa UF membrane at varied salt concentration (15 mgL^{-1} NOM concentrate).*

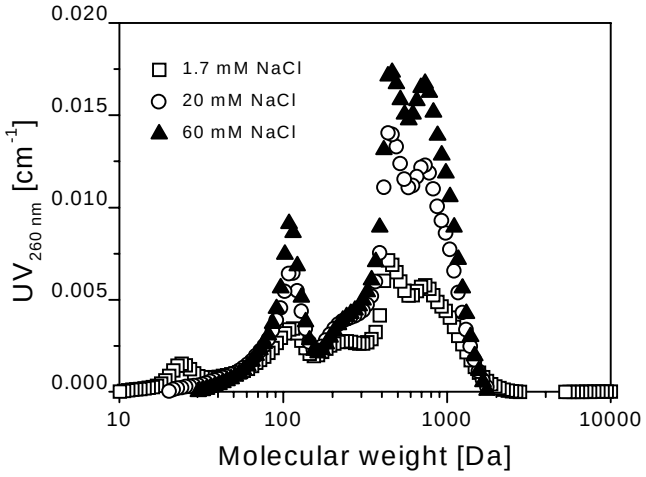


Figure 6.15 *SEC results of permeates of the 5 kDa UF membrane at varied salt concentration (15 mgL^{-1} NOM concentrate).*

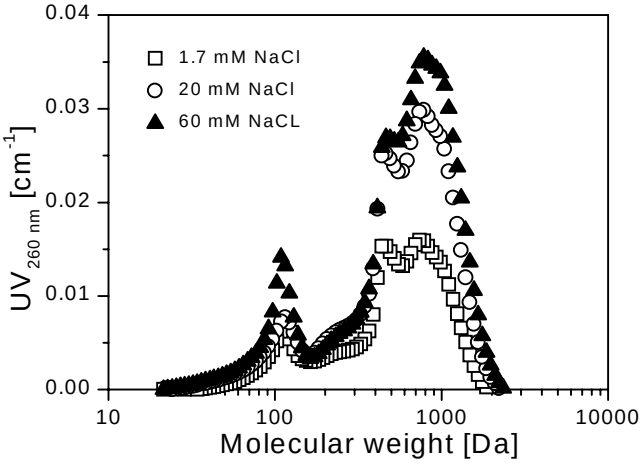


Figure 6.16 *SEC results of permeates of the 10 kDa UF membrane at varied salt concentration (15 mgL^{-1} NOM concentrate).*

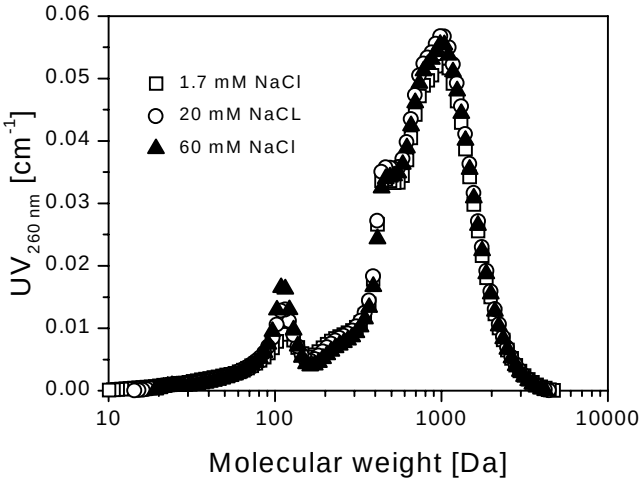


Figure 6.17 *SEC results of permeates of the 30 kDa UF membrane at varied salt concentration (15 mgL^{-1} NOM concentrate).*

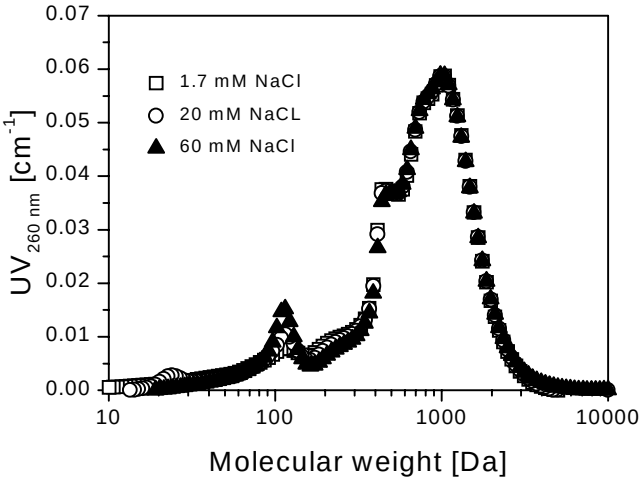


Figure 6.18 *SEC results of permeates of the feed solutions at varied salt concentration (15 mgL^{-1} NOM concentrate).*

Overall, the apparent molecular weight measured with SEC is smaller than that measured with UF fractionation. There are several factors contributing to this. First of all, the ionic strength of the eluent is very high in the SEC method (see Chapter 4 for details of the method) possibly leading to coiling of the molecules. Secondly, charge interactions may cause a higher rejection of the UF membranes than implied by the nominal MWCO alone. It was shown above that some charge effects are evident. Thirdly, the calibration of the methods is very different. While the MWCO of the UF membranes was determined using dextran, the SEC was calibrated with a range of compounds (see Chapter 4), which do not necessarily reflect the characteristics of humic substances and NOM. It should be noted that the feed solutions had identical peak heights for the three experiments, which clearly demonstrated the different retentions achieved as a function of salt concentration.

6.4.9 Chemical Analysis of the UF Fractions using LC-OCD

The feed sample and the five permeates at 20 mL NaCl were further analysed using LC-OCD analysis (see Chapter 4 for method desciption).

The results given in Figure 6.19 for the fractionation samples (NOM concentrate, fractionated at 20 mM NaCl) show three distinct components of NOM in the samples; humics, HS-hydrolysates and low molecular mass acids. In the feed sample some polysaccharides are present which is typical for a surface water source.

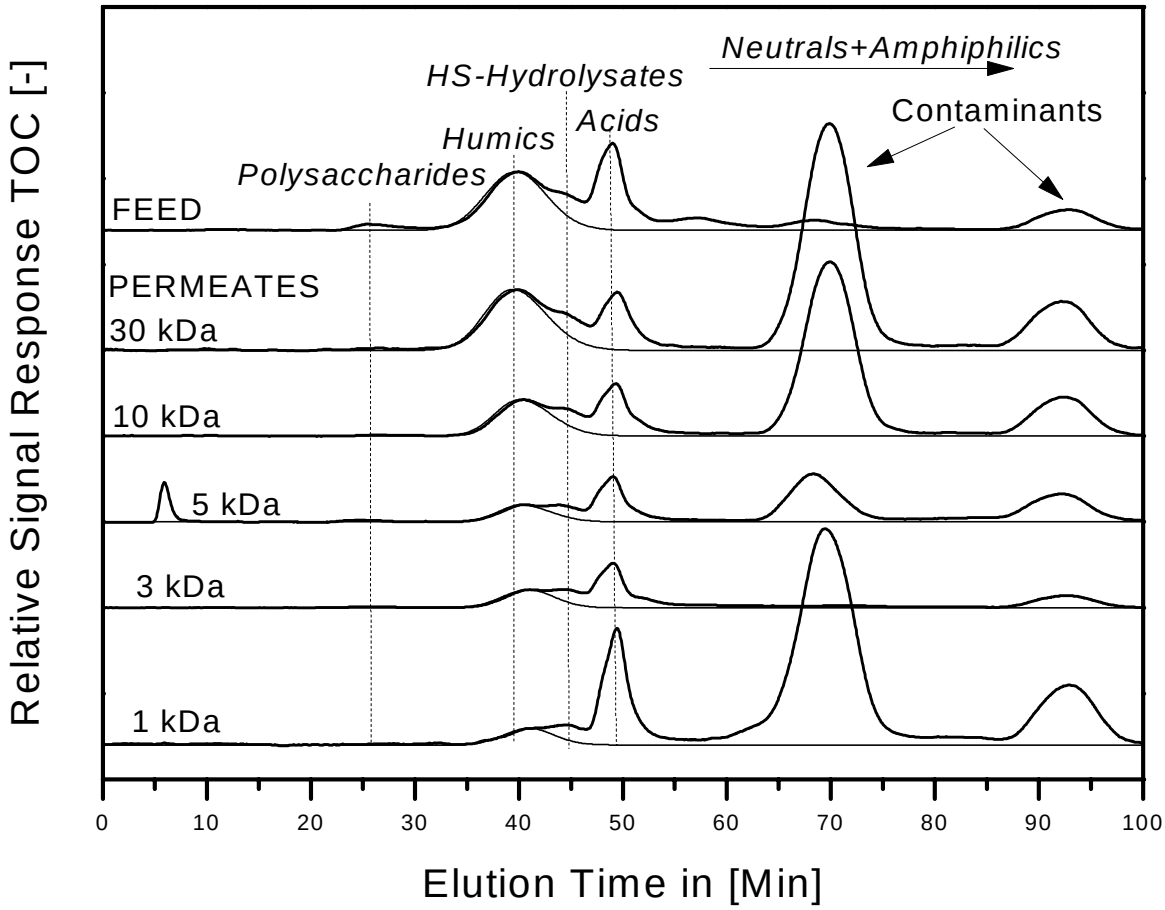


Figure 6.19 *Results of LC-OCD analysis of UF fractions and feed solution at 20 mM NaCl of NOM concentrate.*

The UF membranes reduce the different compounds to varying extents. The humics are retained most with an overall shift towards smaller sizes (peak maximum drifts towards higher elution times). This also shows in lower molecular weights of these fractions and lower UV/DOC ratios as shown in Table 6.4. However, the molecular weights measured are not related to the MWCO of these membranes. Values are much smaller and comparable to SEC results. Comparing the peaks of LC-OCD and SEC, it can be assumed that the largest SEC peak are the humics. This peak was reduced most in size with fractionation. The second peak seen in the SEC graphs (Figure 6.13 to Figure 6.18) is most likely related to the low molecular mass acids. The peaks and their changes in the different permeates, however, do not correspond in the LC-OCD and SEC analysis. It should be noted here that the MW of the LC-OCD samples is determined from the humics peak.

There are contaminants suspected in the neutrals and amphiphilics region. While these could come from the membranes, these contaminants are also visible in the feed sample which was never in contact with the membrane. Further, the NOM contained 8.2% of these compounds (see Chapter 4), which were mostly isolated in the hydrophilic fraction. The origin of these "contaminants" remains unclear and is most likely a combination of compounds leaching from the membranes, even after thorough cleaning, and natural components of the NOM which are less retained by the membranes.

Table 6.4 *Quantitative analysis of LC-OCD results.*

Parameter	Feed	30 kDa	10 kDa	5 kDa	3 kDa	1 kDa
CDOC* [%]	71.6	98.2	95.0	88.7	82.9	86.0
HOC [%]	28.2	1.6	4.9	11.1	17.0	13.7
POC [%]	0.2	0.2	0.1	0.2	0.1	0.2
Humics [% of CDOC]	41.4	19.7	15.2	15.5	27.1	6.7
HS-Hydrolysates [% of CDOC]	14.6	6.0	6.5	9.6	23.2	4.8
LMM Acids [% of CDOC]	12.9	3.3	4.4	8.9	9.5	8.7
LMM Neutrals and Amphophilics [% of CDOC]	28.4	70.3	73.6	64.9	38.6	79.3
Polysaccharides [% of CDOC]	2.8	0.7	0.3	1.0	1.6	0.4
M_W [gmol^{-1}]	972	952	793	751	724	716
M_N [gmol^{-1}]	664	644	568	567	552	539
M_W /M_N [-]	1.46	1.48	1.40	1.32	1.31	1.33
UV_{254nm}/OC [Lmg^{-1}m^{-1}]	4.10	3.99	3.72	3.23	3.42	3.05

* for explanation of abbreviations see Chapter 4 and glossary.

6.5 FILTRATION OF INORGANIC AGGREGATES

Through investigations over the last ten years, a close association between aggregation conditions and the fractal properties of the resulting aggregate are now recognised and reasonably well understood (Jullien and Botet (1987), Lin *et al.* (1989), Klein *et al.* (1990)). While issues such as aggregate restructuring and compression on cake formation must be addressed, this relationship between aggregation conditions and resulting aggregate structure opens the way to design of cake properties through control of suspension conditions.

Many investigators have recognised the importance of aggregation conditions either in suspension or at the membrane surface to cake properties (Grace (1953), McDonogh *et al.* (1984, 1989), Wiesner *et al.* (1989), Schmitz *et al.* (1993), Kim *et al.* (1993), Bacchin *et al.* (1995, 1996), Zhu and Elimelech (1995, 1997), Meagher *et al.* (1996)). Indeed, some workers have recently suggested that the fractal properties of aggregates formed may be influencing membrane filtration behaviour (Khatib *et al.* (1997)). No studies however have been undertaken where the fractal properties of aggregates formed are carefully controlled and the implications to membrane filtration investigated. In this study, aggregates of well-characterised hematite under carefully controlled suspension conditions similar to those used in previous investigations (Amal *et al.* (1990), Zhang and Buffle (1996), Bushell *et al.* (1996)) were prepared (see Chapter 4 for methods). The impact of the resulting cakes formed on permeate flux through UF membranes of sufficiently small pore size that pore clogging effects are minimised was examined. Given our interest in application of UF membranes in water treatment, attention is focussed on the effects of ionic strength, pH and the presence of adsorbing natural organic acids on aggregate structure and thence UF behaviour.

6.5.1 Theoretical Considerations

The flux J of fluid across a membrane free of deposited materials may be described by Darcy's law; i.e.

$$J = \frac{\Delta P}{\eta R_m} \tag{6.3}$$

where ΔP is the pressure drop across the membrane (the trans-membrane pressure drop, or TMP), μ is the absolute viscosity of the fluid and R_m is the hydraulic resistance of the clean membrane with dimension of reciprocal length. Reductions in permeate flux may result from accumulation of materials i) within membrane pores as a result of adsorption or blocking processes, ii) at the membrane surface forming a gel and/or a porous "cake", and iii) near the membrane surface in the concentration boundary (the so-called concentration-polarisation) layer (Mallevialle *et al.* (1996)).

While size reduction or blockage of pores may be considered to increase the resistance of the membrane (R_m) to permeate flux, accumulation of materials in the cake and concentration-polarization layers (so-called "polarised" solids) presents additional resistances to permeation (denoted here as R_c and R_{cp} respectively). These resistances vary as a function of the composition and thickness of each layer, which in turn are determined by the feed water quality and the characteristics of mass transfer in the membrane module. In most instances encountered in water and wastewater treatment, it appears that the concentration-polarisation layer, if it is formed, contributes negligible resistance to permeate flux; i.e. $R_{cp} << R_c$ and, therefore, R_{cp} may be neglected (Mallevialle *et al.* (1996)). While this is in reality not always the case (as shown in later sections of this chapter and in Chapter 7) for the filtration of

inorganic colloids this assumption is considered valid. The flux through a UF membrane containing a deposited layer may thus be written as

$$J = \frac{\Delta P}{\eta\ (R_m + R_c)} \qquad (6.4).$$

According to filtration theory (Bowen and Jenner (1995)), the resistance of cake solids (assuming solids in the concentration-polarisation layer to be negligible) can be written as

$$R_c = \alpha \frac{m_p}{A} \qquad (6.5)$$

where m_p is the mass of deposited particles, A the membrane area and α the specific resistance of the deposit, which can be approximated for cakes formed from uniform, spherical particles by the Carman-Kozeny relationship (equation (6.4))

$$\alpha = \frac{180\,(1-\varepsilon)}{\rho_p\, d_p^2\, \varepsilon^3} \qquad (6.6)$$

where ε is the void volume of the cake, ρ_p the density of the particles and d_p is the mean diameter of the particles. For such a cake, the resistance would thus be expected to increase in proportion to the cake mass and as the inverse of the square of the primary particle size. A strong dependence on cake porosity is also predicted; for example, a change in ε from 0.2 to 0.1 would be expected to induce a 10-fold increase in α.

The Carman-Kozeny relationship is recognized to be valid for media with porosities less than 0.5 Veerapaneni and Wiesner (1996)) and incompressible cakes (Belfort *et al.* (1994)). As such, this semi-empirical expression is well suited to description of the permeability of relatively compact cakes formed by deposition in non-aggregating systems where the particles would be expected to pack uniformly on the membrane surface. More porous cakes are commonly formed when particles aggregate prior to deposition on the membrane surface. Whilst corrections to the Kozeny relationship for high porosity cakes have been deduced (Coulson and Richardson (1978)), these apply to fibres and "ring packing's" and their applicability to aggregrates has not been tested. Aggregates are now recognized to exhibit fractal properties (Lin *et al.* (1990)) and, as such, may be expected to form membrane cakes of somewhat different behavior to a cake formed from non-aggregated particles. One implication of the fractal nature of particulate aggregates is that the porosity of the aggregate (ε_a) is not spatially uniform but increases as the radius of the aggregate (r) increases according to the relationship (Lin *et al.* (1990), Jiang and Logan (1991))

$$\varepsilon_a = 1 - \rho = 1 - \left(\frac{r}{a_p}\right)^{D-3} \qquad (6.7)$$

where a_p is the radius of the primary particle and ρ is the density and D is the fractal dimension of the aggregate (note: D=3 for a solid sphere, 2 for a solid sheet and 1 for a line). Such behaviour is certain to influence the permeability of the cake (subject to diminution by compaction effects) and suggests that factors such as fractal dimension coupled with aggregate size will be important determinants of cake properties.

For example a low fractal number will produce a higher voidae aggregate (equation (6.7)), which should have higher permeability. Lower fractal numbers are favoured by diffusion limited aggregation (DLA) and higher numbers by reaction limited (RLA). A more detailed analysis is given in section 6.5.6. Aggregates are also described in Chapter 4.

6.5.2 Effect of KCl

The effect of suspension KCl concentration on permeate flux is shown in Figure 6.20 (with all initial feed fluxes given in Table 6.5). Two different flux regimes are observed. For KCl concentrations between 0 and 60 mM, rapid flux decline is seen with the flux decreasing to less than 50 % of the initial flux after passage of 2.8 L of permeate. A remarkably similar pattern of flux decline is observed for salt concentrations of 0, 20, and 60 mM KCl. In comparison very little flux decline is observed for 70 and 100 mM KCl.

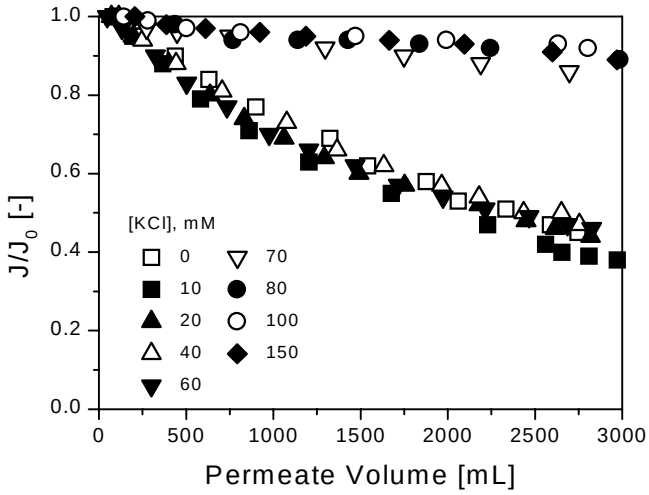


Figure 6.20 *Permeate flux (J) as a fraction of initial flux (J_o) over the course of UF of suspensions of hematite aggregates prepared and filtered at various KCl concentrations ([α-Fe_2O_3] = 10 mgL^{-1}, pH = 3, ΔP = 300 kPa, UF cell stirrer speed = 520 rpm).*

The effect of the KCl concentration on the cake resistance after filtration of 2.8 L feed suspension is presented in Figure 6.21. The calculation of the resistance is based on the "resistance in series" model presented in equation (6.4) which is further described in Chapter 3.

Since the single particles with a mean diameter of 70 nm are too large to penetrate the membrane pores which have an estimated pore size of less than 10 nm (Cheryan (1986)), separation of the total resistance into the intrinsic membrane resistance and the resistance due to the hydraulic resistance of the filtration cake would seem reasonable. A high hydraulic cake resistance is observed for concentrations between 0 and 60 mM KCl and a lower hydraulic resistance for concentrations higher than 70 mM. A distinct break between these two regimes is observed at around 65 mM KCl.

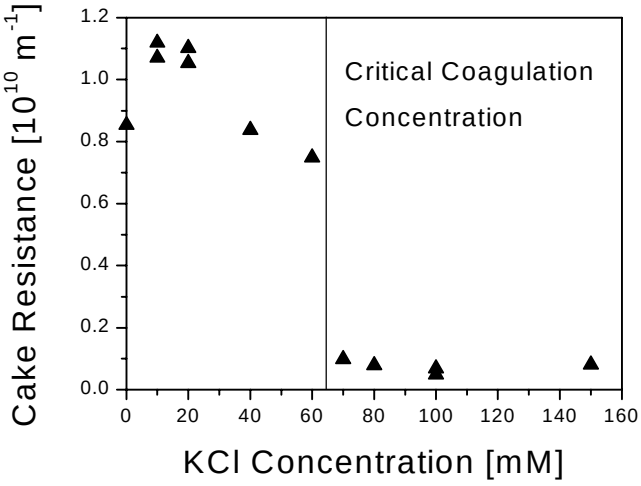


Figure 6.21 *Cake resistance after filtration of 2.8 L of hematite suspension for different KCl concentrations ([α-Fe_2O_3] = 10 mgL^{-1}, pH = 3, ΔP = 300 kPa, stirrer speed = 520 rpm). The critical coagulation concentration at which aggregation is considered to change from reaction limitation to diffusion limitation is also shown.*

Table 6.5 *Initial flux (J_o), flux after passage of 2.8L of permeate (J) and membrane (R_m) and cake (R_c) resistances for the various solution compositions used in studies reported here. (Note: Pure water flux = 1637 ± 47 Lm^{-2}h^{-1}).*

Solution Composition	Initial Flux [Lm^{-2}h^{-1}]	Flux (2.8 L) [Lm^{-2}h^{-1}]	Membrane Resistance [10^{10} m^{-1}]	Total Resistance [10^{10} m^{-1}]	Cake Resistance [10^{10} m^{-1}]
[KCl], mM					
0	1523	690	0.71	1.56	0.85
10	1543	609	0.70	1.77	1.07
10	1444	578	0.75	1.86	1.12
20	1306	574	0.82	1.88	1.05
20	1642	613	0.66	1.76	1.10
40	1437	679	0.75	1.59	0.84
60	1701	780	0.63	1.38	0.75
70	1800	1546	0.60	0.70	0.099
80	1741	1543	0.62	0.70	0.079
100	1820	1681	0.59	0.64	0.049
100	1662	1503	0.65	0.72	0.068
150	1830	1609	0.59	0.67	0.081
[NaCl], mM					
20	1622	646	0.66	1.67	1.00
40	1609	673	0.67	1.60	0.93
60	1543	1278	0.70	0.84	0.14
80	1563	1444	0.69	0.75	0.057
[$CaCl_2$], mM					
20	1543	742	0.70	1.45	0.75
40	1602	1456	0.67	0.74	0.068
60	1642	1424	0.66	0.76	0.10
80	1662	1495	0.65	0.72	0.072
Mean (± std.error)	1612 ± 30		0.67 ± 0.01		
[FA], mgL^{-1} as DOC					
0	1523	690	0.71	1.56	0.85
1	1563	1230	0.69	0.88	0.19
2	1484	1125	0.73	0.96	0.23
5	1530	580	0.70	1.85	1.15
10	1780	571	0.60	1.88	1.28

As can be seen from Figure 6.22, relatively similar cake masses are observed for KCl concentrations either side of the critical coagulation concentration, at least for the first litre of permeate filtered. A

slightly lower cake mass is evident at larger permeate volumes for the high salt compared to the low salt concentration case. These cake masses have been used to obtain the specific cake resistances (α in equation ((6.3))) shown in Table 6.6 for permeate volumes of 1.0, 1.5 and 2.0 L. Averaging of values obtained at these three permeate volumes yields specific cake resistances of $(1.18 \pm 0.09) \cdot 10^{10}$ m.g^{-1} and $(0.092 \pm 0.011) \cdot 10^{10}$ m.g^{-1} for 20 mM and 100 mM KCl, respectively.

The value of $1.18 \cdot 10^{10}$ m.g^{-1} is close to the specific resistance calculated using the Carman-Kozeny equation ((6.4)) for hematite particles of diameter (d_p) 70 nm, density (ρ_p) of 5.2 g.cm^{-3} and packing density of 0.4, i.e. only slightly less compact than that arising from random close packed spheres for which $1-\varepsilon = 0.63$. This value is $1.30 \cdot 10^{10}$ m.g^{-1}.

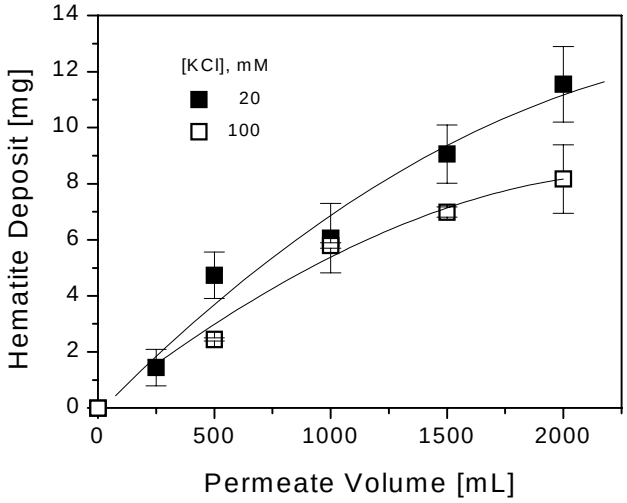


Figure 6.22 *Mass of cake formed on membrane filtration of hematite suspensions formed (and suspended) in 20 mM and 100 mM KCl. Cake masses deduced from both direct weight measurement and from amount of α-Fe_2O_3 retained (as determined by iron analysis) are shown ([α-Fe_2O_3] = 10 mgL^{-1}, pH = 3, ΔP = 300 kPa, UF cell stirrer speed = 520 rpm).*

Table 6.6 *Specific cake resistances for 20 mM and 100 mM KCl studies for permeate volumes of 1.0, 1.5 and 2.0 L. Cake masses as reported in Figure 6.22.*

KCl Conc. [mM]	Permeate Volume [mL]	Cake Mass [mg]	Flux [Lm^{-2}h^{-1}]	Flux Ratio [-]	Membrane Resistance [10^{10} m^{-1}]	Cake Resistance [10^{10} m^{-1}]	Specific Resistance [10^{10} m.g^{-1}]
20	1000	7	901	0.7	0.83	0.37	1.07
20	1500	9	783	0.6	0.83	0.55	1.24
20	2000	11.5	708	0.53	0.83	0.70	1.23
100	1000	5	1745	0.96	0.59	0.025	0.103
100	1500	7	1738	0.95	0.59	0.028	0.081
100	2000	8	1715	0.94	0.59	0.036	0.092

6.5.3 Effect of $CaCl_2$

A similar dramatic effect of salt concentration as for KCl is observed when using $CaCl_2$. As can be seen from Figure 6.23, two different flux regimes are again observed. Concentrations of 0 and 20 mM cause a rapid flux decline during the UF with consistent fouling behavior. Little flux decline is found for $CaCl_2$ concentration higher than 40 mM. As for the higher KCl concentrations, concentrations of 40, 60 and 80 mM $CaCl_2$ show a remarkably similar flux decline.

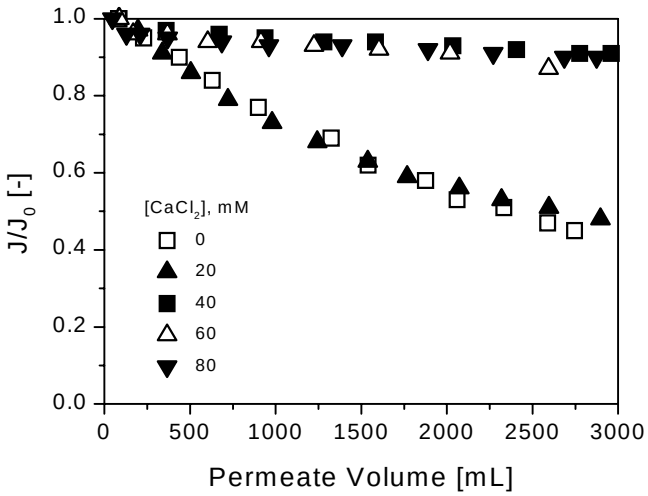


Figure 6.23 *Permeate flux (J) as a fraction of initial flux (J_o) over the course of UF of suspensions of hematite aggregates prepared and filtered at various $CaCl_2$ concentrations ([α-Fe_2O_3] = 10 mgL^{-1}, pH = 3, ΔP = 300 kPa, UF cell stirrer speed = 520 rpm).*

The effect of different $CaCl_2$ concentrations in the feed suspension on the cake resistance after filtration of 2.8 L feed suspension can be seen in Figure 6.24. A high hydraulic cake resistance is evident for $CaCl_2$ concentrations of 0 to 20 mM and low hydraulic resistance for concentrations greater than 40 mM.

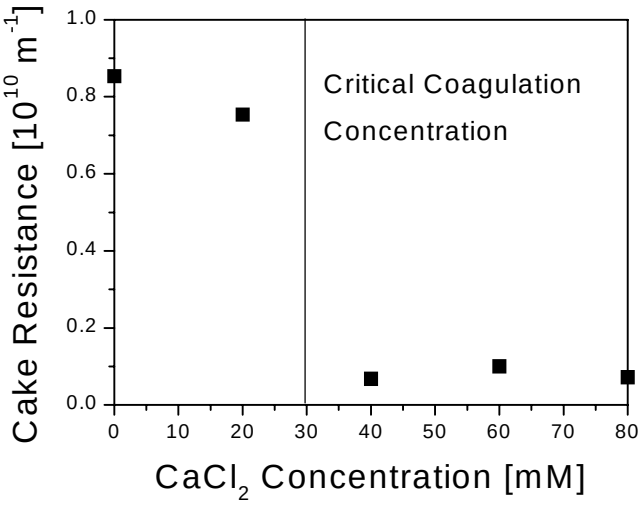


Figure 6.24 *Cake resistance after filtration of 2.8 L of hematite suspension for different $CaCl_2$ concentrations ([α-Fe_2O_3] = 10 mgL^{-1}, pH = 3, ΔP = 300 kPa, UF cell stirrer speed = 520 rpm). The critical coagulation concentration at which aggregation is considered to change from reaction limitation to diffusion limitation is also shown.*

6.5.4 Effect of pH

While change in salt concentration is effective in inducing change of the inter-particle repulsion barrier and thus rate of aggregation, change in suspension pH will alter the hematite zeta potential and may also be used to control the rate of hematite aggregation (and thus the structure of the resulting flocs). The zeta potential of hematite particles identical to those used in this study has been examined by both acid-base titration and mobility measurements (Amal (1991)) and found to decrease relatively linearly between pH 3 and 12 with a point of zero charge around pH 9.

The implications of the pH dependence of zeta potential on aggregation kinetics has been investigated by Amal (1991) who reported that, at low salt concentrations, diffusion limited aggregation could only be induced at around pH 9 (in accord with the low interparticle repulsion barrier at this pH). In accord with the recognised effect of salt in reducing the electrostatic repulsion at larger interparticle distances through double layer compression, rapid (transport or diffusion limited) aggregation could be extended to a wider range of pH around the isoelectric point by increasing the salt concentration. Thus, while

slow (reaction limited) aggregation producing dense aggregates was maintained at pH 3, rapid (diffusion limited) aggregation producing loose aggregates could be induced at pH 5.5 and 11.5 by increasing the KCl concentration to 40 mM.

Co-incident with the effect of pH on hematite aggregation kinetics, we observe significant flux decline on UF of hematite aggregates formed (and filtered) in 40 mM KCl at pH 3 (slow aggregation) but significantly less flux decline on filtration of aggregates formed at pH 5.6, 7.5 and 10.5 (again, in 40 mM KCl) where rapid aggregation has been observed (Figure 6.25).

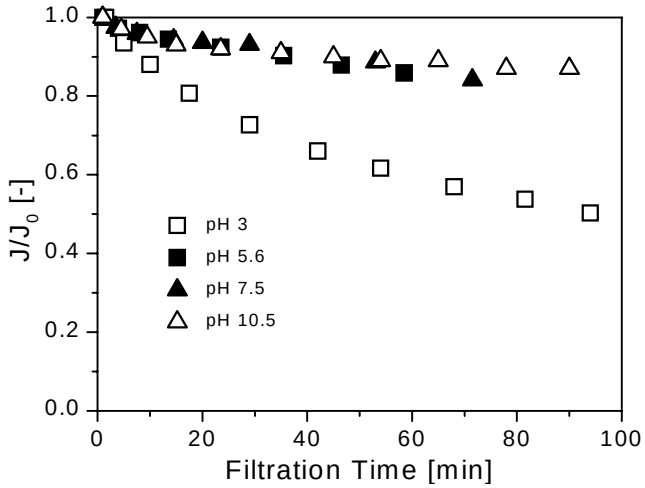


Figure 6.25 *Permeate flux (J) as a fraction of initial flux (J_o) over the course of UF of suspensions of hematite aggregates prepared and filtered at various pH ([α-Fe_2O_3] = 10 mgL^{-1}, [KCl] = 40 mM, ΔP = 300 kPa, UF cell stirrer speed = 520 rpm).*

6.5.5 Effect of IHSS Fulvic Acid

As can be seen from the permeation velocity data presented in Figure 6.26, the presence of the naturally occurring fulvic acid, and the variation of its concentration over a relatively narrow range, has a dramatic impact on permeate throughput in the presence of hematite. In the absence of fulvic acid and at a salt concentration ([KCl] = 40 mM) below the critical coagulation concentration of hematite (at pH 3), significant flux decline occurs over the course of the study with J/J_o reduced to 0.5 after passage of about 2.5 L of permeate In the presence of just 1 mgL^{-1} of fulvic acid, the flux decline is substantially reduced with J/J_o dropping to only 0.8 on filtration of 2.5 L of solution. Slightly greater fouling is evident for 2 mgL^{-1} fulvic acid and use of 5 and 10 mgL^{-1} fulvic acid produces permeation velocities that are substantially lower than the no organic case (J/J_o dropping to 0.4 and lower after filtration of 2.5 L). In the presence of 10 mgL^{-1} pH 3 buffered fulvic acid alone, a slightly lower extent of reduction in permeation velocity over the course of filtering 1.4 L of fluid than that found in the presence of rapidly aggregated particles (i.e. minimal fouling) was observed.

These membrane filtration results are presumably again correlated with the different aggregation behaviour of the hematite colloids for different concentrations of fulvic acid. Indeed, as shown in Figure 6.27, the cake resistance is at a minimum at the fulvic acid concentration (approximately 1 mg.L^{-1}) where the zeta potential of the hematite particles is close to zero and where rapid aggregation has previously been observed to occur (Amal *et al.* (1992)). At fulvic acid concentrations either side of this critical concentration, aggregation has been seen to be retarded due to the presence of high residual surface charge.

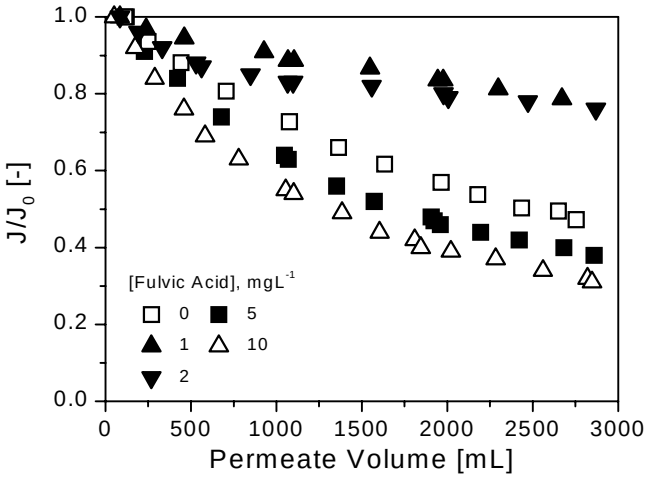


Figure 6.26 *Permeate flux (J) as a fraction of initial flux (J_0) over the course of UF of suspensions of hematite aggregates prepared and filtered in the presence of various concentrations of fulvic acid ([α-Fe_2O_3] = 10 mgL^{-1}, [KCl] = 40 mM, pH = 3, ΔP = 300 kPa, UF cell stirrer speed = 520 rpm).*

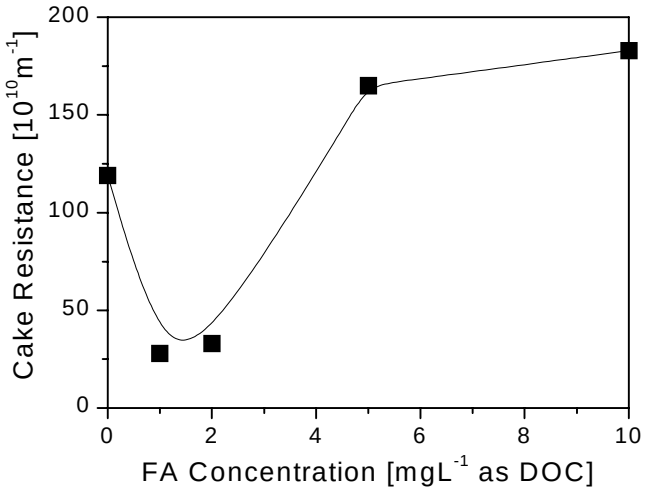


Figure 6.27 *Cake resistance after filtration of 2.8 L of hematite suspension for different fulvic acid concentrations ([α-Fe_2O_3] = 10 mgL^{-1}, [KCl] = 40 mM, pH = 3, ΔP = 300 kPa, UF cell stirrer speed = 520 rpm).*

6.5.6 Aggregate Characteristics and their Effect on Membrane Filtration

The size distribution results obtained for hematite aggregates coagulated under diffusion limited and reaction limited aggregation conditions are of considerable interest in their own right but are only considered briefly here. Some details of characteristics were given in Chapter 4. In essence, it appears (as would be expected from investigations of floc strength vs. floc break-up studies by other workers Mühle (1993)) that the more tenuous flocs generated rapidly under DLA conditions (i.e. high salt concentrations or near zero surface potential) are more prone to breakup, most likely through floc fragmentation or splitting.

Indeed, the mode size of 8 – 10 μm (data is shown in Chapter 4) attained is in the same size range as that estimated for the Kolmogoroff microscale in the peak energy dissipation region (within the vicinity of the radial jet) in the stirred cylindrical membrane filtration chamber (Schafer *et al.* (1997), Dong *et al.* (1994), Ciofalo *et al.* (1996)). These estimations are explained in detail in Appendix 2.

The steady state size distribution observed is quite narrow (also shown in Chapter 4) in accord with previously reported effects of shear-induced fragmentation (Spicer and Pratsinis (1996)). In comparison, a portion of the aggregates generated under RLA conditions are of significantly larger size than the DLA aggregates presumably because their more compact structure is less prone to fragmentation. It should be noted that while there are some large aggregates present under RLA conditions (indeed, enough to contribute to more than half the volume of solids present), a large number of flocs remain in the sub-micron size ranges. These aggregates have presumably formed

slowly and essentially remain immune from orthokinetic coagulation effects. Only the larger aggregates in this size range will begin to experience the effects of mixing and be induced to grow to larger size. These larger aggregates will also experience the dis-aggregative effects of shear but possibly through surface-erosion and loss of individual particles or small groupings of particles rather than the floc splitting that appears to be operative for flocs generated rapidly (Parker *et al.* (1972)). The absence of intermediate-sized aggregates is supportive of such a mechanism.

While the implications of the aggregation regime (i.e. reaction or diffusion limited) to the eventual size distribution(s) attained in the stirred UF cell are reasonably clear, the implications of aggregation kinetics in the colloidal size range to the structure of the eventual distribution of aggregates is less certain. Our major tool for structure determination is small angle light scattering but as stated earlier, the results in the supra-colloidal region are far from simple. Thus, while interpretation of the small angle light scattering results should not be taken too far given the uncertainties present, the results are suggestive of maintenance of the structural regimes developed in the colloidal size range (i.e. compact for RLA and less compact for DLA) but with some modifications due to mixing-induced restructuring. Jung *et al.* (1995) have previously reported an increase in scattering exponent from 1.73 to 2.23 for an identical hematite suspension induced to aggregate at diffusion controlled rates in a stirred cell. Restructuring effects have been reported by Oles (1992), and Lin *et al.* (1990) have reported a similar departure in linearity in log I vs. log q plots to that described in Chapter 4 for the 100 mM KCl aggregates and attributed the result to a compaction at large scale (small q) where shear effects are significant but maintenance of looser structure at small length scales (high q) where the aggregates are strong enough to withstand the shear imposed. Thus, a difference in scattering exponents between hematite aggregates formed under low and high salt conditions of 2.35 and 2.20 (or even 1.8 if considering the high q region) respectively could be claimed as indicative of compact and less compact assemblages in each case but caution must be exercised in drawing such conclusions given the subjectiveness of the data analysis.

It is reasonably apparent from the results presented earlier that minimal flux decline is observed when filtering hematite particles that have been induced to aggregate quickly (by salt addition, adjustment of pH or adsorbing ion addition) compared to the significant decline in permeate flux that is observed when filtering hematite particles that have been induced to aggregate slowly. That coagulation of colloidal suspensions affects the extent of membrane fouling has been well documented (Wiesner *et al.* (1989), Schmitz *et al.* (1993), Kim *et al.* (1993), Bacchin *et al.* (1995, 1996), Zhu and Elimelech (1995, 1997), Meagher *et al.* (1996), Khatib *et al.* (1997)) with a variety of factors shown (or proposed) to account for the observed effects of coagulation on membrane flux. Thus, Kim *et al.* (1993) found that aggregation of silver particles lowered the extent of fouling of UF membranes and concluded that non-aggregated silver particles caused significant flux decline because of pore blocking by the individual particles whereas aggregation retained the particles in a surface cake. Such a mechanism is not likely to be of importance here since the primary hematite particles are significantly larger (approx. 70 nm in diameter) than the membrane pores (approx. 10 nm in diameter) and would not be expected to penetrate the membrane in either the aggregated or (particularly) the non-aggregated states.

Coagulation has also been suggested to lead to a reduction in cake thickness (i.e. lowered fouling) as a result of generation of larger particles that are more susceptible to shear-induced diffusion and (for larger particles) inertial lift (Wiesner *et al.* (1989), Lahoussine-Turcaud (1990), Belfort *et al.* (1994)). Indeed, a number of authors have satisfactorily modelled the reduction in extent of fouling as a result of the lowered cake mass arising from occurrence of these back-transport processes (Bacchin *et al.* (1995, 1996). At the high permeation velocities occurring in the studies reported here (10^{-1} – 10^{-2} cm/s), shear-induced diffusion and (particularly) inertial lift effects would be expected to only have an influence on aggregates of size greater than a few microns in diameter with increasing effect at larger aggregate sizes (Belfort *et al.* (1994)). It would appear from Figure 6.22 however, that these back-transport effects, while undoubtedly retarding deposition of the larger aggregates, are not exerting a dominant influence in the studies reported here. Relatively similar cake masses are seen to accumulate for both slowly and rapidly aggregated systems, particularly through passage of the first 1000 mL of permeate. A reduction in rate of cake accumulation is observed in both cases at higher permeate volumes and may reflect the increasing impact of inertial lift as permeate flux drops in response to increasing cake thickness. The slightly lower rate of accumulation of hematite flocs on the membrane in the case of rapid aggregation (compared to aggregates generated more slowly) may result from the fact that almost all of the rapidly formed aggregates are of a size (3-10 μm) that might be expected to experience some impact of back-transport processes (particularly shear induced diffusion) while only a portion of the more slowly formed aggregates (i.e. those in the larger sized cohort) would be expected to experience the impact of inertial lift

Given that neither a pore blocking mechanism nor a reduced cake thickness due to aggregate back-transport can account for the observed differences in flux for cakes formed from rapidly-formed compared to slowly-formed aggregates, we must conclude that the differences in permeation velocity arise from differences in permeability of the cakes formed under the different aggregation regimes. The order of magnitude difference in specific resistances of cakes developed at 20 mM and 100 mM KCl concentrations (approx. $1 \cdot 10^{10}$ m.g^{-1} versus approx. $0.1 \cdot 10^{10}$ m.g^{-1} respectively) supports the contention that the cakes formed under different aggregation regimes have fundamentally different permeabilities. Given that coagulation occurs at both low (less than the c.c.c.) and high (above c.c.c.) salt concentrations, simple particle/aggregate size arguments (and the concomitant effects on cake porosity) would seem insufficient to account for the observed behaviour.

A possible approach is to consider that the fractal properties of the suspended aggregates are retained (to some extent) by the filter cake. While further consideration must be given to compaction effects, aggregate structure characteristics can be incorporated into the Carman-Kozeny equation ($\alpha \propto (1 - \varepsilon)/\varepsilon^3$) using equation (6.5) ($\varepsilon = 1 - (r/a_p)^D$). The ratio of specific resistances expected for hematite cakes made up of aggregates of various sizes (r/a_p) and fractal dimensions (D) formed in the presence and absence of significant interparticle repulsion (i.e. slow and fast aggregation) are shown in Table 6.7. In all cases we have assumed that the permeability of the cake produced from aggregates formed slowly (in the presence of a repulsion barrier) is controlled by the smaller cohort of aggregates present. As shown in Chapter 4, these aggregates have sizes on the order of 0.4 to 1 μm. Ratios of aggregate to primary particle size (r/a_p) of either 10 (Cases 1 and 4), 5 (Case 2) or 20 (Case 3) have thus been considered as possibly being representative of these slowly formed aggregates. Larger particles are also

present but it is likely that the smaller aggregates would deposit preferentially given their insensitivity to back-transport processes. Aggregates formed rapidly assume an average size in the range 3 to 8 μm (Chapter 4). Two possibilities have thus been examined, one in which aggregates are 100 times the size of the primary particles (Cases 1, 2 and 3) and one in which aggregates are 50 times the size of primary particles (Case 4). We have also assumed that aggregates once deposited in the cake retain similar fractal dimensions to that measured in suspension. While compaction effects may well induce structural change, we have assumed a fractal dimension of 2.4 for aggregates formed in the presence of a repulsion barrier and either 2.2, 2.0 or 1.8 for more rapidly formed aggregates (recall that fractal dimensions of 2.35 and 2.20 were measured by small angle light scattering for aggregates formed slowly and rapidly respectively).

Table 6.7 *Ratio of specific cake resistances (α) calculated using the Carman-Kozeny equation resulting from aggregates of various size and structure formed in the presence and absence of significant interparticle repulsion (slow and rapid aggregation).*

Case	Aggregation Rate	r/a_p [–]	D [–]	ε [1] [–]	α [2] [10^{10} m.g^{-1}]	$\frac{\alpha^{slow}}{\alpha^{rapid}}$
1	Slow	10	2.4	0.749	0.42	
A	Rapid	100	2.2	0.975	0.019	22.1
B	Rapid	100	2.0	0.990	0.007	59.8
C	Rapid	100	1.8	0.996	0.003	149.5
2	Slow	5	2.4	0.619	1.13	
A	Rapid	100	2.2	0.975	0.019	59.5
B	Rapid	100	2.0	0.990	0.007	160.6
C	Rapid	100	1.8	0.996	0.003	401.5
3	Slow	20	2.4	0.834	0.20	
A	Rapid	100	2.2	0.975	0.019	10.6
B	Rapid	100	2.0	0.990	0.007	28.6
C	Rapid	100	1.8	0.996	0.003	71.5
4	Slow	10	2.4	0.749	0.42	
A	Rapid	50	2.2	0.956	0.035	11.9
B	Rapid	50	2.0	0.980	0.015	28.1
C	Rapid	50	1.8	0.991	0.006	64.7

1 $\varepsilon = 1 - (r/a_p)^D$ where D = fractal dimension

2 $\alpha = k(1-\varepsilon)/\varepsilon^3$ where $k = 180/\rho_P d_P^2$ (=7.07 x 10^9 m.g^{-1} for 70 nm diameter hematite particles).

It is clear from the results of calculations presented in Table 6.7 that both aggregate size and structure have a substantial effect on ease of fluid flow through the (assumed) fractal aggregates making up the cake. Aggregates characterised by Case 4A (r = 0.7 μm and D=2.4 for slowly formed aggregates and r =3.5 μm and D=2.2 for rapidly formed aggregates) are considered most similar to the hematite

assemblages investigated here and are estimated to exhibit an approximately order of magnitude decrease in specific cake resistance on change from slow to rapid aggregation similar to that found in this study.

Use of a modified Carman-Kozeny equation may not be the best way to account for effects of aggregate structure on cake permeability. Indeed, Veerapeni and Wiesner (1996) have examined various formulations for describing the hydrodynamics of flow through fractal aggregates and show significant departure from experiment (and the predictions of other models) at high porosities when using the Carman-Kozeny formulation. Thus, both the method of accounting for the effect of fractal structure on aggregate permeability and (perhaps more importantly) the extent of retention of fractal structure of aggregates once deposited as a cake require further attention. However, the results presented here do suggest some retention of structure effects imbued through coagulation conditions once aggregates are deposited as a cake and suggest that control of cake permeability via control of coagulation kinetics is an avenue worthy of further investigation.

Cakes formed on UF membranes as a result of collection of hematite aggregates generated rapidly in stirred suspension (in the absence of a repulsion barrier) exhibit a similar rate of cake accumulation as those formed slowly (in the presence of a repulsion barrier) but possess specific resistances that are an order of magnitude lower. This dramatic difference in cake resistance is considered to arise from the size and fractal properties of the hematite assemblages. The porosity of these assemblages will be influenced both by the fractal dimensions of the aggregates and by their size relative to primary particle size (since, for fractal aggregates, porosity increases as the size of the aggregate increases). The size and strength of aggregates are also important determinants of the relative effects of permeation drag, shear induced diffusion and inertial lift and result, in the studies reported here, in relatively similar rates of particle deposition for both rapidly and slowly formed aggregates.

While compaction effects may act to minimise some of the differences, it appears likely that the differences in size and fractal properties are induced by the kinetics of aggregation of hematite particles in suspension. Slowly formed aggregates possess a cohort of sub-micron sized aggregates of relatively high fractal dimension which form a reasonably impermeable cake while rapidly formed aggregates are generally of larger size and lower fractal dimension and thus create a substantially more permeable cake.

While the Carman-Kozeny equation is recognised to possess some weaknesses, particularly for cakes of high porosity, it does appear to provide a reasonable description of the proportional differences in specific resistances that might be expected for cakes formed from aggregates of differing size and fractal dimension. The results presented here suggest that control of cake permeability via control of coagulation kinetics is an avenue worthy of further investigation though the nature and extent of compaction effects in modifying the fractal properties of aggregates generated in suspension requires further attention.

6.6 FILTRATION OF ORGANICS AND CALCIUM

The aim of filtration experiments with organics and calcium present was to study two effects; (i) the effect of organic size and type on rejection and fouling, and (ii) the effect of coagulation of the organics by calcium and subsequent surface or pore fouling.

Two membranes were examined, the 10 kDa (PLGC) and the 100 kDa (PLHK). Pure water fluxes and filtration protocols were described earlier in this chapter. The flux ratios shown in this section are the fluxes over the initial flux at the start of the experiment (not pure water flux). This compensates for any initial osmotic effects of the feed solutions.

6.6.1 Calcium Concentration

Calcium can cause aggregation of organics. If this was the case, flux decline would increase with calcium concentration and subsequently rejection would increase as the aggregates are retained. Flux results are shown in Figure 6.28A and B for the 100 and 10 kDa membranes, respectively. For the 100 kDa membrane, the flux indeed decreases with calcium concentration and reaches a value of 0.1 as flux ratio (90% flux decline). This flux decline can be attributed to retention of organics, thus the formation of a gel layer or deposit and possibly due to pore plugging. Pore plugging can be expected when the aggregates or molecules are close to membrane pore size, then initial rejection is low and increases as pores become blocked.

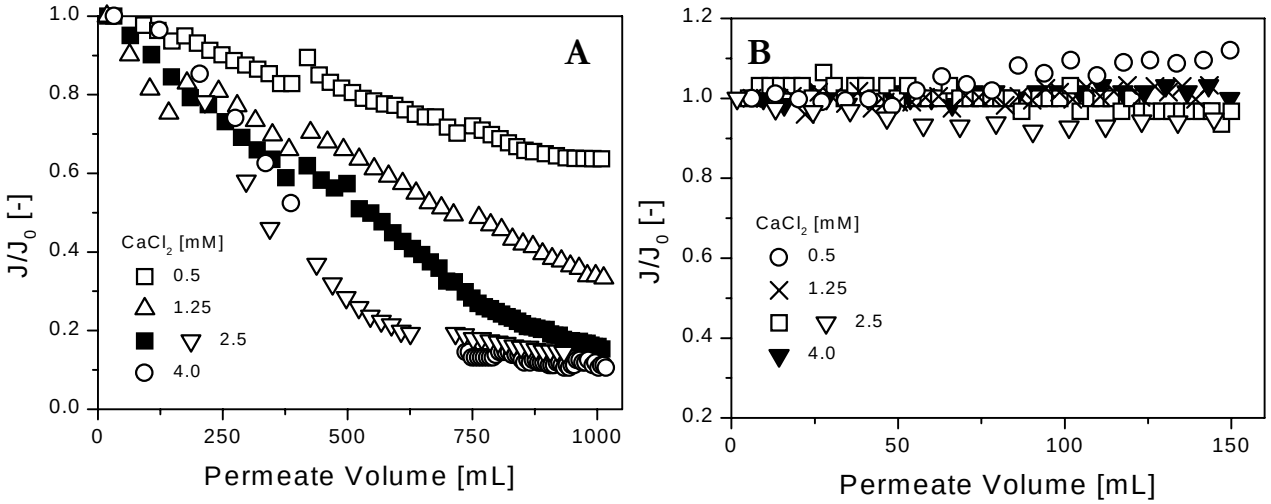


Figure 6.28 *Flux ratios over filtration volume of the (A) 100 kDa and (B) 10 kDa membranes as a function of calcium concentration (pH 7.5, 12.5 mgL^{-1} as DOC IHSS HA). For the 100 kDa membrane permeate was recirculated twice. The experiments at 2.5 mM $CaCl_2$ were repeated.*

For the 10 kDa membrane no substantial flux decline is observed. These results are summarised in Figure 6.29. The 10 kDa membrane also has a much lower pure water flux and operational flux. The fluxes of the 10 kDa and 100 kDa membranes are very similar at a calcium concentration of 4 mM; 50 and 63 Lm^{-2}h^{-1} for the 100 kDa and 10 kDa membranes, respectively. It should be noted that the transmembrane pressures were 100 kPa (100 kDa) and 300 kPa (10 kDa). The effect of flux on fouling

is investigated in more detail in 6.6.3. At the high calcium conditions rejection is also very similar; results are summarised in Table 6.8.

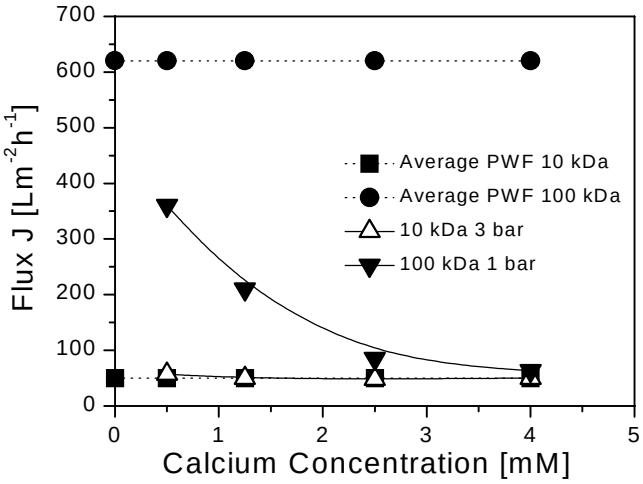


Figure 6.29 *Flux as a function of calcium concentration in comparison with average pure water flux for the 100 kDa and 10 kDa membranes (pH 7-8, 12.5 mgL^{-1} IHSS HA as DOC).*

Table 6.8 *Rejection for the 100 kDa and 10 kDa membranes (pH 7-8, 4 mM $CaCl_2$, 12.5 mgL^{-1} IHSS HA as DOC). Values are for the last sample (at maximum flux decline).*

	DOC [%]	UV_{254nm} [%]
100 kDa	72	66
10 kDa	87	80

The rejection of DOC and UV absorbance at 254 nm for the different calcium concentrations is shown in Figure 6.30 and Figure 6.31 for the 100 kDa and 10 kDa membranes, respectively.

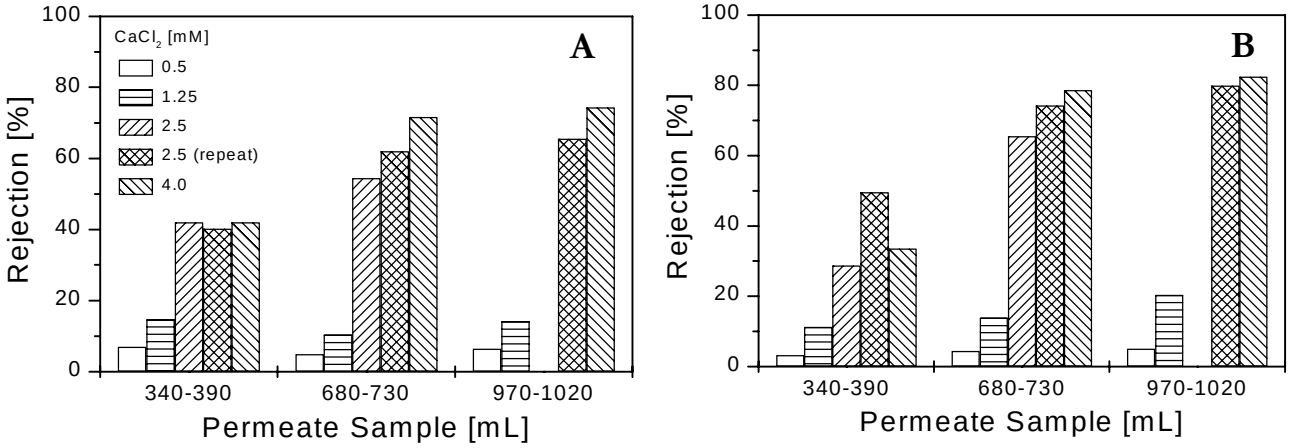


Figure 6.30 *Rejection of the 100 kDa membrane as a function of calcium concentration (A) DOC and (B) $UV_{254\ nm}$ (pH 7.5, 12.5 mgL^{-1} as DOC IHSS HA).*

For the 100 kDa membrane, the rejection increases with calcium concentration and permeate volume. The higher the calcium concentration, the more organic molecules aggregate and are retained by the membrane. Over time, as a deposit forms in the pores and on the surface, rejection increases. The changes in rejection are great; while at a low calcium concentration about 5% of DOC and UV are

retained, at high calcium concentrations these values increase to 70% for DOC and 80% for UV. This difference again demonstrates a selective rejection of UV absorbing compounds, which are larger and more hydrophobic, by UF. The high organic rejections achieved with this membrane at high calcium concentrations are comparable to those of the tighter membrane. While the final fluxes were shown to be similar, the transmembrane pressure is three times as high.

No significant change in rejection was observed for the 10 kDa membrane as a function of calcium concentration for UV rejection (Figure 6.31). Values vary between 60 and 80% for DOC removal and 80 to 90% for UV. The relative error in these measurements is estimated to be about 10%. DOC rejection confirms the trend with salt concentration, which was shown with fractionation experiments in the previous section, i.e. that rejection decreases with increase in ionic strength.

DOC rejection reaches a minimum at the critical coagulation concentration of HA of 2.5 mM $CaCl_2$ (Tipping (1981), Tipping and Ohnstad (1984a)). This can by a compaction of the humic molecules at higher ionic strength (Ghosh and Schnitzer (1980)). The trend is not confirmed with UV rejection which shows that it is the smaller compounds that pass through the membrane. The rejection then increases once aggregation takes place and some of the smaller molecules are probably retained within the aggregates or the deposit formed.

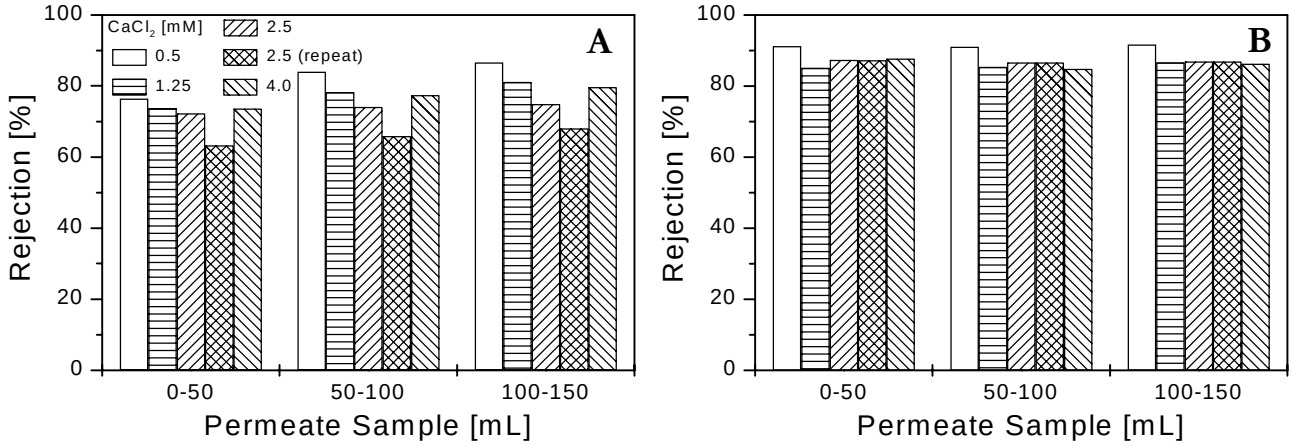


Figure 6.31 *Rejection of the 10 kDa membrane as a function of calcium concentration (A) DOC and (B) $UV_{254\ nm}$ (pH 7.5, 12.5 mgL^{-1} as DOC IHSS HA).*

In summary, calcium concentration plays a significant role in fouling and rejection behaviour of UF. Calcium changes the molecular conformation of the HA, and causes aggregation (see also solubility of calcium and organic compounds in Chapter 4). Flux is also a very critical parameter, although the performance of the high flux membrane appears to be better, in terms of flux at a similar rejection and lower transmembrane pressure.

6.6.2 Organic Type

The three different organic types (IHSS HA & FA, NOM) and the three NOM fractions (humic, fulvic and hydrophilic) were compared at the high calcium concentration of 2.5 mM $CaCl_2$. This study was undertaken in order to investigate if the different organics respond differently to aggregation with calcium.

The flux ratios for both membranes are shown in Figure 6.32A and B. The 100 kDa membrane (Figure 6.32A) shows flux declines which are very dependent on the organic type. The IHSS HA causes most severe flux decline (similar results were obtained in a repeat experiment). This flux decline cannot be reversed by permeate recirculation, indicating a solid deposit. IHSS FA causes least flux decline and is fully reversible. The other organics lie between these extremes, with the humic acid fraction of NOM also causing significant decline and irreversible fouling. The hydrophilic fraction shows a surprisingly steep decline, however it is mostly reversible. This can be explained by concentration polarisation and an osmotic effect, possibly due to the high salt content of this sample, which results from the fractionation method used (see Chapter 4 for details). However no significant osmotic effect is expected for the 100 kDa membrane.

The 10 kDa membrane, again, does not show flux decline for any of the organics. The IHSS FA appears to slightly increase the flux ratio, possibly acting like a surfactant. The rejection results for the 100 kDa membrane are shown in Figure 6.33 for DOC (A) and UV (B).

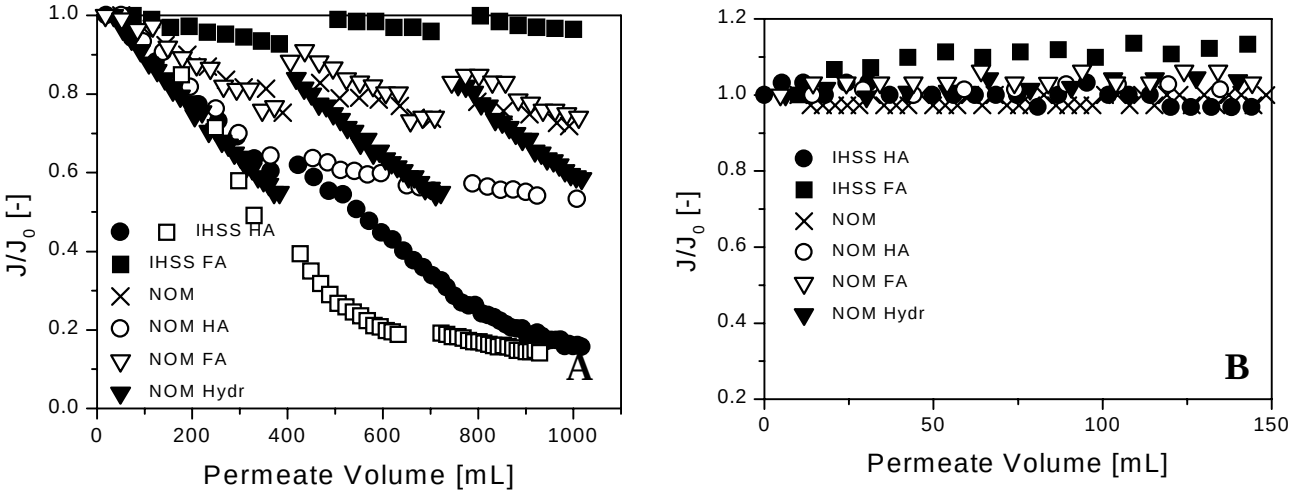


Figure 6.32 *Flux ratios over filtration volume of the (A) 100 kDa and (B) 10 kDa membranes as a function of organic type (pH 7.5, 12.5 mgL^{-1} as DOC organic, 2.5 mM $CaCl_2$). For the 100 kDa membrane permeate was recirculated twice.*

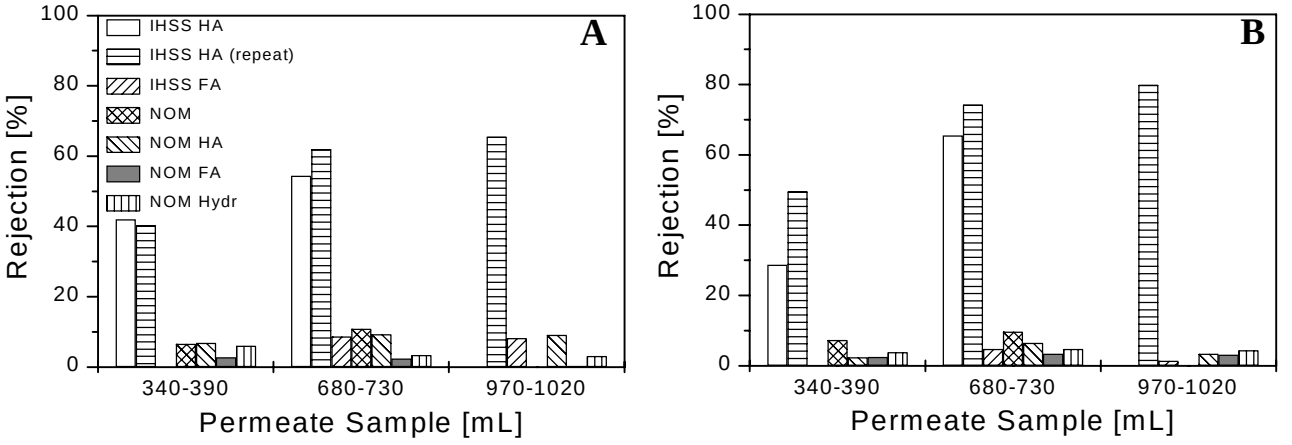


Figure 6.33 *Rejection of the 100 kDa membrane as a function of organic type (A) DOC and (B) $UV_{254\ nm}$ (pH 7.5, 12.5 mgL^{-1} as DOC, organic, 2.5 mM $CaCl_2$).*

While the rejection of IHSS HA is high (40 to 60% DOC and 30 to 80% UV), the rejection of all other organics is below 10%. As the size of the IHSS HA molecule was estimated to be in the order of 1.35 nm and the pores of this membrane about 9.1 nm, aggregation of this compound must be invoked to explain such high rejections. In fact, in the solubility studies (Chapter 4), it was found that only IHSS HA forms aggregates. This is confirmed with the UF rejection observations. The rejection increases over time, which also shows a rejection effect due to blocked pores or a deposit layer on the membrane surface.

The 10 kDa membrane (Figure 6.34A and B) also shows a dependence on the organic type, though in this case the behaviour appears to be determined by organic size and possibly charge, rather than aggregation. Rejection of the largest (and partly aggregated) compound, IHSS HA, remains highest and stable over permeate volume (70 to 80% DOC and 80 to 90% UV). The rejection of the smallest compound, the NOM hydrophilic fraction, is lowest (20% for DOC, 30% for UV). All other organics lie in a similar range with the more aromatic compound, the humic acid fraction of NOM, being rejected most. These organics are smaller than the estimated pore size of 2.6 nm, however the pore size and the organic sizes are both size distributions, which explains the partial retention.

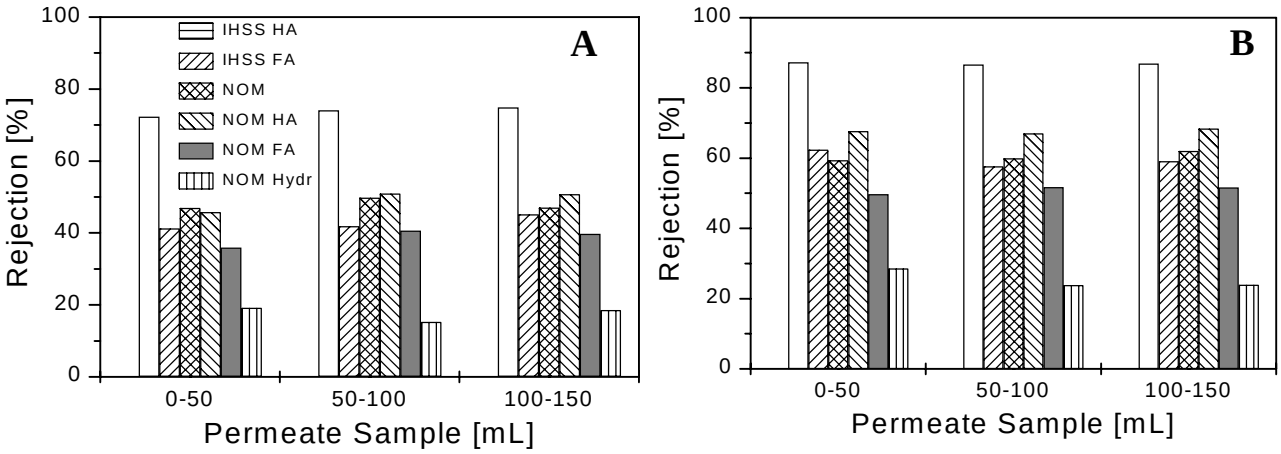


Figure 6.34 *Rejection of the 10 kDa membrane as a function of organic type (A) DOC and (B) $UV_{254\ nm}$ (pH 7.5, 12.5 mgL^{-1} as DOC, organic, 2.5 mM $CaCl_2$).*

6.6.3 Effect of Flux on Fouling

During these experiments the 100 kDa membrane consistently exhibited flux decline depending on the filtration conditions, whereas the 10 kDa membrane showed no such decline. Several factors could explain this.

First of all, pore blocking could cause more severe flux decline of the 100 kDa membrane. This is addressed in the blocking law analysis in the following section.

Secondly, the high flux of this membrane could cause severe concentration polarisation and membrane-solute interaction, or fouling (thus reach a 'critical flux' where deposition starts to control flux). This effect can be controlled by variation of the transmembrane pressure and thus flux.

Thirdly, the higher filtrate volumes used for this membrane could simply increase the cake mass and thus the resistance. The filtrate volume effect can also be examined very easily.

Figure 6.35 shows the flux of the 100 kDa membrane at 8 and 100 kPa and that of the 10 kDa membrane at 300 kPa, but with a filtration volume identical to that of the 100 kDa membrane. The results show that volume is not a critical parameter. The flux remains constant for the 10 kDa membrane even at a filtrate volume comparable to that of the 100 kDa membrane. The small filtrate volumes used in the experiments are thus an appropriate representative of flux decline.

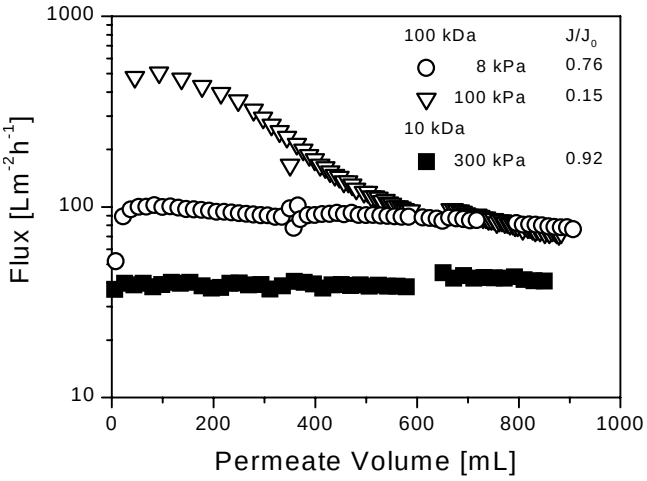


Figure 6.35 *Flux as a function of permeate volume for the two membranes (12.5 mgL^{-1} as DOC IHSS HA, 2.5 mM $CaCl_2$, pH 7-8).*

Lower flux indeed decreased the amount of fouling by reducing possibly pore penetration and gel formation on the membrane. If the 100 kDa membrane is operated at a lower pressure and therefore lower flux, the decline is reduced and the final value is identical, at a much lower pressure. This clearly indicates the importance of 'critical flux' and this requires further studies for surface water systems. Flux is obviously not proportional to pressure at these conditions (a pressure increase from 8 to 100 kPa should cause a 12.5 fold flux increase).

This demonstrates that flux is a critical parameter in membrane fouling, along with the calcium concentration which appears to enhance aggregate formation. If adsorption was the major cause of fouling as suggested by Jucker and Clark (1994), then flux would not have such a strong effect. It should be noted that flux influences concentration polarisation and thus the wall concentration which influences adsorption. Values of organics required to cover the membrane by adsorption are given in Chapter 7. There it was shown that adsorption alone cannot explain the large amounts of organics deposited.

6.6.4 Blocking Law Analysis

The blocking law theory was described in detail in Chapter 3 and summarised in Chapter 5. In this section the blocking law analysis is used to see if a pore fouling mechanism can be identified for the 100 kDa membrane. Experiments were carried out at 2.5 mM $CaCl_2$ under stirred and unstirred conditions. At this calcium concentration aggregation of the organics occurs. It should be noted that the blocking laws are only valid for unstirred filtration. For high permeate fluxes stirring may have a negligible effect.

Figure 6.36 shows the complete blocking and cake filtration relationships for both stirred and unstirred conditions. The results only show the first cycle of the recycle experiments. The analysis is not valid for the further cycles as the feed concentration varies if deposition occurs during the first cycle.

The effect of stirring is large. This means that the blocking law analysis for these conditions is invalid. Initial fluxes were about 500 $Lm^{-2}h^{-1}$ and fluxes after the first cycle were 346 and 152 $Lm^{-2}h^{-1}$ for stirred and unstirred conditions, respectively (this corresponds to flux declines of 40 and 70%).

Neither the cake filtration nor the complete blocking law show a linear relationship when considering that the analysis is invalid for stirred filtration.

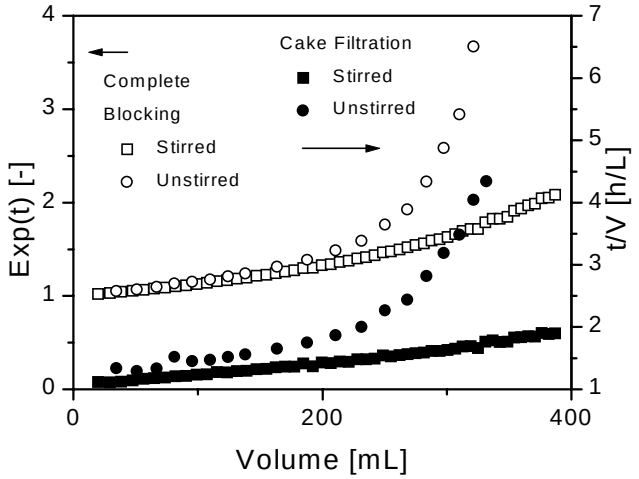


Figure 6.36 *Complete blocking and cake filtration analysis for the 100 kDa membrane at 2.5 mM $CaCl_2$, pH 7-8 and 12.5 mgL^{-1} IHSS HA at stirred (270 rpm) and unstirred conditions.*

Intermediate blocking and standard blocking laws are illustrated in Figure 6.37. Intermediate blocking represents the sealing of pores by an accumulation of 'particles'. This relationship is not linear. Standard blocking is the deposition of solute on the internal pore walls, inducing a reduction in pore diameter. This relationship is the only which can be considered as linear over a considerable range.

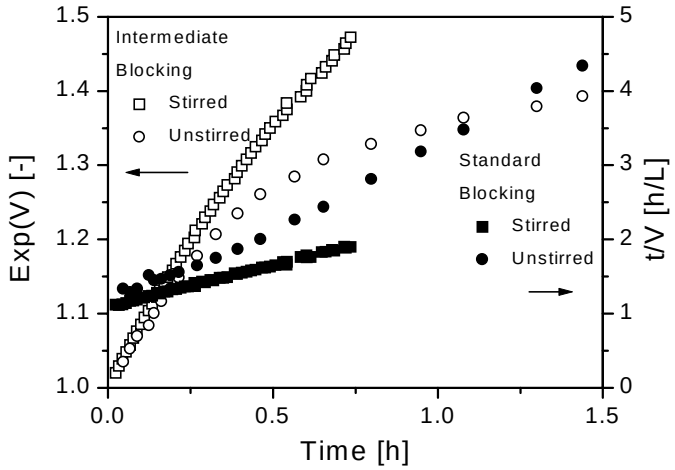


Figure 6.37 *Intermediate and standard blocking analysis for the 100 kDa membrane at 2.5 mM $CaCl_2$, pH 7-8 and 12.5 mgL^{-1} IHSS HA at stirred (270 rpm) and unstirred conditions.*

This means that the blocking law analysis was successful in the distinction between pore and surface fouling. Pore fouling is the dominant mechanism for the 100 kDa membrane as was suggested considering the pore size and the estimated size of organics after aggregation (see Chapter 4 and 7 for organic solubility).

6.7 FILTRATION OF INORGANIC COLLOIDS AND ORGANICS

After the investigation of filtration behaviour of well defined colloidal systems and organics, colloids are now examined in solutions which are closer to surface water conditions. In a preliminary section the effect of colloid size on flux will be examined. This includes the packing of stable primary colloids. A further section examined the filtration of aggregates in the absence of organics. The aggregates are now formed under conditions closer to surface waters, at a pH 7-8 and in the presence of calcium. Finally, the colloidal systems OPS and SPO as described in Chapter 4 are considered.

6.7.1 Stable Colloids in the Absence of Organics

At the pH extremes, the hematite colloids are stable due to charge repulsion (see Chapter 4). Experiments were conducted at pH 3 and 12 to determine the flux decline by such stable primary colloids, which were later used with organics or in different colloid/organic/salt systems. The two smallest primary colloids (40nm, 75nm) were chosen for these experiments as those colloids are expected to deposit with the highest specific resistance due to their size. For the 100 kDa membrane 250 nm colloids were also investigated. Flux results are shown in Figure 6.38A and B. For the 100 kDa membrane there is a distinct difference between the two pH values. At pH 3, the flux decline is about 10%, whereas at pH 12 it is about 50%. No effect of particle size is obvious.

For the 10 kDa membrane no flux decline was observed for either of the colloids at pH 3 or pH 12. Rejection is complete for both membranes as the colloids are much larger than the membrane pores.

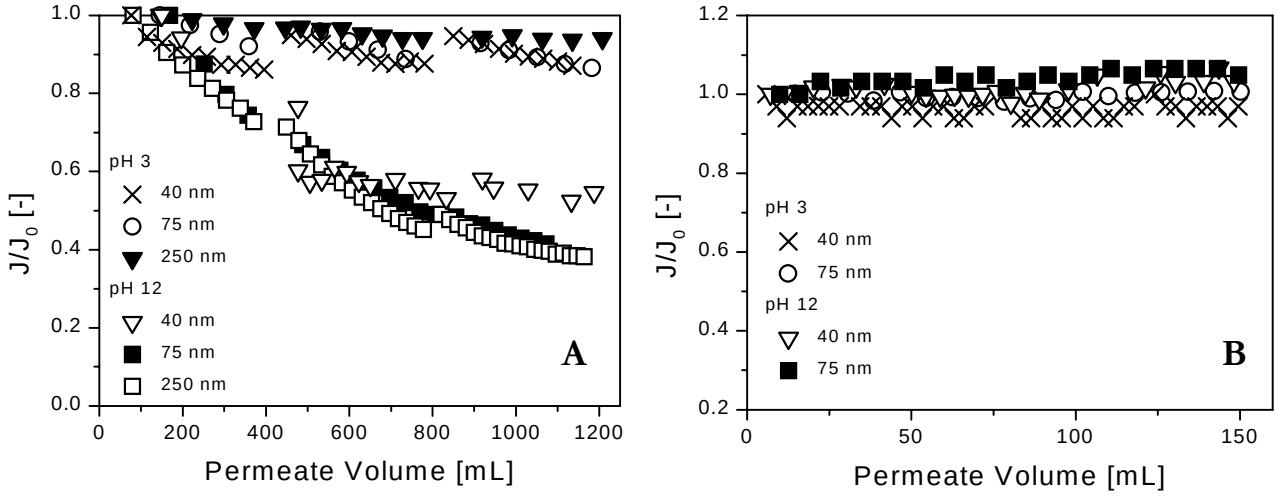


Figure 6.38 *Flux ratios over filtration volume of the (A) 100 kDa and (B) 10 kDa membranes as a function of pH and primary colloid size in MilliQ water.*

As shown in Chapter 4 the charge of the colloids at pH 3 (positive) and pH 12 (negative) is similar. Therefore an electroosmotic effect cannot explain this difference in filtration behaviour at pH 3 and 12. Diffusivity increases as colloid size decreases. This is of importance for the smaller colloids (40nm, 75nm) which are not influenced by lift or shear effects. This increased diffusivity results in a thinner deposit layer due to a increased backtransport as described in Chapter 3. In the absence of charge effects the colloids are expected to pack denser (smaller voids) if the primary colloid size is smaller.

According to Fane (1999) this void can be estimated to be of the order of one-sixth of the colloid size (see values in Table 6.9).

Table 6.9 *Estimated size of voids in a particle packing of various colloid sizes. Compare to estimated membrane pore radii of 2.6 nm (10 kDa) and 9.1 nm (100 kDa).*

Colloid Diameter [nm]	40	75	250	500
Void Size [nm]	6.7	12.5	41.7	83.3

This effect was not observed, although voids and membrane pore sizes are comparable for the 100 kDa membrane (9.1 nm). Particle charge, however, increased with decreasing particle size.

A possible explanation for the effect of pH could be the Debye length, which is the double layer thickness or more applied to membrane filtration the distance at which particles approach each other in a deposit. This distance is determined by the decline of particle charge. The pH of these suspensions was adjusted using HCl and NaOH and a different ionic strength was required to reach pH 3 (1 mM) and pH 12 (10 mM). The Debye length (or double layer thickness) is shown in equation (6.8) (Hiemenz (1986)).

$$\kappa^{-1} = \left(\frac{e^2 \sum_i z_i^{\,2} n_i}{\varepsilon k T} \right)^{-1/2} \qquad (6.8)$$

With $\varepsilon = \varepsilon_0 \cdot \varepsilon_r$; $n_i = 1000 \cdot M_i \cdot N_A$, and $\Sigma\, z_i^2 M_i = 2 \cdot I$ (with I being the ionic strength), and substituting the relevant values for constants, this can be simplified to

$$\kappa^{-1} = 4.31 \cdot 10^{-10} \left(2 \cdot I\right)^{-1/2} \qquad (6.9)$$

where κ is the Debye Hückel parameter and the unit of the Debye length κ^{-1} is m. This calculation results in Debye lengths of 9.64 nm and 3.05 nm for colloids at pH 3 and pH 12, respectively. It has to be noted that there is, by definition of the Debye length, no effect of particle size or charge.

Comparing these lengths with the voids in between colloids shown in Table 6.9 and the calculated membrane pore radii of Table 6.1 (2.6 and 9.1 nm for 10 and 100 kDa membranes, respectively), it is likely that the Debye length may dominate flux decline effects. In the pH 3 case the Debye length is so large, compared to the pore size and void spaces, that no flux decline is to be expected. In the pH 12 case, the Debye length is smaller than the pore size and an effect is well possible. The absence of flux decline for the 10 kDa membrane can be explained with the smaller pore sizes and the lower flux. A lower flux allows more back-diffusion and deposition is therefore reduced.

6.7.2 Aggregates in the Absence of Organics

The effect of different aggregation regimes (rapid versus slow) was discussed in detail in section (6.5). Here, the effect of aggregation under conditions much closer to surface waters (neutral pH and background solution) will be investigated. The experiments were carried out with the smallest colloids (40 nm, 75 nm). At pH 7-8 aggregation is expected in all cases.

The flux ratios obtained are shown in Figure 6.39A and B for the 100 kDa and 10 kDa membrane, respectively. No flux decline was observed. This is possibly due to the rapid aggregation of the colloids resulting in loose aggregate structures, as explained in section 6.5. The salt concentration leading to this fast aggregation is much lower than found necessary for destabilisation of the hematite aggregates at pH3. This is due to the pH. In the experiments shown here, the pH was 7-8. This is close to the point of zero charge and under such conditions fast aggregation would occur even in the absence of salt, and this is indeed the case, as no flux decline was observed even in the absence of calcium.

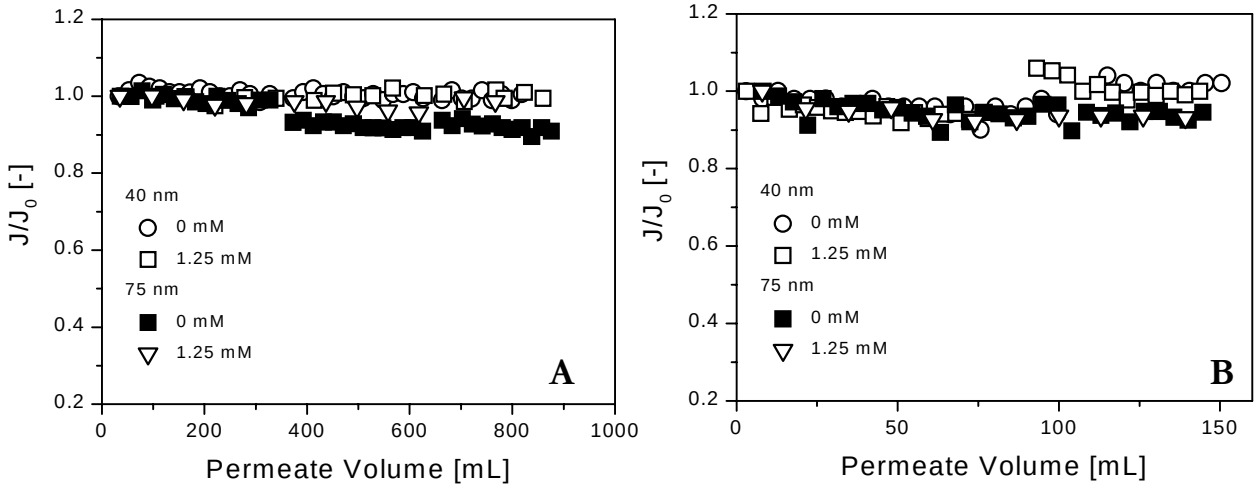


Figure 6.39 *Flux ratios over filtration volume of the (A) 100 kDa and (B) 10 kDa membranes as a function of calcium concentration and primary colloid size in background solution (pH 7-8).*

6.7.3 Colloids Stabilised by Organics (OPS)

It was shown in Chapter 4 how organics may interact with colloids. In the OPS order colloids are mostly stabilised. Calcium can destabilise the colloids, which results in aggregates. Results for flux ratio as a function of primary colloid size and calcium concentration are shown in Figure 6.40A and B. For the 100 kDa membrane, flux ratio decreases with increasing calcium concentration for both colloids. Flux again is lower for the larger colloids. As the calcium concentration becomes greater, an increasing number of colloids aggregate. The Debye length would also change but the calculation is not straight forward, as the adsorbed organic layer would also play a role.

For the 10 kDa membrane, again, no effect is visible. Flux decline is <10% and differences between the different experiments are within experimental error.

Rejection of the 100 kDa membrane is shown in Figure 6.41A and B. The DOC rejection remains low for low calcium concentrations in the presence of colloids. A similar observation was made at low calcium concentration in the absence of colloids (Figure 6.30A). This shows that adsorption on the hematite colloids is minimal and confirms the results of Au *et al.* (1999). At a calcium concentration of 2.5 mM, rejection increases dramatically to values higher than in the absence of colloids. It may be that the colloids enhance the deposition of a layer on the membrane which retains the solute or that the higher calcium concentration enhances aggregation. Note that UV absorption organics is no longer a useful measure of organics rejection as hematite also absorbs UV radiation.

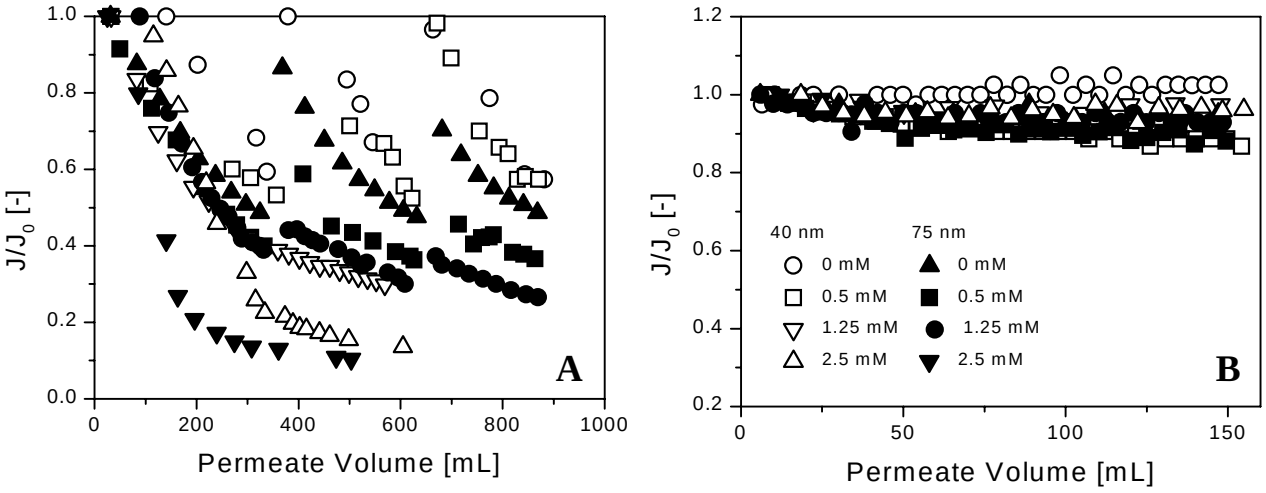


Figure 6.40 *Flux ratios over filtration volume of the (A) 100 kDa and (B) 10 kDa membranes as a function of calcium concentration and primary colloid size (OPS, pH 7-8, 12.5 mgL^{-1} as DOC IHSS HA).*

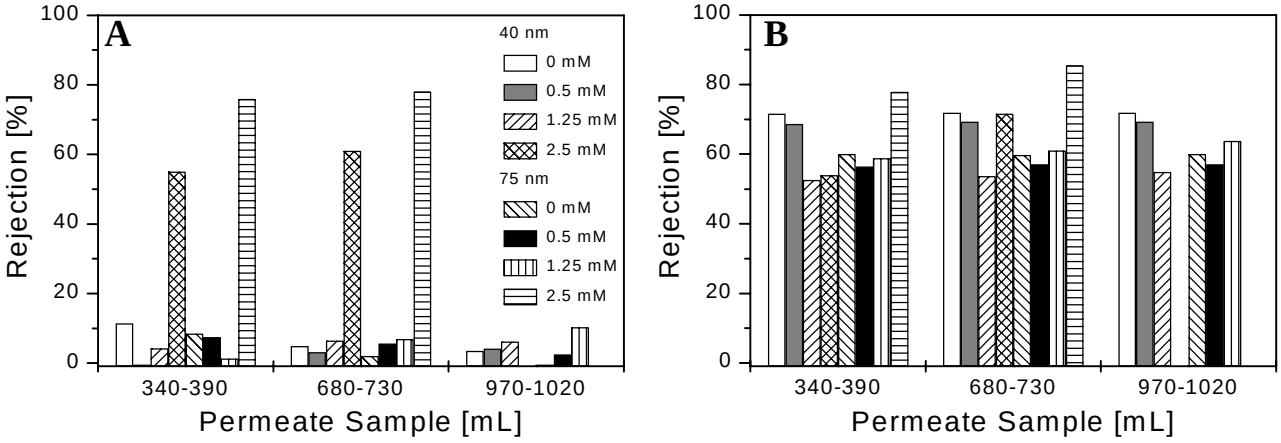


Figure 6.41 *Rejection of the 100 kDa membrane as a function of calcium concentration and primary colloid size (A) DOC and (B) UV$_{254\ nm}$ (OPS, pH 7-8, 12.5 mgL^{-1} as DOC IHSS HA).*

For the 10 kDa membrane (see Figure 6.42) the DOC rejection in the OPS case is similar to that found in the absence of colloids (refer to Figure 6.31). The UV rejection is higher due to the additional rejection of UV absorbing hematite colloids.

The stabilised colloids (OPS) exhibit identical flux decline and organic rejection as in the case without inorganic colloids. For high calcium concentrations, flux decline is greatest with a simultaneous increase in rejection. This is due to aggregation effects combining the organics, the colloids, and the calcium. Since only very little organic adsorbs on the hematite surface (Au *et al.* (1999)), most organics would be aggregating as in the absence of colloids, but it is likely that the colloids will interact in some way with the aggregates formed, for example by allowing interstitial deposition within a colloid cake.

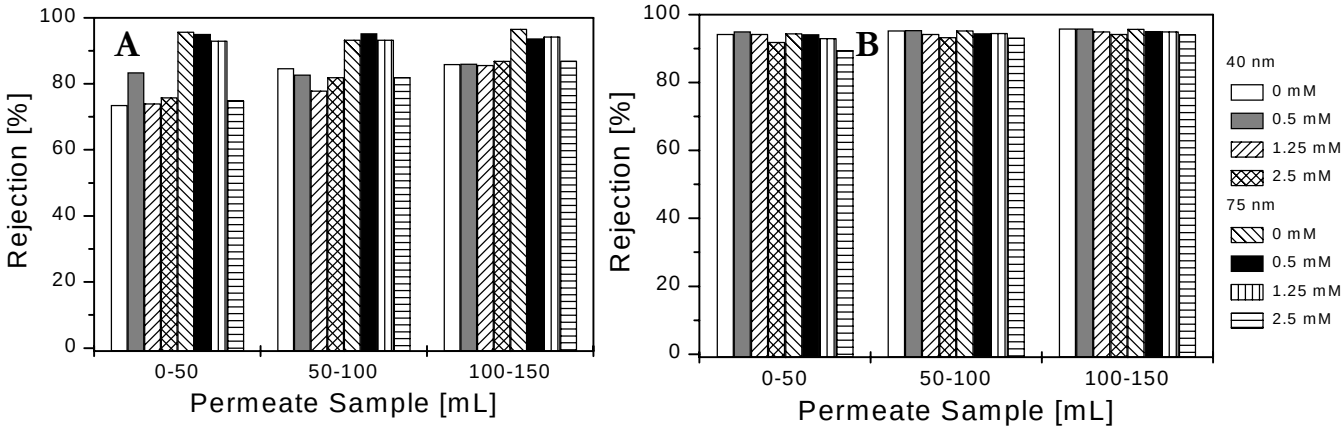


Figure 6.42 *Rejection of the 10 kDa membrane as a function of calcium concentration and primary colloid size (A) DOC and (B) $UV_{254\ nm}$ (OPS, pH 7-8, 12.5 mgL^{-1} as DOC IHSS HA).*

6.7.4 Aggregates in Presence of Organics (SPO)

In the SPO order, the inorganic colloids are allowed to aggregate prior to adsorption of organics on their surface (see Chapter 4). The impact of organics on aggregates formed under such conditions is described below.

The flux ratios are shown in Figure 6.43A and B. For the 100 kDa membrane, the flux decline is about 20% for calcium concentrations lower than 2.5 mM. This is less than in the absence of hematite (Figure 6.28A) and more than in the absence of organics (Figure 6.39A). While the inorganic aggregates themselves do not cause flux decline, and not many organics would be adsorbed on the colloids, it is very likely that the organic-calcium aggregates formed become entrained with the aggregates and result in a higher specific resistance deposit. Furthermore, some of the aggregates may still be able to penetrate into the membrane pores. However, the aggregates appear to protect the membrane partly from this deposition since flux decline was worse in the absence of aggregates. For the 10 kDa membrane flux decline is less than 10%.

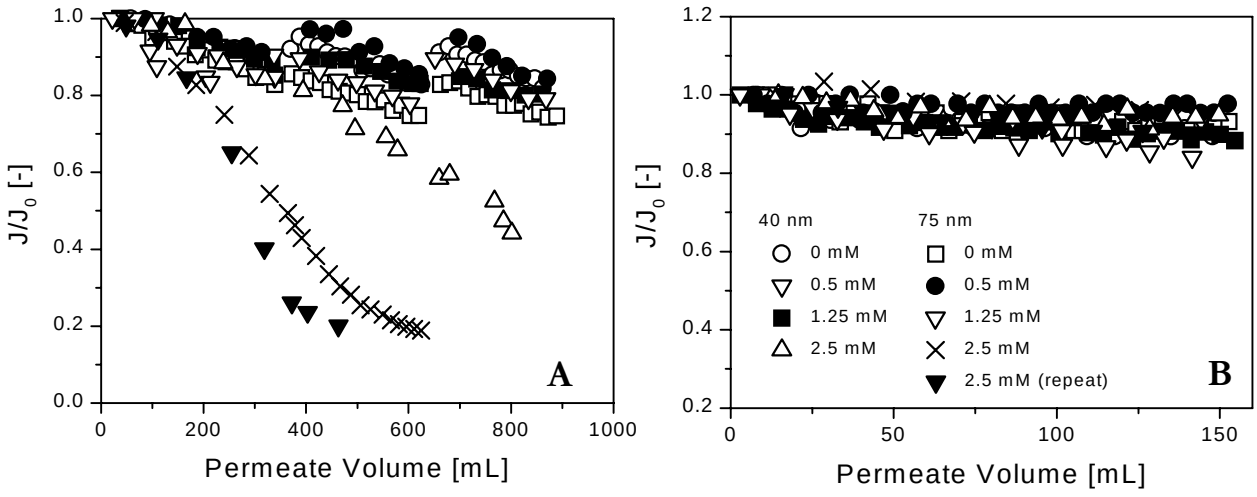


Figure 6.43 *Flux ratios over filtration volume of the (A) 100 kDa and (B) 10 kDa membranes as a function of calcium concentration and primary colloid size (SPO, pH 7-8, 12.5 mgL^{-1} as DOC IHSS HA).*

Rejection for the 100 kDa membrane is shown in Figure 6.44. For all calcium concentrations below 2.5 mM the organic rejection is low. As in the absence of inorganic colloids (Figure 6.30), the DOC rejection increases dramatically for calcium concentrations above 2.5 mM. UV rejection is initially higher than the DOC rejection due to the colloids. UV rejection at 2.5 mM calcium was not measured. Overall the organic rejection is lower than in the absence of colloids. This is most likely due to the formation of a thick unstirred deposit layer in which organics accumulate and rejection decreases due to a concentration polarisation effect. A similar effect was observed in NF (see Chapter 7).

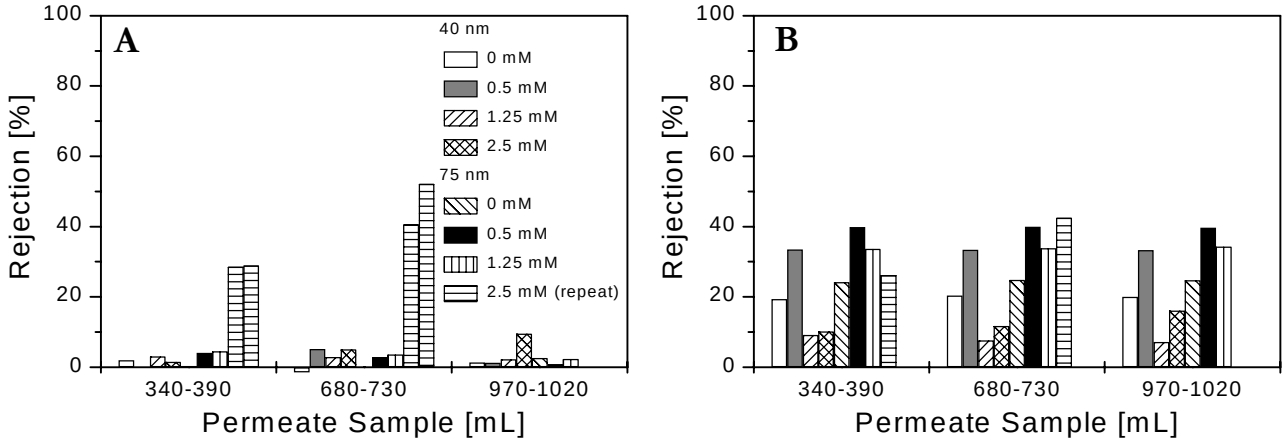


Figure 6.44 *Rejection of the 100 kDa membrane as a function of calcium concentration and primary colloid size (A) DOC and (B) $UV_{254\ nm}$ (SPO, pH 7-8, 12.5 mgL^{-1} as DOC IHSS HA).*

For the 10 kDa membrane, organic rejection (see Figure 6.45) is similar to the case where inorganic colloids were absent. Concentration polarisation effects does not occur to the same extent or has no effect, possibly due to the lower fluxes experienced.

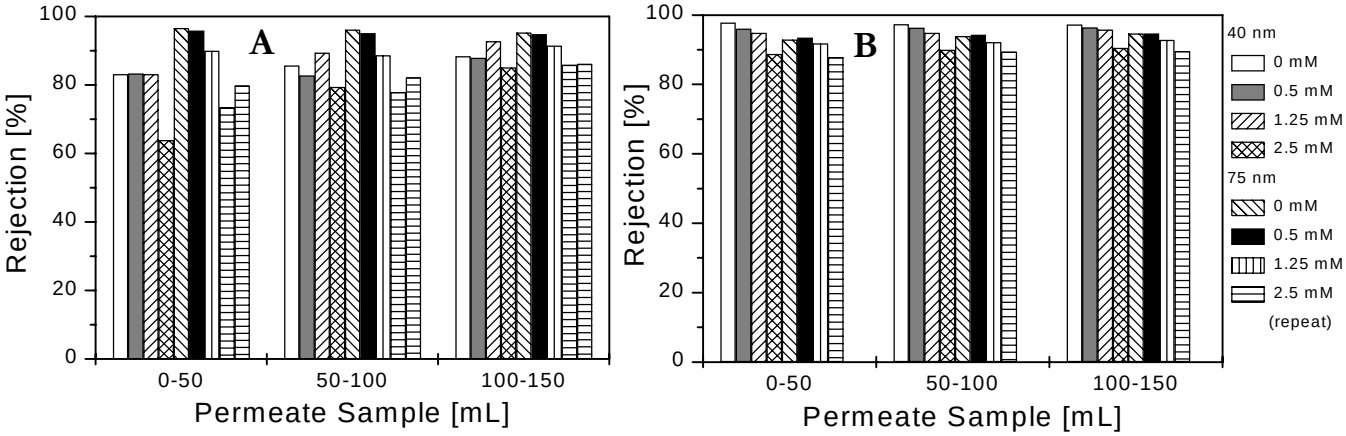


Figure 6.45 *Rejection of the 10 kDa membrane as a function of calcium concentration and primary colloid size (A) DOC and (B) $UV_{254\ nm}$ (SPO, pH 7-8, 12.5 mgL^{-1} as DOC IHSS HA).*

The SPO particles behaviour lies inbetween that of "pure aggregates" and organic calcium aggregates. This suggests that the organic aggregates somehow accumulate inbetween the hematite aggregates and, this to some extent, protects the membrane from excess organic calcium aggregates. Apart from some

concentration polarisation effects with the 100 kDa membrane (enhanced by its high flux) rejection remains the same as in the absence of colloids.

6.7.5 Comparison of Membrane Deposits formed by OPS and SPO Systems

Electronmicrographs of two membrane deposits are shown in Figure 6.46. The deposit of the aggregated systems (SPO) in Figure 6.46B is clearly more porous than that of the OPS systems in Figure 6.46A. This can explain the differences observed in flux decline (see Figure 6.40A (OPS) and Figure 6.43A (SPO)). Values for flux decline were 60% for OPS and 15% for SPO. This is a very similar effect to that observed for different aggregation states in the absence of organics (see section 6.5). While in the SPO case the colloids aggregate rapidly (see also section 6.7.2) and form loose aggregates that subsequently adsorb organics (which cannot be seen in the electronmicrographs due to their small size), in the OPS case the colloids are stabilised and do not aggregate. This appears to correspond to the case where colloids aggregate slowly and form dense aggregates, which is similar to a dense packing of stable colloids on a membrane.

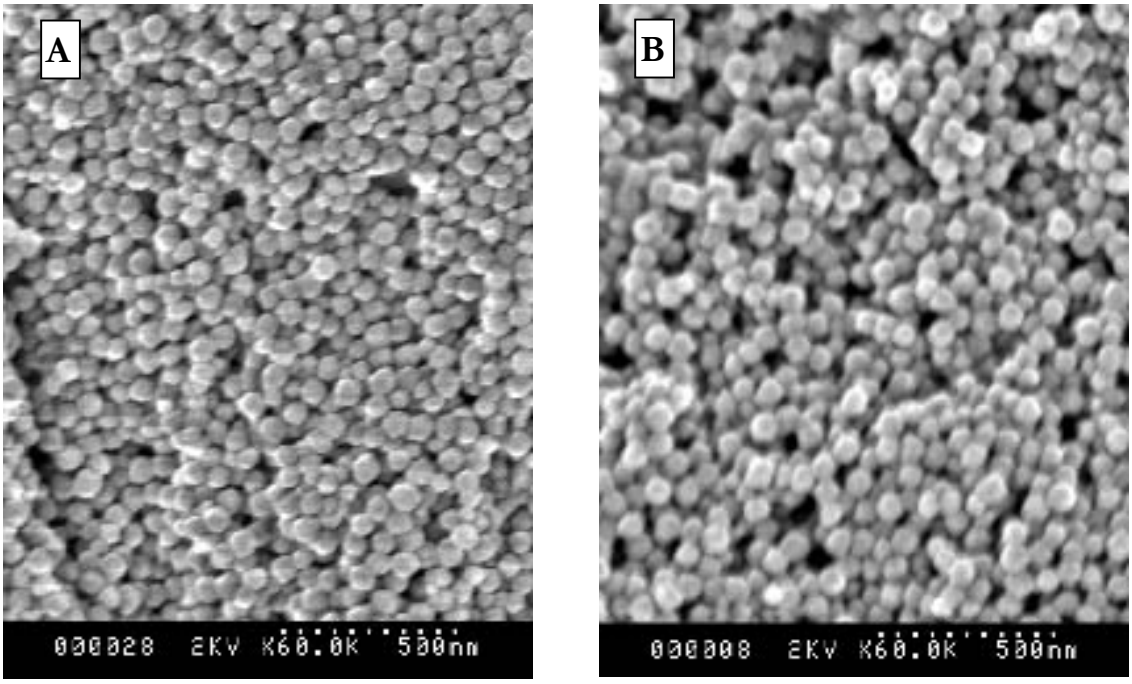


Figure 6.46 *Electronmicrographs of deposits on the 100 kDa membranes of (A) OPS and (B) SPO systems (12.5 mgL^{-1} as DOC IHSS HA, pH 7-8, 10 mgL^{-1} hematite, primary colloid size 75 nm, in background solution).*

6.8 COAGULATION PRETREATMENT

Coagulation is a means of adsorbing organic molecules (which would otherwise not be retained by the membrane) onto a precipitate and thus increase rejection. As in MF, ferric chloride was chosen as the coagulant. After an investigation of the effect of coagulant precipitates on the membrane in the absence of organics, coagulation was examined under the conditions previously described (organics, calcium, OPS, SPO).

The method of solution preparation is described in Chapter 4. The ferriic chloride dosages used were adapted from coagulation papers which did not necessarily foresee membrane separation of the flocs (Dennett *et al.* (1996)).

6.8.1 Effect of Ferric Hydroxide Flocs on Flux in the Absence of Organics

$FeCl_3$ was added to background solution without pH adjustment at three concentrations. The ferric chloride addition resulted in a pH decrease. Final pH values were between 7 at 25 mgL^{-1} and 3 at 100 mgL^{-1}. This leads to the formation of ferric hydroxide precipitates, as described by Lo and Waite (1998). The size and charge of these precipitates depends on the dosage and the equilibrium pH, which is determined by the strongly acidic $FeCl_3$.

Flux ratios are shown in Figure 6.47A and B. Dosage has a strong effect on the flux of the 100 kDa membrane, with flux decline being negligible at 25 mgL^{-1} $FeCl_3$ and strongest at 50 mgL^{-1}. The high dosage of 100 mgL^{-1} lies in between the flux declines of the other dosages. For the 10 kDa membrane flux decline is low, but the 50 mgL^{-1} also shows the strongest decline.

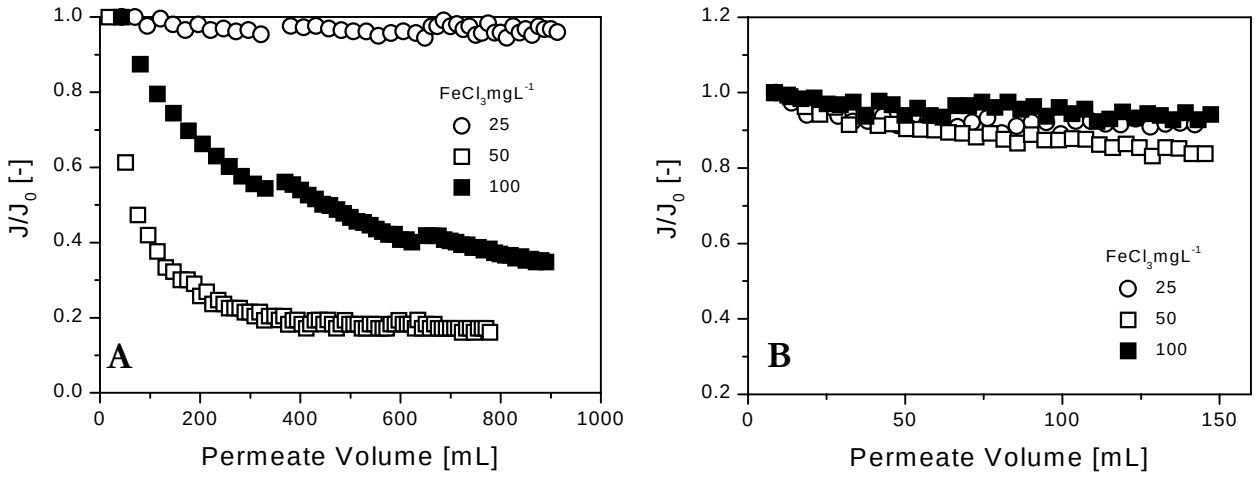


Figure 6.47 *Flux ratio over filtrate volume of the (A) 100 kDa and (B) 10 kDa membranes as a function of ferric chloride concentration.*

As explained previously, at the low dosage the flocs are relatively low in charge and form large visible flocs, probably of a loose structure due to the rapid coagulation. At the high dosage very small particles precipitate, which have a strong positive charge and do not aggregate due to this charge repulsion. Consequently the "flocs" are a lot smaller and more rigid. However, it is likely that they do not form a very dense cake as a result of the charge repulsion between the highly charged colloids. At 50 mgL^{-1} an intermediate behaviour can be expected, possibly small particles precipitate, but pack more densely on

the membrane due to less repulsion. This aspect requires more work to characterise the precipitates and flocs formed, and is considered to be outside the scope of this study.

6.8.2 Effect of Ferric Chloride on Rejection and Flux

In these experiments three membranes are tested -the 30 kDa membrane in addition to the 10 kDa and 100 kDa membranes. The effect of organic type, dosage, and stirring are also investigated. The results are shown in Figure 6.48A, B, and C for the 100, 10, and 30 kDa membranes, respectively. At 25 mgL^{-1} ferric chloride, flux decline is minimal for all organics and all membranes if the cell is stirred. If stirring is stopped (NS) concentration polarisation effects increase and the flux decline is greater. This effect, however, depends on the membrane (as concentration polarisation is strongly dependent on flux) and is strongest for the 100 kDa membrane, whereas for the 10 kDa membrane stirring has no effect at this dosage.

At the high ferric chloride dosage (100 mgL^{-1}), the flux decline is high and, again, the membranes with a higher flux exhibit a greater flux decline. If stirring is stopped for these conditions, flux decline is about 90% for all membranes.

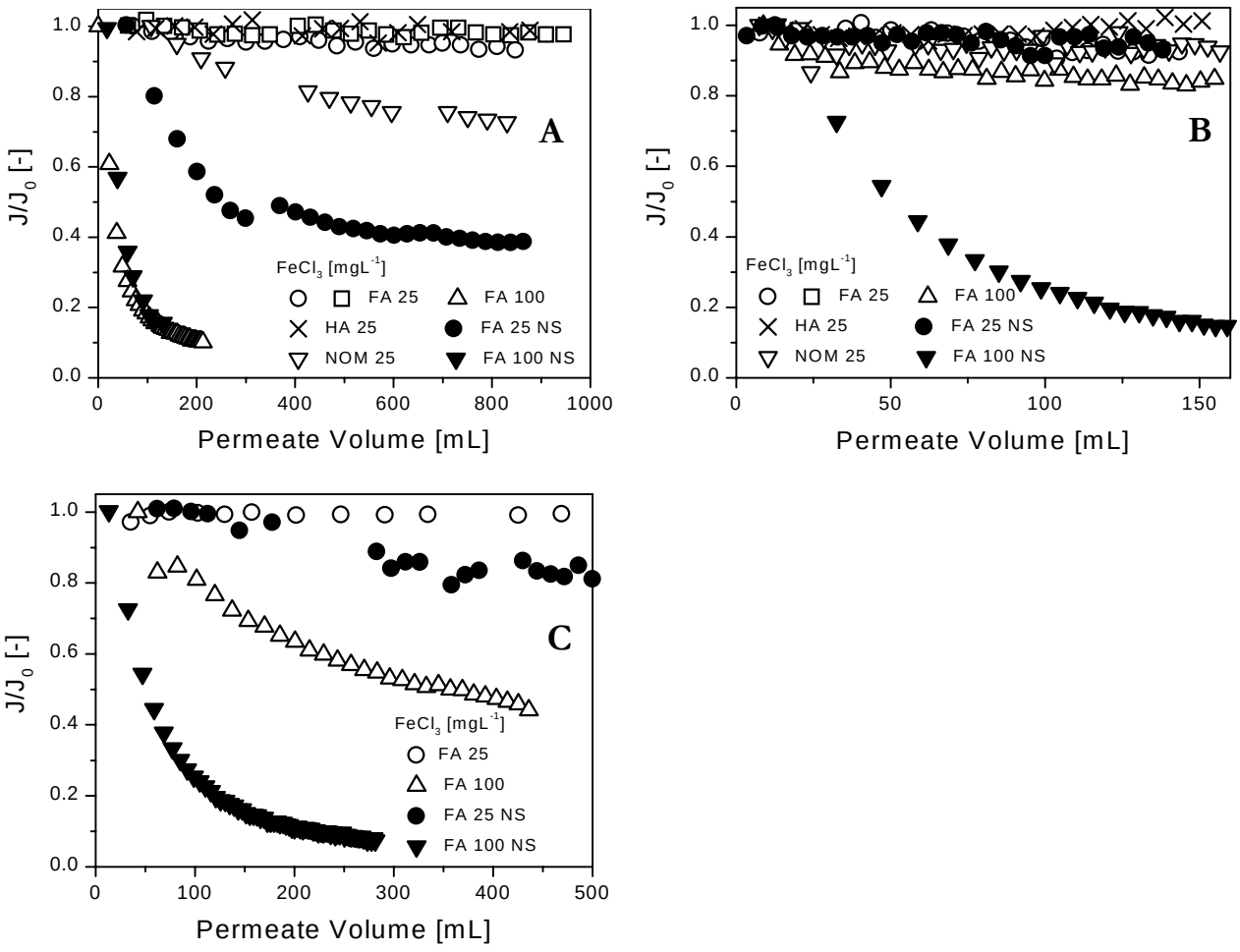


Figure 6.48 *Flux ratios over filtration volume of the (A) 100 kDa, (B) 10 kDa and (C) 30 kDa membranes as a function of ferric chloride dosage, organic type and stirring. NS stands for 'no stirring' (5 mgL^{-1} as DOC IHSS FA).*

Compared to the results obtained in the absence of organics (Figure 6.47), flux decline is worse at the highest dosage. This confirms the charge effect suggested at the dosage of 50 mgL^{-1} in the absence of

organics. The organics would interact with the ferric hydroxide precipitates to some extent and decrease their high positive charge. This would allow denser packing on the membrane. The increased load of particles due to the higher ferric chloride concentration cannot explain the effect observed alone, but this would also play a role.

Table 6.10 *DOC rejection of the 10, 30, and 100 kDa membranes at different ferric chloride dosages. pH was not adjusted after coagulant addition. Organic concentration 5 mgL^{-1} as DOC. N stands for 'stirred' (270 rpm), NS for 'no stirring'.*

$FeCl_3$ [mgL^{-1}]	Organic Type	Stirring	10 kDa	30 kDa	100 kDa
25	FA	S	84	50	29
25	HA	S	80	-	90
25	NOM	S	67	-	10
25	FA	NS	26	21	-
100	FA	S	86	94	77
100	FA	NS	82	81	30

As for MF (see Chapter 5), rejection depends on the organic type. This dependence is stronger for the looser (100 kDa) membrane than for the tight 10 kDa membrane. Stirring reduces rejection and ferric chloride dosage increases rejection for all membranes. This effect is also stronger for the looser membranes.

HA is retained more than FA or NOM, due to stronger interaction with the precipitates. UV results are not presented here since the rejection based on UV is near complete due to the high UV absorbance of $FeCl_3$, which is retained.

6.8.3 Coagulation of OPS Systems

The OPS systems which were previously filtered as a separate system were now also coagulated by addition of ferric chloride. The organics in the OPS system were 5 mgL^{-1} as DOC IHSS FA. Flux ratios are shown in Figure 6.49A and B. Again no flocs were visible at dosages of 50 and 100 mgL^{-1} ferric chloride and pH was not adjusted.

The flux shows little decline at 25 mgL^{-1} $FeCl_3$ for both membranes. At higher dosages flux decline is detrimental (80 to 95%) and for the 50 mgL^{-1} $FeCl_3$ it is less detrimental that 100 mgL^{-1}. This does not correspond to the result observed in the absence of organic and colloids (Figure 6.47). For the 10 kDa membrane up to 20% flux decline is observed at the higher dosages.

The rejection (Figure 6.50) increases with dosage but has dropped to 40-80% for the HA for both membranes. This decline is probably due to concentration polarisation effects as a result of deposition of a particle layer on the membrane. Rejection is now similar for both membranes. Very interestingly, at high dosages the fluxes are also similar (see Table 6.11). At low dosage the 100 kDa membrane retains the same amount of HA, but at a higher flux.

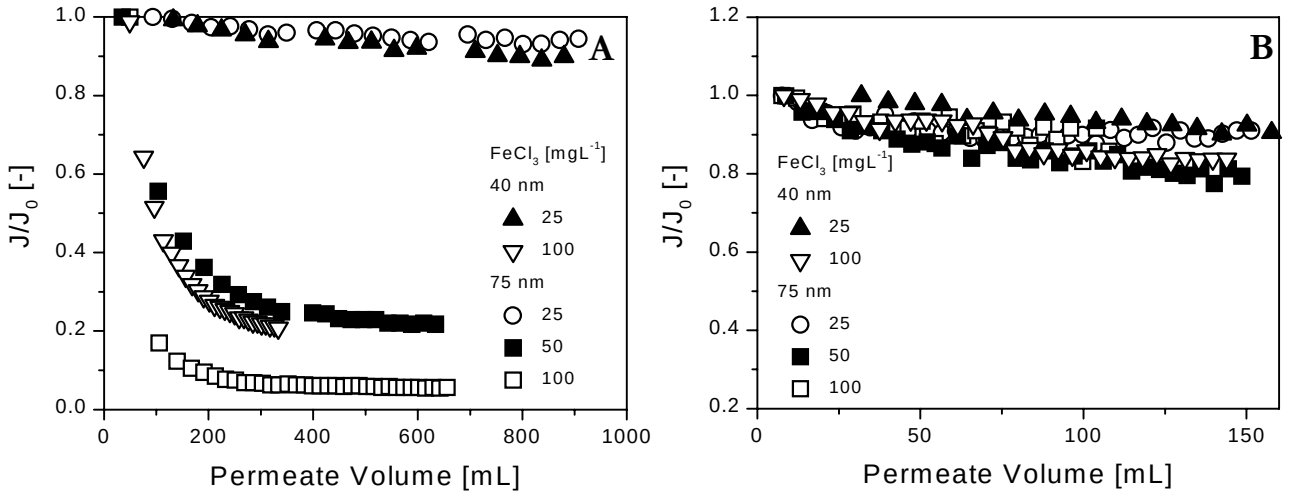


Figure 6.49 *Flux ratios over filtration volume of the (A) 100 kDa and (B) 10 kDa membranes as a function of ferric chloride dosage and primary colloid size (OPS, pH 7-8, 5 mgL^{-1} as DOC IHSS FA).*

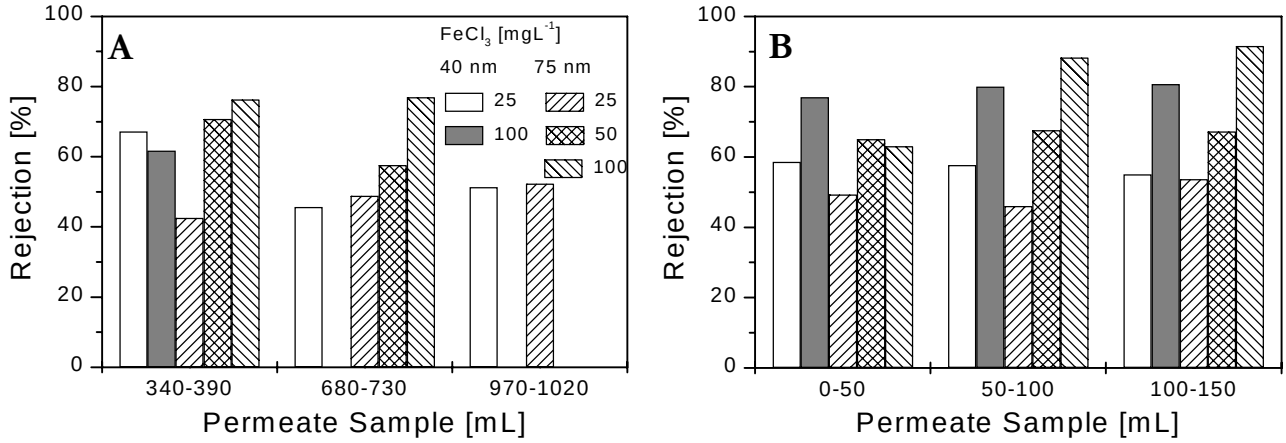


Figure 6.50 *Organic rejection of the (A) 100 kDa and (B) 10 kDa membranes as a function of ferric chloride dosage and primary colloid size (OPS, pH 7-8, 5 mgL^{-1} as DOC IHSS FA). Not all experiment were sampled three times.*

Table 6.11 *Flux values for 50 and 100 mgL^{-1} ferric chloride dosages for the 10 and 100 kDa membranes. The organic type is IHSS FA at a concentration of 5 mgL^{-1} as DOC. OPS systems with primary colloid sizes as indicated.*

$FeCl_3$ [mM]	Primary particle size [nm]	10 kDa J_i [$Lm^{-2}h^{-1}$]	10 kDa J_F [$Lm^{-2}h^{-1}$]	100 kDa J_i [$Lm^{-2}h^{-1}$]	100 kDa J_F [$Lm^{-2}h^{-1}$]
100	40	55	46	619	41
50	75	56	45	619	91
100	75	49	45	787	45

6.8.4 Coagulation of SPO Systems

SPO systems were also coagulated (using ferric chloride) and fluxes are shown in Figure 6.51. Again, flux decline is high for the high dosage for the 100 kDa membrane. For the 10 kDa membrane flux decline is a little greater than in previous experiments.

Rejection also increases with dosage (Figure 6.52) and values are comparable for the two membranes and to the OPS case. Rejection seems higher for the larger primary colloids (OPS and SPO). While the reasons for this are unclear, one possible explanation could be the higher consumption of coagulant for the smaller colloids.

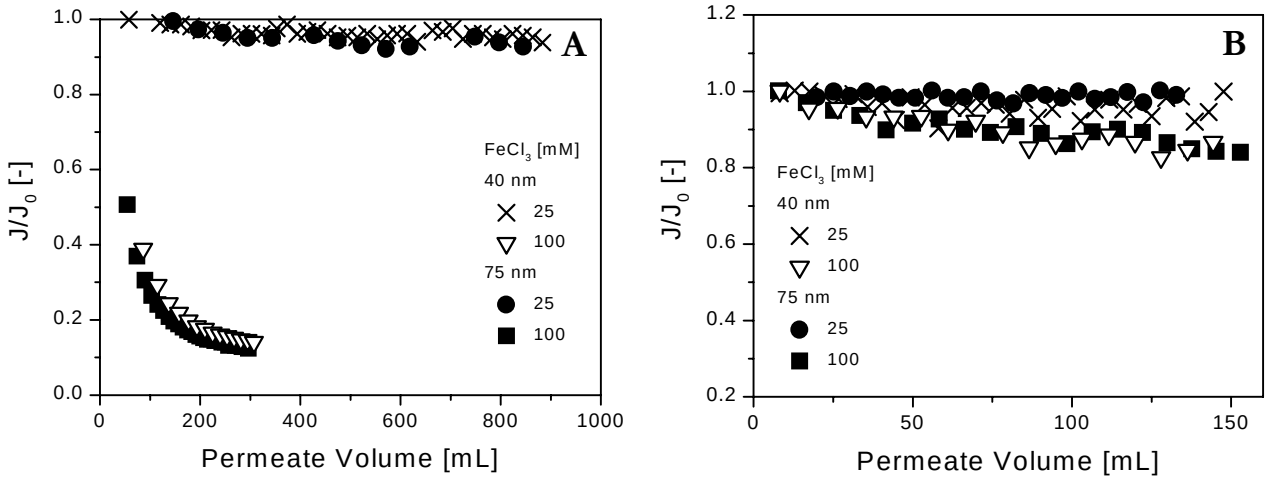


Figure 6.51 *Flux ratios over filtration volume of the (A) 100 kDa and (B) 10 kDa membranes as a function of ferric chloride dosage and primary colloid size (SPO, pH 7-8, 12.5 mgL^{-1} as DOC IHSS HA).*

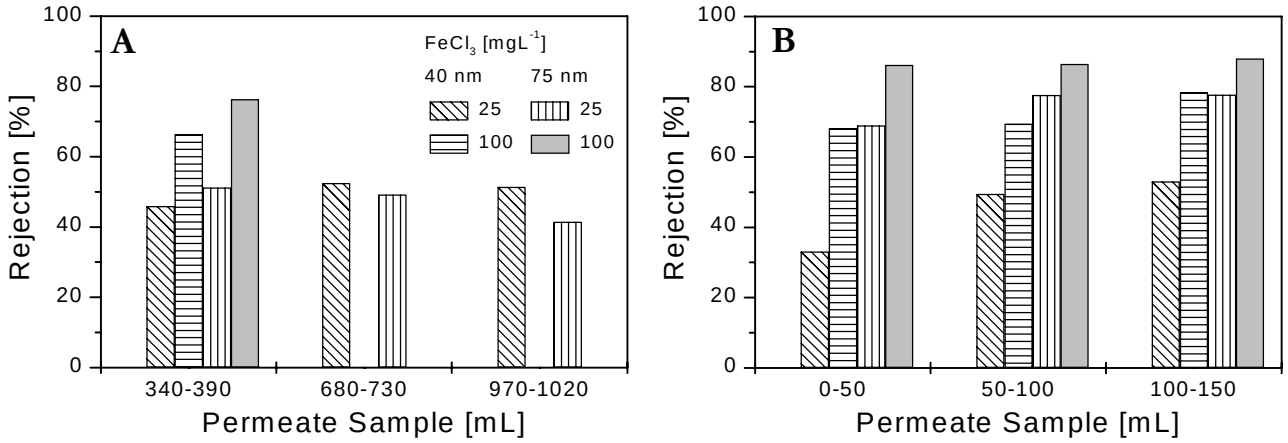


Figure 6.52 *Organic rejection of the (A) 100 kDa and (B) 10 kDa membranes as a function of ferric chloride dosage and primary colloid size (SPO, pH 7-8, 5 mgL^{-1} as DOC IHSS FA). Not all experiment were sampled three times.*

6.8.5 Blocking Law Analysis

For selected experiments blocking law analysis is carried out as for the calcium-organic systems in section 6.6.4. The mechanisms for flocs formed at the two different dosages of ferric chloride were compared for the 100 kDa membrane. The results are shown in Figure 6.53 and Figure 6.54 for dosages of 25 and 100 mgL^{-1} ferric chloride, respectively.

The experiments at high ferric chloride dosage (100 mgL^{-1}) were chosen for the investigation of the pore size effect and again stirred and unstirred experiments are compared. The results are illustrated in Figure 6.54, Figure 6.55, and Figure 6.56 for the 10, 30, and 100 kDa membranes, respectively.

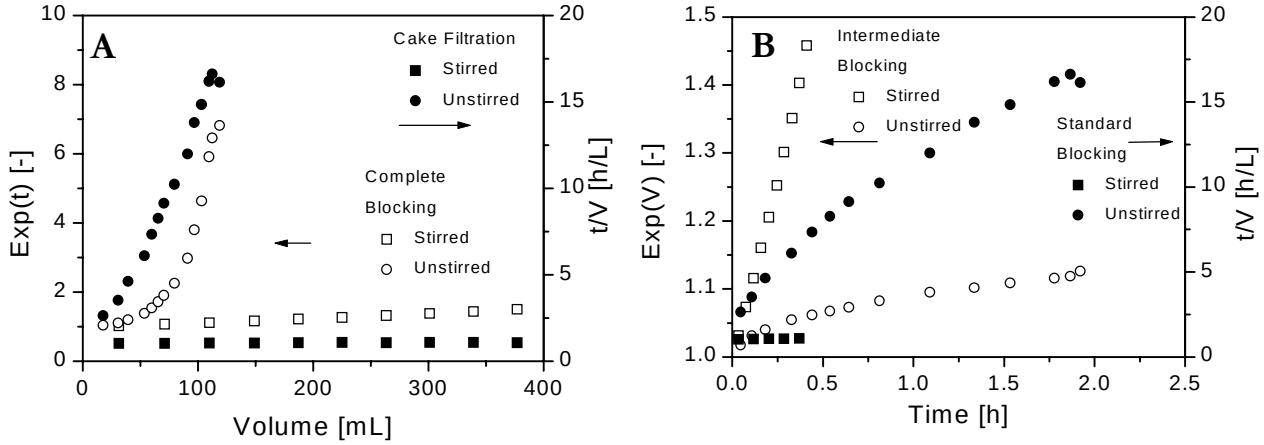


Figure 6.53 *Blocking law analysis for the 100 kDa membrane (25 mgL^{-1} $FeCl_3$, 5 mgL^{-1} as DOC FA, S=stirring at 270 rpm, NS=unstirred), (A) complete blocking and cake filtration and (B) intermediate blocking and standard blocking.*

Figure 6.53 shows cake filtration and to some extent intermediate blocking to be valid mechanisms for filtration of flocs formed at the low ferric chloride dosage. Intermediate blocking implies a long term adsorption process which leads to complete pore blockage. The individual particles cannot block pores on their own, but they accumulate on each other and block pores. Standard blocking, which would be expected to be a precursor of intermediate blocking shows also a linear relationship. The slope drops off after a filtration period of about two hours and the slopes of cake filtration and intermediate blocking increase. The use of the stirred experiment results requires further investigation, as the validity is uncertain.

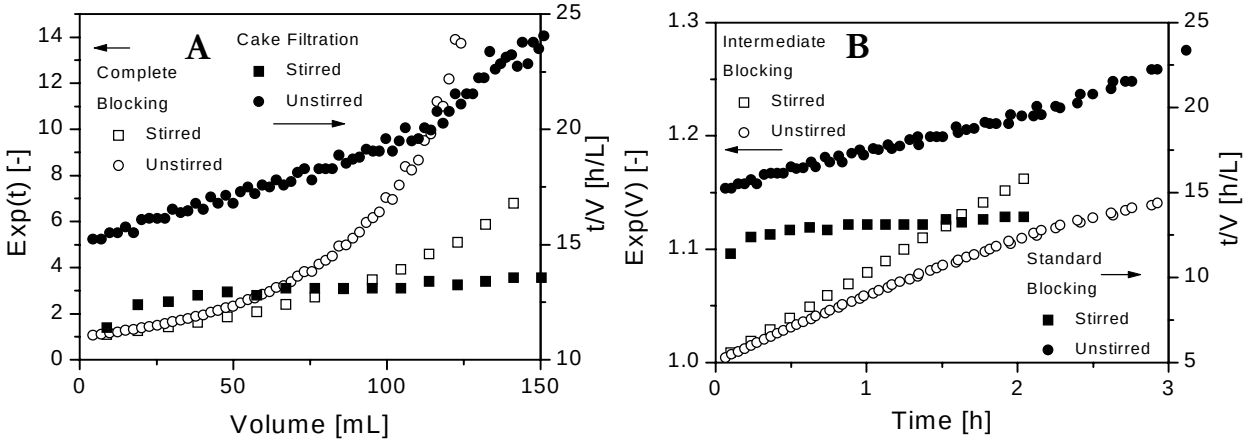


Figure 6.54 *Blocking law analysis for the 100 kDa membrane (100 mgL^{-1} $FeCl_3$, 5 mgL^{-1} as DOC FA, S=stirring at 270 rpm, NS=unstirred), (A) complete blocking and cake filtration and (B) intermediate blocking and standard blocking.*

It appears that for the 100 kDa membrane both cake filtration and standard blocking (particle deposition on internal pore walls) are valid mechanisms, although the slope of the lines changes during the experiment. This implies that the particles which deposit are somewhat smaller or their interaction is reduced as the adsorption leads, according to the model, only to a reduction of the pore diameter. For the lower dosage this adsorption lead to pore blocking. Stirred and unstirred experiments do again show different results which shows that either the filtration laws are not valid and/or the cake is limited successfully by the stirring.

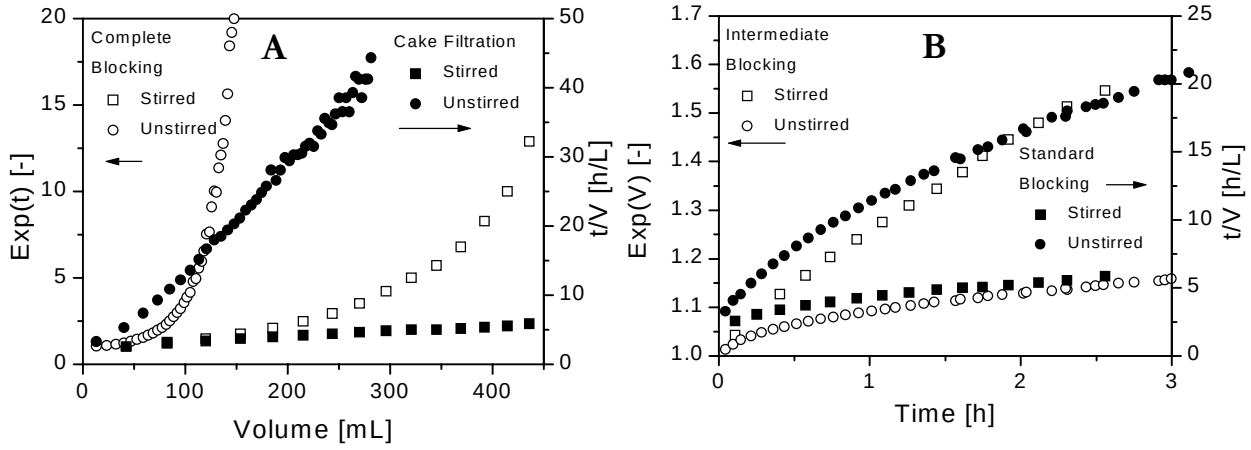


Figure 6.55 *Blocking law analysis for the 30 kDa membrane (100 mgL^{-1} $FeCl_3$, 5 mgL^{-1} as DOC FA, S=stirring at 270 rpm, NS=unstirred), (A) complete blocking and cake filtration and (B) intermediate blocking and standard blocking.*

As the membrane pores become smaller, the standard blocking law is no longer valid (Figure 6.55B). The cake filtration model remains valid, which indicates prevention of the ferric hydroxide precipitates from entering pores and subsequent internal deposition. Membrane pore radii were tabulated in Table 6.1 as 2.6, 4.8, and 9.1 nm for the 10, 30 and 100 kDa membranes, respectively. Lo and Waite (1998) reported iron hydroxide precipitates to be as small as 10 nm. Nevertheless, complete blocking (pore blocking by the particulates) is not a valid mechanism. Possibly cake formation prevents pore blockage.

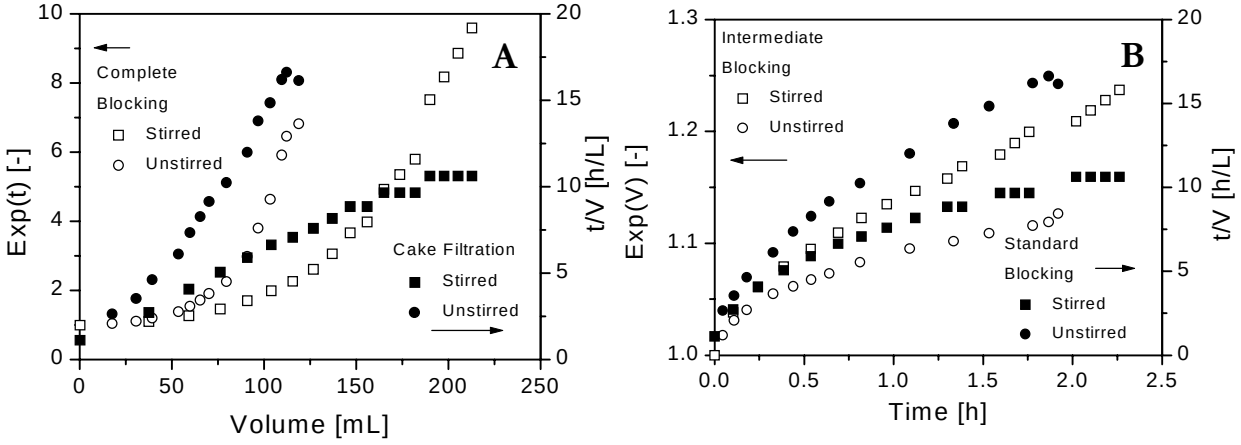


Figure 6.56 *Blocking law analysis for the 10 kDa membrane (100 mgL^{-1} $FeCl_3$, 5 mgL^{-1} as DOC FA, S=stirring at 270 rpm, NS=unstirred), (A) complete blocking and cake filtration and (B) intermediate blocking and standard blocking.*

When the pore size is further reduced, cake filtration remains the only valid mechanism as depicted in Figure 6.56. The slope of the line is reduced significantly compared to the 30 kDa membrane. This illustrates the lower resistance of the cake compared to the resistance of the clean membrane to filtration. This was observed in the flux behaviour (see Figure 6.48).

In summary, coagulation increases rejection for the 100 kDa membrane. Flux and rejection now approach that of the 10 kDa membrane. The rejection of the 10 kDa membrane was slightly increased in some cases. At 25 mgL^{-1} $FeCl_3$ flux decline was lower than in the absence of colloids and $FeCl_3$. This demonstrates that $FeCl_3$ pretreatment can, under certain circumstances, prevent flux decline. This can be attributed to the binding of organic calcium complexes, which otherwise could penetrate into pores and lead to the deposition of a more porous cake, which is determined by the floc structure.

6.9 SUMMARY

Due to the availability of six membranes over a MWCO range from 1 to 100 kDa, UF proved to be an ideal way to investigate the effects of membrane pore size on rejection and flux.

This study was divided into five major sections, (a) fractionation and rejection studies of natural organics under varied solution chemistries, (b) colloid and aggregate studies under controlled aggregation regimes, (c) filtration of calcium-organic aggregates, (d) particulate systems (SPO, OPS), and (e) ferric chloride flocs combined with the above systems.

Rejection studies showed a charge effect in organic rejection. As the ionic strength increased, the rejection dropped. This was presumably due to a decrease in charge repulsion between the negatively charged membranes and organics. Rejection also depends on the organic type. Aromatic compounds were retained preferentially. This was shown by UV/DOC ratios and SEC. LC-OCD exhibited an increase in humics retention with decreasing MWCO, while low molecular weight acids and neutral and amphiphilic substances were little retained.

The filtration of inorganic aggregates in carefully controlled aggregation states related fractal structure of the aggregates to flux. Aggregates formed rapidly in a RLA regime are loose (of low fractal dimension) and the flux decline is low. Aggregates found in the DLA regime are compact (high d_F) and resistance to filtration drops at the transition point between DLA and RLA. This transition point is the critical coagulation concentration. While this effect of increased flux at high ionic strength has been reported frequently in the literature, it has to date not been linked to aggregate structure.

Adsorption of FA on the hematite colloids may have a similar effect if charge is neutralised before being reversed. The aggregate structure effect could only be observed at certain primary particle to pore size ratios. While the effect is strong for the 100 kDa membrane when looking at the 75 nm primary colloid size, the same effect was not observed with the 10 kDa membrane. Therefore,

membrane pore size does play a major role. This solute-solute interaction with implication on cake porosity needs to be considered in future models of particle deposition and charge interactions.

When filtering organics with high calcium concentrations, aggregation of some organics was observed. This aggregation lead to an increased deposition of aggregates, likely to be inside the membrane pores, which gradually increased the membrane pore size. Only the largest organics (IHSS HA) readily formed aggregates with calcium. The decrease in pore size was confirmed by an increased rejection and by blocking law analysis. The relatively large aggregates formed (see Chapter 4 for characterisation) only caused flux decline for the 100 kDa membrane. This can be attributed to, firstly, size exclusion of the aggregates from the small pores of the 100 kDa membrane, and, secondly, the lower flux of the latter membrane. Rejection of the 10 kDa membrane is higher than that of the 100 kDa, as expected. Operation of the 100 kDa membrane at a lower flux resulted in fouling prevention.

Filtration of the OPS and SPO particle systems showed a large flux decline for the stable colloids (OPS). In the SPO systems, flux decline was only significant when calcium concentration was high, and thus the presence of calcium-organic aggregates was likely.

While structure analysis of these complex systems is not possible, electron micrographs of the deposits indicated a structural difference – a very compact structure is formed by the OPS systems, while large voids are visible for the SPO systems.

UF of ferric chloride flocs proved a strong effect of dosage, and presumably floc structure on flux. This effect required further study of well characterised ferric chloride systems. Throughout the study, fouling of the small pore size and low flux membrane (10 kDa) was negligible compared to the 100 kDa membrane. The observation mode with ferric chloride pretreatment was that flux decline was detrimental at high ferric chloride dosages, when small iron oxyhydroxide particles are formed. In this case, fouling was observed with both membranes.

Rejection of natural organics was increased by ferric chloride addition, but scatter in the data was great, presumably due to the dependence of the precipitate-organic interactions on many parameters. These parameters are doseage, organic characteristics, solution chemistry – leading to a process which is difficult to control. Coagulation of OPS systems showed that final fluxes of the 10 kDa and 100 kDa membranes and their rejections are very similar. In this case, the stable nature of the colloids allows close packing of the hematite colloids together with the iron oxyhydroxide flocs, and results in a self-rejecting layer. This is similar in the SPO case. Blocking law analysis now shows a cake filtration effect (which was not the case for the calcium-organic systems). It appears as if, despite significant fouling, the cake prevents pore closure. This supports the assumption of the self-rejecting layer.

6.10 CONCLUSION

In this chapter, rejection and fractionation results have been presented for a fundamental study of the effect of inorganic aggregate structure on flux, the filtration of surface water like systems, and finally pretreatment of UF with coagulation.

Rejection was dependent on membrane and organic type. Further, it was found that UF membranes may retain cations and that charge effects can be important.

An effect of aggregate structure on flux was observed repeatedly during the filtration of well defined aggregates, surface water systems, and coagulated suspensions. Aggregates or flocs that form rapidly have a loose structure and their induced flux decline is mostly negligible. Slowly forming aggregates or stable colloids deposit as a very dense layer and cause severe flux decline.

Rejection was influenced by stirring, membrane type and calcium concentration. Calcium lead to the aggregation of IHSS HA, which increased both flux decline and rejection. A similar effect was observed with coagulation pretreatment. Rejection increased, and, depending on the dosage, the flux decline was either negligible (low dosage) or severe (high dosage). This behaviour was also attributed to the structure of the flocs. A low dosage of ferric chloride had, for example, a positive effect on flux, whereas a similar concentration of calcium caused detrimental decline.

The 100 kDa membrane showed initially a higher flux and lower rejection than the 10 kDa membrane. However a fouled 100 kDa membrane showed a similar rejection to a 10 kDa membrane at a higher flux. Fouling of the 100 kDa membrane could be prevented by operating at a lower flux which lead to fluxes similar to that of the 10 kDa membrane, but at significantly lower pressures (and thus energy requirements).

Chapter 7

NANOFILTRATION

Nanofiltration rejection depends on solute charge, concentration and size, as well as membrane characteristics. Consequently, the membranes used were thoroughly characterised and then tested with salt solutions and a model organic compound. Then organics rejection as a function of pH, organic type, salt concentratio,n and hydrodynamic conditions was determined.

Rejection of four membranes was studied for salt solutions and three organic types. The TFC membranes showed a high rejection of organics, which was determined by size exclusion. Salt rejection varied with membrane type. The TFC-SR membrane showed a high selectivity between sodium and calcium, whereas the TFC-S and TFC-ULP membranes rejected large amounts of calcium and sodium. The Ca-UF membrane rejected little salt, and organics rejection varied with solution chemistry.

The presence of calcium and humic substances or natural organic matter (NOM) in surface waters can cause severe fouling of nanofiltration (NF) membranes. Conditions of fouling were studied as a function of solution chemistry, organic type, calcium concentration, hydrodynamic conditions, and membrane type.

Deposition of organic matter was determined by mass balance in feed and concentrate samples. Electron microscopy and X-ray photoelectron spectroscopy (XPS) were used to study the morphology and composition of the fouling layer.

During permeate recycle experiments, which were used for fouling studies, it was found that calcium concentration (as a representative of multivalent ions) and the type of organic play a major role in fouling. The calcium forms complexes with some of the organics and deposits on the membrane surface. Depending on the solution conditions the organic or calcite (on which organics adsorb) precipitate. Factors, which influence the concentration of organics and ions at the membrane surface, such as stirring, flux, and transmembrane pressure, influenced the deposition of organic matter significantly. Irreversible fouling occurred with all membranes at high calcium concentrations, although the cellulose acetate (CA) membrane showed an overall better performance, possibly due to its low salt rejection and smooth surface. IHSS humic acid (HA) is the organic which deposits most easily. A comparison of UV absorbance and DOC data showed that the fraction which absorbs UV strongest, and is more hydrophobic, deposits preferentially on the membranes. These substances also have the lowest solubility, stressing the importance of concentration polarisation effects.

Inorganic colloids (hematite, 75 nm) did not cause irreversible flux decline. Pretreatment of the solutions using ferric chloride not only prevented flux decline under critical fouling conditions (high calcium concentration and IHSS HA), but also influenced rejection. The latter depends on the charge of the ferric hydroxide precipitates. Cation rejection increased when positive ferric hydroxide colloids were deposited on the membrane, which the organic rejection decreased.

7.1 INTRODUCTION

In the nanofiltration (NF) of surface waters, organic solutes and multivalent ions are removed via a combination of charge interaction and size exclusion. The conformation of the organic molecules (coiled at low pH, linear chains at high pH) is believed to be important for both rejection and flux decline (Ghosh and Schnitzer (1984), Braghetta (1995)). For natural organic matter (NOM) both charge and size mechanisms may be important, especially for compounds which are smaller than the NF 'pores'.

NF membranes may be porous or non-porous depending on the material (Peeters (1997)). While NF of surface waters generally achieves a removal of >90 % of organics, high flux decline is common. Hong and Elimelech (1997) have previously shown that fouling by NOM is increased in the presence of calcium ions, and that permeation drag and electrostatic double layer repulsion control fouling. Elimelech *et al.* (1997) have noted the importance of membrane roughness on colloid fouling of membranes, however the mechanism of fouling is poorly understood. In this study, experiments were carried out under various solution chemistries, and organic and membrane types in order to identify critical fouling conditions.

Jucker and Clark (1994) have demonstrated a preferential adsorption of hydrophobic compounds on hydrophobic UF membranes. However, Childress and Elimelech (1996) showed that humic substances adsorb on hydrophilic membranes very rapidly and that the membrane surface potential becomes more negative due to the humic substances. Calcium facilitates the adsorption of negatively charged organics onto negative surfaces.

The adsorption of organic compounds is an important process; however, adsorption would only be responsible for a relatively thin deposit layer. The objective of this study is to understand the role of concentration polarisation (influenced by hydrodynamic conditions) and solution chemistry on the morphology of the fouling layers. The interactions of calcium and NOM are studied over a wide of pH and concentration range, contributing to an understanding of the interactions and the impact on NF.

7.2 FILTRATION PROTOCOL

7.2.1 Membrane Compaction and Baseline

Very tight membranes such as those in NF and RO may compact when relatively high pressures are applied, and flux may also be influenced by the wettability of the polymer. Compaction can also occur as a result of the repulsive forces between membrane functional groups, which as shown by Braghetta (1995), will be dependent on the solution chemistry. However, in this section only compaction by pressure is considered.

To determine long term water flux behaviour or compaction due to an applied pressure, MilliQ water was filtered over night and the baseline measured. This flux decline is not due to fouling. Values of 13%, 5%, 10%, and 1-2% were obtained for the TFC-ULP, TFC-SR, TFC-S, and CA-UF membranes, respectively. The filtered volume was 1.5L (about 5 to 10 times the volume used in rejection and recycle experiments) after the compaction of the membranes.

As a result of these preliminary studies, membranes are compacted at 10 bar for one hour, then the pure water flux (J_0) is usually measured at 5 bar for about half an hour. When analysing experimental

data, the measured flux is normalised to this pure water flux in forming the ratio J/J_0. Table 7.1 shows the membrane resistance, average permeability, and average pure water fluxes of the four membranes used. All symbols are defined at the end of the thesis. Pure water flux increased with pressure for all four membranes used, as shown in Figure 7.1.

Table 7.1 *Nanofiltration membrane resistance, permeability, and average pure water fluxes.*

Membrane	R_M [m^{-1}]	Average Permeability [$Lm^{-2}h^{-1}bar^{-1}$]	Average Pure Water Flux at 5 bar [$Lm^{-2}h^{-1}$]
TFC-ULP	$9.3 \cdot 10^{10}$	3.9	19.4 ± 2.6
TFC-SR	$3.9 \cdot 10^{10}$	9.2	45.8 ± 6.1
TFC-S	$3.6 \cdot 10^{10}$	9.9	49.4 ± 5.9
CA-UF	$3.6 \cdot 10^{10}$	10.0	49.9 ± 4.2

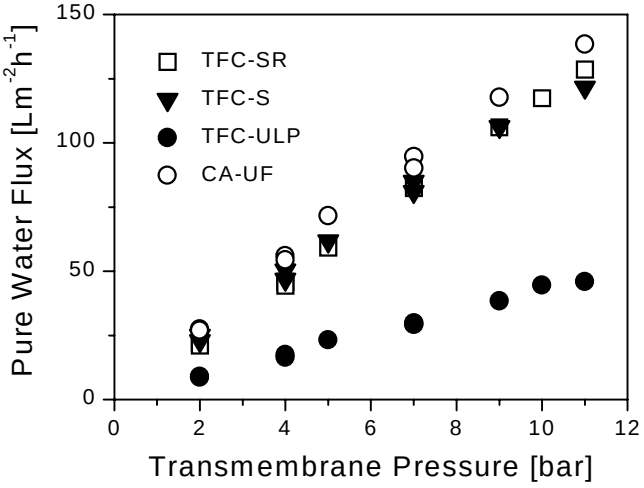


Figure 7.1 *Membrane pure water flux as a function of transmembrane pressure.*

7.2.2 Protocol for Rejection Experiments

A standard protocol for rejection experiments is shown in Table 7.2. A standard rejection experiment took 4 to 7 hours, depending on the membrane used. 120 mL of the permeate were collected from a feed volume of 185 mL, which, at 100% rejection, leads to a threefold concentration in the cell.

7.2.3 Protocol for Recycle Experiments

Recycle experiments were designed to determine membrane fouling. Steps 1, 2, and 4 for the recycle experiments are identical to rejection experiments, as shown in Table 7.2. In recycle experiments, step 3 involves the same amount of feed being added. No permeate samples are taken. After this cycle is completed, the permeate is returned to the stirred cell. This is repeated two times, so that the permeate has been filtered three times. At the end, one permeate sample is taken to calculate overall rejection and the concentrate is weighed and also sampled.

Figure 7.2 shows the flux for a typical recycle experiment, showing the different stages of fouling. The different stages of the experiment are explained in the legend. The information gained from this experiment can be summarised as follows, I: flux reduction due to osmotic pressure and concentration polarisation. Both effects increase during the experiment and irreversible fouling causes further flux decline; II: osmotic pressure, concentration polarisation and irreversible fouling; III: irreversible

fouling; and IV: irreversible fouling after water wash. It should be noted that the solute wall concentration changes with flux, which may be different for each membrane sample.

Table 7.2 *Standard protocol for rejection experiments in the stirred cell.*

Step	Objective	Medium	Pressure	Duration	Procedure
1	compaction	MilliQ	10.0 bar	1 h	place a new membrane into stirred cell, fill cell with MilliQ and fill about 185 mL into reservoir
2	initial pure water flux determination	MilliQ	5.0 bar	30 min	at end of pure water flux determination, pure water samples are taken to check for organics leaching from membrane
3	experiment	Feed	5.0 bar	until 120 mL permeate are produced	empty reservoir, weigh feed volume filled into cell, take feed as sample, put three permeate sample vials onto balance, tare balance. Change sample vials every 40 mL of permeate. After experiment, release pressure instantly, when 120 mL permeate are collected, open cell, weigh concentrate and take concentrate sample. Rinse cell and membrane with pure water.
4	pure water flux determination after experiment	MilliQ	5.0 bar	> 30 min	membrane is stored in a petrie dish at 4°C for fouling analysis after pure water rinse.

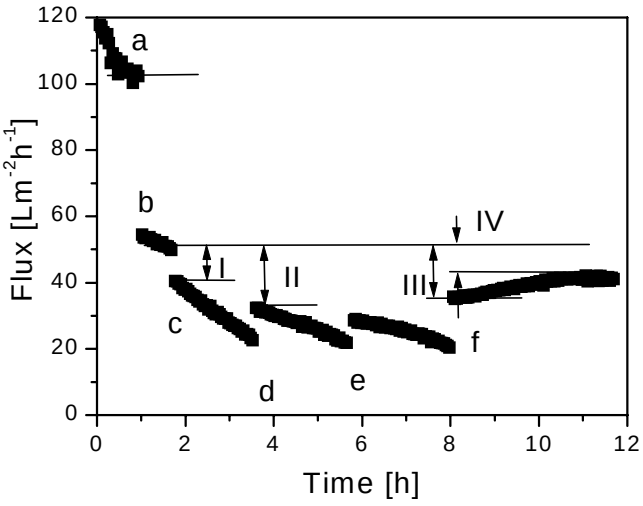


Figure 7.2 *Typical recycle experiment: a: compaction at 10 bar; b: initial pure water flux determination at 5 bar; c: first filtration cycle; d: second filtration cycle; e: third filtration cycle; f: pure water flux determination after filtration.*

7.3 MEMBRANE CHARACTERISATION

7.3.1 Effect of Temperature on Water Flux

Temperature in the stirred cell is measured with a PT100 probe and is accurately adjusted to 20 ^{0}C ± 1 ^{0}C using a waterbath. To study temperature effects, the beaker water temperature was adjusted between 15 ^{0}C and 40 ^{0}C using ice or a hot water bath, respectively and flux measured as a function of wall temperature. Solvent dynamic viscosity changes with temperature follow the equation by Worch (1993)

$$\eta = \frac{0.001002566}{10^{\frac{(1.37023\cdot(T-20)+0.00836\cdot(T-20)^2)}{109+T}}}\cdot 1000. \qquad (7.1)$$

The unit of viscosity is mPa s and that of temperature ^{0}C. The dynamic viscosity and the membrane fluxes as a function of temperature are shown in Figure 7.3.

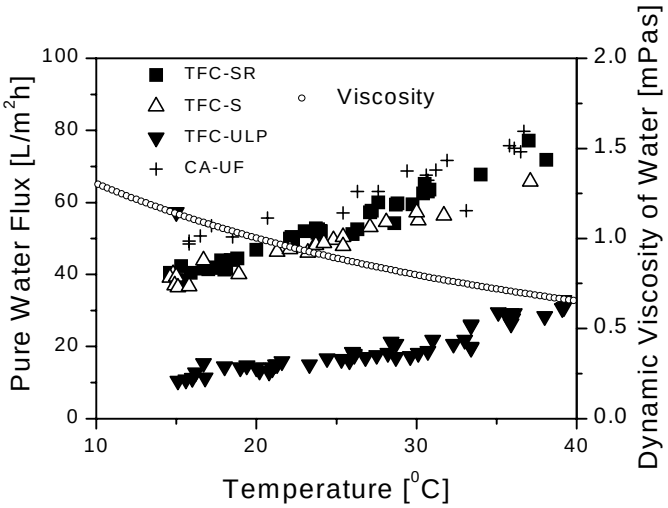


Figure 7.3 *Variation of flux with temperature for the NF membranes used and variation of dynamic viscosity with temperature.*

Permeate flux increases on decreasing viscosity and therefore a higher permeability is achieved at higher temperatures. A common method to account for this change with temperature is to multiply the obtained flux with the viscosity ratio with respect to a reference temperature. If temperature effects on flux are only influenced by changes in viscosity, then the product of flux and viscosity should be constant.

This was the case for the CA-UF membrane only, indicating that the CA-UF membrane has micropores. For membranes with larger pores the flow is high and the water viscosity is controls the flux, whereas for tighter membranes changes in the membrane matrix occur with temperature variation and control flux. For all other membranes, the product of flux and viscosity still increased with temperature. Another correction is suggested by Mallevialle *et al.* (1996), using an Arrhenius equation

$$\frac{J_T}{J_{20}} = \exp\left(\frac{s}{T}\right) \qquad (7.2)$$

with s being an empirical constant to be determined for each membrane. This equation can be rearranged to

$$\ln(J_T) = \frac{P_1}{T} + P_2 \qquad P_2 = ln\, J_{20};\ P_1 = s \tag{7.3}$$

and was fitted for the TFC-ULP membrane. The function can fit the data, but the result is not better than an approximate linear fit. Additionally, there is no correspondence between parameter P_2 and $\ln(J_{20})$. Table 7.3 shows the empirical fitting curves determined from the results obtained in this study.

Table 7.3 *Temperature dependence for the four NF membrane fluxes.*

Membrane	Relationship Flux = f(T) [T in ^{0}C]
TFC-ULP	0.73*T / (4.25+0.58*T)
TFC-S	20.5+1.18*T
TFC-SR	13.2+1.65*T
CA-UF	29.5+1.23*T

It can be seen that temperature effects are significant for the NF membranes. As a consequence, temperature was controlled using a waterbath (see Chapter 4 for details).

7.3.2 Membrane 'Pore Size'

The membranes used and their characteristics such as salt rejection and marker test results as supplied by the manufacturer were described in Chapter 4. Since test conditions are different for the three membranes, here a characterisation is carried out to achieve comparable results. In summary, the CA-UF membrane has a cut-off of 5 kDa, whereas the TFC membranes rejected >90% of lactose. This results in pore diameters (as calculated after Worch (1993) and the Stokes Einstein equation) of 3.72 nm and <0.64 nm for the CA-UF and TFC membranes, respectively.

The aim of the pore size measurement was not to produce an absolute value for pore size or molecular weight cut off, but rather to determine which of the four membranes is more open. A dextran 1000 standard was chosen and rejection experiments were carried out at a dextran concentration of about 50 mgL^{-1} and pH 8. The feed DOC was 19.4 mgL^{-1}. Dextran was chosen as it is not expected to interact strongly with membrane material (Combe *et al.* (1999)).

The results in Table 7.4 show that in terms of dextran rejection, the TFC-SR membrane is the 'tightest' membrane, followed by the TFC-S. The TFC-ULP membrane is also reasonably tight (it should be noted here that the flux of the TFC-ULP membrane is considerably lower which could cause a decreased rejection), whereas the CA-UF membrane is clearly a UF membrane with a very low dextran rejection.

Table 7.4 *Dextran 1000 rejection of four membranes.*

Membrane	TFC-SR	TFC-S	TFC-ULP	CA-UF
Permeate Concentration [mgL^{-1} DOC]	0.55	1.04	2.28	16.05
Rejection [%]	97.2	94.6	88.3	17.3

It was shown in Chapter 4, that the organics size, determined by size exclusion chromatography (SEC), was 1200, 1800, and 3000 Da for NOM, IHSS FA, and IHSS HA, respectively. The rejection of these organics would thus be expected to be greater than that of dextran 1000. The radius of a dextran 1000 molecule was estimated to be about 0.94 nm (see also Table 7.20).

The CA-UF membrane has a very low rejection. This membrane was classified as a NF membrane by the manufacturer, due to its high colour removal and some salt rejection.

7.3.3 Membrane Surface Charge

The membrane surface charges were first measured in background solution as used in the experiments, but in the absence of organics. Results are shown in Figure 7.4. The TFC-SR membrane has the highest charge, followed by the TFC-ULP membrane. The TFC-S membrane has the lowest charge and the CA-UF membrane is somewhat in between. All membranes have a slight positive charge at low pH and are negatively charged in the pH range relevant to surface water treatment. The pH_{pzc} for the four membranes are summarised in Table 7.5 and the zeta potential at pH 8 in Table 7.6.

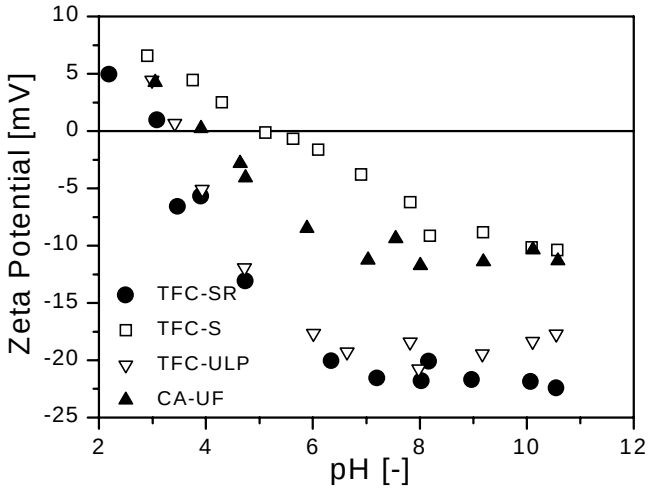


Figure 7.4 *Membrane zeta potential measured in background solution (10 mM NaCl, 0.5 mM $CaCl_2$, and 1 mM $NaHCO_3$).*

Table 7.5 *pH_{pzc} of the NF membranes in different salt solutions.*

Membrane	TFC-SR	TFC-S	TFC-ULP	CA-UF
pH_{pzc} in background solution	3.2	5.0	3.5	4.1
pH_{pzc} in 1 mM KCl	5.7	4.0	3.5	4.0
pH_{pzc} in 1 mM $NaHCO_3$	5.7	4.0	4.5	4.0
pH_{pzc} in 0.5 mM $CaCl_2$	5.7	4.0	4.2	4.2
pH_{pzc} in 10 mM NaCl	5.7	4.0	4.0	5.0

The membranes were then measured with the separate background solution components and the electrolyte, commonly used for zeta potential analysis, 1 mM KCl. Results are shown in Figure 7.5, Figure 7.6, Figure 7.7, and Figure 7.8 for the TFC-SR, TFC-S, TFC-ULP, and CA-UF membranes, respectively.

Table 7.6 *Zeta potential of the NF membranes in different salt solutions at pH 8.*

Membrane	TFC-SR	TFC-S	TFC-ULP	CA-UF
Zeta potential in background solution [mV]	- 22	- 6.5	- 19	- 11
Zeta potential in 1 mM KCl [mV]	- 6	- 9	- 4.5	- 4.5
Zeta potential in 1 mM $NaHCO_3$ [mV]	- 7	- 9	- 6	- 5
Zeta potential in 0.5 mM $CaCl_2$ [mV]	- 3	- 4	- 3	- 2.5
Zeta potential in 10 mM NaCl [mV]	- 14	- 17	- 24	- 8

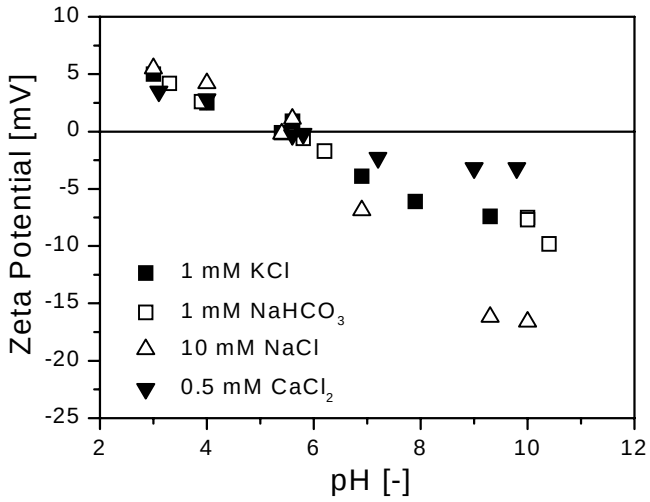


Figure 7.5 *TFC-SR membrane surface potential as a function of solution composition.*

The TFC-SR membrane exhibits the lowest negative charge in calcium chloride solution. This could be due to the presence of divalent positive cations. Potassium chloride and sodium hydrogen carbonate both show an identical zeta potential. The more concentrated sodium chloride solution induces the most negative potential, very similar to those reported in Figure 7.4 for the mixed background electrolyte.

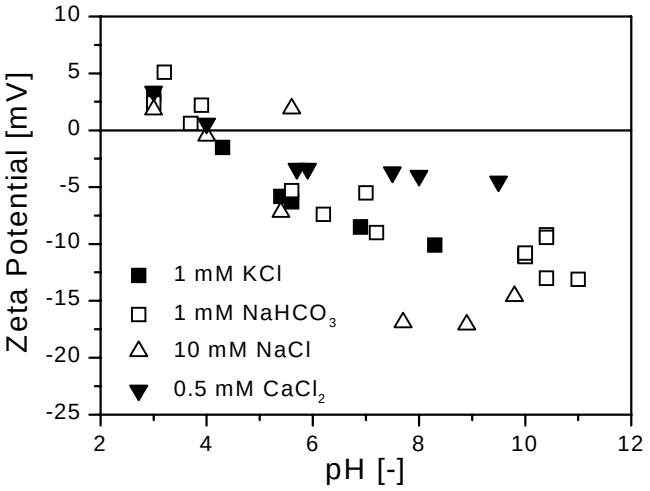


Figure 7.6 *TFC-S membrane surface potential as a function of solution composition.*

The TFC-S membrane demonstrates very similar trends to the TFC-SR membrane as a function of solution chemistry. The least negative charge is evident in calcium chloride solution, while the most negative charge occurs in the more concentrated sodium chloride solution.

The TFC-ULP membrane (Figure 7.7) again confirms the trend with an even larger zeta potential difference at high pH between sodium chloride and calcium chloride solutions. This effect could be explained by adsorption of chloride ions from solution (Jucker and Clark (1994), Hagmeyer (1999)). Ion adsorption depends on the concentration and explains the observed charge dependence very well (Bowen and Mukhtar (1996), Peeters (1997)). Elimelech *et al.* (1994) discuss the increase in charge at increased ionic strength with an increase of Cl^- in solution. Anions adsorb on non-polar or hydrophobic surfaces more easily than cations because they are less hydrated and therefore smaller. This effect applies to CA and TFC membranes. An unchanged isoelectric point indicates that there is no specific adsorption of cations.

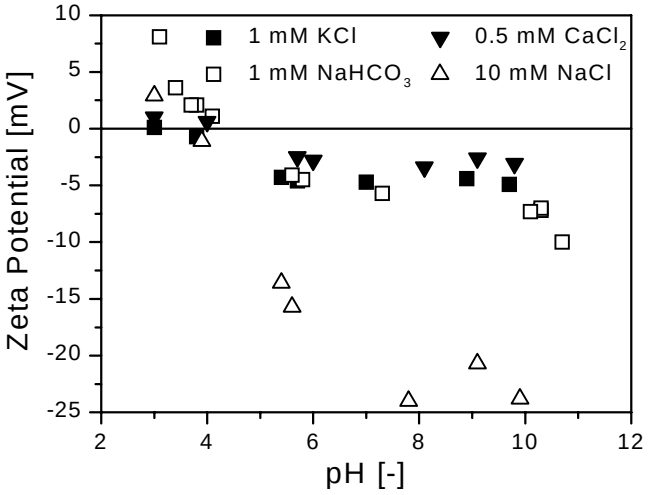


Figure 7.7 *TFC-ULP membrane surface potential as a function of solution composition.*

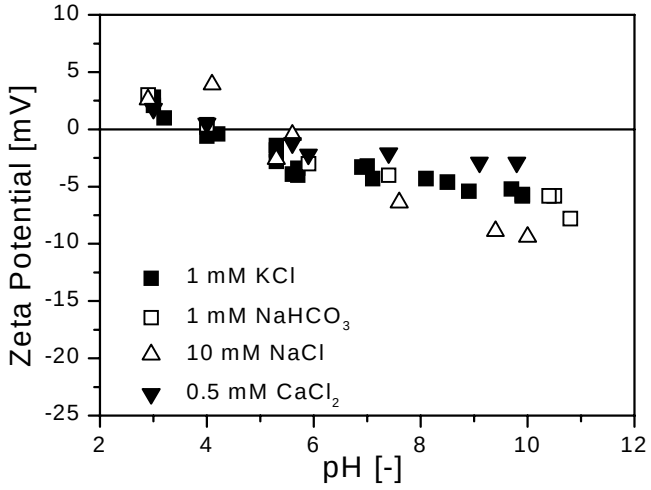


Figure 7.8 *CA-UF membrane surface potential as a function of solution composition.*

For the CA-UF membrane, the zeta potential at any given pH is almost independent of the ionic composition (Figure 7.8). The CA-UF membrane has very low surface potentials compared to the TFC membranes, with values very similar to those published for CA by Combe *et al.* (1999).

Zeta potential only gives the average charge of a surface. In reality, membranes have a heterogeneous surface and charge depends on the local concentrations of functional groups. Also, the surface roughness may have an impact on the measured charge, with an increased surface roughness leading to an underestimation of surface charge. This effect requires further investigation.

Also, fouling may alter zeta potential and rejection behaviour. Elimelech *et al.* (1994) have shown that the adsorption of humic acid on CA and TFC membranes leads to a drastic increase in negative surface charge over the entire pH range.

To compare surface and pore zeta potentials, an alternative method was applied to the most open membrane, the CA-UF. This can be used to calculate pore zeta potential as shown in Figure 7.9.

The charge is close to zero for the pH range measured between 3 and 7. The electrodes used do not allow measurements for higher pH. At 10 mM NaCl, the zeta potential appears slightly lower at about -5mV. This result is surprisingly different to the surface potential measured (see Figure 7.8) and could indicate that the charge in the membrane pores is different to the membrane surface potential. Macoun (1998) explained that a correction for convection and current leakage was required when the potential in pores is measured. Additionally, the pores could be so small that the double layers overlap, thus reducing the measured charge, necessitating further corrections.

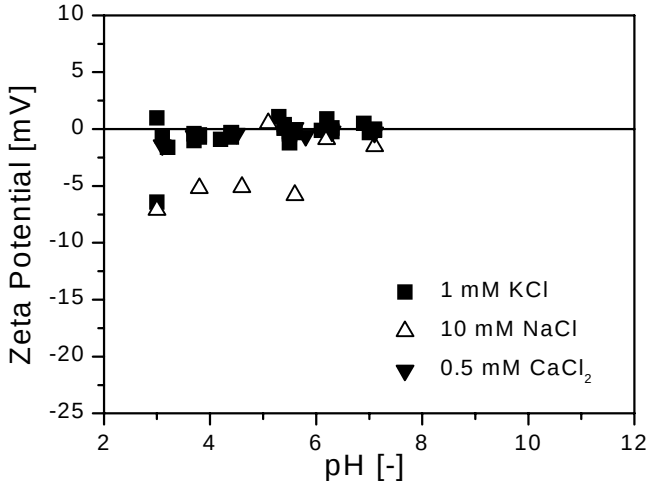


Figure 7.9 *CA-UF membrane pore zeta potential as a function of solution composition.*

In this study, which uses membranes from MF to NF, the most appropriate zeta potential is believed to be the surface-measured value. This parameter is less ambiguous, avoiding pore double layer corrections.

7.3.4 Surface Roughness

Membrane surface roughness has a macroscopic and microscopic scale. Ghayeni *et al.* (1998) have reported large scratches on RO and NF membranes. While these large scale inhomogenities may cause attachment of large particles, we are interested in the microscopic roughness that determines the surface area available for adsorption and the thickness of the boundary layer.

As can be seen in Figure 7.10, the CA-UF membrane has a very smooth surface, whereas the TFC membranes are relatively rough.

7.3.5 Contact Angle

The contact angle is a measure of the wettability of a membrane, and, thus, the membrane hydrophobicity. The angle between a water droplet and the membrane was measured as described in Chapter 4. For an ideally hydrophilic membrane, the angle is 0 degrees. The membranes were cleaned with MilliQ, then stored at 4 ^{0}C and measured dry. Bouchard *et al.* (1997) reported a change in contact

angle with hydration for the TFC-S membrane, whereas the contact angle of a CA membrane was independent of hydration. Chemical heterogeneity and surface roughness can also influence the contact angle measurements. The angles were measured immediately after deposition to avoid errors due to spreading of the drop caused by surface capillary forces. Table 7.7 shows the contact angles for the clean membranes. It can be seen that the TFC-SR membrane is a very hydrophilic membrane, whereas the TFC-S, TFC-ULP and CA-UF membranes are only moderately hydrophilic.

The value measured for the CA-UF membranes corresponds very well to the values of 54 to 58^0 for CA membranes reported by Combe *et al.* (1999).

Table 7.7 *Contact angles of the clean membranes.*

Membrane	TFC-SR	TFC-S	TFC-ULP	CA-UF
Contact Angle [^{0}]	13.1 ± 6.4	52.8 ± 2.9	40.9 ± 2.1	54.0 ± 7.1

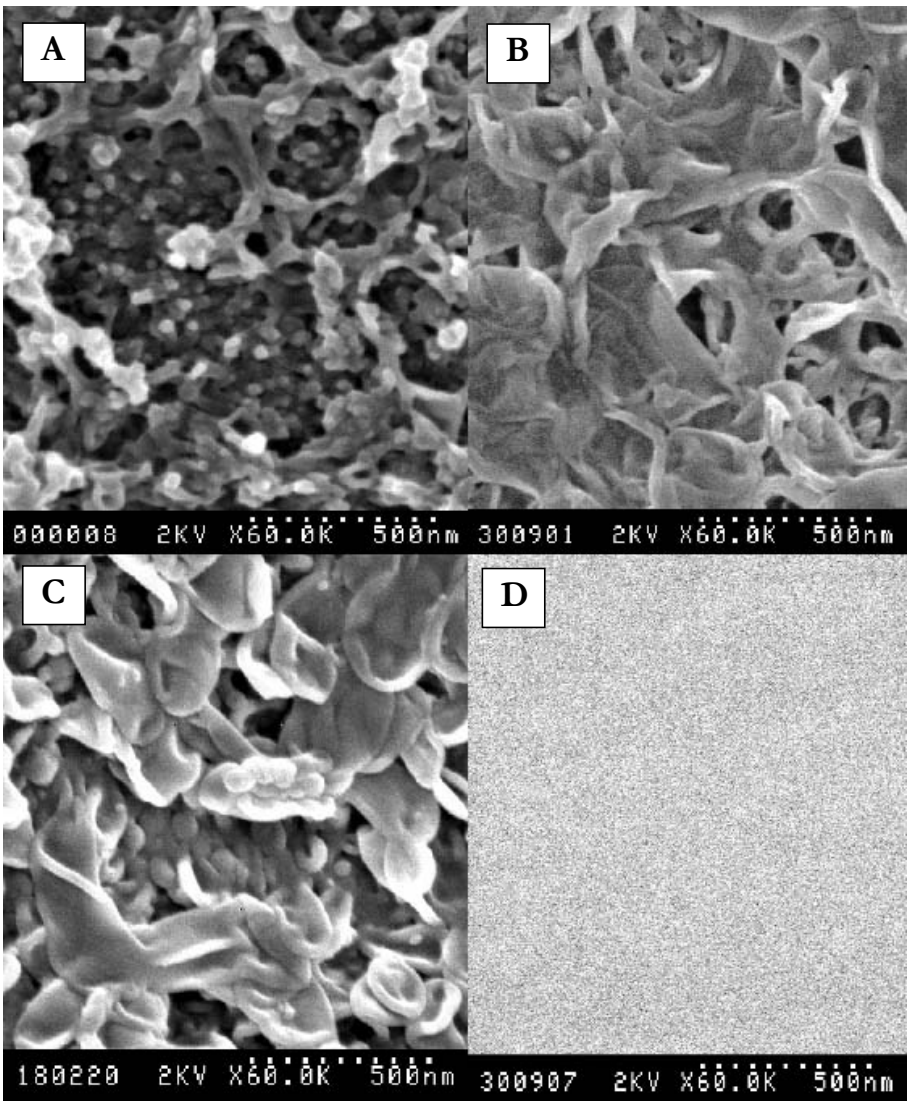


Figure 7.10 *Electron-micrographs of the clean membranes (A) TFC-SR, (B) TFC-S, (C) TFC-ULP, and (D) CA-UF.*

7.4 REJECTION EXPERIMENTS

7.4.1 Salt Rejection in the Absence of Organics

The salt rejection and flux ratio at the end of filtration at pH 4.5, 8, and 10 are shown in Table 7.8. The three values represent the rejection after the collection of 40, 80, and 120 mL of permeate, respectively. J_{W0} is the pure water flux before the experiment. The flux does not change measurably with pH, which is in accordance with the results of Hagmeyer (1999). This means that no change in "pore size" as reported by other workers (Braghetta (1995)) is to be expected.

A high rejection for both calcium and sodium is observed for the TFC-ULP membrane, indicating RO behaviour. Rejection is highest at pH 10, the flux decline is high, which can be explained by concentration polarisation due to high rejection.

Table 7.8 *Cation rejection (20 mM NaCl, 1 mM $NaHCO_3$ and 0.5 mM $CaCl_2$, pH 8, no organics).*

Membrane	pH	J_{W0} [$Lm^{-2}h^{-1}$]	Ca^{2+} Rejection [%]	Na^{+} Rejection [%]	Cl^{-} Rejection[1] [%]	J/J_{W0} [-]	Membrane Charge [mV]
TFC-ULP	4.5	17.0	95 / 95 / 95	90 / 88 / 87	- / 89	0.49	-9.4
TFC-ULP	8	16.4	96 / 95 / 94	90 / 88 / 87	90 / 89	0.46	-19.4
TFC-ULP	10	19.8	99 / 99 / 99	86 / 95 / 96	91 / 93	0.46	-18.5
TFC-S	4.5	53.2	96 / 95 / 96	70 / 70 / 70	27 / 72	0.52	+2.4
TFC-S	8	49.2	92 / 91 / 90	72 / 70 / 95	53 / 71	0.55	-6.5
TFC-S	10	45.1	94 / 89 / 88	69 / 68 / 69	50 / 70	0.52	-10.2
TFC-SR	4.5	39.8	95 / 95 / 95	41 / 37 / 31	45 / 43	0.92	-11.6
TFC-SR	8	45.2	61 / 67 / 70	21 / 22 / 17	27 / 25	0.99	-21.8
TFC-SR	10	40.2	78 / 80 / 94	50 / 47 / 50	63 / 49	0.84	-21.8
CA-UF	4.5	44.6	16 / 12 / 06	13 / 08 / 04	00 / 09	1.02	-2.3
CA-UF	8	46.9	11 / 01 / 01	16 / 09 / 05	19 / 15	1.11	-11.0
CA-UF	10	42.8	00 / 00 / 00	14 / 09 / 08	08 / 08	1.03	-11.0

[1] Numbers in the first column are the result obtained from ion chromatography, while the second column values are and result 2 the calculated rejection from Na and Ca results (neglecting the carbonate system, H^{+} and OH^{-}). Both values are average values.

The TFC-S membrane shows a similar calcium rejection to the TFC-ULP membrane, but a significantly lower sodium rejection, which is more typical of NF. The TFC-S membrane shows a relatively stable performance over the pH range. However, neither membrane shows a pH effect, indicating that the ions are mostly retained due to their size. Sodium and calcium ions occur mostly in their dissociated form up to a pH of 10.

While the TFC-ULP membrane is the membrane with the higher charge, but more open "pores" (see Dextran experiments), it can be concluded that the sodium rejection occurs due to charge, not ion size. This is also confirmed by the pH effect. A higher rejection of cations at pH 10 may be due to solution speciation (carbonate dominates at pH>10.3 as divalent CO_3^{2-} (over HCO_3) which will act as a co-ion

besides Cl^-, sodium as $NaCO_3^-$ and calcium as $CaCO_3$ (aq); see Appendix 5 for speciation). However, very little is known about the speciation in the concentration polarisation layer.

The TFC-SR membrane shows a significantly lower rejection for sodium as well as a strong pH effect. Rejection is lowest at pH 8. This can neither be explained by "pore size", nor charge. The TFC-SR membrane has the highest charge, highest hydrophilicity, and smallest pore size. However, there is no difference in membrane charge between pH 8 and 10. The effect observed can again be explained by solution speciation effects. Carbonate and chloride are the co-ions in solution. At pH 8, carbonate is present in its monovalent form as HCO_3^- and is rejected less than its divalent and undissociated species, at pH 4.5 and 10, respectively. Due to charge balance, cations (or counter-ions) are also rejected less.

The CA-UF membrane behaves like a UF membrane and shows a salt rejection close to zero. The values of 15% observed are probably due to initial ion adsorption in the membranes or due to experimental error, which is high at low rejections.

Overall, the flux ratios (J/J_{W0}, solution flux after filtration of 120 mL of solution relative to the pure water flux before the experiment) correspond well to the salt rejection. This indicates a concentration polarisation and osmotic pressure effect due to the accumulation of ions at the membrane surface and an increase in cell concentration. This flux decline was fully reversible. The flux of the CA-UF membrane consistently increases after salt filtration, probably due to an increased hydrophilicity after ion adsorption in the membrane. Rejection of calcium is stable and generally does not increase with the concentration in the feed cell.

To verify the above results, experiments were carried out with two membrane types (TFC-S, TFC-SR) as a function of pH and ionic strength. One membrane sample was used for the entire series of experiments. For the TFC-S membrane (Figure 7.11A), a stable rejection between pH 4.5 and 10 was confirmed. However, at a pH of about 3.5 this rejection dropped to near zero. This coincides with the point of zero charge of the membrane. A similar effect was reported by Hagmeyer (1999).

The TFC-SR membrane (Figure 7.11B) shows a similar pattern, the sodium rejection drops a little between pH 5.5 and 6.5 (the isoelectric point was measured to be about 5). The low rejection measured at pH 7-8 was not confirmed here.

Both membranes show a general trend of a decrease in rejection with increased NaCl concentration for both ions, although a stable calcium rejection is reached for calcium rejection of the TFC-SR membrane in the presence of NaCl (see Figure 7.12).

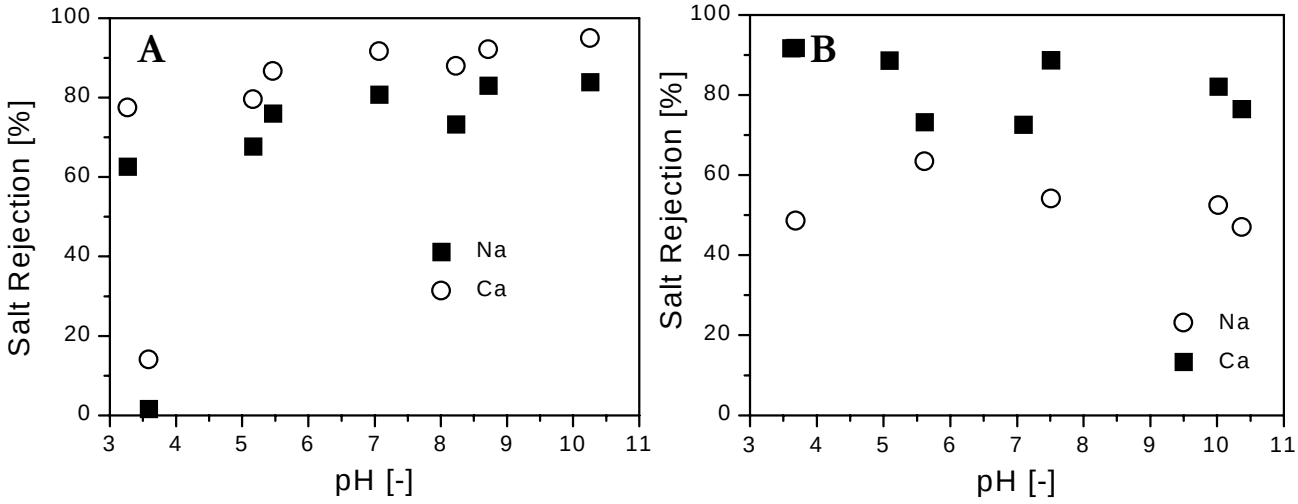


Figure 7.11 *Salt rejection (A) TFC-S and (B) TFC-SR membrane (0.5 mM $CaCl_2$, 1 mM $NaHCO_3$).*

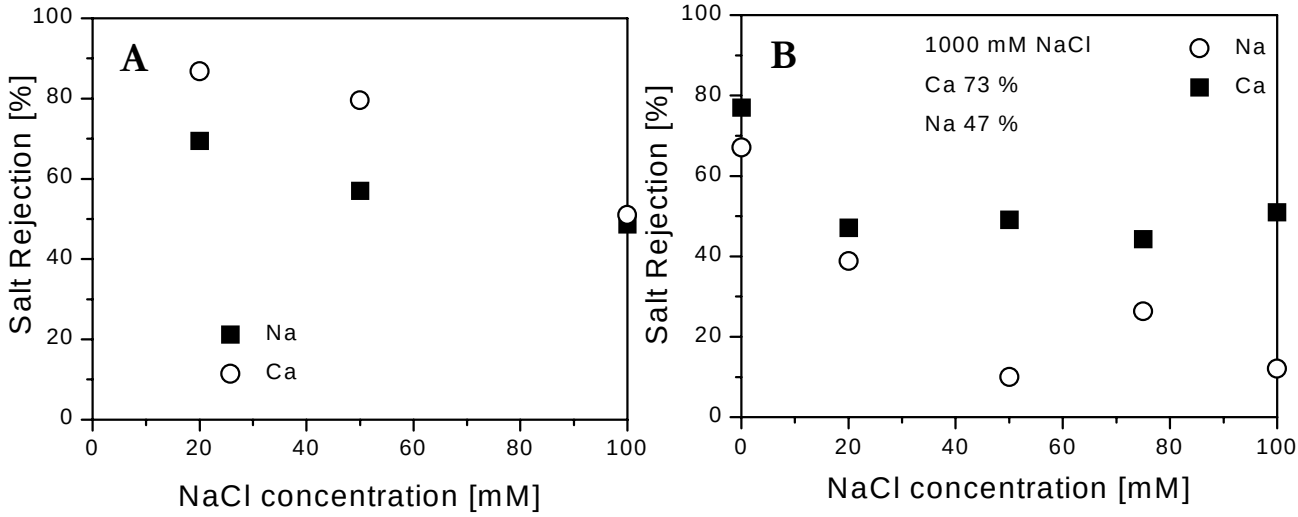


Figure 7.12 *Salt rejection (A) TFC-S and (B) TFC-SR membrane (pH 8, 0.5 mM $CaCl_2$, 1 mM $NaHCO_3$).*

In summary, it appears that the TFC-SR membrane shows very interesting characteristics for water treatment applications, whereas the TFC-ULP and TFC-S membranes may remove more sodium than required.

7.4.2 Organics and Salt Rejection in Synthetic Surface Water Solutions

Fulvic acid (FA) was used for rejection experiments, as FA is smaller than HA. Therefore, the rejection due to size of this compound should be lowest. While the NOM is still smaller than FA, the impurities in the NOM and the fact that its contents are largely uncharacterised make the use of FA more attractive.

Effect of Salt Type

Preliminary experiments were carried out with the TFC-SR membrane to test the impact of background salt composition on flux and rejection. Rejection results are summarised in Table 7.9.

As a general trend, in most experiments the rejection increases from sample 1 to 3. This may have occurred for a number of reasons. Firstly, the concentration in the cell increases during filtration. Secondly, the composition of the feed changes as a function of rejection, with the less rejected

compound being depleted in the cell. Thirdly, the variation of the membrane charge due to adsorption effects may vary the rejection behaviour of the membranes.

Table 7.9 *Rejection as a function of salt composition (TFC-SR, 5 mgL^{-1} DOC FA, pH 8).*

Solution Composition	DOC Rejection [%]	UV_{254nm} Rejection [%]	Ca^{2+} Rejection [%]	Na^{+} Rejection [%]	J/J_{W0} [-]
1 mM $NaHCO_3$	90 / 93 / 96	94 / 99 / 98	-	90 / 89 / 88	0.96
1 mM $NaHCO_3$; 0.5 mM $CaCl_2$	75 / 89 / 92	94 / 97 / 97	54 / 48 / 53	19 / 08 / 06	0.97
1 mM $NaHCO_3$; 1 mM $CaCl_2$	87 / 94 / 95	95 / 98 / 99	48 / 46 / 62	10 / 01 / -45	0.78
1 mM $NaHCO_3$; 2.5 mM $CaCl_2$	85 / 96 / 99	98 / 99 / 99	72 / 66 / 72	-05 / -13 / -21	0.85
1 mM $NaHCO_3$; 0.5 mM $CaCl_2$; 20 mM NaCl	94 / 94 / 94	94 / 96 / 98	67 / 68 / 68	34 / 40 / 38	0.91

The rejection of FA is not influenced significantly by the salt environment. This indicates that size exclusion is the dominant mechanism and that the structure of the molecule (curled at high salt concentration or linear at low salt concentration) is not of importance.

The cation rejection depends strongly on the electrolyte concentration. The calcium rejection increases with calcium concentration and in the presence of 20 mM NaCl. Sodium rejection also increases with concentration, but decreases in the presence of calcium, even reaching negative rejections when the calcium concentration increases to 2.5 mM. Macoun (1998) attributes negative rejection to a faster permeation of ions than water under certain conditions of enhanced driving force, and Hagmeyer (1999) states that the multivalent ion may "pump" the monovalent ion across the membrane. The final flux depends on the electrolyte concentration. Calcium is more effective in reducing flux than sodium chloride.

Effect of Membrane Type

Two membranes of the same type (TFC-S), but different batches were tested for the effect of their significantly different pure water flux on rejection. Rejection of organics decreased from 80 to 65% for a flux increase from 33 to 74 $Lm^{-2}h^{-1}bar^{-1}$. This is an expected trend due to the increase in wall concentration with an increased flux. Therefore a large error can be expected due to variations in membrane quality. However, these problems can be minimised by measuring the water flux of each membrane prior to experiments.

Rejection results at pH 8 for FA (smallest organic used) are summarised in Table 7.10 for the four membranes used in this study.

The TFC-ULP and TFC-S membranes have a very high ion rejection of >80% for sodium and >90% for calcium. Values are comparable to those obtained in the absence of organics.

UV 254nm is rejected at a higher rate than DOC, with a difference of about 10%. This indicates a fractionation of organic matter into more or less absorbing functional groups by the membrane. The smaller organics absorb less UV (with the exception of the relatively large polysaccharides), and it is these small compounds which pass through membranes more easily (Huber (1998)).

Table 7.10 *Rejection (the three values present rejection after 40, 80 and 120 mL filtration, respectively) and final flux to initial pure water flux ratio of membranes (5 mgL^{-1} DOC FA, 0.5 mM $CaCl_2$, 1 mM $NaHCO_3$, 20 mM NaCl, pH 8).*

Membrane	DOC Rejection [%]	UV $_{254nm}$ Rejection [%]	Calcium Rejection [%]	Sodium Rejection [%]	J/J_{W0} Final [-]
TFC-ULP	72 / 83 / 86	80 / 91 / 93	87 / 92 / 92	83 / 87 / 85	0.37
TFC-S	78 / 83 / 90	93 / 95 / 96	92 / 95 / 96	74 / 85 / 87	0.63
TFC-SR	94 / 94 / 94	94 / 96 / 98	67 / 68 / 68	34 / 40 / 38	0.91
CA-UF	68 / 72 / 72	76 / 88 / 85	17 / 13 / 13	17 / 11 / 10	1.11

The TFC-SR membrane rejects a higher percentage of DOC and UV 254nm than the other two membranes. In contrast, cations are rejected far less, sodium to about 40% and calcium to about 70% (which also corresponds to values determined earlier in the absence of organics). The difference between DOC and UV is reduced, as both are rejected almost entirely.

The CA-UF membrane has the lowest rejection of organics, and the ion rejection is slightly increased compared to the absence of organics. This may indicate interactions between the retained organics and the cations. This membrane shows a very interesting flux behaviour, with no decline at all over the experiments and a higher pure water flux after the experiments. This indicates the lack of concentration polarisation or osmotic pressure effect at the low salt rejection. The smooth membrane surface would also influence this. The adsorption of ions or organics render the membrane more hydrophilic.

Effect of Organic Type, Concentration and pH

Increasing solute concentration has been reported to decrease rejection (Macoun (1998)). During the experiments, concentration in the feed solution increases about 3 times if rejection is high. It was observed that cation rejection decreases with time or remains constant.

The DOC and UV 254nm rejection however, increases in all experiments. This indicates some difference in transport mechanisms, or simple fractionation of the organics with time if small compounds pass through the membrane first. To confirm this, experiments were carried out on the TFC-SR membrane as a function of organic type and pH, and the results are given in Table 7.11.

According to DOC measurements, IHSS FA is retained more effectively than either HA or NOM. It is somewhat surprising that FA is retained best, as IHSS HA is larger than FA (see Chapter 4). However, in UF fractionation the differences between HA and FA are small for the 1 kDa membrane. Also, the molecular weight (or size) determined by size exclusion chromatography is an average value. The HA is more polydisperse than the FA and it is the low molecular weight compounds, which are present to a similar extent in both samples, that determine NF rejection. Further, the FA has a significantly higher carboxylic group content than the HA (see Chapter 4), which indicates some charge effects. Structure effects may also play a role, but the knowledge of the structure of FA and HA is insufficient at this stage to draw conclusions. The UV absorbing component of all organics examined are retained almost completely under all conditions.

Table 7.11 *Rejection in the presence of different organic types for the TFC-SR membrane (0.5 mM $CaCl_2$, 1 mM $NaHCO_3$, 20 mM NaCl).*

Conditions	DOC Rejection [%]	UV_{254nm} Rejection [%]	Ca Rejection [%]	Na Rejection [%]	J/J_{W0} [-]
FA pH 4.5	80 / 80 / 70	99 / 98 / 96	96 / 96 / 96	46 / 36 / 22	0.9
FA pH 8	94 / 94 / 94	94 / 96 / 98	67 / 68 / 68	34 / 40 / 38	0.91
FA pH 10	88 / 93 / 94	94 / 97 / 99	72 / 65 / 62	37 / 30 / 21	0.9
HA pH 4.5	66 / 71 / 80	97 / 99 / 98	86 / 91 / 92	50 / 48 / 49	0.8
HA pH 8	72 / 72 / 78	96 / 98 / 98	66 / 58 / 64	28 / 10 / 20	0.93
HA pH 10	71 / 69 / 73	97 / 98 / 99	81 / 76 / 76	55 / 53 / 51	0.82
NOM pH 4.5	66 / 70 / 72	94 / 95 / 97	91 / 93 / 93	49 / 53 / 52	0.8
NOM pH 8	66 / 71 / 70	96 / 97 / 97	74 / 74 / 74	39 / 40 / 40	0.9
NOM pH 10	74 / 83 / 84	64 / 87 / 91	72 / 77 / 73	45 / 58 / 52	0.74

Calcium rejection is highest at low pH, where the membranes are positively charged and the calcium is fully dissociated. Sodium rejection is consistently lower at pH 8 and this confirms the results in Table 7.8.

The rejection of calcium increases with the IHSS HA concentration as shown in Table 7.12. This could either be caused by the more negative charge of the membrane due to the HA adsorption, as shown by Elimelech *et al.* (1994). This would increase anion rejection and therefore show largest cation rejection due to the need to maintain electroneutrality. Alternatively, it could be due to complexation interactions between the retained HA and calcium. The flux ratio goes up, possibly because HA replaces calcium in the boundary layer, which causes a reduction in osmotic pressure.

Table 7.12 *Effect of HA concentration on rejection (pH 8, TFC-SR, 0.5 mM $CaCl_2$, 1 mM $NaHCO_3$, 20 mM NaCl).*

HA Concentration [mgL^{-1} DOC]	DOC Rejection [%]	UV_{254nm} Rejection [%]	Ca Rejection [%]	Na Rejection [%]	J/J_0 [-]
2.5	58 / 91 / 94	96 / 98 / 99	57 / 52 / 56	19 / 10 / 13	0.85
5.0	72 / 72 / 78	96 / 98 / 98	66 / 58 / 64	28 / 10 / 20	0.93
7.5	78 / 91 / 95	99 / 98 / 98	66 / 67 / 68	24 / 21 / 23	0.96

For the TFC-S membrane, rejection of UV absorbance is highest for the IHSS HA, whereas DOC rejection is similar for all compounds (see Table 7.13). Calcium and sodium rejection are increased in the presence of all organics, which indicates an effect of surface charge variation rather than an interaction with the organics. Sodium rejection in the absence of organics is lowest (and similar to results shown in Table 7.8). No effect of pH is apparent.

The increase of FA concentration causes a moderate increase in DOC and UV rejection, as well as calcium rejection (Table 7.14).

Table 7.13 *Rejection in the presence of different organic types for the TFC-S membrane (0.5 mM $CaCl_2$, 1 mM $NaHCO_3$, 20 mM NaCl).*

Conditions	DOC Rejection [%]	UV_{254nm} Rejection [%]	Ca Rejection [%]	Na Rejection [%]	J/J_0 [-]
FA pH 4.5	80 / 81 / 84	92 / 93 / 94	86 / 87 / 88	71 / 69 / 71	0.87
FA pH 8	78 / 83 / 90	93 / 95 / 96	92 / 95 / 96	74 / 85 / 87	0.63
FA pH 10	79 / 82 / 85	91 / 96 / 96	96 / 94 / 94	79 / 76 / 72	0.54
HA pH 4.5	55 / 63 / 78	100 / 100 / 100	97 / 98 / 98	89 / 88 / 87	-
HA pH 8	88 / 91 / 91	99 / 99 / 99	99 / 99 / 99	94 / 92 / 89	-
HA pH 10	70 / 85 / 85	98 / 99 / 100	100 / 100 / 100	91 / 90 / 89	-
NOM pH 4.5	85 / 87 / 88	95 / 98 / 99	98 / 98 / 98	93 / 92 / 91	0.56
NOM pH 8	95 / 95 / 96	95 / 97 / 96	97 / 97 / 97	93 / 92 / 90	0.53
NOM pH 10	85 / 85 / 93	91 / 95 / 97	94 / 86 / 95	69 / 47 / 76	0.58

Table 7.14 *Effect of FA concentration on rejection (pH 8, TFC-S, 0.5 mM $CaCl_2$, 1 mM $NaHCO_3$, 20 mM NaCl).*

FA Concentration [mgL^{-1} DOC]	DOC Rejection [%]	UV_{254nm} Rejection [%]	Ca Rejection [%]	Na Rejection [%]	J/J_0 [-]
2.5	56 / 67 / 80	80 / 83 / 89	76 / 76 / 78	58 / 56 / 58	0.53
5.0	78 / 83 / 90	93 / 95 / 96	92 / 95 / 96	74 / 85 / 87	0.63
7.5	87 / 89 / 89	96 / 97 / 97	89 / 86 / 94	70 / 78 / 77	0.51

Table 7.15 *Rejection in the presence of different organic types for the TFC-ULP membrane (0.5 mM $CaCl_2$, 1 mM $NaHCO_3$, 20 mM NaCl).*

Conditions	DOC Rejection [%]	UV_{254nm} Rejection [%]	Ca Rejection [%]	Na Rejection [%]	J/J_0 [-]
FA pH 4.5	88 / 90 / 92	91 / 95 / 96	92 / 95 / 95	89 / 89 / 88	0.42
repeat	90 / 89 / 89	96 / 98 / 98	96 / 96 / 95	92 / 90 / 89	0.45
FA pH 8	72 / 83 / 86	80 / 91 / 93	87 / 92 / 92	83 / 87 / 85	0.37
FA pH 10	84 / 90 / 92	89 / 93 / 94	98 / 98 / 98	93 / 93 / 93	0.51
HA pH 4.5	39 / 68 / 68	100 / 100 / 100	94 / 96 / 96	87 / 88 / 88	-
HA pH 8	62 / 77 / 88	99 / 99 / 100	98 / 97 / 97	92 / 91 / 90	-
HA pH 10	77 / 91 / 93	92 / 100 / 99	93 / 99 / 99	90 / 93 / 94	-
NOM pH 4.5	79 / 88 / 93	98 / 99 / 98	97 / 95 / 95	80 / 87 / 88	-
NOM pH 8	95 / 95 / 96	95 / 97 / 96	97 / 97 / 97	93 / 92 / 91	0.49
NOM pH 10	81 / 90 / 92	92 / 97 / 98	100 / 99 / 98	93 / 92 / 90	-

The results of replicate studies shown in Table 7.15 indicate very good reproducibility of the experiments. For the TFC-ULP membrane, rejection of DOC, UV, calcium, and sodium are nearly

complete. Ion rejection appears to increase with pH, although the differences are close to the experimental error. No difference between the organics can be observed, indicating that the size of all the organics used is well above the membrane pore size.

The CA-UF membrane (see Table 7.16) shows lower rejection, a much larger gap between DOC and UV rejection, and larger variations as a function of pH. The membrane pore size is obviously very close to the size of the organics, determined to be between 1200 to 3000 $gmol^{-1}$ (dextran of 1000 $gmol^{-1}$ was rejected at 17% by this membrane). The rejection of calcium increases with pH, probably due to increased calcium-organic interaction, as the membrane itself is not likely to retain ions. The reliability of treatment using the CA-UF membrane is reduced, as the rejections measured vary between 17 and 87%. HA rejection is highest, indicating a size effect, which is expected from the low charge of the membrane and the relatively large pores.

Table 7.16 *Rejection in the presence of different organic types for the CA-UF membrane (0.5 mM $CaCl_2$, 1 mM $NaHCO_3$, 20 mM NaCl).*

Conditions	DOC Rejection [%]	UV_{254nm} Rejection [%]	Ca Rejection [%]	Na Rejection [%]	J/J_0 [-]
FA pH 4.5	17 / 19 / 18	57 / 57 / 62	05 / 06 / 01	15 / 08 / 07	1.03
FA pH 8	68 / 72 / 72	76 / 88 / 85	17 / 13 / 13	17 / 11 / 10	1.11
FA pH 10	46 / 64 / 72	75 / 87 / 90	26 / 18 / 20	13 / 08 / 05	1.05
HA pH 4.5	69 / 81 / 87	85 / 89 / 92	19 / 21 / 12	17 / 18 / 10	-
HA pH 8	74 / 75 / 79	94 / 93 / 85	18 / 13 / 12	13 / 09 / 07	-
HA pH 10	28 / 36 / 48	73 / 90 / 91	31 / 26 / 19	18 / 18 / 11	-
NOM pH 4.5	39 / 54 / 59	63 / 58 / 74	10 / 04 / 14	16 / 11 / 13	-
NOM pH 8	54 / 56 / 62	72 / 72 / 73	19 / 14 / 12	13 / 11 / 10	-
NOM pH 10	32 / 50 / 49	74 / 79 / 78	27 / 23 / 12	16 / -01 / 02	-

The organics, similar to the membrane, exhibit higher negative charge with increasing pH. Their pKa values cannot be specified since the mixture of functional groups and the influence of neighbouring functional groups cause continuous "distribution" of pKa values. However, generally the organics are expected to be of higher charge and have a rather long chain structure at high pH, whereas at low pH their functional groups are more protonated, the molecules are less charged and tend to form more "curled-up" structures and aggregate more easily. It has been suggested in the literature (Braghetta (1995)) that the more compact molecular shapes allow the formation of a denser deposit on the membrane, resulting in a greater flux decline but, due to their smaller size, the rejection should also decrease. These trends were not observed in this study, but fouling conditions may be required to observe these effects. pH did not seem to affect rejection behaviour significantly.

The rejection results do not show a clear pH effect. There are a number of reasons which could explain this result. Firstly, membrane flux was not controlled and varies with each membrane sample. This effects rejection, although experiments were reproducible which eliminates this possibility to some extent. Secondly, pH may cause a shift in rejection of certain fractions rather than a change in total DOC rejection. Thirdly, the organics retained could be excluded by size exclusion rather than charge

effects and changes in size and shape of the molecules with pH were above the cut-off of the membranes.

Liquid chromatography organic carbon detection (LC-OCD was performed to investigate possible effects. The method was described in Chapter 4. Figure 7.13 demonstrates the selectivity of the TFC-S membrane towards certain fractions of the NOM. While the humics and hydrolysates are almost completely retained, the acids fraction can pass through the membrane. Polysaccharides which are largely uncharged compounds also permeate through the membranes. It should be noted that the feed sample is diluted 1:25.

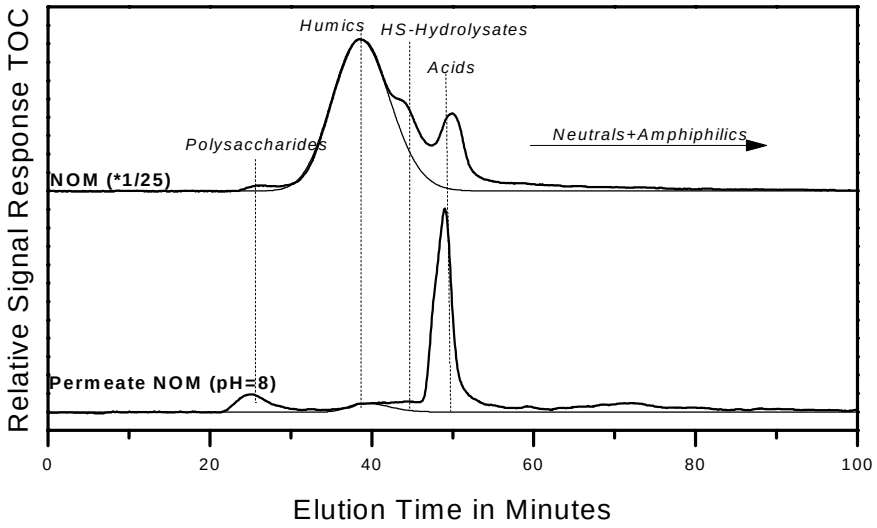


Figure 7.13 *LC-OCD result of NOM permeate of a TFC-S membrane.*

Figure 7.14 shows permeate characteristics as a function of pH for the TFC-S membrane with an IHSS HA feed (also diluted 1:25). The humics and hydrolysates are again fully retained. The rejection of the low molecular weight acids is low and decreases with pH. These acids dissociate with increasing pH and this increased rejection can be attributed to charge interactions. The nature and origin of the neutrals and amphiphilics peak is unclear. While the fraction in the permeate corresponds the amount in the feed, the rejection is much lower than that of the LMW acids.

The results confirm that charge interactions are important for organics rejection. While the humics and hydrolysates are retained by size exclusion effects, the smaller compounds demonstrate pH effects. Rejection experiments in this section failed to show this effect due to the high proportion of organics larger than pore size in the samples.

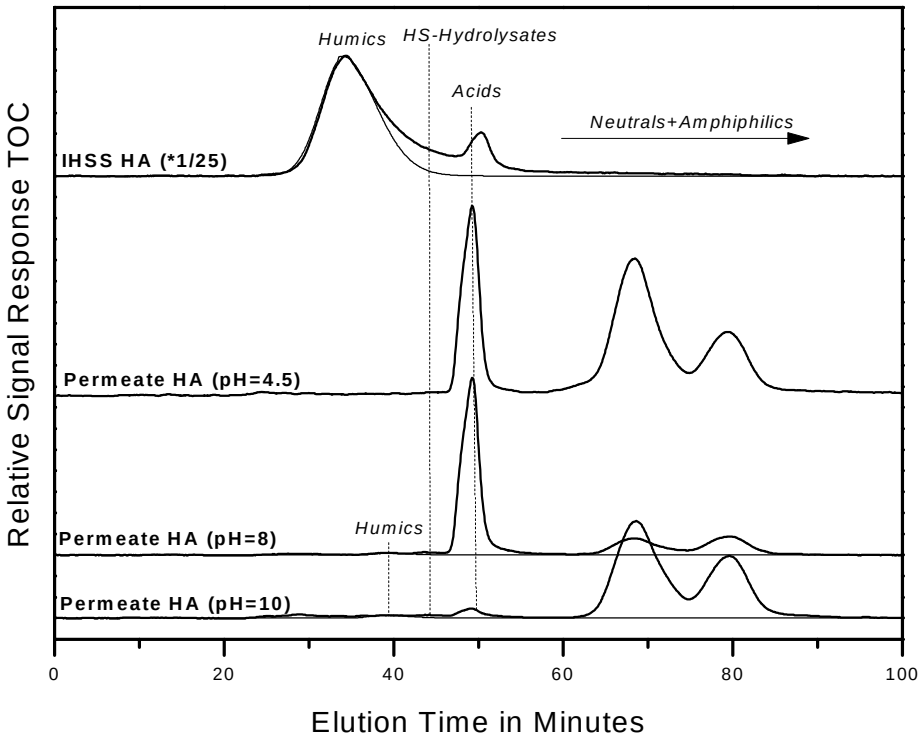


Figure 7.14 *LC-OCD Analysis of IHSS HA permeates obtained at different pH with TFC-S membrane.*

Effect of Stirring and Transmembrane Pressure on Rejection

Stirring (in the stirred cell) influences concentration polarisation and, therefore, mass transfer across the membrane. The wall concentration of solute increases at lower stirring and therefore the rejection is expected to decrease. Table 7.17 shows rejection results of unstirred conditions of the CA-UF membrane.

Table 7.17 *Effect of pH on rejection of CA-UF membrane for unstirred conditions (5mgL^{-1} DOC FA, unstirred, 0.5 mM $CaCl_2$, 1 mM $NaHCO_3$, 20 mM NaCl).*

Conditions	DOC Rejection [%]	UV_{254nm} Rejection [%]	Ca Rejection [%]	Na Rejection [%]	J/J_0 [-]
FA pH 4.5	11 / 09 / 03	36 / 24 / 25	06 / 01 / -01	07 / 01 / 02	1.03
FA pH 8	-36 / -50 / -80	20 / 11 / 11	07 / -04 / -03	09 / -01 / 02	1.00
FA pH 10	-36 / -40 / -60	11 / 08 / 11	16 / 01 / 01	09 / 01 / 02	1.01

The CA-UF membrane has the largest pores and with the solute having a very similar size to the pores, rejection drops from values like 72% for stirred conditions to –80% unstirred. This implies very high "pumping" under unstirred conditions. Similar trends can be seen for UV, calcium and sodium rejection.

These results are of interest considering the tendency to operate water treatment UF membranes under 'dead-end' (unstirred) hydrodynamic conditions to reduce energy costs.

For a tighter membrane (TFC-S, see Figure 7.15), rejection decreases by about 50% without stirring at pH 8. The stirred experiment was repeated to demonstrate reproducibility. While a similar effect is clearly visible for this membrane, the decrease in rejection due to lack of stirring is very dependent on the solute to pore size ratio.

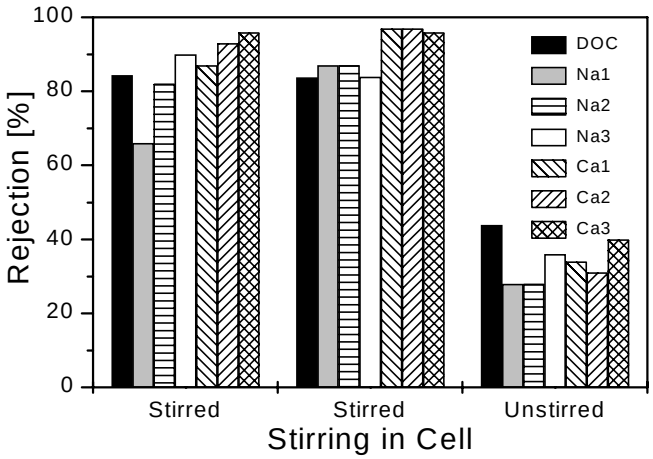


Figure 7.15 *Effect of stirring on DOC and cation rejection (TFC-S membrane, pH 8, 0.5 mM $CaCl_2$, 1 mM $NaHCO_3$, 20 mM NaCl).*

The transmembrane pressure determines the solvent flux through the membrane. Increased flux will cause an increase in solute concentration at the membrane surface until a limiting layer (gel, osmotic pressure, etc) is formed and flux no longer increases with pressure as under pure water conditions.

The effect of transmembrane pressure on the rejection of the TFC-SR membrane was examined and results are shown in Table 7.18. Rejection at all pressures is relatively stable, although at 7.5 bar rejection is initially lower and DOC rejection decreases with increasing pressure.

This indicates that the process in governed by convection and diffusion. While reverse osmosis generally relies on diffusion for solute transport and convection for solvent transport, in ultrafiltration both are convection driven. A lower rejection at higher pressure indicates convection, as the solute is transported faster. This is somewhat surprising for tight membrane pores, and the higher boundary layer concentration may also result in increased diffusion. Braghetta (1995) found that NOM transport was primarily convection controlled. At low pressure a slight diffusion component was visible. However the 'NF' membranes used were tight UF membranes (MWCO 1000 Da). The membrane performs reliably over a range of pressures, but the normalised flux is lower at high pressure, as expected if the boundary layer concentration is higher.

Table 7.18 *Effect of transmembrane pressure on rejection of TFC-SR membrane (5mgL^{-1} DOC FA, pH8, 0.5 mM $CaCl_2$, 1 mM $NaHCO_3$, 20 mM NaCl).*

Conditions	DOC Rejection [%]	UV_{254nm} Rejection [%]	Ca Rejection [%]	Na Rejection [%]	J/J_0 [-]
2.5 bar	80 / 89 / 93	93 / 95 / 97	60 / 55 / 57	21 / 12 / 13	0.96
5.0 bar	94 / 94 / 94	94 / 96 / 98	67 / 68 / 68	34 / 40 / 38	0.91
7.5 bar	63 / 81 / 89	78 / 86 / 92	52 / 51 / 56	21 / 15 / 15	0.87

Rejection at Critical Fouling Conditions

Critical fouling conditions were established during recycling experiments (see later section). The critical fouling condition are not conditions where fouling starts, but rather conditions at which fouling is particularly bad. These conditions are large organics (IHSS HA) at a concentration of 12.5 mgL^{-1} as DOC and 2.5 mM $CaCl_2$.

The objective here is to compare the rejection at these conditions (Table 7.19) to previous results at lower organic and calcium concentration (see Table 7.11, Table 7.13, Table 7.15, and Table 7.16 for TFC-SR, TFC-S, TFC-ULP, and CA-UF membranes, respectively).

Table 7.19 *Rejection and final flux to initial pure water flux ratio of membranes at critical fouling conditions (12.5 mgL^{-1} DOC HA, 2.5 mM $CaCl_2$, 1 mM $NaHCO_3$, 20 $mScm^{-1}$, pH 8).*

Membrane	DOC Rejection [%]	UV $_{254nm}$ Rejection [%]	Calcium Rejection [%]	Sodium Rejection [%]	J/J_{W0} Final [-]
TFC-ULP	78 / 90 / 93	96 / 98 / 98	97 / 98 / 98	90 / 91 / 91	0.61
TFC-S	92 / 93 / 97	98 / 99 / 99	96 / 97 / 96	83 / 80 / 77	0.39
TFC-SR	89 / 93 / 96	99 / 100 / 100	58 / 55 / 51	20 / 22 / 29	0.75
CA-UF	72 / 72 / 79	89 / 88 / 89	23 / 16 / 25	21 / 15 / 25	0.83

For the TFC-ULP membrane, DOC and UV rejection have slightly increased, whereas the salt rejection is similar. This shows that concentration polarisation effects are not important for the rejection behaviour of this membrane (a deposit layer would be expected to cause a reduced rejection of ions).

For the TFC-S membrane, the rejection of DOC and UV is also increased. However the rejection of ions is reduced by up to 10% (sodium).

The TFC-SR membrane shows an increase in HA rejection from 78 to 96% as DOC. UV results increase another 2% and reach complete rejection. Flux ratio is reduced from 0.93 to 0.50, whereas calcium and sodium rejection has decreased (up to 10% for calcium).

The CA-UF membrane shows a similar organic rejection, but a clearly higher salt rejection. This shows that calcium and sodium do interact with the organics (by complex formation or gelation) or that the polarised ('gel') layer formed is able to retain salt.

In conclusion for the rejection experiments, the TFC-SR membrane promises best performance in water treatment with a stable flux, and low sodium and high calcium rejection. The organic rejection of this membrane is the highest overall.

For all the TFC membranes, rejection is high. Sodium rejections of the TFC-S and TFC-ULP membranes are greater than normally necessary in a surface water application, but certainly these membranes have a great application potential for brackish water or water reclamation. The higher salt rejection causes a larger reduction in flux, and therefore these membranes may be economically less interesting.

The CA-UF membrane has a low charge, large pores, and a low salt rejection. It is on the fringe of being classed as a UF membrane. The organic rejection can be high, but is dependent on the solution

chemistry. Hydrodynamic conditions can reduce the rejection to below zero and therefore this membrane is not as reliable as the TFC membranes (at a similar flux). However, flux decline is near zero and the membrane performed well, even outside the pH range specified by the manufacturer.

Under fouling conditions, the organics rejection increases, whereas the salt rejection increases or decreases depending on the membrane.

7.5 FOULING CONSIDERATIONS

In this section, several parameters of importance in understanding fouling will be explained and their importance estimated.

7.5.1 Mass Balance for Deposit Calculations

The amount of solute deposit M_D on the membranes may be described (using mass balance principles) by

$$M_D = V_F \cdot c_F - V_C \cdot c_C . \qquad (7.4)$$

The concentrate sample is taken after recirculation of the permeate into the cell, and this way the permeate concentration is accounted for in the concentrate. By recirculating the permeate into the cell, concentration polarisation effects would be reversed and only irreversible deposition measured. This deposit can also be described as loss of solute L_D (as percent of mass in the feed solution)

$$L_D = 100 \cdot \frac{M_D}{V_F \cdot c_F} . \qquad (7.5)$$

Deposition and loss can be calculated for calcium, colloids, and organic carbon as DOC or UV.

7.5.2 Estimation of Adsorption of Organics on Membrane Surface

The deposition of organics on the membrane surface as a monolayer was estimated in order to determine the minimum amount of organics required to cover the membrane surface. Several assumptions were made; (i) the membrane surface is perfectly smooth (adsorption will increase with surface roughness), (ii) the organics are of spherical shape (the conformation of the molecules in reality depends on the solution chemistry and aggregation), and (iii) the organic carbon content of the molecules is 50% (see Chapter 4 and Appendix 1 for details on NOM characterisation). The estimation also neglects the fact that large amounts of water would be present in the molecules, which would affect the amount adsorbed. Table 7.20 describes the molecular diameter and diffusion coefficients, calculated by two methods (different size/molecular weight relationships) for comparison, and the number of moles as well as mass of organics adsorbed as a function of postulated molecular weight.

The masses of about 5 μg adsorbed correspond to only 0.2% of organic carbon in a fouling experiment, where the membrane (surface of $21.2 \cdot 10^{-4}$ m^2) is brought in contact with a feed that contains a total of 2.5 mg organic carbon (12.5 mgL^{-1} DOC).

The amount of ions adsorbed can also be estimated. Hagmeyer (1999) estimated the distance between point charges on an NF membrane. An estimated distance of 4nm, for example (depends on membrane charge), would imply that with the size of the organic molecules, only one functional group

of the molecule would interact with a membrane functional group. Due to the mostly identical charge of membranes and organics this would require a cation for bridging (Jucker and Clark (1994)). The amount of calcium needed for such bridging is minimal (0.1 ng for a charge distance of 4nm; 0.3 mg if each HA molecule adsorbed (as calculated in Table 7.20 co-adsorbs one calcium ion)).

Table 7.20 *Estimated organic carbon adsorbed as a monolayer on a membrane as used in the experiments (membrane area 21.2 · 10^{-4} m^2).*

Molecular weight of organic [$gmol^{-1}$]	500	1000	5000	10000
Diameter of molecule [nm]*	0.69	0.94	1.91	2.59
Diameter of molecule [nm]⁰	0.55	0.79	1.86	2.69
Diffusion Coefficient [m^2s^{-1}] ¹	$6.22 \cdot 10^{-10}$	$4.56 \cdot 10^{-10}$	$2.25 \cdot 10^{-10}$	$1.66 \cdot 10^{-10}$
Diffusion Coefficient [m^2s^{-1}] ⁺	$3.91 \cdot 10^{-10}$	$2.71 \cdot 10^{-10}$	$1.15 \cdot 10^{-10}$	$0.80 \cdot 10^{-10}$
Number of moles adsorbed [-]²	$9.4 \cdot 10^{-9}$	$5.1 \cdot 10^{-9}$	$1.2 \cdot 10^{-9}$	$6.7 \cdot 10^{-9}$
Mass of organic carbon adsorbed [μg]	4.7	5.1	6.2	6.7

* the relationship diameter=0.045 · (molecular weight)$^{0.44}$ was used (Combe *et al.* (1999)).

⁰ the relationship diameter=2.0374 10^{-11} · (molecular weight)$^{0.53}$ determined for molecules between 56 and 405 $gmol^{-1}$ was used (Worch (1993)).

⁺ calculated after Worch (1993).

¹ calculated using Stokes Einstein equation.

² calculated from the packing of the spherical molecules of a diameter as calculated after (Combe *et al.* (1999)) on the surface.

Childress and Elimelech (1996) measured increased adsorption in the presence of bivalent cations and for larger organics. Jucker and Clark (1994) found that IHSS HA adsorbs more onto hydrophobic membranes than does IHSS FA. This would be expected by the above estimation due to the difference in size.

The estimated amounts show how difficult it is to measure such an amount of carbon accurately. Combe *et al.* (1999) reported that this amount adsorbed could not be measured by mass balance (total amount adsorbed about 10 μg on a 28.7 · 10^{-4} m^2 membrane section (Clark (1999)). This amount is very close to the estimated monolayer adsorption value. The organic carbon was desorbed from the membranes with NaOH and then measured with UV. Despite the results being very close to the calculated monolayer value, this method is subject to errors from (i) the contamination of the NaOH with membrane components, (ii) the erratic concentration determination using UV (the selective adsorption of UV absorbing compounds could lead to an overestimation), and (iii) possibly the modification of UV absorbance characteristics of the organics due to the extreme pH variation.

From these estimates it is clear though, that monolayer adsorption can only account for a small proportion of the organic carbon deposited. Monolayer adsorption was chosen as the the change in charge due to adsorption is large which would reduce further adsorption. It is an objective of the fouling studies to measure and understand the mechanisms of the deposits observed.

7.5.3 Concentration Polarisation and Osmotic Pressure

Concentration polarisation is the accumulation of solute due to solvent convection through the membrane. Concentration polarisation leads to a reduced permeate flux, either in the form of an osmotic pressure on the feed side (thus reducing the effective transmembrane pressure), or due to the

build-up of a region of higher viscosity in the boundary layer (and thus creating an additional resistance to filtration). Concentration polarisation may also increase solute diffusion across the membrane and thus reduce rejection. The principle is explained in detail in Chapter 3.

If concentration polarisation effects are strong, the solute in the boundary layer can reach its solubility limit and cause irreversible fouling. Depending on the concentration of different solutes (in this case, calcium and organics), aggregation, gel formation, coagulation, or precipitation may occur after an initial adsorption. The concentration of solute in the boundary layer is determined by the equilibrium between convective transport of solute to the membrane and the backdiffusion of the solute into the bulk solution, due to the concentration gradient.

The solute mass transfer coefficient is required to calculate the solute concentration at the membrane surface. This mass transfer coefficient is in theory independent of the membrane. Equation *(7.6)* describes the film model relationship between flux and concentration of solute at the membrane surface.

$$J = k_S \cdot \ln \frac{(c_W - c_P)}{(c_B - c_P)} \qquad (7.6)$$

Equation *(7.7)* describes flux as a function of the osmotic pressure, caused by concentration polarisation.

$$J = \frac{\Delta P - \Delta \Pi}{\mu \quad R_M} \qquad (7.7)$$

Concentration polarisation may be of particular importance in NF because of the relatively high flux (compared to RO) and high rejection (compared to UF). Due to low concentrations of solute in surface water treatment applications, concentration polarisation is often neglected. In this study the extent of concentration polarisation is estimated for conditions typical of surface water membrane processing.

7.5.4 Mass Transfer Coefficient and Wall Concentration

The mass transfer coefficient of the stirred cell was estimated using the method described below. Dextran (T-70) was purchased from Pharmacia Biotech (Uppsala, Sweden) and a stock solution of about 60 g/L was used. The molecular weight of Dextran T-70 ($[C_6H_{10}O_5]_n$) is 70.3 kDa. The MW per unit is 162.2 Da, and the carbon content is 44.4%.

Applying the osmotic pressure model, assuming negligible fouling of the membranes with Dextran and a negligible permeate concentration, the wall concentration of Dextran can be calculated using equations *(7.8)* and *(7.9)* and the relationship between osmotic pressure and Dextran concentration developed by Wijmans *et al.* (1985)

$$\Delta\Pi = 0.375\, c + 7.52\, c^2 + 76.4\, c^3 \quad [bar]. \qquad (7.8)$$

This equation can be resolved to calculate the concentration from the measured osmotic pressure

$$c = 0.074 + 1.071 \cdot \left(1 - Exp\left(-\frac{\pi}{104.844}\right)\right) + 0.341 \cdot \left(1 - Exp\left(-\frac{\pi}{3.417}\right)\right) \qquad (7.9)$$

The mass transfer coefficient was determined as a function of membrane type and stirrer speed. Results obtained for various membranes are within ± 5%, and thus no impact of the membrane was found. The average mass transfer coefficient at 400 rpm was (1.81 ± 0.10) · 10^{-6} ms^{-1}. Rejection of Dextran was >99.5% for all membranes used.

Stirring had a large effect on the mass transfer coefficient with the mass transfer coefficients varying from 0.14 · 10^{-6} ms^{-1} at 0 rpm (unstirred) to 2.18 · 10^{-6} ms^{-1} at 560 rpm. This indicates that unstirred filtration will cause significantly higher wall concentrations, which explains the differences observed in rejection and fouling experiments.

Knowing the mass transfer coefficient, it is possible to predict c_W by applying equation *(7.6)*, using c_P = 0. Figure 7.16A and Figure 7.16B show the estimated surface concentration of calcium and humic acid as a function of flux and mass transfer coefficient, respectively. The larger mass transfer coefficients have been adapted from Da Costa (1993) who used a spacer filled channel. The value of 9 ·10^{-6} ms^{-1} is an optimised mass transfer coefficient for an ideal spacer design (hydrodynamic angle of 90^0). Values ranged from 4 to 9 ·10^{-6} ms^{-1} depending on the spacer orientation for a flow of 1 $Lmin^{-1}$. A standard crossflow system would have a mass transfer coefficient in between the optimised and the stirred cell value. It can be seen that the predicted surface concentrations increase rapidly at fluxes approaching 50 $Lm^{-2}h^{-1}$, a value commonly achieved with these membranes.

The calculations do not consider the rise in bulk concentration, c_B, during the stirred cell experiments, which could increase the results by a factor of three. It should be noted that the concentrations will not increase indefinitely (as it appears from Figure 7.16) since a solubility limit will be reached which depends on the solution chemistry and extent of concentration polarisation. The concentration then remains constant, at the so-called gel concentration.

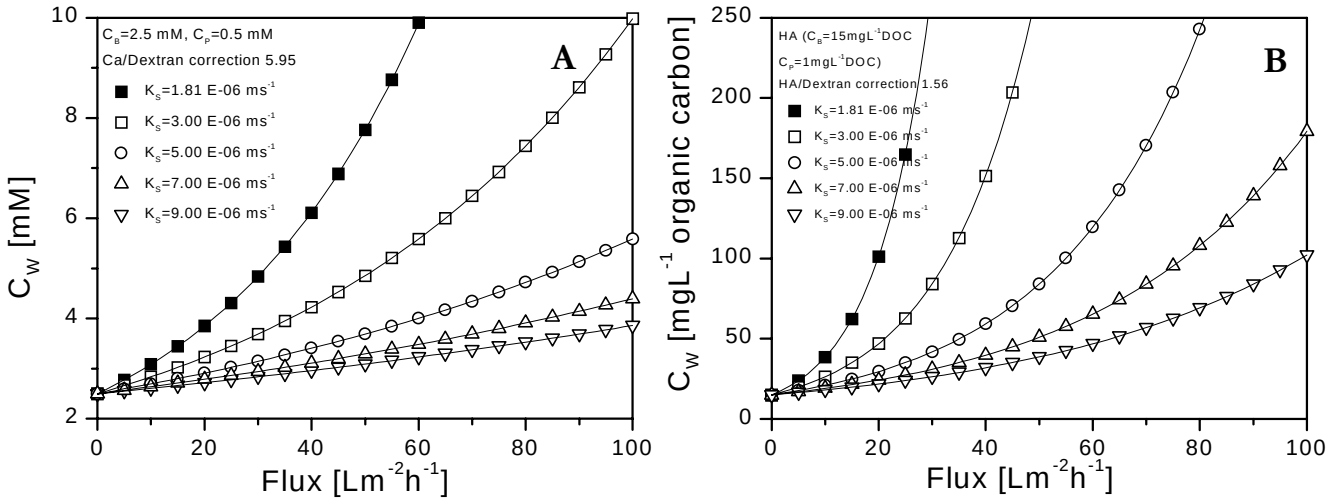


Figure 7.16 *Estimated wall concentration of (A) calcium and (B) humic acid (HA, 10 kDa) as a function of flux and mass transfer coefficient ((■) typical of stirred cell; (○△▽) typical of crossflow or spiral element).*

Using Dextran for mass transfer coefficient estimations probably results in an overestimate of concentration polarisation, due to the larger size of Dextran compared to humic substances and calcium. However the diffusion characteristics of humic acid, calcium-humate complexes, and even calcium in the highly viscous boundary layer are not known, and Dextran is probably a conservative assumption. Corrections for calcium and HA (molecular weight 1 and 10 kDa) were performed using

the hydrodynamic correlations for stirred cells summarised by Suki (1984), Blatt *et al.* (1970) and Goldsmith (1971), as described below. Laminar conditions were assumed in the stirred cell, thus

$$Sh = 0.285 \cdot Re^{0.55} \cdot Sc^{0.33} \tag{7.10}$$

With Re being constant for different solutes, $Sc = \nu D^{-1}$ and $k_S = Sh \cdot D \cdot r^{-1}$, where ν is the kinematic viscosity, D is the solute diffusivity and r the cell radius. This gives correction factors as the ratio of the two mass transfer coefficients with D_1 and D_2 being the different solute diffusivities.

$$\frac{k_{S1}}{k_{S2}} = \left(\frac{D_1}{D_2} \right)^{0.67} \tag{7.11}$$

The diffusion coefficients were calculated using the Stokes-Einstein equation at 20^0C after correlating molecular weight and size. This correlation lead to correction factors for the k_{S1} versus Dextran (k_{S2}) as shown in Table 7.21.

Table 7.21 *Size, diffusion coefficients and correction factor used for mass transfer calculation ([1] Peeters (1997), [2] Schweitzer (1979)).*

	Calcium	HA (1 kDa)	HA (10 kDa)	Dextran T-70 (70 kDa)
Size [Å]	2.37 [1]	17 [2]	35 [2]	68 [2]
Diffusion coefficient [m^2s^{-1}]	$1.355 \cdot 10^{-9}$	$3.779 \cdot 10^{-10}$	$1.835 \cdot 10^{-10}$	$9.446 \cdot 10^{-11}$
Correction factor [-]	5.95	2.53	1.56	1

Note that these initially estimated values are slightly larger than those calculated in Table 7.20. The diffusivities are likely to change in the boundary layer, and Bhattacharjee *et al.* (1999) predicted an increase in diffusivity with an increase of concentration. This means that backdiffusion would be enhanced and the estimated boundary layer concentration would be lower. It is evident from the results that modules with high mass transfer coefficients are important to avoid excessively high values of c_W. Alternatively, low flux operation (or larger membrane area) will also reduce c_W.

7.5.5 Osmotic Pressure in Solutions and Boundary Layer

The osmotic pressure of solutions and especially the osmotic pressure in the boundary layer reduces the effective transmembrane pressure. To estimate the possible effect, ionic strength and osmotic pressure values for various salt solution compositions are summarised in Table 7.22.

The osmotic pressure for the worst case, a calcium concentration of 10 mM in the boundary layer, causes a transmembrane pressure reduction of 14.4%. If the flux is proportional to applied pressure, then this should result in no more than a 14.4% flux reduction. However, if one considers the concentration in the cell (up to a factor of 3) then the flux reduction may be greater (up to 43.2%).

According to Braghetta (1995), molecules with a molecular weight of less than 10 kDa can also contribute considerably to flux decline due to osmotic pressure. This effect would increase for smaller molecules with a higher charge. However, the concentrations of organics are very low (few mgL^{-1}, equivalent to micromoles) and inorganics would thus be expected to dominate osmotic pressure.

Table 7.22 *Osmotic pressure as a function of solution composition.*

Solution Composition	Ionic Strength [mM] $I = 0.5 \cdot \sum (c_i \cdot z_i^2)$	Osmotic Pressure [bar] $\Pi = \sum j_i \frac{n_i}{V_i} RT$
20 mM NaCl, 1 mM $NaHCO_3$, 0.5 mM $CaCl_2$	22.5	1.060
1 mM $NaHCO_3$, 0.5 mM $CaCl_2$	2.5	0.085
0.5 mM $CaCl_2$	1.5	0.036
1 mM $NaHCO_3$	1	0.049
20 mM NaCl	20	0.974
2.5 mM $CaCl_2$	7.5	0.180
10 mM $CaCl_2$ (extreme concentration polarisation)	30	0.720

7.5.6 Solubility of Calcium and Natural Organic Matter (NOM)

Having estimated the wall concentration of calcium and organics, it would be useful to know the solubility of these compounds to predict when precipitation can be expected. However, the solubility product of natural organics is largely unknown and very difficult to determine due to the complex mixture of compounds present in NOM. Some components of NOM may form insoluble complexes with multivalent ions such as calcium and precipitate on the membrane surface. NOM is expected to contain about 40% FA, 10% HA, and 50% undefined compounds, of which about 40% are hydrophilic acids. Fulvic acid (FA) is soluble under acidic and basic conditions, while humic acid (HA) is insoluble at low pH (Thurman (1985)). Multivalent ions and pH reduction decrease the solubility of compounds such as HA. This is, principally, a result of charge neutralisation effects. Tipping *et al.* (1988) showed that humic solubility increases with increase in its charge. FA has a higher charge than HA. Complexation of NOM with calcium increases with pH due to a higher dissociation of carboxylic groups (Hong and Elimelech (1997), Matlack (1992)). The complexation also leads to a charge neutralisation and floc formation.

Another process likely to occur is calcite precipitation, when pH and calcium concentration are both high. The NOM then adsorbs on the calcite surface. Suess (1973a, 1973b) measured the selective adsorption of organics onto calcite and mentioned the possibility of hydrated organo-calcium complexes on calcite surfaces. He described the thick layer of organics on the calcite surface as nitrogen-rich, possibly protein-like substances.

Chemical equilibrium calculations using the speciation code MinteqA2 (Allison *et al.* (1991)) of calcium solubility under the conditions used in the experiments indicate that calcite will precipitate at the higher pH's investigated, though some supersaturation may occur. In the absence of organics and at a pH of 8 calcite precipitation is expected at a concentration of about 3 mM (see Appendix 5). This value will increase in the presence of organics due to interactions with calcium. However, Matlack (1992) indicated that the dissolved organic matter (DOM)-metal complexation is drastically underestimated by MinteqA2 at high pH. Organics can inhibit inorganic precipitation, but, given the high degree of uncertainty in calcium-organic complexation constants, definitive prediction of the effect of NOM on calcite precipitation is not possible. As shown in Chapter 4, the solubility of HA at low pH and in the

presence of calcium, at the concentrations predicted in Figure 7.16, is low and precipitation of organics (low pH) and calcium-organic complexes or organics associated with calcium (high pH) can be expected.

7.6 FOULING EXPERIMENTS

In this section, the critical fouling conditions, which lead to the establishment and verification of fouling mechanisms, will be determined. Experiments were carried out under enhanced fouling conditions, namely 12.5 mgL^{-1} organic carbon and, for most experiments, calcium concentration of 2.5 mM. These conditions are extreme for surface waters but help understand and accelerate fouling, and are not unrealistic if one considers the conditions of modules in a filtration plant operating at 80 to 90% recovery (i.e. feed concentrated 5 to 10 times).

7.6.1 Effect of Background Electrolyte

The rejection experiments have shown that flux depends on the salt solution composition. Figure 7.17 shows results for the different components of the chosen background solution with FA for the TFC-S membrane which, due to its high salt rejection, should be most sensitive to the salt used.

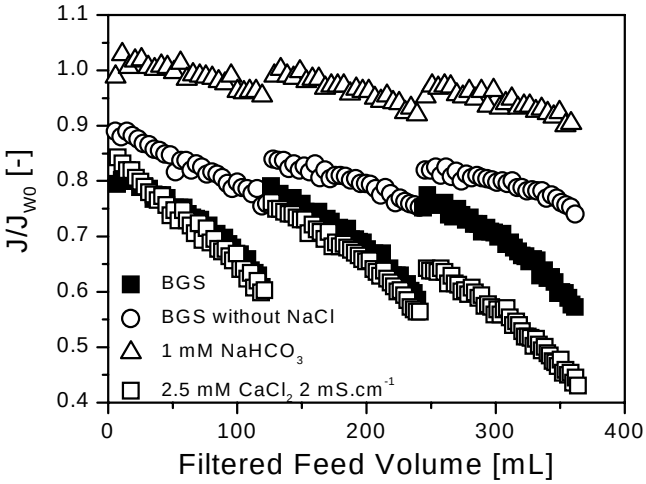


Figure 7.17 *Flux ratio for solutions at variable ionic compostion (TFC-S membrane, 12.5 mgL^{-1} DOC FA, pH 8, BGS contains 0.5 mM $CaCl_2$, 1 mM $NaHCO_3$, 20 mM NaCl).*

It can be seen that calcium chloride and sodium chloride (at a much higher concentration) contribute to a similar extent to flux decline. This flux decline in the presence of FA is most likely caused by concentration polarisation due to an increased concentration in the stirred cell (the concentration increases by a factor of up to 3 during the experiment) and the resulting osmotic pressure increase. The deposit values show that calcium increases deposition of DOC and UV (see 2.5 mM $CaCl_2$), but no significant difference in deposition is visible for the other solutions (see Table 7.23).

To compare the osmotic effect on membranes, the four membranes were tested in the presence of FA and background solution. The result is shown in Figure 7.18. It can be seen that the membranes with a lower salt rejection (CA-UF and TFC-SR) show a significantly lower flux decline. In the case of the CA-UF membrane, the flux increases after filtration. This is most likely due to a small amount of adsorption of ions or FA to the membrane material, which may render the surface more hydrophilic.

Table 7.23 *Flux and solute deposition as a function of ionic composition (conditions as Figure 7.17).*

Salt	After Recycle 3 J/J_{W0}	After Experiment J_W/J_{W0}	After Water Rinse J_W/J_{W0}	DOC Loss [%] ([mg])	UV_{254nm} Loss [%]([cm^{-1}])	Calcium Loss [%]([mg])
20 mM NaCl, 1 mM $NaHCO_3$, 0.5 mM $CaCl_2$	0.57	0.98	0.93	1 (0.014)	4 (0.020)	0.9 (0.20)
1 mM $NaHCO_3$, 0.5 mM $CaCl_2$	0.74	0.91	0.91	7 (0.15)	4 (0.021)	1.5 (0.61)
2mS/cm Cond (NaCl), 1 mM $NaHCO_3$, 2.5 mM $CaCl_2$	0.42	0.88	0.90	8 (0.14)	11 (0.052)	2.7 (6.1)
1 mM $NaHCO_3$	0.90	1.05	1.00	4 (0.08)	4 (0.021)	-

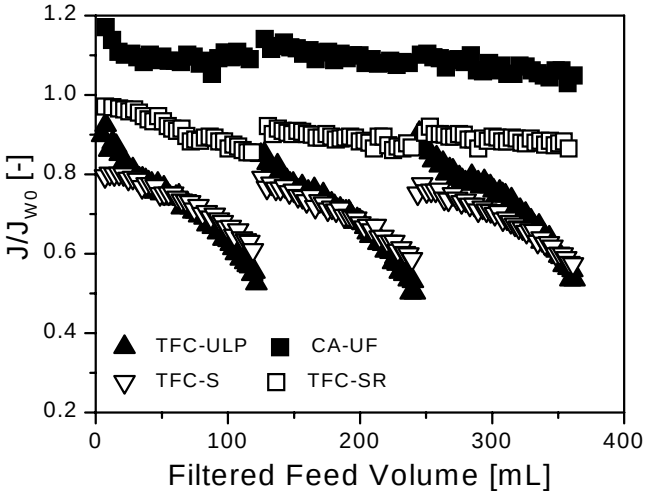


Figure 7.18 *Effect of membrane type at 0.5 mM $CaCl_2$, 1 mM $NaHCO_3$, 20 mM NaCl and 12.5 mgL^{-1} DOC FA.*

It is surprising that the TFC-SR membrane does not show this osmotic pressure effect as much as the other membranes, as this membrane also retains a considerable amount of salt (but less sodium). It was calculated in Table 7.22 that sodium is the main contributor to osmotic pressure. However, the flux behaves as if sodium and calcium were virtually absent (compare with TFC-S membrane in absence of sodium and calcium in Figure 7.17).

As can be seen from Table 7.24, very small amounts of material are deposited on the membranes (close to the measurable limit of this method). Relatively large values of calcium losses (in mg) are measured for the TFC membranes.

To investigate the lower osmotic pressure effect on the TFC-SR membrane, an experiment was carried out in the absence of stirring, which would increase concentration polarisation effects. The results are shown in Figure 7.19.

The lack of stirring indeed showed that concentration polarisation (which is increased in the absence of stirring) increases flux decline tremendously, even though the membrane appeared less sensitive to osmotic pressure effects. With the flux decline at unstirred conditions, a very significant deposit was formed on the membrane, as summarised in Table 7.25. Given the method by which this deposit was measured, it includes material which can be removed with a water wash, but not the polarised layer.

Table 7.24 *Flux and deposit as a function of membrane type (0.5 mM $CaCl_2$, 1 mM $NaHCO_3$, 20 mM NaCl and 12.5 mgL^{-1} DOC FA).*

Membrane	After Recycle 3 J/J_{W0}	After Experiment J_W/J_{W0}	After Water Rinse J_W/J_{W0}	DOC Loss [%] ([mg])	UV_{254nm} Loss [%] ([cm^{-1}])	Calcium Loss [%] ([mg])
TFC-ULP	0.54	1.12	1.07	0 (0.008)	3 (0.013)	1.4 (0.33)
TFC-S	0.57	0.98	0.93	1 (0.014)	4 (0.020)	0.9 (0.20)
TFC-SR	0.87	0.98	-	2 (0.056)	1 (0.007)	1.1 (0.24)
CA-UF	1.05	1.04	1.01	1 (0.030)	1 (0.003)	0

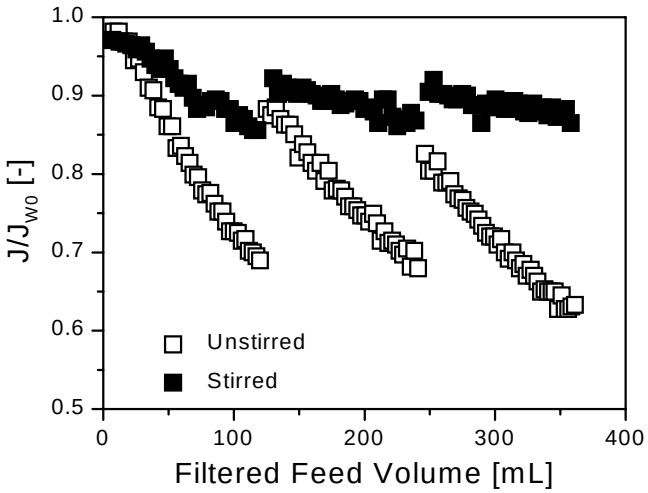


Figure 7.19 *Effect of stirring on flux of TFC-SR membrane (0.5 mM $CaCl_2$, 1 mM $NaHCO_3$, 20 mM NaCl and 12.5 mgL^{-1} DOC FA, pH 8).*

Table 7.25 *Flux ratios and solute deposition as a function of stirring (conditions as in Figure 7.19).*

Membrane	After Recycle 3 J/J_{W0}	After Experiment J_W/J_{W0}	After Water Rinse J_W/J_{W0}	DOC Loss [%] ([mg])	UV_{254nm} Loss [%] ([cm^{-1}])	Calcium Loss [%] ([mg])
Stirred (400 rpm)	0.89	0.95	0.99	2 (0.056)	1 (0.007)	1.1 (0.24)
unstirred	0.63	0.86	0.96	23 (0.53)	22 (0.118)	2.8 (0.65)

Very similar amounts (%) of UV absorbing material and DOC are deposited. The deposition of calcium also increases in the absence of stirring, but to a much smaller extent. The flux decline is largely reversible with a pure water wash which indicates a physical (polarisation), rather than chemical, association of the solute with the membrane.

Neither of the membranes exhibited any irreversible fouling in the presence of FA (except in unstirred conditions), and the deposition of ions and FA was minimal under these conditions (12.5 mgL^{-1} DOC in 0.5 mM $CaCl_2$, 1 mM $NaHCO_3$, 20 mM NaCl).

7.6.2 Effect of Organic Type

The organics were extensively characterised, as described in Chapter 4. Differences such as functional group content, size, charge, and hydrophobicity will influence the fouling behaviour if these properties are responsible for flux decline. Figure 7.20 shows a comparison of the different organics filtered through a TFC-S membrane.

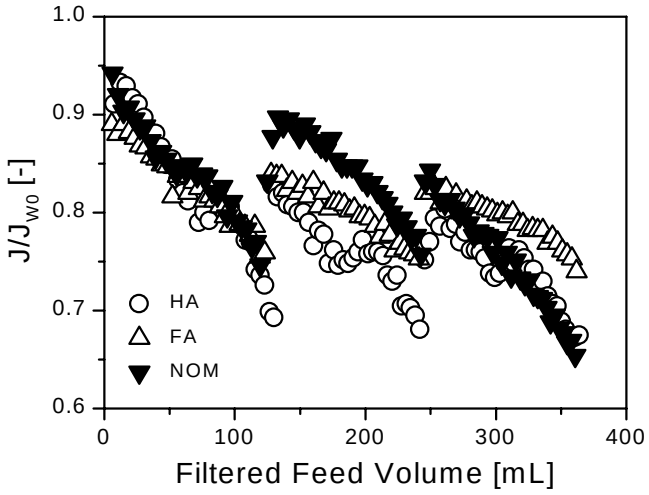


Figure 7.20 *Effect of organic type on flux decline of TFC-S membrane (0.5 mM $CaCl_2$, 1 mM $NaHCO_3$, no NaCl and 12.5 mgL^{-1} DOC).*

Table 7.26 *Deposit and flux as a function of organic type (TFC-S, 0.5 mM $CaCl_2$, 1 mM $NaHCO_3$, no NaCl and 12.5 mgL^{-1} DOC).*

Organic	After Recycle 3 J/ J_{W0}	After Experiment J_W/J_{W0}	After Water Rinse J_W/J_{W0}	DOC Loss [%] ([mg])	UV_{254nm} Loss [%] ([cm^{-1}])	Calcium Loss [%] ([mg])
NOM	0.65	0.93	0.93	3 (0.09)	14 (0.076)	0.8 (0.39)
IHSS HA	0.68	0.85	0.91	8 (0.12)	4 (0.026)	0.7 (0.35)
IHSS FA	0.74	0.91	0.91	7 (0.15)	4 (0.021)	1.5 (0.61)

The NOM shows the largest flux decline. This is not due to the type of organic, but due to the presence of salts that were concentrated with the organics as described in Appendix 1. Since this experiment was carried out in the absence of NaCl, the difference due to this salt content of the NOM is clearly visible, while at a higher NaCl concentration the effect disappears. IHSS HA shows a greater flux decline than IHSS FA which can be attributed to the organic itself, as both compounds are purified. The contribution of the HA in the NOM to flux decline is clarified later. The flux decline cannot be fully attributed to concentration polarisation, as the starting values of the cycles decrease. Neither can it be related to irreversible deposition as shown in Table 7.26, as the deposition of organics is well above the values estimated for monolayer adsorption.

It is not obvious from these results that the amount deposited of IHSS HA is higher than that of IHSS FA, as decribed by Jucker and Clark for hydrophobic membranes (Jucker and Clark (1994)). It may be that with hydrophilic membranes charge effects become more important. The flux ratio was lowest for HA and, therefore, further fouling studies were carried out with HA, since HA appeared to be the critical fraction responsible for fouling.

7.6.3 Effect of Calcium Concentration

Calcium may complex organic substances, cause coagulation of the organics, or chemically interact with organics and/or the membrane. It is therefore important to study the effect of calcium on fouling. In Appendix 5 it is shown that the calcium in the system will commence to precipitate in solution at a concentration of about 3 mM in the absence of organics (assuming calcite does not supersaturate).

Concentrations in the boundary layer are expected to be significantly higher than those in the bulk, as shown in Figure 7.16. Figure 7.21 and Figure 7.22 show the observed effect of the calcium concentration on flux decline for TFC-S and TFC-SR membranes, respectively. While flux declines steadily with increasing calcium concentration up to 2.5 mM for both, TFC-S and TFC-SR membranes, variable results are observed for 4 mM $CaCl_2$.

For the TFC-S membrane (Figure 7.21 and Table 7.27) the flux increases again to values similar to 0 mM. This can be attributed to precipitation of calcite. As will be seen in the membrane deposit morphology studies section, a different structure of the deposit is observed with increased calcium concentration.

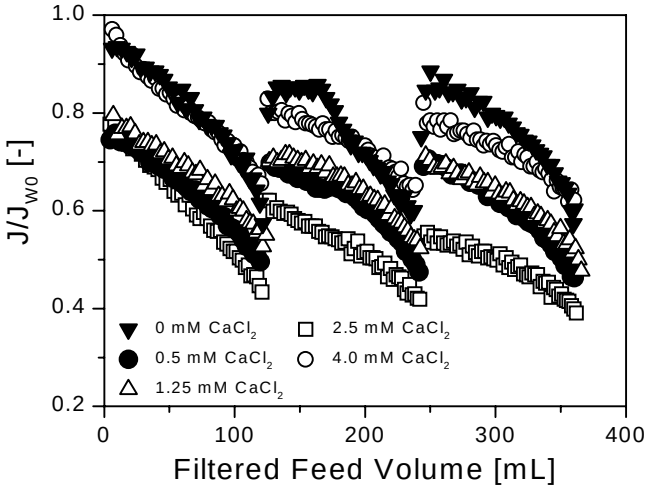


Figure 7.21 *Effect of calcium concentration on flux decline of TFC-S membrane, pH 8, 1 mM $NaHCO_3$, conductivity 2 mScm^{-1} adjusted with NaCl.*

Table 7.27 *Deposition and flux as a function of calcium concentration (TFC-S, pH 8, 1 mM $NaHCO_3$, conductivity 2 mScm^{-1} adjusted with NaCl).*

Ca Concentration [mM]	After Recycle 3 J/ J_{W0}	After Experiment J_W/J_{W0}	After Water Rinse J_W/J_{W0}	DOC Loss [%] ([mg])	UV_{254nm} Loss [%] ([cm^{-1}])	Calcium Loss [%] ([mg])
0	0.60	1.13	1.13	1 (0.023)	2 (0.016)	0
0.5	0.46	0.92	0.87	2 (0.039)	4 (0.023)	0.1 (0.05)
1.25	0.48	0.88	-	4 (0.05)	9 (0.054)	0.3 (0.28)
2.5	0.39	0.68	0.79	1 (0.016)	16 (0.09)	0.4 (0.21)
4	0.62	0.87	0.87	9 (0.116)	23 (0.134)	2.3 (8.3)

For the TFC-SR membrane this increase is not observed. Indeed, the flux is lowest at 4 mM $CaCl_2$ (Figure 7.22), however the deposit is quite reversible in this case (Table 7.28). An explanation for this

may be the lower retention of calcium by the membrane so that the precipitates formed are not quite as "porous" as those formed with the TFC-S membrane, as the concentration built-up in the boundary layer is not as great. Figure 7.23 summarises final flux for the TFC-S and TFC-SR membranes. The larger flux ratios of the TFC-SR membrane compared to the TFC-S membrane are evident.

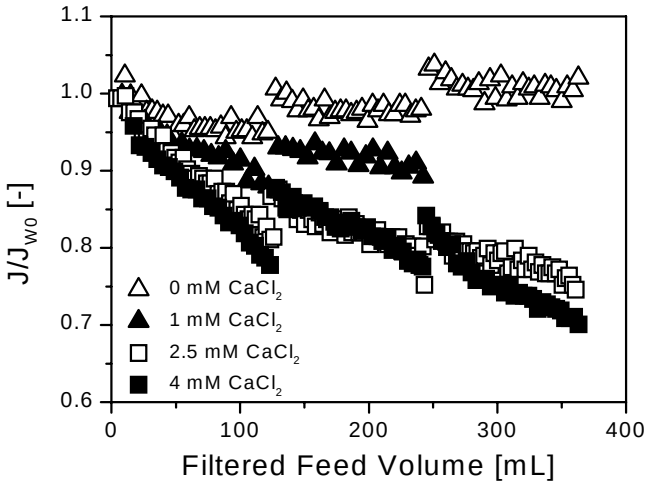


Figure 7.22 *Effect of calcium concentration on flux decline of TFC-SR membrane, pH 8, 1 mM $NaHCO_3$, conductivity 2 mScm^{-1} adjusted with NaCl.*

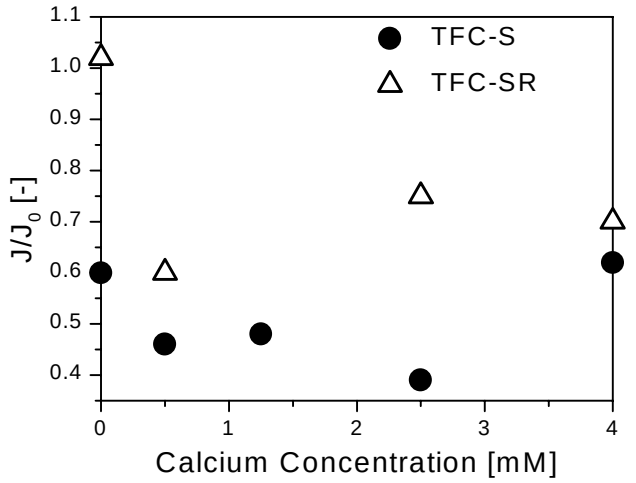


Figure 7.23 *Effect of calcium concentration on final flux of the TFC-S and TFC-SR membranes.*

Table 7.28 *Deposition and flux as a function of calcium concentration (TFC-S, pH 8, 1 mM $NaHCO_3$, conductivity 2 mScm^{-1} adjusted with NaCl).*

Ca Concentration [mM]	After Recycle 3 J/ J_{W0}	After Experiment J_W/J_{W0}	After Water Rinse J_W/J_{W0}	DOC Loss [%] ([mg])	UV_{254nm} Loss [%] ([cm^{-1}])	Calcium Loss [%] ([mg])
0	1.02	1.05	1.01	1 (0.012)	3 (0.021)	-
1	0.60	0.70	0.83	10 (0.18)	9 (0.063)	0.7 (0.24)
2.5	0.75	0.83	0.93	15 (0.18)	16 (0.086)	1.3 (2.86)
4	0.70	0.84	0.96	18 (0.28)	26 (0.194)	1.2 (1.56)

The effect of calcium concentration on the deposition of organics (as DOC and UV) and calcium for the TFC-S membrane is shown in Figure 7.24 and Table 7.27. For higher calcium concentrations the flux is lower. The deposition of calcium increases rapidly between 2.5 and 4 mM feed concentration, whereas the deposition of organics is increasing continuously with calcium concentration. At 4 mM the amount of humic acid (or the fraction of HA that interacts readily with calcium) is too small to inhibit calcite precipitation. For the TFC-SR membrane (Figure 7.25 and Table 7.28) the difference between UV and DOC deposition is smaller than for the TFC-S membrane, and becomes more apparent at high calcium concentration. This may be related to the deposition mechanism, but further work is needed to understand the precipitation of calcium and organics.

The higher flux ratio in the absence of calcium indicates that the HA makes the membrane more hydrophilic. This implies that interactions, other than calcium bridging are occurring. A similar increase was observed by Elimelech *et al.* (1997). The flux has a minimum at 2.5 mM $CaCl_2$ and increases at higher calcium concentrations. This is due to precipitation and the structural changes in the deposit.

Hydrated complexes (which Suess (1973a) described in detail) are expected to induce a higher flux decline than precipitate. This may explain the lower flux decline when solid precipitates are formed at 4 mM $CaCl_2$, although the deposition of calcium and organics are higher (see Figure 7.24).

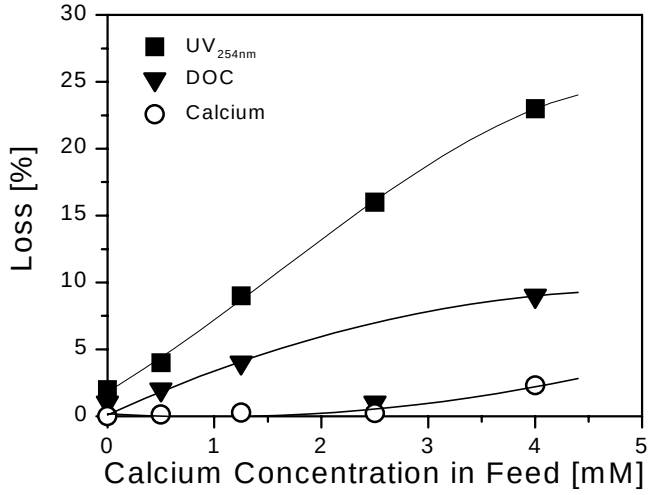


Figure 7.24 *Loss of humic acid (as DOC and UV) and calcium as a function of calcium concentration for TFC-S membrane; note that at 4 mM $CaCl_2$ the 8.3 mg of Ca and 0.62 mg DOC are lost (deposited).*

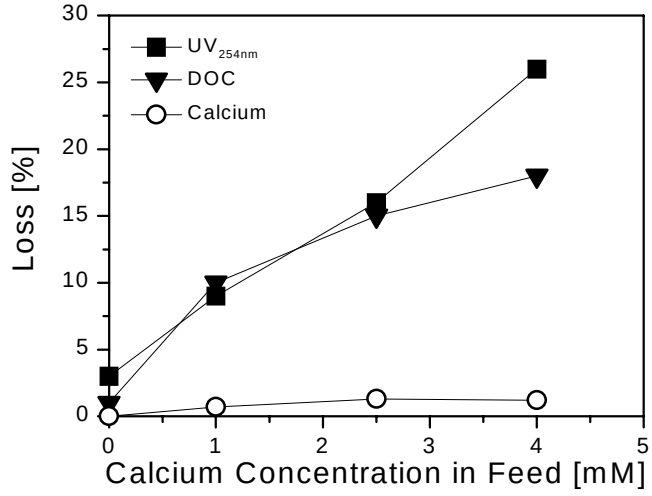


Figure 7.25 *Loss of humic acid (as DOC and UV) and calcium as a function of calcium concentration for TFC-SR.*

Braghetta (1995) reported an increase in deposition with ionic strength (KCl, NaCl), but HA adsorption on the membranes was higher with $CaCl_2$. The reasons for this were given as interfacial charge neutralisation, salt bridges and coagulation of NOM). This is confirmed here with observations of coagulation and precipitation of the HA with calcium in the boundary layer.

The above studies now allow the definition of 'critical fouling conditions' in NF. Further studies of parameters at these conditions will enable to understand the underlying mechanisms of deposition and fouling.

7.6.4 Critical Fouling Conditions

Following the previous findings with studies on organic type and calcium concentration, critical fouling conditions were identified and will be used for fouling characterisation experiments, i.e. 12.5 mgL^{-1} DOC HA and 2.5 mM $CaCl_2$, pH 8. These 'critical conditions' are not conditions below which now fouling occurs, but rather conditions which were identified to cause most severe fouling. The occurrence of fouling is a continuum.

The effect of this feed on the different membranes was examined. Results are shown in Table 7.29 and Figure 7.26. One would expect increased deposition and flux decline for the membranes with a higher surface roughness (Elimelech *et al.* (1997)). Surface roughness contributes to increased concentration polarisation. It was shown in Figure 7.10 that the surface roughness of the three TFC membranes was similar, whereas the CA-UF membrane is a lot smoother.

The increased flux decline at higher surface roughness was verified, except for the TFC-ULP membrane. The discrepancy can be explained with the lower flux of the TFC-ULP membrane compared to the other membranes, which counteracts deposition and thus flux decline.

The TFC-SR membrane, which is the membrane with the most negative surface charge and exclusively negative functional groups (see Chapter 4 for details), showed greatest deposition, but only moderate flux decline. However, the TFC-S membrane exhibited greatest flux decline and irreversibility, possibly due to compaction effects during the experiments (see Baseline at the start of this chapter).

Table 7.29 *Effect of membrane type (12.5 mgL^{-1} DOC HA, 2.5 mM $CaCl_2$).*

Membrane	After Recycle 3 J/J_{W0}	After Experiment J_W/J_{W0}	After water Rinse J_W/J_{W0}	DOC Loss [%] ([mg])	UV_{254nm} Loss [%] ([cm^{-1}])	Calcium Loss [%] ([mg])
TFC-ULP	0.61	0.93	0.92	9 (0.11)	12 (0.065)	0.8 (1.72)
TFC-S	0.39	0.68	0.79	1 (0.016)	16 (0.09)	0.2 (0.41)
TFC-SR	0.75	0.83	0.93	15 (0.18)	16 (0.286)	1.3 (2.86)
CA-UF	0.83	0.90	0.97	6 (0.078)	10 (0.054)	0.4 (0.92)

Figure 7.27 shows electronmicrographs of the deposits formed on the different membranes. The deposits on the TFC-SR and CA-UF membranes look very similar, with a very smooth deposit, covering the membrane surface structure.

For the TFC-S membrane the deposit is very rough, indicating some crystalline precipitation. For the TFC-ULP membrane the deposit is even more porous and the membrane structure still seems visible to

some extent, although this is unlikely with the amount deposited (5 μg were estimated to be a monolayer deposit). It must be assumed that a lower flux results in a more porous deposit on the TFC-ULP membrane and, despite the high rejection, a lower irreversible flux decline than the TFC-S membrane. The deposit formed on this membrane is also looser and flux can be mostly recovered with a pure water flush.

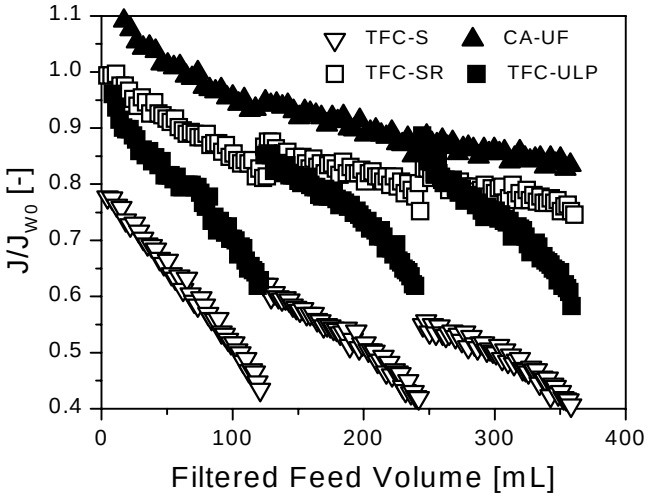


Figure 7.26 *Flux ratio for the four membranes at critical fouling conditions (12.5 mgL^{-1} HA as DOC, 2.5 mM $CaCl_2$, 1 mM Na HCO_3, 2 mScm^{-1} adjusted with NaCl).*

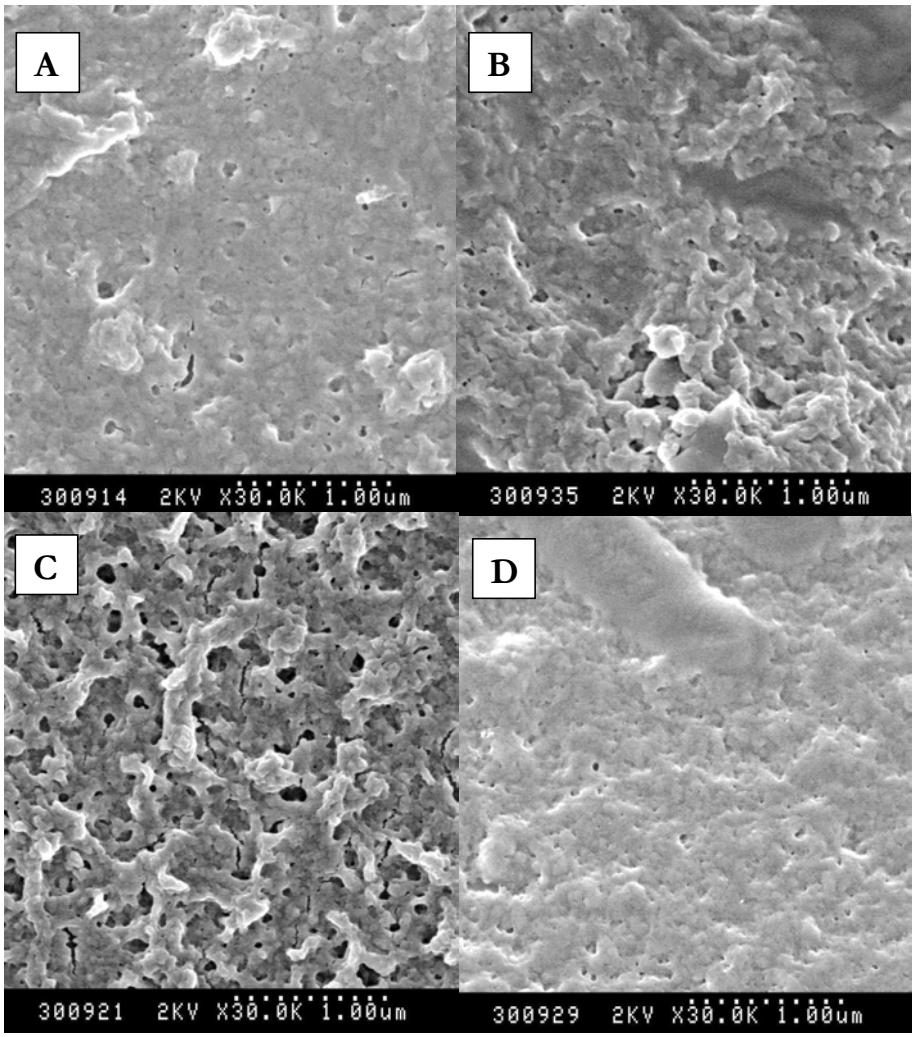


Figure 7.27 *Electron-micrographs of the membranes after recycle experiment at critical fouling conditions (12.5 mgL^{-1} HA as DOC, 2.5 mM $CaCl_2$, 1 mM Na HCO_3, 20 mM NaCl) (A) TFC-SR, (B) TFC-S, (C) TFC-ULP, and (D) CA-UF.*

7.6.5 Effect of Organic Concentration and Type

As described above, at the selected critical fouling conditions, of high calcium concentration in the presence of HA, a deposit was formed on the membrane surface. Further studies were undertaken to examine if this flux-decline-causing deposit also formed in the presence of other organics.

Figure 7.28 shows the flux ratio for the three different organics used with the TFC-S membrane. Figure 7.29 shows a comparison between flux decline for high calcium concentrations in the presence and absence of organics. Results obtained for a similar study at pH 10 are shown in Figure 7.30. The results, presented in Table 7.30, show a larger flux decline in the presence of organics compared to pure calcium, although the deposition of calcium is generally higher in the absence of organics (which can be explained by precipitation). It can be seen clearly from Figure 7.28 and Table 7.30. that the IHSS HA causes the most severe flux decline. This is similar to the result obtained at low calcium concentration.

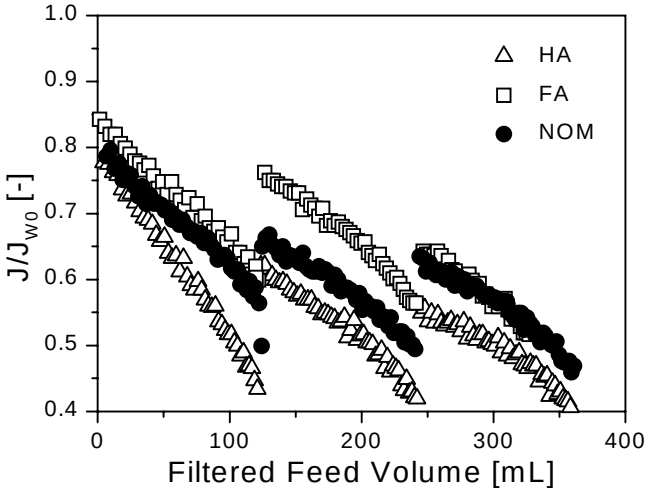


Figure 7.28 *Flux ratio for various organics (TFC-S, 2.5 mM $CaCl_2$, pH 8, 2 mS/cm, 12.5 mgL^{-1} DOC).*

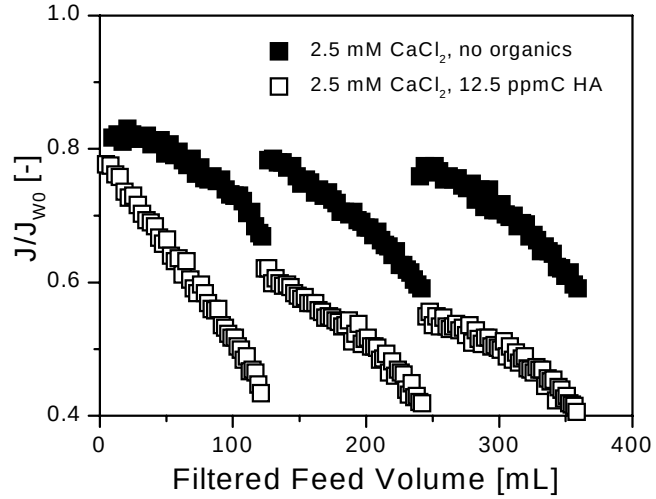


Figure 7.29 *Effect of HA on flux decline of TFC-S membrane at pH 8, with and without $CaCl_2$.*

These experiments show the effect of inhibition of calcite precipitation by the organics at pH 8. At pH 10 (Figure 7.30) the inhibition is less effective because the solubility of calcium carbonate is lower and no difference in flux can be seen. Further studies of the deposit morphologies are illustrated in section 7.8.

Comparing the deposition of calcium with the organic type, two possibilities exist: the stronger interaction between calcium and FA (rather than HA), or the higher efficiency of HA in the inhibition

of calcite precipitation. Jucker and Clark (1994) suggested stronger interaction between HA and calcium, which is also supported by the fact that more hydrophobic compounds are preferentially deposited (larger deposit of UV than DOC). The trace metal content is also generally higher in HA than in FA, which supports greater interaction between HA and calcium (Klein *et al.* (1990) and Chapter 4). Of the organics used, HA has the largest molecular weight and is more hydrophobic than FA and NOM (see Chapter 4). It is thus suggested, that HA is more efficient in the inhibition of calcite precipitation.

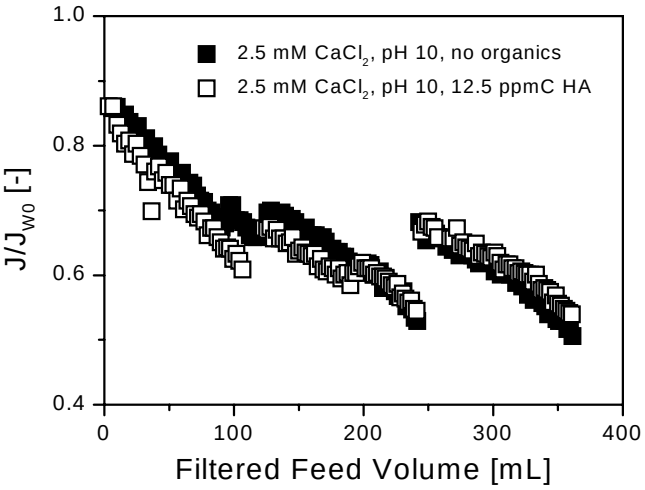


Figure 7.30 *Effect of HA on flux decline of TFC-S membrane at pH 10, with and without $CaCl_2$.*

The reason for this is the higher concentration of large molecular weight compounds in the boundary layer, which is evident from mass transfer coefficient estimations. The ks increases significantly with a decreasing size of the solute, and, therefore, the concentration polarisation in the boundary layer is significantly lower for smaller compounds.

This was supported by size exclusion chromatography of feed and concentrate samples, where a clear shift towards smaller sizes was observed due to deposition of larger compounds (see Figure 7.31). In this case, samples were taken of the feed and then of the concentrate, into which the permeate was recirculated after filtration. The difference between the two samples is the deposit on the membrane, called 'loss' in the legend. The 'loss' size distribution was calculated and was clearly shifted towards larger molecular weights showing a selective deposition.

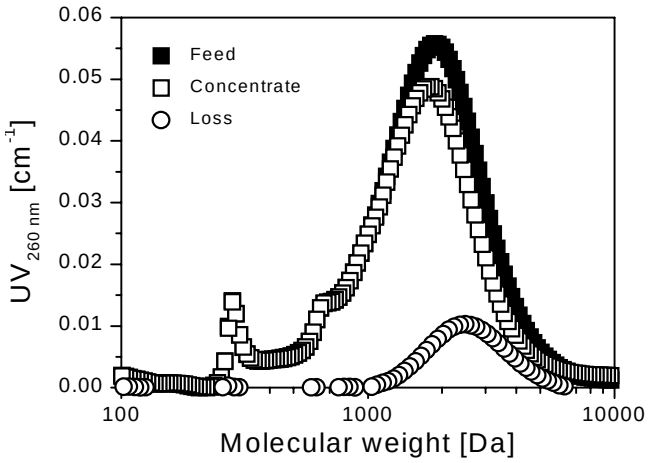


Figure 7.31 *Size exclusion result of feed, concentrate and calculated deposit on the CA-UF membrane (12.5 mgL^{-1} DOC HA, 2.5 mM $CaCl_2$).*

From the results of deposition shown in Table 7.30, it appears as if the IHSS FA forms a consistently greater deposit, with more calcium associated. The IHSS HA and Aldrich samples show a lower deposition as DOC, but a much higher deposition as UV. This indicates that it is the aromatic fraction of these samples which deposits preferentially.

Table 7.30 *Effect of organic type and concentration with TFC-S membrane (12.5 mgL^{-1} DOC, 2.5 mM $CaCl_2$).*

Organic	After Recycle 3 J/J_{W0}	After Experiment J_W/J_{W0}	After water Rinse J_W/J_{W0}	DOC Loss [%]([mg])	UV_{254nm} Loss [%] ([cm^{-1}])	Calcium Loss [%] ([mg])
NOM	0.47	0.84	0.84	2 (0.059)	14 (0.073)	1.7 (3.85)
IHSS HA	0.39	0.68	0.79	1 (0.016)	16 (0.09)	0.2 (0.41)
IHSS FA	0.42	0.88	0.90	8 (0.14)	11 (0.052)	2.7 (6.13)
Aldrich 100 kDa	0.59	0.89	1.00	2 (0.057)	61 (0.888)	0.5 (1.10)
No organic	0.61	0.98	0.93	-	-	1.9 (3.70)

The two membranes that exhibited no flux decline with FA were also tested as a function of organic type. As shown in Figure 7.32, and Figure 7.33 for the TFC-SR and CA-UF membranes, respectively, HA is the organic which causes detrimental fouling for all membranes.

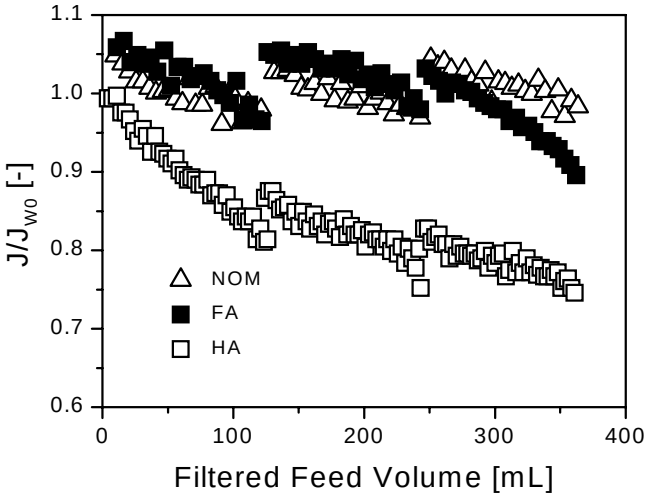


Figure 7.32 *Effect of organic type on flux decline on TFC-SR membrane (12.5 mgL^{-1} DOC, 2.5 mM $CaCl_2$, pH 8, conductivity 2 mScm^{-1}).*

Table 7.31 *Deposition and flux as a function of organic type (TFC-SR, 12.5 mgL^{-1} DOC, 2.5 mM $CaCl_2$, pH 8, conductivity 2 mScm^{-1}).*

Organic	After Recycle 3 J/J_{W0}	After Experiment J_W/J_{W0}	After Water Rinse J_W/J_{W0}	DOC Loss [%] ([mg])	UV_{254nm} Loss [%] ([cm^{-1}])	Calcium Loss [%] ([mg])
NOM	0.98	1.13	1.06	7 (0.17)	12 (0.066)	-
IHSS HA	0.75	0.83	0.93	15 (0.18)	16 (0.286)	1.3 (2.86)
IHSS FA	0.90	1.17	1.16	11 (0.21)	10 (0.043)	2.2 (1.84)

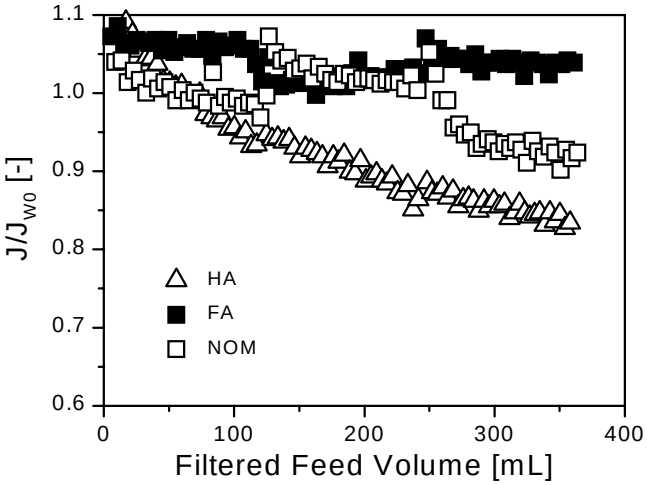


Figure 7.33 *Effect of organic type on flux decline on CA-UF membrane (12.5 mgL^{-1} DOC, 2.5 mM $CaCl_2$, pH 8, conductivity 2 mScm^{-1}).*

Table 7.32 *Deposition and flux as a function of organic type (CA-UF membrane, 12.5 mgL^{-1} DOC, 2.5 mM $CaCl_2$, pH 8, conductivity 2 mScm^{-1}).*

Organic	After Recycle 3 J/J_{W0}	After Experiment J_W/J_{W0}	After Water Rinse J_W/J_{W0}	DOC Loss [%] ([mg])	UV_{254nm} Loss [%] ([cm^{-1}])	Calcium Loss [%] ([mg])
NOM	0.92	0.99	0.96	10 (0.26)	16 (0.084)	1.3 (1.16)
IHSS HA	0.83	0.90	0.97	6 (0.078)	10 (0.054)	0.4 (0.92)
IHSS FA	1.04	1.07	1.04	13 (0.22)	14 (0.054)	-

These results lead to the conclusion that it is the hydrophobic character and the size which leads to such distinctive behaviour. As a result, the NOM was fractionated into the HA, FA, and hydrophilic fractions. The method by which these fractions were obtained was described in detail in Chapter 4. The same experiment was then carried out with these fractions, and results are shown in Figure 7.34 and Table 7.33.

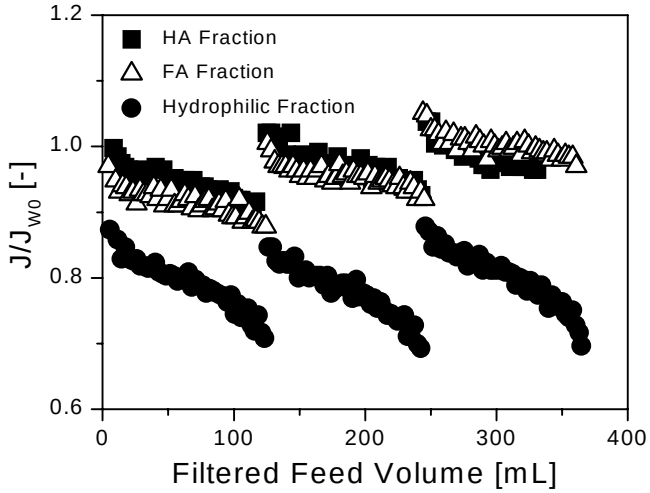


Figure 7.34 *Effect of NOM fractions on flux decline on TFC-SR membrane (12.5 mgL^{-1} DOC HA, 2.5 mM $CaCl_2$, pH 8, conductivity 2 mScm^{-1}).*

Table 7.33 *Flux and deposition of NOM fractions (TFC-SR, 12.5 mgL^{-1} DOC HA, 2.5 mM $CaCl_2$, pH 8, conductivity 2 mScm^{-1}).*

Organic	After Recycle 3 J/J_{W0}	After Experiment J_W/J_{W0}	After Water Rinse J_W/J_{W0}	DOC Loss [%] ([mg])	UV_{254nm} Loss [%] ([cm^{-1}])	Calcium Loss [%] ([mg])
NOM HA	0.96	1.15	1.13	31 (0.77)	14 (0.096)	0.7 (0.98)
NOM FA	0.97	1.19	1.14	19 (0.60)	58 (0.296)	-
NOM Hydr.	0.72	1.15	1.04	29 (0.96)	61 (0.246)	0.8 (1.55)

Only a very slight flux decline is observed for the hydrophobic fractions, FA and HA. Surprisingly, the hydrophilic fraction of NOM causes flux decline. This can probably be attributed to the high ionic strength of this fraction though (see Chapter 4 for details), especially given the high reversibility of this flux decline. The argument that the small compounds may cause pore plugging, due to their smaller size and lower rejection, cannot be supported due to the reversibility of this flux decline. This result contradicts the observations of Cho *et al.* (1998) who found both hydrophilic and hydrophobic compounds were significant foulants.

Since there seems to be a definite relationship between hydrophobicity and flux decline, this would seem to indicate that there are specific chemical characteristics of the IHSS HA, which cause the observed flux decline. The solubility of the compounds, which is related to molecular size, is most likely responsible for the difference. In fact, the sizes of the NOM fractions are not very different, although large enough for a change in rejection. The hydrophilic fraction is retained less than the FA and HA fractions (see Table 7.34).

Table 7.34 *Rejection of the NOM fractions during recycle experiments (TFC-SR, 12.5 mgL^{-1} DOC HA, 2.5 mM $CaCl_2$, pH 8, conductivity 2 mScm^{-1}).*

	DOC [%]	UV_{254nm} [%]	Calcium [%]	Sodium [%]
NOM HA	95.6	98.8	70.8	3
NOM FA	96.5	97.7	75.4	0
NOM Hydrophilic	83.8	87.3	74.0	3

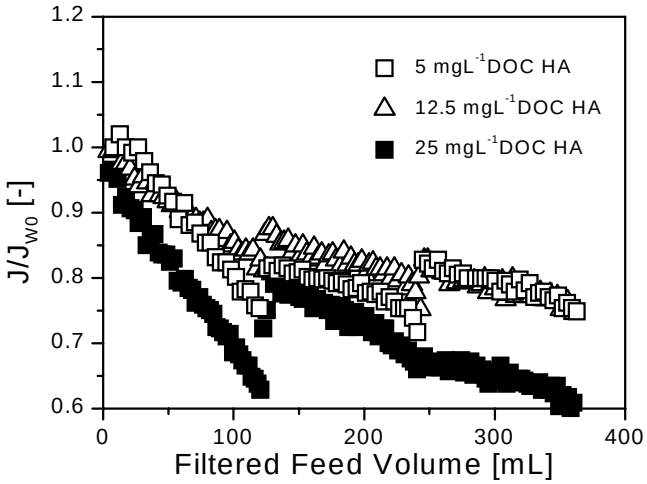


Figure 7.35 *Effect of HA concentration on flux decline of TFC-SR membrane (2.5 mM $CaCl_2$, pH 8, conductivity 2 mScm^{-1}).*

If solubility of the organic compound is critical, then deposition should increase with organic concentration. This is indeed the case, as shown in Figure 7.35 and Table 7.35. Note that this experiment was carried out with IHSS HA and the TFC-SR membrane which shows less fouling than the other membranes. The amount of cake/gel formed is limited by the amount of high molecular weight organic available. It is likely that only a certain fraction of the HA interacts strongly with cations.

Table 7.35 *Deposition and flux as a function of HA concentration (TFC-SR, 2.5 mM $CaCl_2$, pH 8, conductivity 2 $mScm^{-1}$).*

HA Concentration [mgL^{-1}] as DOC	After Recycle 3 J/J_{W0}	After Experiment J_W/J_{W0}	After Water Rinse J_W/J_{W0}	DOC Loss [%] ([mg])	UV_{254nm} Loss [%] ([cm^{-1}])	Calcium Loss [%] ([mg])
0	0.95	1.05	1.00	-	-	-
5	0.75	0.88	0.99	14 (0.09)	11 (0.30)	0.9 (0.69)
12.5	0.75	0.83	0.93	15 (0.18)	16 (0.286)	1.3 (2.86)
25	0.61	0.70	0.85	29 (1.11)	32 (0.407)	4.4 (3.75)

7.6.6 Effect of pH

The pH effects both solubility of calcium and that of organics. While the organics are more soluble at high pH, the calcium ions are more soluble at low pH and a best compromise at neutral pH values would be expected.

The results of pH on flux are presented in Figure 7.36 and Table 7.36, as well as Figure 7.37 and Table 7.37, for the TFC-S and TFC-SR membranes, respectively.

The amount of deposit on the TFC-S and TFC-SR membranes as a function of pH is shown in Figure 7.38. The deposit of organics and calcium for both membranes increases with increasing pH. If charge repulsion was the dominating effect, the deposition would be highest at low pH, when both membrane and organics have a low charge. This would also favour hydrophobic interactions. However, deposition is low at low pH (4.5), indicating that solubility effects and calcium interactions are crucial as those interactions are strongest at high pH (see Figure 7.38). At pH 8 the deposit is only loosely bound to the membrane since 50 % of the flux decline can be recovered by a water wash. At pH 4 and 10 the water wash is ineffective, indicating a strong bond between solute and membrane, as well as a dense deposit in itself (strong interactions within the cake).

Flux decline is not related to the amount of deposit, so it must be assumed that the structure of the deposit is responsible for flux decline rather than the amount. It is suggested that at pH 4.5 the organics are coiled and pack very densely on the membrane, at pH 8 complexes form a gel on the membrane that can be removed/dissolved by pure water, and at pH 10 calcite precipitation occurs, which is irreversible, but of a more porous structure. The flux prior to water wash is lowest at pH 8. The hypothesis of a different structure of the deposit was verified by electronmicrographs (see section 7.8). The greater amount of deposit on the TFC-SR membrane at pH 10 shows that deposition increases with membrane charge, which may be due to a higher attraction of calcium to the membrane surface.

The deposition and flux ratios, shown in Table 7.36, suggest that at pH 4.5 the organics that precipitate do so by interaction with calcium, as at this pH 1.23 mg of calcium also precipitates. This interaction could be simply an enhancement of the aggregation of the colloidal organics formed at this pH, as HA is not soluble at low pH. Overall, the deposition of organics at this pH is lowest, as also shown in Figure 7.38.

At pH 10 calcite precipitates and adsorbs a considerable amount of HA. This appeared in the solubility tests (see Chapter 4) as a coagulation process with observed floc formation. With the TFC-SR membrane this effect was not observed. Both organic and calcium deposition increase steadily with pH as shown in Figure 7.38 and Table 7.37. The low value for DOC on TFC-S at pH 7.5 is believed to be experimental error.

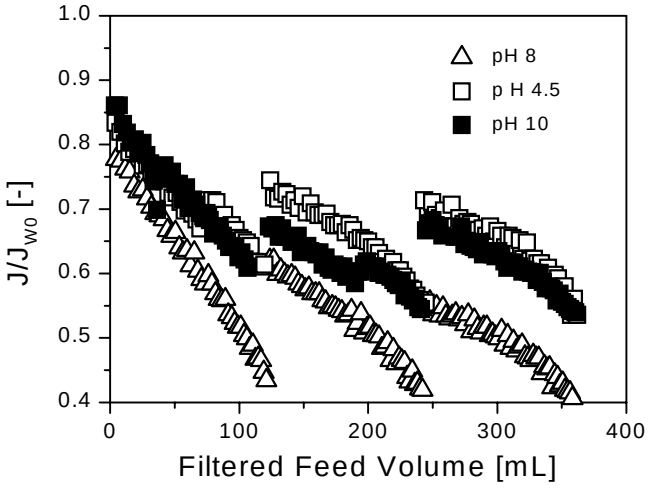


Figure 7.36 *Effect of pH on flux decline of TFC-S membrane (2.5 mM $CaCl_2$, conductivity 2 mScm^{-1}).*

Table 7.36 *Deposition and flux ratios as a function of pH (TFC-S, 2.5 mM $CaCl_2$, conductivity 2 mScm^{-1}).*

pH	After Recycle 3 J/J_{W0}	After Experiment J_W/J_{W0}	After Water Rinse J_W/J_{W0}	DOC Loss [%] ([mg])	UV_{254nm} Loss [%] ([cm^{-1}])	Calcium Loss [%] ([mg])
4.5	0.54	0.80	0.83	3 (0.04)	10 (0.064)	0.6 (1.23)
8	0.39	0.68	0.79	1 (0.016)	16 (0.09)	0.4 (0.21)
10	0.52	0.78	0.75	18 (0.227)	32 (0.168)	2.9 (5.14)

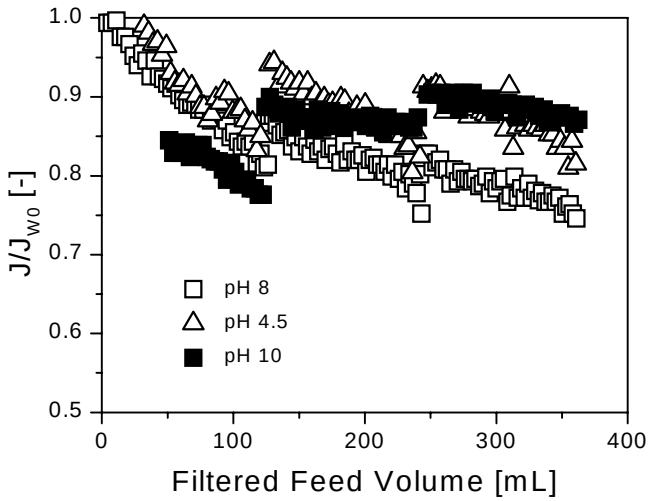


Figure 7.37 *Effect of pH on flux decline of TFC-SR membrane (2.5 mM $CaCl_2$, conductivity 2 mScm^{-1}).*

Table 7.37 *Deposition and flux as a function of pH (TFC-SR, 2.5 mM $CaCl_2$, conductivity 2 $mScm^{-1}$).*

pH	After Recycle 3 J/J_{W0}	After Experiment J_W/J_{W0}	After Water Rinse J_W/J_{W0}	DOC Loss [%] ([mg])	UV_{254nm} Loss [%] ([cm^{-1}])	Calcium Loss [%] ([mg])
4.5	0.82	0.88	0.87	6 (0.066)	9 (0.052)	0.3 (0.76)
8	0.75	0.83	0.93	15 (0.18)	16 (0.086)	1.3 (2.86)
10	0.87	0.89	0.89	30 (0.350)	46 (0.206)	1.0 (1.62)

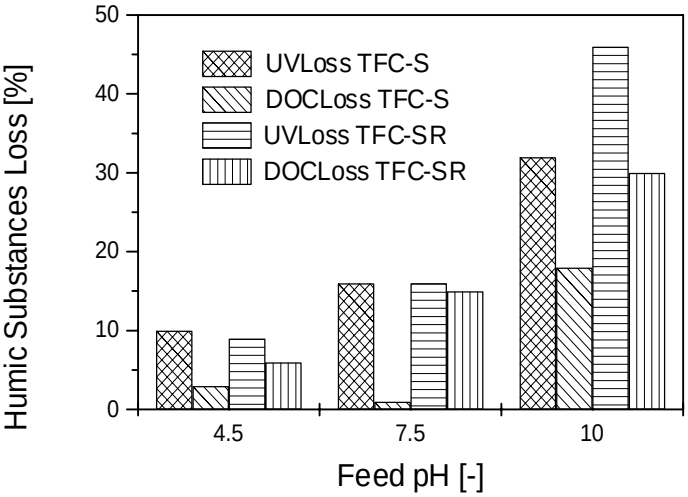


Figure 7.38 *Effect of pH on deposition of DOC and UV absorbing matter on two membranes (TFC-S and TFC-SR).*

Braghetta (1995) reported a higher flux decline at low pH due to changes in the membrane matrix, and a larger deposit at low pH due to charge neutralisation and a higher packing density of the NOM. This was a relatively hydrophobic (PS) membrane (tight UF, MWCO 1 kDa) and NOM was filtered in a phosphate buffer medium (phosphate was found to enhance membrane fouling by NOM). Braghetta however confirmed low flux decline at high pH due to the high solubility of NOM.

In all cases, more UV than DOC is deposited, showing that the high molecular weight, more hydrophobic and more aromatic compounds are preferentially depositing at all pH conditions.

7.6.7 Effect of Transmembrane Pressure

Increased transmembrane pressure causes increased flux and concentration polarisation. Permeation drag, the force which drags colloids to the membrane surface, increases with the higher imposed flux. Reduced stirring has a very similar impact since backtransport effects are reduced. The effect of pressure was examined at 12.5 mgL^{-1} HA and 2.5 mM $CaCl_2$. The results are shown in Table 7.38, Figure 7.39, and Figure 7.40. Increased pressure has a strong effect on deposition and flux. Very interestingly, the flux decline with reduced stirring (see Table 7.24) was reversible with pure water. This indicates that a large portion of the flux decline is due to concentration polarisation, whereas for increased pressure, the flux cannot be recovered. At reduced stirring levels, the boundary layer would be thicker, whereas at a higher flux the concentration in the boundary layer is increased.

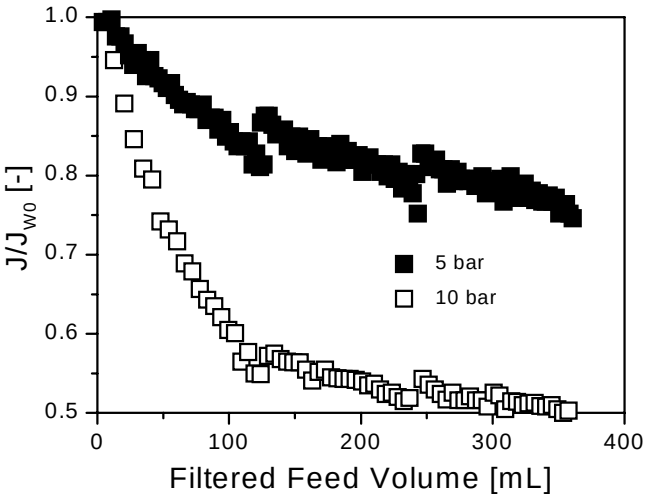


Figure 7.39 *Effect of transmembrane pressure on flux decline of TFC-SR membrane (12.5 mgL^{-1} HA and 2.5 mM $CaCl_2$, pH 8).*

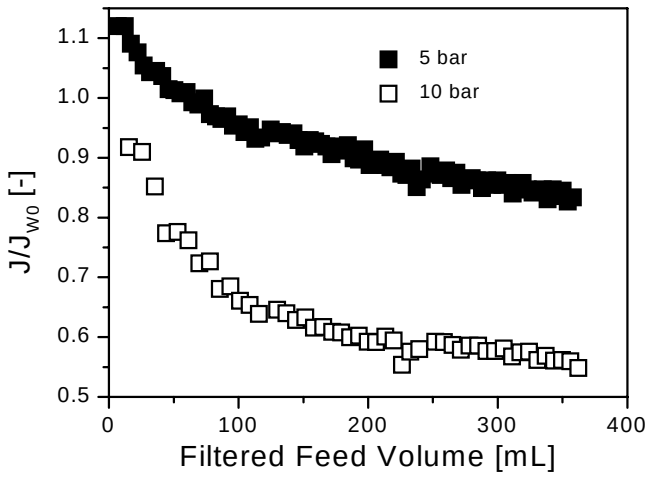


Figure 7.40 *Effect of transmembrane pressure on flux decline of CA-UF membrane (12.5 mgL^{-1} HA and 2.5 mM $CaCl_2$, pH 8).*

Table 7.38 *Effect of transmembrane pressure (12.5 mgL^{-1} HA and 2.5 mM $CaCl_2$) on flux and deposition of solute on TFC-SR and CA-UF membrane.*

Membrane	Stirring [rpm]	Pressure [bar]	After Recycle 3 J/ J_{W0}	After Experiment J_W/J_{W0}	DOC Loss [%] ([mg])	UV_{254nm} Loss [%] ([cm^{-1}])	Calcium Loss [%] ([mg])
CA-UF	400	5	0.83	0.90	6 (0.08 mg)	10	0.44 (0.92 mg)
CA-UF	400	10	0.55	0.58	13 (0.17 mg)	16	-
TFC-SR	400	5	0.75	0.83	15 (0.18 mg)	16	1.33 (2.86 mg)
TFC-SR	400	10	0.50	0.56	20 (0.32 mg)	19	-

The flux decline is larger than 40% for CA-UF and TFC-SR at a pressure of 10 bar. This may indicate the presence of a critical flux phenomenon, as previously explained for microfiltration. This is defined by Howell *et al.* (1995) as the flux below which there is no deposition of colloids on the membrane. For NF, this critical flux may be the flux below which concentration polarisation does not reach the solubility limit of the solute species or it could be the flux at which the deposition of nanometer size

colloids occurs. Such particles are small enough to cause flux decline on the membrane as described by Bhattacharjee *et al.* (1999).

To further investigate the characteristics on the organics deposited LC-OCD analysis was performed for the feed and concentrate samples at 5 and 10 bar. Experimental conditions were critical fouling conditions.

The lower peaks in the concentrate samples (note that the feed sample is diluted) indicates a deposition of organic matter. Additionally, the peaks shift to the right, which for the humics means a lower molecular weight. In fact, the IHSS HA molecular weight has shifted from initially 2747 Da to 1661 and 1664 Da at 10 and 5 bar, respectively.

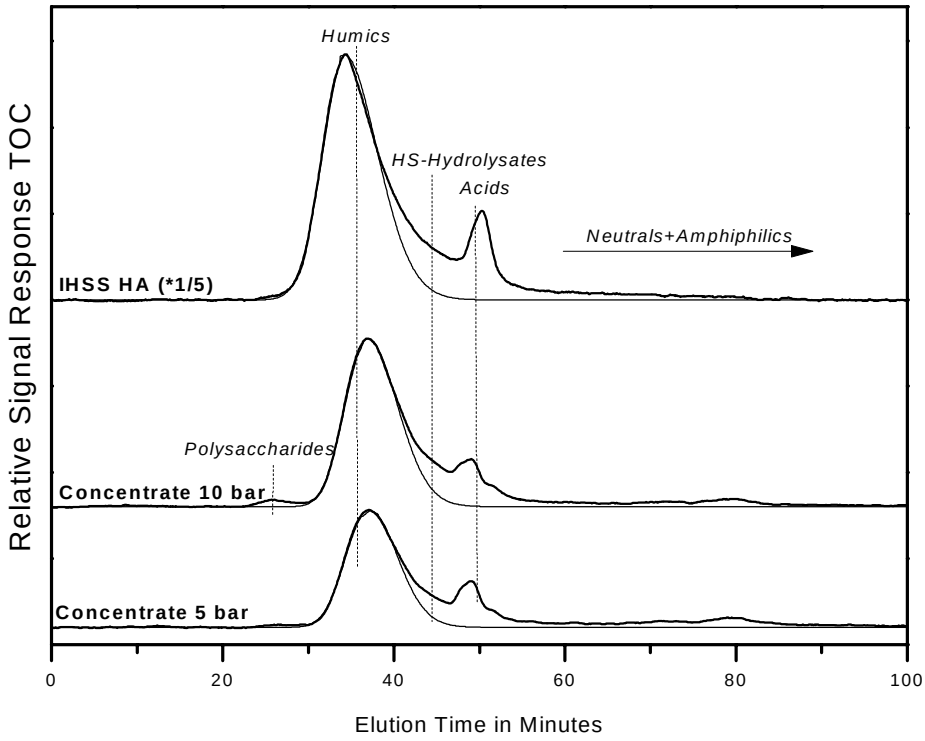


Figure 7.41 *LC-OCD results of TFC-SR membrane at critical fouling conditions and 10 bar (12.5 mgL^{-1} as DOC IHSS HA, 2.5 mM $CaCl_2$, pH 7-8).*

7.6.8 Effect of Inorganic Colloids

In the previous chapters, the effects of colloidal fouling of MF and UF membranes was thoroughly studied. Whilst the effect of these relatively large colloids on NF were not expected to be significant, a brief series of experiments were performed to check this.

The experiments were carried out at pH 3 with the two smallest colloids (see Appendix 3 for preparation and characterisation). This extreme pH was required in order to obtain stable (non-aggregating) primary colloids, rather than their aggregates in the absence of organics (see Chapter 4 for characterisation of colloidal systems). Results are shown in Figure 7.42. At pH 3 the colloids have a high positive charge. This should lead to a significant repulsion between the colloids, increased backdiffusion, and therefore lower concentration polarisation of colloids (Bhattacharjee *et al.* (1999)).

This is indeed the case. Flux decline is minimal, and for the larger particles the flux even increases slightly. Flux is generally expected to increase with particle size (see Chapter 3), but the colloids are also very large compared to the membrane "pores". A red deposit is visible on the membranes after the experiments, indicating some membrane-colloid interactions.

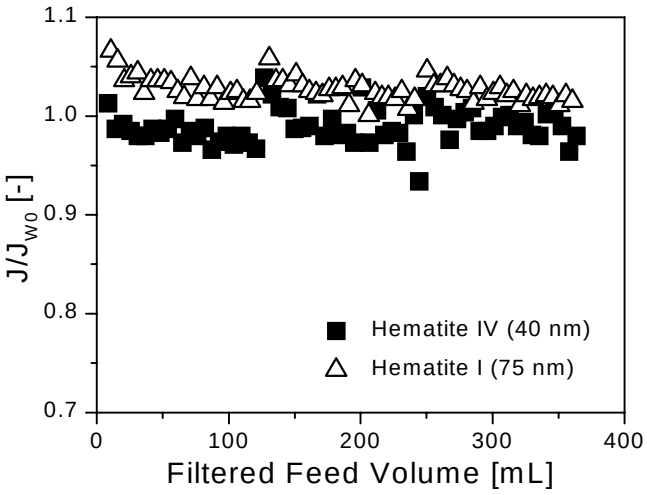


Figure 7.42 *Flux ratio for two particle sizes at pH 3 (stable colloids) with TFC-SR membrane.*

Experiments were then carried out in the OPS mixing order (colloids stabilised by organics) at pH 4.5, 8 and 10. Figure 7.43 shows the OPS colloids at pH 4.5, 8, and 10, and the relevant data are given in Table 7.39. At pH 4.5 and 8 flux declines slightly during each cycle, but is fully restored by water washing, signifying negligible fouling. Greater flux decline was observed in the absence of the colloids (Figure 7.35, Table 7.35) for 5 mgL^{-1} HA at pH 8. This is not surprising, as the colloids adsorb organics which may be responsible for flux decline (and which were precipitating with calcium in the absence of colloids).

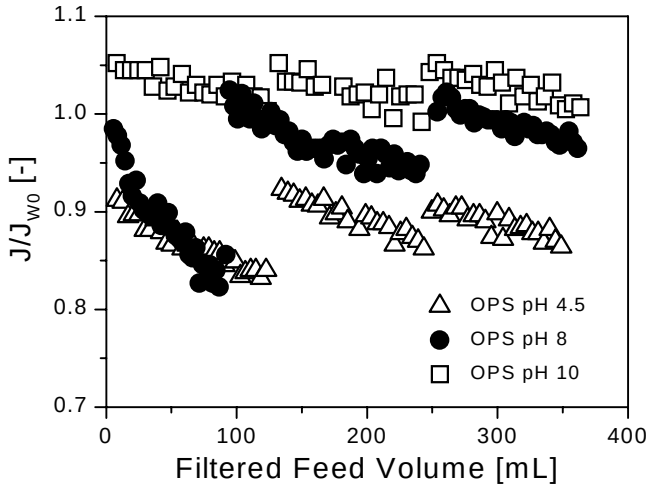


Figure 7.43 *Flux ratio for the filtration of OPS systems with TFC-SR membrane as a function of pH (Hematite I (75 nm), BGS, 5 mgL^{-1} DOC HA).*

Rejection (see Table 7.40) is highest at pH 8. This is probably attributable to the deposit morphology and charge, and requires further investigation before conclusions can be drawn.

As shown in Chapter 6 (UF), the aggregates (SPO) did not cause flux decline on the tight membranes. This was attributed to the fact that the aggregates are too large to deposit or cause flux decline. For this reason no experiments were carried out with the SPO aggregates/systems.

Table 7.39 *Flux ratios and deposition of colloids and organics on the membranes (OPS).*

pH	After Recycle 3 J/J_{W0}	After Experiment J_W/J_{W0}	After Water Rinse J_W/J_{W0}	DOC Loss [%] ([mg])	UV_{254nm} Loss [%] ([cm^{-1}])	Calcium Loss [%] ([mg])	Iron Loss [%] ([mg])
4.5	0.87	1.02	1.00	0	75 (0.551)	2.8 (0.46)	18 (0.21)
8	0.97	1.08	1.08	27 (0.176)	53 (0.434)	37.2 (3.40)	70 (1.29)
10	1.01	1.10	1.08	30 (0.217)	66 (0.486)	1.4 (0.24)	17 (0.20)

Table 7.40 *Rejection of DOC, UV_{254nm} and cations during colloid filtration (OPS).*

pH	DOC [%]	UV_{254nm} [%]	Calcium [%]	Sodium [%]
4.5	68.5	98.8	89.2	0
8	85.2	98.6	85.5	76
10	63.4	99.2	55.0	1

7.7 COAGULATION PRETREATMENT

Coagulation using ferric chloride was used in MF and UF to increase organic rejection. The interest in NF is to examine the effect of ferric chloride on the membrane flux and to assess if the presence of amorphous iron hydroxide particles causes severe flux decline.

7.7.1 Effect of Organic Type

The effect of organic type was studied under identical conditions to those used in the MF and UF studies. As shown in Figure 7.44A and B, flux decline does not depend on organic type (HA, FA or NOM), but is affected by ferric chloride concentration (25, 100 mgL^{-1}). The flocs formed at 25 mgL^{-1} $FeCl_3$ do not cause any significant flux decline for any of the organics. At 100 mgL^{-1} $FeCl_3$, an osmotic pressure effect is apparent (the initial flux ratio is 0.9) and a definite flux decline is observed. The osmotic pressure increases as particles are smaller and have a higher charge, which is expected at such a high dosage.

This effect is attributed to the presence of highly charged colloidal iron oxyhydroxide species. The pH was not adjusted after $FeCl_3$ addition and at the high dosage no visible flocs formed.

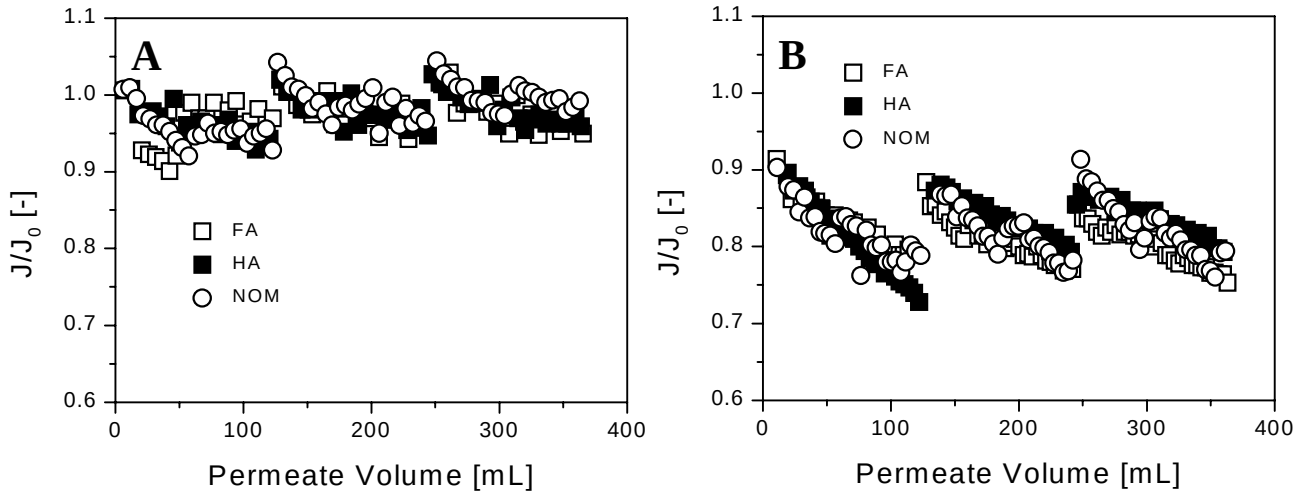


Figure 7.44 *Effect of organic type on coagulation (A) 25 mgL^{-1} $FeCl_3$ (pH 7) and (B) 100 mgL^{-1} $FeCl_3$ (pH 3). TFC-SR, 5 mgL^{-1} DOC.*

The deposition and flux ratios are shown in Table 7.41 and rejection in Table 7.42. The extent of organics deposition in these experiments is difficult to measure as the initial concentration was low (5 mgL^{-1} DOC). However, it is clear that the flux decline is minimal in the 25 mgL^{-1} $FeCl_3$ case, and fully reversible even at 100 mgL^{-1} $FeCl_3$, which confirms concentration polarisation effects.

The rejection shows significant variations depending on the $FeCl_3$ dosage. At 25 mgL^{-1} $FeCl_3$, when flocs are relatively neutral and large, the DOC rejection is about 70%, UV rejection is complete (due to the UV absorbing characteristics of the fully retained iron), calcium rejection varies from 40 to 60%, and sodium rejection is zero. In the case of 100 mgL^{-1} $FeCl_3$, when the flocs are small and positively charged, DOC rejection drops to about 45%, UV rejection is complete, calcium rejection increased to >90%, and sodium rejection increased to about 30%.

These results suggest that the positively charged deposit of small ferric hydroxide flocs induces cation rejection due to its positive charge. DOC is retained less than in the absence of ferric chloride, most likely due to the presence of a thick concentration polarisation layer that reduces rejection.

Rejection results for the TFC-SR membrane in the absence of $FeCl_3$ were also shown in Table 7.11.

Table 7.41 *Deposition and flux as a function of organic type and $FeCl_3$ concentration (25 mgL^{-1} $FeCl_3$ or 100 mgL^{-1} $FeCl_3$, TFC-SR, 5 mgL^{-1} DOC).*

	After Recycle 3 J/J_{W0}	After Experiment J_W/J_{W0}	After Water Rinse J_W/J_{W0}	DOC Loss [%] ([mg])	UV_{254nm} Loss [%] ([cm^{-1}])	Calcium Loss [%] ([mg])	Iron Loss [%] ([mg])
25 FA	0.97	1.04	1.03	36 (0.55)	21 (0.083)	3.8 (0.65)	3.0 (0.036)
25 HA	0.97	1.14	1.06	40 (0.68)	-	-	2.0 (0.022)
25 NOM	0.98	1.10	1.05	-	-	-	-
100 FA	0.76	1.07	1.02	-	-	-	-
100 HA	0.80	1.06	1.04	47 (0.29)	26 (0.234)	2.0 (0.32)	12 (0.56)
100 NOM	0.77	1.10	1.03	-	-	-	-

Table 7.42 *Rejection as a function of organic type and $FeCl_3$ concentration (25 mgL^{-1} $FeCl_3$ or 100 mgL^{-1} $FeCl_3$, TFC-SR, 5 mgL^{-1} DOC).*

	DOC [%]	UV_{254nm} [%]	Calcium [%]	Sodium [%]
0 FA	94	96	68	36
0 HA	74	98	63	19
0 NOM	69	97	74	40
25 FA	72.4	94.6	44.3	0
25 HA	69.4	93.8	71.2	0
25 NOM	68.8	96.7	63.4	0
100 FA	45.1	99.7	96.1	31.2
100 HA	45.9	98.4	93.2	31.4
100 NOM	47.6	96.8	93.7	21.9

7.7.2 Effect of Ferric Chloride on Treatment of Solutions containing Colloids and HA

Colloids and aggregates are present in natural waters. The systems used were described in Chapter 4, and their MF and UF filtration behaviour described thoroughly in Chapters 5 and 6, respectively.

In NF, the presence of stable colloids (OPS) and 25 mgL^{-1} $FeCl_3$ results in little flux decline as in the absence of colloids (see Figure 7.45). At 100 mgL^{-1} $FeCl_3$ the flux is lower, and this indicates greater concentration polarisation effects due to the built-up of a particle layer. In the case of aggregates (SPO), there is strictly no flux decline and even a slight flux increase at low $FeCl_3$ concentration. At high $FeCl_3$ concentration the flux is also higher than in the absence of aggregates.

In MF, it was found that the presence of SPO aggregates loosens the structure of the cake. Here the relatively large aggregates possibly act as turbulence promoters, which disturb the formation of a thick boundary layer.

Table 7.43 and Table 7.44 show flux ratios, deposition, and rejection in the presence of colloids. Deposition is overall high and flux decline remains fully reversible. Rejection shows similar patterns for calcium and sodium as in the absence of colloids. DOC rejection is about 30% except at low $FeCl_3$ concentration with OPS colloids.

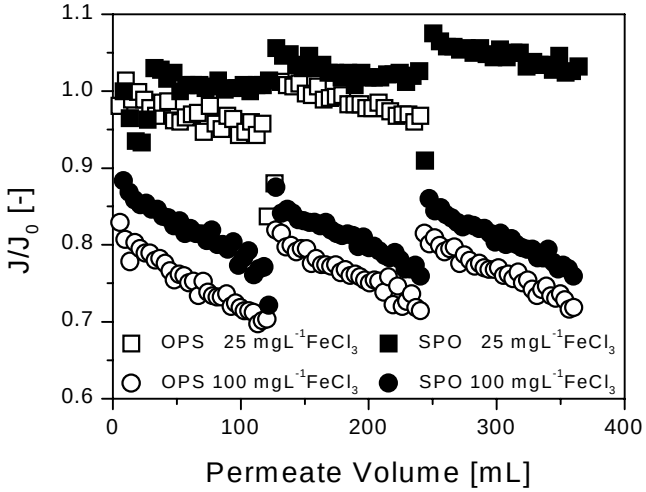


Figure 7.45 *Ferric chloride addition in the presence of stabilised (OPS) and aggregated (SPO) colloids (TFC-SR membrane, 2.5 mM $CaCl_2$, 5 mgL^{-1} DOC HA, 10 mgL^{-1} hematite (75 nm)).*

Table 7.43 *Deposition and flux as a function of colloid aggregation state and $FeCl_3$ concentration in the presence of colloids (25 mgL^{-1} $FeCl_3$ or 100 mgL^{-1} $FeCl_3$, TFC-SR, 5 mgL^{-1} DOC).*

	After Recycle 3 J/J_{W0}	After Experiment J_W/J_{W0}	After Water Rinse J_W/J_{W0}	DOC Loss [%] ([mg])	UV_{254nm} Loss [%] ([cm^{-1}])	Calcium Loss [%] ([mg])	Iron Loss [%] ([mg])
OPS 25	0.95	1.00	0.99	71 (0.73)	93 (1.54)	4.8 (0.86)	17 (0.47)
OPS 100	0.72	1.05	1.00	57 (0.40	-	1.8 (0.33)	12 (0.62)
SPO 25	1.04	1.11	1.11	65 (0.43)	45 (0.21)	5.7 (1.07)	-
SPO 100	0.77	1.05	1.02	47 (0.35)	57 (1.41)	2.8 (0.48)	10 (0.55)

Table 7.44 *Rejection as a function of colloid aggregation state and $FeCl_3$ concentration (25 mgL^{-1} $FeCl_3$ or 100 mgL^{-1} $FeCl_3$, TFC-SR, 5 mgL^{-1} DOC).*

	DOC [%]	UV_{254nm} [%]	Calcium [%]	Sodium [%]
25 OPS	66.2	99.0	70.2	0
100 OPS	30.9	99.2	96.2	17.5
25 SPO	37.8	98.8	70.6	1.2
100 SPO	32.9	97.6	94.9	36.7

7.7.3 Effect of Ferric Chloride Addition at Critical Fouling Conditions

Ferric chloride precipitates in solution as amorphous ferric oxyhydroxide and the colloids formed adsorb organics. The interest in adding ferric chloride to the solutions is to remove the organics which were found to cause irreversible fouling due to adsorption on the membrane and precipitation with calcium on the membrane surface.

Aggregates formed in the bulk solution or colloids that adsorb organics do not cause irreversible fouling, compared to organic-calcium complexes, which form a gel precipitate in the boundary layer. In the case of coagulation this results overall in larger colloid sizes. Naturally, this results in a higher flux, due to the lower specific resistance of the cake formed, or an overall more porous structure of the deposit. This theory was confirmed with the addition of $FeCl_3$. Figure 7.46 shows the dramatic impact of $FeCl_3$ on flux improvement. The $FeCl_3$ indeed removes the organics which precipitate on the membrane.

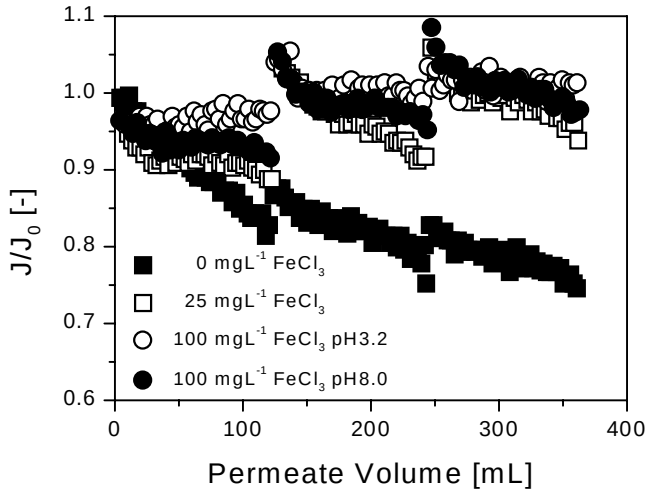


Figure 7.46 *Ferric chloride addition at critical fouling conditions (TFC-SR membrane, 2.5 mM $CaCl_2$, 12.5 mgL^{-1} DOC HA).*

$FeCl_3$ readily complexes or adsorbs the large organics (see Chapter 5), which were shown to be the organics causing most flux decline in NF. Deposition of iron is lower at pH 8, when the flocs are larger and of a lower charge. There is apparently a charge effect, since at pH 3 when the colloids are smaller and highly charged, less organics deposit (Table 7.45). The rejection of iron at pH 3 is low (0.34 mgL^{-1} iron in permeate), while in all other experiments no iron was detected in the permeate. This is expected since Fe is slow to hydrolyse at pH 3.

The deposit gives the membrane a positive charge (a bare membrane is slightly positive at pH 3 (Figure 7.4) when clean, but expected to become negative in the presence of organics (Childress and Elimelech (1996)) and the rejection changes. Calcium and sodium rejection both increase considerably under these conditions (Table 7.46). This confirms that ions are retained by charge effects. The deposition of calcium is lower at pH 3. The sodium rejection drops to below zero when the pH at 100 mgL^{-1} $FeCl_3$ is adjusted from pH 3 to pH 8. This indicates some 'pumping' effect, possibly due to the lower concentration of hydrogen ions at this pH.

The extent of organics deposition depends on the iron concentration. This is similar to the effects observed with calcium concentration, except that no flux decline is observed with $FeCl_3$. This may indicate that the structure of the complexes formed is different due to the higher charge of the iron colloids. In the next section deposit morphology studies are reported.

Table 7.45 *Deposition and flux as a function of $FeCl_3$ concentration (TFC-SR, 12.5 mgL^{-1} DOC HA, 2.5 mM $CaCl_2$, 2mScm^{-1}).*

$FeCl_3$ [mgL^{-1}]	After Recycle 3 J/J_{W0}	After Experiment J_W/J_{W0}	After Water Rinse J_W/J_{W0}	DOC Loss [%] ([mg])	UV_{254nm} Loss [%] ([cm^{-1}])	Calcium Loss [%] ([mg])	Iron Loss [%] ([mg])
0 pH 8	0.75	0.83	0.93	15 (0.18)	16 (0.086)	1.3 (2.86)	5.4 (6.7)
8 pH 8	1.02	1.05	1.04	43 (0.62)	74 (0.65)	9.3 (1.4)	16 (0.07)
25 pH 8	0.97	1.20	1.12	49 (0.52)	-	5.4 (6.7)	4 (0.056)
100 pH3	0.71	1.17	1.03	65 (0.66)	32 (0.172)	0.5 (0.58)	14 (0.61)
100 pH8	0.97	1.20	1.14	73 (1.52)	81 (0.67)	14 (0.61)	9.3 (18.4)

Table 7.46 *Rejection as a function of colloid aggregation state and $FeCl_3$ concentration (25 mgL^{-1} $FeCl_3$ or 100 mgL^{-1} $FeCl_3$, TFC-SR, 5 mgL^{-1} DOC).*

$FeCl_3$ Concentration [mgL^{-1}]	DOC [%]	UV_{254nm} [%]	Calcium [%]	Sodium [%]
0 pH 8	93.0	100	55.0	24
8 pH 8	99.0	96.5	58.1	10.4
25 pH 8	93.7	97.9	82.6	3
100 pH 3	79.0	98.5	98.5	42.7
100 pH 8	90.6	99.2	83.8	-12

7.7.4 Permeate LC-OCD Analysis

The DOC rejection varies in the presence of colloids or ferric chloride. While in the absence of colloids the TFC-SR membrane rejects 74% of IHSS HA at pH 8 (Table 7.11). With a ferric chloride dosage of 25 mgL^{-1} this HA rejection is reduced to 69% and at a dosage of 100 mgL^{-1} to 46% (Table 7.42). In the presence of OPS colloids (no ferric chloride) the rejection is 85% (Table 7.40).

To investigate the selective deposition of removal of specific organic compounds LC-OCD analysis of the permeates was carried out. The results are presented in Figure 7.41.

At the high ferric chloride dosage the rejection of humics is complete, while at the low dosage and in the presence of stable colloids (OPS) a small amount of humics permeates through the membrane. LMW acid retention at the high dosage is low. One hypothesis (which requires further investigation) is that the non-hydrolysed ferric chloride complexes with the acids or causes charge neutralisation, which reduces retention. Huber (1998) explains this with a destruction of the acidic hull of such compounds under certain conditions. The hydrolysates are not retained with the ferric chloride pretreatment and can generally not be retained in flocculation processes. Polysaccharides are destabilised in the flocculation process and thus better retained with the flocculation pretreatment.

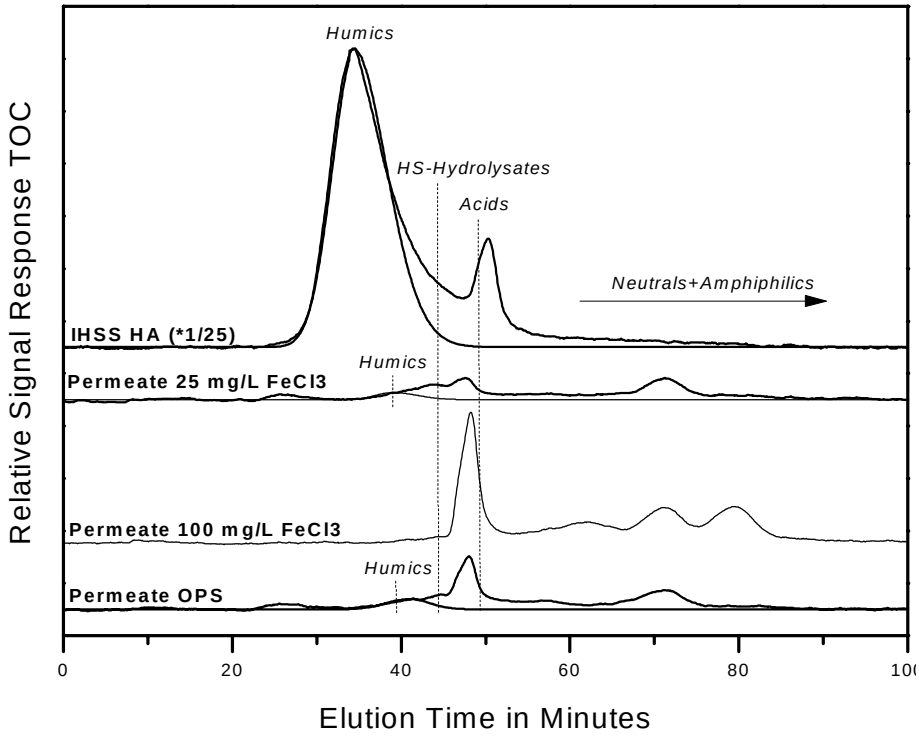


Figure 7.47 *LC-OCD analysis of permeate samples of ferric chloride pretreated NF and with feedwater containing OPS colloids compared to feed HA characteristics for TFC-SR membrane.*

7.7.5 Suggested Mechanisms

To explain the results in the previous sections some possible mechanisms are suggested, which are partly a repetition from Chapter 3. The pores of a NF membrane are in the order of 1 nm. Solutes larger than these pores are rejected by a size exclusion mechanism. Solutes much smaller than these pores are rejected if the charge is the same as that of the membrane, and the higher the charge the stronger the rejection. This explains the selectivity of NF between monovalent ions, like sodium, and multivalent ions, such as calcium or iron. Figure 7.48 shows a schematic of this latter mechanism.

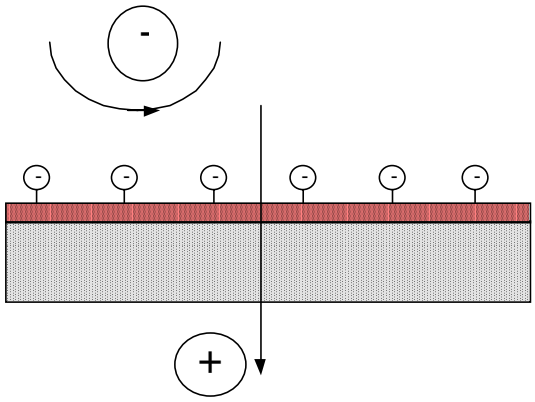


Figure 7.48 *Charge rejection mechanism in nanofiltration.*

If solutes are rejected, their boundary layer concentration increases due to a balance between backdiffusion into the bulk and convection to the membrane with the feed (concentration polarisation; Figure 7.49A). When a deposit of solids accumulates on the membrane surface, as is expected during

ferric chloride treatment, the thickness of the unstirred boundary layer increases (see Figure 7.49B). This means the concentration of solutes at the membrane surface increases and the overall rejection decreases. However, if the solids deposit has a positive charge (which is the case for the ferric hydroxide precipitates) then an additional barrier is added to the membrane. Solutes now have to pass through a positively charged and a negatively charged barrier, and the overall rejection will increase for some compounds.

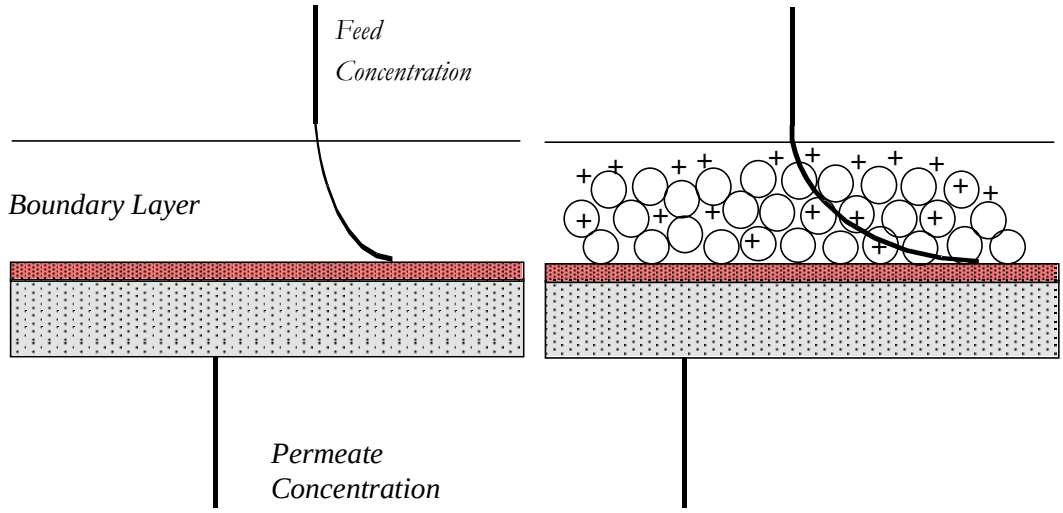


Figure 7.49 *Boundary layer and concentration profile (A) during NF without solids and (B) with an accumulation of positively charge solids.*

These phenomena explain the changes in rejection observed due to ferric chloride pretreatment. Calcium and sodium rejection increase when small (10nm, Lo and Waite (1998)) are deposited on the membrane. However, this barrier decreases the rejection of DOC. This can be explained with the increased concentration polarisation effect. The concentration of DOC in the boundary layer would increase and, due to the organics being a mixture of compounds of different sizes, the small organics permeate through the membrane at a higher rate.

7.8 MEMBRANE DEPOSIT MORPHOLOGY STUDIES

7.8.1 Electronmicroscopy

Electronmicrographs of clean membranes were shown in Figure 7.10. The deposits formed at critical fouling conditions were shown in Figure 7.27. In this section further electronmicrographs as a function or organic type, pH and calcium concentration are shown.

Effect of Organic Type

The characteristics of the organics used are presented in Chapter 4. Figure 7.50A, Figure 7.50B, and Figure 7.50C show the deposit of NOM, FA and Aldrich 100 kDa permeate, respectively, on a TFC-S membrane. The results compare with Figure 7.51B for IHSS HA. For IHSS HA and the Aldrich sample, a thick cake deposit is visible. This can be explained by the high aromaticity and molarity of these samples (see Chapter 4).

For both NOM and IHSS FA (both considerably smaller and less aromatic organics than IHSS HA), the membrane structure is still visible. This confirms that there is only minimal deposition of these compounds.

Effect of Calcium Concentration

The thickness of the deposit increases with calcium concentration, which confirms the mass balance results. Electron micrographs of calcium concentrations of 0.5, 2.5, and 4 mM are shown in Figure 7.51A, B, and C, respectively. At 0.5 mM, no deposit can be identified (compare electronmicrograph of clean membrane in Figure 7.10B). At 2.5 mM, the deposit is thick and relatively smooth, although some porous crystals are visible. At 4 mM the deposit becomes very rough. Large "lumps" are visible. It appears that if the precipitates form larger aggregates. This explains the higher flux shown in Figure 7.21, and demonstrates the effect of deposit structure on the flux.

The electronmicrographs confirm the results of the wall concentration estimation - the solutes surpass their solubility limit and form a solid deposit on the membrane.

Effect of pH

At pH 10 in the absence of organics, large (up to 5 μm, square) calcite crystals are visible (Figure 7.52A). These crystals are very large (note that the length scale of the electronmicrograph is different for these three photos). The size of the crystals explains the high flux observed despite a high calcium deposition.

In the presence of organics, aggregated spherical colloids of about 100 nm can be seen. The organics influence the precipitation of the calcite and change the shape of the crystals, which explains the observed difference in flux. At pH 8 (see Figure 7.52B) the calcite crystals are smaller than at pH 10 and more organics appear to be associated with the deposit.

At pH 4.5 the deposit is smoother. As expected, no calcite precipitation is evident due to the high solubility of calcium carbonate at this pH (Figure 7.52C).

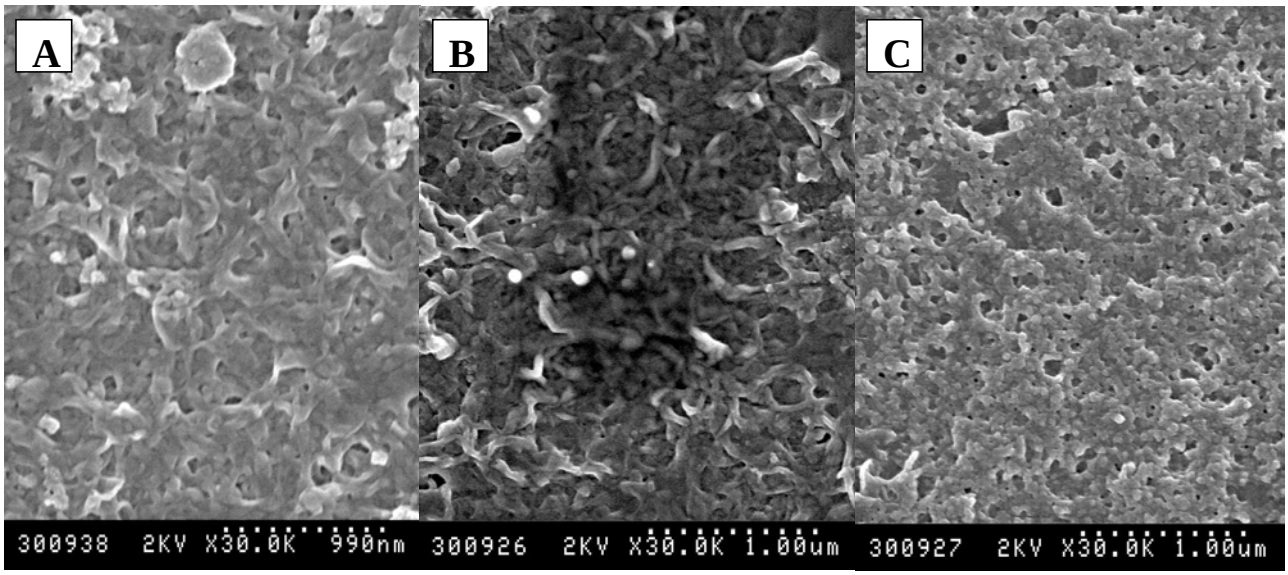


Figure 7.50 *Variation of deposit as a function of organic type at critical fouling conditions on TFC-S membrane (A) NOM, (B) FA, and (C) Aldrich 100 kDa permeate (12.5 mgL^{-1} DOC, pH 8, 2.5 mM $CaCl_2$).*

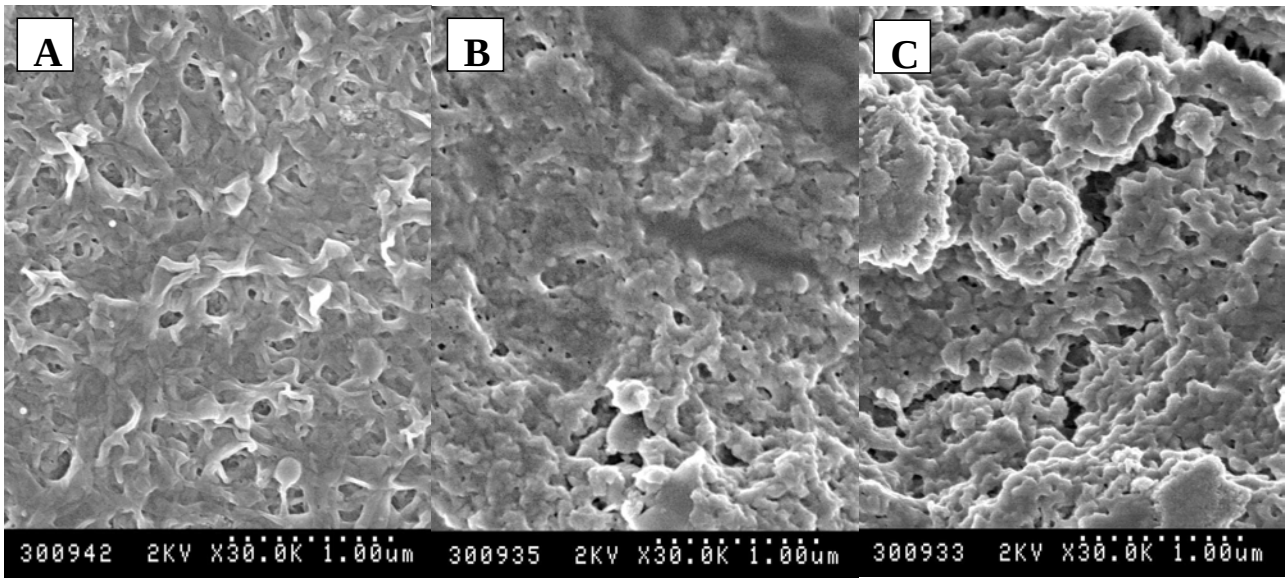


Figure 7.51 *Electronmicrographs of TFC-S membrane deposits as a function of calcium concentration (A) 0.5 mM, (B) 2.5 mM, and (C) 4 mM (12.5 mgL^{-1} DOC HA, pH 8).*

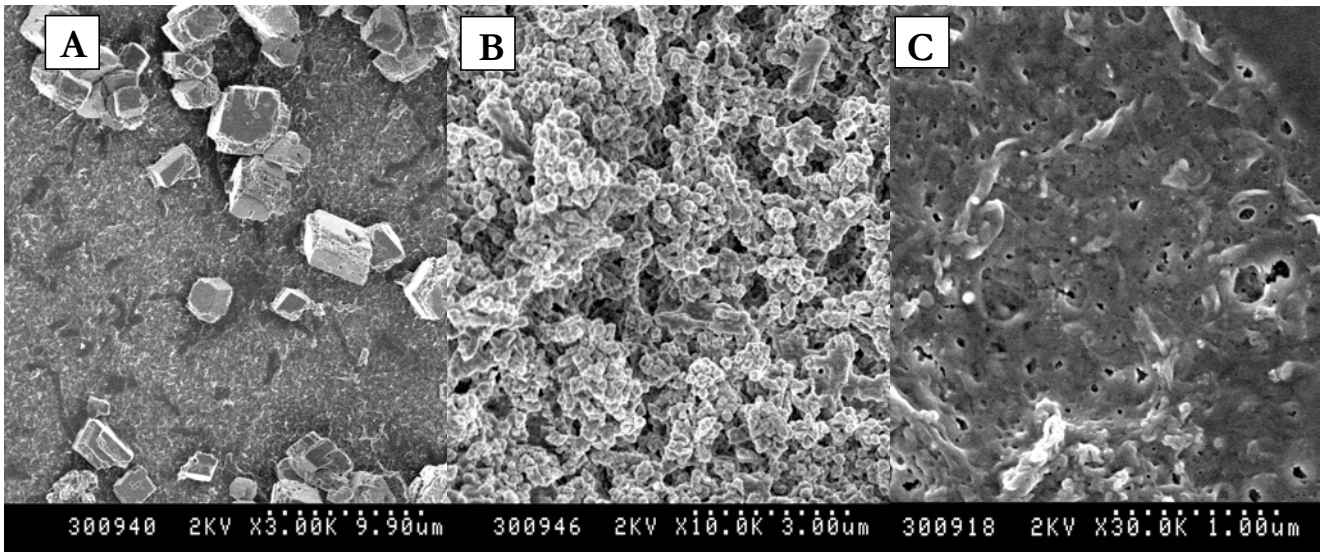


Figure 7.52 *Electronmicrographs (A) calcite crystals (pH 10, 2.5 mM $CaCl_2$),(B) calcite and organic aggregates (12.5 mgL^{-1} DOC HA, pH 10, 2.5 mM $CaCl_2$), and (C) smooth deposit at pH 4.5 on TFC-S membrane (12.5 mgL^{-1} DOC HA, 2.5 mM $CaCl_2$); (note the different magnifications according to different object sizes).*

7.8.2 XPS Analysis

XPS analysis was carried out on the TFC-S membranes with a calcite deposit, calcium-humate flocs, and on clean membranes, calcium-humate precipitates, and pure HA. No calcium was found on the clean membrane. The identification of peaks is difficult, due to the complexity of the structure of humic acid and the similarity to the membrane (carboxylic groups). Jucker and Clark (1994) suggested the presence of a Ca-humic bond in their measurements at 349.8 eV. This result was confirmed with the calcium-humate complex sample of this study (349.6 eV). On the membranes the chemical shift is different, possibly indicating the presence of a calcite precipitate (346.7 eV) and a calcium-humate complex, but the peaks cannot be resolved due to the small amount of calcium present.

Table 7.47 *XPS results for various samples; composition in % mass concentration.*

Sample	C [%]	O [%]	N [%]	Ca [%]	Cl [%]	Ca chemical shift [eV]
TFC-S (clean)	57	26	10	0	5	N/A
IHSS HA (pure)	54	41	1	1	0	352.4
IHSS HA + Ca	61	20	0	7	10	349.6
Calcite	-	-	-	-	-	346.7
TFC-S+HA+Ca	66	27	5	3	0	347.7
TFC-S+Ca	67	21	10	1	1	348.3

7.8.3 Contact Angle

The adsorption or deposition of organics changes the surface of the membranes. A change in hydrophobicity is therefore expected. It is often reported that hydrophilic membranes reduce adsorption (Gourley *et al.* (1994), Jucker and Clark (1994)). Table 7.48 shows contact angles for different membranes after recycle experiments at fouling conditions.

Table 7.48 *Contact angles of the membranes at critical fouling conditions (12.5 mgL^{-1} as DOC HA, 2.5 mM $CaCl_2$, pH 8).*

Membrane	TFC-SR	TFC-S	TFC-ULP	CA-UF
Contact Angle (clean) [^{0}]	13.1 ± 6.4	52.8 ± 2.9	40.9 ± 2.1	54.0 ± 7.1
Contact Angle (fouled) [^{0}]	34.9 ± 5.8	43.8 ± 4.8	-	55.0 ± 9.0

Comparing the contact angles of membranes with a deposit in Table 7.48 with the contact angles of the clean membranes, it can be seen that the membrane type determines whether the organics render the membrane more hydrophilic or more hydrophobic. The TFC-SR membrane, which is a very hydrophilic membrane, is made more hydrophobic by the HA. For the more hydrophobic TFC-S membrane the opposite is true, while the hydrophobicity of the CA-UF membrane remains more or less unchanged. Combe *et al.* (1999) confirmed the dependence on the membrane material with their finding that different bonds are involved for TFC and CA membranes. A hydration layer, which was found responsible for a decrease in the effectiveness of long-range (non-polar) forces, is formed less on hydrophobic membranes. These authors also found that dipole interactions are an important factor in HS adsorption. However, the hydrophobicity of the membrane was not affected by the foulant. This contradicts the findings in this study in addition to the results of Jucker and Clark (1994), who reported a decrease of hydrophobicity of the membranes due to the deposit. Jucker and Clark used hydrophobic membranes and the results confirm the findings of this study.

Table 7.49 *Contact angles of the TFC-S membrane as a function of organic type and calcium concentration (12.5 mgL^{-1} as DOC organic, pH 8).*

Contact Angle [^{0}]	HA	FA	NOM
0.5 mM $CaCl_2$	53.2 ± 4.2	-	42.4 ± 3.4
0.5 mM $CaCl_2$, no NaCl	53.3 ± 6.9	60.0 ± 6.0	-
1.25 mM $CaCl_2$	53.5 ± 4.2	-	-
2.5 mM $CaCl_2$	43.8 ± 4.8	53.5 ± 5.5	49.9 ± 3.0

The higher hydrophobicity of the deposit using FA, as shown in Table 7.49, is surprising. FA at 2.5 mM $CaCl_2$ on the TFC-SR membrane showed a contact angle of 51.5 ± 3.6^0 and confirms the trend observed with the TFC-S membrane. Increasing the FA concentration from 12.5 to 25 mgL^{-1} as DOC leads to a further increase of contact angle to 63.0 ± 2.8^0.

7.9 SUMMARY

Rejection and fouling analysis in NF is more difficult than that of more open membranes such as MF and UF due to an increased interplay of colloids and natural organics with salt, which is retained to a greater extent. Osmotic effects become important.

A detailed investigation into the effect of different salt components on membrane charge revealed that adsorption of anions plays a major role. The charge (measured as zeta potential) was highest at high ionic strength.

Cation rejection confirmed the RO nature of the TFC-S and TFC-ULP membranes, with a high rejection of Na and Ca. On the other hand, the CA-UF membrane confirmed the UF nature, with very low Na and Ca rejections. The TFC-SR membrane can be seen as a 'real' NF membrane, exhibiting a high Ca but low Na rejection. This salt rejection reflected itself in the flux behaviour – high salt rejection ultimately lead to lower fluxes due to the high osmotic pressures in the boundary layer.

Neither organic type nor pH had a measurable effect on rejection. This indicates that the organics are too large for molecular conformation or charge repulsion to play a major role. Size exclusion dominates the bulk rejection measured as DOC. A more detailed analysis of the permeate organics, however, revealed that charge does play a role for the low molecular weight acid fraction. At pH 10, where charge repulsion is maximised, the permeate concentration in these low molecular weight acids is lowest. DOC measurements failed to detect this difference due to the high content of organics, such as humics, which are retained by size exclusion. Rejection decreased for unstirred conditions and increased when the membranes were fouled. In the unstirred conditions the reduced rejection is due to concentration polarisation effects, while the fouling changes the membrane surface charge and effective pore size.

Prior to fouling studies, a number of effects needed to be estimated in order to allow interpretation of the fouling mechanisms. Firstly, adsorption on the membranes was estimated assuming monolayer adsorption. The estimates achieved results that were very close to literature values of static adsorption, and were generally very low. Such adsorption could not explain the large amounts of deposits observed during filtration.

Secondly, concentration polarisation and mass transfer coefficients were used to estimate expected wall concentrations of calcium and organics. Concentrations of large organic compounds were indeed likely to reach their solubility limit in the vicinity of the membrane. This supported the hypothesis of a deposition/precipitation rather than chemical adsorption.

Fouling experiments confirmed the hypothesis of precipitation. Large compounds, which are slower in their diffusion away from the membrane, did foul more readily, especially in the presence of calcium. The effect was stronger in the absence of stirring when the boundary concentration is even higher.

Additionally, the dependence of organic concentration supported this effect. The deposition of natural organics was very selective, and larger, UV-absorbing compounds deposited preferentially. Membrane characteristics and operating parameters did influence deposition, with flux and salt rejection appearing to be more important than surface roughness or hydrophobicity. Once again, this result confirmed the precipitation mechanism, as opposed to chemical adsorption.

The pH did influence deposition, as at high pH calcium carbonate is likely to precipitate, while at low pH the organics precipitate. A selective deposition of large compounds was confirmed with SEC and LC-OCD analysis.

In the presence of OPS colloids, the flux decline is fully reversible and the particles themselves do not cause flux decline. This is because the hematite colloids are very large compared to the membrane pores. The colloids may adsorb some of the larger molecules which are responsible for fouling.

Ferric chloride addition prevented fouling, due to the preferential adsorption of the large organics on the ferric chloride precipitates. While there is no flux decline at the low dosage, where large flocs are formed, at high dosage reversible flux decline occurred, presumably due to an osmotic pressure build-up arising from the very small, highly positively charged precipitates. These colloids with a high positive charge induce a large sodium rejection. This was attributed to the deposition of a positively charged layer on the membrane. Organics rejection is reduced and LC-OCD analysis revealed that the low molecular weight acids permeate the membranes to a greater extent at these conditions.

Ferric chloride pretreatment of the solutions which also included hematite colloids confirmed the trends of low organic, but high cation rejection at the high dosage.

At critical fouling conditions ferric chloride successfully prevented fouling at any dosage. At the higher organic concentration the iron oxyhydroxide precipitates are neutralised and the osmotic effects observed are smaller. The impact on rejection of these less positively charged colloids is also reduced.

Finally, membrane morphology studies gave insights into the nature of the fouling layers formed. More deposition is observed for the largest compound, IHSS HA. The amount of deposit increased with calcium concentration. Further, calcium concentration also influences the structure of the formed layer. The anticipated solubility effects are confirmed, as precipitates od calcium-organic compounds and calcium carbonates are visible.

The effect of organics on calcium carbonate precipitation was also confirmed. While in the absence of organics large calcite crystals deposit, in the presence of organics the precipitates are smaller and of spherical shape. At the low pH, where calcium carbonate is more soluble, a very smooth deposit formed.

Contact angle measurements showed that it depends on the membrane material if the fouling layer makes the membranes more hydrophilic or hydrophobic.

7.10 CONCLUSION

In this chapter NF was characterised in terms of membrane characteristics, solute rejection, fouling behaviour, and deposit analysis.

The TFC-SR membrane, the most charged and most hydrophilic membrane, showed excellent rejection and flux performance with a high selectivity between calcium and sodium. The TFC membranes all demonstrated high organics rejection, with size exclusion being the dominant rejection mechanism. Both TFC-S and TFC-ULP membranes showed a high sodium rejection, which makes these membranes less attractive for surface water applications. Salt rejection determined the flux of these membranes. It is, therefore, necessary to select a membrane well suited to the desired product quality. The CA-UF membrane had a very low salt rejection, while organics rejection was comparably high. The pore size of this membrane is very similar to the size of the organics and therefore treatment is not as reliable as with the TFC membranes.

It can be concluded from the above experiments that characterisation of the NOM and the inorganics in a surface water is essential in predicting fouling potential. Hydrophobic organics deposit preferentially on the membranes due to their larger size and hydrophobicity. At high calcium concentrations fouling is significant, with the mechanism depending on solution chemistry.

Calcium-humate complexes cause highest flux decline, due to their highly compactable floc-like structure, compared to calcite precipitates. Deposition of calcium and organics increases with pH, due to the precipitation of calcite and adsorption of organics on the calcite surface. HA caused highest flux decline of the three organics used, probably due to its higher concentration in the boundary layer. This related to the largest molecular weight of HA and, thus, a slower diffusion away from the membrane. As a result precipitation occurred.

Fouling could be related to concentration polarisation, which has been calculated for the stirred cell mass transfer coefficient and crossflow systems. Solubility tests showed that in both systems the solubility of calcium and organics is exceeded at the fluxes typical for NF. Operation at low flux, low transmembrane pressure and high shear reduces the deposition of insoluble matter at the membrane surface and thus minimises fouling.

Inorganic colloids did not cause flux decline as they adsorb the organics, which are likely to deposit on the membrane, on their surface. However, the build-up of a colloidal cake-layer results in a reduced solute rejection, but flux decline is fully reversible. This shows that pore fouling is not important, and it is surface deposit which causes detrimental flux decline in NF.

It was found that the flux decline, even at critical fouling conditions is completely avoided by addition of ferric chloride. For large dosages (100 mgL^{-1} $FeCl_3$), an osmotic pressure builds up and this reduces flux reversibly. The positive ferric hydroxide colloids deposit on the membrane and their charge appears to govern rejection. Cation rejection increases considerably, while the rejection of organics decreases. This demonstrates that the deposit on a fouled membrane can change rejection characteristics.

Chapter 8

PROCESS COMPARISON

The aim of Chapter 8 is to bring Chapters 5 (MF), 6 (UF) and 7 (NF) together and compare filtration behaviour against a number of criteria. The first criterium will be the clean membrane characteristics such as flux, permeability, operational pressure, membrane resistance, and MWCO or pore size.

Further, rejection of organics will be investigated as a function of membrane pure water flux, MWCO or pore size. This is followed by fouling under fouling conditions where resistances of the fouling layers will be compared. Then particulate fouling is investigated and similar comparisons of resistances and rejection are made. The next section is dedicated to the effect of ferric chloride pretreatment on flux and rejection of a number of membranes.

From the information gained, the membrane area requirements per m^3 product water at typical recoveries will be calculated. This translates directly into cost.

While a detailed cost analysis is not carried out, the final section is an alternative approach to the conventional cost analysis and is concerned with environmental considerations. These have been neglected in many previous cost studies and the aim is to raise issues for further investigations into a complete cost analysis. The section includes energy requirements, chemicals consumption, concentrate characteristics, health and water quality aspects, and suggestions for future water treatment.

8.1 INTRODUCTION

As shown in the previous chapters, the removal of natural organics achieved with MF, UF, and NF can be relatively similar, depending on pretreatment applied and organic characteristics. Operating fluxes and transmembrane pressures, however, are different and a comparison of the processes against a number of criteria is required to make a judgement as to the most appropriate treatment approach.

Additionally, fouling mechanisms are different. Fouling layer resistances were used to compare fouling for the different processes to overcome the problem of different initial fluxes.

8.2 PURE WATER MEMBRANE CHARACTERISTICS

Pure water flux at the indicated operating pressure, permeability, membrane resistance, MWCO, and pore diameter (as calculated with the relationship of Worch (1993) and the Stokes Einstein equation) are shown in Table 8.1. Membrane characteristics such as permeability overlap for UF and NF.

Table 8.1 *Pure water membrane characteristics of the membranes used in Chapters 5, 6 and 7.*

Process	Membrane	Pure Water Flux [$Lm^{-2}h^{-1}$]	Water Permeability [$Lm^{-2}h^{-1}bar^{-1}$]	Pressure [bar]	Membrane Resistance [m^{-1}]	MWCO [kDa]	Pore Diameter [nm]
MF	GVWP	7968 ± 288	7968	1	$4.51 \cdot 10^{7}$	-	220*
MF	GVHP	7803 ± 308	7803	1	$4.60 \cdot 10^{7}$	-	220*
UF	PLHK	1320 ± 40	1320	1	$0.03 \cdot 10^{10}$	100*	18.20
UF	PLTK	390 ± 20	390	1	$0.09 \cdot 10^{10}$	30*	9.62
UF	PLGC	65 ± 5	21.7	3	$1.66 \cdot 10^{10}$	10*	5.18
UF	PLCC	28 ± 3	9.3	3	$3.85 \cdot 10^{10}$	5*	3.72
UF	PLBC	22 ± 2	7.3	3	$4.90 \cdot 10^{10}$	3*	2.84
UF	PLAC	15 ± 2	5.0	3	$7.18 \cdot 10^{10}$	1*	1.88
NF	CA-UF	49.9 ± 4.2	10.0	5	$3.6 \cdot 10^{10}$	5#	3.72
NF	TFC-SR	45.8 ± 6.1	9.2	5	$3.9 \cdot 10^{10}$	< 0.18#	< 0.64
NF	TFC-S	49.4 ± 5.9	9.9	5	$3.6 \cdot 10^{10}$	< 0.18#	< 0.64
NF	TFC-ULP	19.4 ± 2.6	3.9	5	$9.3 \cdot 10^{10}$	<0.18#	< 0.64

* information supplied by Millipore.

\# determined by Fluid Systems using lactose marker tests. Rejections for MWCO as >90% at 1% glucose in MilliQ. CA-UF determined with 5 kDa dextran at 100 mgL^{-1}. Rejection of 10 kDa dextran was 76% (Takigawa (1999)).

8.3 REJECTION OF ORGANICS AND CALCIUM

Rejection values at comparable conditions are given in Table 8.2. Rejection of colloids is not considered, as the rejection of colloids is complete for all processes except MF, where the rejection of OPS colloids was 0, 8.4, 83.2, and 93.2% for 40, 75, 250, and 500 nm primary colloids, respectively. Rejection of SPO aggregates was complete.

8.3.1 Rejection of Organics and Cations

Table 8.2 shows rejection values of the different organics and their fractions as DOC and UV, as well as cation rejection. Cation rejection increases for tighter membranes. Organic rejection varies with membrane and organic type and will be illustrated as a function of clean membrane parameters in the following figures.

Table 8.2 *Rejection of DOC, UV absorbance at 254 nm and cations as a function of membrane at pH 7-8, 5-15 mgL^{-1} organics as DOC, 0.5 mM $CaCl_2$. Cation rejection is in the absence of organics .*

	DOC Rejection [%] / UV_{254} Rejection [%]						Rejection [%]	
	IHSS HA	IHSS FA	NOM	NOM HA	NOM FA	NOM Hyd	Ca^{2+}	Na^{+}
MF GVWP	10/4#	7/0#	17/2#	-	-	-	0	0
UF 100 kDa	6/4	8/4#	9/9#	8/5#	3/4#	4/5#	0	0
UF 30 kDa	11/12	12/13	10/8	2/7	0/4	14/26	2.8	0
UF 10 kDa	66/88	56/53	51/55	65/76	58/64	41/50	2.6	0
UF 5 kDa	88/91	82/63	74/71	79/87	77/81	60/66	2.0	0
UF 3 kDa	86/93	84/94	77/73	79/90	78/86	60/73	13.6	0
UF 1 kDa	90/96	87/97	86/84	82/79	81/89	68/80	13.2	0
NF CA-UF	76/83	71/91	57/72	-	-	-	14.4	12.6
NF TFC-SR	74/97	94/96	69/97	96/99#	96/98#	84/87#	67.6	37.4
NF TFC-S	90/99	84/95	95/96	-	-	-	94.4	82.0
NF TFC-ULP	76/99	80/88	95/96	-	-	-	90.4	85.0

values are at 2.5 mM $CaCl_2$, 5-15 mgL^{-1} organics as DOC. Rejection of IHSS HA at these conditions is 92.7% (TFC-SR) and 57% (UF 100 kDa), for comparison.

Rejection of UV and DOC as a function of membrane pore size is illustrated in Figure 8.1 and Figure 8.2, respectively. While UV rejection is about 10% higher on average than DOC rejection for the lower pore sizes, it appears as if UV is not as selective as DOC. This is particularly clear for the hydrophilic fraction of NOM, which is retained about 20% less than the other fractions. UV does not show this difference as clearly because it does not measure the hydrophilic fraction easily. A clear cut-off for a pore size of 6 to 7 nm shows a drastic reduction in rejection. This cut-off lies between the 30 kDa and 5 kDa UF membranes.

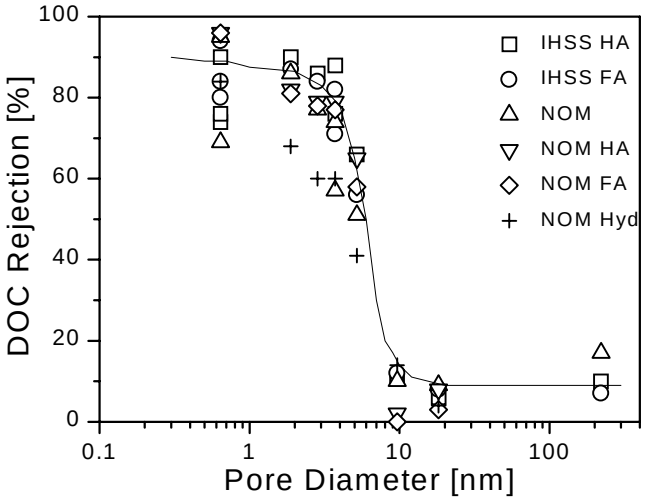


Figure 8.1 *DOC rejection as a function of pore diameter for values reported in Table 8.1 and Table 8.2.*

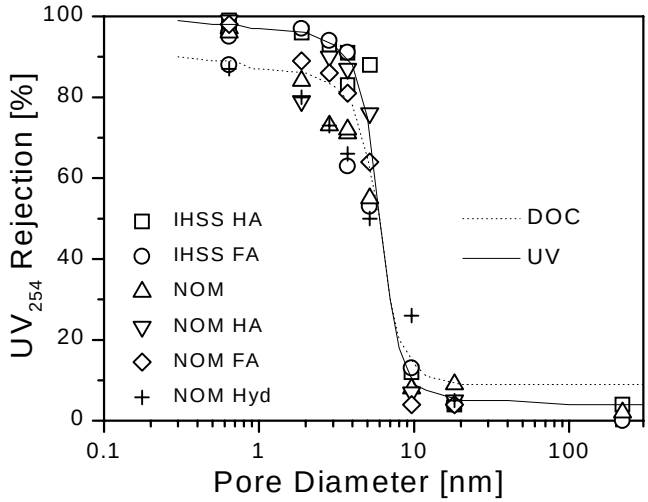


Figure 8.2 *UV_{254} rejection as a function of pore diameter for values reported in Table 8.1 and Table 8.2. The DOC curve is adapted from Figure 8.1.*

Alternatively, rejection can be presented as a function of permeability and membrane resistance. Permeability did not show a very interesting relationship (figure not shown), but results of DOC rejection as a function of membrane resistance are shown in Figure 8.3. While rejection generally increases with increasing membrane resistance, four membranes are found at a resistance of $4 \cdot 10^{10}$ m^{-1}. The CA-UF and 5 kDa UF membranes are at the lower end of rejection, the TFC-S and TFC-SR show a high rejection at comparable resistance.

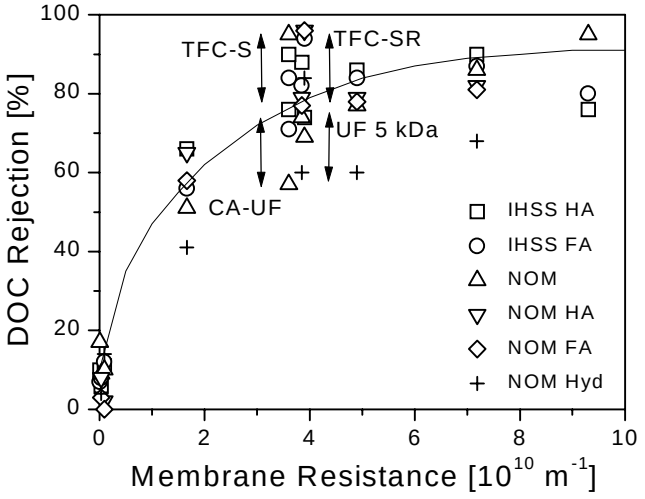


Figure 8.3 *DOC rejection as a function of membrane resistance for values reported in Table 8.1 and Table 8.2.*

It should be noted here that the pore size and membrane resistance are clean water characteristics. Fouling and concentration polarisation may alter their value, but the use of fouled membrane resistance for example seems unsuitable to predict filtration behaviour. Salt rejection for example, would shift the apparent resistance of TFC-S and TFC-SR membranes to larger values.

8.3.2 Rejection Mechanisms

In MF, where sieving is believed to dominate rejection, charge effects were observed. However, it is the colloid stability that determines rejection for colloids which were smaller than membrane pore size. Aggregates that form in the absence of organics are retained, but exhibit reduced rejection at high fluxes, pressures and after a backwash.

In UF, charge (of membrane and solute) and sieving are important. Colloids in the size range investigated are fully retained. Aggregation of the organics has the greatest influence on rejection. Aggregates of IHSS HA and calcium adsorb inside membrane pores and cause a pore size reduction. This increases rejection. At higher ionic strength, but prior to the onset of aggregation, rejection decreases which indicates that charge effects are important in UF.

In NF, it is also charge and sieving that are important. While in MF colloid interactions and in UF organic interactions are important, in NF it is the speciation, ion dissociation, organic-cation complexation, as well as the structure and size of compound that have a significant impact on rejection. Solute-solute interactions of decreasing size scale are determining rejection as membrane pore size decreases.

Fouling also affects rejection. In MF and UF pores gradually fill up, while in NF a deposit of a higher charge than the membrane may form and enhance rejection. Colloid fouling can also increase the thickness of the unstirred boundary layer and increase concentration polarisation, which adversely affects rejection.

The general conclusion for all processes and their rejection mechanisms is that solute-solute interactions are important. The size of the 'solute' of interest varies with process (or pore size).

8.4 FOULING BY ORGANICS, CALCIUM AND COLLOIDS

8.4.1 Organics and Calcium

Organics, specifically the large and hydrophobic fraction, and calcium cause fouling of all processes. Suggested mechanisms are surface modification, aggregation and pore blocking, or gel formation on the surface. Detailed studies under typical fouling conditions (in this thesis also called 'critical fouling conditions', 12.5 mgL^{-1} IHSS HA and 2.5 mM $CaCl_2$) have been undertaken. As summarised in Chapter 2, 2.5 mM calcium is approximately the critical coagulation concentration for HA. At these conditions adsorption of large HA aggregates on the membrane material causes severe fouling of MF, UF and NF. In UF this is due to pore size reduction (Chapter 6), and in NF due to the precipitation of a calcium-organic species on the membrane surface and the subsequent formation of a high resistance deposit. Results of flux decline and membrane resistance are summarised in Table 8.3.

The clean membrane resistance R_M is calculated for pure water flux, while the fouling resistance R_F is the total resistance minus the membrane resistance (see equations (8.1) and (8.2)). ΔP is the

transmembrane pressure, η the water viscosity, J_{W0} the initial pure water flux, and J_F the final flux at the end of the experiment.

$$R_M = \frac{\Delta P}{J_{W0} \cdot \eta} \tag{8.1}$$

$$R_F = \frac{\Delta P}{J_F \cdot \eta} - R_M \tag{8.2}$$

The fouling resistance is high for the membranes with a high salt rejection (TFC-S, TFC-ULP) and low for the MF membranes. However, in MF, only a very small resistance is required to cause considerable flux decline. The results show that the morphologies of the various fouling layers are very different.

Table 8.3 *Flux, flux decline, permeability, membrane resistance and rejection at 2.5 mM $CaCl_2$ and IHSS HA at pH 7-8. Filtration protocols are described in Chapters 5,6 and 7 for MF, UF, and NF, respectively.*

	Flux					Rejection			
Process	J_F [$Lm^{-2}h^{-1}$]	J_F/J_0 [-]	L_F [$Lm^{-2}h^{-1}bar^{-1}$]	R_M [10^{10} m^{-1}]	R_F [$10^{10}m^{-1}$]	DOC [%]	UV_{254} [%]	Ca^{2+} [%]	Na^+ [%]
MF GVWP	1732	0.22	1732	0.0046	0.0162	10	4	0	0
MF GVHP	1981	0.25	1981	0.0045	0.0181	16	6	0	0
UF 100 kDa	76	0.12	76	0.057	0.416	57	70	0	0
UF 10 kDa	32	0.94	11	3.168	0.198	70	87	6	4
NF CA-UF	41	0.83	8	3.600	0.780	74	89	98	20
NF TFC-SR	34	0.75	7	3.920	1.360	93	100	96	24
NF TFC-S	19	0.39	4	3.625	5.815	94	99	55	80
NF TFC-ULP	12	0.61	2	9.255	5.710	87	98	21	91

The results are illustrated in Figure 8.4 and compared to UV and DOC rejection of unfouled membranes.

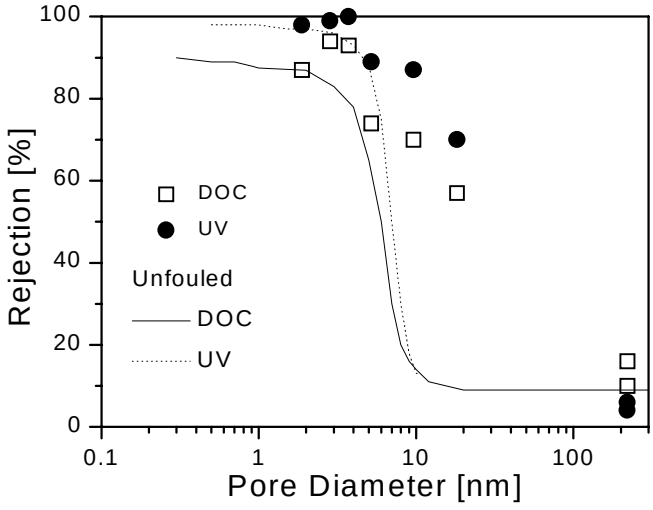


Figure 8.4 *Rejection at critical fouling conditions as a function of pore diameter. The line graphs are rejection of unfouled membranes.*

The cut-off, which was between 6 and 8 nm under unfouled conditions, has shifted to >20 nm under fouling conditions. The increase in rejection can be attributed to the larger solute size due to aggregation and pore adsorption which was demonstrated for UF in Chapter 6. This shows a clear increase in membrane rejection as fouling proceeds.

8.4.2 Colloidal Systems

Results of OPS systems with 75 nm primary colloids are shown in Table 8.4. Membrane resistance is reduced in the presence of colloids compared to the critical fouling conditions (Table 8.3). The change in resistance possibly resulted from decreased rejection. For the 10 kDa membrane resistance and rejection increase in the presence of colloids.

Table 8.4 *Flux, flux decline, permeability, membrane resistance and rejection of OPS systems with a primary colloid size of 75 nm, 0.5 mM $CaCl_2$ and IHSS HA.*

	Flux					Rejection			
Process	J_F [$Lm^{-2}h^{-1}$]	J_F/J_0 [-]	L_F [$Lm^{-2}h^{-1}bar^{-1}$]	R_M [10^{10} m^{-1}]	R_F [$10^{10}m^{-1}$]	DOC [%]	UV_{254} [%]	Ca^{2+} [%]	Na^+ [%]
MF GVWP	6142	0.78	6142	0.0046	0.0012	1	-	0	0
UF 100 kDa	215	0.37	215	0.057	0.110	5	57	0	0
UF 30 kDa	253	1.00	253	0.142	0	11	-	0	0
UF 10 kDa	51	0.88	17	3.168	1.056	95	95	10	0
NF TFC-SR	44	0.97	9	3.920	0.120	85	99	86	76

For the SPO system, resistances are also lower compared to critical fouling conditions. Results are tabulated in Table 8.5. The 10 kDa membrane has again a higher resistance at higher rejection.

Table 8.5 *Flux, flux decline, permeability, membrane resistance and rejection of SPO systems with a primary colloid size of 75 nm, 0.5 mM $CaCl_2$ and IHSS HA.*

	Flux					Rejection			
Process	J_F [$Lm^{-2}h^{-1}$]	J_F/J_0 [-]	L_F [$Lm^{-2}h^{-1}bar^{-1}$]	R_M [10^{10} m^{-1}]	R_F [$10^{10}m^{-1}$]	DOC [%]	UV_{254} [%]	Ca^{2+} [%]	Na^+ [%]
MF GVWP	2047	0.26	2047	0.0046	0.0129	17	-	0	0
UF 100 kDa	421	0.87	421	0.057	0.028	8	40	0	0
UF 30 kDa	225	1.00	225	0.142	0	83	-	0	0
UF 10 kDa	45	1.00	15	3.168	0.753	97	95	0	0

8.5 FERRIC CHLORIDE PRETREATMENT

Ferric chloride is used in MF and UF to increase rejection. In Chapter 7 it has been demonstrated that ferric chloride can also be used to reduce fouling in NF. In this section the effect on rejection, flux, and the cost of such a pretreatment are compared.

8.5.1 Effect on Rejection

Table 8.6 and Table 8.7 show the rejection of organics and cations with coagulant addition. The results are compared to rejection without coagulation in Figure 8.5. The UV results are a combination of ferric chloride and organic absorption and cannot be used to interpret organics rejection.

Comparing rejection with and without ferric chloride pretreatment, the rejection can be increased considerably by ferric chloride addition for the larger pores. However, results scatter a lot and the treatment may need to be carefully optimised if it is to be able to provide a reliable barrier for the organics. Rejection for the NF membrane (already at >90%) appears unchanged with ferric chloride pretreatment.

Table 8.6 *Rejection in percent of various processes with two ferric chloride dosages. Solutions contain 5 mgL^{-1} IHSS FA and 0.5 mM $CaCl_2$ (MF and UF) and 12.5 mgL^{-1} IHSS HA and 2.5 mM $CaCl_2$ (NF). pH adjusted to pH 7-8 prior to ferric chloride addition.*

Rejection [%]	25 mgL^{-1} $FeCl_3$				100 mgL^{-1} $FeCl_3$			
Process	DOC	UV_{254nm}	Ca^{2+}	Na^+	DOC	UV_{254nm}	Ca^{2+}	Na^+
MF GVWP	39	89	-	-	48	79	-	-
UF 100 kDa	35	-	-	-	77	-	-	-
UF 30 kDa	50	-	-	-	94	-	-	-
UF 10 kDa	84	-	-	-	86	-	-	-
NF TFC-SR	94	98	83	3	79	99	99	43

Table 8.7 *Variation of DOC rejection with organic type in coagulation and MF/UF. Ferric chloride dosage 25 mgL^{-1} and solution as indicated in Table 8.6.*

Process	Organic Type	Ferric Chloride [mgL^{-1}]	DOC Rejection [%]
MF GVWP	IHSS FA	25/100	39/48
	IHSS HA	25/100	10/57
	NOM	25/100	39/83
UF 100 kDa	IHSS FA	25	35
	IHSS HA	25	90
	NOM	25	-
UF 10 kDa	IHSS FA	25	84
	IHSS HA	25	80
	NOM	25	67

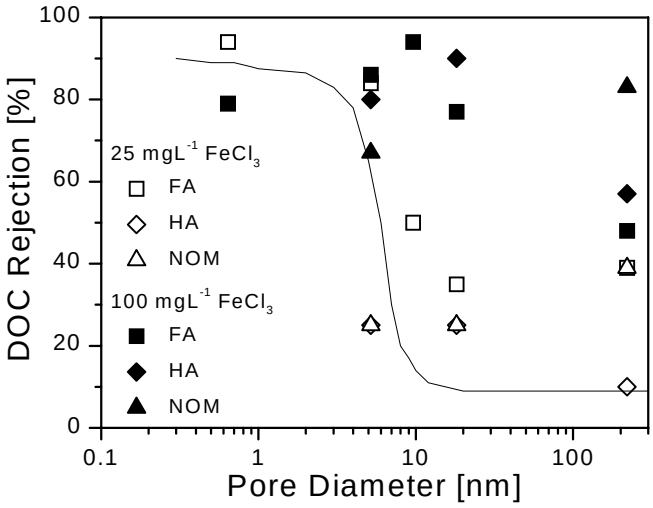


Figure 8.5 *DOC rejection as a function of pore diameter with coagulation pretreatment compared to rejection with no pretreatment (shown as a line).*

In the presence of pre-prepared hematite colloids (OPS and SPO systems as described in Chapter 4), rejection is as shown in Table 8.8. The rejection compared to organic rejection of membranes without pretreatment in Figure 8.6. In the presence of these colloids the scatter in the data is reduced, possibly due to the formation of a more stable deposit. The rejections with MF are now comparable to those obtained with NF.

Table 8.8 *Rejection in percent of various processes with two ferric chloride dosages. Solutions contain 5 mgL^{-1} IHSS FA and 0.5 mM $CaCl_2$ (MF and UF) and 12.5 mgL^{-1} IHSS HA and 2.5 mM $CaCl_2$ (NF) and colloidal systems with 10 mgL^{-1} hematite I (75 nm). pH adjusted to pH 7-8 prior to ferric chloride addition.*

Rejection [%]		25 mgL^{-1} $FeCl_3$				100 mgL^{-1} $FeCl_3$			
Process	Colloids	DOC	UV_{254nm}	Ca^{2+}	Na^{+}	DOC	UV_{254nm}	Ca^{2+}	Na^{+}
MF GVWP	OPS	79	97	-	-	68	70	-	-
MF GVWP	SPO	90	97	-	-	82	90	-	-
UF 100 kDa	OPS	55	-	0	-	83	-	4	0
UF 100 kDa	SPO	20	-	2	0	79	-	34	0
UF 10 kDa	OPS	50	-	0	0	80	-	0	0
UF 10 kDa	SPO	75	-	0	0	87	-	1	0

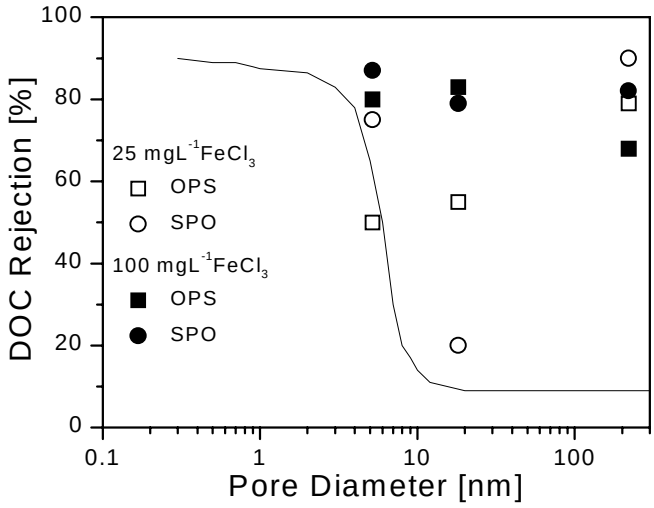


Figure 8.6 *DOC rejection as a function of pore diameter with coagulation pretreatment compared to rejection with no pretreatment (shown as a line) in the presence of colloidal systems (OPS/SPO).*

8.5.2 Effect on Flux

Table 8.9 and Table 8.10 show flux decline and membrane resistances with two ferric chloride dosages. Comparing flux ratio and fouling resistance, there is no direct relationship between the two. For the 10 kDa membrane the flux decline observed is small, while the resistance of the fouling layer is quite high. The fouling layer resistance increases with applied pressure and is not necessarily a function of membrane pure water flux. This effect is stronger at the high ferric chloride doses where a lot of small coagulant precipitates are deposited in the absence of hematite colloids.

Table 8.9 *Flux, flux decline, permeability, as well as membrane and fouling resistance of various processes with two ferric chloride dosages.*

	25 mgL^{-1} $FeCl_3$					100 mgL^{-1} $FeCl_3$				
Process	J_F	J_F/J_0	L_F	R_M	R_F	J_F	J_F/J_0	L_F	R_M	R_F
	[Lm^{-2}h^{-1}]	[-]	[Lm^{-2}h^{-1}bar^{-1}]	[10^{10} m^{-1}]		[Lm^{-2}h^{-1}]	[-]	[Lm^{-2}h^{-1}bar^{-1}]	[10^{10} m^{-1}]	
MF GVWP	1708	0.19	1708	0.005	0.016	299	0.043	299	0.004	0.116
UF 100 kDa	588	0.93	588	0.057	0.004	59	0.10	59	0.058	0.551
UF 30 kDa	286	0.99	286	0.125	0.001	112	0.44	112	0.141	0.180
UF 10 kDa	53	0.99	18	2.033	0.015	49	0.84	16	1.867	0.332
NF TFC-SR	44	0.97	8.8	3.920	0.160	37	0.80	7.4	3.920	0.933

When colloidal hematite particles are present (Table 8.10) the effect of ferric chloride dosing is smaller and resistances are highest for the 100 kDa membrane. In the presence of the hematite colloids it appears as if permeation drag becomes important and pressure plays a minor role.

Table 8.10 *Flux, flux decline, permeability, as well as membrane and fouling resistance of various processes with two ferric chloride dosages in the presence of particle systems.*

	25 mgL^{-1} $FeCl_3$					100 mgL^{-1} $FeCl_3$				
Process	J_F	J_F/J_0	L_F	R_M	R_F	J_F	J_F/J_0	L_F	R_M	R_F
	[Lm^{-2}h^{-1}]	[-]	[Lm^{-2}h^{-1}bar^{-1}]	[10^{10} m^{-1}]		[Lm^{-2}h^{-1}]	[-]	[Lm^{-2}h^{-1}bar^{-1}]	[10^{10} m^{-1}]	
MF GVWP, OPS	996	0.12	996	0.0042	0.0319	363	0.042	363	0.0042	0.0947
MF GVWP, SPO	2238	0.25	2238	0.0041	0.0120	209	0.025	209	0.0043	0.1675
UF 100 kDa, OPS	562	0.94	562	0.0599	0.0039	45	0.057	45	0.0456	0.752
UF 100 kDa, SPO	761	0.93	761	0.0437	0.0034	33	0.053	33	0.0580	1.030
UF 10 kDa, OPS	47	0.91	16	2.109	0.2085	45	0.92	15	2.220	0.198
UF 10 kDa, SPO	57	0.99	19	1.866	0.0195	40	0.84	13	2.253	0.432

8.6 PROCESS RELIABILITY AND WATER QUALITY

8.6.1 Dependence of Product Quality on Organic Type and Solution Chemistry

It was shown in section 8.3 that rejection of the individual membranes depends on organic type. Further, rejection also depends on solution chemistry and solute-solute interactions as is investigated in Chpaters 5, 6, and 7. These parameters are likely to continuously change for a raw water. While for MF the changes affect solutes and colloids, in UF they affect the natural organics, and in NF ions. This means that a stable product quality in terms of natural organics can only be guaranteed for NF. A

8.6.2 Water Quality

Fane (1996) proposed an overall water quality index for treatment based on pathogen, turbidity, colour and salt removal. This criterion was modified to suit the study in this project and is presented in Table 8.11. The equation for the water quality parameter (WQP) used in this study, is the sum of the rejections of "solute" of interest, in this study colloids, organics and cations. For experiments where several colloids, organics and cations were tested, the average is taken (see last equation).

$$WQP = \sum R'_j$$

$$WQP = R'_{Colloid} + R'_{Organic} + R'_{Cation} \qquad (8.3)$$

$$WQP = \frac{R'_{40} + R'_{75} + R'_{250} + R'_{500}}{4} + \frac{R'_{FA} + R'_{HA} + R'_{NOM}}{3} + \frac{R'_{Na} + R'_{Ca}}{2}$$

Pathogens were not included in this study. However, for MF this may not be achieved under all operating conditions as reported by Jacangelo *et al.* (1995a). Log removals of the virus *MS2 bacteriophages* (0.025 μm) reported were as low as 0.4 (60%) for MF (0.2 μm), while an UF membrane (100 kDa) removed > 6 log. *Cryptosporidium parvum* (4 to 6 μm in diameter) and *Giardia muris* (7 to 14 μm) cysts was complete (> 6 log, below detection limit) by both MF and UF. The removal of viruses is thus a criteria which needs to be considered in the process choice.

The total score for each parameter suite (colloids, DOC, and ions) is 100. The columns are subdivided into equal fractions, resulting in total points of 25 for the individual colloid fraction, for the organic fraction, and 50 for the major cations (Na^+, Ca^{2+}). For colloids stable primary colloids (OPS system) are assumed as these appear most abundant in a natural water. Ion rejection is represented by sodium and calcium rejection in the absence of organics and DOC rejection of solutions containing 0.5 mM $CaCl_2$ (except for MF where calcium concentration is 2.5 mM). As a sum criterion, the water quality parameter (WQP) is introduced. The maximum score for WQP is 300.

The WQP values increase with membrane tightness as expected. The CA-UF membrane performs overall as an UF membrane in the 5 kDa cut-off range. This shows that its classification as a NF membrane is not justified. This is indicated in Chapter 7 also.

MF and UF membranes with a MWCO below 10 kDa achieve a WQP below 150, thus only 50% of the maximum score while the NF membranes achieve values in the range 230 to 280.

Table 8.11 *Water quality criteria for process evaluation and water quality parameter. The numbers are fractions of the rejection achieved. The sum of each parameter suite of 100 corresponds to a rejection of 100% of all fractions. Experimental conditions were pH 7-8, 5-15 mgL^{-1} organic as DOC, 0.5 mM $CaCl_2$ (except for MF where calcium concentration is 2.5 mM).*

	Colloids				DOC			Ions		**TOTAL**
	40 nm	75 nm	250 nm	500 nm	HA	FA	NOM	Na^+	Ca^{2+}	**WQP (300 max)**
MF GVWP	0	2.1	20.8	23.3	3.4	2.4	5.7	0	0	**57.7**
UF 100 kDa	25	25	25	25	2.0	2.8	3.0	0	0	**107.8**
UF 30 kDa	25	25	25	25	3.7	4.0	3.3	0	1.4	**112.4**
UF 10 kDa	25	25	25	25	22.0	18.7	17.0	0	1.3	**159.0**
UF 5 kDa	25	25	25	25	29.3	27.3	24.7	0	1.0	**182.3**
UF 3 kDa	25	25	25	25	28.7	28.0	25.7	0	6.8	**189.2**
UF 1 kDa	25	25	25	25	30.0	29.0	28.7	0	6.6	**194.3**
NF CA-UF	25	25	25	25	25.3	23.6	19.1	6.3	7.2	**181.5**
NF TFC-SR	25	25	25	25	24.7	31.3	23.0	18.7	33.8	**231.5**
NF TFC-S	25	25	25	25	30.0	27.9	31.8	41.0	47.2	**277.9**
NF TFC-ULP	25	25	25	25	25.2	26.8	31.8	42.5	45.2	**271.5**

This WQP is plotted as a function of membrane characteristics such as pore diameter, permeability, and resistance (as shown in Table 8.1) in Figure 8.7, Figure 8.8, and Figure 8.9, respectively.

WQP as a function of log pore diameter decreases linearly with increasing pore diameter. Pore diameter, which was calculated from the MWCO and marker tests, varies linearly with the WQP and the correlation of the relationship obtained is 0.94. Pore diameter represents the effective pore diameter, not necessarily a physical value in the case of NF.

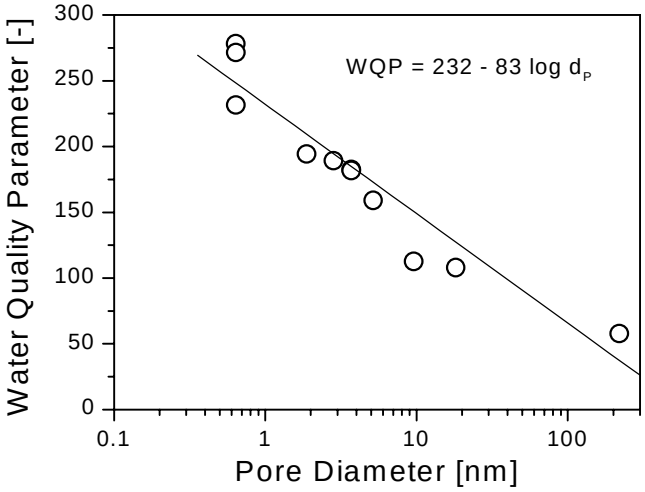


Figure 8.7 *Water quality parameter as a function of clean membrane pore diameter.*

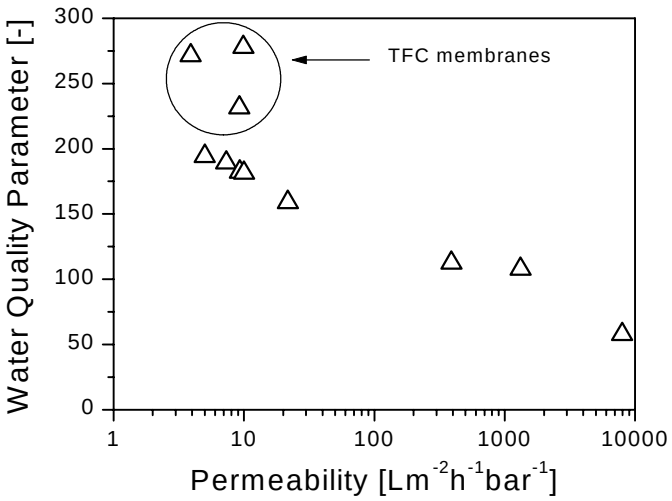


Figure 8.8 *Water quality parameter as a function of clean membrane permeability.*

WQP shows a linear relationship as a function of log permeability - i.e., the WQP increases exponentially with decreasing permeability. The TFC membranes show a disproportional increase in WQP with decreasing permeability compared to the other membranes. At comparable permeability the WQP is higher than that of the UF membranes.

The WQP as a function of clean membrane resistance does not show a clear relationship for the different membranes. The TFC-S and TFC-SR membranes lie above most other values and the MF membrane lies below.

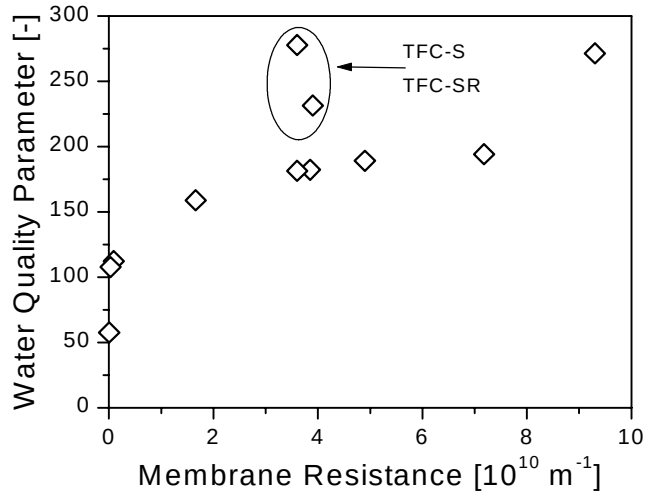


Figure 8.9 *Water quality parameter as a function of clean membrane resistance.*

In summary, the established WQP is a useful measure of membrane performance. It appears that membrane pore diameter is the best criterion to predict achievable water quality. While pore diameter is easily accessible for MF, a calculation using a molecular weight and size relationship (such as that used in this study; see Chapter 4) is required for UF. For NF, where the presence of pores is moot, the application of theoretical models (as described in Chapter 3) is required. The use of marker tests is useful for a pore diameter estimation, but solute molecule structure is an issue for such small membrane polymer voids.

A schematic for the selection of a suitable technology is shown in Figure 8.10. While some of this schematic is obvious from Table 3.1, the distinctions between aggregates and stable colloids as well as between organics are new.

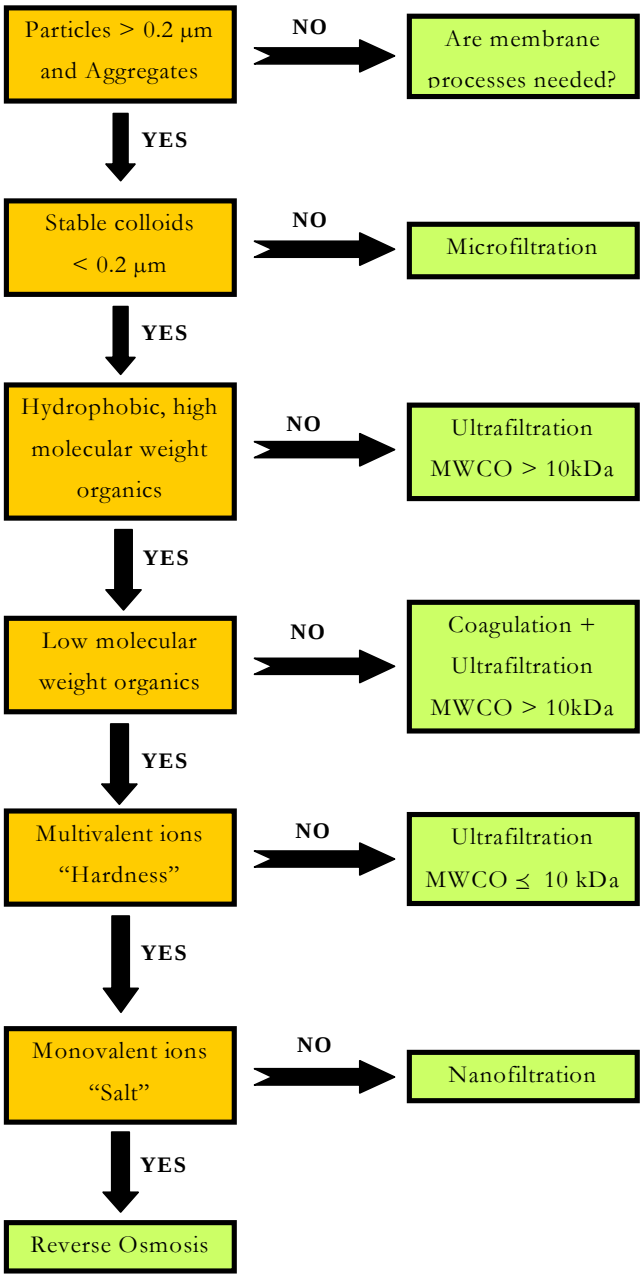


Figure 8.10 *Schematic for process selection. Boxes represent "solutes" to be removed and the process of choice.*

8.7 MEMBRANE AREA REQUIREMENTS AND COST

8.7.1 Membrane Cost

Membrane module costs for a typical municipal plant (4 to 20 · 10^3 m^3/d) are as shown in Table 8.12. Polypropylene is the cheapest option for MF, while RO membranes are cheaper than all other membrane types due to a much larger market (as was shown in Chapter 3).

The membranes selected for cost estimates are the MF PVDF, the UF CA, and the NF PA. The selection was based on the comparability to membrane materials used in this study. The cost for MF is high, but PVDF is chosen as this appears to be the best membrane material despite other materials being installed currently. For polypropylene the cost will be about one third of the estimate and possibly lower for a submerged membrane system (Johnson (1999)).

Table 8.12 *Membrane cost (Leslie (1999)).*

Process	Module Size [m²]	Average Module Cost [US$]	Membrane Cost [US$/m²]
MF Polypropylene	31	650	21.0
MF PVDF	40	2500	62.5
UF CA	90	1500	16.7
UF X*	72	2000	27.8
NF Polyamide	48	750 - 1000	15.6 – 20.8
RO Polyamide	50	< 500	< 10
RO CA	50	< 500	< 10

* X = Proprietary (ZENON)

8.7.2 Membrane Requirements

The membrane surface requirements and resulting total membrane cost (which is proportional to membrane replacement cost) is estimated from the final flux achieved during experiments. Membrane replacement is estimated to be required every four years (identical for each process). Results are presented in Table 8.13 for a plant capacity of 1000 m^3/d.

Table 8.13 *Fluxes, required membrane area for a plant capacity of 1000 m^3/d and membrane cost.*

Process	Initial Flux [$Lm^{-2}h^{-1}$]	Final Flux [$Lm^{-2}h^{-1}$]	Membrane Area Clean [m²]	Membrane Area Fouled [m²]	Membrane Cost Clean [US$]	Membrane Cost Fouled [US$]
MF	7968	1753	5.2	23.8	325	1488
MF#	797	175	52	238	3250	14880
UF 100 kDa	587	80	71.0	521	1185	8698
UF 30 kDa	254	112*	164	372	2740	6213
UF 10 kDa	34	32	1225	1302	20466	21745
UF 5 kDa	28	27*	1488	1543	24851	25771
UF 3 kDa	22	21*	1894	1984	31629	33135
UF 1 kDa	15	14*	2778	2976	46389	49702
NF CA-UF	50	42	833	992	17333	20635
NF TFC-SR	46	34	906	1225	18841	25490
NF TFC-S	49	19	850	2193	17687	45614
NF TFC-ULP	19	12	2193	3472	45614	72222

\# MF flux adapted to a more realistic value as reported in Chapter 3. Flux of MF in the experiments is high due to the use of flat sheet membranes, where permeate side pressure drop is negligible compared to hollow fibre systems.

* estimated values or extrapolated from other experiments for comparison. Fouling experiments were not conducted with these membranes.

The conditions chosen are the fouling conditions used in this study (12.5 mgL^{-1} as DOC IHSS HA, 2.5 mM $CaCl_2$).

Flux decline under these conditions were generally higher than in the presence of OPS colloids and thus represent a conservative estimate. Average membrane costs adapted from Table 8.12 are 62.5 US$/$m^3$ for PVDF MF, 16.7 US$/$m^3$ for CA UF, and 20.8 US$/$m^3$ for PA NF. The selection is based on the material (comparable to the current study).

8.7.3 Water Quality and Membrane Cost

As expected, membrane cost goes up as water quality goes up. Not surprisingly, membrane cost increases as flux decreases. The relationship between water quality achieved by the different process options and the membrane cost has to date not been examined. Estimated membrane cost for clean and fouled membranes is shown for a plant capacity of 1000 m^3/day in Table 8.13. In Figure 8.11 and Figure 8.12 the relationship between WQP and membrane cost is shown. The processes are different in terms of WQP, while membrane costs overlap for both clean and fouled conditions.

Membrane costs for MF and open UF membranes are comparable, at an increased WQP for UF. A similar trend is observed for tighter UF membranes and NF, while membrane cost is comparable at a much higher WQP. This shows that NF is very competitive with UF, especially if a high flux membrane is chosen (the high cost membrane is the TFC-ULP membrane which has a low flux and high salt rejection). The TFC-S membrane performs a lot better at higher flux and identical salt rejection.

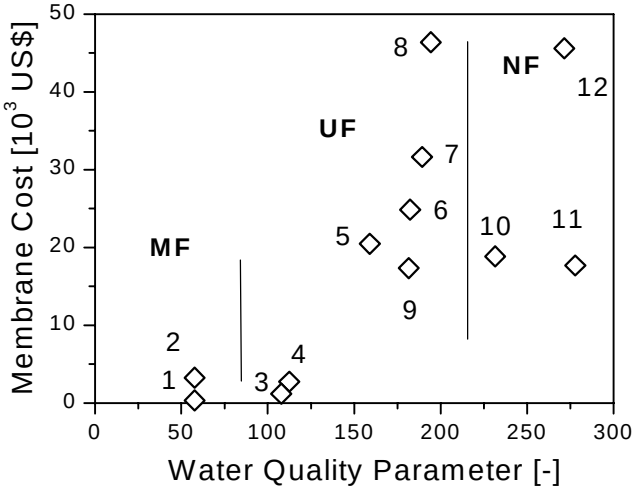


Figure 8.11 *Membrane cost at clean water conditions over water quality parameter. Membranes are 1-GVWP at high flux, 2-GVWP at low flux, 3-100kDa UF, 4-30 kDa UF, 5-10 kDa UF, 6-5 kDa UF, 7-3 kDa UF, 8-1 kDa UF, 9-CA-UF, 10-TFC-SR, 11-TFC-S, 12-TFC-ULP.*

Figure 8.12 depicts the scenario when the membranes are fouled. The membrane cost increases as a result of the lower throughput. Low flux MF is now higher in membrane cost than loose UF. The high salt retention NF membranes are also identical or higher in cost than tight UF. However, the NF membrane with high calcium, but low sodium rejection is very competitive with medium range UF (10 kDa) and low flux MF.

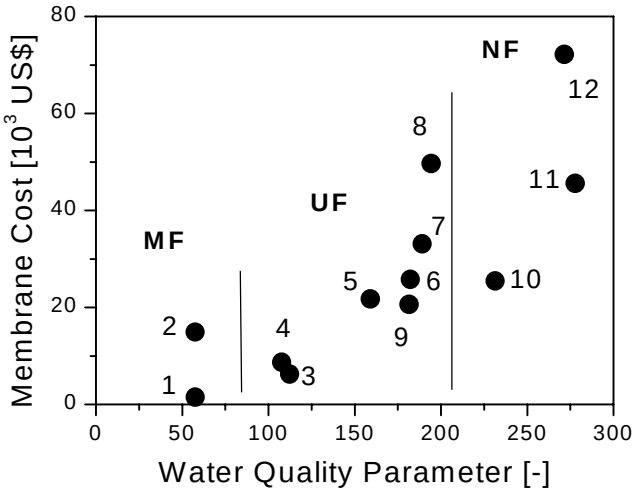


Figure 8.12 *Membrane cost at fouling conditions over water quality parameter. Membranes are 1-GVWP at high flux, 2-GVWP at low flux, 3-100kDa UF, 4-30 kDa UF, 5-10 kDa UF, 6-5 kDa UF, 7-3 kDa UF, 8-1 kDa UF, 9-CA-UF, 10-TFC-SR, 11-TFC-S, 12-TFC-ULP.*

8.7.4 Effect of Ferric Chloride Pretreatment

The cost of ferric chloride on treatment is determined by consumption of $FeCl_3$. The cost of ferric chloride depends on location of the treatment plant (transport cost), quality of the ferric chloride (solid/liquid/imported/purity) and quantity purchased. Quoted prices (per kg $FeCl_3$) ranged from about 0.29 US$/kg for a 20 ton local delivery of liquid $FeCl_3$ to US$7.10/kg for imported, high purity and low quantity $FeCl_3$. It should be noted here that experiments in this study were performed with analytical grade $FeCl_3$. The impurities in $FeCl_3$ produced from spent pickle liquor from iron and steel production may not be of concern when used for conventional treatment, but for membrane applications this effect should be investigated. For this reason both ends of the range are used for comparison.

The variation in flux and thus membrane area required, and the treatment of sludge produced also impact on the treatment cost. While the production of sludge is addressed in section 8.8.2, the information available does not allow a cost estimation. The cost induced by ferric chloride consumption is tabulated in Table 8.14. At the high dosages (100 mgL^{-1}) which are used in enhanced coagulation the cost becomes substantial if high cost (high purity or low quantities) ferric chloride was required. If such dosages are required prior to MF then the process becomes economically comparable to NF, without including the cost of the higher operating pressure and sludge treatment (see Chapter 3 for details on treatment costs). If low cost ferric chloride can be used then costs are minimal.

Table 8.14 *Ferric chloride cost as a function of dosage for a 1000 m^3/day plant capacity.*

	Ferric Chloride Dosage as $FeCl_3$ [mgL^{-1}]		
	5	25	100
Ferric Chloride Consumption [kg/d]	5	25	100
Ferric Chloride Cost [US$/d]	1.47 - 35.50	7.34 - 177.50	29.40 - 710.00
Ferric Chloride Cost [US$/$m^3$]	0.001 - 0.036	0.007 - 0.178	0.029 - 0.71

The variation of membrane area due to ferric chloride dosage is listed in Table 8.15. The sample experiments chosen are those in the absence of additional hematite colloids. For MF and UF, organic

concentration and type are 5 mgL^{-1} IHSS FA, and for NF 12.5 mgL^{-1} IHSS HA. Note that the fluxes at the low dosage have increased to above normal levels for the high MWCO membranes.

Table 8.15 *Membrane cost as a function of ferric chloride dosage 1000 m^3/day plant capacity.*

	25 $FeCl_3$ [mgL^{-1}]			100 $FeCl_3$ [mgL^{-1}]		
Process	Final Flux [$Lm^{-2}h^{-1}$]	Membrane Area [m^2]	Membrane Cost [US$]	Final Flux [$Lm^{-2}h^{-1}$]	Membrane Area [m^2]	Membrane Cost [US$]
MF	1708	24	1525	299	139	8710
MF#	171	240	15250	30	1390	87100
UF 100 kDa	588	71	1183	59	706	11794
UF 30 kDa	286	146	2433	112	372	6213
UF 10 kDa	53	786	13129	49	850	14201
NF TFC-SR	44	947	19697	37	1126	23424

adjusted to a flux closer to normal MF flux. Divided by ten in assuming identical fouling.

Ferric chloride pretreatment leads to a higher WQP due to the higher organic and colloid rejection. While the value is stable in NF (although minor changes can occur as shown in Chapter 7), a correction of WQP due to the improved rejection is carried out for MF and UF.

A total colloid rejection due to coagulation in MF increases the WQP from 57.7 to 111.5. With an average organic rejection of 30% and 63% at ferric chloride dosages of 25 and 100 mgL^{-1} (calculated from Table 8.7), the WQP further increases to 130 and 163, respectively.

Assuming similar rejections for UF, the WQP increases from 107.8 to 130 and 163 for the three UF membranes. Figure 8.13 shows the altered cost and WQP due to ferric chloride pretreatment. The cost for low flux MF is prohibitive, while NF is not much higher than MF and UF with pretreatment, but it produces a much higher WQP. The higher cost due to fouling at higher ferric chloride dosage is not very important, but it should be remembered that at this dosage the ferric chloride cost becomes important. Further, the energy for the higher operating pressures are lower than the costs for ferric chloride dosage. As soon as the ferric chloride cost increases, the operating costs for NF are lower.

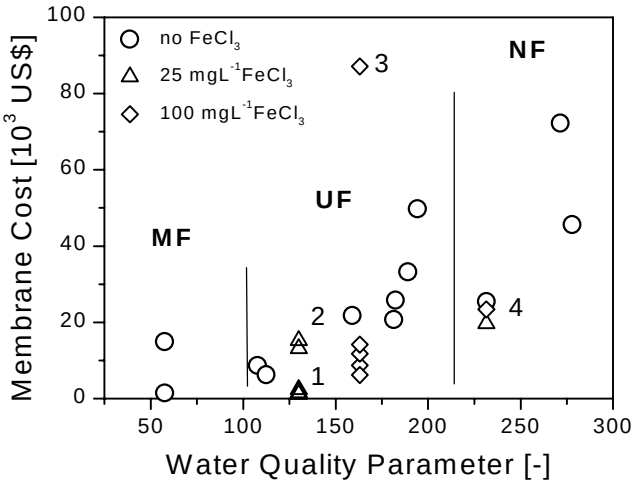


Figure 8.13 *Membrane cost as a function of WQP. Membranes with no ferric chloride as shown in Figure 8.12. 1-GVWP high flux and 30kDa UF, 2-10 and 100 kDa UF, 3-GVWP low flux, 4-TFC-SR.*

8.8 ENVIRONMENTAL CONSIDERATIONS

8.8.1 Energy Requirements

Energy requirements can be an important cost in membrane applications due to the requirement of a transmembrane pressure. The power input is determined by water or feed flow Q_F and applied pressure P (see equation (8.1)).

$$Power = Q_F \cdot P \tag{8.4}$$

This relationship can be modified to include product water flow Q_P by introducing recovery R into equation (8.1).

$$R = \frac{Q_P}{Q_F} \tag{8.5}$$

$$Power = \frac{Q_P}{R} \cdot P \tag{8.6}$$

Assuming a plant production capacity of 1000 m^3/d for all processes, the power consumption depends solely on plant recovery and transmembrane pressure (permeate pressure is neglected). Typical recoveries are adapted from Chapter 3. The transmembrane pressure values used in this study are in the common range also shown in Chapter 3. For RO, a comparative value of 1000 kPa was assumed. Electricity costs of US$0.05 per kWh were adapted from Clair *et al.* (1997) and operation times of 24 hours a day were assumed. Results are shown in Table 8.16. Electricity costs in Australia are about US$0.077 per kWh, the energy cost per m^3 is thus about 50% higher.

Table 8.16 *Typical recoveries, transmembrane pressures, power requirements, consumption and resulting energy costs based on applied pressures with an overall motor/pump efficiency of 40%..*

Process	Recovery [%]	Pressure [kPa]	Power [kW]	Consumption [kWh/d]	Energy cost [US$/1000 m^3]	Energy cost [US$/$m^3$]
MF	90 - 98	100	1.29 – 1.18	77.5 - 70.8	1.5 - 1.4	0.004 – 0.0035
UF	90 - 98	100	1.29 – 1.18	77.5 - 70.8	1.5 - 1.4	0.004 – 0.0035
UF	90 - 98	300	3.86 – 3.54	231.5 - 212.5	4.6 - 4.2	0.012 – 0.011
NF	75 - 95	500	7.72 – 6.09	463.3 – 365.5	9.3 - 7.3	0.023 – 0.018
RO	50 - 80	1000	23.15 – 14.47	1389 – 868.3	27.8 - 17.4	0.070 – 0.043

As expected, energy cost increase exponentially from MF to RO. The values for MF are likely to be an overestimate, due to an identical operating pressure as open UF membranes in the stirred cell experiments. This value can probably be halved. While the energy requirements double between UF and NF, they triple from NF to RO. This supports the argument that a membrane with the appropriate rejection should be selected for the task at hand.

8.8.2 Chemicals Addition

Chemicals are added to adjust pH, to clean membranes, and as a coagulant to increase rejection in MF and UF or to reduce fouling in RO. In this section only coagulant addition will be considered. Coagulation imposes two costs on water treatment, firstly, the consumption of coagulant (in this case ferric chloride) and, secondly, by sludge production or a higher particle load of the concentrate or backwash stream. Concentrations were taken from this study, with 25 to 100 mgL^{-1} $FeCl_3$ for removal of natural organics (MF and UF) and 5 to 25 mgL^{-1} for fouling reduction (NF and RO). This fouling prevention cannot be applied to the commonly used spiral wound modules due to their unsuitability to a high particulate load, but can be applied to hollow fibre or tubular systems.

The ferric chloride consumption per product is calculated with recovery (see Table 8.16 for values). The ferric chloride consumption per day (or per 1000 m^3 product) gives an indication of the quantities of coagulant to be transported to the plant.

The ferric chloride concentration in the waste stream varies from 20 g to 5 kg, depending on dosage and recovery. A high consumption of ferric chloride should be avoided, not only for cost, but also for environmental reasons.

Table 8.17 *Ferric chloride consumption and sludge production.*

Process	Ferric chloride dosage [mgL^{-1}]	Ferric chloride consumption per product [$g\ m^{-3}$]	Ferric chloride consumption per day [$kg\ d^{-1}$]	Ferric chloride concentration in "waste" [$kg\ m^{-3}$]
MF	25 - 100	28 - 102	25 - 100	0.25 - 5
UF	25 - 100	28 - 102	25 - 100	0.25 - 5
NF	5 - 25	7 - 26	5 - 25	0.02 – 0.50
RO	5 - 25	10 - 31	5 - 25	0.02 – 0.50

8.8.3 Concentrate Disposal

The amount of concentrate produced is calculated for a plant capacity of 1000 m^3/d and recoveries from Table 8.12. The loading of the concentrate streams for a water quality as used in the experiments is calculated as a function of rejection and recovery. This leads to the concentrate concentration c_c as shown in equation (8.7), where V_F is the feed volume, c_F the feed concentration, R recovery as defined in equation (8.2) and the rejection R' as defined in Chapter 3. Rejection values for the different solutes and membranes are tabulated in Table 8.11.

$$c_c = \frac{V_F \cdot c_F}{V_C} (1 - R \cdot (1 - R')) \tag{8.7}$$

The waste streams generated require treatment, which adds to process costs. The sodium concentrations in Table 8.18 are very high due to the use of a background electrolyte in the experiments, but they reflect the increase in salinity of the concentrates when NF is used. The NF recovery is limited by this salt content due to possible precipitation and osmotic pressure effects. A production of a 250 m^3/day waste stream would appear to be excessive.

Electrodialysis can be used to further concentrate the volumes produced and increase recovery (Schäfer (1993)), but the high concentration of organics could cause severe fouling of the ED membranes. A hybrid process which removes organics prior to NF (such as coagulation + MF, or UF) could be used.

Table 8.18 *Amount of concentrate produced and loading of the concentrate as a function of rejection for a plant capacity of 1000 m^3/d and feed concentrations of 12.5 mgL^{-1} DOC (HA), 10 mgL^{-1} hematite, 0.5 mM (20 mgL^{-1}) calcium and 20 mM (460 mgL^{-1}) sodium. Colloid concentrations in MF are for 40, 75, 250 and 500 nm colloids respectively. Assumed recoveries are 90-98% for MF and UF and 75-95% for NF.*

Process	Volume of concentrate [m^3d^{-1}]	DOC [mgL^{-1}]	Colloids [mgL^{-1}]				Calcium [mgL^{-1}]	Sodium [mgL^{-1}]
			40 nm	75 nm	250 nm	500 nm		
MF	20 - 100	75 - 24	10	51-18	418 - 85	465 - 94	20	460
UF 100 kDa	20 - 100	49 - 19	500 - 100				20	460
UF 30 kDa	20 - 100	80 - 25	500 - 100				47 – 25	460
UF 10 kDa	20 - 100	417 - 87	500 - 100				45 – 25	460
UF 5 kDa	20 - 100	551 - 111	500 - 100				40 – 24	460
UF 3 kDa	20 - 100	540 - 109	500 - 100				153 – 44	460
UF 1 kDa	20 - 100	564 - 114	500 - 100				149 - 44	460
NF CA-UF	50 - 250	226 - 46	400 - 200				75 – 29	1561-634
NF TFC-SR	50 - 250	193 - 41	400 - 200				277 – 61	3470-976
NF TFC-S	50 - 250	188 - 38	400 - 200				379 – 77	7627-1592
NF TFC-ULP	50 - 250	192 - 41	400 - 200				364 - 74	7889-1633

8.8.4 Health Aspects

The choice of process depends on the importance of health versus cost criteria. Crucial relationships in decision making are

- the risks associated with certain water components such as viruses and by-products and thus the critical concentration of such compounds required to cause illness or death
- the monetary value the general population regards as acceptable to pay for the prevention of illness and death.

While the assessment of microbiological risks factors is possible and the subject of a number of studies, a similar assessment for chlorination by-products and their effects as carcinogens or mutagens is presently not possible due to the long term nature of the effects and the importance of many other parameters.

The evaluation of the value of health and a human life are rather subjective. A way to translate this relationship into a consumer view may be to look at the amount consumers are willing to pay for safe drinking water. An increase in consumption of bottled water was observed during the 1998 *Cryptosporidium* and *Giardia* 'outbreak' in Sydney. While tap water is priced at about A\$0.80/m^3 (US\$ 0.52/m^3), bottled water is sold at a cost of around A\$1000/m^3. This reflects a very high willingness of the consumer to pay for safe drinking water.

8.8.5 Treatment Considerations

Safe drinking water comes at a price, and while water is cheap (though scarce) in Australia (US$0.52/m^3), in Europe or the US water prices can be up to three times this value. Although consumers are willing to pay a tremendous price for bottled drinking water, the extent to which water can be treated is (at least in Australia) limited by the low water price.

Treatment of all water to near perfect standards may not be required if an alternative approach to water supply was taken. An option well worth consideration, is localised treatment of water for human consumption. Treatment systems could be installed in the basements of large buildings, while the feed water for these systems could be rain water, conventional drinking water, or, for the more open-minded population, from a reuse source.

This means that distribution systems can be bypassed, disinfection reduced, and more sophisticated treatment systems applied on a small scale which would not be affordable on large scale. Simultaneously, the environmental impact of treatment would be reduced as the 'concentrate' of such systems with a relatively clean intake could be used for irrigation, toilet flushing or car washing.

8.9 CONCLUSION

Rejection shows a cut-off for natural organics rejection at a pore diameter of clean membranes of about 6 to 8 nm. Below this pore diameter rejection is <20%, while above it is mostly >80%. All twelve membranes lie on this cut-off curve. When the membranes are fouled this cut-off is shifted to >20 nm and the cut-off itself is not as distinct. This can be attributed to a pore size reduction due to internal pore adsorption, the formation of self-rejecting cake layers, and solute-solute interactions in the boundary layer. If ferric chloride is added this cut-off ceases in existence. Rejection of natural organics for the more open membranes can reach the levels achieved with NF. However, the scatter in data is large due to the dependence of rejection on solution chemistry, organic type and concentration, coagulant dosage and the presence of colloids. This renders this system, while potentially being a very economic alternative. To processes requiring intensive monitoring and quality adjustment. More reliable performance requires excessive dosages and is accompanied by detrimental flux decline.

A water quality parameter (WQP), which considers colloid, organics and salt rejection, was established for the membranes investigated. A linear relationship between WQP and log pore diameter was found. Finally, a complete cost analysis was replaced by the evaluation of A) membrane cost as a function of clean water flux and operation at fouled conditions, B) WQP as a function of membrane cost, C) ferric chloride cost, and D) energy costs.

A complete cost analysis has not been performed as some parameters require detailed analysis, such as life cycle, environmental impact, or risk assessment and need to be incorporated into cost values in a sensible way.

Very interestingly the cost for ferric chloride dosage is identical to the energy cost for RO treatment. This means that if a high ferric chloride dosage is required a process of MF or UF is not necessarily more economic than NF. This somewhat contradicts the common assumption that energy costs of tighter membranes are prohibitive.

Chapter 9

SUMMARY & CONCLUSION

The focus of this thesis is a comparison of natural organics rejection potential and fouling mechanisms of three membrane processes which are commonly used in water treatment - micro- (MF), ultra- (UF), and nanofiltration (NF). This comparative treatment study is combined with the science of natural organics and surface water systems, including an examination of natural organic-colloid-calcium interactions and solution speciation.

An extensive literature review on organics characterisation lead to the conclusion that a combination of MF and RO followed by freeze drying is the state of the art technique to concentrate surface water to produce a stock of natural organic matter (NOM). This technique was applied to concentrate 5000 L of a local Australian surface water. Further, 'model' compounds of the surface water systems to be examined were selected. These are well characterised and purified organics (IHSS FA & HA), and inorganic colloids (40 – 500 nm in diameter) in a carbonate buffer system containing mono- and multivalent cations.

A range of characterisation and fractionation techniques is required to thoroughly characterise the organics used. This lead to the selection of UF fractionation and chromatographic techniques for size determination, MALDI and DRIFT for absolute size and functional group content determination, scattering techniques for measurement of structure and size of aggregates, XAD for fractionation, and titration and zeta potential measurements for determination of the charge of organics and colloids.

A further literature review of membrane processes, led to the conclusion that the selection of hydrophilic membranes is essential for reduced fouling by natural organics. Consequently, the membrane materials of choice were hydrophilic and hydrophobic PVDF (MF), regenerated cellulose (UF), and both thin film composite (TFC) and cellulose acetate (CA) for NF. A total of twelve membranes were selected, with over a pore diameters ranging from less than 0.64 nm to 220 nm. It became evident that an understanding of solute-solute interactions is critical in understanding rejection and fouling. Subsequently, a number of organic and colloidal systems were chosen for a study on small scale (stirred cell system), which allowed the variation of sufficient parameters and enabled operation in a small, controlled system. Membranes were characterised thoroughly with zeta potential measurements, surface roughness examination, contact angle, salt rejection, pure water flux and pore diameter calculation.

The first process to be investigated was MF. Well-defined systems were investigated including (a) organics in the absence of inorganic colloids, (b) stable (non-aggregating) primary particles, (c) primary particles at pH extremes with organics, (d) particles stabilised with organics, (e) particles pre-aggregated in electrolyte solution prior to adsorption of organics, and (f) organics solutions and hematite suspensions coagulated with ferric chloride ($FeCl_3$).

Natural organics rejection was less than 20%. While natural organics caused fouling at high calcium concentrations, presumably due to the aggregation of particulate organics, the behaviour of colloids smaller than the pore size is of particular interest. Stable colloids in the absence of organics deposited on the membrane material, and colloids of a size closest to membrane pores caused highest flux decline due to pore plugging. In the presence of organics these colloids aggregated at low pH as their charge was neutralised. At ambient pH the colloids were stabilised by organics as a result of the high net negative surface charge. Under these conditions, a dramatic decrease in rejection was observed. Due to their small size and stable nature such systems are likely to be the most abundant in natural waters. When colloids were pre-aggregated prior to organics adsorption, rejection of colloids increased to near complete levels. Ferric chloride addition increased the rejection of natural organics and initially stable colloids. However, rejection and flux depend on solution chemistry, organic type, presence of colloids, coagulant dosage, and floc characteristics. Blocking law analysis of selected results showed the simultaneous occurrence of pore adsorption, plugging, and cake filtration processes.

In UF, rejection and fractionation experiments showed that a molecular weight cut-off (MWCO) of smaller than 10 kDa is required to remove a substantial amount of natural organics. Rejection depends on organic type and solution chemistry. The importance of charge effects between organics and membranes was demonstrated.

An effect of aggregate structure on flux was observed repeatedly during the filtration of well defined aggregates, surface water systems, and coagulated suspensions. Aggregates or flocs that form rapidly have a loose structure and their induced flux decline is mostly negligible. Slowly forming aggregates or stable colloids deposit as a very dense layer and cause severe flux decline.

Rejection was influenced by stirring, membrane type, and calcium concentration. Calcium led to the aggregation of IHSS HA, which increased both flux decline and rejection. A similar effect was observed with coagulation pretreatment. Rejection increased, and, depending on the dosage, the flux decline was either negligible (low dosage) or severe (high dosage). This behaviour was also attributed to the structure of the flocs. A low dosage of ferric chloride had, for example, a positive effect on flux, whereas a similar concentration of calcium caused detrimental decline.

The 100 kDa membrane showed initially a higher flux and lower rejection than the 10 kDa membrane. However, a fouled 100 kDa membrane exhibited a similar rejection to a 10 kDa membrane at a higher flux. Fouling of the 100 kDa membrane could be prevented by operating at a lower flux. This lead to fluxes similar to that of the 10 kDa membrane, but at significantly lower pressures (and thus energy requirements).

Blocking law analysis in UF indicated internal pore adsorption to be the principal mechanism by which natural organic aggregates were retained and resulted in a pore size reduction. When ferric chloride is added cake filtration becomes important.

In NF, rejection depends on size and charge, for both salt and organics. The TFC-SR membrane showed excellent rejection and flux performance with a high selectivity between calcium and sodium. The TFC membranes all demonstrated high organics rejection, with size exclusion being the dominant rejection mechanism. However, LC-OCD analysis showed that charge effects are important for some fractions of organics. Both TFC-S and TFC-ULP membranes showed a high sodium rejection, which makes these membranes less attractive for surface water applications. Salt rejection determined the flux of these membranes. It is, therefore, necessary to select a membrane well suited to the desired product quality. The CA-UF membrane had a very low salt rejection, while organics rejection was comparably high. The pore size of this membrane is very similar to the size of the organics and therefore treatment is not as reliable as with the TFC membranes.

Large and hydrophobic organics deposit preferentially on the membranes. At high calcium concentrations fouling is significant, with the mechanism depending on solution chemistry.

Calcium-humate complexes cause the greatest flux decline in NF, presumably due to their highly compactable floc-like structures, compared to calcite precipitates. Deposition of calcium and organics increases with pH, due to the precipitation of calcite and adsorption of organics on the calcite surface. Humic acid (HA) caused the highest flux decline of the three organics used, probably due to its higher concentration in the boundary layer. This is related to the larger molecular weight of HA and, thus, a slower diffusion away from the membrane. As a result, precipitation occurred.

Fouling could be related to concentration polarisation, which has been calculated for the stirred cell mass transfer coefficient and crossflow systems. Solubility tests demonstrated that in both systems, the solubility of calcium and organics is exceeded at the fluxes typical for NF. Operation at low flux, low transmembrane pressure, and high shear reduces the deposition of insoluble matter at the membrane surface and thus minimises fouling.

Inorganic colloids did not cause flux decline as they adsorb the organics, which are otherwise to deposit on the membrane. However, the build-up of a colloidal cake-layer results in a modified (lower) solute rejection, but flux decline is fully reversible.

It was found that the flux decline, even under the so-called critical fouling conditions on the NF membranes, is completely avoided by the addition of a low dosage of ferric chloride. For large dosages (100 mgL^{-1} $FeCl_3$), an osmotic pressure builds up and this reduces flux reversibly. The positive ferric hydroxide colloids deposit on the membrane and their charge appears to govern rejection. Cation rejection increases considerably, while the rejection of organics decreases. This demonstrates that the deposit on a fouled membrane can change rejection characteristics. Charge effects were confirmed again by LC-OCD analysis, which showed the rejection of different fractions as a function of pretreatment by NF.

A number of key issues are highlighted through direct comparison of the three processes. Firstly, a cut-off for natural organics rejection at a pore diameter of clean membranes of about 6 to 8 nm is observed. Below this pore diameter rejection is <20%, while above it is mostly >80%. All twelve membranes lie on this cut-off curve. When the membranes are fouled this cut-off is shifted to >20 nm and the cut-off itself is not as distinct. This can be attributed to a pore size reduction due to internal pore adsorption, the formation of self-rejecting cake layers, and solute-solute interactions in the boundary layer. If ferric chloride is added this cut-off ceases to exist. With chemical addition, rejection

of natural organics for the more open membranes can reach the levels achieved with NF. However, the scatter in data is large due to the dependence of rejection on solution chemistry, organic type and concentration, coagulant dosage and the presence of colloids. This variability in rejection introduces an element of risk into such an approach, which is potentially a very economic alternative. If a process involving choice of a more open membrane coupled with chemical addition were to be adopted, intensive monitoring would be essential. More reliable performance requires excessive dosages and is accompanied by detrimental flux decline.

Secondly, for the three membrane processes fouling could not be attributed to any organic characteristic other than size. It was the largest organic (IHSS HA) which had the lowest solubility in the presence of calcium and caused the most severe fouling in all processes. This fouling was a solubility related phenomenon though in the case of MF and UF, aggregation of the precipitants had an impact on the fouling mechanism and resultant flux characteristics.

Thirdly, a water quality parameter (WQP), which considers colloid, organics, and salt rejection, was developed for the membranes investigated. A linear relationship between WQP and log pore diameter was found. Finally, a partial cost analysis of various options was undertaken by evaluation of a) membrane cost as a function of clean water flux and operation at fouled conditions, b) WQP as a function of membrane cost, c) ferric chloride cost, and d) energy costs.

The 'ideal' process depends on the raw water quality and the product water requirements. While MF and UF with a high MWCO can achieve comparable natural organics removal to NF and UF with a low MWCO (provided chemical adsorbents/coagulants such as ferric chloride are added), process reliability is an issue. Smaller compounds are retained to a lesser extent than large and hydrophobic compounds due to their reduced interaction with ferric chloride. The lower treatment costs needed, in this case, to be balanced against a more expensive monitoring system. NF is more economic than UF with a low MWCO. However, compared with MF or UF with high MWCO a salt rejection requirement is needed to justify the additional expense for a higher achievable WQP.

Looking back at the aims laid out in the introduction to this thesis, the following conclusions can be drawn.

(1) All processes investigated have the potential to remove a large amount of natural organics. While this is largely independent of solution chemistry and organic type for NF, it depends strongly on pretreatment and organic type in MF.

(2) Fouling by pore plugging can be most severe in MF. The solution chemistry can vary the aggregation state of the colloids and/or natural organics and dramatically affect fouling.

(3) In UF, fouling by natural organics is mainly influenced by pore adsorption. Colloid fouling is dominated by the aggregate structure. Fouling can significantly improve NOM rejection. With coagulation pretreatment the fouling mechanism shifted from pore adsorption to cake formation.

(4) NF experiments showed that fouling was caused by precipitation of a calcium-organic complex. This precipitation and fouling could be prevented with coagulation pretreatment.

(5) In all processes, large and hydrophobic organic compounds caused most severe fouling.

(6) Structure effects were important in all processes, but on a different scale. The structural dimension which influenced flux decline decreased with membrane pore size from large colloidal aggregates to molecular aggregates.

(7) The final comparison showed that treatment of waters with NF can be done at a competitive cost to MF with pretreatment, if large amounts of natural organics are to be removed.

Chapter 10

FURTHER RESEARCH

Research tends to open more new questions than it answers. Therefore, at the end of this extensive project, there is a long list of areas where further research is needed. The list was divided into two areas, (i) fundamentals, and (ii) process design & evaluation.

On a fundamental level, some of the current research is limited by analytical techniques. This is mostly in the particle analysis field. While it is currently unproblematic to measure colloids in the submicron range which are monodisperse and spherical, there are no reliable techniques which allow the analysis of size, shape and structure of polydisperse systems at concentrations of surface waters. Similar limitations apply to the structural analysis of natural organics and their aggregates. Light scattering together with modelling of colloidal systems may allow the modification of existing techniques.

Further development of these methods will allow the examination of structural effects of systems, such as iron oxyhydroxides or natural organics, on filtration behaviour. In this thesis it was shown that there are structural effects, but their quantification for these systems (that is, oxyhydroxide flocs and organic-calcium aggregates) was not possible.

While methods exist to observe in situ deposition of visible, supermicron particles, these methods need to be further developed for applications to submicron colloids. The observation of deposition of such colloids, their structure and conformation, as well as the properties of the deposit formed cannot be observed in situ at this stage. Measuring these characteristics in situ is important due to the effect shear has on particle size, shape and deposition.

Also, very little is known about the heterogeneous nature of membrane surfaces. While average parameters such as zeta potential and surface roughness can be measured, the nature and distribution of sites is unknown. This 'black box' treatment of membranes limits the application of sophisticated methods of surface analysis. Adsorption studies generally yield only vague insight into possible mechanisms.

More chemical speciation work is needed with the incorporation of various natural organics, complexes, micropollutants and precipitates into the database. Solution speciation is of particular importance in NF.

Some researchers believe that membranes are at the end of their development stage. However, it is obvious when comparing commercial polymeric membranes, that these membranes are far inferior in performance to "natural" (biologically generated and managed) membranes. Such natural membranes adapt their characteristics to their environment. Natural membranes operate at very low 'fluxes' – this low flux appears to be also a trend in commercial applications which can be seen in the critical flux concept – and high surface areas. Also these membranes are usually 'immersed' in their system – a further trend in current treatment. More development is needed to stabilise membrane performance and extend membrane lifetimes.

Module design, especially in RO, has suffered significant neglect over an extended period for a long time. The development of hollow fibre thin film composite NF membranes could be of great advantage for surface water treatment. The spiral wound design limits the particle load permitted onto the membrane, requiring extensive pretreatment. Improved spacer design may also overcome these problems.

Additionally, a careful re-evaluation of the critical flux concept as a function of membrane pore size and foulant characteristics should be possible to establish a more general relationship. The blocking laws should also be re-evaluated for membrane applications.

Pretreatment processes need to be optimised for their adsorption capacity of natural organics and micropollutants. While most adsorptive processes are selective towards a certain fraction, there may be options to enhance the removal of the smaller and more hydrophilic compounds as well as that of micropollutants.

On a process design & evaluation level, a number of careful analyses are required. Firstly, with deteriorating water quality on the planet and water scarcity, the question needs to asked how much water needs to be treated to extremely high standards. It may be the time to treat water for immediate consumption only using more localised facilities thus avoiding troublesome distribution systems.

Secondly, an analysis such as life cycle analysis or environmental impact assessment should be performed on water treatment systems. This analysis should include issues such as treatment plant construction, membrane manufacturing, chemicals consumption, waste production (concentrate streams, sludge, membranes), energy consumption (with the option to apply alternative energies), as well as health aspects and risk assessment.

Thirdly, based on the previous two studies, a complete cost analysis should be carried out which includes long term use of resources and health effects, rather than the typical short-sighted accounting process in which immediately apparent factors such as pumping costs, chemical usage, and capital costs are included.

Fourthly, an evaluation of hybrid membrane processes and coupling of different stages is yet been adequately studied. This implies the use of gradually tighter membranes to remove solutes sequentially. For example, this could be a MF or UF membrane as a first stage with NF or RO at a later stage. The advantage of such treatment would be a possible reduction in precipitation in early stages where fluxes are high.

Concentrate generation and treatment and, - including the trade-off between increased recovery and treatment cost, is an entire field of study which has been addressed very little.

And finally, water mining or water reuse are going to be future issues which raise a set of new questions such as risk, consumer acceptance, retention of micropollutants (hormones, pharmaceuticals, pesticides), and very different type of organics. While rivers in Europe are mostly reuse-streams, with sewage works feeding in and water works taking out, such closed systems will not be readily accepted by the consumer.

Appendix 1

CONCENTRATION OF NATURAL ORGANIC MATTER (NOM)

The concentration of NOM from Mooney Mooney Dam in the Brisbane Water National Park (NSW, Australia) using microfiltration (MF), reverse osmosis (RO) and freeze drying is described. Characterisation of the product is shown in Chapter 4.

The recovery of the RO process was 99.7 %, and a concentration factor of 250 was achieved. No chemical modifications of the samples were carried out and no precipitation occurred during operation of the RO. A total volume of 5000L of surface water was concentrated and dried to produce 230g of powder with a carbon content of approximately 12%.

The performance of the two membrane processes in terms of rejection and flux was monitored throughout operation and the results are shown in this Appendix. This concentration experiment has lead to the further understanding of membrane performance and initiated some of the more fundamental studies carried out in the course of this PhD.

4.1 SELECTION OF CONCENTRATION METHOD

4.1.1 Conventional Methods

Historically, NOM or humic substances have been concentrated from soils or water using adsorptive techniques. Humic substances (HS) are by definition the hydrophobic compounds of NOM, which adsorb to specific resins (such as XAD8 and XAD4). They are extracted from water with an anion exchange resin as described by Leenheer (1981, 1996). This "XAD-Method" fractionates NOM and compounds are possibly modified by the extreme pH changes used. Fractions which may be major fouling precursors or fractions which are extremely difficult to retain with various membrane processes may be lost. The disadvantages of this technique, apart from being very slow, are that only a certain fraction of NOM is retained and that severe modifications of the solution conditions are necessary which may alter the characteristics of the organics. Generally the ion exchange resins adsorb hydrophobic compounds preferentially (Serkiz and Perdue (1990)). Abbt-Braun *et al.* (1991) clearly state that available HS and their fractions are operationally defined.

4.1.2 Concentration using Membranes

In 1990 the use of membranes for NOM concentration was first reported (Serkiz and Perdue (1990)). Since then RO has been used actively (Sun *et al.* (1994), Sun *et al.* (1995), Gjessing (1996), Gjessing *et al.* (1998), Croué *et al.* (1996)) and RO concentrates are now also offered by IHSS. Most compounds in surface water may be concentrated using RO with only a minimal loss of very small organics in the permeate and volatile organics during concentration and freeze drying.

Drawbacks reported are the possible presence of plankton and bacteria in the samples and the abundance of inorganic colloids and salt (Clair *et al.* (1996)). Crum *et al.* (1996) used ultrafiltration after RO to remove salt from the concentrate. This method, however, sacrifices a fraction of NOM which is smaller than the UF pores which will be lost in the permeate and the desalting step is probably incomplete. NOM and multivalent cations form complexes which are not expected to separate in the diafiltration process. Crum *et al.* (1996) also used a cation exchange resin to replace major inorganic cations (Ca^{2+}, Mg^{2+}, Na^{+}, K^{+}) with H^{+}. This also eliminates HCO_3^- as CO_2, which leads to a decrease in solution pH and possibly a precipitation of HA, due to the low solubility of HA at low pH. Ødegaard and Kooftatep (1982) studied the effect of operating conditions on the permeate quality and thus the loss of organics during concentration. They found that pressure was not a crucial parameter, whereas increased membrane 'pore size' and organic concentration lead to a greater loss. It should be noted that some of the membranes used were rather 'open' RO membranes.

Clair *et al.* (1996) reported major losses of concentrate due to the plumbing of their RO plant and observed precipitation in most samples. It was further reported that polycondensation reactions in the concentrate occurred which modified the acid-base characteristics. Phenolic compounds appeard to be lost with the permeate, but most likely, aliphatic carbon is lost. Clair *et al.* (1996) considered the application of a cation exchange resin as a possible fractionation step. Sun *et al.* (1995) suggested the use of a Na^{+} resin to avoid pH variation which leads to increased loss of organics in the permeate and enhances precipitation.

4.1.3 Comparison of Membrane and Adsorption Concentrates

As a result of the selective removal of hydrophobic compounds by resins, RO concentrates contain more polar and aliphatic substances such as proteinaceous compounds. Shuman (1990) anticipates that the hydrophilic fraction which is lost in the XAD process may carry important information and it is believed that this fraction is essential to study membrane filtration, since this small size fraction may be the most difficult part to retain. Serkiz and Perdue (1990) reported significant differences in the elemental composition of HA and FA (concentrated using XAD resins) and DOM concentrated from the same source using RO. Croué *et al.* (1996) compared resin adsorption and membrane filtration and found that the major differences to be the ash content (high purity of adsorbates versus erroneous elemental analysis and low carbon content for membrane concentrates). Furthermore, the XAD concentrate is more aromatic in nature, whereas, the RO concentrate is more hydrophilic and possesses more carboxyl functional groups, and also contains more proteinaceous and sugar type structures. Amino structures were poorly isolated by both techniques. Although RO may modify the NOM only slightly, the freeze drying step ultimately transfers the NOM into solids. This step is required in any concentration method. Depending on the modification, redissolution may be difficult. However, Gjessing (1996) reported no modification in the coagulation properties as a result of freeze drying concentration.

4.1.4 Method Selection

In this study, "real" NOM was obtained using the least invasive and, at least at the beginning of this project, "state-of-the-art" method for NOM extraction: MF combined with RO.

Reverse osmosis will concentrate all constituents of surface water, except some ions, allowing the most wholistic approach. In order to remove large organic matter such as bacteria and particles which are undesirable components of a NOM stock, the surface water was pretreated using MF. This method, however, will selectively remove some organics which are associated with particulates. In order to retain the fraction of organics which may be complexed with multivalent ions and to reduce modifications, it was decided not to use an ion exchange resin.

4.2 SURFACE WATER SOURCE

4.2.1 Choice of Location

Surface water from the Gosford Mooney Mooney pump station in the Brisbane Water National Park in New South Wales was chosen as a source material. It is rich in iron and is soft as are many New South Wales waters and is therefore an ideal representative of a local water. Figure A1.1 shows an aerial photograph of the two Mooney Mooney Dams, on the left the large or upper dam, with the pump station next to the dam. This dam was chosen as the source, as the pump station allowed 2WD access and had power available. The area surrounding the dam is extensive Australian Eucalypt forest of the Brisbane Water National Park.



Figure A1.1 *Aerial photo of the catchment of Mooney Mooney Dam and the Upper and Lower Dams in the Brisbane Water National Park (Gosford, NSW, Australia).*

Figure A1.2 shows a photograph of the dam. However, part of the catchment is used for agricultural activities, which could potentially cause pollution problems.



Figure A1.2 *Photograph of Mooney Mooney Upper Dam (view from near the dam wall).*

4.2.2 Raw Water Characteristics

Raw water characteristics were partly supplied by the Gosford City Council and partly analysed during the month of operation. An average composition can be summarised as follows.

Table A1.1 *Cation composition of raw water.*

Cation	K	Mg	Mn	Ca	Fe	Al	Cu	Na
Concentration [mgL^{-1}]	2.0	2.7	0.05	2.9	1.3	0.5	0.05	10.7

The Mooney Mooney Dam water is known to be high in manganese and iron due to low dissolved oxygen levels in the bottom water associated with thermal stratification. Since the concentration of NOM in 1996 a mechanical stirrer has been installed at the Dam to counteract this problem.

Table A1.2 *Analytical parameters of raw water.*

Parameter	Unit	Value
pH	(-)	6.0
Conductivity	(µS/cm)	120
TOC	(ppm)	6
Turbidity	(NTU)	1.5 - 15
Suspended Solids (as Non-Filterable Residue)	(ppm)	1-7
Hardness (Mg and Ca)	(ppm)	5.6
Alkalinity	(ppm)	9 - 10
Total Phosphorous	(ppb)	10 - 150
Total Inorganic Nitrogen	(ppb)	5 - 80
Ammonia	(ppb)	2 - 30
Oxidised Nitrogen	(ppb)	3 to 50

4.3 MEMBRANE PROCESS OPERATION

4.3.1 Microfiltration and Reverse Osmosis Equipment

A photograph of the two units and the concentration tank in the pump station is displayed in Figure A1.3.

A Memcor microfiltration unit with automated air backflush was used for pretreatment. The membrane area of the hollow fibre module is 1 m^2.

The Permutit Liberator 1 reverse osmosis unit contains two spiral wound modules of 0.96 m^2 each with Filmtec BW30 membranes, a crosslinked aromatic polyamide. These were selected based on low adsorption and high rejection characteristics.



Figure A1.3 *Equipment used to concentrate NOM; a Memcor MF unit and a Permutit Liberator I reverse osmosis unit.*

MF pretreatment was chosen to eliminate particulate matter such as bacteria and inorganic particles, which were not part of the target material. MF would not normally remove natural organics, due to their small size, but NOM often adsorbs on inorganic particulate matter, which is removed and causes a loss of the target material. However, it was considered more important to remove inorganic particles and bacteria.

The whole operation was carried out on-site in eight batches distributed over a period of one month. Operation parameters were monitored and samples of all process streams analysed, which provided initial insights about the surface water behaviour.

Schematics of both processes are shown in Figure A1.4 and Figure A1.5.

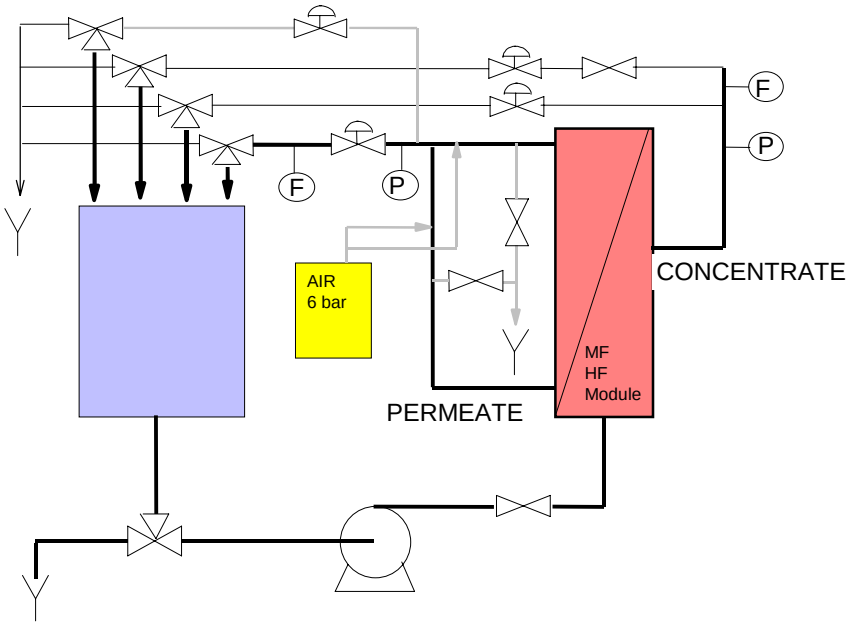


Figure A1.4 *Microfiltration process as a pretreatment in the concentration step (Memcor).*

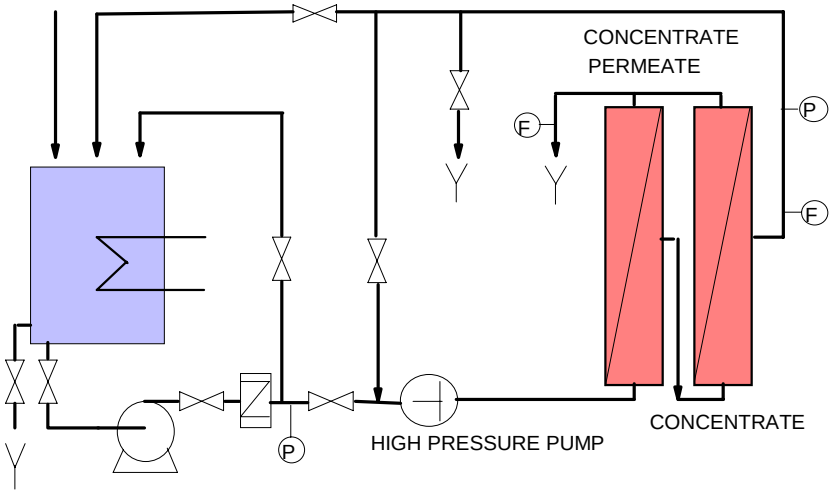


Figure A1.5 *Reverse Osmosis Process as the main concentration step (Liberator I).*

4.3.2 Membrane Process Operation

The MF unit was operated at 0.6 bar with the feed tank continuously fed with surface water directly from the bottom of the dam. Concentrate and excess permeate were both recycled to the feed tank, generating a continuous overflow. Filtration cycles were of 4 to 10 minutes and samples were taken immediately after backwash in order to have a comparable water quality with lowest losses of organic material due to filter cake built-up.

The RO unit was operated at 13 bar, permeate was discharged and concentrate recycled into the feed tank for further concentration. The final volume of a batch was limited by the inner volume of the unit with about 15 L usually obtained, including concentrate washed out of the unit at the end of cycle. The concentration in this final liquid changed depending on the volume of the batch treated at that time.

These volumes varied from 300 L to 1500 L per batch. The feed tank was cooled to 18±2 ^{0}C with a cooling coil supplied with fresh raw water.

Once 5000 L of surface water was attained, all previously concentrated batches were added into the feed tank for further concentration. All batches were stored in a refrigerator.

4.3.3 Freeze Drying

The material obtained from 5000 L of surface water was further concentrated using a Lyovac GT2 (Leybold Heraeus) Freeze Dryer. Quick freezing was applied to minimise damage to the structure of the molecules. The concentrate was filled into four aluminium plates of a diameter of approximately 20 cm to a height of 5 mm. After operation for about 15 hours the powder was removed from the plates with a spatula and refilled without cleaning (to avoid loss of NOM). The operation was repeated until all the concentrate was dried.

4.3.4 Analysis

Standard parameters were flux, temperature, pH, conductivity, TOC/DOC, cations and UV spectra. Further characterisation was carried out with the freeze dried material and is reported in the NOM characterisation section of Chapter 4.

4.4 RESULTS

Results of two batches are shown, the first batch is in standard operation while the last batch is the final concentration step of all previous concentrate batches. In the last concentration step a concentration factor of approximately 250 was attained.

4.4.1 Flux and Water Permeability

Microfiltration flux decreased by approximately 60 % (630 to 385 L $m^{-2}h^{-1}$) during the initial batch and then stabilised. No flux variation during the filtration cycle due to backflush was measurable. Since the MF served as a pretreatment step, and therefore the flux was not continuously monitored. However, serious flux decline soon became apparent which encouraged further investigations.

The flux during RO was of more interest with regard to possible precipitation, and was continuously monitored. The permeability (flux per pressure) for the first and last experiment are shown Figure A1.6 and Figure A1.7, respectively.

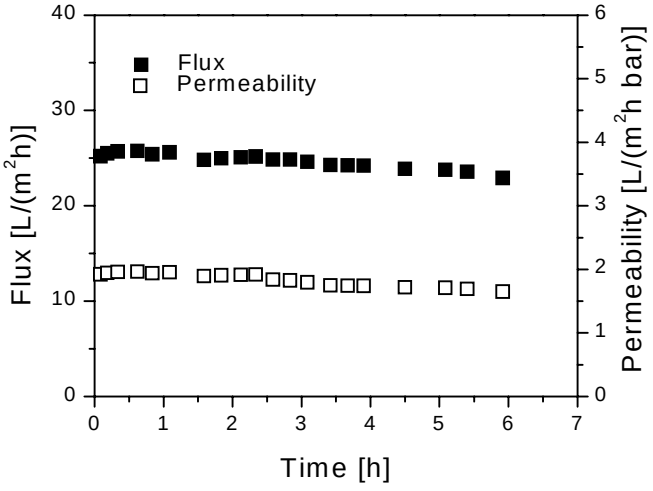


Figure A1.6 *Flux and permeability during first RO batch (25/09/96).*

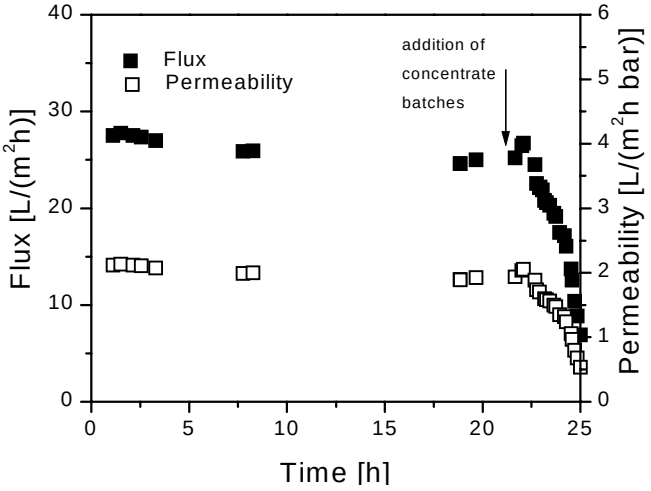


Figure A1.7 *Flux and permeability during last RO batch (25/10/96).*

No significant flux decline occurred during normal batches with concentration factors of up to 100. A small flux decline that was observed can probably be attributed to osmotic effects due to the salt concentration. The osmotic pressure of the salt solution (which is of a higher concentration in the boundary layer) reduces the effective transmembrane pressure.

When the concentrate batches were added flux declined rapidly. This could be due to an increased osmotic pressure, increased viscosity of the solutions, or adsorption of material on the membrane or, more likely, a combination of all of these effects. No precipitation occurred in the tank. After the last batch was concentrated, the RO was rinsed with pure water (permeate). Flux was strongly influenced by temperature, which was responsible for most flux changes occurring during usual operation. The graph showing temperature dependence is shown in Figure A1.8.

Pressure dependence was measured and compared to the initial behaviour. The result is shown in Figure A1.9. The changes were insignificant. The fitting curves were extended to 10 ^{0}C since this temperature is in the surface water range.

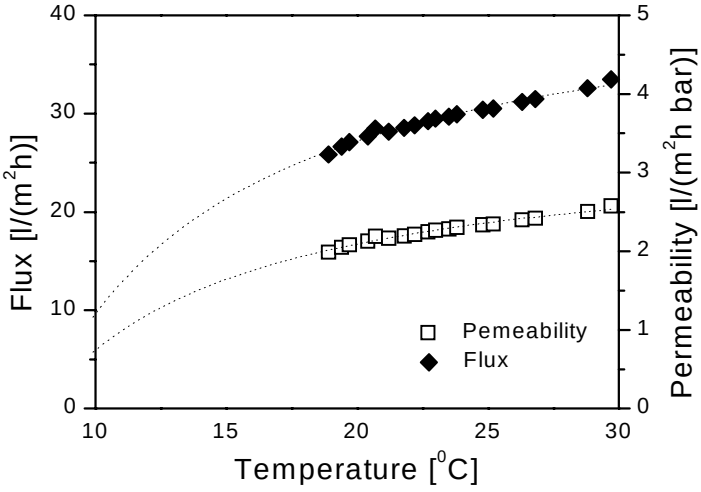


Figure A1.8 *Temperature dependence of flux and water permeability for RO.*

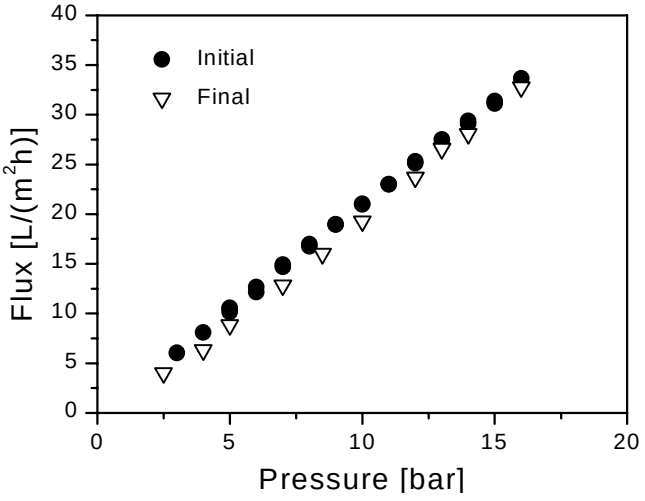


Figure A1.9 *Pressure dependence of RO clean water flux before and after concentration.*

However, cleaning solutions (water and KOH solution) contained substantial amounts of organic matter. The RO unit was first flushed with 30 L of clean water (permeate) and then for 1 hour with 20 L of 0.1% KOH (pH 11.7) at low pressure and high flow to avoid permeate production. Unfortunately, it was not possible to distinguish between material adsorbed on the membrane and organics which accumulated in other parts of the equipment, when operating at such a relatively large scale.

4.4.2 Organic Carbon Rejection

Dissolved organic carbon (DOC) is by definition the organic carbon content of a sample which was prefiltered through a 0.45 μm filter, whereas total organic carbon (TOC) is the carbon content of an

untreated sample. Due to this definition, the organic carbon measured in the raw water represents TOC, whereas all other samples are DOC values, even though all were measured with the same method. Organic carbon contents in all process streams are shown in Figure A1.10 and Figure A1.11.

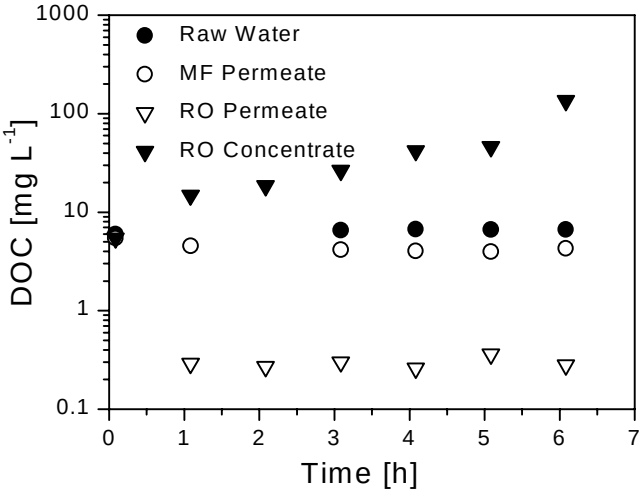


Figure A1.10 *Organic carbon content of process streams (25/09/96).*

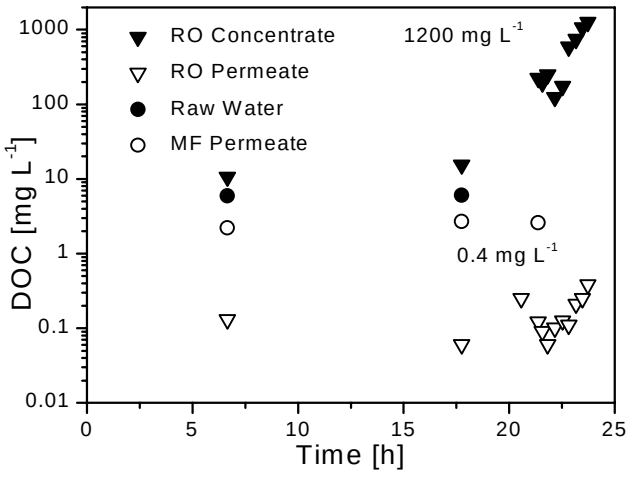


Figure A1.11 *Organic carbon content of process streams (25/10/96).*

In the study, two interesting observations were made; firstly, MF organic carbon rejection increased significantly during the period of interest (from 10 to 55 % as is shown in section 4.4.6) and an increase of rejection could be observed during a filtration cycle. This indicates that a kind of 'dynamic membrane' or self rejecting layer is formed during surface water filtration, which is responsible for flux decline, and also increased rejection. This increase in rejection is of concern, since organic matter is probably lost. This issue has relevance to the nature of the target NOM stock. This is further discussed in the membrane backflush efficiency section below.

For water treatment applications the flux decline was significant. Rejections may be comparable to those obtained with the use of some ultrafiltration membranes and thus it would be interesting to compare which process is more economic at a similar water quality.

Secondly, RO rejection decreased with very high DOC concentrations of the feed solution after being constant for concentration factors up to about 100. Permeate concentration increased approximately four times from normal operation to higher concentration factors of about 300. However, losses due to these relatively high permeate concentrations are very low, since only a small amount of permeate

was produced at this last stage of operation. This is further illustrated in the mass balance section below.

4.4.3 Rejection of Conductivity

Conductivity is an indicator of total dissolved solids (TDS) in water. In this case conductivity was used to observe overall salt rejection of the RO membrane during operation. Conductivity in all process streams at the start and at the completion of operation is shown Figure A1.12 and Figure A1.13. During the first concentration cycle the RO concentrate conductivity increased due to the low permeability of the membrane towards ions. The start value was about 100 μS, and the final value was 2.2 mS representing an increase of approximately 20 times, corresponding to the concentration factor of that day.

The raw water conductivity decreased 5 to 10 % during microfiltration. No rejection of salt is expected with MF, however, the ions may be associated with the particulates or retained organics. The RO permeate was very low in conductivity, as expected, and is not very concentration dependent. During the concentration experiment, the permeate conductivity increased from 3 to 10 μS.

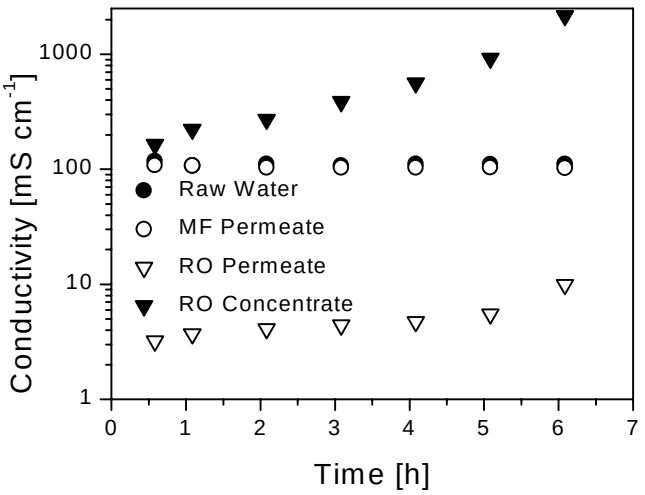


Figure A1.12 *Conductivity in process streams (25/09/96).*

After one month of experiments, the MF conductivity rejection did not increase significantly. The layer formed on the MF membrane which increased DOC rejection, had no major influence on salt rejection. This is also shown in the backwash efficiency section.

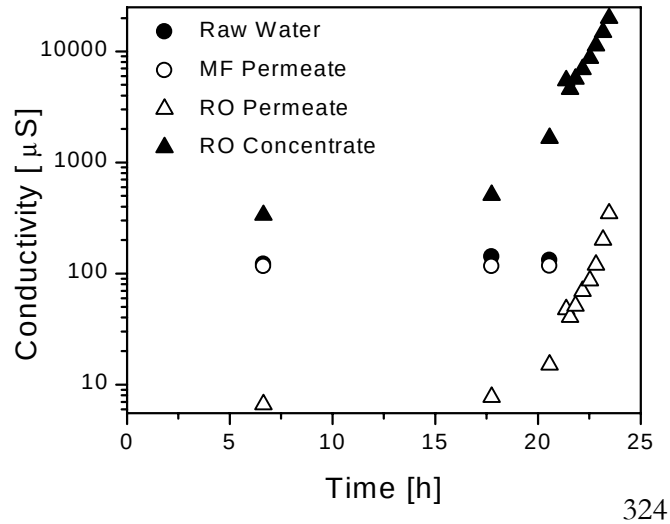


Figure A1.13 *Conductivity in process streams (25/10/96).*

The RO permeate quality decreased slightly from a start value of 3 to 5 µS. The changes during the final experiment with very high concentrate concentrations are more significant; the permeate conductivity and the rejection of conductivity as a function of concentrate conductivity are shown in Figure A1.14. After a slight initial increase in rejection, it decreased during the final concentration step.

The last measured conductivities were 20 mS in the concentrate, corresponding to a concentration factor of about 330 and a permeate concentration of 350 µS. The effect of concentration on the diffusion of solute through the membrane is far more important for inorganic than organic ions, since the permeate DOC did not increase significantly.

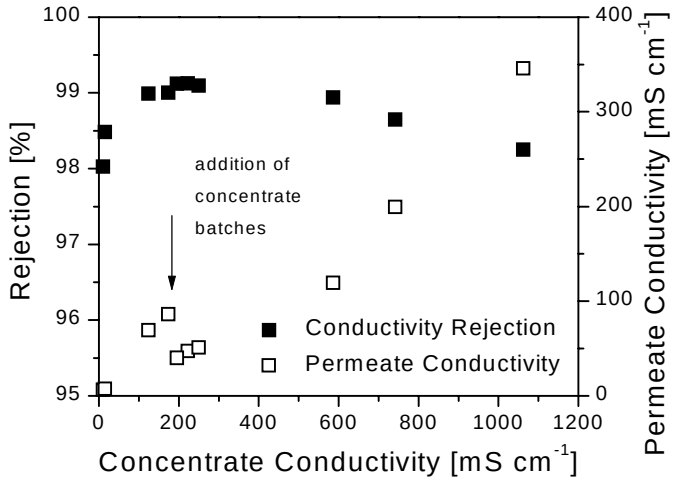


Figure A1.14 *Rejection of conductivity and permeate conductivity as a function of concentrate conductivity (25/10/96).*

4.4.4 pH Value

The raw water and MF filtrate pH were relatively constant ranging between 5.5 and 6.0. Both RO permeate and concentrate pH values increased with the concentrate pH increasing from 5.8 to 7.3. These increases are most probably related to the behaviour of carbonate species, since in the concentrate tank the development of gas was observed. Also, changes in ions which permeate through the membrane and thus change the solution chemistry may influence pH.

With increasing concentration, the dissociation of ions might decrease. These changes are even more significant for the last experiment, where permeate pH increased from 5.3 to 6.5 and concentrate pH from 6.2 to 8.2. The pH over time is shown in Figure A1.15 and Figure A1.16.

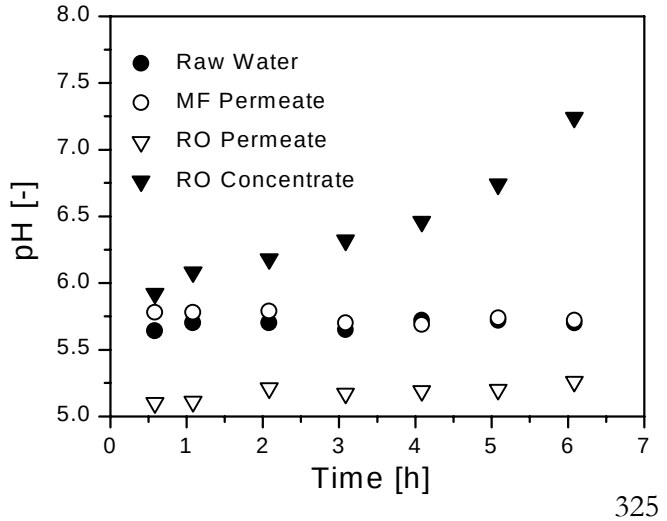


Figure A1.15 *pH for different process streams (25/09/96).*

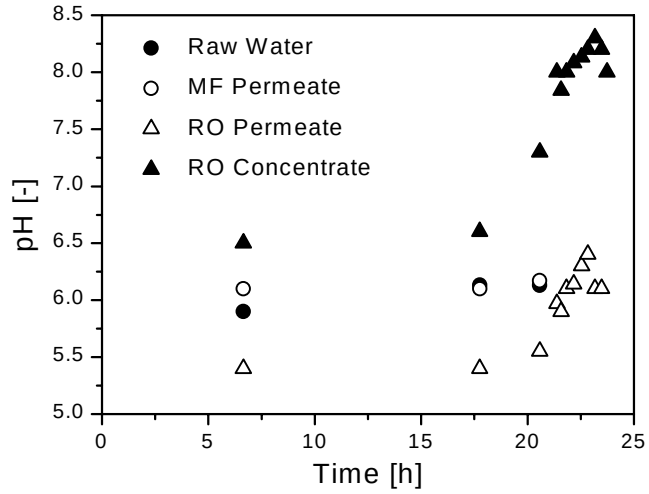


Figure A1.16 *pH for different process streams (25/10/96).*

A change in temperature was not observed and can therefore not be an explanation for the pH variation (calcium carbonate is more soluble at low pH). However some precipitation may have occurred.

4.4.5 Cation Analysis

To further understand membrane selectivities and solution characteristics, an ICP-AES analysis was carried out. Eight cations were analysed: K, Mg, Mn, Ca, Fe, Al, Cu and Na.

Results show that the raw water (see Figure A1.17) composition was constant over the experiment period. During MF (Figure A1.18), Fe and Al were retained in significant proportions (about 85 %), since these elements probably occur as particles. Up to 10 % of the other ions are retained, probably due to their association with organic and inorganic particulate matter. Fe concentration in the MF permeate dropped during the first two hours of operation. This was accompanied by a rapid flux decline, thus indicating a higher rejection, probably of smaller particles due to the build-up of a filter cake. MF permeate concentration of Fe and Al is also lower for the final concentration experiment.

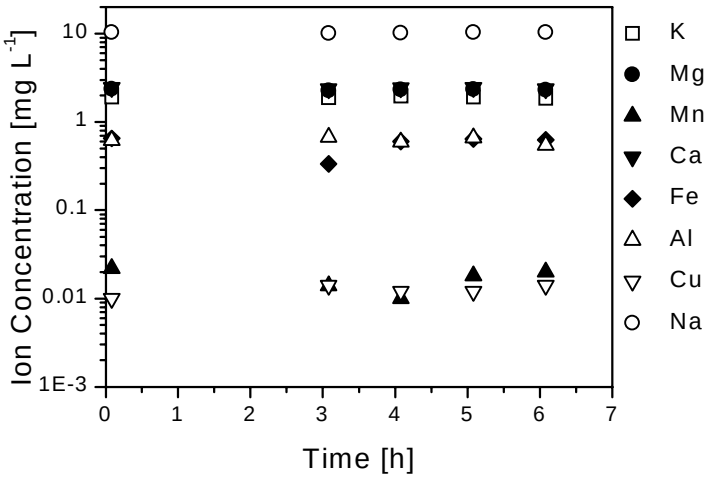


Figure A1.17 *Concentration of cations in the raw water (batch 25/09/96).*

The increase in the RO concentrate cation concentration is shown in Figure A1.19 and Figure A1.20 for the first batch and the final concentration step, respectively. The concentration increased for all cations steadily, as expected, at such high rejections.

The RO permeate cation concentration increased for Na, but remained constant for all other cations in the first batch (see Figure A1.21). At higher feed concentrations all ions permeated through the membrane depending on their size, charge and concentration in the concentrate (see Figure A1.22). The cation concentration in the permeate was Na>K>Ca>Mg>Al>Mn>Fe>Cu.

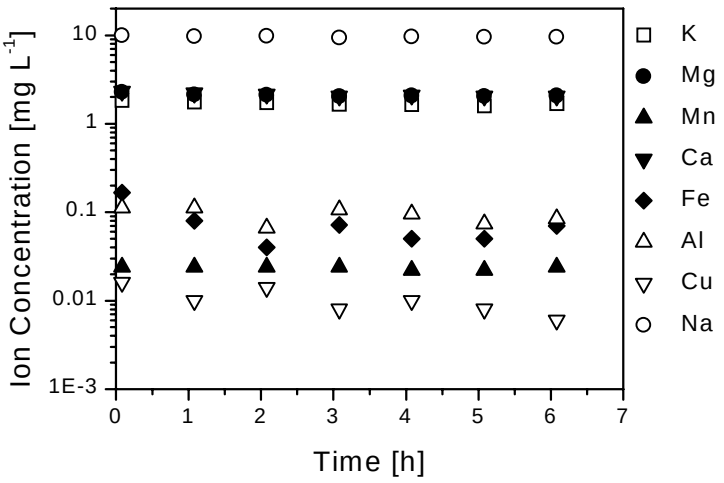


Figure A1.18 *Concentration of cations in the MF Permeate (batch 25/09/96).*

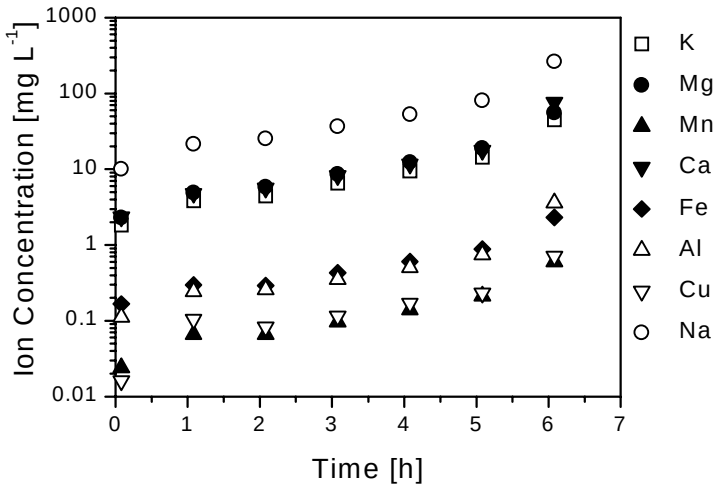


Figure A1.19 *Concentration of cations in the RO concentrate (batch 25/09/96).*

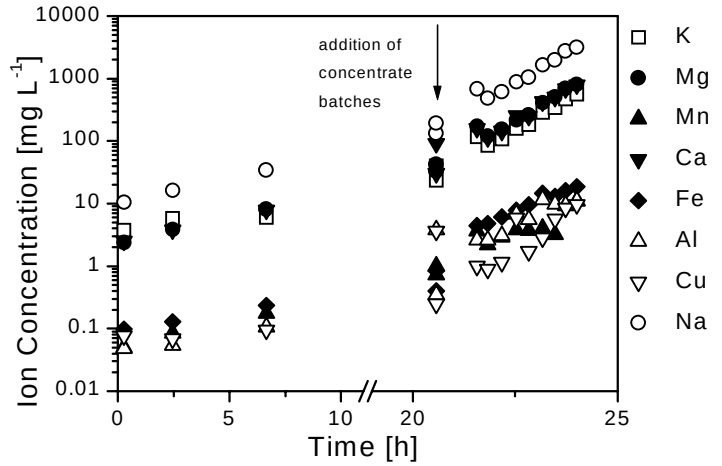


Figure A1.20 *Concentration of cations in the RO concentrate (batch 25/10/96).*

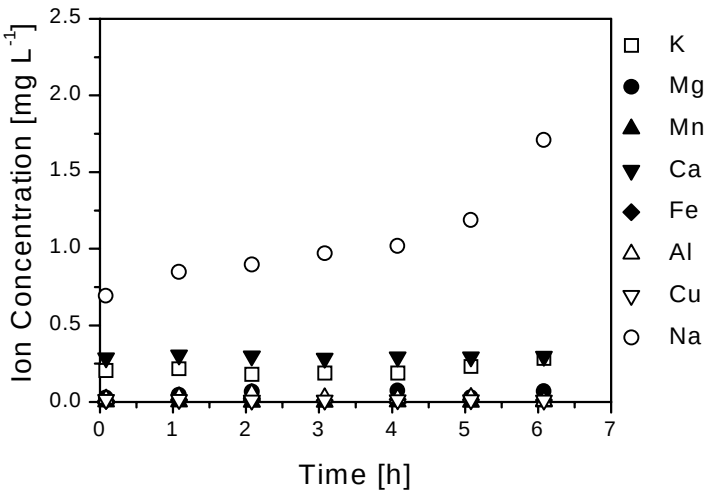


Figure A1.21 *Concentration of cations in the RO permeate (batch 25/09/96).*

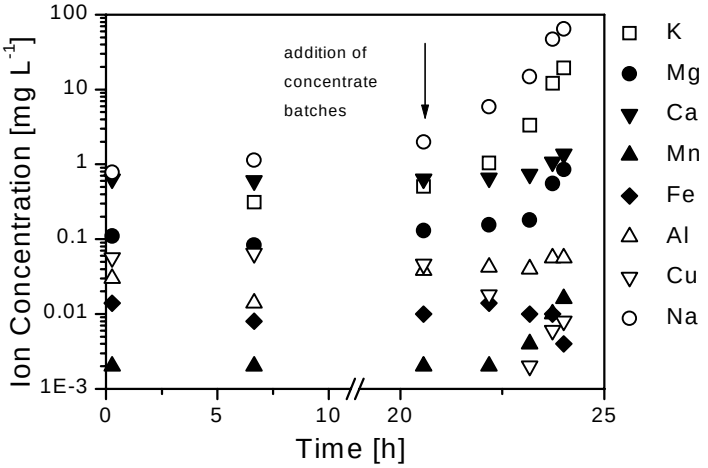


Figure A1.22 *Concentration of cations in the RO permeate (batch 25/10/96).*

4.4.6 Overall Rejection

The rejection of both systems, MF and RO, is summarised in Table A1.3. There is a large increase in DOC rejection during the MF operation, from 9.5 to 55.5%, and in colloid rejection reflected in Fe and Al. This increase in colloid rejection is probably due to retention of small colloids (smaller than the membrane pore size) as shown in Figure 5.1 and also characterised in Chapter 2. Feed concentrations during MF operation are stable and no concentration occurred as in RO. The RO rejection increased with feed concentration to almost 100% for all parameters.

Table A1.3 *Rejection of RO Membrane in normal operation (25/09/96) and at end of last concentration cycle (25/10/96)*

Rejection [%]	DOC	UV_{254nm}	Cond	Na	K	Ca	Mn	Mg	Fe	Al	Cu
MF Initial[o]	9.5	19.0	8.1	2.9	4.5	4.1	0	3.4	74.4	38.2	28.6
MF Final[*]	55.5	69.0	17.6	3.7	6.1	8.4	6.7	10.8	96.3	89.5	40.6
RO Initial[o]	98.04	97.4	98.05	93.22	88.76	87.67	91.67	98.77	95.18	82.14	86.54
RO Final[*]	99.97	99.24	98.25	97.99	96.55	99.83	99.85	99.89	99.98	99.49	99.92

[o] 25/09/96 first sample

[*] 25/10/96 last sample

4.4.7 MF Backwash Efficiency

The MF air backwash system did not induce major flux improvement as shown in Figure A1.23. However, a part of the fouling layer would have been removed since the rejection of DOC and some solids decreased after the backwash.

Rejection before and after backwash is shown in Table A1.4. DOC rejection varied most with backwash and some of the more colloidal metals (Al, Fe) also decreased. This shows the effectiveness of the membrane cake deposit in retaining solute or particles.

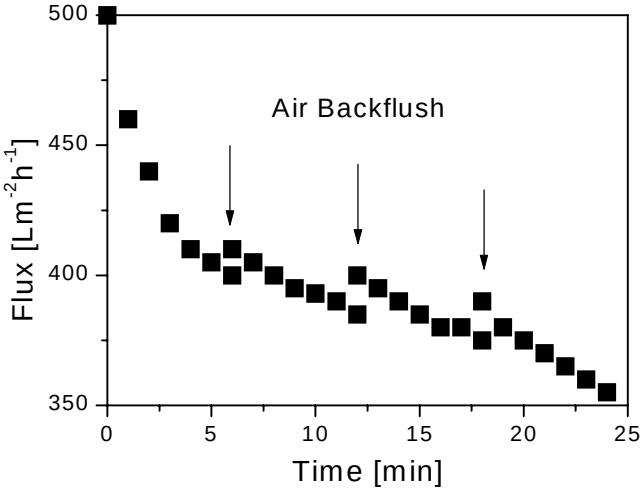


Figure A1.23 *MF Backflush efficiency as flux over time. The arrows indicate backflushes.*

Table A1.4 *Effect of air backwash on MF rejection (samples were taken on last operation day).*

Rejection [%]	DOC	UV_{254nm}	Na	K	Ca	Mn	Mg	Fe	Al	Cu
Before	57.3	69.3	3.2	6.3	10.1	10.0	11.2	98.0	94.4	50.0
After	49.7	69.0	3.0	14.9	11.4	10.0	9.0	97.5	90.8	21.4

4.4.8 Membrane Cleaning and Storage

After the completion of the concentration operation a chemical clean was carried out for the MF and RO units. Flux was fully restored for both units by this cleaning step.

For the MF unit, Memclean Ex A2, a commercial detergent supplied by Memtec, was used at a concentration of 5%w/w. The membranes are stored dry.

The RO unit was cleaned with a 0.1%w/w KOH solution (pH 12, max. 30^0C) at a transmembrane pressure of 140 kPa. The membranes were then stored in 1% metabisulfite solution.

4.4.9 Mass Balance

The overall mass balance of the concentration of 5000 L of surface water is illustrated in Table A1.5. The MF permeate is used as 100% organics although this neglects the loss of about 32% of organics (on average) by the MF pretreatment step. These organics are microorganisms, algae, and such organics which adsorb on inorganic particulates. Only 5% of organics were lost in the permeate. According to the literature review in Chapter 4 these organics are small aromatic compounds (such as phenols or

volatile organics) which cannot be retained by membranes. Further volatile compounds were likely to be lost from the concentrate by evaporation. Some loss also occurred due to concentrate which remains inside the plumbing of the system.

Table A1.5 *Mass balance on NOM concentration.*

	Volume [L]	Average Concentration [mg L^{-1}]	Total Mass [g]	Total [%]	Comment
Raw Water	5000	6.25	31.25	-	
MF Permeate	5000	4.25	21.25	100	MF retained on average 32% of DOC. This should strictly be considered as loss, but the separation of NOM and particulate organic matter such as microorganisms or algae is not possible.
RO Permeate	4985	0.23	1.15	5.41	Very small compounds are lost with the RO permeate
RO Concentrate	15	1251	18.77	88.32	
Loss during Membrane Concentration	-	-	1.36	6.40	Loss due to volatile organic carbon evapotrating from the concentrate and concentrate lost in plumbing of the system
RO Water Wash	25	19.8	0.5	2.35	
RO KOH Wash	40	12.4	0.5	2.35	Total about 104 % due to error on estimated/averaged concentrations
NOM Powder	-	-	14.49	-	The amount of powder obtained including the salt was 230g. Carbon content was determined to be 6.3 % by IHSS which results in 14.49g. See Chapter 4 for details.
Estimated Loss during Freeze Drying	-	-	4.28	-	The high loss during freeze drying can be attributed to the required spreading of samples on flat plates which needed cleaning if the instrument was used by other users.

The NOM powder obtained after further losses due to the freeze drying process was 230 g including salts. With a carbon content of approximately 6.3 % this accounts for 14.5 g organics in total.

Results of the characterisation of the NOM obtained are shown in Chapter 4. This also includes comments on variation of the NOM due to concentration and freeze drying. The carbon analysis is dependent on the oxidation efficiency of the DOC analyser (see Appendix 2 for details).

4.5 CONCLUSION

This study not only enabled the generation of the crucial "NOM stock" for further experimentation, but also provided an initial experience of use of membranes in water treatment. Some observations need to be followed up in the future as outlined below.

- The extent of MF fouling was far more important for process performance than expected. The reasons for this and possibilities for overcoming this problem need to be examined.
- TOC rejection of the MF was higher than initially assumed possible. The potential of MF for TOC rejection needs to be examined on laboratory scale.
- Colloids seemed to play an important role in MF fouling. Some can pass through the MF and may cause fouling in further processes, such as NF. The effect of colloids needs to be further examined and the effect of using a tighter membrane such as UF as a pretreatment step needs to be investigated. These issues are addressed in Chapter 5.
- RO fouling did not occur for normal operating conditions of water treatment. Treatment efficiency should be examined without pretreatment or an alternative pretreatment. These issues are considered in Chapter 7, for Nanofiltration.

Membrane concentration is currently the best available and certainly most efficient process for NOM concentration. However, it is not clear if organic compounds are modified during this process and if so, what implications of these changes are on their treatability.

The experience gained during the "production of NOM was very valuable for the additional research carried out during the course of this project.

Appendix 2

FILTRATION SYSTEM CHARACTERISATION

In Appendix2, the drawings for the Perspex and stainless steel filtration cells, and the magnetic stirrers are provided. This is of importance as the geometry of the stirred cell and the stirrers used influences the hydrodynamics in the cell and thus floc formation and aggregation. Boundary layer thickness and concentration are also influenced. The effect of stirring on boundary layer concentration is shown in Chapter 7. Appropriate references are also given there.

Further a hydrodynamic analysis of the shear forces in the cell is carried out to understand the impact of shear on agglomerates in the cells.

Dr. David Luketina (Civil and Environmental Engineering, UNSW) performed the hydrodynamic analysis for these stirred cells to estimate the shear stress on agglomerates. The analysis is valid for agglomerates larger than 9 μm. Turbulent shear stress dominates for agglomerates up to a size of 9 mm, when mean shear stress becomes dominating. Results can be used for calculation of aggregate break-up and comments on this have been made in Chapter 6.

In essence, the results show that agglomerates larger than 9 μm are prone to break-up. This may explain the presence of smaller aggregates as shown in Chapter 4.

A2.1 FILTRATION SYSTEM DESIGNS

A2.1.1 Perspex Stirred Cell

The cells were used for micro-and ultrafiltration and their volume is 110 mL. They are designed for pressures ≤ 300 kPa. A drawing of the stirred cell is shown in Figure A2.1, with all dimensions in mm. This cell was used for the hydrodynamic analysis as described below.

A pressure release valve is mounted on top of the stirred cell in case the pressure exceeds 300 kPa. Further, an inlet from the feed reservoir (Perspex, 1.5 L) and a manual pressure release valve are located on top of the cell. The cell is placed on a magnetic stirrer table for stirrer operation (see Figure A2.2 for stirrer calibration). The membrane is fitted on a porous support in the bottom of the cell.

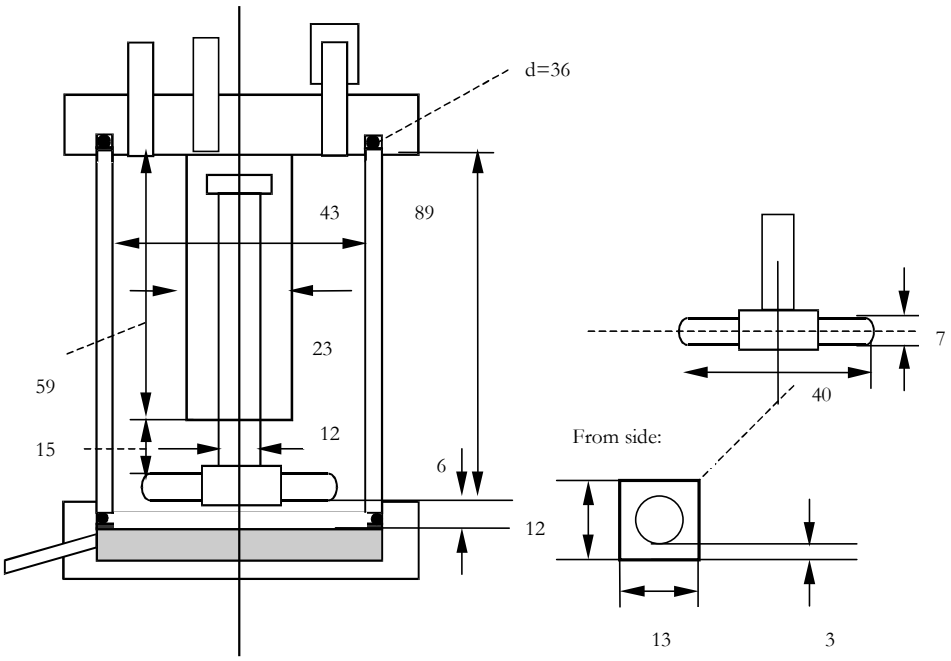


Figure A2.1 *Drawing of Perspex stirred cell. All dimensions are in mm.*

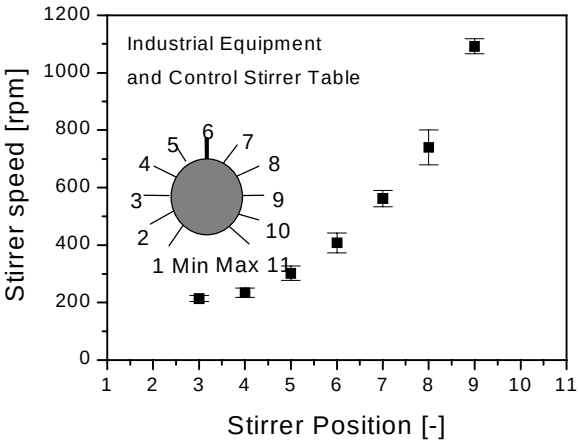


Figure A2.2 *Calibration of stirrer (stirrer speed measured with stroboscope as explained in Materials and Methods Chapter).*

A2.1.2 Stainless Steel Stirred Cell

These systems were designed for up to 20 MPa in nanofiltration and reverse osmosis experiments. The cell volume is 190 mL. The magnetic stirrer is purchased from Amicon. The drawing is shown in Figure A2.3.

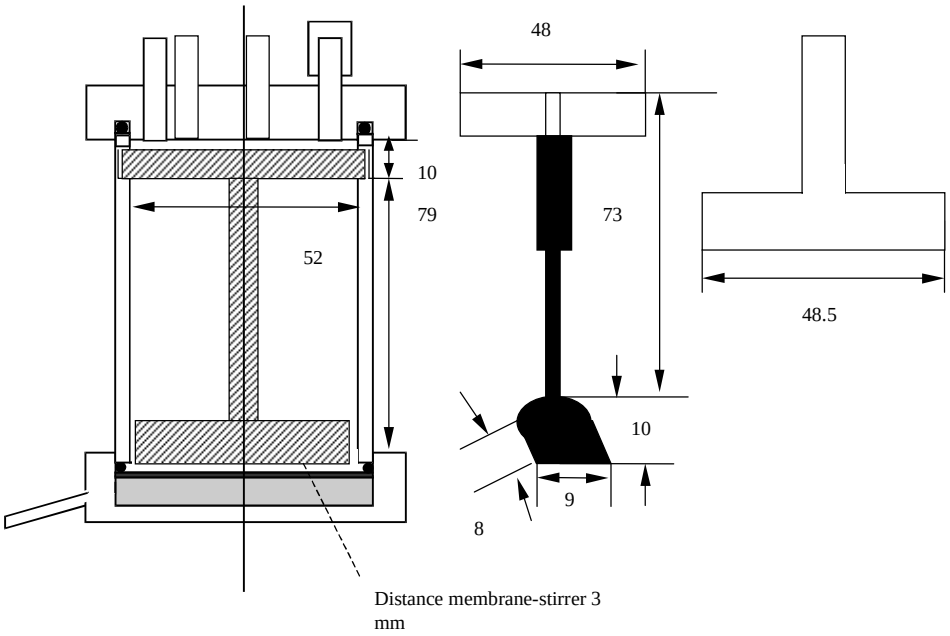


Figure A2.3 *Drawing of stainless steel stirred cell. All dimensions are in mm.*

A2.2 MASS TRANSFER IN STIRRED CELLS

Smith *et al.* (1968) looked at mass transfer of a batch dialyser of similar geometry to those of the stirred cells. In summary, mass transfer reduced as stirrer diameter reduced. Mass transfer is lowest at the centre of the impeller. The transition between laminar and turbulent regimes occurred between Re of 20 000 and 30 000. The closer the impeller to the surface, the higher the mass transfer.

This shows that the mass transfer in the NF (stainless steel) cells is higher than in the MF and UF (perspex), as A) the impeller has a greater diameter and B) the impeller is closer to the surface. Maximum deposition observed in experiments confirms the lower mass transfer at the centre. A more detailed mass transfer analysis is performed in Chapter 7.

A2.3 SHEAR IN A CYLINDRICAL CHAMBER STIRRED BY A RADIAL FLOW IMPELLER

A2.3.1 General Description of Flow

Radial flow impellers discharge fluid in a radial direction. The subsequent low pressure region created at the centre or eye of the impeller causes fluid to enter from an axial direction. The resulting circulation consists of a radial jet or impeller stream at the level of the impeller driving circulation cells above and below the impeller (in this instance, there will be minimal circulation below the impeller due to its close

proximity to the base of the chamber). The radial jet is of comparable thickness to the impeller height and has velocities of around 0.2 of the impeller blade tip velocity U_{tip} (Dong *et al.* (1994), Ciofalo *et al.* (1996)) near the ends of the blades. In addition to the circulation cells and impeller stream, a swirling flow is set up inside the chamber. The highest shears s_m due to mean flows will be in the jet region and can be parameterised by:

$$s_m = 0.2 \frac{U_{tip}}{d} = 0.2 \frac{\omega R}{d} \qquad \text{(A2.1)}$$

where d is the height of the impeller blade, R is the radius of the impeller blade and ω is the rotational rate in rad s^{-1}.

It will be shown that the turbulent shear s_t exceeds the means shear s_m. For this reason we will concentrate on the turbulent shear.

The impeller used in the stirrer is of a type for which hydrodynamic data is relatively lacking. However, a considerable amount of data is available for Rushton turbines and flat bladed paddle stirrers. For this reason, it is necessary to use a theoretical analysis to predict the shear rather than drawing directly on the results of previous studies. This analysis follows.

A2.3.2 Theoretical Analysis for Shear Prediction in Stirred Cell

Turbulent Shear Relationships

Before the relevant turbulent shear can be assessed, it is necessary to know the scale of interest and understand its relevance to the turbulent cascade (transfer of energy from large to small scales). The Kolmogoroff microscale L_k is given by:

$$L_k = \left(\frac{\nu^3}{\varepsilon}\right)^{1/4} \qquad \text{(A2.2)}$$

where ε is the turbulent dissipation of turbulent kinetic energy (per unit mass).

For scales of motion L less than and larger than L_k the turbulent velocity scale u is given by:

$$u = A(\varepsilon L)^{1/3} \qquad L > L_k \qquad \text{(A2.3)}$$

and

$$u = B\left(\frac{\varepsilon}{\nu}\right)^{1/2} L \qquad L < L_k \qquad \text{(A2.4)}$$

respectively, where A and B are constants. A and B are approximately unity and $(1/15)^{1/2}$ respectively, for well developed turbulence.

The turbulent shear $s_t = u/L$, so that:

$$s_t = \left(\frac{\varepsilon}{L^2}\right)^{1/3} \qquad L > L_k \qquad \text{(A2.5)}$$

and

$$s_t = \left(\frac{1}{15}\frac{\varepsilon}{\nu}\right)^{1/2} \qquad L < L_k \tag{A2.6}$$

Particle agglomerates of diameter d_p where $d_p > L_k$ (the most likely case) will be subject to shear associated with the turbulent length scale $L = d_p$. Thus the shear influencing the particle agglomerates will be:

$$s_t = \left(\frac{\varepsilon}{d_p^2}\right)^{1/3} \qquad d_p > L_k \tag{A2.7}$$

In order to estimate the shear, it is necessary to determine the turbulent dissipation.

Turbulent dissipation

The turbulent dissipation can be estimated from:

$$\varepsilon = \frac{u_e^3}{L_e} \tag{A2.8}$$

where the subscript e denotes the energy bearing or integral scales.

If we scale $u_e \approx U$ and $L_e \approx d$ then:

$$\varepsilon \approx \frac{U^3}{d} = \frac{(\omega r)^3}{d} \tag{A2.9}$$

where r is the radial distance from the centre of the impeller. The peak dissipation will be near the impeller tips where $u_e \approx U_{tip}$ so that:

$$\varepsilon_{peak} \approx \frac{\omega^3 R^3}{d} \tag{A2.10}$$

Averaging dissipation along the length of the impeller gives:

$$\varepsilon_{near\ arm} \approx \frac{\omega^3 R^3}{4 d} \tag{A2.11}$$

This dissipation will largely occur within a (downstream) distance d of the impeller blades (Schafer *et al.* (1997)). Distributing this dissipation over the volume occupied by the impeller zone and stream results in:

$$\varepsilon_{impeller} \approx \frac{n d}{2\pi R_c}\frac{\omega^3 R^3}{4 d} = \frac{n \omega^3 R^2}{8\pi} = \frac{n U_{tip}^3}{8\pi R_c} \tag{A2.12}$$

where n is the number of blades and R_c is the chamber radius.

An alternate method is to estimate the dissipation by assuming that the power input is largely expended within the impeller zone and stream (this is justified by the results of Schafer *et al.* (1997) as well as Bakker and Van den Akker (1994). The power input can be approximated using a conventional drag formulation:

$$P \approx n \int_0^R \frac{1}{2} \rho C_D d (\omega r)^3 dr = \frac{n}{8} \rho C_D d \omega^3 R^4 = \frac{n}{8} \rho C_D d R U_{tip}^3 \qquad \text{(A2.13)}$$

where C_D is a drag coefficient. This can be expressed as a Power number P_o as:

$$P_o = \frac{P}{\rho N^3 D^5} = \frac{n \pi^3}{32} C_D \left(\frac{d}{R}\right) \qquad \text{(A2.14)}$$

Power numbers estimated using the above relationship for the radial impellers of Leentvaar and Ywema (1980) tend to be around twice the measured values. From this we can conclude that a more appropriate estimate of the input power is:

$$P \approx \frac{n}{16} \rho C_D d \omega^3 R^4 = \frac{n}{16} \rho C_D d R U_{tip}^3 \qquad \text{(A2.15)}$$

This is not unexpected, as the relative velocity between the impeller blades and the fluid at radius r will be less than ωr due to the swirl induced in the fluid.

For the impeller used in these experiment, with cylindrical arms, $C_D \approx 1$ for $Re = \omega r d/\nu > 400$ where ν is the kinematic viscosity. Averaging the power over the mass occupied by the impeller and substituting $C_D = 1$ results in:

$$\varepsilon_{impeller} \approx \frac{n \omega^3 R^3}{16 \pi R_c} = \frac{n U_{tip}^3}{16 \pi R_c} \qquad \text{(A2.16)}$$

This relationship will provide an upper bound on $\varepsilon_{impeller}$ as some energy will be made available to the mean flow. This mean flow energy is then being dissipated at the boundaries of the chamber. Further, energy will be dissipated outside of the impeller zone and impeller stream. However, laboratory and numerical studies have indicated that the vast majority of dissipation in stirred chambers takes place in the impeller zone and impeller stream (e.g. Cutter (1966), Bakker and Van den Akker (1994), Schafer *et al.* (1997)).

The preceding relationship for $\varepsilon_{impeller}$ has exactly the same form as the earlier estimate except that value is halved. This suggests that the values given by ε_{peak}, as derived earlier, should also be halved. Thus the shear rates now become:

$$s_{t\,peak} = \frac{\omega R}{(2 d d_p^2)^{1/3}} = \frac{U_{tip}}{(2 d d_p^2)^{1/3}} \qquad d_p > L_k \qquad \text{(A2.17)}$$

and

$$s_{t\ impeller} = \omega R \left(\frac{n}{16\pi R d_p^2}\right)^{1/3} = U_{tip} \left(\frac{n}{16\pi R d_p^2}\right)^{1/3} \qquad d_p > L_k \tag{A2.18}$$

A2.3.3 Implications of Shear on Agglomerates in Solution

Circulation

Now that we have a means for estimating the shear, it is of interest to see how often and for what duration, agglomerates will be subject to high levels of shear. The chamber has a throughflow of Q_i. The radial or impeller stream discharge Q_R can be approximated by:

$$Q_R = 0.2\ \alpha\, n\, \omega\, R\, d^2 \tag{A2.19}$$

where it has been assumed that a discharge of velocity $0.2\ U_{tip}$ is occurring over an area of αd^2 behind each impeller where α is a constant. Comparison with a conventional pumping number N_Q:

$$N_Q = \frac{Q}{N D^3} \tag{A2.20}$$

leads to:

$$N_Q = 0.2\pi\, \alpha\, n \left(\frac{d}{D}\right)^2 \tag{A2.21}$$

For an eight bladed radial impeller, Ciofalo (1996) quotes Nagata (1975) as reporting a value for N_Q of 0.34. The above relationship gives the same value if $\alpha = 1.7$. However, the impeller used in our experiments, being cylindrical, is more streamlined than the flat bladed impeller of Nagata (1975). This will result in a reduced radial flow. Given that the drag coefficient for a cylinder is half that of a flat plate, $\alpha \approx 1$ is probably more appropriate.

The ratio $R_Q = Q_i/Q_R$ will determine how often particles recirculate and pass through the high shear impeller zone. For large values of R the inflow will dominate and relatively few particles will recirculate. If the density difference between the particles and fluid is sufficiently small and the particles themselves are small they will follow the fluid motion.

The fraction of particles which will travel directly to the outlet without being recirculated in period T will be $\chi = R_Q/(1+R_Q)$ where $T = V/Q_i$ and V is the volume of the chamber. The fraction of the particles in the inflow left to recirculate one or more times is simply $1-\chi$. In the next period T, of the $1-\chi$ particles recirculating, χ will be the fraction removed. Thus the fraction of particles that recirculate once is $\chi(1-\chi)$. This can be generalised to give the fraction f of particles that have been exposed to the high shear zone m times as:

$$f = \chi\,(1-\chi)^{m-1} \tag{A2.22}$$

The duration of exposure t_{exp} to the high shear on each passage through the impeller can be estimated from:

$$t_{exp} = \frac{Q_i + Q_R}{\pi d R_c^2} \qquad \text{(A2.23)}$$

The Experiments with Perspex Stirred Cells

For the experiments ω = 54 rad s-1, d = 0.007, n = 2, R_c = 0.0215 and R_Q = 0.02. Thus the above become $s_{t\ peak} \approx 4.5\ (d_p)^{-2/3}$ and $s_{t\ impeller} \approx 1.3\ (d_p)^{-2/3}$. Given the approximations made earlier, these estimates are probably accurate to within a factor of two or three.

The Kolmogoroff length in the peak dissipation region is estimated to be around 9 μm. Thus, as long as particle agglomerates are larger than this in size, the preceding analysis will be valid. The Reynolds number Re is well above the required value of 400.

The ratio of the shear stress due to mean and turbulent flows is:

$$\frac{s_{t\ impeller}}{s_m} - 5\,d\left(\frac{n}{16\pi R_c d_p^2}\right)^{1/3} \qquad \text{(A2.24)}$$

Substituting the experimental values yields $s_{t\ impeller} / s_m \approx 0.043\ (d_p)^{-2/3}$. For the mean shear stress to be dominant, d_p would need to exceed 9 mm. Thus the earlier assumption of the mean shear stress not being as significant as the turbulent shear stresses is valid.

Appendix 3

HEMATITE PREPARATION (α - Fe_2O_3)

Spherical, monodisperse hematite (α-Fe_2O_3) colloids are used in this study to simulate naturally occurring inorganic colloids. The interaction of such colloids with organics is described in Chapter 2 and their postulated aggregation behaviour in Chapter 4.

Here the preparation and characterisation of the colloids for four different primary colloid sizes – 40, 75, 250 and 500 nm – is described. Basic characteristics, such as particle size, volume, mass, surface area, and zeta potential are summarised.

The amount of particles required to cover the membrane area, the number of layers if all colloids are deposited and the layer thicknesses assuming a porosity for random closed spheres are calculated.

A3.1 SYNTHESIS OF HEMATITE PARTICLES

Hematite particles were synthesised following the method of Matijevic and Scheiner (1978), also described by Amal (1991), by forced hydrolysis of a homogeneous iron (III) chloride solution. The hematite particles produced with this method are monodispersed and spherical. Four different sizes of hematite were produced and the recipes are shown in Table A3.1. For larger particles, the hematite I was used as a seed sol. For smaller particles (hematite IV) the standard receipe was varied to cause a increased nucleation and shorter growth.

Table A3.1 *Hematite Preparation Procedures and Colloid Characteristics, ferric chloride floc characteristics for comparison.*

	Hematite I	Hematite II	Hematite III	Hematite IV
Fe Source/ Seed Solution	3.65 g $FeCl_3 \cdot 6H_2O$ dissolved in 20 mL 3.75 mM HCl	20 mL Hematite I 3.05 g $FeCl_3 \cdot 6H_2O$	20 mL Hematite II 3.05 g $FeCl_3 \cdot 6H_2O$	4.5 g $FeCl_3 \cdot 6H_2O$ dissolved in 7.5 mL 0.1M HCl
Nucleation in Acid at 100^{0}C	750 mL 3.75 mM HCl	6.3 mL $HClO_2$ (70%) 725 mL H_2O	6.3 mL $HClO_2$ (70%) 725 mL H_2O	700 mL H_2O
Particle Formation in Oven	100 ^{0}C, 24 hrs	100 ^{0}C, 24 hrs	100 ^{0}C, 24 hrs	boil for 20 min then add 6.75 mL 1M HCl and add 35.75 mL H_2O, then 100^{0}C, 1 hr
Cooling	Let Sol cool to room temperature	Let Sol cool to room temperature	Let Sol cool to room temperature	Let Sol cool to room temperature
Cleaning (aggregation and Centrifugation):				
Aggregation (settling of colloids or change of colour will be observed)	Add KCl to a concentration of about 0.1 M	0.1 M KCl	0.1 M KCl	0.1 M KCl (add more if not sufficient)
Centrifugation	2000 rpm 10 min	2000 rpm 10 min	2000 rpm 10 min	2500 rpm 10 min or longer if no separation occurs
repeat cleaning steps 5 times	repeat cleaning steps 5 times	repeat cleaning steps 5 times	repeat cleaning steps 5 times	repeat cleaning steps 5 times
Storage	At 4^{0}C, adjust pH to 3.0 using HCl	At 4^{0}C, adjust pH to 3.0 using HCl	At 4^{0}C, adjust pH to 3.0 using HCl	At 4^{0}C, adjust pH to 3.0 using HCl

All glassware used was cleaned with concentrated HCl (36%) to avoid nucleation at the glass surface. It is essential to use clean vials and wash bottles to avoid contamination of the hematite surface and thus variation of the surface characteristics.

Vigorous stirring was applied during the addition of ferric chloride to the solution. For the small colloids (hematite IV, 40 nm), the solution needs to be excessively saturated to ensure very high nucleation rates. After 20 minutes of nucleation and growth, adjusting the acid concentration, and thus

changing the equilibrium solubility, stopped the process. Further growth is allowed in the oven. Since under these conditions, not all iron is used, after centrifugation the supernatant is dark brown, but clear.

For the larger particles, Hematite I is used as a seed sol, providing the nuclei for further growth on their surface. Seed sol and ferric chloride are added in this case to boiling perchloric acid.

Aggregation of the colloids using KCl was required to facilitate centrifugation. The supernatant was discarded and the "cleaning" step repeated five times. A Clements Model B Universal Centrifuge was used for particle cleaning and an Ultrason Elma Transsonic T460 ultrasonic bath was used for particle redispersion. This washing step is required to eliminate remaining free iron from the solutions. For the smallest colloids (40 nm) this step can be difficult, requiring higher KCl concentrations and longer centrifugation times.

A3.2 CHARACTERISATION OF HEMATITE PARTICLES

The concentration of the sol was determined using ICP-AES. The sol was heated 1:1 with concentrated HCl (36%) until the colloids dissolved. The concentration and size characterisation of the sols is shown in Table A3.2.

Table A3.2 *Hematite batches (different values are for different batches), concentration and primary particle sizes (*the larger size measured by PCS for the smallest primary particles is probably due to the presence of doublets and triplets in solution and the measurement of the hydrate layer).*

Batch	Fe Concentration [mgL^{-1}]	Hematite Concentration [mgL^{-1}]	PCS [nm]	FESEM [nm]
Hem I	755, 406, 636, 895	1080, 580, 909, 1280	$177 \pm 31^*$, 117^*, $193 \pm 20^*$, 136^*	75 ± 10
Hem II	730, 705	1044, 1008	220, 260	250 ± 25
Hem III	808	1155	450	500 ± 50
Hem IV	287	410	-	40 ± 5

Table A3.3 lists the characteristics of the different hematite sizes and compares selected characteristics. Specific surface area decreases with particle size and the ferric chloride flocs have a much higher surface area, most likely due to a smaller precipitate size or amorphous nature. Zeta potential decreases with particle size (see Chapter 4 for method description and charge characterisation as a function of solution chemistry).

Based on the colloid size (and ignoring charge effects and double layer thickness), the number of particles to cover the membrane surface in a monolayer was calculated. Further, the number of layers and the layer thickness were calculated assuming that 1L of solution with a concentration of 10 mgL^{-1} is filtered (and thus 10 mg of colloids deposit) on a membrane. This is the amount of solution filtered in MF experiments.

The resulting layer thicknesses are the maximum values achievable if all colloids deposit. The thichness is dependent on particle packing and cake porosity.

Table A3.3 *Characteristics of hematite colloids and, ferric chloride flocs for comparison ([1] Crosby et al. (1983)).*

	Hematite I	Hematite II	Hematite III	Hematite IV	$FeCl_3$ Floc
Particle Size [nm]	75	250	500	40	N/A
Volume per Particle [m^3]	$220.9 \cdot 10^{-24}$	$8\,181.2 \cdot 10^{-24}$	$6\,5449.8 \cdot 10^{-24}$	$33.5 \cdot 10^{-24}$	N/A
Mass per Particle [g]	$1\,157.5 \cdot 10^{-18}$	$42\,869.5 \cdot 10^{-18}$	$342\,295.2 \cdot 10^{-18}$	$175.5 \cdot 10^{-18}$	N/A
Number of Particles per 10 mg [-]	$8.6 \cdot 10^{12}$	$2.3 \cdot 10^{11}$	$2.9 \cdot 10^{10}$	$5.7 \cdot 10^{13}$	N/A
Surface Area [m^2g^{-1}]	15.1*	4.5*	2.3*	28.7*	160-230[1]
Zeta potential at pH 3 [mV]	+35	+24	+18	+36	N/A
Particles required to cover MF membrane surface [-]	$2.26 \cdot 10^{10}$	$2.03 \cdot 10^{9}$	$5.10 \cdot 10^{8}$	$7.96 \cdot 10^{10}$	N/A
Number of Layers [-]	380	113	57	716	N/A
Layer Thickness [x] [μm]	28.5	28.2	28.5	28.6	N/A
Layer Thickness [x] [μm]	45.2	44.8	45.2	45.4	N/A

* Calculated on the basis of spherical particles of a density of 5.24 $g.cm^{-3}$ (Liang (1988)).

[x] Assuming a solid deposit, thus a cake porosity of zero.

[+] Assuming random close packed spheres, thus a cake porosity of 0.63 (see Chapter 6).

Electronmicrographs of the four different particles are shown in Figure A3.1. A drop of sol was deposited on a clean membrane for analysis and sample preparation was identical to the method described in Chapter 4 for FESEM.

To determine the size of the particles formed the particles were measured on the photographs and the average size determined with an estimated average error. The photographs confirm the spherical and monodisperse nature of the colloids.

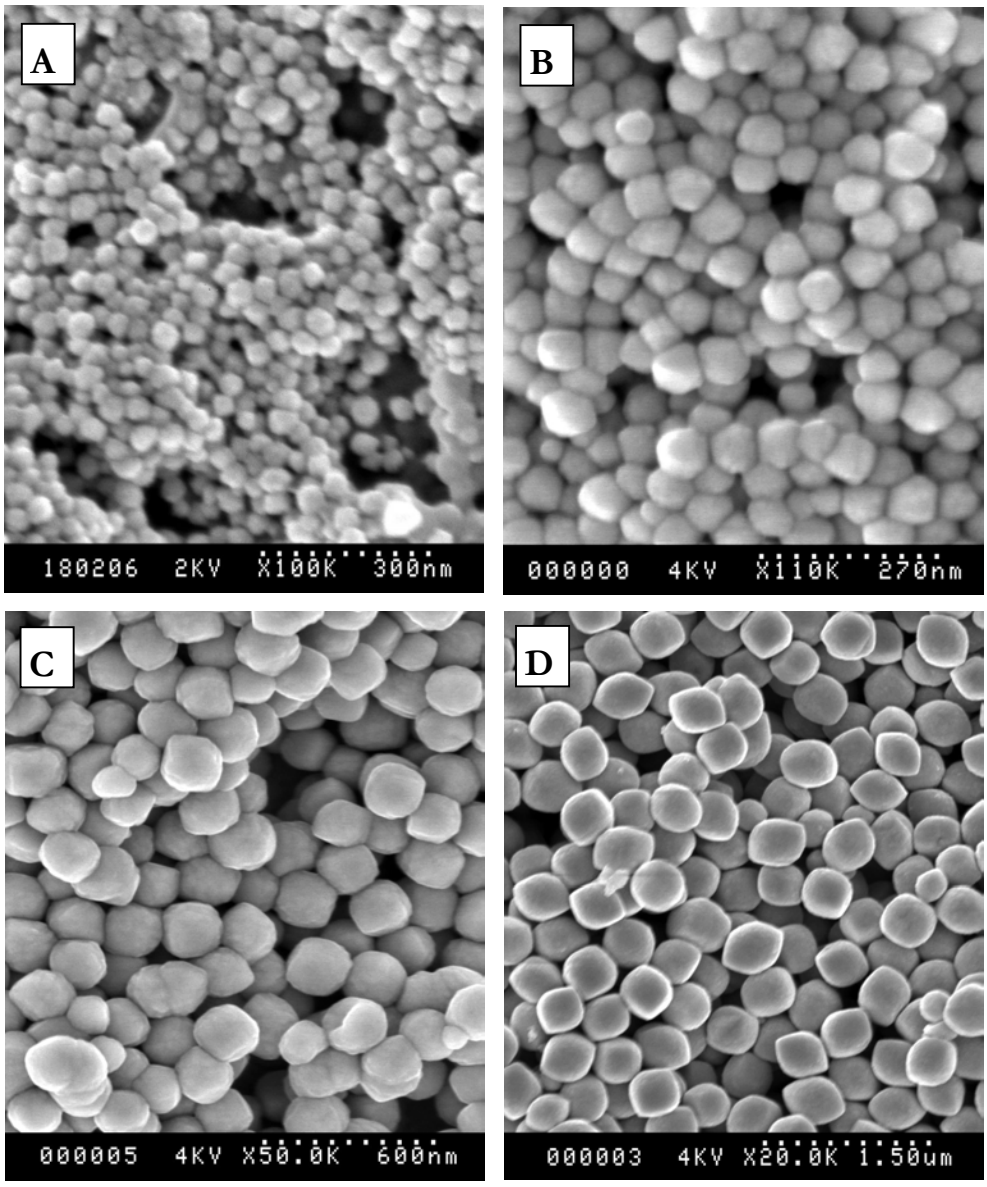


Figure A3.1 *Electronmicrographs of the hematite colloids produced A) hematite IV, 40 nm, B) hematite I, 75 nm, C) hematite II, 250 nm, and D) hematite III, 500 nm (Note different magnification of pictures).*

Appendix 4

INSTRUMENT CALIBRATION

The intention in this Appendix is to point out potential problems of two very commonly used routine techniques for NOM analysis. Both techniques are in principle very simple, but extreme care has to be taken in the interpretation of results.

Both DOC and UV analysers were tested extensively to understand the limitations of these analyses. Care has to be taken when UV analysis is used to determine the organic concentration of solutions, especially in water treatment. Treatment often removes a fraction of the UV absorbing compounds selectively and the measured values are in this case not related to the organic concentration.

Additionally, the oxidation efficiency of the DOC analyser may also depend on the organic characteristics and similar problems may be encountered. It is strongly suggested to couple at least two techniques for organic carbon analysis.

Both UV and DOC respond differently to organic fractions - large, aromatic compounds strongly absorb UV light, whereas DOC has a higher oxidation efficiency for smaller, more aliphatic compounds.

A4.1 ORGANIC CARBON ANALYSIS

The nomenclature of organic carbon is described in detail in Chapter 2 and in the Glossary. While there is a difference in definition between total organic carbon (TOC) and dissolved organic carbon (DOC), which is that the DOC is that part of TOC which passes through a 0.45 μm filter, in this thesis the terms are used interchangeably.

A4.1.1 Introduction

Membranes can remove large amounts of NOM from waters. It is a challenge to correctly measure the organic carbon in waters at very low levels and prior to the purchase of an instrument several instruments were compared. Once a choice was made, the instrument was optimised and extensively tested for potential problems and errors.

A4.1.2 Principle

DOC analysers on the market at the time of purchase, operate based on two different principles; A) high temperature oxidation over a catalyst followed by measurement of the evolved CO_2 by infra-red photometry, or after conversion to methane, by flame ionisation detection, and B) wet oxidation of organic carbon by the action of UV light in the presence of potassium persulphate. The CO_2 produced is stripped from solution and reduced to methane which is measured quantitatively by flame ionisation detection.

It appears from the literature that method A is more suitable for highly concentrated samples (mainly due to generally very low volumes of samples analysed), whereas method B is better for trace analysis. This was confirmed in our testing of two instruments based on method A. Thus an instrument operating with wet oxidation was purchased, which also allowed the injection of up to several mL of samples. This instrument, a Skalar 12 (Skalar, Netherlands) is shown in Figure A4.1.



Figure A4.1 *Skalar 12 DOC analyser with auto-sampler.*

A4.1.3 Oxidation Efficiency and Choice of Standards

The oxidation efficiency of an organic compound is not always 100%. This depends on the UV lamp, the solution chemistry in the analyser, and the stability of the compound. Since different compounds have different oxidation efficiencies, the choice of a standard compound becomes crucial. As the first

step of method evaluation, oxidation efficiencies of commonly used standards and target compounds were evaluated. Results are summarised in Table A4.1.

Table A4.1 *Oxidation efficiencies of different standard compounds.*

Compound	Formula	MW [gmol^{-1}]	Carbon [%]	Oxidation Efficiency [%]
D-Glucose	$CH_2OHCH(CHOH)_4O$	180.2	40.0	99
Benzoic Acid	$C_7H_6O_2$	122.1	68.8	90
Potassium Hydrogen Phthalate	$KHC_8H_4O_4$	204.2	47.1	92
Stream Reference Suwannee Fulvic Acid (IHSS)	undefined	-[3]	53.0	82
Stream Reference Suwannee Humic Acid (IHSS)	undefined	-[3]	52.9	77
NOM	undefined	-[3]	11.9	104[1]
D-Glucose + stock[1]	-	-	-	98
FA + stock	-	-	-	96
HA + stock	-	-	-	95
NOM + stock	-	-	-	110[2]

The oxidation efficiency was calculated from the slope of the measured value over the concentration (concentrations of 0.5, 1, 2, 5 and 10 mg L^{-1} were analysed). An oxidation efficiency of 100% would yield a slope of 1.

The oxidation efficiency for D-glucose was reported to be 100% (Hine and Bursill (1985)), in good agreement with the above results. Results rely on the correctness of information about carbon content of FA and HA received from IHSS, and a comparably small error in making standard solutions for FA and HA.

Higher oxidation efficiencies were obtained for natural organic matter and humic substances in the presence of a carbonate buffer. This indicates that inorganic carbon cannot be fully removed from the samples in the presence of these substances, whereas inorganic carbon in pure carbonate buffer was removed effectively.

An increased sulphuric acid concentration was tested in order to examine its impact on inorganic carbon removal and oxidation efficiency, but no effect over the tested range was observed. Sparging the samples with N_2 showed no improvement. The effect of increased sulphuric acid concentration is shown in Figure A4.2. We believe that the organic carbon interacts with the inorganic carbon not allowing full removal.

For further analysis, it was decided to use D-glucose as a standard exhibiting to 100% oxidation efficiency. Depending on the compound in solution, absolute concentrations can then be calculated using oxidation efficiencies. D-glucose can easily be consumed by micro-organisms, and therefore it is important to always prepare fresh standards.

---

[1] stock is the background salt solution, consisting of 20 mM NaCl, 0.5 mM $CaCl_2$ and 1 mM $NaHCO_3$

[2] the carbon content was determined using this instrument-this is therefore not a real oxidation efficiency

[3] see Chapter 4 for characterisation and average values

The argument that humic substances or NOM should be used as a standard is understandable, but given the difference between the organic samples (HA, FA, NOM) and the difficulties in fully dissolving some of these materials, D-glucose appeared to be the better choice. It has to be noted that absolute concentrations are not required for rejection calculations in membrane experiments.

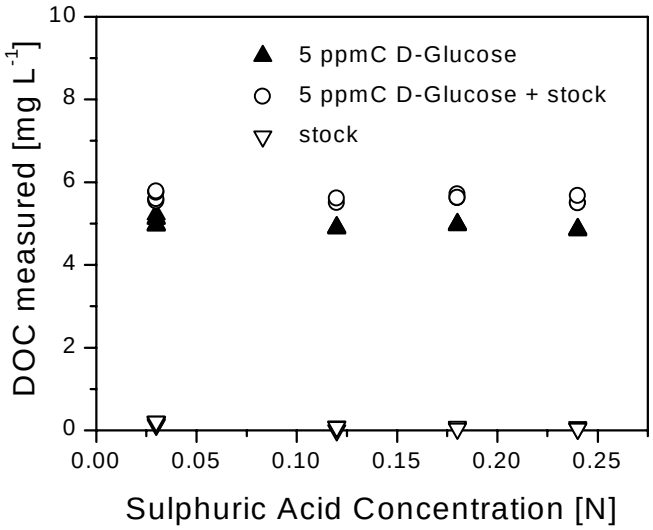


Figure A4.2 *DOC dependence on sulphuric acid concentration and the presence of inorganic carbon (see footnote of previous page for the definition of 'stock').*

As an outcome of these investigations, it is suspected that the oxidation efficiency of fractions of organics (as obtained in samples after treatment) will vary, which will cause an error in the results.

A4.1.4 Operation Mode

The Skalar 12 DOC instrument allows variation of sample and wash water injection times and thus the volume of sample analysed and the period between the samples. This is the main reason why the instrument performs so well at low concentrations. Further, the instrument was never operated at concentrations above 20 mg L^{-1} DOC to avoid contamination of the system. The main operating parameters are listed in Table A4.2, after optimisation of sampling and wash times. Chemicals were freshly prepared for each run, unless the instrument was used on consecutive days. Chemicals are not recirculated in the system.

Table A4.2 *Operation mode of Skalar 12 DOC analyser.*

Parameter	Value
Sample Time	120 s (Volume 4 mL)
Wash Time	240 s (Volume 4 mL)
H_2SO_4 Concentration (acidification of samples to remove inorganic carbon)	0.03 M
Digestion Reagent	22 mM $K_2S_2O_8$ (6g)
	89 mM $Na_2B_4O_7$ $10H_2O$ (34g)
HCl Concentration (acidification of samples to remove CO_2 produced by oxidising organic carbon)	0.45 M

A4.1.5 Detection Limit

Two calibration settings were used, standard (0 to 10 mgL^{-1}) and very low level (0 to 1 mgL^{-1}) of organic carbon. The latter was used mainly for the RO permeate analysis in the concentration of NOM using MF and RO as explained in Appendix 1.

Figure A4.3 shows the calibration for the low range. Although the error in analysis is relatively high (see Table A4.3), the results for these low values measured in this range are far better than if measured in the normal range between 0 and 10 mg L^{-1}. Additionally, measurements of these low concentrations would be impossible with a type 'A' analyser.

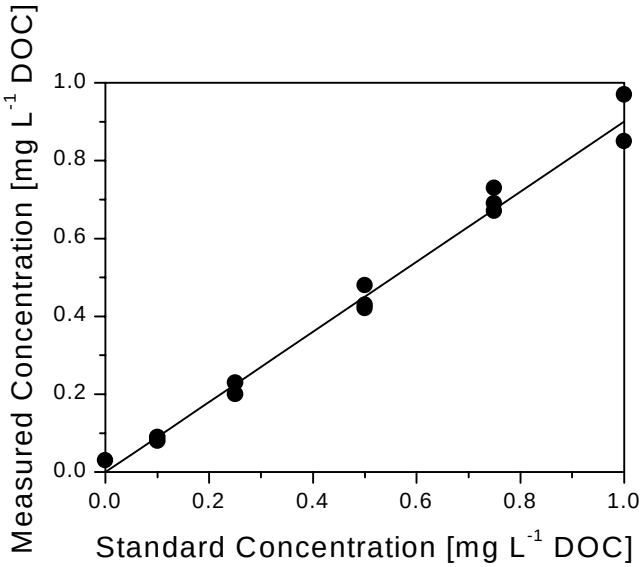


Figure A4.3 *Calibration of the Skalar 12 from 0 to 1 mg L^{-1} organic carbon (using D-Glucose standard).*

The reason for this high error is the automatic correction of the results using "wash" and "drift" samples, the absolute error of the drift samples (usually 5 to 10 mg L^{-1}) is too large for the small samples to be calculated correctly. This was improved significantly by calibrating the instrument in the low level range. Results were excellent.

A4.1.6 Errors and Interferences

To avoid contamination of samples from the air, no organic solvents were used in the laboratory where the DOC analyser was located, and no organic solvents were stored in the same refrigerator as the DOC samples.

All sample vials and glassware were cleaned with MilliQ water after soaking in 1M NaOH for 24 hours. Glassware used to prepare standards or feed solutions was cleaned with 5M KOH to remove any kind of contamination. All vials were covered to avoid dust collection.

High contamination was observed with a pH electrode. Feed solutions were contaminated to a great extent during pH adjustment with a Lutron pH electrode which is a gel filled plastic electrode (pH 207). A Beckman indicator (ϕ50 pH meter) with an Activon glass electrode (Ag/AgCl; 6K6I AEP 311) was used for further solution preparations and no contamination was observed. The electrode was only used in samples after DOC analysis and was cleaned thoroughly prior to use for pH adjustment. The conductivity was measured with a Lutron CD-4303 instrument.

The presence of inorganic particles such as hematite did not influence oxidation efficiency, and the error of analysis was evaluated with 10 samples of a few different concentrations in the range of

interest. For these evaluations, fulvic acid in a background salt solution and carbonate buffer was tested. Hematite does adsorb to the tubing of the DOC analyser, however no impact on the analytical performance was observed.

In the analysis of particulates one problem persists - while the sample awaits analysis in the autosampler, large agglomerates may settle in the vial and the analysis will be incorrect. This problem was overcome by filling the sample into the vial immediately before injection. No loss of agglomerates inside the system and thus loss of DOC was observed.

At high pH the analysis will be overestimated, as the amount of acid dosed to remove inorganic carbon will become insufficient.

The instrument can tolerate high levels of salt (up to 100 gL^{-1} of chloride) and no interference from salt at surface water concentrations is to be expected. In fact the instrument was designed for sea water analysis and was used successfully for samples of concentrations higher than sea water in Antarctica!

The error for small values becomes very high in relative terms. This is partly due to the calibration range, but also due to the proximity to the detection limit. Two calibration ranges were established for the DOC analyser. A standard range of 1 to 10 mgL^{-1} DOC and a very low level range from 0.1 to 1 mgL^{-1} DOC. Very good correlations were obtained for both ranges and samples below 0.5 mgL^{-1} DOC were reanalysed in the second range.

Table A4.3 *Error on DOC analysis (determined based on 10 values per sample).*

Measured FA Concentration [mgL^{-1} DOC]	Absolute Error [mgL^{-1} DOC]	Relative Error [%]
0.15	0.04	26.5
0.26	0.03	11.3
0.7	0.06	8.6
0.82	0.02	2.2
1.0	0.07	6.9
2.0	0.11	5.3
4.5	0.12	2.7
9.2	0.20	2.2

The reproducibility of the absolute values for different runs is poor, due to the calibration and change in flows of gases and chemicals (the flow of chemicals depends on the tubing of the peristaltic pump which is changed every 4 weeks) and the gas flow on the exact pressure adjustment). It is thus important to measure each batch of samples together.

The results obtained with the Skalar 12 instrument were checked with a TOC Analyser 1010 (O I Analytical), which is based on a wet oxidation method with 100 g L^{-1} persulphate at 100 ^{0}C (see Table A4.4) . Carbon is detected by NDIR, this method does not involve a UV source, which is believed to cause the decreased oxidation efficiencies described above. The standard used for this instrument

(CSIRO Melbourne) is potassium hydrogen phthalate. Results were generally higher, but after considering the different standard, the improvement in oxidation efficiency was only about 5%.

Table A4.4 *Oxidation efficiencies of different compounds with the TOC Analyser 1010.*

	D-Glucose	IHSS FA	IHSS HA
Oxidation Efficiency [%]	104	90	87

A4.2 UV/VIS ABSORBANCE

A4.2.1 Method

The UV spectrophotometer measures the light absorbed by a sample at a specific wavelength. For NOM the UV/VIS spectra are somewhat featureless with no distinct peaks in absorbance. This is due to the fact that NOM is a mixture of many compounds.

The wavelengths of 395 to 430 nm are commonly used for colour analysis, with a Hazen unit being calculated as

$$HU = 231 \cdot UV_{395\,nm}. \tag{A4.1}$$

The absorbance of a sample being

$$UV_{\lambda} = \frac{A}{b} \cdot D \tag{A4.2}$$

where A is the measured absorbance at wavelength λ , b the path length of quartz cell, and D the dilution factor of the sample. The wavelength of 254 nm is the most commonly used in the literature and is described as an indirect carbon measurement (Hine and Bursill (1985)).

Alternatively a number of ratios can be used such as

$$E_4 / E_6 = \frac{465\,nm}{665\,nm}, \tag{A4.3}$$

which indicates a higher degree of humification or condensation as the ratio becomes smaller. In usual surface waters the values at such high wavelengths are usually very small, so the error would be very high.

The most commonly used ratio is the UV/DOC ratio which gives an indication of the "freshness" of the DOC. If the ratio is lower, the sample contains a large proportion of phenolic, benzene and carboxylic groups which are gradually oxidised or biodegraded. This is shown in the humification diagram in Chapter 4.

Since many publications use very different wavelengths to measure UV, it was decided to scan samples from 190 nm to 500 nm to observe possible changes in the spectra, but 254 nm was used for calculations.

A4.2.2 Absorbance Characteristics of NOM

The absorption characteristics were determined for four organics and three NOM XAD fractions in calibrating absorbance over DOC. The absorbance as a function of wavelength for these compounds is shown in Figure A4.4. The slope of DOC versus UV absorbance at 254 nm plots are given in Table A4.5. HA absorbs significantly more than FA over the whole range, with Aldrich HA (purified with a 100 kDa UF membrane) being the strongest absorber. Aldrich HA is a commercial product (Sigma) which is probably extracted from soil and commonly used as a representative of aqueous HA in engineering research. The humic fraction of NOM behaves very similarly to the IHSS HA.

NOM shows very similar behaviour to FA indicating the predominance of FA and other low molecular weight compounds in surface water. The hydrophilic fraction (which is often the one left in a permeate) has a very low absorbance- thus the rejection of a membrane filter is easily overestimated).

For wavelengths smaller than 250 nm an interference of inorganic compounds is observed. This is more significant for NOM, where no salts have been removed in the concentration procedure, compared to FA and HA. Figure A4.4 also indicates the limits of the absorption scan towards low wavelengths due to interferences and towards higher wavelengths (>400 nm) due to low absorbance which results in a high error.

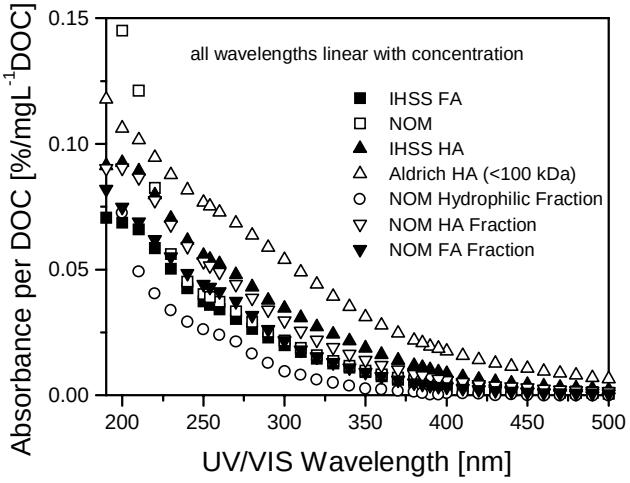


Figure A4.4 *Absorbance of FA, HA, Aldrich HA, NOM, and NOM XAD fractions over wavelength. Each point represents the slope of a calibration curve for different concentrations.*

From the above results it was decided to use 254 nm results for experiments, but with complete wavelength scans performed for each sample as a routine procedure. MilliQ water was used as a reference in a 1 cm quartz cuvette and samples were measured at room temperature. Samples were analysed prior to refrigeration to avoid changes due to coagulation or precipitation, which was enhanced at low temperature.

The correlations for UV over DOC were very linear and are summarised in Table A4.5 and, again, the presence of salt changed the results. The interference of salt can also be seen very clearly for non-purified NOM in Figure A4.4 at around 200 nm. However, the use of UV to determine organics concentration of samples is not possible (at least not to replace DOC analysis) because of the change in composition of organics during water treatment (membrane filtration).

Table A4.5 *Correlation of UV absorbance over DOC for different organics (254 nm).*

Substance	Slope [1/(cm mg L^{-1} as DOC)]	Correlation Coefficient
FA (IHSS)	0.036	0.999
HA (IHSS)	0.054	0.999
NOM	0.039	0.999
FA + stock	0.037	0.999
HA + stock	0.050	0.999
NOM + stock	0.043	0.999

A4.2.3 Errors and Interferences

Interferences are expected from colloids (not retained by the 0.45 μm filter), and various UV absorbing inorganics such as ferrous iron. When hematite colloids or ferric chloride coagulant were added to samples, the UV measurement did not give any information about carbon content, as the absorbance of hematite or ferric chloride was identical or higher than that of the organics.

Eaton investigated the UV method in detail and found that UV absorption of organics may vary in the pH range <4 and >10 and such samples should be treated with care. The absorbance of a sample should be in the range of 0.005 to 0.9. Precision ranged from 0.9 to 6% (Eaton (1995)).

UV absorbance was tested in the pH range from 2.5 to 11 for the HA used in this study and no dependence on pH could be found for HA in between pH 4 and 11. At lower pH values solubility may be a problem. Reproducibility of the UV measurements was excellent and far superior to DOC analysis.

Turbidity measurements are a very common analysis of surface water treatment. For turbidity scattering rather than absorbance is measured at a certain wavelength and angle, usually 90^0. Hongve and Åkesson (1998) described the interference of absorbing substances in turbidity measurements. There is little interest in turbidity measurements in this study, as this parameter was not considered, however, obviously particles that scatter light will cause overestimation of absorbance of a sample. This effect can only be partially prevented by filtration of samples with a 0.45 μm filter, as this step will not retain small colloids and may also fractionate the organics by adsorption (see MF Chapter for more detail).

Appendix 5

SOLUTION SPECIATION USING MINTEQA2

In Appendix 5, a geochemical speciation package (MinteqA2) was used to characterise the electrolyte systems used in the experiments. Results are shown as a function of pH for the carbonate buffer, sodium, and calcium.

The solution species were characterised in terms of ionic molar mobility, diffusivity, mobility, and hydrated ion radius prior to speciation. Equilibrium pH of the background solution was estimated as a function of gas type and operating pressure.

Calcium solubility as a function of calcium concentration and pH was investigated and the concentrations of calcium species in solution as well as calcite precipitate shown.

In the last section, a rough estimate for the solution speciation in the presence of a dissolved organic matter (DOM) was attempted. DOM is the MinteqA2 equivalent of DOC. This involved the speciation of DOM as a function of pH for two calcium concentrations. Subsequently the impact of DOM on calcium solubility and calcite precipitation was examined. Again, the calcium speciation was determined as a function of pH.

Although the results obtained with the DOM are limited, a reasonable understanding of the system was obtained. These results are essential in developing an understanding of membrane filtration behaviour.

A5.1 INTRODUCTION

The importance of speciation of solutes was pointed out by Simpson *et al.* (1987) in a study of nanofiltration of solutions at different pH values. Urase *et al.* (1998) studied the effect of speciation on arsenic removal by nanofiltration and explained a change of rejection with the presence of a species of different charge.

Different species of solutes alter charge, size and mobility (see Table A5.2), and it is thus no surprise that the rejection of the membranes varies. Therefore, it is important to understand the changes in speciation of the solutions used under the conditions of the experiments.

A5.2 MINTEQA2 SPECIATION CODE

A5.2.1 Availability of software and data input

MinteqA2 is a geochemical speciation code which was released by the U.S. EPA. Version 3.11 was used in this study. The software is available on the internet from the U.S. EPA Center for Exposure Assessment and Modeling (CEAM) as are several manuals (Allison *et al.* (1991)).

Useful sites are http://www.cee.odu.edu/model.html
http://www.cee.odu.edu/cee/model/minteq.html
http://www.und.ac.za/und/prg/projects/speciat.html

ProdefA2 was used to generate the input files for MinteqA2. The chemical recipes are given in Table A5.1.

Table A5.1 *Recipes used for speciation calculations.*

Parameter	Value	Comment
H^+	1.00E-02 to 1.00 E-12	Equilibrium pH was fixed
Ca^{2+}	0.5 to 5 mM	
Cl^-	21 mM	
Na^+	21 mM	
CO_3^{2-}	1 mM	
Temperature	20 ^{0}C	

The characteristics of species in solution are given in Table A5.2. Ion radii were calculated from the diffusion coefficient using the Stokes Einstein equation

$$r = \frac{k_B T}{6\pi\eta D}. \qquad \text{(A5.1)}$$

The ionic molar mobility (Perry and Chilton (1973)) is defined as

$$\omega_i = \frac{\lambda_i}{F^2 * |z_i|} . \qquad \text{(A5.2)}$$

Values for the systems used are tabulated in Table A5.2.

Table A5.2 *Characteristics of species in solution ([1]Urase et al. (1998), [2] Cussler (1995), [3] Peeters (1997), [4] Moulin et al. (1999)).*

Ion	Ionic Molar Mobility [mol m² J⁻¹ s⁻¹] [1]	Diffusivity [m² s⁻¹] [2, 3]	Mobility [m² s⁻¹ V⁻¹] [4]	Hydrated Ion Radius [nm]
H^+	$3.76 * 10^{-12}$	$9.31 * 10^{-9}$	$3.63 * 10^{-7}$	0.026
OH^-	$2.13 * 10^{-12}$	$5.38 * 10^{-9}$	$2.06 * 10^{-7}$	0.464
Cl^-	$8.20 * 10^{-13}$	$2.03 * 10^{-9}$	$7.91 * 10^{-8}$	0.121. 0.099, 0.107
Na^+	$5.38 * 10^{-13}$	$1.33 * 10^{-9}$	$5.19 * 10^{-8}$	0.184, 0.186, 0.164
Ca^{2+}	$3.20 * 10^{-12}$	$0.92 * 10^{-9}$	$6.18 * 10^{-8}$	0.309, 0.197, 0.237
HCO_3^-	$4.78 * 10^{-12}$	$1.18 * 10^{-9}$	$4.61 * 10^{-8}$	0.207
CO_3^{2-}	[1/2 CO_3^{2-}] $3.72 * 10^{-12}$	$0.92 * 10^{-9}$	$7.18 * 10^{-8}$	0.266

The molar mobilities of species like $NaCO_3^{2-}$ or $CaCO_3^-$ are not available, but values are expected to be lower than for HCO_3^{2-} due to the larger size of these species.

A5.3 SPECIATION RESULTS

A5.3.1 pH calculations as a function of partial CO_2 pressure

The equilibrium pH of the solutions was estimated for stirred cell 'atmospheres' as shown in Table A5.1. Both N_2 and instrument air can be used to pressurise the stirred cell solutions. Due to its inert nature N_2 is commonly used for this purpose. However, when a carbonate buffer is used in a system, the buffer depends on the partial pressure of CO_2 in the air above the solution. To provide this partial pressure instrument air can be used. When the system is operated at high pressures such as in NF, the partial pressure of CO_2 increases. The equilibrium pressure calculation was carried out for background solution without pH adjustment (0.5 mM $CaCl_2$, 1 mM $NaHCO_3$, 20 mM NaCl) in the absence of organics.

Table A5.3 *equilibrium pH as a function of type of gas used and applied pressure.*

Gas	Pressure [bar]	Equilibrium pH [-]
Nitrogen	1	10.39
Instrument Air	1	8.49
Instrument Air	5	7.81

The equilibrium pH with instrument air at 5 bar, which was the operating pressure for NF appears most realistic for a surface water system.

A5.3.2 Solution Speciation

To determine species in solution, calculations as a function of pH were carried out in the range from 2 to 12. The calcium concentration was in this case fixed at 0.5 mM. At this calcium concentration no calcite precipitation occurs over the entire pH range.

Figure A5.1, Figure A5.2, and Figure A5.3 show the speciation of the carbonate system, sodium and calcium, respectively. It can be seen that the speciation of the carbonate system is extremely pH dependent under the pH conditions (4.5, 7-8, 10) used in the experiments. At low pH neutral H_2CO_3 would form, at pH 7 to 9 monovalent HCO_3^-, and from pH 10 divalent CO_3^{2-} predominates.

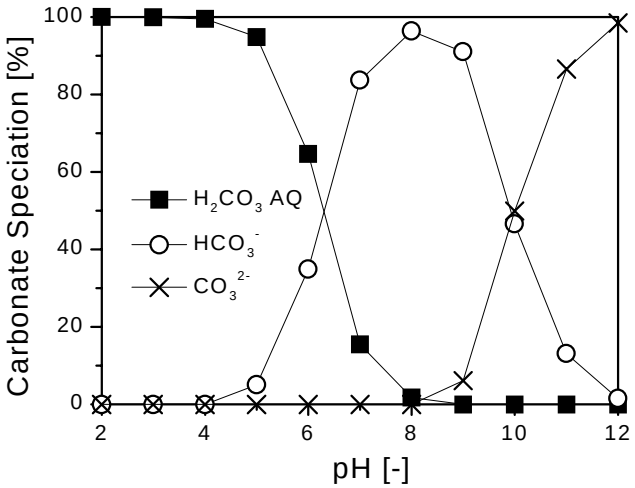


Figure A5.1 *Carbonate speciation pH dependence.*

The speciation of sodium is not quite as spectacular, with sodium being completely dissolved as monovalent Na^+. However, at pH 10, sodium begins to be present in the form of the anionic ion pair $NaCO_3^-$.

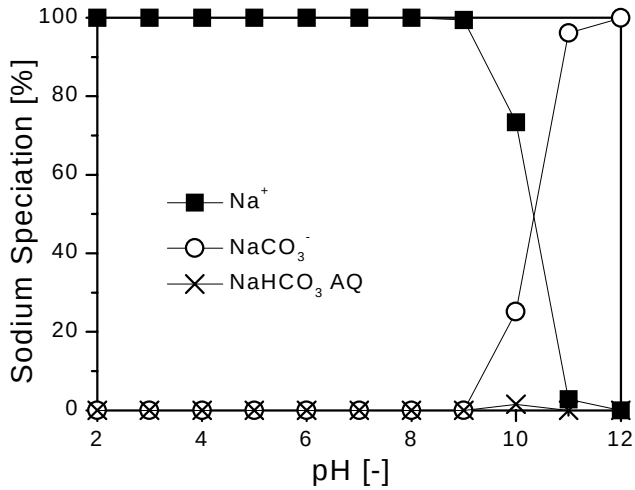


Figure A5.2 *Sodium speciation pH dependence.*

For calcium the transition from divalent Ca^{2+} to neutral $CaCO_3$ (aq) occurs above pH 8, thus below the pH value of 10 used in the experiments.

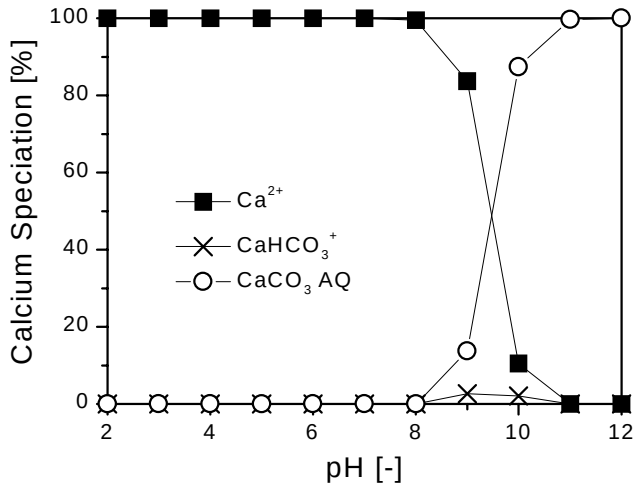


Figure A5.3 *Calcium speciation pH dependence.*

These effects affect rejection of sodium and calcium as a function of pH and need to be considered in the interpretation of results.

A5.3.3 Calcium Precipitation

The calcium concentrations used in some of the experiments were close to (and sometimes beyond) solubility limits. To determine the solubility of calcium in the systems used, calculations were carried out, firstly for calcium concentrations between 0.5 and 5 mM, and, secondly, pH values of 2 to 12 for all calcium concentrations. The solubility of calcium is obviously higher at low pH up to pH 8, where precipitation occurs at a concentration of 3 mM $CaCl_2$. Figure A5.4 shows the calcite concentration as a function of calcium concentration at pH 8 where the transition between the soluble form and the precipitate occurs.

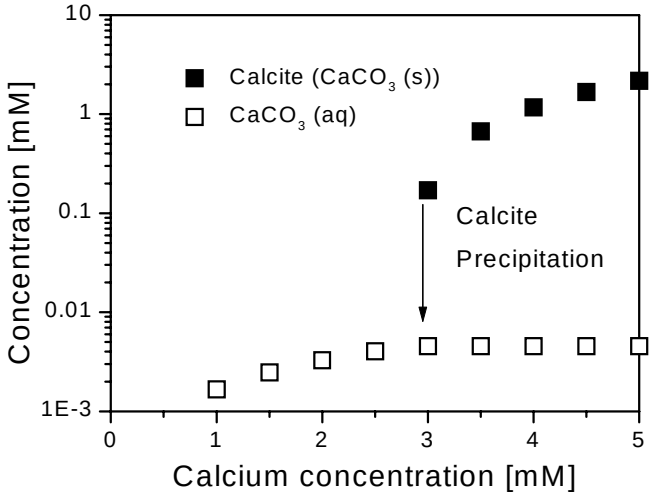


Figure A5.4 *Calcium solubility (at pH 8). Calcite concentrations are 0.17 mM at 3 mM calcium and 2.17 mM at 5 mM calcium.*

Figure A5.5 gives the concentration of all calcium species present as a function of pH for a calcium concentration of 2.5 mM, which was the concentration of the "critical fouling condition" in some experiments.

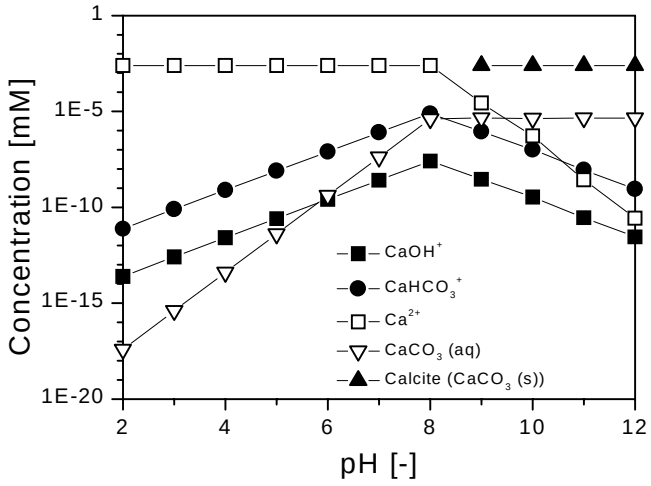


Figure A5.5 *Speciation of calcium as a function of pH at a calcium concentration of 2.5 mM.*

The predominant species in terms of concentration are soluble calcium up to pH 8 to 9 and calcite precipitate at a higher pH. From pH 9 to 12 calcite (or calcium carbonate) precipitates fully at all concentrations as the only solid, except for the 0.5 mM calcium case, when calcite and aragonite coexist. Both precipitates have the same formula, $CaCO_3$, and the difference between the two is probably insignificant (Morel and Hering (1993)) for the membrane experiments.

Morel and Hering (1993) state that the calcium carbonate is usually supersaturated in surface waters. Further, pressure has an effect on the free energies on the ions (in this case in the water column, but this is also applicable to high pressure membrane systems) and the solubility is decreased at lower pressures. Solubility of calcite also increases with CO_2 partial pressure (which would have increased in the NF stirred cell since air was used to pressurise the system).

A5.3.4 Speciation of Systems Containing Organics

NOM or humic substances interact with ions, especially multivalent ions such as calcium, and thus introduce a range of additional species. Matlack (1992) modelled the interactions of dissolved organic carbon with cations using MinteqA2. It is clear that there are many problems involved in this work due to the unknown parameters associated with the organic matter and thus the lack of constants required to achieve meaningful modelling results. Ion binding by humic and fulvic acids depends on the type of organic (Tipping (1993)) which requires measurements for each individual organic type used.

The complexation capacity also varies with pH, ionic strength, organic concentration, and the nature of the metal ion. The heterogeneity of ligands in these organic molecules makes it nearly impossible to obtain accurate complexation results (Perdue (1989)). To get accurate results, measurements with the system of interest are required and the DOM in the MinteqA2 database cannot replace these measurements (Allison and Perdue (1994)).

The MinteqA2 database contains dissolved organic matter (DOM) as a component (number 145). The DOM was isolated from the Suwannee River by Serkiz and Perdue (1990) by reverse osmosis. It was not fractionated into humic and fulvic fractions and is thus not identical to the IHSS Suwannee River FA and HA used in this study.

Metal binding studies were conducted at the U.S. EPA, and DOM-metal complexes (H, Al, Ba, Be, Ca, Cd, Cr, Cu, Fe, Mg, Ni, Pb, Zn) are also included in the database. Unfortunately, Na is missing, as the DOM was pretreated with an H^+ ion exchange resin (Serkiz and Perdue (1990)).

This DOM is different to the three samples used in this study and for this reason and the uncertainty in the values in the database the speciation results in the presence of organics must be treated with care. Further, no data are available for the interaction of DOM with other system components such as carbonate species or precipitates.

It is clear that H^+ competes with the metal ions for binding sites and thus metal-DOM complexation would be higher at high pH. Due to the interaction of ions and organics, some of the ions which are likely to precipitate will be bound and thus the apparent solubility of these ions will be higher. In order to examine trends, the DOM present in the MinteqA2 database was used for speciation calculations. The results cannot be applied as absolute values for the systems used in experiments. The molar site concentration required by ProdefA2 was determined to be 100 μeq L^{-1}. This was calculated for a organic concentration of 12.5 mg L^{-1} as DOC and a carboxylic group content of 4 meq g^{-1} (IHSS HA). The molar concentration for an estimated organic molecular weight of 1000 Da (or g mol^{-1}) would be 25 μM.

Figure A5.6 and Figure A5.7 show the speciation of DOM as a function of pH for calcium concentrations of 0.5 mM and 2.5 mM, respectively.

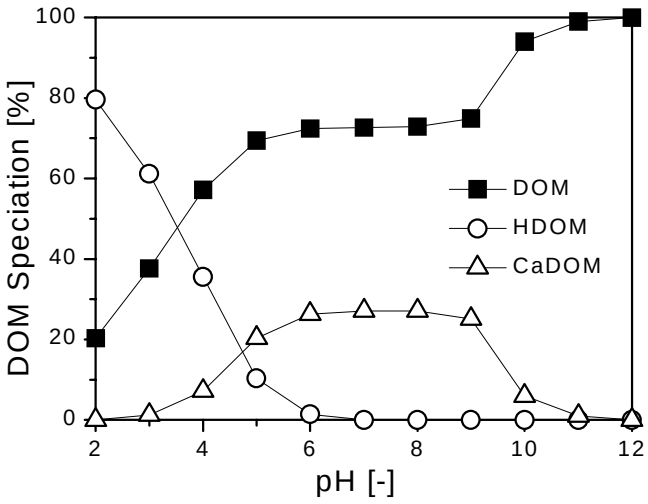


Figure A5.6 *DOM speciation pH dependence at a calcium concentration of 0.5 mM (100 μeq L^{-1} organic matter (12.5 mg L^{-1} as DOC)).*

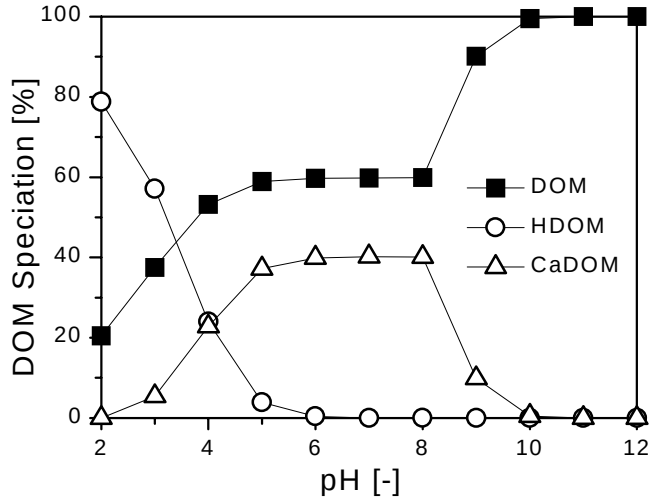


Figure A5.7 *DOM speciation pH dependence at a calcium concentration of 2.5 mM (100 μeq L^{-1} organic matter (12.5 mg L^{-1} as DOC)).*

At low pH the DOM is not very soluble and thus present in the form H-DOM. As the pH increases, DOM fully dissolves and dissolved DOM as well as Ca-DOM complexes co-exist. At a higher pH, the

organics are more negatively charged and thus the complexation increases. The model, however, does not include any ternary interactions involving calcium, organics, and organic complexes with carbonate, and thus the complexed species decrease with a further increase in pH. This result most probably does not correspond to reality, as a precipitation of the DOM with the calcium would be expected rather than an increase in dissolved concentration from pH 8 where calcite precipitates.

The effect of DOM on calcium solubility is less apparent than expected. Calcite precipitates, as in the absence of DOM (Figure A5.4), from a calcium concentration of 3 mM, as shown in Figure A5.8. However, the calcite concentration is now varied with a concentration of 0.12 at 3 mM and 2.12 at 5 mM. The calcite concentration is reduced by the concentration of the Ca-DOM complex (see Figure A5.9).

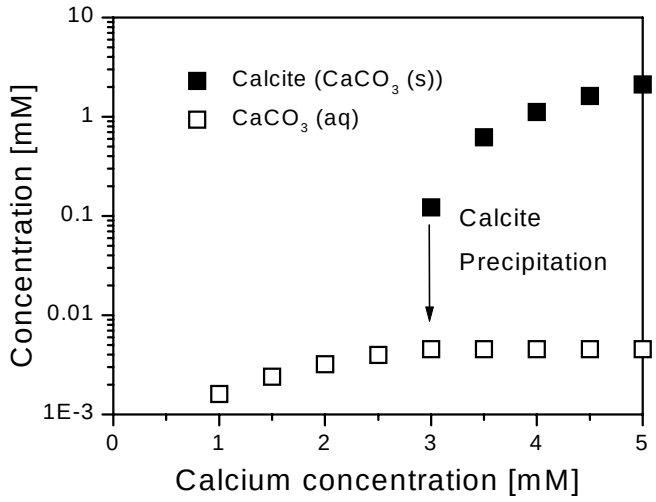


Figure A5.8 *Calcium solubility (at pH 8) in the presence of 100 μeq L^{-1} organic matter (12.5 mg L^{-1} as DOC).*

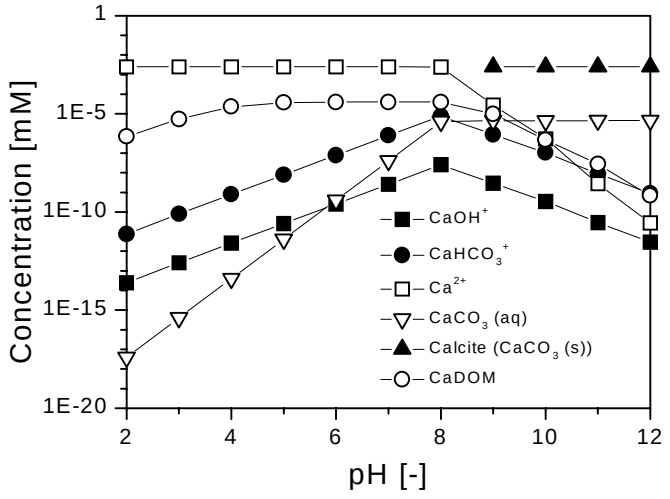


Figure A5.9 *Speciation of calcium as a function of pH at a calcium concentration of 2.5 mM and the presence of 100 μeq L^{-1} organic matter (12.5 mg L^{-1} as DOC).*

A5.3.5 Comments on the membrane boundary layer concentrations

Speciation calculations were carried out for the feed solutions. The issue of increased concentrations in the membrane boundary layer (where the precipitation is most likely to occur) was addressed in the NF Chapter (Chapter 7). It should be noted here that the local pH in the boundary layer is very likely to be different, due to the different mobility of H^+ and OH^-. For this reason (the larger mobility of H^+) the pH of permeate is often lower. It is possible that the pH of the boundary layer will be larger than the bulk solution which could lead to higher precipitation.

A5.4 CONCLUSION

The speciation results presented here contribute to improved understanding of the electrolyte solution. This is essential in understanding the pH dependence of rejection in membrane filtration, specifically nanofiltration.

Limitations to the model are the DOM. The default DOM of the database was used due to the lack of data for the organics used in the experiments. While the results obtained up to pH 8 appear reasonable, once calcite precipitation occurs, the DOM results appear incorrect. DOM will precipitate with calcite, if not as a Ca-DOM complex (as shown in Chapter 7). The lack of data and understanding at these pH conditions make the modelling impossible and further work is needed in updating the database before reliable results can be obtained.

GLOSSARY

A/C	Activated Carbon
AFM	Atomic Force Microscopy
AOM	Aquatic Organic Matter
ARMCANZ	Agricultural Research Management Council of Australia and New Zealand
ATR-FTIR	Attenuated Total Reflection Fourier Transformation Infrared Spectroscopy
BDOC	Biodegradable Dissolved Organic Carbon
CA	Cellulose Acetate
CCC	Critical Coagulation Concentration
CDOC	Chromatographable Organic Carbon
CHFP	Chloral Hydrate Forming Potential
DBP	Disinfection By-Product
DEAE	Diethylaminoethyl
DLA	Diffusion Limited Aggregation
DOC	Dissolved Organic Carbon
DOM	Dissolved Organic Matter
DOTM	Direct Observation through the Membrane Technique
DRIFT	Diffusive Reflectance Fourier Transform Infrared Spectroscopy
EC	Electronic Conductive Carbon Black
EDS	Electron Dispersive Spectra
EDTA	Ethylene Diamine Tetra Acetic Acid
FA	Fulvic Acid
FESEM	Field Emission Scanning Electron Microscopy
FFF	Flow Field Fractionation
FI	Fouling Index
FID	Flame Ionisation Detector
FTIR	Fourier Transform Infrared Spectroscopy
GAC	Granular Activated Carbon
GPC, GFC	Gel Permeation Chromatography
GVWP	Hydrophilic 0.22 μm MF Membrane
GVHP	Hydrophobic 0.22 μm MF Membrane
HA	Humic Acid
HAA	Haloacetic Acid
HAA5	Five Haloacetic Acids
HAAFP	Haloacetic Acid Forming Potential
H/C	Hydrogen to Carbon Ratio
HIOP	Heated Iron Oxide Particles
HOC	Hydrophobic Organic Carbon
HPLC	High Pressure/Performance Liquid Chromatography
HPLC-SEC	High Pressure/Performance Liquid Chromatography Size Exclusion Chromatography
HS	Humic Substances
IC	Ion Chromatography
ICP-AES	Inductively Coupled Plasma Atomic Emission Spectroscopy
ICR	Information Collection Rule
IOP	Iron Oxide Particles
IEP	Isoelectric Point
IHSS	International Humic Substances Society
KA	Kaolin
LC-OCD	Liquid Chromatography Organic Carbon Detection
LD-FTMS	Laser Desorption Fourier Transform Mass spectrometry
LMM	Low Molecular Mass
LMW	Low Molecular Weight
LSI	Lamgelier Saturation Index
MALDI	Matrix Assisted Laser Desorption Ionisation
MCL	Major Contaminant Level
MF	Microfiltration
MFI	Modified Fouling Index
MIB	2-Methylisoborneol
M_n	Number Average MW
M_w	Weight Average MW
MTC	Mass Transfer Coefficient
MS	Mass Spectroscopy
MW	Molecular Weight
MWCO	Molecular Weight Cut-Off
NF	Nanofiltration
NHMRC	National Health and Medical Research Council
NMR	Nuclear Magnetic Resonance Spectroscopy
NOM	Natural Organic Matter
OC	Organic carbon
O/C	Oxygen to Carbon Ratio
OPS	Particles Stabilised with Organics
PA	Polyamide
PAC	Powdered Activated Carbon

PAC	Polyaluminiumchloride
PCR	Polymerase Chain Reaction
PCS	Photon Correlation Spectroscopy
PEG	Polyethylene Glycol
PLAC	1 kDa Regenerated Cellulose UF Membrane
PLBC	3 kDa
PLCC	5 kDa
PLGC	10 kDa
PLTK	30 kDa
PLHK	100 kDa
POC	Particulate Organic Carbon
PS	Polysulfone
PSS	Polystyrene Sulfonate
PVDF	Polyvinylidene Fluoride
Py-FTMS	Pyrolysis-field Ionisation Mass Spectrometry
Py-GC/MS	Pyrolysis Gas Chromatography Mass Spectroscopy
PZC	Point of Zero Charge
RBSMT	Rapid Bench Scale Membrane Test
RLA	Reaction Limited Aggregation
RO	Reverse Osmosis
SANS	Small Angle Neutron Scattering
SEC	Size Exclusion Chromatography
SDI	Silt Density Index
SOC	Synthetic Organic Compounds
SPFC	Stabilised Polyferric Chloride
SPO	Aggregates with Organics Adsorbed
TDS	Total Dissolved Solids
TFC	Thin Film Composite
THM	Trihalomethanes
THMFP	Trihalomethane Forming Potential
THMP	Trihalomethane Precursors
TOC	Total Organic Carbon
TOX	Total Organic Halogen
UF	Ultrafiltration
ULP	Ultra Low Pressure
UV_{254nm}	Ultra Violet Absorption at 254 nm
VOC	Volatile Organic Carbon
WHO	World Health Organisation
WQP	Water Quality Parameter
XAD	Non-ionic, Macroporous Resin
XAD4	Acrylic Ester Copolymer Resin (Hydrophilic)
XAD8	Acrylic Ester Copolymer Resin (Hydrophobic)
XPS	X-Ray Photoelectron Spectroscopy

SYMBOLS

Chapters 2, 3 and 4

A	Membrane area [m^2]
B	Pure water permeability of membrane [$m^3m^{-2}s^{-1}bar^{-1}$]
b	Constant describing characteristics of sublayer
c_{BL}	Solute concentration in boundary layer [$molL^{-1}$]
c_i	Concentration of ion i in the membrane [$molm^{-3}$]
c_{Bi}	Bulk concentration for sample i [$molL^{-1}$]
c_F	Solute concentration in feed solution [$molL^{-1}$]
c_{mS}	Average solute concentration across membrane [$molL^{-1}$]
$c_{m,W}$	Concentration of water in the membrane [$molm^{-3}$]
c_P	Permeate concentration [$molL^{-1}$]
c_{Pi}	Permeate concentration of sample i [$molL^{-1}$]
c_S	Electrolyte concentration [$molL^{-1}$]
Δc_S	Solute concentration gradient across membrane [$molL^{-1}$]
c_W	Solute concentration at membrane wall [$molL^{-1}$]
c_G	Gel layer concentration [$molL^{-1}$]
$d_{Particle}$	Particle diameter [m]
d_{Pore}	Pore diameter [m]
d_{Solute}	Solute diameter [m]
D	Diffusion coefficient of water [m^2s^{-1}]
$D_{i,p}$	Diffusivity of ion i in the membrane (hindered diffusivity) [m^2s^{-1}]
D_M	Diffusion coefficient of solute in membrane [m^2s^{-1}]
D_S	Solute diffusion coefficient in bulk solution [m^2s^{-1}]
e	Fundamental electron charge [$1.602\ 10^{-19}$ C]
F	Faraday constant [$9.648\ 10^4$ $Cmol^{-1}$]
J	Permeate flux [$Lm^{-2}h^{-1}$]
J_0	Initial permeate flux [$Lm^{-2}h^{-1}$]
J_{crit}	Critical flux [$Lm^{-2}h^{-1}$]
J_{lim}	Limiting flux [$Lm^{-2}h^{-1}$]
J_{si}	Flux of ion i [$molm^{-2}s^{-1}$]
k	Distribution coefficient [-]
k'	Fluid consistency index [kg $s^N m^{-2}$]
k_B	Boltzmann's constant [$1.380\ 10^{-23}$ JK^{-1}]
k_M	Mass transfer coefficient in membrane [$m^2m^{-2}s^{-1}$]
k_S	Overall mass transfer coefficient of solute in the boundary layer [$m^2m^{-2}s^{-1}$]
$K_{i,c}$	Hindrance factor for convection in the membrane (depending on ion and pore radii) [-]
L_S	Solute permeability [$molm^{-2}s^{-1}Pa^{-1}$]
L_V	Hydrodynamic permeability [$m^3m^{-2}s^{-1}bar^{-1}$ or $mPa^{-1}s^{-1}$]
M	Molecular weight [$gmol^{-1}$]
N_A	Avogadro constant [$6.022\ 10^{23}$ mol^{-1}]
n_P	Number of pores [-]
ΔP	Pressure difference across membrane [Pa]
Q_P	Permeate volume flow [m^3h^{-1}]
r	Molecule radius [m]
r_P	Pore radius [m]
R	Gas constant [$3.814\ Jmol^{-1}K^{-1}$]
R	Rejection [-]
R_C	Resistance due to external (cake) deposition [m^{-1}]
R_{CP}	Resistance due to concentration polarisation [m^{-1}]
R_M	Resistance of clean membrane [m^{-1}]
R_P	Resistance due to internal (pore) fouling [m^{-1}]
T	Absolute temperature [K]
$V_{m,W}$	Partial molar volume of water [m^3mol^{-1}]
x	Distance normal to membrane [m]
Δx	Membrane thickness [m]
z_i	Valence of ion [-]

Greek Symbols

δ	Thickness of the concentration polarisation / boundary layer [m]
ε	Dielectric constant [-]
η	Dynamic water/solvent viscosity [Pas]
κ	Debye length parameter [m^{-1}]
λ	Ratio of solute/pore diameter [-]
π	Osmotic pressure [bar]
$\Delta\Pi$	Osmotic pressure difference across membrane [Pa]
$\Delta\Pi_W$	Osmotic pressure difference between boundary layer and permeate side [Pa]
σ	Reflection coefficient (independent of fluid velocity and solute concentration); Staverman refection coefficient [-]
τ	Tortuosity factor [-]
Φ_S	Solids volume fraction in feed
Ψ	Electric potential [V]

Chapter 5

A Membrane area [m^2]
c_0 Initial feed concentration [mgL^{-1}]
c_F Final feed concentration [mgL^{-1}]
c_C Concentrate concentration [mgL^{-1}]
c_{bi} Bulk concentration (concentration in the batch cell) [mgL^{-1}]
c_{pi} Permeate concentration of i^{th} sample [mgL^{-1}]
I Intensity [photoncounts]
J Flux [$Lm^{-2}h^{-1}$]
J_0 Initial feed flux [$Lm^{-2}h^{-1}$]
J_{W0} Initial pure water flux [$Lm^{-2}h^{-1}$]
J_{Wf} Final pure water flux (after experiment) [$Lm^{-2}h^{-1}$]
J_{800mL} Membrane flux after 800 mL feed filtration [$Lm^{-2}h^{-1}$]
k_{CB} Complete blocking filtration constant [-]
k_{CF} Cake formation filtration constant [-]
k_{IB} Intermediate blocking filtration constant [-]
k_{SB} Standard blocking filtration constant [-]
ΔP Transmembrane pressure [10^5 Pa]
Q Scattering vector or momentum transfer [m^{-1}]
R Rejection [%]
t Time [h]
V Total filtrate volume [L]
V_{cell} Cell volume [L]
V_F Feed volume [L]
V_P Permeate sample volume [L]

Chapter 6

a_P Radius of primary particle [m]
A Membrane area [m^2]
D Fractal dimension [-]
k constant
$M_{\%}$ Mass deposit [%]
m_P Mass of deposited particles [g]
r Aggregate radius [m]
R_C Cake resistance [m^{-1}]
R_{CP} Resistance of concentration polarisation layer [m^{-1}]
R_M Membrane resistance [m^{-1}]

Greek Symbols

α Specific cake resistance [mkg^{-1}]
ε Cake porosity [-]
ε_a Aggregate porosity [-]
ρ_P Particle density [kgm^{-3}]

Chapter 7

A Membrane surface [m^2]
c_B Bulk concentration [mgL^{-1}]
c_C Concentrate concentration [mgL^{-1}]
c_F Feed concentration [mgL^{-1}]
c_i ion concentration [$molL^{-1}$]
c_P Permeate concentration [mgL^{-1}]
c_W Wall concentration [mgL^{-1}]
D Diffusion coefficient [m^2h^{-1}]
D_1 Diffusion coefficient of solute 1 [m^2h^{-1}]
D_2 Diffusion coefficient of solute 2 [m^2h^{-1}]
j Factor for mole increase due to dissociation [-]
J Flux [$Lm^{-2}h^{-1}$]
J_{20} Flux at 20^0C [$Lm^{-2}h^{-1}$]
J_T Flux at any temperature [$Lm^{-2}h^{-1}$]
J_{W0} Pure water flux prior to experiment [$Lm^{-2}h^{-1}$]
J_W Pure water flux after experiment [$Lm^{-2}h^{-1}$]
k_S Solute mass transfer coefficient [ms^{-1}]
L_D Loss of solute in percent of mass in feed solution [%]
L_S Loss of solute [%]
M_D Mass deposit of solute on membrane [mg]
n number of moles [-]
P_1 Fitting parameter 1
P_2 Fitting parameter 2
ΔP Transmembrane pressure [bar]
r Radius of stirred cell [m]
R Rejection [%]
R Gas constant [3.814 $Jmol^{-1}K^{-1}$]
Re Reynolds number [-]
R_M Membrane resistance [ms^{-1}]
s Empirical constant
Sc Schmid number [-]
Sh Sherwood number [-]
t Time [h]
T Temperature [^{0}C]
v_B Potential barrier between particles [L]
V Permeate volume [L]
V_C Concentrate volume [L]
V_F Feed volume [L]
V_i Solent volume [L]
z_i Ion valence [-]

Greek Symbols

η Viscosity of solvent (water) [Pa s]
ν Kinematic viscosity [L^2s^{-1}]
$\Delta\Pi$ Osmotic pressure difference [bar]

Chapter 8

c_c Concentrate concentration [mgL^{-1}]
J_0 Initial flux [$Lm^{-2}h^{-1}$]
J_F Final flux [$Lm^{-2}h^{-1}$]
J_{W0} Initial pure water flux [$Lm^{-2}h^{-1}$]
L_F Final membrane permeability [$Lm^{-2}h^{-1}bar^{-1}$]
P Operating pressure [kPa]
ΔP Transmembrane pressure [kPa]

Power Power [W]
Q_F Feed flow [m^3h^{-1}]
Q_P Permeate flow [m^3h^{-1}]
R Recovery [-]
R' Rejection [-]
R_M Membrane resistance [m^{-1}]
R_F Fouling layer resistance [m^{-1}]

Greek Symbols

η Dynamic water/solvent viscosity [Pas]

Appendix 2

A constant [-]
B constant [-]
c_D Drag coefficient [-]
d Height of impeller blade [m]
d_P Agglomerate diameter [m]
L Scales of motion [m]
L_k Kolmogoroff microscale [m]
N_Q Conventional pumping number [-]
n number of impeller blades [-]
P Power input [W]
P_0 Power number [-]
Q_i Chamber throughflow [m^3s^{-1}]
Q_R Radial or impeller stream discharge [m^3s^{-1}]
R Radius of impeller blade [m]
R_C Chamber radius [m]
R_Q Recirculation ratio [-]
r Radial distance from centre of impeller [m]
Re Reynolds number [-]
s_t Turbulent shear [s^{-1}]
s_m Means shear [s^{-1}]
T Time period [s]
u Turbulent velocity scale [ms^{-1}]
U_{tip} Impeller blade tip velocity [$radms^{-1}$]
V Volume of chamber [m^3]

Greek Symbols

α Constant [-]
ε Turbulent dissipation (per kg of fluid) [m^2s^{-3}]
ρ Fluid density [kgm^{-3}]
ω Rotational rate [$rads^{-1}$]
ν Kinematic viscosity [L^2s^{-1}]
χ Fraction of particles travelling to outlet without recirculation [-]

Appendix 4

A Measured absorbance value [-]
b Pathlength of quartz cell [m]
D Dilution factor of sample [-]
E_4 Absorbance at 465 nm [m^{-1}]
E_6 Absorbance at 665 nm [m^{-1}]
HU Hazen unit [m^{-1}]
UV_λ Absorbance of a sample at wavelength λ [m^{-1}]

Greek Symbols

λ Wavelength [nm]

Appendix 5

D Diffusivity [m^2h^{-1}]
F Faraday constant [$9.648\ 10^4$ $Cmol^{-1}$]
k_B Boltzmann's constant [$1.380\ 10^{-23}$ JK^{-1}]
r Hydrated ion radius [m]
T Absolute temperature [K]
z_i Ion charge [-]

Greek Symbols

λi mobility [$m^2s^{-1}V^{-1}$]
ω_i Ionic molar mobility [$molm^2J^{-1}s^{-1}$]

REFERENCES

Abbt-Braun G., Frimmel F.H., Lipp P. (1991), **Isolation of organic substances from aquatic and terrestrial systems-comparison of some methods**, Z. Wasser- Abwasser-Forsch., 24, 285-292.

Abbt-Braun G., Frimmel F.H., Schulten H.-R. (1990), **Strukturelle Charakterisierung isolierter aquatischer Huminstoffe - Anwendbarkeit, Grenzen und Vergleich ausgewählter Methoden**, Vom Wasser, 74, 325-338.

Afonso M.D., Geraldes V., Rosa M.J., de Pinho M.N. (1992), **Nanofiltration removal of chlorinated organic compounds from alkaline bleaching effluents in a pulp and paper plant**, Water Research, 26, 12, 1639-1643.

Agbekodo M.K.A. (1994), **Élimination par nanofiltration des composés organiques d'une eau de surface prétraité. Caractérisation du carbone organique dissous avant et après nanofiltration**, Thèse, Université de Poitiers.

Agbekodo K., Legube B., Côté P., Bourbigot M.-M. (1994), **Performance de la nanofiltration pour l'élimination de la matière organique naturelle: essais sur l'usine de Méry/Oise**, Revue des Sciences de l'Eau, 7, 183-200.

Agbekodo K.M., Legube B., Dard S. (1996), **Atrazine and simazine removal mechanisms by nanofiltration: Influence of natural organic matter concentration**, Water Research, 30, 11, 2535-2542.

Agbekodo M.K., Legube B. (1995), **Distribution du CODB d'une eau de surface ayant subi deux types de traitements différents**, Environmental Technology, 16, 7, 657-666.

Agui W., Tamura S., Abe M., Ogino K. (1992), **Removal of dissolved humic substances from water with a reverse osmosis membrane**, The Science of the Total Environment, 117/118, 543-550.

Aiken G.R. (1984), **Evaluation of ultrafiltration for determining molecular weight of fulvic acid**, Environmental Science & Technology, 18, 12, 978-981.

Aiken G.R. (1985), **Isolation and concentration techniques for aquatic humic substances**, in: Aiken G.R., McKnight D.M., Wershaw R.L., MacCarthy P. (Eds.), Humic Substances, in Soil, Sediment, and Water, John Wiley & Sons, Inc., 363-386.

Aiken G.R., Brown P.A., Noyes T.I., Pinckney D.J. (1989), **Molecular size and weight of fulvic and humic acids from the Suwannee River**, in: Averett R.C., Leenheer J.A., McKnight D.M., Thorn K.A. (Eds.), **Humic Substances in the Suwannee River, Georgia: Interactions, Properties, and Proposed Structures**, U.S. Geological Survey, Open-File Report 87-557, 163-178.

Alarcon Herrera M.T. (1994), **Removal of trihalomethane precursors in drinking water treatment processes**, Dissertation, University of Windsor, Canada.

Alberts J.J., Griffin C., Gwynne K., Leversee G.J. (1994), **Binding of natural humic matter to polycyclic aromatic hydrocarbons in rivers of the United States**, Water Science & Technology, 30, 10, 199-205.

Alberts J.J., Miano T., Nelson J., Ertel J. (1995), **Fluorescence spectral characteristics of humic, fulvic and hydrophilic acid fractions isolated along a salinity gradient from the Savannah River, Georgia**, in: IHSS, Humic Substances in the Environment, New Challenges and Approaches, IHSS Conference, Aug/Sept 95, Atlanta, Georgia, 80.

Alborzfar M., Jonsson G., Gron C. (1998), **Removal of natiral organic matter from two types of humic ground waters by nanofiltration**, Water Research, 32, 10, 2983-2994.

Allegrezza A.E., Parekh B.S., Parise P.L., Swiniarski E.J., White J.L. (1987), **Chlorine resistant polysulfone reverse osmosis modules**, Desalination, 64, 285-304.

Allgeier S.C. (1996), **ICR membrane Systems: Demonstration of the RBSMT**, Proc. of AWWA Annual Conference, Toronto, Canada, 105-122.

Allgeier S.C., Summers R.S. (1995a), **Development of a rapid bench-scale membrane test for the evaluation of nanofiltration performance**, Proc. AWWA Membrane Technology Conf., Reno, Nevada, Aug 95, 207-227.

Allgeier S.C., Summers R.S. (1995b), **Effect of mass transfer resistance and system recovery on membrane permeation**, Proc. AWWA Membrane Technology Conf., Reno, Nevada, Aug 95, 39-66.

Allgeier S.C., Summers R.S. (1995c), **Evaluating NF for DBP control with the RBSMT**, Journal AWWA, Mar 95, 87-99.

Allison J.D., Brown D.S., Novo-Gradac K.J. (1991), **MINTEQA2/PRODEFA2, A Geochemical Assessment Model for Environmental Systems: Version 3.0 User's Manual**, Environmental Research Laboratory, U.S. EPA, Athens, Georgia.

Allison J.D., Perdue E.M. (1994), **Modeling metal-humic interactions with MINTEQA2**, Humic Substances in the Global Environment and Implications on Human Health, (Ed. N. Senesi, T.M. Miano), Elsevier Science, 927-942.

Altmann J., Ripperger S. (1997), **Particle deposition and layer formation at the crossflow microfiltration**, Journal of Membrane Science, 124, 119-128.

Amal R. (1991), **Fractal structure and kinetics of aggregating colloidal hematite**, PhD Thesis, UNSW, Chemical Engineering, 1991.

Amal R., Raper J.A., Waite T.D. (1990), **Fractal structure of hematite aggregates**, J of Colloid and Interface Science, 140, 1, Nov 1990, 158-168.

Amal R., Raper J.A., Waite T.D. (1992), **Effect of fulvic acid adsorption on the aggregation kinetics and structure of hematite particles**, Journal of Colloid and Interface Science, 151, 1, 244-257.

Amirbahman A., Olson T.M. (1993), **Transport of humic matter - coated hematite in packed beds**, Environ. Sci. Technol., 27, 2807-2813.

Amirbahman A., Olson T.M. (1995), **Deposition kinetics of humic matter-coated hematite in porous media in the presence of Ca^{2+}**, Colloids and Surfaces, A: Physicochemical and Engineering Aspects, 99, 1-10.

Amy G., Cho J. (1999), **Interactions between natural organic matter (NOM) and membranes: rejection and fouling**, in: Ødegaard H. (Ed), Removal of humic substances from water, Conference Proceedings, Trondheim, Norway, 141-148.

Amy G., Jacangelo J., Odem W., Adams J. (1993a), **Membrane separation of disinfection by-product (DBP) Precursors: The U.S. Experience**, Chapter 15, Drinking Water Quality Management, Technomic Publishing, 291-311.

Amy G., Siddiqui M., Ryan J. (1993b), **Membrane separation of DBP precursors from low-turbidity surface waters**, Proc. of AWWA Membrane Technology Conf., Baltimore, Aug 93, 651-663.

Amy G.L., Alleman B.C., Cluff C.B. (1990), **Removal of dissolved organic matter by nanofiltration**, Journal of Environmental Engineering, 116, 1, 200-205.

Amy G.L., Collins M.R., Kuo C.J., King P.H. (1987), **Comparing gel permeation chromatography and ultrafiltration for the molecular weight characterization of aquatic organic matter**, Journal AWWA, Research and Technology, Jan 87, 43-49.

Amy G.L., Sierka R.A., Bedessem J., Price D., Tan L. (1992), **Molecular size distributions of dissolved organic matter**, J AWWA, Research and Technology, June 92, 67-75.

Aoyama M. (1996a), **Fractionation of water-soluble organic substances formed during plant residue decomposition and high performance size exclusion chromatography of the fractions**, Soil Sci. Plant Nutr., 42, 1, 31-40.

Aoyama M. (1996b), **Use of high performance size exclusion chromatography to monitor the dynamics of water-soluble organic substances during the decomposition of plant residues in soil**, Soil Sci. Plant Nutr., 42, 1, 21-30.

Aptel P., Bersillon J.L., Mallevialle J. (1995), **Six years of experience in the production and distribution of ultrafiltered water**, International Workshop, Membranes in Drinking Water Production, Paris, Mar 95, 87-89.

Aptel P., Laîné J.-M. (1998), **Ten years of experience in the use of ultrafiltration in France for drinking water production**, in: Rautenbach R., Melin T., Dohmann M., Membrantechnik in der öffentlichen Wasseraufbereitung und Abwasserbehandlung, Bemessung, umsetzung, Kosten, 2. Aachener Tagung siedlungswasserwirtschaft bund Verfahrenstechnik, 15.-16. Sept., A1, 1-14.

Aptel P., personal communication (07/1998).

Arenillas A., Luque S., Rodríguez M., Alvarez J.R., Coca J. (1995), **Comparison of nano- and low MWCO ultrafiltration membranes for the treatment of bleaching effluents from an ECF pulp production process**, Proc. of Euromembrane '95, I, 373-376.

Aster B., Burba P., Broekaert J.A.C. (1996), **Analytical fractionation of aquatic humic substances and their metal species by means of multistage ultrafiltration**, Fresenius J. Analytical Chemistry, 354, 722-728.

Au K.-K., Penisson A.C., Yang S., O'Melia C. (1999), **Natural organic matter at oxide/water interfaces: complexation and conformation**, Geochimica and Cosmochimica Acta, (accepted).

Averett R.C., Leenheer J.A., McKnight D.M., Thorn K.A. (1989), **Humic substances in the Suwannee River, Georgia: interactions, properties, and proposed structures**, U.S. Geological Survey, Open-File Report 87-557.

Bacchin P. (1994), **Formation et resistance au transfert d'un depot de colloides sur une membrane d'ultrafiltration**, PhD Thesis, Université Paul Sabatier de Toulouse, Genie Chimique.

Bacchin P., Aimar P., Sanchez V. (1995), **Model for colloidal fouling of membranes**, AIChE Journal, 41, 2, 368-376.

Bacchin P., Aimar P., Sanchez V. (1996), **Influence of surface interaction on transfer during colloid ultrafiltration**, Journal of Membrane Science, 115, 49-63.

Bailey G.W., Shevchenko S.M., Yu Y.S., Kamermans H. (1997), **Combining scanning tunneling microscopy and computer simulation of humic substances: citric acid, a model**, Soil Sci. Soc. Am. J., 61, 92-101.

Bailey G.W., Yu Y.S., Shevchenko S.M. (1995), **Characterizing and visualizing the micromorphology of humic substances**, in: IHSS, Humic Substances in the Environment, New Challenges and Approaches, IHSS Conference, Aug/Sept 95, Atlanta, Georgia, 61.

Baker J., Stephenson T., Dard S., Côté P. (1995), **Characterisation of fouling of nanofiltration membranes used to treat surface waters**, Environmental Technology, 16, 977-985.

Bakker A., Van den Akker H.E.A. (1994), **Single-phase flow in stirred reactors**, Trans IChemE, 72, Part A, 583-593.

Baudin I., Anselme C. (1995), **Combining PAC and ultrafiltration**, World Water and Environmental Engineering, Nov 95, 12-13.

Becher G., Carlberg G.E., Gjessing E.T., Hongslo J.K., Monarca S. (1985), **High-performance size exclusion chromatography of chlorinated natural humic water and mutagenicity studies using the microscale fluctuation assay**, Environ. Sci. Technol., 19, 422-426.

Beckett R. (1989), **Analysis of humic substances using flow field-flow fractionation**, Aquatic Humic Substances, 5, Influence on Fate and Treatment of Pollutants, American Chemical Society, 65-80.

Beckett R., Hart B.T. (1988), **Molecular weight distributions of humic substances using flow field-flow fractionation**, Proc. Science, Technology and Utilisation of Humic Acids, CSIRO North Ryde, Nov 88, 42-52.

Beckett R., Jue Z., Giddings J.C. (1987), **Determination of molecular weight distribution of fulvic and humic acids using flow field-flow fractionation**, Environmental Science & Technology, 21, 3, 289-295.

Beckett R., Le N.P., (1990), **The role of organic matter and ionic composition in determining the surface charge of suspended particles in natural waters**, Colloids and Surfaces, 44, 35-49.

Bedwell W.B., Yates S.F., Brubaker I.M. (1988), **Crossflow microfiltration-fouling mechanisms studies**, Separation Science and Technology, 23, 6/7, 531-548.

Belfort G. (1980), **Artificial particulate fouling of hyperfiltration membranes IV. Dynamic protection from fouling**, Desalination, 34, 159-169.

Belfort G., Alexandrowicz G., Marx B. (1976), **Artificial particulate fouling of hyperfiltration membranes**, Desalination, 19, 127-138.

Belfort G., Davis R.H., Zydney A.L. (1994), **The behaviour of suspensions and macromolecular solutions in crossflow microfiltration**, Journal of Membrane Science, 96, 1-58.

Belin C., Quellec C., Lamotte M., Ewald M., Simon Ph. (1993), **Characterization by fluorescence of the dissolved organic matter in natural water. Application to fractions obtained by tangential ultrafiltration and XAD resin isolation**, Environmental Technology, 14, 1131-1144.

Ben-Aim R., Peuchot M.M. (1991), **Membranes for water and wastewater treatment**, Water Supply, 9, 185-194.

Berg P., Hagmeyer G., Gimbel R. (1997), **Removal of Pesticides and other micropollutants by nanofiltration**, Desalination, 113, 205-208.

Bhattacharjee C., Datta S. (1996), **Analysis of mass transfer during ultrafiltration of PEG-6000 in a continuous stirred cell: effect of back transport**, Journal of Membrane Science, 119, 39-46.

Bhattacharjee S., Kim A.S., Elimelech M. (1999), **Concentration polarization of interacting solute particles in cross-flow membrane filtration**, Journal of Colloid and Interface Science, 212, 81-99.

Bhattacharjee S., Ko C.-H., Elimelech M. (1998), **DLVO interactions between rough surfaces**, Langmuir, 14, 12, 3365-3375.

Bian R., Watanabe Y., Tambo N., Ozawa G. (1999), **Removal of humic substances by UF and NF membrane systems**, in: Ødegaard H. (Ed), Removal of humic substances from water, Conference Proceedings, Trondheim, Norway, 131-139.

Binovi R. (1983), **A replacement for the silt density index: permanganate demand to predict reverse osmosis membrane fouling**, Dissertation, University of Cincinnati.

Blatt W.F., Dravid A., Michaels A.S., Nelsen L. (1970), **Solute polarisation and cake formation in membrane ultrafiltration: causes, consequences and control techniques**, in: Flinn J. (Ed), Membrane Science and Technology, Plenum Press, 47.

Boerlage S.F.E., Kennedy M.D., Bonne P.A.C., Galjaard G., Schippers J.C. (1997), **Modified fouling index for the prediction of the rate of flux decline in reverse osmosis, nano- and ultrafiltration systems**, Proc. AWWA Membrane Technology Conference, New Orleans, Feb. 97, 979-999.

Boerlage S.F.E., Kennedy M.D., Witkamp G.J., van der Hoek J.P., Schippers J.C. (1997), **Prediction of $BaSO_4$ solubility in reverse osmosis systems**, Proc. AWWA Membrane Technology Conference, New Orleans, Feb. 97.

Boffardi B.P. (1997), **Scale deposit control for reverse osmosis systems**, Proc. AWWA Membrane Technology Conference, New Orleans, Feb. 97, 681-693.

Boller M., Blaser S. (1998), **Particles under stress**, Water Science & Technology, 37, 10, 9-29.

Bouchard C.R., Jolicoeur J., Kouadio P., Britten M. (1997), **Study of humic acid adsorption on nanofiltration membranes by contact angle measurements**, The Canadian Journal of Chemical Engineering, 75, April, 339-345.

Bourbigot M.M. (1996), **Non-desalting applications of membranes for drinking water treatment in France**, Proc. of WaterTECH, AWWA, Sydney, May 96, 422-427.

Bourbigot M.-M., Bablon G. (1993), **Traitement des eaux et filtration sur membranes**, Point Sciences et Techniques, 4, 1, 5-8.

Bourbigot M.M., Coté P., Agbekodo K. (1993), **Nanofiltration: An advanced process for the production of high quality drinking water**, Proc. of AWWA Membrane Technology Conf., Baltimore, Aug 93, 207-211.

Bourbonniere R.A., van Halderen T. (1989), **Fractional precipitation of humic acid from colored natural waters**, Water, Air, and Soil Pollution, 46, 187-198.

Bowen W.R., Cao X. (1998), **Electrokinetic effects in membrane pores and the determination of zeta-potential**, Journal of Membrane Science, 140, 267-273.

Bowen W.R., Hilal N., Lovitt R.W., Wright C.J. (1998), **A new technique for membrane characterisation: direct force measurement of the force of adhesion of a single particle using an atomic force microscope**, Journal of Membrane science, 139, 269-274.

Bowen W.R., Jenner F. (1995), **Theoretical descriptions of membrane filtration of colloids and fine particles: An assessment and review**, Advances in Colloid and Interface Science, 56, 141-200.

Bowen W.R., Mohammad A.W., Hilal N. (1997), **Characterisation of nanofiltration membranes for predictive purposes - use of salts, uncharged solutes and atomic force microscopy**, Journal of Membrane Science, 126, 91-105.

Bowen W.R., Mukhtar H. (1996), **Characterisation and prediction of separation performance of nanofiltration membranes**, Journal of Membrane Science, 112, 263-274.

Bowen, W.R., Calvo, J.I., Hernández, A. (1995), **Steps of membrane blocking in flux decline during protein microfiltration**, Journal of Membrane Science, 101, 153-165.

Braghetta A. (1995), **The influence of solution chemistry and operating conditions on nanofiltration of charged and uncharged organic macromolecules**, Dissertation, University of North Carolina, Chapel Hill.

Braghetta A., DiGiano F.A. (1994), **Organic solute association with nanofiltration membrane surface: influence of ph and ionic strength on membrane permeability**, AWWA Annual Conference, Denver, Jun 94, 1009-1029.

Braghetta A., DiGiano F.A., Ball W.P. (1997), **Nanofiltration of natural organic matter: pH and ionic strength effects**, Journal of Environmental Engineering, 123, 7, 628-641.

Brun G., Sayag D.R., Andre L. (1994), **The potentiometric and conductimetric characterization of the complexing power of humic substances**, Humic Substances in the Global Environment and Implications on Human Health, (Ed. N. Senesi, T.M. Miano), Elsevier Science, 193-198.

Buffle J., Deladoey P., Haerdi W. (1978), **The use of ultrafiltration for the separation and fractionation of organic ligands in fresh waters**, Analytica Chimica Acta, 101, 339-357.

Burba P., Aster B., Nifant'eva T., Shkinev V., Spivakov B.Ya. (1998), **Membrane filtration studies of aquatic humic substances and their metal species: a concise overview Part 1. Analytical fractionation by means of sequential-stage ultrafiltration**, Talanta, 45, 977-988.

Bushell G.C., Amal R., Raper J.A. (1996), **The effect of a bimodal particle size distribution on scattering from hematite aggregates**, Physica A, 233, 859-866.

Cabaniss, S.E. (1995), **Infrared and model compound studies of the acidity of humic substances**, in: IHSS, Humic Substances in the Environment, New Challenges and Approaches, IHSS Conference, Aug/Sept 95, Atlanta, Georgia, 9.

Cabaniss S.E., Shuman M.S. (1988), **Copper binding by dissolved organic matter**, Geochim. Cosmochim. Acta 52, 185-200.

Calvo J.I., Hernández A., Prádanos P., Tejerina F. (1996), **Charge adsorption and zeta potential in cyclopore membranes**, J. Colloid Interface Sci., 181, 2, 399-412.

Campbell W.L., Malcolm M.J. (1985), **Preparation, homogenisation, and storage of earth standards used and distributed by the International Humic Substances Society**, Organic Geochemistry, 8, 1, 109.

Carman P.C. (1938), **Fundamental principles of industrial filtration- A critical review of present knowledge**, Trans Inst Chem Eng, 16, 168-188.

Causserand C., Nyström M., Aimar P. (1994), **Study of streaming potentials of clean and fouled ultrafiltration membranes**, Journal of Membrane Science, 88, 211-222.

Champlin T.L, Hendricks D.W. (1995), **Pilot testing NF membranes for direct treatment of low-turbidity surface waters**, Proc. AWWA Membrane Technology Conf., Reno, Nevada, Aug 95, 229-249.

Chandrakanth M.S., Amy G.L. (1998), **Effects of NOM source variations and calcium complexation capacity on ozone-induced particle destabilisation**, Water Research, 32, 1, 115-124.

Chandrakanth M.S., Honeyman B.D., Amy G.L. (1996), **Modeling the interactions between ozone, natural organic matter, and particles in water treatment**, Colloids and Surfaces A: Physicochemical and Engineering Aspects, 107, 321-342.

Chang D., Hsu F., Hwang S.-I. (1995), **Steady-state permeate flux of cross-flow microfiltration**, Journal of Membrane Science, 98, 97-106.

Chang J.S., Tsai L.J., Vigneswaran S. (1996), **experimental investigation of the effect of particle size distribution of suspended particles on microfiltration**, Water Science & Technology, 34, 9, 133-140.

Chang S.D., Ruiz H., Bellamy W.D., Spangenberg C.W., Clark D.L. (1994), **Removal of arsenic by enhanced coagulation and membrane technology**, Proc. Of the 1994 National Conference on Environmental Engineering, American Society of Civil Engineers, 632-639.

Chang Y., Benjamin M.M. (1995), **A combined iron oxide adsorption and ultrafiltration process for natural organic matter removal and fouling control**, Proc. AWWA Annual Conference, Anaheim, CA, 657-666.

Chang Y., Benjamin M.M. (1996), **Iron oxide adsorption and UF to remove NOM and control fouling**, Journal AWWA, Dec 96, 74-88.

Chang Y., Li C.-W., Benjamin M.M. (1997), **Iron oxide-coated media for NOM sorption and particulate filtration**, Journal AWWA, 89, 5, 100-113.

Chang Y.-J. (1996), **A combined iron oxide adsorption and ultrafiltration process for natural organic matter removal and fouling control**, Dissertation, University of Washington, Civil Engineering.

Chang Y.-J., Choo K.-H., Benjamin m.M., Reiber S. (1998), **Combined adsorption-UF process increases TOC removal**, J AWWA, 90, 5, 90-102.

Chellam S., Jacangelo J.G., Bonacquisti T.P., Long B.W. (1997a), **Effect of operating conditions and pretreatment for nanofiltration of surface water**, Proc. AWWA Membrane Technology Conference, New Orleans, Feb. 97, 215-231.

Chellam S., Jacangelo J.G., Bonacquisti T.P., Schauer B.A. (1997b), **Effect of pretreatment on surface water nanofiltration**, J AWWA, 89, 10, 77-88.

Chellam S., Serra C.A., Wiesner M.R. (1998), **Estimating costs for integrated membrane systems**, J AWWA, 90, 11, 96-104.

Chellam S., Wiesner M.R. (1997), **Particle back-transport and permeate flux behaviour in crossflow membrane filters**, Environmental Science and Technology, 31, 3, 819-824.

Chellam S., Wiesner M.R. (1998), **Evaluation of crossflow filtration models based on shear-induced diffusion and particle adhesion: Complications induced by feed suspension polydispersity**, Journal of Membrane Science, 138, 83-97.

Chen S.-H., Lu M.-C., Hsu C.-S. (1998), **Effect of metal ions on humic acid removal in ultrafiltration systems**, 11th IWSA-ASPAC Regional Conference, 224-228.

Chen V., Fane A.G., Madaeni S., Wenten I.G. (1997), **Particle deposition during membrane filtration of colloids: transition between concentration polarization and cake formation**, Journal of Membrane Science, 125, 109-122.

Cheryan, M. (1986), **Ultrafiltration Handbook**, Technomic Publishing Company, Inc., USA.

Chian E.S.K., Fang H.H.P. (1976), **Physicochemical criteria of removal of trace organics by reverse osmosis**, Physical, Chemical Wastewater Treatment, American Institute of Chemical Engineers, . Water 1, 152-160.

Childress A.E. (1997), **Characterization and performance of polymeric reverse osmosis and nanofiltration membranes**, Dissertation, University of California.

Childress A.E., Elimelech M. (1996), **Effect of solution chemistry on the surface charge of polymeric reverse osmosis and nanofiltration membranes**, Journal of Membrane Science, 119, 253-268.

Childress A.E., Elimelech M. (1997), **Effects of natural organic matter and surfactants on the surface characteristics of low pressure reverse osmosis and nanofiltration membranes**, Proc. AWWA Membrane Technology Conference, New Orleans, Feb. 97, 717-725.

Chin, Y.-P. (1995), **A new paradigm for size of humic materials: The molecular weight of purified humic substances and unfractionated aquatic organic matter**, in: IHSS, Humic Substances in the Environment, New Challenges and Approaches, IHSS Conference, Aug/Sept 95, Atlanta, Georgia, 8.

Chin Y.P., Aiken G., Oloughlin E. (1994), **Molecular weight, polydispersity, and spectroscopic properties of aquatic humic substances**, Environmental Science and Technology, 28, 11, 1853-1858.

Cho J., Amy G., Pellegrino J., Yoon Y. (1998), **Characterization of clean and natural organic matter (NOM) fouled NF and UF membranes, and foulants characterization**. Desalination, 118, 101-108.

Chudacek M.W., Fane A.G. (1984), **The dynamics of polarisation in unstirred and stirred ultrafiltration**, Journal of Membrane Science, 21, 145-160.

Ciofalo M., Brucato A., Grisafi F., Torraca N. (1996), **turbulent flow in closed and free-surface unbaffled tanks stirred by radial impellers**, Chemical Engineering Science, 51(14), 3557-3573.

Clair D.H., Adams P.V., Shreve S. (1997), **Microfiltration of a high-turbidity surface water with post-treatment by nanofiltration and reverse osmosis**, Proc. AWWA Membrane Technology Conference, New Orleans, Feb. 97, 233-268.

Clair T.A., Kramer J.R., Sydor M., Eaton D. (1991), **Concentration of aquatic dissolved organic matter by reverse osmosis**, Water Research, 25, 9, 1033-1037.

Clair T.A., Sayer B.G., Kramer J.R., Eaton D.R. (1996), **Seasonal variation in the composition of aquatic organic matter in some Nova Scotian brownwaters: a nuclear magnetic resonance approach**, Hydrobiologica, 317, 141-150.

Clark M.M. personal communication 03/99.

Clark M.M., Heneghan K.S. (1991), **Ultrafiltration of lake water for potable water production**, Desalination, 80, 243-249.

Clark M.M., Jucker C. (1993), **Interactions between hydrophobic ultrafiltration membranes and humic substances**, Proc. of AWWA Membrane Technology Conf., Baltimore, Aug 93, 259-272.

Clark M.M., Lucas P. (1998), **Diffusion ands partitioning of humic acid in a porous ultrafiltration membrane**, Journal of Membrane Science, 143, 13-25.

Cohen R.D., Probstein R.F. (1986), **colloidal fouling of reverse osmosis membranes**, Journal of Colloid and Interface Science, 114, 1, 194-207.

Collins M.R., Amy G.L., Steelink C. (1986), **Molecular weight distribution, carboxylic acidity, and humic substances content of aquatic organic matter: implications for removal during water treatment**, Environmental Science & Technology, 20, 10, 1028-1032.

Combe C., Molis E., Lucas P., Riley R., Clark M.M. (1999), **The effect of CA membrane properties on adsorptive fouling by humic acid**, Journal of Membrane Science, 154, 73-87.

Cornel P.K., Summers R.S., Roberts P.V. (1986), **Diffusion of humic acid in dilute aqueous solution**, Journal of Colloid and Interface Science, 110, 1, 149-164.

Côté P. (1995), **State-of-the-art techniques in reverse osmosis, nanofiltration and electrodialysis in drinking-water supply**, 20th International Water Supply Congress & Exhibition IWSA, Durban, South Africa, 9-15 Sept 95, 9, 1-13.

Côté P., Kopp V., Tanghe N., Faivre M. (1993), **Nanofiltration for surface water post-treatment: the case of Mery-Sur-Oise in the suburb of Paris**, Proc. of AWWA Membrane Technology Conf., Baltimore, Aug 93, 777-782.

Cotsaris E., Nelson P., Bursill D., Oades M. (1988), **organic carbon in water, its sources and role in nutrient transport**, Proc. Science, Technology and Utilisation of Humic Acids, CSIRO North Ryde, Nov 88, 106-112.

Coulson J.M., Richardson J.F. (1978), **Chemical Engineering**, 3rd Edition, ume 2, Pergamon Press.

Cowie C., Pilotto L., Douglas R., Bursill D., Wade A., Reynolds C., Rouch G., Ho W., Chapman M., Bree D., Jones R. (1996), **A national drinking water quality database**, Proc. of WaterTECH, AWWA, Sydney, May 96, 433-438.

Crosby S.A., Glasson D.R., Cuttler A.H., Butler I., Turner D.R., Whitfield M., Millward G.E. (1983), **Surface areas and porosities of Fe(III)- and Fe(II)-derived oxyhydroxides**, Environmental Science & Technology, 17, 709-713.

Croué J.-P., Labouyrie-Rouillier L., Violleau D., Lefèbvre E., Legube B. (1996), **Isolation and characterisation of natural organic matter from surface water / comparison of resin adsorption and membrane filtration isolation procedures**, Natural Organic Matter Workshop, Poitiers, France, September '96, 6.

Crozes G., Anselme C., Mallevialle J. (1993a), **Effect of adsorption of organic matter on fouling of ultrafiltration membranes**, Journal of Membrane Science, 84, 61-77.

Crozes G., Anselme C., Mallevialle J. (1993b), **Impact of adsorption on ultrafiltration membrane fouling**, Proc. of AWWA Membrane Technology Conf., Baltimore, Aug 93, 803-831.

Crozes G., Jacangelo J., Anselme C., Laîné, J.M. (1995a), **Impact of ultrafiltration operating conditions on membrane irreversible fouling**, Proc. AWWA Membrane Technology Conf., Reno, Nevada, Aug 95, 457-485.

Crozes G., White P., Marshall M. (1995b), **Enhanced coagulation: its effect on NOM removal and chemical costs**, Journal AWWA, 87, 78-89.

Crum R.H., Murphy E.M., Keller C.K. (1996), **A non-adsorptive method for the isolation and fractionation of natural dissolved organic carbon**, Water Research, 30, 5, 1304-1311.

Cussler E.L. (1995), **Diffusion mass transfer**, Cambridge University Press. (p.147)

Cutter L.A. (1966), **Flow and turbulence in a stirred tank**, American Institute of Chemical Engineers Journal, 12, 35-45.

Da Costa, A.R. (1993), **Fluid flow and mass transfer in spacer-filled channels for ultrafiltration**, PhD Thesis, University of New South Wales, Chemical Engineering, Sydney.

Dal-Cin M.M., Kumar A., Capes C.E. (1995), **Natural organic matter and disinfection by-product reduction in drinking water using membrane technology: a literature review**, internat NRC Report, No. ER-1354-95S, 07/95, Ottawa, Canada.

Dard S., Côté P., Seberac P., Ortiz R.S. (1995), **Drinking water production from high sulfate mine water by nanofiltration**, Proc. AWWA Membrane Technology Conf., Reno, Nevada, Aug 95, 365-373.

De Nobili M., Contin M. (1994), **Determination of carboxyl groups content in fulvic acids by the CTA (Cetyltrimethylammonium) method**, Humic Substances in the Global Environment and Implications on Human Health, (Ed. N. Senesi, T.M. Miano), Elsevier Science, 263-268.

De Nobili M., Fornasier F. (1994), **Polyacrilamide gel electrophoresis of humic substances fractionated by ultrafiltration**, Humic Substances in the Global Environment and Implications on Human Health, (Ed. N. Senesi, T.M. Miano), Elsevier Science, 269-272.

De Nobili M., Fornasier F. (1996), **Assessment of the effect of molecular size on the electrophoretic mobility of humic substances**, European Journal of Soil Science, 47, 223-229.

De Witte J.-P. (1996), **Surface water potabilisation by means of a novel nanofiltration element**, Desalination, 108, 153-157.

Deen W.M., Satvat B., Jamieson J.M. (1980), **Theoretical model for glomerular filtration of charged solutes**, Am. J. Physiol., 238, F126-139.

Dennett K.E., Amirtharajah A., Moran T.F., Gould J.P. (1996), **Coagulation: its effect on organic matter**, J AWWA, Apr 96, 129-142.

Devitt E. C., Wiesner M. R. (1998), **Dialysis investigations of atrazine-organic matter interactions and the role of a divalent ion**, Environmental Science and Technology, 32, 2, 232-237.

Devitt E.C., Ducellier F., Côté P., Wiesner R. (1998), **Effects of natural organic matter and the raw water matrix on the rejection of atrazine by pressure-driven membranes**, Water Research, 32, 9, 2563-2568.

Devitt E.C., Wiesner M.R., Côté P. (1994), **Atrazine removal by ultrafiltration and nanofiltration enhanced by natural organic matter**, AWWA Annual Conference, New York, June 94, 517-529.

DiGiano F.A. (1996), **Evaluation of Natural Organic Matter Fouling in Bench-scale, Batch Recycle Tests of Nanofiltration**, ICR Workshop on Bench-scale and Pilot-scale Evaluations, AWWA, Cincinnati, Ohio, March 1996.

DiGiano F.A., Braghetta A., Nilson J., Utne B. (1994), **Fouling of nanofiltration membranes by natural organic matter**, National Conference on Environmental Engineering, American Society of Civil Engineers, 320-328.

DiGiano F.A., Braghetta A., Utne B., Nilson J. (1993), **Nanofiltration fouling by natural organic matter and role of particles in flux enhancement**, Proc. of AWWA Membrane Technology Conf., Baltimore, Aug 93, 273-291.

Dittrich J., Gnirß R. (1995), **Mikrofiltration zur Keim- und P-Entfernung sowie katalytische Denitrifikation**, Weitgehende Reinigung von kommunalem Abwasser, Teilprojekt B, Berliner Wasserbetriebe.

Dong L., Johansen T., Engh T.A. (1994), **Flow induced by an impeller in an unbaffled tank – I. Experimental.**, Chemical Engineering Science, . 49,. 4, 549-560.

Doyen W. (1997), **Latest developments in ultrafiltration for large-scale drinking water applications**, Desalination, 113, 165-177.

Duranceau S.J., Taylor J.S., Mulford L.A. (1992), **SOC Removal in a Membrane Softening Process**, Journal AWWA, Jan 92, 68-78.

Duranceau S.J., Taylor J.S. (1993), **Solute charge and molecular weight modeling for prediction of solute mass transfer coefficients**, Proc. of AWWA Membrane Technology Conf., Baltimore, Aug 93, 243-249.

Durham B. (1997), **Membrane pretreatment of reverse osmosis – long term experience on difficult waters**, Desalination, 110, 49-58.

Eaton A. (1995), **Measuring UV - absorbing organics: a standard method**, Journal AWWA, Feb 95, 86-90.

Edwards M., Benjamin M.M., Ryan J.N. (1996), **Role of organic acidity in sorption of natural organic matter (NOM) to oxide surfaces**, Colloids and Surfaces A: Physicochemical and Engineering Aspects, 107, 297-307.

Eisenberg T.N., Middlebrooks E.J. (1985), **Reverse osmosis treatment of drinking water**, Butterworth Publishers.

Elimelech M. personal communication (09/1999).

Elimelech M., Chen W.H., Waypa J.J. (1994), **Measuring the zeta (electrokinetic) potential of reverse osmosis membranes by a streaming potential analyzer**, Desalination, 95, 269-286.

Elimelech M., Zhu X., Childress A.E., Hong S. (1997), **Role of membrane surface morphology in colloidal fouling of cellulose acetate and composite aromatic polyamide reverse osmosis membranes**, Journal of Membrane Science, 127, 101-109.

Engebretson R.R., von Wandruszka R. (1994), **Microorganization in dissolved humic acids**, Environ. Sci. Technol., 28, 1934-1941.

Engel A. (1978), **Molecular weight determination by scanning transmission electron microscopy**, Ultramicroscopy, 3, 273-281.

Ephraim J.H., Mathuthu A.S., Marinsky J.A. (1994), **Calcium binding by fulvic acids studied by an ion selective electrode and an ultrafiltration method**, Humic Substances in the Global Environment and Implications on Human Health, (Ed. N. Senesi, T.M. Miano), Elsevier Science, 1125-1130.

Ephraim J.H., Pettersson C., Allard B. (1996), **Correlations between acidity and molecular size distributions of an aquatic fulvic acid**, Environment International, 22, 5, 475-483.

Ericsson B., Hallberg M., Wachenfeldt J. (1996), **Nanofiltration of highly colored raw water for drinking water production**, Desalination, 108, 129-141.

Ericsson B., Trägårdh G. (1996), **Treatment of surface water rich in humus - Membrane filtration vs. conventional treatment**, Desalination, 108, 117-128.

Fairhurst A.J., Warwick P., Richardson S. (1995), **The influence of humic acid on the adsorption of europium onto inorganic colloids as a function of pH**, Colloids and Surfaces A: Physicochemical and Engineering Aspects, 99, 187-199.

Faivre M., Dard S., Tanghe N., Kopp V., Agbekodo K. (1992), **Elimination de la matière organique des eaux a potabiliser par nanofiltration**, JIE 92, Conférence no 9, 9, 1-13.

Fane A. G., Hodgson P. H., Leslie G. L. (1993), **Crossflow microfiltration of biofluids and biomass - new perspectives**, 6th World Filtration Congress, Nagoya, 5-13.

Fane A.G. (1984), **Ultrafiltration of Suspensions,** Journal of Membrane Science, 20, 3, 249-260.

Fane A.G. (1996), **Membranes for water production and waste water reuse**, Desalination, 106, 1-9.

Fane A.G. (1997), **Membrane technology in the process industries**, UNSW, CEIC 5341 Lecture Notes.

Fane A.G., personal communication (06/98).

Fane A.G., Fell C.J.D., Hoogland M.R., McDonogh R. (1988), **Crossflow membrane filtration of slurries**, Chemeca '88, Australia's Bicentennial International Conference for the Process Industries, Sydney, 887-891.

Fane A.G., Fell C.J.D., Nor M.T. (1982), **Ultrafiltration of mixtures containing macrosolutes and suspended solids**, The Second ASEAN Membrane Technology Workshop, Bangkok, Oct 82.

Fane A.G., Fell C.J.D., Waters A.G. (1983), **Ultrafiltration of protein solutions through partially permeable membranes - The effect of adsorption and solution environment**, Journal of Membrane Science, 16, 211-224.

Fang H.H.P., Chian E.S,K. (1975), **Removal of alcohols, amines, and aliphatic acids in aqueous solution by NS-100 membrane**, Journal of Applied Polymer Science, 19, 1347-1358.

Field R.W., Aimar P. (1993), **Ideal limiting fluxes in ultrafiltration: comparison of various theoretical relationships**, Journal of Membrane Science, 80, 107-115.

Filella M., Buffle J. (1993), **Factors controlling the stability of submicron colloids in natural waters**, Colloids and Surfaces A: Physicochemical and Engineering Aspects, 73, 255-273.

Filella M., Buffle J., Leppard G.G. (1993), **Characterization of submicrometre colloids in freshwaters: Evidence for their bridging by organic structures**, Water Science & Technology, 27, 11, 91-102.

Filteau G., Moss P. (1997), **Ultra-low pressure RO membranes: an analysis of performance and cost**, Desalination, 113, 147-152.

Frimmel F.H., Abbt-Braun G., Hambsch B., Huber S., Scheck Ch., Schmiedel U. (1994), **Behaviour and functions of freshwater humic substances - some biological, physical and chemical aspects**, Humic Substances in the Global Environment and Implications on Human Health, (Ed. N. Senesi, T.M. Miano), Elsevier Science, 735-755.

Frimmel F.H., Hesse S. (1996), **Size-resolved DOC and UV-Absorbance as tools for characterization of NOM**, Natural Organic Matter Workshop, Poitiers, France, September '96, 8.

Fu L.F., Dempsey B.A. (1997), **Effects of charge and coagulant dose on nom removal and membrane fouling mechanisms**, Proc. AWWA Membrane Technology Conference, New Orleans, Feb. 97, 1043-1058.

Fu P., Ruiz H., Lozier J., Thompson K., Spangenberg C. (1995), **A pilot study on groundwater natural organics removal by low-pressure membranes**, Desalination, 102, 47-56.

Fu P., Ruiz H., Thompson K., Spangenberg C. (1994), **Selecting membranes for removing NOM and DBP precursors**, Journal AWWA, Dec 94, 55-72.

Gagliardo P., Adham S., Trussell R. (1997), **Water purification using reverse osmosis: thin film composite versus cellulose acetate membranes**, Proc. AWWA Membrane Technology Conference, New Orleans, Feb. 97, 597-608.

Gauthier V., Gérard B., Portal J.-M., Block J.-C., Gatel D. (1999), **Organic Matter as loose deposits in a drinking water distribution system**, Water Research, 33, 4, 1014-1026.

Ghayeni S.B., Beatson P.J., Schneider R.P., Fane A.G. (1998), **Adhesion of waste water bacteria to reverse osmosis membranes**, Journal of Membrane Science, 138, 29-42.

Ghosh K., Schnitzer M. (1980), **Macromolecular structures of humic substances**, Soil Science, 129, 5, 266-276.

Gill W.N., Wiley D.E., Fell C.J.D., Fane A.G. (1988), **Effect of viscosity on concentration polarization in ultrafiltration**, AIChE Journal, 34, 9, 1563-1567.

Gjessing E.T. (1996), **Multi-method characterisation of natural organic matter (NOM) isolated from water: characterisation of RO-isolates from water of two semi-identical dystrophiclakes in Norway**, Natural Organic Matter Workshop, Poitiers, France, September '96, 5.

Gjessing E.T., Alberts J.J., Bruchet A., Egeberg P.K., Lydersen E., McGown L.B., Mobed J.J., Münster U., Pempkowiak J., Perdue M., Ratnawerra H., Rybacki D., Takacs M., Abbt-Braun G. (1998), **Multi-method characterisation of natural organic matter isolated from water: characterisation of reverse osmisis-isolates from water of two semi-identical dystrophic lakes in Norway**, Water Research, 32, 10, 3108-3124.

Glater J., Hong S.-K., Elimelech M. (1994), **The search for a chlorine-resistant reverse osmosis membrane**, Desalination, 95, 325-345.

Glucina K., Laîné J.-M., Robert C. (1997), **Integrated, Multi-Objective Membrane Systems for Surface Water Treatment**, Proc. AWWA Membrane Technology Conference, New Orleans, Feb. 97, 327-353.

Goldberg M.C., Weiner E.R.. (1989), **Fluorescence measurements of the volume, shape, and fluorophore composition of fulvic acid from the Suwannee River**, in: Averett R.C., Leenheer J.A., McKnight D.M., Thorn K.A. (Eds.), **Humic Substances in the Suwannee River, Georgia: Interactions, Properties, and Proposed Structures**, U.S. Geological Survey, Open-File Report 87-557, 179-204.

Goldsmith R.L. (1971), **Macromolecular ultrafiltration with microporous membranes**, Ind. Eng. Chem. Fundam., 10, 1, 113-120.

Gourley L., Britten M., Gauthier S.F., Pouliot Y. (1994), **Characterisation of adsorptive fouling on ultrafiltration membranes by peptides mixtures using contact angle measurements**, Journal of Membrane Science, 97, 283-289.

Grace H.P. (1953), **Resistance and compressibility of filter cakes**,Chem. Eng. Prog., 49, 6, 303-318.

Greenberg A.E., Clesceri L.S., Eaton A.D. (1992), **Standard methods for the examination of water and wastewater**, 18th Edition, American Public Health Association.

Gregory J. (1998), **The density of particle aggregates**, Water Science & Technology, 36, 4, 1-13.

Grout H., Tarquis A.M., Wiesner M.R. (1998), **Multifractal analysis of particle size distribution in soil**, Environ. Sci. Technol., 32, 9, 1176-1182.

Gu B., Mehlhorn T.L., Liang L., McCarthy J.F. (1996a), **Competitive adsorption, displacement, and transport of organic matter on iron oxide: I. Competitive adsorption**, Geochimica et Cosmochimica Acta, 60, 11, 1943-1950.

Gu B., Mehlhorn T.L., Liang L., McCarthy J.F. (1996b), **Competitive adsorption, displacement, and transport of organic matter on iron oxide: II. Displacement and transport**, Geochimica et Cosmochimica Acta, 60, 16, 2977-2992.

Gu B., Schmitt J., Chen Z., Liang L., McCarthy J.F. (1994), **Adsorption and deposition of natural organic matter in iron oxide: mechanisms and models**, Environ. Sci. Technol., 28, 1, 38-46.

Guizard C., Ajaka N., Garcia F., Larbot A., Cot L. (1991), **Nouvelles membranes pour la nanofiltration - Influence de la structure mésoporeuse sur les performances en filtration**, Industrie Minérale, Mines et Carrières, Les Techniques, Jui 91, 111-114.

Gusses A.M., Allgeier S.C., Speth T.F., Summers R.S. (1996), **Verification and use of the rapid bench-scale membrane test**, Proc. of AWWA Annual Conference, Toronto, Canada, 743-777.

Gusses A.M., Speth T.F., Allgeier S.C., Summers R.S. (1997), **Evaluation of surface water pretreatment processes using rapid bench-scale membrane test**, Proc. AWWA Membrane Technology Conference, New Orleans, Feb. 97, 765-782.

Hagmeyer G. (1999), **Rückhaltung von binären und ternären Elektrolytmischungen durch Nanofiltrationsmembranen unter besonderer Berücksichtigung der Kohlensäurespezies**, Dissertation, Mechanical Engineering, Gerhard-Mercator University Duisburg.

Hagmeyer G., Gimbel R. (1993), **Rejection of carbonic acid species in (reverse osmosis) and nanofiltration**, Proc. of AWWA Membrane Technology Conf., Baltimore, Aug 93, 251-257.

Hagmeyer G., Panglisch S., Gimbel R. (1996), **Ultrafiltration for drinking water treatment of reservoir water**, Proc. of WaterTECH, AWWA, Sydney, May 96, 621-627.

Hagstrom J.P. (1988), **Performance of polysulfone membranes in the ultrafiltration of a surface water**, Master Thesis, Civil Engineering, University of Illinois.

Hall M.S., Lloyd D.R., Starov V.M. (1997a), **Reverse osmosis of multicomponent electrolyte solutions - Part II. Experimental verification**, Journal of Membrane Science, 128, 39-53.

Hall M.S., Starov V.M., Lloyd D.R. (1997b), **Reverse osmosis of multicomponent electrolyte solutions - Part I. Theoretical development**, Journal of Membrane Science, 128, 23-37.

Hambsch B. (1992), **Untersuchungen zu mikrobiellen Abbauvorgängen bei der Uferfiltration**, Dissertation, Universität Karlsruhe.

Harmant P. (1996), **Controle de la structure de depots de particules colloidales en filtration frontale et tangentielle**, PhD Thesis, Université Paul Sabatier de Toulouse (Sciences), Genie des Procédés.

Harmant P., Aimar P. (1996), **Coagulation of colloids retained by porous wall**, AIChemE Journal, 42, 12, 3523-3532.

Hart B.T., Day G., Beckett R. (1988), **Influence of dissolved organic matter on the uptake of heavy metals and toxic organics by suspended particulate matter in natural waters**, Proc. Science, Technology and Utilisation of Humic Acids, CSIRO North Ryde, Nov 88, 64-72.

Hashimoto A. (1995), **Status of chlorine disinfection and its by-products in Japan**, Chapter 4, Drinking Water Quality Management, Technomic Publishing, 67-85.

Hazlett T. (1990), **Standard test method for molecular weight cut-off evaluation of flat sheet ultrafiltration membranes**, American Society for Testing and Materials, Annual Book of ASTM Standards, E 1343-90.

Hepplewhite C. (1995), **Fractionation and characterisation of dissolved natural organic matter from Hope Reservoir water**, CRC Report Australian Water Quality Centre, Bolivar, SA.

Hering J.G., Morel F.M.M. (1988), **Humic acid complexation of calcium and copper**, Environ. Sci. Technol., 22, 10, 1234-1237.

Hermia J. (1982), **Constant pressure blocking filtration laws-application to power-law non-newtonian fluids**, Trans IChemE, 60, 183-187.

Hiemenz P.C. (1986), **Principles of colloid and surface chemistry**, 2nd Edition, New York, Marcel Dekker.

Hiemstra P., Van Paassen J., Rietman B., Nederlof M., Verdouw J. (1997), **Reduction of color and hardness of groundwater with nanofiltration - Is pilot plant investigation really important?**, Proc. AWWA Membrane Technology Conference, New Orleans, Feb. 97, 857-881.

Higa M., Tanioka A., Kira A. (1998), **A novel measurement method of Donnan Potential at an interface between charged membrane and mixed salt solution**, Journal of Membrane Science, 140, 213-220.

Hillis P. (1997), **Full-Scale Application of Membrane Microfiltration in North West Water Huntington Stage 4, Provision of an 80 Mld Plant**, Desalination, 113, 267-272.

Hillis P., Padley M., Le M.S. (1996), **Removal of natural organic matter by coagulation and microfiltration in potable water treatment**, Proc. of Colloidal Science in Membrane Engineering, Toulouse, May 96, O25.

Hine P.T., Bursill D.B. (1985), **The characterisation of organics in water**, Department of Resources and Energy Australian Water Resources Council, Research Project No. 80/140.

Ho B., Kumar P., Eslake J. (1995), **Performance evaluation of membrane microfiltration plant at Kangaroo Valley**, AWWA 16th Federal Convention, Vol 2, Sydney, Apr 95, 613-620.

Ho W.S.W., Sirkar K.K. (1992), **Membrane Handbook**, van Nostrand Reinhold, New York.

Hoffmann E., Marko-Varga G., Csiky I., Jönsson J. Å. (1986), **Multicolumn ion chromatographic determination of nitrate and sulfate in waters containing humic substances**, Int. J. Environ. Anal. Chem., 25, 161.

Hoffmann M.R., Yost E.C., Eisenreich S.J., Maier W.J. (1981), **Characterization of soluble and colloidal-phase metal complexes in river water by ultrafiltration. A mass-balance approach**, Environmental Science & Technology, 15, 6, 655-661.

Hofman J.A.M.H., Beerendonk E.F., Folmer H.C., Kruithof J.C. (1997), **Removal of pesticides and other micropollutants with cellulose-acetate, polyamide and ultra-low pressure reverse osmosis membranes**, Desalination, 113, 209-214.

Hofman J.A.M.H., Beerendonk E.F., Kruithof J.C. (1995), **Modelling of the rejection of organic micropollutants by nanofiltration and reverse osmosis systems**, Proc. AWWA Membrane Technology Conf., Reno, Nevada, Aug 95, 733-746.

Holland M., Nash C. (1995), **Nagambie's new 3.5 MLPD drinking water plant uses non-chemical microfiltration to treat Goulburn river water**, AWWA 16th Federal Convention, Vol 2, Sydney, Apr 95, 107-114.

Hong S., Elimelech M. (1997), **Chemical and physical aspects of natural organic matter (nom) fouling of nanofiltration membranes**, Journal of Membrane Science, 132, 159-181.

Hongve D., Åkesson G. (1998), **Comparison of nephelometric turbidity measurements using wavelengths 400-600 and 860 nm**, Water Research, 32, 10, 3143-3145.

Howell J.A. (1995), **Sub-critical flux operation of microfiltration**, Journal of Membrane Science, 107, 165-171.

Huang J., Guo Q., Ohya H., Fang J. (1998), **The characteristics of crosslinked PAA composite membrane for separation of aqueous organic solutions by reverse osmosis**, Journal of Membrane Science, 144, 1-11.

Huber S.A. (1998), **Organics – The value of chromatographic characterisation of TOC in process water plants**, Ultrapure Water, 16-20.

Huber S.A., **Direct-injection size-exclusion chromatography (DISEC) of dissolved natural organic matter (NOM) using high-sensitiuvity organic carbon detection: empiric chromatographic studies**, (unpublished).

Huisman I.H., Dutré B., Persson K.M., Trägårdh G. (1997), **Water permeability in ultrafiltration and microfiltration: viscous and electroviscous effects**, Desalination, 113, 95-103.

Hwang K.-J., Liu H.-C., Lu W.-M. (1998), **Local properties of cake in cross-flow microfiltration of submicron particles,** Journal of Membrane Science, 138, 181-192.

Jacangelo J.G., Adham S.S., Laîné J.-M. (1995a), **Mechanisms of Cryptosporidium, Giardia, and MS2 virus removal by MF and UF**, J AWWA, 07, 107-121.

Jacangelo J.G., Cummings E.W., Coté P., Mallevialle J. (1993), **Influence of feedwater characteristics on ultrafiltration and nanofiltration permeate water quality**, Proc. of AWWA Membrane Technology Conf., Baltimore, Aug 93, 293-322.

Jacangelo J.G., DeMarco J., Owen D.M., Randtke S.J. (1995b), **Selected Processes for removing NOM: An overview**, Journal AWWA, Jan 95, 64-77.

Jacangelo J.G., Laîné J.-M., Cummings E.W., Adham S.S. (1995c), **UF with pretreatment for removing DBP precursors**, Journal AWWA, Mar 95, 100-112.

Jacangelo J.G., Patania N.L., Laîné J.-M., Montgomery J.M., Booe W., Mallevialle J. (1992), **Low pressure membrane filtration for particle removal**, AWWA Research Foundation and American Water Works Association.

Jacangelo J.G., Trussell R.R., Watson M. (1997), **Role of membrane technology in drinking water treatment in the United States**, Desalination, 113, 119-127.

Jacangelo J.G., Watson M., Herndon V. (1999), **Basis concepts for the use of membrane technology in drinking water treatment**, ICOM '99, Workshop od Membrane Treatment for Drinking Water, Toronto, Canada.

Jackson J.M., Landolt D. (1973), **About the mechanism of formation of iron hydroxide fouling layers on reverse osmosis membranes**, Desalination, 12, 361-378.

Jeantet R., Maubois J.L. (1995), **Sélectivité de membranes de nanofiltration: effet du pH, de la nature et de la concentration des solutions**, Lait, 75, 595-610.

Jensen K., Thorsen T. (1995), **Treatment of water containing humic substances. - status and prospects.**, International Workshop, Membranes in Drinking Water Production, Paris, Mar 95, 63-65.

Jiang Q., Logan B.E. (1991), **Fractal dimensions of aggregates determined from steady-state size distributions**, Environ. Sci. Technol., 25, 12, 2031-2038.

Jiminez M.C.S., Domínguez P.A., Silverio J.M.C. (1993), **Reaction kinetics of humic acid with sodium hypochlorite**, Water Research, 27, 5, 815-820.

Johannsen K. (1993), **Untersuchungen und Berechnungen zur Huminstoffadsorption**, Dissertation, University of Karlsruhe, Germany.

Johns M.M., Skogley E.O., Inskeep W.P. (1993), **Characterization of carbonaceous adsorbents by soil fulvic and humic acid adsorption**, Soil Sci. Am. J., 57, 1485-1490.

Johnson W.T. (1999), **Recent advances in microfiltration for drinking water treatment**, AWWA Annual Meeting, Chicago, June '99.

Jönsson A.-S. (1993), **Influence of shear rate on the flux during ultrafiltration of colloidal substances**, Journal of Membrane Science, 79, 93-99.

Jönsson A.-S., Jönsson B. (1996a), **Colloidal fouling during ultrafiltration**, Separation Science and Technology, 31, 19, 2611-2620.

Jönsson A.-S., Jönsson B. (1996b), **Ultrafiltration of colloidal dispersions - a theoretical model of the concentration polarization phenomena**, Journal of Colloid and Interface Science, 180, 504-518.

Jucker C., Clark M.M. (1994), **Adsorption of aquatic humic substances on hydrophobic ultrafiltration membranes**, Journal of Membrane Science, 97, 37-52.

Julien F., Gueroux B., Mazet M. (1994), **Comparison of organic compounds removal by coagulation-flocculation and by adsorption onto preformed hydroxyde flocs**, Water Research, 28, 12, 2567-2574.

Jullien R., Botet R. (1987), **Aggregation and fractal aggregates**, World Scientific: Singapore.

Jung S.-j., Amal R., Raper J.A. (1995), **The use of small angle light scattering to study structure of flocs**, Part. Part. Syst. Charact., 12, 274-278.

Kabsch-Korbutowicz M., Winnicki T. (1996), **Application of modified polysulfone membranes to the treatment of water solutions containing humic substances and metal ions**, Desalination, 105, 41-49.

Kaeding U. (1998), **The kinetics of coagulation of natural organic matter with alum**, CRC for Water Quality and Treatment, Postgraduate Student Conference 1998, 109-114.

Kainulainen T., Tuhkanen T., Vartiainen T., Heinonen-Tanski H., Kalliokoski P. (1994), **The effect of different oxidation and filtration processes on the molecular size distribution of humic material**, Water Science & Technology, 30, 9, 169-174.

Kaiya Y., Itoh Y., Takizawa S., Fujita K. (1996), **Fouling analysis and control in membrane treatment process for potable purpose**, World Filtration Congress, Budapest, Hungary, May 96, 526-530.

Kamp i.r.P.C. (1995), **Integral approach of surface water treatment using ultrafiltration and reverse osmosis**, Proc. AWWA Membrane Technology Conf., Reno, Nevada, Aug 95, 31-37.

Kango R.A., Zutshi D.P. (1986), **Interaction of certain heavy metals with lake humic acids**, Intern. J. Environ. Anal. Chem., 26, 51-59.

Kaplan L.A., Gremm T.J. (1995), **Bioavailability of humic substances in stream ecosystems**, in: IHSS, Humic Substances in the Environment, New Challenges and Approaches, IHSS Conference, Aug/Sept 95, Atlanta, Georgia, 115.

Kasper D.R. (1993), **Pre- and posttreatment processes for membrane water treatment systems**, Proc. of the AWWA Membrane Technology Conference, Aug 93, Baltimore, 105-137.

Kastelan-Kunst L., Kosutik K., Dananic V., Kunst B. (1997), **FT30 Membranes of characterized porosities in the reverse osmosis organics removal from aqueous solutions**, Water Research, 31, 11, 2878-2884.

Kastelan-Macan M., Petrovic M. (1996), **The role of fulvic acids in phosphorous sorption and release from mineral particles**, Water Science & Technology, 34, 7-8, 259-265.

Kawada I., Inoue K., Kazuse Y., Ito H., Shintani T., Kamiyama Y. (1987), **New thin-film composite low pressure reverse osmosis membranes and spiral wound modules**, Desalination, 64, 387-401.

Kedem O., Katchalsky A. (1958), **Thermodynamic analysis of the permeability of biological membranes to non-electrolytes**, Biochimica and Biophysica Acta, 27, 229.

Khatib K., Rose J., Barres O., Stone W., Bottero J.-Y., Anselme C. (1997), **Physico-chemical study of fouling mechanisms of ultrafiltration membrane on Biwa lake (Japan)**, Journal of Membrane Science, 130, 53-62.

Khow J.H., Bernard I.A., Rachwal A.J., Jefferies M., O'Donnell J. (1997), **Technical and economic feasibility of nanofiltration membranes for removal of metals and organics from potable water supplies**, AWWA Annual Conference, Feb 97.

Kilduff J., Weber W.J. Jr. (1992), **Transport and separation of organic macromolecules in ultrafiltration processes**, Environmental Science & Technology, 26, 3, 569-577.

Kim C.H., Hosomi M., Murakami A., Okada M. (1994a), **Effects of clay on the fouling by organic substances in potable water treatment by ultrafiltration**, Water Science & Technology, 30, 9, 159-168.

Kim C.-H., Hosomi M., Murakami A., Okada M. (1996a), **characteristics of fouling due to clay-organic substances in potable water treatment by ultrafiltration**, Water Science & Technology, 34, 9, 157-164.

Kim K.-J., Chen V., Fane A.G. (1993), **ultrafiltration of colloidal silver particles: flux, rejection, and fouling**, J. of Colloid and Interface Science, 155, 347-359.

Kim K.J., Chen V., Fane A.G. (1994b), **Characterization of clean and fouled membranes using metal colloids**, Journal of Membrane Science, 88, 93-101.

Kim K.-J., Dickson M.R., Chen V., Fane A.G. (1992a), **Applications of field emission scanning electron microscopy to polymer membrane research**, Micron and Microscopica Acta, 23, 3, 259-271.

Kim K.J., Fane A.G., Fell C.J.D. (1990), **Quantitative microscopic study of surface characteristics of ultrafiltration membranes**, Journal of Membrane Science, 54, 89-102.

Kim K.J., Fane A.G., Fell, C.J.D., Joy D.C. (1992b), **Fouling mechanisms of membranes during protein ultrafiltration**, Journal of Membrane Science, 68, 79-91.

Kim K.J., Fane A.G., Nyström M., Pihlajamaki A., Bowen W.R., Mukhtar H. (1996b), **Evaluation of electroosmosis and streaming potential for measurement of electric charges of polymeric membranes**, Journal of Membrane Science, 116, 149-159.

Klein R., Weitz D.A., Lin M.Y., Lindsay H.M., Ball R.C., Meakin P. (1990), **Theory of scattering from colloidal aggregates**, Progress in Colloid and Polymer Science, 81, 161-168.

Knoell T., Safarik J., Cormack T., Riley R., Lin S.W., Ridgway H. (1999), **Biofouling potentials of microporous polysulfone membranes containing a sulfonated polyether-ethersulfone/polyethersulfone block copolymer: correlation of membrane surface properties with bacterial attachment**, J Membrane Science, 157, 117-138.

Ko M.K., Pellegrino J.J. (1992), **Determination of osmotic pressure and fouling resistances and their effects on performance of ultrafiltration membranes**, Journal of Membrane Science, 74, 141-157.

Kopp V., Chantriaux T. (1993), **Nanofiltration d'une eau de surface: la première phase industrielle de Méry-sur-Oise**, Point Sciences et Techniques, 4, 1, 12-14.

Kopp V., Tanghe N., Faivre M. (1993), **Tertiary refining by nanofiltration of surface water in the Paris region**, Water Supply, 11, 3/4, 271-280.

Koprivnjak J.-F., Blanchette J.G., Bourbonniere R.A., Clair T.A., Heyes A., Lum K.R., McCrea R., Moore T.R. (1995), **The underestimation of concentrations of dissolved organic carbon in freshwaters**, Water Research, 29, 1, 91-94.

Korshin G. V., Benjamin M.M., Sletten R.S. (1997a), **Adsorption of natural organic matter (NOM) on iron oxide: effects on NOM composition and formation of organo-halide compounds during chlorination**, Water Research, 31, 7, 1643-1650.

Korshin G.V., Li C.-W., Benjamin M.M. (1996), **UV spectra of NOM: A consistent description and practical applications**, Natural Organic Matter Workshop, Poitiers, France, September '96, 7.

Korshin G.V., Li C.-W., Benjamin M.M. (1997b), **Monitoring the properties of natural organic matter through UV spectroscopy: a consistent theory**, Water Research, 31, 7, 1787-1795.

Kotelyanskii M.J., Wagner N.J., Paulaitis M.E. (1998), **Atomistic simulation of water and salt transport in the reverse osmosis membrane FT-30**, Journal of Membrane Science, 139, 1-16.

Krasner S.W., Amy G. (1995), **Jar testing evaluations of enhanced coagulation**, Journal AWWA, Oct 95, 93-107.

Krasner S.W., Croué J.-P., Buffle J., Perdue E.M (1996), **Three approaches for characterizing NOM**, Journal AWWA, June, 66-79.

Kretzschmar R., Hesterberg D., Sticher H. (1997), **Effect of adsorbed humic acid on surface charge and flocculation of kaolinite**, Soil Sci. Soc. Am. J., 61, 101-108.

Kronberg L. (1999), **Water treatment practice and the formation of genotoxic chlorohydroxyfuranones**, in: Ødegaard H. (Ed), Removal of humic substances from water, Conference Proceedings, Trondheim, Norway, 35-42.

Küchler I.L., Miekeley N. (1994), **Ultrafiltration of humic compounds through low molecular mass cut-off level membranes**, The Science of the Total Environment, 154, 23-28.

Küchler I.L., Miekeley N., Forsberg B.R. (1994), **Molecular mass distributions of dissolved organic carbon and associated metals in waters from Rio Negro and Rio Solimões**, The Science of the Total Environment, 156, 207-216.

Kulkarni A., Mukherjee D., Gill W.N. (1996), **Flux enhancement by hydrophilization of thin film composite reverse osmosis membranes**, Journal of Membrane Science, 114, 39-50.

Kumar P., Keetch K., Walkom G., Williams R. (1998), **Operating experience of a portable microfiltration plant with highly turbid chlorinated water**, 11th IWSA-ASPAC Regional Conference, 451-457.

Kunikane S., Magara Y., Itoh M., Tanaka O. (1995), **A comparative study on the application of membrane technology to the public water supply**, Journal of Membrane Science, 102, 149-154.

Kwak J.C.T., Nelson R.W.P. (1977), **Ultrafiltration of fulvic and humic acids, a comparison of stirred cell and hollow fiber techniques**, Geochimica and Cosmochimica Acta, 1977, 41, 993-996.

Lahoussine-Turcaud V., Wiesner M.R., Bottero J.-Y. (1990), **Fouling in tangential-flow ultrafiltration: the effect of colloid size and coagulation pretreatment**, Journal of Membrane Science, 52, 173-190.

Laîné J.-M., Clark M.M., Mallevialle J. (1990), **Ultrafiltration of lake water: effect of pretreatment on the partitioning of organics, THMPF, and flux**, Journal AWWA, Dec 90, 82-87.

Laîné J.-M., Hagstrom J.P., Chark M.M., Mallevialle J. (1989), **Effects of ultrafiltration membrane composition**, J AWWA, Nov 89, 61-67.

Laufenberg G., Hausmanns S., Kunz B. (1996), **The influence of intermolecular interactions on the selectivity of several organic acids in aqueous multicomponent systems during reverse osmosis**, Journal of Membrane Science, 110, 59-68.

Ledin A., Karlsson S., Düker A., Allard B. (1995), **Characterization of the submicrometre phase in surface waters - a review**, Analyst, 120, 3, 603-608.

Leenheer J.A, McKniht D.M., Thurman E.M., MacCarthy P. (1989), **Structural components and proposed structural models of fulvic acid from the Suwannee River**, in: Averett R.C., Leenheer J.A., McKnight D.M., Thorn K.A. (Eds.), **Humic Substances in the Suwannee River, Georgia: Interactions, Properties, and Proposed Structures**, U.S. Geological Survey, Open-File Report 87-557, 331-360.

Leenheer J.A. (1981), **Comprehensive approach to preparative isolation and fractionation of dissolved organic carbon from natural waters and wastewaters**, Environmental Science & Technology, 15, 5, 578-587.

Leenheer J.A. (1985), **Fractionation techniques for aquatic humic substances**, in: Aiken G.R., McKnight D.M., Wershaw R.L., MacCarthy P. (Eds.), Humic Substances, in Soil, Sediment, and Water, John Wiley & Sons, Inc., 409-429.

Leenheer J.A. (1996), **Fractionation, isolation and characterisation of hydrophilic constituents of dissolved organic matter in water**, Natural Organic Matter Workshop, Poitiers, France, September '96, 4.

Leenheer J.A., Brown P.A., Noyes T.I. (1989), **Implications of mixture characteristics on humic-substance chemistry**, Aquatic Humic Substances, 2, Influence on Fate and Treatment of Pollutants, American Chemical Society, 25-40.

Leentvaar J., Ywema T.S.J. (1980), **Some dimensionless parameters of impeller power in coagulation-floculation processes**, Water Research, 14, 135-140.

Legube B., Agbekodo K., Coté P., Bourbigot M.M. (1995), **Removal of organohalide precursors by nanofiltration**, Water Supply, 13, 2, 171-181.

Legube B., Xiong F., Croue J.-P., Doré M. (1990), **Étude sur les acides fulviques extraits d'eaux superficielles françaises, extraction, caractérisation et réactivité avec le chlore**, Revue des Sciences de l'Eau, 3, 4, 399-424.

Leppard G.G., Burnison B.K., Buffle J. (1990), **Transmission electron microscopy of the natural organic matter of surface waters**, Analytica Chimica Acta, 232, 107-121.

Leslie G., personal communication (10/1999).

Levenstein R., Hasson D., Semiat R. (1996), **Utilization of the Donnan effect for improving electrolyte separation with nanofiltration membranes**, Journal of Membrane Science, 116, 77-92.

Levi Y., Pernette S., Wable O., Kiene L. (1997), **Demonstration unit of satellite treatment in distribution system using ultrafiltration and nanofiltration**, Proc. AWWA Membrane Technology Conference, New Orleans, Feb. 97, 581-597.

Li H., Fane A.G., Coster H.G.L, Vigneswaran S. (1998), **Direct observation of particle deposition on the membrane surface during crossflow microfiltration**, Journal of Membrane Science, 149, 83-97.

Li H., Fane A.G., Coster H.G.L., Vigneswaran S. (1999), **An assessment of polarisation models of crossflow microfiltration by direct observation through the membrane**, submitted to Journal of Membrane Science.

Liang L. (1988), **Effects of surface chemistry on kinetics of coagulation of submicron iron oxide particles (α-fe_2o_3) in water**, PhD Thesis, California Institute of Technology, May 88.

Liang L.,. Morgan J.J. (1990), **Chemical aspects of iron oxide coagulation in water: Laboratory studies and implications for natural systems**, Aquatic Sciences, 52, 1, 32-55.

Liao M.Y., Randtke S.J. (1986), **Predicting the removal of soluble organic contaminants by lime softening**, Water Research, 20, 27-35.

Lin M.Y., Klein R., Lindsay H.M., Weitz D.A., Ball R.C., Meakin P. (1990), **The structure of fractal colloidal aggregates of finite extent**, J Colloid and Interface Science, 137, 1, 263-280.

Lin M.Y., Lindsay H.M., Weitz D.A., Ball R.C., Klein R., Meakin P. (1989), **Universality in colloid aggregation**, Nature, 339, 360-362.

Lipp P. (1993), **Zum Einfluß der Rohwasserzusammensetzung auf das Trennverhalten von Membranen bei der Umkehrosmose wäßriger Lösungen**, Dissertation, Technische Hochschule Karlsruhe, Nov 1993.

Lipp P., Gimbel R., Frimmel F.H. (1994), **Parameters influencing the rejection properties of FT30 membranes**, Journal of Membrane Science, 95, 185-197.

Lipp P., Schmitt A., Baldauf G. (1997), **Treatment of soft reservoir water by limestone filtration in combination with ultrafiltration**, Desalination, 113, 285-292.

Lo B., Waite T.D. (1998), **Structure of ferric oxyhydroxide aggregates – a light scattering study**, Chemeca '98 Conference, Port Douglas, Sept 1998, CD Rom.

Logan B., Jiang Q. (1990), **Molecular size distributions of dissolved organic matter**, Journal of Environmental Engineering, 116, 6, 1046-1062.

Lozier J., Jones G. (1997), **Meeting the challenges of the new drinking water regulations with dual-membrane treatment**, Proc. AWWA Membrane Technology Conference, New Orleans, Feb. 97.

Maartens A., Swart P., Jacobs E.P. (1998), **Humic membrane foulants in natural brown water: characterisation and removal**, Desalination, 115, 215-227.

MacCarthy P., Malcolm R.L. (1989), **The nature of commercial humic acids**, Aquatic Humic Substances, 4, Influence on Fate and Treatment of Pollutants, American Chemical Society, 55-64.

MacCormick A.B. (1995), **The application of microfiltration in water and wastewater treatment**, in: Kolarik L.O., Priestly A.J. (eds.), Modern Techniques in Water and Wastewater Tratment, 45-51.

Mackey E.D. (1999), **Fouling of ultrafiltration and nanofiltration membranes by dissolved organic matter**, Dissertation, Rice University, Environmental Science and Engineering, Houston.

Macoun R.G. (1998), **The mechanisms of ionic rejection in nanofiltration**, PhD thesis, UNSW, Chemical Engineering.

Macoun R.G., Shen Y.R., Fane A.G., Fell C.J.D. (1991), **Nanofiltration: theory and applications to ionic separations**, Chemeca, Sep 91, 398-405.

Malcolm R.L. (1985), **Geochemistry of stream fulvic and humic substances**, in: Aiken G.R., McKnight D.M., Wershaw R.L., MacCarthy P. (Eds.), Humic Substances, in Soil, Sediment, and Water, John Wiley & Sons, Inc., 181-210.

Malcolm R.L., MacCarthy P. (1986), **Limitations in the use of commercial humic acids in water and soil research**, Environmental Science & Technology, 20, 9, 904-911.

Mallevialle J., Anselme C., Marsigny O. (1989), **Effects of humic substances on membrane processes**, 41, Aquatic Humic Substances, Influence on Fate and Treatment of Pollutants, American Chemical Society, 749-767.

Mallevialle J., Odendaal P.E., Wiesner M.R. (1996), **Water treatment membrane processes**, McGraw-Hill.

Mallubhotla H., Hoffmann S., Schmidt M., Vente J., Belfort G. (1998), **Flux enhancement during dean vortex tubular membrane nanofiltration. 10. Design, construction, and system characterisation,** Journal of Membrane Science, 141, 183-195.

Martin-Mousset B., Croué J.P., Lefebvre E., Legube B. (1997), **Distribution et caractérisation de la matière organique dissoute d'eaux naturelles de surface**, Water Research, 31, 3, 541-553.

Matijevic E., Schreiner P. (1978), **Ferric hydrous oxide sols III. preparation of uniform particles by hydrolysis of Fe(III)-chloride, -nitrate, and -perchlorate solutions**, Journal of Colloid and Interface Science, 63, 3, 509-523.

Matlack K.S. (1992), **Modeling the interaction of dissolved organic matter with cations**, Dissertation, Georgia Institute of Technology.

Matthiasson E. (1983), **The role of macromolecular adsorption in fouling of ultrafiltration membranes**, Journal of Membrane Science, 16, 23-36.

Mayer L.M. (1985), **Geochemistry of humic substances in estuaries**, in: Aiken G.R., McKnight D.M., Wershaw R.L., MacCarthy P. (Eds.), Humic Substances, in Soil, Sediment, and Water, John Wiley & Sons, Inc., 211-232.

Mazid M.A. (1988), **Separation and fractionation of macromolecular solutions by ultrafiltration**, Separation Science and Technology, 23, 14&15, 2191-2210.

McCann B. (1999), **By-product blues**, Water21, July/August, 15-18.

McCoy G.A. (1993), **Characterization of natural organic matter and its relation to removal by chemical coagulation**, Dissertation, University of Colorado, Boulder.

McDonogh R.M., Fane A.G., Fell C.J.D. (1989), **Charge effects in the cross-flow filtration of colloids and particulates**, Journal of Membrane Science, 43, 69-85.

McDonogh R.M., Fell C.J.D., Fane A.G. (1984), **Surface charge and permeability in the ultrafiltration of non-flocculating colloids**, Journal of Membrane Science, 21, 285-294.

McDonogh R.M., Welsch K., Fane A.G., Fell C.J.D. (1995), **Flux and rejection in the ultrafiltration of colloids**, Desalination, 70, 251-264.

Meagher L., Klauber C., Pashley R.M. (1996), **The influence of surface forces on the fouling of polypropylene microfiltration membranes**, Colloids and Surfaces, A: Physicochemical and Engineering Aspects, 106, 63-81.

Milonjic S.K., Vucic N.B., Vujosevic S.I. (1996), **Ultrafiltration of hematite sol**, Separation Science and Technology, 31, 10, 1515-1521.

Moaddeb M., Koros W.J. (1997), **Occlusion of pores of polymeric membranes with coloidal silica**, Short Communication, Journal of Membrane Science, 136, 273-277.

Morel F.M.M., Hering J.G. (1993), **Principles and applications of aquatic chemistry**, Wiley-Interscience, New York.

Mori S. (1988), **Determination of chemical composition and molecular weight distributions of high-conversion styrene-methyl methacrylate copolymers by liquid adsorption and size exclusion chromatography**, Anal. Chem., 60, 1125-1128.

Morran J.Y., Bursill D.B., Drikas M., Nguyen H. (1996), **A new technique for the removal of natural organic matter**, Proc. of WaterTECH, AWWA, Sydney, May 96, 428-432.

Moulin C. (1993), **Membranes: agrément et normalisation**, Point Sciences et Techniques, 4, 1, 9-11.

Moulin C., Tazi-Pain A. (1993), **Use of organic microfiltration membranes for groundwater treatment**, Proc. of AWWA Membrane Technology Conf., Baltimore, Aug 93, 361-372.

Moulin P., Manno P., Rouch J.C., Serra C., Clifton M.J., Aptel P. (1999), **Flux improvement by Dean vortices: ultrafiltration of colloidal suspensions and macromolecular solutions**, Journal of Membrane Science, 156, 109-130.

Mühle K. (1993), **Floc stability in laminar and turbulent flow**, In: Coagulation and flocculation: theory and applications, Dobias B. (Ed.), Marcel Dekker, New York, 8, 355-390.

Mulford L.A., Jones P.S., Taylor J.S. (1990), **Disinfection By-product control by nanofiltration**, EPA, DWRD, Cincinnati.

Munch W.D., Zestar L.P., Anderson J.L. (1979), **Rejection of polyelectrolytes from microporous membranes**, J Membrane Science, 5, 77-102.

Murphy D., de Pinho M.N. (1995), **An ATR-FTIR study of water in cellulose acetate membranes prepared by phase inversion**, Journal of Membrane Science, 106, 245-257.

Murphy E.M., Zachara J.M., Smith S.C. (1990), **Influence of mineral-bound humic substances on the sorption of hydrophobic organic compounds**, Environmental Science & Technology, 24, 10, 1507-1516.

Nagata S. (1975), **Mixing: Principles and Applications**, Wiley, New York.

Nakao S., Kimura S. (1982), **Models of membrane transport phenomena and their application for ultrafiltration data**, J. Chem. Eng. Japan, 15, 200-205.

Nakatsuka S., Ase T. (1995), **Ultrafiltration of river water for drinking water production**, Proc. AWWA Membrane Technology Conf., Reno, Nevada, Aug 95, 621-639.

Nazzal F.F., Wiesner M.R. (1993), **The effect of pH and ionic strength on the cross-flow filtration of colloidal silica and humic solutions using ceramic membranes**, Proc. of AWWA Membrane Technology Conf., Baltimore, Aug 93, 93-104.

Newcombe G., Drikas M. (1996), **Characterisation of natural organic material from Myponga Reservoir and the effect on activated carbon adsorption**, Proc. of WaterTECH, AWWA, Sydney, May 96, 442-447.

Newcombe G., Drikas M., Assemi S., Beckett R. (1996), **The influence of characterised natural organic material on activated carbon adsorption: I characterisation of concentrated reservoir water**, (supplement to WaterTech '96 paper).

Newman M.E., Fiella M., Chen Y., Nègre J.-C., Perret D., Buffle J. (1994), **Submicron particles in the River Rhine-II. Comparison of field observations and model predictions**, Water Research, 28, 1, 107-118.

Nilson J.A., DiGiano F.A. (1996), **Influence of NOM composition on nanofiltration**, Journal AWWA, May '96, 53-66.

Noble R.D., Stern S.A. (1995), **Membrane separations technology-principles and applications**, Elsevier.

Norwood D.L., Christman R.F. (1987), **Structural characterisation of aquatic humic material. 2. Phenolic content and its relationship to chlorination mechanism in an isolated aquatic fulvic acid**, Environmental Science & Technology, 21, 8, 791-798.

Nyström M., Kaipia L., Luque S. (1995a), **Fouling and retention of nanofiltration membranes**, Journal of Membrane Science, 98, 249-262.

Nyström M., Pihlajamäki A., Ehsani N., Kareinen P., Vanhanen S. (1995b), **Characterisation of fouled and clean membranes increases the understanding of membrane material and model substance interaction**, Proc. of Euromembrane '95, I, 101-106.

Nyström M., Ruohomäki K., Kaipia L. (1994), **Humic acid as a fouling agent in filtration**, International Specialist Conference on Desalination and Water Reuse, Perth, Dec 94, 1, 119-128.

Nyström M., Ruohomäki K., Kaipia L. (1996), **Humic acid as a fouling agent in filtration**, Desalination, 106, 79-87.

O'Melia C.R. (1989), **Particle-particle interactions in aquatic systems**, Colloids and Surfaces, 39, 255-271.

O'Melia C.R., Becker W.C., Au K.-K. (1999), **Removal of humic substances by coagulation**, in: Ødegaard H. (Ed), Removal of humic substances from water, Conference Proceedings, Trondheim, Norway, 55-64.

Ødegaard H., Eikebrokk B., Storhaug R. (1999), **Processes for the removal of humic substances from water- an overview based on Norwegian experiences**, in: Ødegaard H. (Ed), Removal of humic substances from water, Conference Proceedings, Trondheim, Norway, 43-52.

Ødegaard H., Koottatep S. (1982), **Removal of humic substances from natural waters by reverse osmosis**, Water Research, 16, 613-620.

Ødegaard H., Thorson T. (1989), **Removal of humic substances by membrane processes**, 42, Aquatic Humic Substances, Influence on Fate and Treatment of Pollutants, American Chemical Society, 769-782.

Oles V.J., (1992), **Shear induced aggregation and breakup of polystyrene latex particles**, J Colloid Interface Sci, 154, 2, 351-358.

Österberg R., Mortensen K. (1994), **Fractal geometry of humic acids. Temperature-dependent restructuring studied by small-angle neutron scattering**, Humic Substances in the Global Environment and Implications on Human Health, (Ed. N. Senesi, T.M. Miano), Elsevier Science, 127-132.

Page D. (1998), **Characterisation of dissolved organic matter (DOM) from selected South Australian Reservoirs**, CRC for Water Quality and Treatment, Postgraduate Student Conference 1998, 91-96.

Parker D.S., Kaufman W.J., Jenkins D. (1972), **Floc break-up in turbulent flocculation processes**, ASCE J. San Eng Div, 98, 79-99.

Patel R., Penisson A.C., Hill R.D., Wiesner M.R. (1994), **Membrane microfiltration of secondary wastewater effluent**, Chemical Water and Wastewater treatment III, 29-36.

Peeters J.M.M. (1997), **Characterization of nanofiltration membranes**, Dissertation, University of Enschede, Netherlands.

Peeters J.M.M., Mulder M.H.V., Keizer K., Strathmann H. (1995), **Relation between membrane charge and rejection characteristics of nanofiltration membranes**, Proc. of Euromembrane '95, Vol I, 107-112.

Peeters J.M.M., Mulder M.H.V., Keizer K., Strathmann H., Verweij H. (1996), **Streaming potential measurements as a characterisation method for nanofiltration membranes**, Proc. of Colloid Science in Membrane Engineering, Toulouse, May 96, O24.

Perdue M. (1989) **Effects of humic substances on metal speciation**, Aquatic Humic Substances, Influence on Fate and Treatment of Pollutants, American Chemical Society, 281-295.

Perie C., Bailly J.-R., Labbe H., Guiresse M. (1995), **Is there a relation between molecular dimension of humic acids and their isoelectric point**, in: IHSS, Humic Substances in the Environment, New Challenges and Approaches, IHSS Conference, Aug/Sept 95, Atlanta, Georgia, 57.

Perret D., Newman M.E., Nègre J.-C., Chen Y., Buffle J. (1994), **Submicron particles in the Rhine River-I. physico-chemical characterisation**, Water Research, 28, 1, 91-106.

Perry R.H., Chilton C.H. (1973), **Chemical Engineer's Handbook**, 5th Edition, New York, McGraw-Hill.

Petersen R.J. (1993), **Review: Composite reverse osmosis and nanofiltration membranes**, Journal of Membrane Science, 83, 81-150.

Pettersson C., Ephraim J., Allard B. (1994), **On the composition and properties of humic substances isolated from deep groundwater and surface waters**, Organic Geochemistry, 21, 5, 443-451.

Peuravuori J., Pihlaja K. (1998), **Multimethod characterisation of lake aquatic humic matter isolated with sorbing solid and tangential membrane filtration**, Analytical Chimica acta, 364, 203-221.

Pickering K.D., Wiesner M.R. (1993), **Cost model for low-pressure membrane filtration**, Journal of Environmental Engineering, 119, 5, 772-797.

Pihlajamäki A. (1998), **Electrochemical characterisation of filter media properties and theiir exploitation in enhanced filtration**, PhD Thesis, Lappeenranta University of Technology, Finland.

Pontalier P.-Y., Ismail A., Dodds J., Ghoul M. (1995), **Modelling of convective and diffusive transports in nanofiltration process**, Proc. of Euromembrane '95, Vol I, 197-200.

Potts D.E., Ahlert R.C., Wang S.S. (1981), **A critical review of fouling of reverse osmosis membranes**, Desalination, 36, 235-264.

Prasanthi H., Ngo H.H., Vigneswaran S. (1995), **Effects of organics on filtration and their removal**, AWWA 16th Federal Convention, Vol 2, Sydney, Apr 95, 139-146.

Rachwal A.J., Khow J., Colbourne J.S., O'Donnell J. (1994), **Water treatment for public supply in the 1990's - a role for membrane technology?**, Desalination, 97, 427-436.

Raman L.P., Cheryan M., Rajagopalan N. (1994), **Consider nanofiltration for membrane separations**, Chemical Engineering Progress, Mar 94, 68-74.

Randon G., Portugues P., Côté P., Cavard J. (1994), **Etude du comportement d'un réseau de distribution alimente par une filière de nanofiltration: L'experience d'Auvers-sur-Oise**, Journées Information Eaux, Poitiers, Sept 94, 7, 1-10.

Rasyid U., Johnson W.D., Wilson M.A., Hanna J.V. (1992), **Changes in organic structural group composition of humic and fulvic acids with depth in sediments from similar geographical but different depositional environments**, Organic Geochemistry, 18, 4, 521-529.

Ratanatamskul C., Yamamoto K., Urase T., Ohgaki S. (1996), **Effect of operating conditions on rejection of anionic pollutants in the water environment by nanofiltration especially in very low pressure range**, Water Science & Technology, 34, 9, 149-156.

Rautenbach R., Gröschl A. (1990), **Separation potential of nanofiltration membranes**, Desalination, 77, 73-84.

Ravindran V., Badriyha B.N. (1993), **Crossflow membrane filtration for the removal of natural organic matter**, Proc. of AWWA Membrane Technology Conf., Baltimore, Aug 93, 587-599.

Readman J. (1991), **A rejection profile test for ultrafiltration membranes & devices**, Biotechnology, 9, Oct 91, 941-946.

Reedy M.M., Leenheer J.A., Malcolm R.L. (1989), **Elemental analysis and heat of combustion of fulvic acid from the Suwannee River**, in: Averett R.C., Leenheer J.A., McKnight D.M., Thorn K.A. (Eds.), **Humic**

Substances in the Suwannee River, Georgia: Interactions, Properties, and Proposed Structures, U.S. Geological Survey, Open-File Report 87-557, 147-161.

Regli S., Means E.G., Lykins B.W. (1995), **Disinfection and disinfection by-products regulations in the united states**, Chapter 5, Drinking Water Quality Management, Technomic Publishing, 87-109.

Reinhard M. (1984), **Molecular weight distribution of dissolved organic carbon and dissolved organic halogen in advanced treated wastewaters**, Environ. Sci. Technol., 18, 410-415.

Reiss C.R., Robert C., Taylor J.S. (1997), **Multi-contaminant removal by integrated membrane systems**, Proc. AWWA Membrane Technology Conference, New Orleans, Feb. 97, 289-306.

Reiss C.R., Taylor J.S. (1995), **Prediction of nanofilter productivity decline using fouling indices**, Proc. AWWA Membrane Technology Conf., Reno, Nevada, Aug 95, 433-448.

Rice J.A., Lin J.S. (1994), **Fractal dimensions of humic materials**, Humic Substances in the Global Environment and Implications on Human Health, (Ed. N. Senesi, T.M. Miano), Elsevier Science, 115-120.

Rice J.A., Weil D.A. (1994), **Absolute molecular-weight distribution of fulvic acid**, Humic Substances in the Global Environment and Implications on Human Health, (Ed. N. Senesi, T.M. Miano), Elsevier Science, 355-359.

Rios G.M., Sarrade S.J., Carlès M. (1995), **Rejection characteristics of nanofiltration for small organic and ionic compounds**, Proc. of Euromembrane '95, Vol I, 113-118.

Rohe D.L., Blanton T.C., Mariñas B.J. (1990), **Drinking Water Treatment by Nanofiltration**, National Conference on Environmental Engineering, 707-716.

Rosa M.J., de Pinho M.N. (1994), **Separation of organic solutes by membrane pressure-driven processes**, Journal of Membrane Science, 89, 235-243.

Ryan J.N., Elimelech M. (1996), **Review - Colloid mobilisation and transport in groundwater**, Colloids and Surfaces A: Physicochemical and engineering Aspects, 107, 1-56.

Schäfer A.I. (1993), **Bewertung und verfahrenstechnische Optimisierung der Verfahrenskombination Elektrodialyse/Umkehrosmose zur Aufbereitung von Brunnenwasser**, Diplomarbeit, Fachhochschule Heilbronn.

Schafer M., Hofken M., Durst F. (1997), **Detailed measurements for visualisation of the flow field within a stirred–tank reactor equipped with a rushton turbine**, Trans IchemE, Vol 75, Part A, 729-736.

Schmitz P., Wandelt B., Houi D., Hildenbrand M. (1993), **Particle aggregation at the membrane surface in crossflow microfiltration**, Journal of Membrane Science, 84, 171-183.

Schulten H.-R. (1994), **A chemical structure for humic acid. Pyrolysis-gas chromatography/mass spectrometry and pyrolysis-soft ionisation mass spectrometry evidence**, Humic Substances in the Global Environment and Implications on Human Health, Elsevier Science, 43-56.

Schulten H.-R., Schnitzer M. (1993), **A chemical structure for humic substances**, Naturwissenschaften, 80, 29-30.

Schulten H.-R., Schnitzer M. (1995), **Three-dimensional models for humic acids and soil organic matter**, Naturwissenschaften, 82, 487-498.

Schultz M.F., Benjamin M.M., Ferguson J.F. (1987), **Adsorption and desorption of metals on ferrihydrite: reversibility of the reaction and sorption properties of the regenerated solid**, Environmental Science & Technology, 21, 863-869.

Schweitzer P.A. (1979), **Handbook of separation techniques for chemical engineers**, McGraw-Hill.

Senesi N. (1994), **The fractal approach to the study of humic substances**, Humic Substances in the Global Environment and Implications on Human Health, (Ed. N. Senesi, T.M. Miano), Elsevier Science, 3-41.

Senesi N., Lorusso G.F., Miano T.M., Maggipinto G., Rizzi F.R., Capozzi V. (1994), **The fractal dimension of humic substances as a function of pH by turbidity measurements**, Humic Substances in the Global Environment and Implications on Human Health, (Ed. N. Senesi, T.M. Miano), Elsevier Science, 121-126.

Senesi N., Rizzi F.R., Dellino P., Acquafredda P. (1996), **Fractal dimension of humic acids in aqueous Suspension as a Function of pH and time**, Soil Sci. Am. J., 60, 1773-1780.

Senesi N., Rizzi F.R., Dellino P., Acquafredda P. (1997), **Fractal humic acids in aqueous suspensions at various concentrations, ionic strengths, and pH values**, Colloids and Surfaces, A: Physicochemical and Engineering Aspects, 127, 57-68.

Serkiz S.M., Perdue E.M. (1990), **Isolation of dissolved organic matter from the Suwannee River using reverse osmosis**, Water Research, 24, 7, 911-916.

Sethi S., Wiesner M.R. (1995), **Performance and cost modeling of ultrafiltration**. J of Environmental Engineering, Dec '95, 874-883.

Sethi S., Wiesner M.R. (1997), **Modeling of transient permeate flux in cross-flow membrane filtration incorporating multiple particle transport mechanisms**, J Membrane Science, 136, 191-205.

Shaw D.J. (1991), **Introduction to Colloid and Surface Chemistry**, 4th Edition, Butterworth-Heinemann Ltd..

Shaw P.J., de Haan H., Jones R.I. (1994), **Applicability and reliability of gel filtration to study aquatic humic substances revisited; the effects of pH on molecular size distributions**, Environmental Technology, 15, 753-764.

Shaw P.J., Jones R.I., DeHaan H. (1994), **Separation of molecular size classes of aquatic humic substances using ultrafiltration and dialysis**, Environmental Technology, 15, 765-774.

Sherwood T.K., Brian P.L.T., Fisher R.E., Dresner L. (1965), **Salt concentration at phase boundaries in desalination by reverse osmosis**, 4, 113-118.

Shinozuka N., Nihei Y. (1994), **Size of humic substances in aqueous solution studied by light scattering**, Humic Substances in the Global Environment and Implications on Human Health, (Ed. N. Senesi, T.M. Miano), Elsevier Science, 889-894.

Shuman M.S. (1990), **Carboxyl acidity of aquatic organic matter: possible systematic errors introduced by XAD extraction**, Organic Acids in Aquatic Ecosystems, John Wiley & Sons, 97-109.

Simpson A.E., Kerr C.A., Buckley C.A. (1987), **The effect of pH on the nanofiltration of the carbonate system in solution**, Desalination, 64, 305-319.

Singer P.C. (1999), **Humic substances as precursors for potentially harmful disinfection by-products**, in: Ødegaard H. (Ed), Removal of humic substances from water, Conference Proceedings, Trondheim, Norway, 27-33.

Smith K.A., Colton C.K., Merrill E.W., Evans L.B. (1968), **Convective Transport in a Batch Dialyzer: Determination of True Membrane Permeability from a Single Measurement**, Chemical Engineering Progress Symposium Series, The Artificial Kidney, 84, 64, 45-58.

Solomon T.L., Summers R.S., Speth T.F. (1993), **The reduction of membrane fouling by physical, chemical and biological pretreatment**, Proc. of AWWA Membrane Technology Conf., Baltimore, Aug 93, 159-186.

Sombekke H.D.M., Voorhoeve D.K., Hiemstra P. (1997), **Environmental impact assessment of groundwater treatment with nanofiltration**, Desalination, 113, 293-296.

Song L. (1998), **Flux decline in cdrossflow microfiltration and ultrafiltration: mechanisms and modeling of membrane fouling**, Journal of Membrane Science, 139, 183-200.

Song L., Elimelech M. (1995), **Theory of concentration polarization in crossflow filtration**, J. Chem. Soc. Faraday Trans., 91, 19, 3389-3398.

Song L., Johnson P.R., Elimelech M. (1994), **Kinetics of colloid deposition onto heterogeneously charged surfaces in porous media**, Environmental Science & Technology, 28, 1164-1171.

Sourirajan S., Matsuura T. (1985), **Reverse osmisis and ultrafiltration process principles**, Div. of Chemistry, National Research Council of Canada, Report No. 24188, Ottawa.

Speth T.F., Summers R.S., Gusses A.M. (1996), **Evaluating membrane foulants from conventionally-treated drinking waters**, Natural Organic Matter Workshop, Poitiers, France, September '96, 44.

Spicer P.T., Pratsinis S.E. (1996), **shear-induced flocculation: the evolution of floc structure and the shape of the size dfistribution at steady state**, Water Research, 30, 1049-1056.

Sposito G. (1997), **Scaling invariance of the von Smoluchovski rate law**, Colloids Surfaces A, 120, 101-110.

Staub C., Buffle J., Haerdi W. (1984), **Measurement of complexation properties of metal ions in natural conditions by ultrafiltration: Influence of various factors on the retention of metals and ligands by neutral and negatively charged membranes**, Analytical Chemistry, 56, 2843-2849.

Staude, E. (1992), **Membranen und Membranprozesse**, Grundlagen und Anwendungen, VCH.

Steinberg C., Muenster U. (1985), **Geochemistry of and ecological role of humic substances in lakewater**, in: Aiken G.R., McKnight D.M., Wershaw R.L., MacCarthy P. (Eds.), Humic Substances, in Soil, Sediment, and Water, John Wiley & Sons, Inc., 105-145.

Stevenson F.J. (1985), **Geochemistry of soil humic substances**, in: Aiken G.R., McKnight D.M., Wershaw R.L., MacCarthy P. (Eds.), Humic Substances, in Soil, Sediment, and Water, John Wiley & Sons, Inc., 13-52.

Suess E. (1973a), **Interaction of organic compounds with calcium carbonate-I. Association phenomena and geochemical implications**, Geochimica et Cosmochimica Acta, 34, 157-168.

Suess E. (1973b), **Interaction of organic compounds with calcium carbonate-II. Organo-carbonate association in Recent sediments**, Geochimica et Cosmochimica Acta, 37, 2435-2447.

Suki A.B. (1984), **Factors affecting flux in protein ultrafiltration**, PhD Thesis, UNSW, Sydney, Chemical Engineering.

Sun L., Perdue E.M., McCarthy J.F. (1994), **Using reverse osmosis to obtain organic matter from surface waters**, Humic Substances in the Global Environment and Implications on Human Health, (Ed. N. Senesi, T.M. Miano), Elsevier Science, 901-910.

Sun L., Perdue E.M., McCarthy J.F. (1995), **Using reverse osmosis to obtain organic matter from surface and ground waters**, Water Research, 29, 6, 1471-1477.

Suratt W.B. (1993), **Pretreatment for membrane processes**, Proc. of AWWA Membrane Technology Conf., Baltimore, Aug 93, 9-19.

Suratt W.B., Pinto T.G., O'Keefe B. (1993), **Low cost membrane softening-two years of operation with a hybrid membrane system**, Proc. of AWWA Membrane Technology Conf., Baltimore, Aug 93, 491-512.

Swift R.S. (1985), **Fractionation of soil humic substances**, in: Aiken G.R., McKnight D.M., Wershaw R.L., MacCarthy P. (Eds.), Humic Substances, in Soil, Sediment, and Water, John Wiley & Sons, Inc., 387-408.

Szabó G.T., Móré Gy. Ramadan Y. (1996), **Filtration of organic solutes on reverse osmosis membrane. Effect of counter-ions**, Journal of Membrane Science, 118, 295-302.

Takagi R., Hori M., Gotoh K., Tagawa M., Nakagaki M. (1996), **Membrane charge distribution of cellulose acetate membrane around the interface between the membrane and bulk solution**, World Filtration Congress, Budapest, Hungary, May 96, 395-399.

Takigawa D., personal communication (07/1999).

Takigawa D.Y., Metcalfe P.F., Chu H.C., Light W.G. (1995), **Ultra-low pressure reverse osmosis membranes**, Proc. AWWA Membrane Technology Conf., Reno, Nevada, Aug 95, 69-82.

Tan L., Amy G.L. (1991), **Comparing ozonation and membrane separation for colour removal and disinfection by-product control**, Journal AWWA, May 91, 74-79.

Tan L., Sudak R.G. (1992), **Removing color from a groundwater source**, Journal AWWA, Jan 92, 79-87.

Tang H.X., Tian B.Z., Luan Z.K., Zhang Y. (1994), **Inorganic polymer flocculant polyferric chloride, it's properties, efficiency and production**, Chemical Water and Wastewater Treatment III, 57-69.

Tanizaki Y., Shimokawa T., Nakamura M. (1992), **Physiochemical speciation of trace elements in river waters by size fractionation**, Environmental Science & Technology, 26, 7, 1433-1444.

Tarleton E.S., Wakeman, R.J. (1993), **Understanding flux decline in crossflow microfiltration Part I - Effects of particle and pore size**, Trans IChemE, Vol 71, Part A, 399-409.

Tarleton E.S., Wakeman R.J. (1994a), **Understanding flux decline in crossflow microfiltration: Part II - Effects of process parameters**, Trans IChemE, Vol 72, Part A, 431-440.

Tarleton, E. S., Wakeman, R. J. (1994b), **Understanding flux decline in crossflow microfiltration: Part III- Effects of membrane morphology**, Trans IChemE, Vol 72, Part A, 521-529.

Taylor H.E., Garbarino J.R. (1989), **Occurrence and distribution of selected trace metals in the International Humic Substances Society's standard and reference fulvic and humic acids isolated from the Suwannee River**, in: Averett R.C., Leenheer J.A., McKnight D.M., Thorn K.A. (Eds.), **Humic Substances in the Suwannee River, Georgia: Interactions, Properties, and Proposed Structures**, U.S. Geological Survey, Open-File Report 87-557, 81-98.

Taylor J.S., Mulford L.A. (1995), **Membrane protocol to meet the IRC**, Proc. AWWA Membrane Technology Conf., Reno, Nevada, Aug 95, 195-205.

Taylor J.S., Thompson D.M., Carswell J.K. (1987), **Applying membrane processes to groundwater sources for trihalomethane precursor control**, Journal AWWA, Aug 87, 72-82.

Thill A., Veerapaneni S., Simon B., Wiesner M., Bottero J.Y., Snidaro D. (1998), **Determination of structure of aggregates by confocal scanning laser microscopy**, J of Colloid and Interface Science, 204, 357-362.

Thompson, M.J. (1994), **The effect of flocculation prior to membrane filtration of surface water**, Thesis, UNSW School of Chemical Engineering.

Thorsen T., Harz A., Ødegaard H. (1997), **Influence of raw water characteristics and membrane pore size on the performance of ultra-filters for NOM (humic substances) removal**, IWSA World Congress, SS13, 5-8.

Thorson T., Krogh T., Bergan E. (1993), **Removal of humic substances with membranes system, use and experiences**, Proc. of AWWA Membrane Technology Conf., Baltimore, Aug 93, 131-143.

Thurman E.M. (1985), **Organic geochemistry of natural waters**, Martinus Nijhoff/Dr W. Junk Publishers, Dordrecht.

Thurman E.M., Malcolm R.L. (1981), **Preparative isolation of aquatic humic substances**, Environmental Science & Technology, 15, 4, 463-466.

Tiller C.L., O'Melia C.R. (1993), **Natural organic matter and colloidal stability: models and measurements**, Colloids and Surfaces A: Physicochemical and Engineering Aspects, 73, 89-102.

Tipping E. (1981), **The adsorption of aquatic humic substances by iron oxides**, Geochimica et Cosmochimica Acta, 45, 191-199.

Tipping E. (1993), **Modelling ion binding by humic acids**, Colloids and Surfaces A: Physicochemical and Engineering Aspects, 73, 117-131.

Tipping E., Backes C.A., Hurley M.A. (1988), **The complexation of protons, aluminium and calcium by aquatic humic substances: A model incorporating binding-site heterogeneity and macroionic effects**, Water Research, 22, 5, 597-611.

Tipping E., Heaton M.J. (1983), **The adsorption of aquatic humic substances by two oxides of manganese**, Geochimica et Cosmochimica Acta, Vol 47, 1393-1397.

Tipping E., Ohnstad M. (1984a), **Aggregation of humic substances**, Chemical Geology, 44,. 349-357.

Tipping E., Ohnstad M. (1984b), **Colloid stability of iron oxide particles from a freshwater lake**, Nature, 308, 266-268.

Tombacz E., Meleg E. (1990), **A theoretical explanation of the aggregation of humic substances as a function of pH and electrolyte concentration**, Organic Geochemistry, 15, 4, 375-381.

Tombácz E., Regdon I. (1994), **Humic substances as various colloidal systems**, Humic Substances in the Global Environment and Implications on Human Health, (Ed. N. Senesi, T.M. Miano), Elsevier Science, 139-144.

Trägårdh G. (1989), **Membrane cleaning**, Desalination, 71, 325-335.

Tran C.N., Chu H.C., Light W.G. (1989), **Chlorine-resistant semipermeable membranes**, U.S. Patent, No 4830885.

Tsatsaronis S., Durham B. (1996), **Preparation of process water with microfiltration**, World Filtration Congress, Budapest, Hungary, May 96, 501-506.

Tsuru T., Nakao S-i. Kimura S. (1991a), **Calculation of ion rejection by extended Nernst-Planck equation with charged reverse osmosis membranes for single and mixed electrolyte solutions**, Journal of Chemical Engineering of Japan, 24, 4, 511-517.

Tsuru T., Urairi M., Nakao S.-i., Kimura S. (1991b), **Reverse Osmosis of single and mixed electrolytes with charged membranes: experiment and analysis**, Journal of Chemical Engineering of Japan, 24, 4, 518-524.

Tu S.-C., Ravindran V., Badriyha B.N., Pirbazari M. (1997), **A membrane transport model for predicting permeate flux in nanofiltration processes**, Proc. AWWA Membrane Technology Conference, New Orleans, Feb. 97, 487-498.

Urase T., Oh J.-i., Yamamoto K. (1998), **Effect of pH on rejection of different species of arsenic by nanofiltration**, Desalination, 117, 11-18.

US EPA (1998), **Safe Drinking Water is in our hands**, Existing standards and future priorities, US EPA, Office of Water, http://www.epa.gov/safewater.

Van den Berg G.B., Smolders C.A. (1989), **Concentration polarization phenomena during dead-end ultrafiltration of protein mixtures. The influence of solute-solute interactions**, Journal of Membrane Science, 47, 1-24.

Van der Bruggen B., Schaep J., Maes W., Wilms D., Vandecasteele C. (1998), **Nanofiltration as a treatment method for the removal of pesticides from ground waters**, Desalination, 117, 139-147.

Van der Bruggen B., Schaep J., Wilms D., Vandecasteele C. (1999), **Influence of molecular size, polarity and charge on the retention of organic molecules by nanofiltration**, Journal of Membrane Science, 156, 29-41.

van der Hoek J.P., Bonné P.A.C., van Soest E.A.M., Graveland A. (1995), **Application of hyperfiltration at the Amsterdam waterworks: effect of pretreatment on operation and performance**, Proc. AWWA Membrane Technology Conf., Reno, Nevada, Aug 95, 277-294.

van der Meer W.G.J., Aeijelts Averink C.W., van Dijk J.C. (1996), **Mathematical model of nanofiltration systems**, Desalination, 105, 25-31.

Van der Meer W.G.J., van Dijk J.C. (1997), **Theoretical optimization of spiral-wound and capillary nanofiltration modules**, Desalination, 113, 129-146.

van Duijn A. (1996), **Membrane fouling - no problem**, Membrane Technology, 69, 6-8.

Veerapaneni S., Wiesner M.R. (1994), **Particle deposition on an infinitely permeable surface-dependence od deposit morphology on particle size**, J of Colloid and Interface Science, 162, 110-122.

Veerapaneni S., Wiesner M.R. (1996), **Hydrodynamics of fractal aggregates with radially varying permeability**, J of Colloid and Interface Science, 177, 45-57.

Veerapaneni S., Wiesner M.R. (1997), **Deposit morphology and head loss development in porous media**, Environ. Sci. Technol., 31, 10, 2738-2744.

Ventresque C., Bablon G. (1996), **Drinking water treatment: the use of nanofiltration for polishing surface waters**, World Filtration Congress, Budapest, Hungary, May 96, 490-495.

Ventresque C., Turner G., Bablon G. (1997), **From prototype to full scale**, J AWWA, 89, 10, 65-76.

Vickers J.C., Braghetta A., Hawkins R.A. (1997), **Bench scale evaluation of microfiltration-nanofiltration for removal of particles and natural organic matter**, Proc. AWWA Membrane Technology Conference, New Orleans, Feb. 97, 369-387.

Vickers J.C., Johnson P.E., Willinghan G.A. (1993), **Meeting the surface water treatment rule using continuous microfiltration**, Proc. of AWWA Membrane Technology Conf., Baltimore, Aug 93, 61-75.

Vickers J.C., Thompson M.A., Kelkar U.G. (1995), **The use of membrane filtration in conjunction with coagulation processes for improved NOM removal**, Desalination, 102, 57-61.

Vigneswaran S., Fane A.G. (1998), **Membrane technologies for water treatment**, Indian Chem. Eng., Section B., 40, 3, CHE102-110.

Vitanage D.C., Doolan C., Bliss P., Bowen L. (1996), **Water quality managenent in distribution systems**, Proc. of WaterTECH, AWWA, Sydney, May 96, 633-640.

Volchek K., Keller L., Velicogna D., Whittaker H. (1993), **Selective removal of metal ions from ground water by polymeric binding and microfiltration**, Desalination, 89, 247-262.

Wale R.T., Johnson P.E. (1993), **Microfiltration principles and applications**, Proc. of AWWA Membrane Technology Conf., Baltimore, Aug 93, 1-8.

Wang X.-L., Tsuru T., Togoh M., Nakao S.-i., Kimura S. (1995a), **Evaluation of pore structure and electrical properties of nanofiltration membranes**, Journal of Chemical Engineering of Japan, 28, 2, 186-192.

Wang X.-L., Tsuru T., Togoh M., Nakao S.-i., Kimura S. (1995b), **Transport of organic electrolytes with electrostatic and steric-hindrance effects through nanofiltration membranes**, Journal of Chemical Engineering of Japan, 28, 4, 372-380.

Watson B.M., Hornburg C.D. (1989), **Low energy membrane nanofiltration for removal of color, organics and hardness from drinking water supplies**, Desalination, 72, 11-22.

Wershaw R.L., Aiken G.R. (1985), **Molecular size and weight measurements of humic substances**, in: Aiken G.R., McKnight D.M., Wershaw R.L., MacCarthy P. (Eds.), Humic Substances, in Soil, Sediment, and Water, John Wiley & Sons, Inc., 477-492.

Wetterau G.E., Clark M.M., Anselme C. (1995), **A dynamic model for predicting fouling during ultrafiltration of a natural water**, Proc. AWWA Membrane Technology Conf., Reno, Nevada, Aug 95, 593-608.

White D. A., Lesecq P. (1993), **Optimisation of intermittently operated microfiltration processes**, The Chemical Engineering Journal, 52, 73-77.

Wiesner M.R., Clark M.M., Jacangelo J.G., Lykins B.W., Marinas B.J., O'Melia C.R., Rittmann B.E., Semmens M.J. (1992), **Committee report: membrane processes in potable water treatment**, Journal AWWA, Jan 92, 59-67.

Wiesner M.R., Clark M.M., Mallevialle J. (1989), **Membrane filtration of coagulated suspensions**, Journal of Environmental Engineering, 115, 1, 20-40.

Wiesner M.R., Hackney J., Sethi S., Jacangelo J.G., Laîné J.-M. (1994), **Cost estimates for membrane filtration and conventional treatment**, Journal AWWA, Dec 94, 33-41.

Wijmans J.G., Nakao S., Smolders C.A. (1984), **Flux limitation in ultrafiltration: osmotic pressure model and gel layer model**, Journal of Membrane Science, 20, 115-124.

Wijmans J.G., Nakao S., Van Den Berg J.W.A., Troelstra F.R. F.R., Smolders C.A. (1985), **Hydrodynamic resistance of concentration polarization boundary layers in ultrafiltration**, Journal of Membrane Science, 22, 117-135.

Wilkinson A.E., Hesketh N., Higgo J.J.W., Tipping E., Jones M.N. (1993), **The determination of the molecular mass of humic substances from natural waters by analytical ultracentrifugation**, Colloids and Surfaces A: Physicochemical and Engineering Aspects, 73, 19-28.

Wilkinson K.J., Stoll S., Buffle J. (1995), **Characterization of NOM-colloid aggregates in surface waters: Coupling transmission electron microscopy staining techniques and mathematical modeling**, Fresenius J. Anal. Chem., 351, 54-61.

Wilson M.A. (1988), **What we know and what we don't know about humic materials**, Proc. Science, Technology and Utilisation of Humic Acids, CSIRO North Ryde, Nov 88, 1-10.

Worch E. (1993), **Eine neue Gleichung zur Berechnung von Diffusionskoeffizienten gelöster Stoffe**, Vom Wasser, 81, 289-297.

Xu X., Spencer H.G. (1997), **Transport of electrolytes through a weak acid nanofiltration membrane: effects of flux and crossflow velocity interpreted using a fine-porous membrane model**, Desalination, 113, 85-93.

Yaroshchuk A., Staude E. (1992), **Charged membranes for low pressure reverse osmosis properties and applications**, Desalination, 86, 115-134.

Yiantsios S.G., Karabelas A.J. (1998), **The effect of colloid stability on membrane fouling**, Desalination, 118, 143-152.

Yuan W., Zydney A.L. (1999), **Humic acid fouling during microfiltration**, Journal of Membrane Science, 157, 1, 1-12.

Zander A.K., Cleveland C., Curry N.K. (1995), **Measurement of membrane surface hydrophobicity and charge as affected by solution characteristics**, Proc. AWWA Membrane Technology Conf., Reno, Nevada, Aug 95, 609-619.

Zhang J., Buffle J. (1996), **Multi-method determination of the fractal dimension of hematite aggregates**, Colloids and Surfaces, A: Physicochemical and Engineering Aspects, 107, 175-187.

Zhou J.L., Rowland S.J. (1997), **Evaluation of the interactions between hydrophobic organic pollutants and suspended particles in estuarine waters**, Water Research, 31, 7, 1708-1718.

Zhu X., Elimelech M. (1995), **Fouling of reverse osmosis membranes by aluminium oxide colloids**, Journal of Environmental Engineering, 121, 884-892.

Zhu X., Elimelech M. (1997), **Colloidal fouling of reverse osmosis membranes: measurements and fouling mechanisms**, Environmental Science and Technology, 31, 3654-3662.

Zhu X., Hong S., Childress A.E., Elimelech M. (1995), **Colloidal fouling of reverse osmosis membranes: experimental results, fouling mechanisms, and implications for water treatment**, Proc. AWWA Membrane Technology Conf., Reno, Nevada, Aug 95, 251-263.

Zhu, X. (1996), **Colloidal fouling of thin film composite and cellulose acetate reverse osmosis membranes**, Dissertation, University of California, Civil Engineering, Los Angeles.

Ziechmann W. (1980), **Huminstoffe**, Verlag Chemie, Weinheim, Germany.

THESIS RELATED PUBLICATIONS

JOURNAL PAPERS

Schäfer, A.I. ; Fane, A.G. ; Waite, T.D.

Nanofiltration of Natural Organic Matter: Removal, Fouling and the Influence of Multivalent Ions, Desalination, 118 (1998), 109-122.

Waite, T.D. ; Schäfer, A.I. ; Fane, A.G. ; Heuer, A.

Colloidal Fouling of Ultrafiltration Membranes: Impact of Aggregate Structure and Size, Journal of Colloid and Interface Science, 212 (1999), 264-274.

Schäfer, A.I. ; Schwicker, U. ; Fischer, M.M. ; Fane, A.G. ; Waite, T.D.

Microfiltration of Colloids and Natural Organic Matter, J Membrane Science, (accepted 08/99)

Aoustin, E. ; Schäfer, A.I. ; Fane, A.G. ; Waite, T.D.

Effect of Humic Sustance and Colloid Interactions on Ultrafiltration Behaviour, Separation and Purification Technology, (accepted 03/2000)

Schäfer, A.I. ; Waite, T.D. ; Fane, A.G.

Effect of Solution Preparation Method on Stabilisation and Aggregation of Colloids with Natural Organic Matter, Environmental Science and Technology, (submitted 04/2000)

Schäfer, A.I. ; Pihlajamäki, A. ; Fane, A.G. ; Nyström, M. ; Waite, T.D.

Nanofiltration of Solutions containing Natural Organic Matter (NOM), Journal of Membrane Science, (in preparation)

Schäfer, A.I. ; Fane, A.G. ; Waite, T.D.

Direct Coagulation Pretreatment in Nanofiltration of Waters rich in Organic Matter and Calcium, Water Science and Technology, (accepted 02/2000)

Schäfer, A.I. ; Mauch, R. ; Fane, A.G. ; Waite, T.D.

Charge Effects in the Fractionation of Humic Substances and Natural Organic Matter using Ultrafiltration, Journal AWWA, (in preparation)

Schäfer, A.I. ; Fane, A.G. ; Waite, T.D.

Comparing Membrane Processes for Natural Organics Removal, Water Research, (submitted 01/2000)

CONFERENCE PAPERS

Schäfer, A.I. ; Fane, A.G. ; Waite, T.D.

A Review on the Options for Removal of Natural Organics from Water by Membranes, Proc. IMSTEC '96 (International Membrane Science and Technology Conference), UNSW, Sydney, Nov 1996, Volume 2, 7-9.

Heuer, A. ; Schäfer, A.I. ; Waite, T.D. ; Fane, A.G.

Effect of Aggregate Structure on Ultrafiltration of Colloidal Hematite for the Removal of Colloids and Organic Substances from Surface Water, A.J.B. Kemperman and G.H. Koops (Eds.) Abstracts of the Third International Symposium of the European Society for Membrane Science and Technology (Euromembrane'97), University of Twente, June 1997. ISBN 90-365-09726475.

Schäfer, A.I. ; Fischer M.M. ; Fane A.G. ; Waite T.D.

Microfiltration (MF) of Dilute Suspensions of Colloids and Humic Substances, WaterTECH, Brisbane, April 1998, CD-ROM, ISBN 0-908255-41-1.

Schäfer, A.I. ; Fane, A.G. ; Waite, T.D.

Nanofiltrations of Solutions containing Natural Organic Matter (NOM), in: Proc. Environmental Engineering Research Event, C. Biggs, G. Swain, P. Lant (Eds), Noosa, Queensland, Dec 1997, 159-164. ISBN 09827 222 85

Schäfer, A.I.

Natural Organic Matter Removal Using Membranes, CRC for Water Quality and Treatment, Postgraduate Student Conference, Warburton, Victoria, 15-18 June 1998, 23-28 (confidential).

Schäfer, A.I. ; Fane, A.G. ; Waite, T.D.

Chemical Addition prior to Membrane Processes for Natural Organic Matter (NOM) Removal, in: Chemical Water and Wastewater Treatment V, H.H. Hahn, E.Hoffman, H.Ødegaard (Eds.), Springer, 8th International Gothenburg Symposium, Prague, Sept 1998, 125-137.

Schäfer, A.I. ; Fane, A.G. ; Waite, T.D.

Nanofiltration of Natural Organic Matter: Removal, Fouling and the Influence of Multivalent Ions, Proc. "Membranes in Drinking and Industrial Water Production", Amsterdam, Sept 1998, 109-122.

Schäfer, A.I. ; Fane, A.G. ; Waite, T.D.

Membrane Processes for Removal of Natural Organic Matter (NOM) in Water Treatment, Chemeca '98 Conference, Port Douglas, Sept 1998, CD-ROM.

Schäfer, A.I. ; Fane, A.G. ; Waite, T.D.

Nanofiltration of Natural Organic Matter (NOM): Precipitation and Coagulation Effects on Fouling, in: Proc. EERE'98, A.I. Schäfer, L. Basson, B.S. Richards (Eds.), Avoca Beach, Dec 1998, ISBN 0 7334 0519 3, 315-320.

Schäfer, A.I. ; Fane, A.G. ; Waite, T.D.

Nanofiltration of Natural Organic Matter (NOM): Precipitation and Coagulation Effects on Fouling, ICOM '99, 12-18 June 1999, Toronto, Canada.

Aoustin, E. ; Schäfer, A.I. ; Fane, A.G. ; Waite, T.D.

Effect of Humic Sustance and Colloid Interactions on Ultrafiltration Behaviour, Euromembrane '99, Book of Abstracts, Volume 1, Lectures, I. Genné, R. Leysen, J. Schaep, C. Vandecasteele (Eds.), Leuven, Belgium, ISBN 90-5682-202-0, 75-76.

Schäfer, A.I. ; Fane, A.G. ; Waite, T.D.

Coagulation Pretreatment and Nanofiltration, Environmental Engineering Research Event, Melbourne, 11/99, CD Rom, ISBN 064638256X.

Schäfer, A.I. ; Fane, A.G. ; Waite, T.D.

Membrane Processes for Natural Organic Matter Removal in Water Treatment, Water 2000, Auckland, (accepted 11/1999).

Schäfer, A.I. ; Fane, A.G. ; Waite, T.D.

Direct Coagulation Pretreatment in Nanofiltration of Waters rich in Organic Matter and Calcium, 1st World Congress of the International Water Association, Paris 07/2000, (accepted 02/2000)

Schäfer, A.I. ; Fane, A.G. ; Waite, T.D.

Fouling Effects on Rejection in the Membrane Filtration of Natural Waters, Membranes in Drinking and Industrial Water Production, Paris 10/2000, (abstract submitted).



Andrea Iris **SCHÄFER** 21/03/1970, German

"A dynamic & multi-lingual environmental engineer committed to innovative, sustainable and economically feasible solutions"

1996-1999: **REMOVAL OF NATURAL ORGANIC MATTER USING MEMBRANES (PhD)**
University of NSW, Chemical Engineering, UNESCO Centre for Membrane Science and Technology, Sydney, Australia. Main sponsor: Cooperative Research Centre for Water Quality and Treatment (CRC WQ&T)

1998: *ENVIRONMENTAL ENGINEERING RESEARCH EVENT 1998 (EERE '98)*
6-9 December 1998, Avoca Beach, Australia (Conference Organisation).

1997: *TREATMENT OF ZINC MINING EFFLUENT USING REVERSE OSMOSIS*
(1 month) University of NSW, UNESCO Centre for MST for Industrial Client

1995: *SEPARATION OF ORGANIC ACIDS USING BIPLOLAR ED MEMBRANES*
(4 months) Fraunhofer Gesellschaft, FhG/IGB, Stuttgart, Germany.

1994-1995: *MICROFILTRATION OF PARTICLE SUSPENSIONS*
(3 months) Savoie University, ESIGEC, Chambéry, France.

1994-1995: **PROCESS ENGINEERING (D.E.A., equivalent PhD prep.)**
Savoie University, ESIGEC, Chambéry, France.

1994: *SUPPORTED LIQUID MEMBRANE EXTRACTION OF ORGANIC ACIDS*
(4 months) Industrial Research Limited (IRL), Wellington, New Zealand

1993-1995: **ENVIRONMENTAL ENGINEERING (equivalent Masters)**
Savoie University, ESIGEC, Chambéry, France.

1993: *GROUND WATER DESALINATION WITH RO/ED HYBRID MEMBRANE*
(6 months) *PROCESS,* Dürr GmBH, Process Engineering, Stuttgart, Germany.

1992: *HEAT EXCHANGE SIMULATIONS FOR SPENT FUEL TRANSPORT CASKS &*
(6 months) *FIRE RISK ASSESSMENT FOR KOEBERG NUCLEAR POWER PLANT,* ESKOM (Electricity Supply Commission), Johannesburg, South Africa.

1989-1993: **PHYSICAL & INTRUMENTAL ENGINEERING (MAJOR PROCESS ENGINEERING) (equivalent Honours)**
Fachhochschule Heilbronn, Germany.

1989: *INSTRUMENTAL ANALYSIS, MEMBRANE TECHNOLOGY, METAL*
(6 months) *WORKING,* Berghof GmbH Process Engineering, Eningen, Germany.

1989: *HIGH SCHOOL LEAVING CERTIFICATE (Major Maths and Physics)*
Isolde Kurz Gymnasium, Reutlingen, Germany.

Membership European Society for Membrane Science and Technology (ESMST) since 09/1995
International Association on Water Quality (IAWQ) since 01/1996
Australian Water & Wastewater Association (AWWA) since 1996-1999

Languages German (native), English (fluent, TOEFL 01/1995: 630), French (fluent), Spanish.